

# Tidd Hot Gas Clean Up Program

## Final Report

October 1995

Work Performed Under Contract No.: DE-FC21-89MC26042

For  
U.S. Department of Energy  
Office of Fossil Energy  
Morgantown Energy Technology Center  
Morgantown, West Virginia

By  
Ohio Power Company  
Columbus, Ohio

**MASTER**

DISTRIBUTION OF THIS DOCUMENT IS UNLIMITED

*DCE*

## **DISCLAIMER**

This report was prepared as an account of work sponsored by an agency of the United States Government. Neither the United States Government nor any agency thereof, nor any of their employees, makes any warranty, express or implied, or assumes any legal liability or responsibility for the accuracy, completeness, or usefulness of any information, apparatus, product, or process disclosed, or represents that its use would not infringe privately owned rights. Reference herein to any specific commercial product, process, or service by trade name, trademark, manufacturer, or otherwise does not necessarily constitute or imply its endorsement, recommendation, or favoring by the United States Government or any agency thereof. The views and opinions of authors expressed herein do not necessarily state or reflect those of the United States Government or any agency thereof.

This report has been reproduced directly from the best available copy.

Available to DOE and DOE contractors from the Office of Scientific and Technical Information, 175 Oak Ridge Turnpike, Oak Ridge, TN 37831; prices available at (615) 576-8401.

Available to the public from the National Technical Information Service, U.S. Department of Commerce, 5285 Port Royal Road, Springfield, VA 22161; phone orders accepted at (703) 487-4650.

DOE/MC/26042 -- 5130

TIDD HOT GAS CLEAN UP PROGRAM

DOE

# **Tidd Hot Gas Clean Up Program**

## **Final Report**

Work Performed Under Contract No.: DE-FC21-89MC26042

For  
U.S. Department of Energy  
Office of Fossil Energy  
Morgantown Energy Technology Center  
P.O. Box 880  
Morgantown, West Virginia 26507-0880

By  
Ohio Power Company  
1 Riverside Plaza  
Columbus, Ohio 43216-6631

October 1994

## Forward

---

This Final Report on the Tidd Hot Gas Clean Up Program covers the period from initial Proof-of-Concept testing in August, 1990, through final equipment inspections in May, 1995.

The Tidd Hot Gas Clean Up (HGPU) system was installed in the Tidd Pressurized Fluidized Bed Combustion (PFBC) Demonstration Plant, which is the first utility-scale PFBC plant in the United States. The plant is owned and operated by Ohio Power Company and is located on the banks of the Ohio River, approximately 75 miles downstream of Pittsburgh, Pennsylvania.

This project was funded by the U. S. Department of Energy (DOE), administered by the Morgantown Energy Technology Center (METC) in accordance with DOE Cooperative Agreement No. DE-FC21-89MC26042. Westinghouse Science and Technology Center (STC) of Pittsburgh, Pennsylvania, also contributed 20% cost share for their portion of the project.

The METC Project Manager was Richard A. Dennis. The Contractor Project Manager was Michael J. Mudd and the Principal Investigator was John D. Hoffman. The Westinghouse Project Manager was Thomas E. Lippert.

Detailed design work on the project began in July, 1990, and site construction began in December, 1991. Initial operation of the system occurred in May, 1992, and the hot gas filter was commissioned in October, 1992. The test program ended in March, 1995, when the Tidd Plant was shut down following its four-year test program.

Section 1.0 of this report is an executive summary of the project covering the project background, system description, test results and conclusions. Section 2.0 is an introduction covering the program objectives and schedule. Section 3.0 provides detailed descriptions of the system and its major components. Section 4.0 provides detailed results of all testing including observations and posttest inspection results. Sections 5.0 and 6.0 list the program conclusions and recommendations, respectively. Appendix I is a report prepared by Southern Research Institute on the properties of Tidd PFBC ash sampled during the test program. Appendix II is a report prepared by Westinghouse STC on the performance of candle filter fail-safe regenerator devices.

This report was prepared by American Electric Power Service Corporation (AEPSC) as agent for Ohio Power Company. The portions of the report covering material surveillance test results (Sections 4.9.1 and 4.9.2) were prepared by Westinghouse STC. The following individuals prepared this report:

American Electric Power Service Corporation, Columbus, Ohio:

John D. Hoffman  
Michael J. Mudd  
William P. Reinhart

Westinghouse Science and Technology Center, Pittsburgh, Pennsylvania:

Gerald J. Bruck  
Mary Ann Alvin  
Dennis M. Bachovchin

Southern Research Institute, Birmingham, Alabama:

Todd R. Snyder

## Table of Contents

---

1.0 EXECUTIVE SUMMARY .....	1
1.1 Background .....	1
1.2 Project Description .....	1
1.3 Results .....	2
1.4 Conclusions .....	7
2.0 INTRODUCTION .....	9
2.1 Program Objectives .....	9
2.2 Program Schedule and Milestones .....	9
3.0 PROJECT DESCRIPTION .....	13
3.1 System Description .....	13
3.2 Filter Vessel .....	17
3.3 Filter Internals .....	17
3.4 Backpulse System .....	24
3.5 Backup Cyclone .....	28
3.6 Ash Removal System .....	30
3.6.1 Screw Cooler .....	33
3.6.2 Surge Hopper and Lockhopper .....	34
3.7 Hot Gas Piping .....	35
3.8 Controls and Data Acquisition .....	36
4.0 RESULTS .....	38
4.1 Proof-of-Concept Testing .....	38
4.1.1 Thermal Transient Tests .....	38
4.1.2 HTHP Array Backpulse Tests .....	38
4.1.3 Alkali Attack .....	39
4.1.4 Pulse Valve Testing .....	39
4.1.5 Cold Flow Modelling .....	39
4.1.6 Gasket Tests .....	39
4.1.7 Filter Cake Properties .....	40
4.1.8 Karhula Testing .....	40
4.2 Initial System Operation .....	41
4.2.1 System Modifications (5/92-10/92) .....	42
4.3 Test Period I: 10/92 - 12/92 .....	47
4.3.1 Test Run 1 - 10/28 to 11/1/92 .....	47
4.3.2 Test Run 2 - 11/17/92 .....	48
4.3.3 Test Run 3 - 11/21 to 11/24/92 .....	48
4.3.4 Test Run 4 - 11/25 to 12/7/92 .....	50
4.3.5 Posttest Inspection and Modifications (12/92-6/93) .....	50
4.4 Test Period II: 6/93 - 9/93 .....	71
4.4.1 Test Runs 5 and 6 - 6/30 to 7/5/93 .....	71
4.4.2 Test Run 7 - 7/18 to 8/5/93 .....	71
4.4.3 Test Runs 8 and 9 - 8/9 to 8/14/93 .....	73
4.4.4 Test Run 10 - 8/19 to 8/24/93 .....	73
4.4.5 Test Run 11 - 8/29 to 9/23/93 .....	74

## Table of Contents

---

4.4.6	Posttest Inspection and Modifications (9/93-1/94)	77
4.5	Test Period III: 1/94 - 4/94	85
4.5.1	Test Run 12 - 1/10 to 1/11/94	85
4.5.2	Test Run 13 - 1/15 to 1/29/94	86
4.5.3	Test Run 14 - 2/17 to 2/18/94	86
4.5.4	Test Run 15 - 2/19 to 2/25/94	89
4.5.5	Test Run 16 - 3/3 to 3/9/94	89
4.5.6	Test Run 17 - 3/16 to 3/23/94	89
4.5.7	Test Run 18 - 3/31 to 4/18/94	90
4.5.8	Posttest Inspection and Modifications (4/94-7/94)	96
4.6	Test Period IV: 7/94 - 10/94	113
4.6.1	Test Runs 19 and 20 - 7/16/94	113
4.6.2	Test Run 21 - 7/20/94 to 7/27/94	113
4.6.3	Test Run 22 - 7/28/94 to 8/25/94	115
4.6.4	Posttest Inspection (8/94)	115
4.6.5	Test Run 23 - 9/3/94 to 9/10/94	117
4.6.6	Posttest Inspection (9/94)	117
4.6.7	Test Run 24 - 9/22/94 to 10/21/94	117
4.6.8	Posttest Inspection (10/94)	120
4.7	Test Period V: 1/95-3/95	137
4.7.1	Test Runs 25, 26, and 27 - 1/13/95 to 1/21/95	137
4.7.2	Test Run 28 - 1/27/95 to 2/2/95	137
4.7.3	Posttest Inspection (2/95)	140
4.7.4	Test Runs 29 and 30 - 2/9/95 to 2/10/95	140
4.7.5	Test Run 31 - 2/11/95 to 2/12/95	140
4.7.6	Test Run 32 - 2/13/95 to 2/16/95	140
4.7.7	Posttest Modifications (2/95)	142
4.7.8	Test Run 33 - 2/18/95 to 3/8/95	142
4.7.9	Test Run 34 - 3/14/95 to 3/30/95	142
4.7.10	Posttest Inspection (4/95-5/95)	144
4.8	Final Equipment Inspections	156
4.8.1	Filter Vessel	156
4.8.2	Filter Internals	156
4.8.3	Backpulse System	157
4.8.4	Backup Cyclone	164
4.8.5	Ash Removal System	164
4.8.6	Hot Gas Piping	164
4.9	Materials Surveillance Test Results	180
4.9.1	Metal Structures and Test Coupons	182
4.9.2	Candle Filters	197
5.0	CONCLUSIONS	218
6.0	RECOMMENDATIONS	220

## Table of Contents

---

APPENDIX I (Prepared by Southern Research Institute) .....	222
APPENDIX II (Prepared by Westinghouse STC) .....	238

## Table of Contents

---

### List of Tables

Table 2.2.1 - Tidd HGCU Test Periods .....	10
Table 2.2.2 - Tidd HGCU Runs Summary .....	11
Table 3.1 - APF Design Basis .....	14
Table 3.7 - Hot Gas Piping Design .....	36
Table 4.1.7 - PFBC Ash Properties .....	40
Table 4.3 - Summary of HGCU Operation - Test Period I .....	47
Table 4.4 - Summary of HGCU Operation - Test Period II .....	71
Table 4.5 - Summary of HGCU Operation - Test Period III .....	85
Table 4.6 - Summary of HGCU Operation - Test Period IV .....	113
Table 4.7 - Summary of HGCU Operation - Test Period V .....	137
Table 4.9.1 - Summary of Internal Structural Component Performance Issues and Corrective Actions .....	184
Table 4.9.2 - Surveillance Tree Coupon Weight Comparisons .....	187
Table 4.9.3 - Elongation of Clay Bonded Silicon Carbide Candle Filters .....	201
Table 4.9.4 - Posttest Candle Filter Time-Of-Flight Measurements .....	202
Table 4.9.5 - Filter Candle Materials .....	204
Table 4.9.6 - Candle Filter Failure Mechanisms Experienced During Operation at Tidd .....	205
Table 4.9.7 - Candle Filter Bulk Matrix Strength .....	208
Table I-1 - Sedigraphic Analyses of Tidd Ashes .....	228
Table I-2 - Sieve Analyses of Tidd Ashes .....	228
Table I-3 - Chemical Analyses of Tidd Ashes Collected in May 1995, % wt. ....	230
Table I-4 - Acid/Base Ratios of Ashes Collected at Tidd on May 11, 1995 .....	231
Table I-5 - Chemical Analyses of Tidd Ashes Collected in 1993, % wt. ....	232
Table I-6 - Physical Analyses of Ashes Collected at Tidd on May 11, 1995 .....	233
Table II-1 - Head Loss Across Fail-Safe Regenerator Devices .....	240

## Table of Contents

### List of Figures

Figure 2.2 - Program Schedule .....	10
Figure 3.1.1 - HGCU Slipstream Schematic .....	15
Figure 3.1.2 - Isometric View of HGCU System .....	16
Figure 3.2 - Photograph of APF Vessel During Erection .....	19
Figure 3.3.1 - APF Internal Arrangement .....	20
Figure 3.3.2 - Photograph of Filter Internals During Initial Installation .....	21
Figure 3.3.3 - Photograph of Filter Internals During Initial Installation .....	22
Figure 3.3.4 - Photograph of Filter Internals During Initial Installation .....	23
Figure 3.4.1 - Schematic Diagram of Backpulse System .....	25
Figure 3.4.2 - Photograph of Backpulse Skid .....	26
Figure 3.4.3 - Photograph of Backpulse Skid .....	27
Figure 3.5 - Cross Section of Backup Cyclone .....	29
Figure 3.6 - Ash Removal System Schematic .....	32
Figure 3.6.1 - Screw Cooler Schematic .....	34
Figure 4.2.1 - Photograph of Hastelloy Liner in Hot Gas Pipe Spool .....	44
Figure 4.2.2 - Typical Expansion Joint After Modifications .....	45
Figure 4.2.3 - Cross Section of Typical Hot Gas Piping Joint .....	46
Figure 4.3.1 - Photograph of Bottom Filter Candles Following Test Run 1 .....	49
Figure 4.3.2 - Photograph of Filter Internals Following Test Run 4 .....	51
Figure 4.3.3 - Photograph of Filter Internals Following Test Run 4 .....	52
Figure 4.3.4 - Photograph of Filter Internals Following Test Run 4 .....	53
Figure 4.3.5 - Photograph of Filter Internals Following Test Run 4 .....	54
Figure 4.3.6 - Photograph of Filter Internals Following Test Run 4 .....	55
Figure 4.3.7 - Photograph of Filter Internals Following Test Run 4 .....	56
Figure 4.3.8 - Photograph of Filter Internals Following Test Run 4 .....	57
Figure 4.3.9 - Photograph of Filter Internals Following Test Run 4 .....	58
Figure 4.3.10 - Photograph of Filter Internals Following Test Run 4 .....	59
Figure 4.3.11 - Graphs of Filter Parameters During Test Run 4 .....	66
Figure 4.3.12 - Photograph of Filter Internals Before Test Period II .....	67
Figure 4.3.13 - Photograph of Filter Internals Before Test Period II .....	68
Figure 4.3.14 - Photograph of Filter Internals Before Test Period II .....	69
Figure 4.3.15 - Photograph of Filter Internals Before Test Period II .....	70
Figure 4.4.2 - Filter DP and Temperature During Test Run 7 .....	72
Figure 4.4.5 - Filter DP and Temperature During Test Run 11 .....	76
Figure 4.4.6 - Photograph of Filter Internals Following Test Run 11 .....	79
Figure 4.4.7 - Photograph of Filter Internals Following Test Run 11 .....	80
Figure 4.4.8 - Photograph of Filter Internals Following Test Run 11 .....	81
Figure 4.4.9 - Photograph of Filter Internals Following Test Run 11 .....	82
Figure 4.4.10 - Photograph of Filter Internals Following Test Run 11 .....	83
Figure 4.4.11 - Photograph of Filter Internals Following Test Run 11 .....	84
Figure 4.5.2 - Filter DP and Temperature During Test Run 13 .....	87
Figure 4.5.4 - Filter DP and Temperature During Test Run 15 .....	88

## Table of Contents

Figure 4.5.5 - Filter DP and Temperature During Test Run 16 .....	91
Figure 4.5.6 - Filter DP and Flow During Test Run 16 .....	92
Figure 4.5.7 - Filter DP and Temperature During Test Run 17 .....	93
Figure 4.5.8 - Filter DP and Flow During Test Run 17 .....	94
Figure 4.5.9 - Filter DP and Temperature During Test Run 18 .....	95
Figure 4.5.10 - Photograph of Filter Internals Following Test Run 18 .....	98
Figure 4.5.11 - Photograph of Filter Internals Following Test Run 18 .....	99
Figure 4.5.12 - Photograph of Filter Internals Following Test Run 18 .....	100
Figure 4.5.13 - Photograph of Filter Internals Following Test Run 18 .....	101
Figure 4.5.14 - Photograph of Filter Internals Following Test Run 18 .....	102
Figure 4.5.15 - Photograph of Filter Internals Following Test Run 18 .....	103
Figure 4.5.16 - Photograph of Filter Internals Following Test Run 18 .....	104
Figure 4.5.17 - Photograph of Filter Internals Following Test Run 18 .....	105
Figure 4.5.18 - Photograph of Filter Internals Following Test Run 18 .....	106
Figure 4.5.19 - Photograph of Filter Internals Before Test Period IV .....	107
Figure 4.5.20 - Photograph of Filter Internals Before Test Period IV .....	108
Figure 4.5.21 - Photograph of Filter Internals Before Test Period IV .....	109
Figure 4.5.22 - Photograph of Filter Internals Before Test Period IV .....	110
Figure 4.5.23 - Photograph of Filter Internals Before Test Period IV .....	111
Figure 4.5.24 - Photograph of Filter Internals Before Test Period IV .....	112
Figure 4.6.2 - Filter DP and Temperature During Test Run 21 .....	114
Figure 4.6.3 - Filter DP and Temperature During Test Run 22 .....	116
Figure 4.6.5 - Filter DP and Temperature During Test Run 23 .....	118
Figure 4.6.7 - Filter DP and Temperature During Test Run 24 .....	119
Figure 4.6.8 - Photograph of Filter Internals Following Test Run 24 .....	122
Figure 4.6.9 - Photograph of Filter Internals Following Test Run 24 .....	123
Figure 4.6.10 - Photograph of Filter Internals Following Test Run 24 .....	124
Figure 4.6.11 - Photograph of Filter Internals Following Test Run 24 .....	125
Figure 4.6.12 - Photograph of Filter Internals Following Test Run 24 .....	126
Figure 4.6.13 - Photograph of Filter Internals Following Test Run 24 .....	127
Figure 4.6.14 - Photograph of Filter Internals Following Test Run 24 .....	128
Figure 4.6.15 - Photograph of Filter Internals Following Test Run 24 .....	129
Figure 4.6.16 - Photograph of Filter Internals Following Test Run 24 .....	130
Figure 4.6.17 - Photograph of Crack in Back Pulse Tube .....	131
Figure 4.6.18 - Location of Filter Candle Materials Before Test Period V .....	132
Figure 4.6.19 - Photograph of Filter Internals Before Test Period V .....	133
Figure 4.6.20 - Photograph of Filter Internals Before Test Period V .....	134
Figure 4.6.21 - Photograph of APF Shroud Following Test Run 24 .....	135
Figure 4.6.22 - Photograph of APF Shroud After Replacement of Upper Portion .....	136
Figure 4.7.2 - Filter DP and Temperature During Test Run 28 .....	139
Figure 4.7.6 - Filter DP and Temperature During Test Run 32 .....	141
Figure 4.7.8 - Filter DP and Temperature During Test Run 33 .....	143
Figure 4.7.9 - Filter DP and Temperature During Test Run 34 .....	145
Figure 4.7.10 - Photograph of Filter Internals Following Test Run 34 .....	147
Figure 4.7.11 - Photograph of Filter Internals Following Test Run 34 .....	148
Figure 4.7.12 - Photograph of Filter Internals Following Test Run 34 .....	149

## Table of Contents

Figure 4.7.13 - Photograph of Filter Internals Following Test Run 34 .....	150
Figure 4.7.14 - Photograph of Filter Internals Following Test Run 34 .....	151
Figure 4.7.15 - Photograph of Filter Internals Following Test Run 34 .....	152
Figure 4.7.16 - Photograph of Filter Internals Following Test Run 34 .....	153
Figure 4.7.17 - Photograph of Filter Internals Following Test Run 34 .....	154
Figure 4.7.18 - Photograph of Filter Internals Following Test Run 34 .....	155
Figure 4.8.1 - Photograph of Corrosion of APF Head Under Insulation Near Outlet Nozzle .....	158
Figure 4.8.2 - Photograph of APF Shroud During Final Removal .....	159
Figure 4.8.3 - Photograph of Shroud Impingement Plate .....	160
Figure 4.8.4 - Photograph of APF Liner .....	161
Figure 4.8.5 - Photograph of Tubesheet Cone .....	162
Figure 4.8.6 - Photograph of Tubesheet Cone .....	163
Figure 4.8.7 - Photograph of Backpulse Valve Internals .....	166
Figure 4.8.8 - Photograph of Backpulse Valve Internals .....	167
Figure 4.8.9 - Photograph of Backup Cyclone Internals .....	168
Figure 4.8.10 - Photograph of Backup Cyclone Internals .....	169
Figure 4.8.11 - Photograph of Backup Cyclone Internals .....	170
Figure 4.8.12 - Photograph of Backup Cyclone Internals .....	171
Figure 4.8.13 - Photograph of Alternate Ash Line Restrictive Orifice .....	172
Figure 4.8.14 - Photograph of Alternate Ash Line Restrictive Orifice .....	173
Figure 4.8.15 - Photograph of Hastelloy Liner After Removal From Pipe Section .....	174
Figure 4.8.16 - Photograph of Inside Surface of Carbon Steel Pipe Under Hastelloy Liner .....	175
Figure 4.8.17 - Photograph of Inside of Pipe Spool Following Removal of Section .....	176
Figure 4.8.18 - Photograph of Inside of Pipe Spool Following Removal of Section .....	177
Figure 4.8.19 - Photograph of Inside of Pipe Spool Following Removal of Section .....	178
Figure 4.8.20 - Photograph of Inside of Pipe Spool Following Removal of Section .....	179
Figure 4.9 - Tidd HGCU APF Operating Temperature History .....	181
Figure 4.9.1 - Cross Section of 0.005-inch Wire from Fine Fail-safe Mesh As New-700X .....	188
Figure 4.9.2 - Cross Section of 0.005-inch Wire from Fine Fail-safe Mesh After 1329 hours at Karhula-700X .....	189
Figure 4.9.3 - Cross Section of 0.005-inch Wire from Fine Fail-safe Mesh After 1110 hours at Tidd-700X .....	190
Figure 4.9.4 - Cross Section of Alloy 333 Coupon-700X .....	191
Figure 4.9.5 - Cross Section of Alloy 617 Coupon-700X .....	192
Figure 4.9.6 - Cross Section of Alloy 556 Coupon-700X .....	193
Figure 4.9.7 - Cross Section of Alloy 188 Coupon-700X .....	194
Figure 4.9.8 - Cross Section of Alloy 253MA Coupon-700X .....	195
Figure 4.9.9 - Cross Section of Alloy 310 Coupon-700X .....	196
Figure 4.9.10 - Room Temperature Gas Flow Resistance of the First Generation Monolithic and Advanced Second Generation Candle Filters .....	198
Figure 4.9.11 - Room Temperature Gas Flow Resistance Measurements Across As-Manufactured Clay Bonded Silicon Carbide Filter Elements. Measurements Were Repeated After Operation at Tidd. ....	200
Figure 4.9.12 - Correlation of Time-of-Flight and Burst Strength with Room Temperature C-Ring Compressive Strength for Candle Filters Exposed for 464 Hours of PFBC Operating Conditions in Test Period I. ....	203

## Table of Contents

---

Figure 4.9.13 - Schumacher Strength Profile .....	206
Figure 4.9.14 - Photo Micrograph Showing Crystallization of the Schumacher Dia Schumalith F40 Filter Matrix .....	210
Figure 4.9.15 - Crystallization of the Coors Alumina/Mullite Filter Matrix after 1110 hrs of Operation in Test Period IV .....	213
Figure 4.9.16 - Crystallization of the Coors Alumina/Mullite Filter Matrix after 2816 hrs of Operation in Test Period IV and V .....	214
Figure 4.9.17 - Thermal Coefficient of Expansion of the Tidd PFBC Ash and Select Porous Ceramic Filter Materials .....	217
Figure I-1 - SEM Photograph of a Fresh Fracture Surface of an Ash Agglomerate Taken from an Ash Shed in the Tidd APF in October 1994 .....	226
Figure I-2 - Cumulative Size Distribution Data Measured with a Sedigraph and Sieves for Five Ashes Collected from the Tidd APF .....	229
Figure II-1 - Fraction of Flow Through Broken Positions Versus Percent Broken .....	241

## Acronyms and Abbreviations

---

<b>acfm</b>	Actual Cubic Feet Per Minute
<b>AEP</b>	American Electric Power Company, Inc.
<b>APF</b>	Advanced Particle Filter
<b>ANSI</b>	American National Standards Institute
<b>ASME</b>	American Society of Mechanical Engineers
<b>BUC</b>	Backup Cyclone
<b>CaO</b>	Calcium Oxide
<b>cm</b>	Centimeter
<b>CVI-SiC</b>	Chemical Vapor Infiltration-Silicon Carbide
<b>Δ</b>	Delta
<b>DP</b>	Differential Pressure
<b>EDAX</b>	Energy Dispersive X-Ray Analyses
<b>F</b>	Degrees Fahrenheit
<b>FSRD</b>	Fail-Safe Regenerator Device
<b>fps</b>	Feet Per Second
<b>gm/cc</b>	Grams Per Cubic Centimeter
<b>gpm</b>	Gallons Per Minute
<b>GT</b>	Gas Turbine
<b>HGCU</b>	Hot Gas Clean Up
<b>hp</b>	Horsepower
<b>hr</b>	Hour

## Acronyms and Abbreviations

---

<b>HTHP</b>	High Temperature High Pressure
<b>ID</b>	Inside Diameter
<b>in.</b>	Inches
<b>in. H<sub>2</sub>O</b>	Inches of Water
<b>in.-lbf.</b>	Inch-Pounds of Torque
<b>lbm</b>	Pounds Mass
<b>mm</b>	Millimeter
<b>MWe</b>	Megawatt Electric
<b>MWt</b>	Megawatt Thermal
<b>OD</b>	Outside Diameter
<b>PCFB</b>	Pressurized Circulating Fluidized Bed
<b>PFBC</b>	Pressurized Fluidized Bed Combustion
<b>POPS</b>	Plant Operations and Performance System
<b>ppmw</b>	Parts Per Million by Weight
<b>psi</b>	Pounds Per Square Inch
<b>psig</b>	Pounds Per Square Inch Gauge
<b>PT</b>	Penetrant Test
<b>QA/QC</b>	Quality Assurance/Quality Control
<b>scfm</b>	Standard Cubic Feet Per Minute
<b>SEM</b>	Scanning Electron Microscopy
<b>SSH</b>	Secondary Superheater

## Acronyms and Abbreviations

---

<b>ST</b>	Steam Turbine
<b>TOF</b>	Time of Flight
<b><math>\mu\text{m}</math></b>	Microns
<b>UNS</b>	Unified Numbering System
<b>XJ</b>	Expansion Joint
<b>XRD</b>	X-Ray Diffraction

## Executive Summary

---

### 1.0 EXECUTIVE SUMMARY

#### 1.1 Background

The objective of this program was to evaluate the design and obtain operating experience for a commercial size Advanced Particle Filter (APF) through long-term testing on a slipstream at Ohio Power Company's Tidd Pressurized Fluidized Bed Combustion (PFBC) Demonstration Plant. The 70 MWe Tidd PFBC Demonstration Plant in Brilliant, Ohio was completed in late 1990, and operated through March 1995 as part of the Department of Energy's Clean Coal Technology Program. Provisions were included as part of the original design to install a one-seventh slipstream on the PFBC exhaust gases between the fluidized bed and the gas turbine to test an APF system. In July 1990, AEP awarded a contract to Westinghouse Science and Technology Center to provide a candle-based APF. Detailed engineering and material procurement were completed by the end of 1991 when installation began. Initial operation of the system occurred in May, 1992, and the APF was commissioned in October, 1992. The HGCU system operated during five separate test periods between October, 1992, and March, 1995, compiling a total of 5854 hours of operation on coal fire.

#### 1.2 Project Description

In the original design, the Tidd PFBC Demonstration Plant utilized seven strings of primary and secondary cyclones to remove 98% of the particulate matter from the gases between the fluidized bed and the gas turbine. The HGCU slipstream replaced one of the seven secondary cyclones by taking the discharge gas of one of the primary cyclones to outside of the combustor vessel and into the APF. After passing through the APF, the gas flowed through a backup cyclone and then returned to the combustor vessel, where the slipstream flow rejoined the combustor gas at the discharge of the other six cyclone strings.

Under the original maximum load design conditions, gas at approximately 150 psig, 1550F flowed into the filter at 7600 acfm with a dust loading of approximately 600 ppmw. In January 1994, the dust loading to the filter was increased from approximately 600 ppmw to 3400 ppmw by detuning the primary cyclone upstream of the APF. In January 1995, the primary cyclone was bypassed which increased the ash loading to approximately 20,000 ppmw. Ash collected in the APF was discharged to a screw cooler and into a lockhopper system which fed a vacuum pneumatic ash transport system. A backup cyclone

## Executive Summary

---

downstream of the filter was included to clean the gas in case of a filter malfunction, and to balance the pressure drop of the slipstream with the other six cyclone strings.

The system was designed to remove virtually all entrained particulates discharged from one of the seven parallel primary cyclones on the outlet of the PFBC combustor. Ash collected on the outside surface of ceramic filter elements (candles), resulting in a gradual increase in the overall flow resistance of the slipstream. The filter cake was periodically dislodged by injecting a high pressure air pulse to the clean side of the candles. The ash cake on the candles then fell to the conical discharge hopper where it was removed from the filter vessel and cooled by an ash screw cooler which discharged into a lockhopper system.

The main elements of the system included the filter vessel and its internals; back pulse skid, including secondary accumulators and valves; back pulse air supply skid, including compressor, dryer and primary accumulator; backup cyclone; ash screw cooler, surge hopper, lockhopper, piping, and instrumentation.

The filter vessel was 10 feet in diameter and 44 feet high. The vessel was internally insulated with a 7 to 9-inch thick layer of alumina-silica ceramic fiber insulation to keep the vessel shell temperature below 250F. The filter contained 384 filter elements which were referred to as candles because of their long cylindrical shape. Each candle was nominally 2.36 inches in outside diameter and 4.92 feet long. The candles were made of two layers of sintered silicon carbide.

The Backpulse System was comprised of a compressor skid, valve skid, and interconnecting piping.

There were three control modes available for the filter system, namely manual mode, automatic differential pressure (DP) mode and automatic timer mode. The system was normally operated in the timer mode. In this mode, filter cleaning occurred at uniform time intervals, typically thirty minutes. A Bailey Net 90 control system was used to monitor and control the system parameters and provide operator interfaces. Data collected included pressure, temperature, flowrate, differential pressure, level, etc. throughout the system.

### 1.3 Results

During the design phase of the project, Westinghouse conducted proof-of-concept testing to verify the design basis of various system components. The tests included thermal transient tests of filter elements,

## Executive Summary

---

high temperature high pressure tests of an eleven candle array, cold flow modeling, pulse valve tests, gasket tests, alkali attack tests on silicon carbide, and ash characterization.

During initial operation of the system in May, 1992, using a bypass cyclone with the APF not in service, an expansion joint in the hot gas piping system ruptured due to stress corrosion from chemical attack by condensed flue gas. Hot spots also were detected in the piping system during this test. As a result of the problems noted during initial testing, several modifications were made to the piping system before the APF was commissioned. The stainless steel expansion joint bellows were replaced with two-ply Hastelloy C-22 material which had much better corrosion resistance to condensed flue gas. The ceramic fiber material used to internally insulate the hot gas piping and expansion joints was replaced with cast refractory to prevent hot gas from flowing to the outer pipe and creating hot spots. Hastelloy cladding was added to the inside surface of the hot gas pipe to protect it from corrosion. The modifications described above proved successful, and the piping system performed very well during subsequent testing. However, corrosion of expansion joint bellows remained a problem until additional steps were taken later in the project.

The filter was commissioned on coal fire on October 28, 1992. During the first test period from October to December, 1992, the system operated 464 hours during four test runs, with the longest run of 286 hours. The major problem during this test period was unreliable ash removal from the APF and lockhopper system. In addition, another expansion joint bellows (inner ply only) developed a pinhole leak due to corrosion, the backpulse air compressor failed resulting in a 17-hour interruption in filter cleaning, and the APF pressure drop was unstable at operating temperatures above 1400F. Upon shutdown, the APF hopper was full of ash above the level of the lower candles which resulted in the breakage of 21 bottom candles. The HGCU system was bypassed and Tidd continued to operate on six cyclone strings until the next test period.

Prior to the next test period, several modifications were made to address the problems encountered during the first test period. All of the bottom filter candles were replaced. The ash removal system was modified to improve the operation of the lockhopper system, a vibrator was added to the APF hopper liner to aid in ash removal, the expansion joints were heat traced and insulated to maintain them above the flue gas acid dew point, and backup compressors were added to ensure continuous filter cleaning in case a future compressor failures.

## Executive Summary

---

The second test series began in June, 1993, and lasted until September, 1993. During this period, the system operated for 1295 hours on coal fire over seven separate runs with the longest run of 597 hours. During this period problems with ash removal from the APF hopper persisted and the filter pressure drop was unstable during some of the runs. It was possible to clean the ash from the filter candles at reduced load (temperature) and thereby lower the filter pressure drop; however, the high filter pressure drop recurred after two days of operation at higher temperatures.

Posttest inspection revealed 62 broken candles and very heavy ash bridging between candles and support pipes. Microcracking was detected in the high temperature portion of the backpulse tubes. Galling was found on the backpulse valve internals. Modifications made to the system prior to the next test series included replacing all of the filter candles, replacing the backpulse tubes with a different material, adding hardened surfaces to the backpulse valve internals, and adding nine purge air nozzles to the APF hopper to aid in ash removal.

In an effort to overcome the ash bridging problem, it was decided to detune the primary cyclone upstream of the filter during the next test series. It was believed that the resulting coarser ash would be easier to remove from the filter candles and less likely to accumulate on the hopper walls. All testing during the next test period was conducted with the cyclone detuned.

The third test period was from January to April, 1994, and covered 1279 hours of operation with seven runs, the longest being 444 hours. Ash sampling was performed upstream and downstream of the APF using specially designed sampling probes. The results showed that by detuning the primary cyclone, the ash loading to the filter increased from a design value of 600 ppmw to about 3400 ppmw, and the mass mean particle size of the ash increased from about 3 to 7 microns. The higher ash concentration resulted in significantly higher ash loading. Despite the higher ash loading, the filter pressure drop was stable during this period up to 1450F operating temperature.

Hazardous Air Pollutant testing was conducted by Radian Corporation in April, 1994, and the results of the testing are documented in Report Number DCN 94-633-021-03, dated October, 1994. As part of Hazardous Air Pollutant testing, SO<sub>2</sub> data were obtained upstream and downstream of the APF. Results indicated that the SO<sub>2</sub> level in the gas was reduced approximately 40% by the APF. Post-test analysis of ash samples retrieved from the APF and precipitator hoppers confirmed this observation.

## Executive Summary

---

The filter internals were removed from the APF vessel following this test series, and 28 broken candles were found. Very heavy ash bridging was observed between the inner rows of candles and the support pipe on the top and middle plenums. All of the candle breaks except one appeared to be fresh breaks judging from the clean fracture surfaces. All of the breaks occurred at the top of the candles just below the candle holders. The breaks appeared to result from bending forces from ash bridging from the inner candles to the outer candles. The outlet side of the filter was very clean with virtually no ash deposits. This indicated that the failures occurred during or after plant shutdown, and that the filter was not leaking ash to the clean side during operation.

All of the candles in the upper and middle plenums were removed, cleaned, and inspected. The bottom plenum candles were not removed and cleaned since they did not exhibit significant bridging. The upper and middle plenums were reassembled with an assortment of new and used candles. Thirty of the new replacement candles were second generation materials.

Since ash bridging between the support pipes and inner rows of candles remained a problem, it was decided to remove the inner row of candles from the six upper and middle plenums to determine if this would eliminate the ash bridging. Removal of the inner rows reduced the number of candles from 384 to 288 and increased the face velocity from 7.1 ft/min to 8.9 ft/min. In addition, provisions were added to totally spoil the primary cyclone ahead of the filter to evaluate operation with a higher mean particle size.

The fourth test period began in July, 1994 and ended in October, 1994. Operation totaled 1706 hours of coal fire over six runs, the longest being 691 hours. After operating for 844 hours, the filter was inspected using a boroscope to determine if removal of the inner rows of candles from the upper and middle plenums had eliminated ash from accumulating on the ash sheds and bridging over to the candles. This was believed to be the root cause of the candle failures in the previous tests. Ash bridging, while less than before, had still occurred. The APF hopper was clean two days following shutdown, but when inspected again four days following shutdown, ash was found in the hopper. During the inspection with a boroscope, 14 broken filter candles were seen, and candle pieces were later removed from the hopper. It was decided to continue this test series with 14 broken candles.

During the following test run, the primary cyclone was completely spoiled for 90 hours causing all of the ash entering it to flow into the APF. The APF was again inspected using a boroscope following this run, and it was found that most of the ash bridges seen in the previous inspection had disappeared, and

## Executive Summary

---

the few that remained appeared smaller. This indicated that the coarser ash was cleaning the ash accumulation from the ash sheds. The liner and hopper also were very clean of ash deposits. No additional broken candles were observed.

At the end of this test series the APF internals were removed from the vessel for inspection and candle replacement. A total of 30 candles were observed to be broken. Ten of the 30 breaks had clean fracture surfaces indicating that the breaks occurred after shutdown or during removal from the vessel. Heavy ash bridging was apparent near the bottoms of some of the candles. It was evident that the ash accumulation that occurred during the first 600 hours of this run was not removed during the last 90 hours of operation with the cyclone spoiled.

Two of the nine backpulse tubes were found to have longitudinal cracks, believed to be due to thermal fatigue. All nine tubes were replaced in kind following this test series.

All of the filter candles in the APF were replaced prior to the next (and final) test series. In order to broaden the base of candle filter material testing, the filter was fitted with a combination of silicon carbide, alumina mullite, and two other second generation materials. The inner rows of candles in the upper and middle plenums were left out, the same as in the prior test series. The primary cyclone upstream of the APF was modified to force all the gas and ash to flow through it and not collect any ash. This was done to determine whether the APF would operate at full load gas temperature (1550F) without ash bridging and without unstable pressure drop. As a precautionary measure to protect the gas turbine from erosion by the coarse ash if a candle broke, fail-safe devices were installed above each candle. The devices were designed to plug when exposed to ash, but otherwise not interfere with the normal flow of gas and backpulse cleaning air.

The final test series ran from January through March, 1995, and totaled 1110 hours over 10 runs, the longest being 427 hours. All tests during this period were conducted with the primary cyclone bypassed resulting in heavy, coarse ash loading to the APF. This was the first test series in which the APF operated above 1500F for sustained periods. Filter pressure drop was stable during most of this period, with indications of a slight increase near the end of the period. Inspection after 173 hours of operation revealed no ash bridging and very clean filter internals. Later in the test period fragments from one type of second generation filter candle were removed from the ash removal system. Posttest inspection revealed that 20 of 22 Dupont PRD66 second generation candles and two Coors alumina-mullite candles

## Executive Summary

---

were broken. No ash bridging was seen. Some of the candles were found to have internal ash accumulation in the bottom. Three candles were found to be cracked in the bottom portion.

Following completion of the test program, equipment inspections were performed to assess the condition of the hardware. The APF vessel was in good condition except for significant corrosion in the top of the head where hot gas had contacted the metal surface. The shroud was in good condition, but the liner appeared warped in some locations. The tubesheet and support cone were in excellent condition. The backpulse valves, backup cyclone, ash removal system, and hot gas piping were all found to be in good to excellent condition.

Westinghouse conducted a materials surveillance program during the project. This program included both metal structures (and coupons) and filter candle material monitoring. The metal structures in general exhibited few problems. Creep data and penetrant testing of welds did not reveal problems. Some embrittlement of 310 stainless steel was noted. Candle surveillance data included pretest dimensional checks, gas flow resistance, burst testing, time-of-flight testing, and visual examination. Posttest data included dimensional checks for creep and bowing, bulk strength measurements by C-ring testing, and photo micrograph examination for phase changes in the material.

The bulk strength of Schumacher Dia Schumalith F40 filter surveillance candles was measured at various points during the program. The bulk strength decreased approximately 50% during the initial 1000-2000 hours of operation, but remained relatively stable during remaining operation. Two of the surveillance candles remained in service for the full test duration of 5854 hours.

### 1.4 Conclusions

The Tidd Hot Gas Clean Up Program provided valuable information for the future design and operation of ceramic barrier filters in a PFBC flue gas environment. The most important conclusions reached from this program are listed below.

1. The basic design of the candle-based APF was structurally adequate. The hot metal structures of tubesheet, plenums, and candle holders operated without problems.

## Executive Summary

---

2. Clay-bonded silicon carbide candle material exhibited approximately 50% loss of strength after 1000-2000 hours of exposure to the PFBC environment. The strength level stabilized upon further exposure time.
3. Nearly all of the silicon carbide candle breakage observed in this program was attributed to ash bridging in the APF. Ash bridging was strongly affected by the size and temperature of the ash entering the filter. Very small ash (mass mean particle size 1 to 3 microns) passing through from a well-tuned cyclone formed an ash cake on the filter candles that was extremely difficult to remove at operating temperatures over 1400F. Ash from a partially detuned cyclone (about 7 microns) was more easily removed than the smaller ash, but still difficult to remove at operating temperatures over 1450F. Ash from a completely spoiled cyclone (above 27 microns) was easily removed and did not tend to bridge.
4. It is important to prevent ash from entering the inside of the filter candles to avoid blinding them on the inside surfaces which have larger pore size than the outer surfaces. Also, ash accumulation in the inside bottom of candles can induce cracking in the candles.
5. The design of hot gas piping is critical. Cast refractory thermal insulation was required to protect the pipe from the hot gas. Ceramic fiber insulation proved unsatisfactory as internal thermal insulation in the hot gas piping.
6. Flue gas which contacts metal surfaces below the acid dew point forms a very corrosive liquid. Metal surfaces that were not protected from contact with the gas experienced corrosion.
7. It is important to have reliable continuous ash removal from the filter. Ash buildup in the APF hopper resulted in candle breakage.
8. Based on very limited data, the APF reduced the SO<sub>2</sub> concentration in the gas passing through it approximately 40%. This is believed to result from the gas reacting with ash cake on the filter candles as evidenced by a higher degree of sulfation of the APF ash than the precipitator ash.

## Introduction

---

### 2.0 INTRODUCTION

#### 2.1 Program Objectives

The objective of this program was to evaluate the design and obtain operating experience for a commercial size Advanced Particle Filter (APF) through long-term testing on a slipstream at Ohio Power Company's Tidd Pressurized Fluidized Bed Combustion (PFBC) Demonstration Plant. Performance and reliability of commercial-scale filter modules were monitored to assess of the readiness and economic viability of this technology for commercial PFBC applications.

At the beginning of the program, it was intended to test two different filters. However, the program scope was narrowed to evaluate different filter candle materials in the same filter vessel. It was not feasible within the cost and time constraints of the program to completely replace the filter with another of a different configuration.

#### 2.2 Program Schedule and Milestones

The 70 MWe Tidd PFBC Demonstration Plant in Brilliant, Ohio was completed in late 1990, and operated through March 1995 as part of the Department of Energy's Clean Coal Technology Program. Provisions were included as part of the original design to install a one-seventh slipstream on the PFBC exhaust gases between the fluidized bed and the gas turbine to test an APF system. In November 1988, AEP submitted a proposal to the DOE for the Hot Gas Clean Up (HGCU) Program, and in August 1989, a cooperative agreement was signed. In July 1990, AEP awarded a contract to Westinghouse Science and Technology Center to provide a candle-based APF. Detailed engineering and material procurement were completed by the end of 1991 when installation began. Initial operation of the system occurred in May, 1992, and the APF was commissioned in October, 1992.

## Introduction

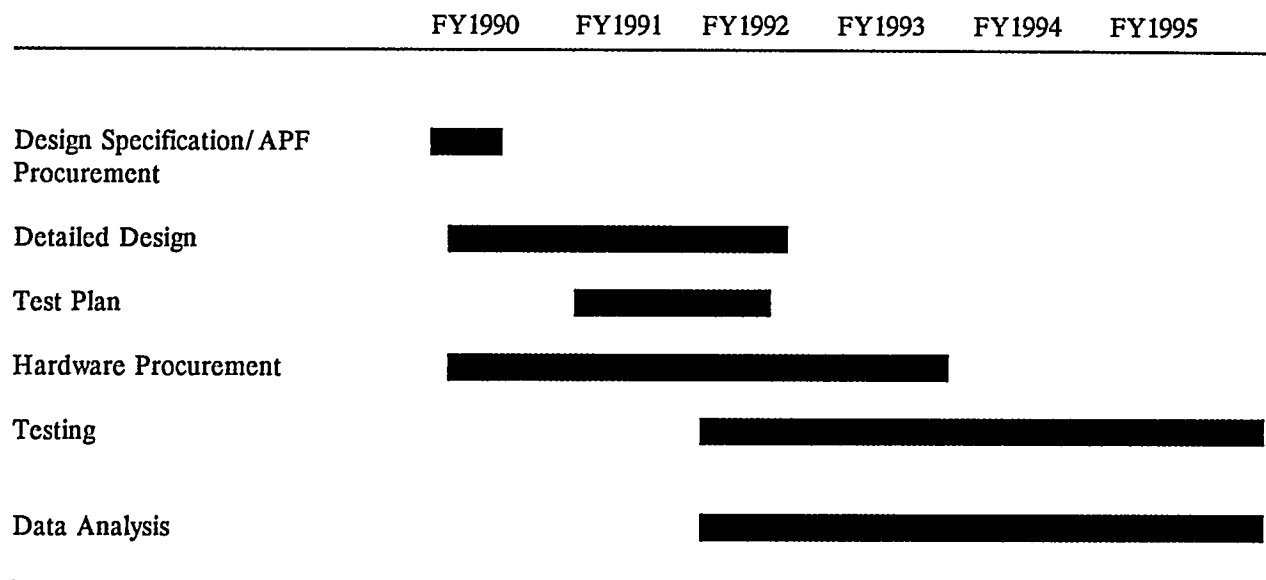


**Figure 2.2 - Program Schedule**

The HGPU system was operated during five separate test periods between October, 1992, and March, 1995, as listed in Table 2.2.1. Table 2.2.2 presents a summary of all HGPU test runs for the entire program. Figure 2.2 shows the duration of each of the program's major activities.

**Table 2.2.1 - Tidd HGPU Test Periods**

Test Period	I	II	III	IV	V
Date	10/92-12/92	6/93-9/93	1/94-4/94	7/94-10/94	1/95-3/95
Run No.	1-4	5-11	12-18	19-24	25-34
Test Period Total Hours	464	1295	1279	1706	1110
Longest Run, Hours	286	597	444	691	427

## Introduction

### Table 2.2.2 - Tidd HGCU Runs Summary

RUN NO.	COAL FIRE		UNIT TRIP		COAL FIRE HOURS	NOTES
	DATE	TIME	DATE	TIME		
0	05/21/92	20:26	05/23/92	07:41	35.3	Bypass mode. Coal fire hours not included in totals. Unit trip due to XJ-4 failure.
1	10/28/92	18:10	11/01/92	23:32	101.4	Unit trip due to HGCU ash lockhopper pluggage.
2	11/17/92	09:33	11/17/92	10:50	1.3	Unit trip due to plugged primary cyclones.
3	11/21/92	18:41	11/24/92	22:50	76.2	Unit trip due to coal paste problems.
4	11/25/92	12:11	12/07/92	09:56	285.8	Warm startup. Unit trip due to XJ7 failure. 21 candles found broken during outage.
<b>TOTAL FOR RUNS 1 - 4</b>					<b>464.6</b>	
5	06/30/93	17:28	07/03/93	05:04	59.6	Shutdown to change GT telemetry instrumentation.
6	07/05/93	00:35	07/05/93	17:17	16.7	Completed GT testing.
7	07/18/93	18:20	08/05/93	12:22	426.0	Shutdown due to ash buildup in APF hopper.
8	08/09/93	10:18	08/09/93	11:37	1.3	GT trip due to bearing vibration.
9	08/10/93	22:29	08/14/93	05:27	79.0	Warm startup. Shutdown due to low O2 resulting from high coal paste excursion.
10	08/19/93	17:48	08/24/93	13:28	115.7	Manual combustor trip due to unstable bed conditions after switching to limestone.
11	08/29/93	23:31	09/23/93	20:12	596.7	Combustor trip due to leak in sorbent transport pipe. 62 candles found broken during outage.
<b>TOTAL FOR RUNS 5 - 11</b>					<b>1295.0</b>	
12	01/10/94	06:41	01/11/94	01:36	18.9	Manual combustor trip due to plugged primary cyclone.
13	01/15/94	23:42	01/29/94	20:31	332.8	Manual combustor trip due to boiler tube leak.
14	02/17/94	14:58	02/18/94	14:14	23.3	Manual combustor trip due to leak in HGCU gas sample connection.
15	02/19/94	06:12	02/25/94	13:09	151.0	Manual combustor trip due to loss of sorbent air compr.
16	03/03/94	10:22	03/09/94	11:30	145.1	Manual combustor trip due to loss of two paste pumps.
17	03/16/94	14:48	03/23/94	10:50	164.0	GT trip due to low lube oil pressure.
18	03/31/94	09:04	04/18/94	20:43	443.7	Manual combustor trip due to internal sorbent injection pipe leak. 28 candles found broken during outage.
<b>TOTAL FOR RUNS 12 - 18</b>					<b>1278.8</b>	

## Introduction

RUN NO.	COAL FIRE		UNIT TRIP		COAL FIRE HOURS	NOTES
	DATE	TIME	DATE	TIME		
19	07/16/94	01:56	07/16/94	04:27	2.5	Manual combustor trip due to loss of three paste pumps.
20	07/16/94	12:59	07/16/94	13:55	0.9	Manual combustor trip due to plugged primary cyclones.
21	07/20/94	19:18	07/27/94	12:08	160.8	Shutdown due to GT vibration.
22	07/28/94	09:59	08/25/94	17:47	679.8	Manual combustor trip due to bad signal relay from the ST generator. 14 candles found broken during outage.
23	09/03/94	01:01	09/10/94	04:07	171.1	Manual combustor trip due to sorbent pipe leak. Operated part-time with P11 cyclone totally spoiled.
24	09/22/94	17:02	10/21/94	11:39	690.6	Operated part-time with P11 cyclone totally spoiled. Planned outage. 30 candles found broken during outage.
<b>TOTAL FOR RUNS 19 - 24</b>					<b>1705.8</b>	
25	01/13/95	13:24	01/13/95	17:47	4.4	Manual combustor trip due to plugged primary cyclone
26	01/18/95	15:53	01/19/95	08:39	16.8	GT trip due to low control fluid pressure.
27	01/20/95	17:35	01/21/95	00:44	7.2	Manual combustor trip due to unstable bed conditions.
28	01/27/95	00:58	02/02/95	02:05	145.1	Manual comb. trip due to hot spot on HGCU pipe flange.
29	02/09/95	00:30	02/09/95	15:09	14.7	Combustor trip due to high SSH outlet temperature.
30	02/10/95	04:05	02/10/95	18:34	14.5	Hot restart. Manual combustor trip due to gasket leak on HGCU surge hopper.
31	02/11/95	09:26	02/12/95	17:51	32.4	Hot restart. Manual combustor trip due to plugged HGCU alternate ash removal line.
32	02/13/95	11:40	02/16/95	12:43	73.1	Hot restart. Combustor trip due to plugged paste nozzles.
33	02/18/95	19:29	03/08/95	14:40	427.2	Manual combustor trip due to loss of two paste pumps.
34	03/14/95	17:15	03/30/95	08:27	375.2	Planned final shutdown.
<b>TOTAL FOR RUNS 25 - 34</b>					<b>1110.4</b>	
<b>TOTAL FOR RUNS 1 - 34</b>					<b>5854.5</b>	

## Project Description

---

### 3.0 PROJECT DESCRIPTION

#### 3.1 System Description

In the original design, the Tidd PFBC Demonstration Plant utilized seven strings of primary and secondary cyclones to remove 98% of the particulate matter from the gases between the fluidized bed and the gas turbine. The HGCU slipstream replaced one of the seven secondary cyclones by taking the discharge gas of one of the primary cyclones to outside of the combustor vessel and into the APF. After passing through the APF, the gas flowed through a backup cyclone and then returned to the combustor vessel, where the slipstream flow rejoined the combustor gas at the discharge of the other six cyclone strings.

Figure 3.1.1 provides a simplified schematic of the HGCU system, and Figure 3.1.2 shows an isometric view of the system.

Under the original maximum load design conditions, gas at approximately 150 psig, 1550F flowed into the filter at 7600 acfm with a dust loading of approximately 600 ppmw. In January 1994, the dust loading to the filter was increased from approximately 600 ppmw to 3400 ppmw by detuning the primary cyclone upstream of the APF. In January 1995, the primary cyclone was bypassed which increased the ash loading to approximately 20,000 ppmw. Ash collected in the APF was discharged to a screw cooler and into a lockhopper system which fed a vacuum ash transport system. In December, 1994, an alternate ash line was installed at the screw cooler outlet to handle the heavy ash loading resulting from bypassing the primary cyclone.

## Project Description

Table 3.1 provides the design basis of the APF system.

**Table 3.1 - APF Design Basis**

Maximum Temperature	1670 F
Operating Temperature	1550 F
Maximum Pressure	185 psig
Operating Pressure	150 psig
Gas Flow Rate	100,700 lb/hr
Inlet Dust Loading	5000-500 ppm
Outlet Dust Loading	<15 ppm
Mass Mean Particle Size	1.5 microns
Temperature Drop	5 F
Pressure Drop	3 psi
Face Velocity	7.1 ft/min

The main elements of the system included the filter vessel and its internals; back pulse skid, including secondary accumulators and valves; back pulse air supply skid, including compressor, dryer and primary accumulator; backup cyclone; ash screw cooler, surge hopper, lockhopper, piping, and instrumentation.

The system was designed to remove virtually all entrained particulates discharged from one of the seven parallel primary cyclones on the outlet of the PFBC combustor. Ash collected on the outside surface of ceramic filter elements (candles), resulting in a gradual increase in the overall flow resistance of the slipstream. The filter cake was periodically dislodged by injecting a high-pressure air pulse to the clean side of the candles. The ash cake on the candles then fell to the conical discharge hopper. Back pulse air was routed individually to nine plenums (3 clusters, each with 3 plenum levels), via injection tubes mounted on the top head of the filter vessel. Back pulsing was controlled by means of high-speed pilot-assisted solenoid valves and air-actuated isolation valves. The pressure in the secondary accumulator tanks typically ranged from 800 to 1200 psig. The electrical pulse duration was 0.2 to 0.7 second, and the corresponding air pressure pulse duration was 0.5 to 1.0 second. The pulse air supply system, located in the combustor building basement, provided high pressure dried and filtered air on as-needed basis to five secondary accumulators, via a primary accumulator on the discharge side of the compressor.

## Project Description

---

An air preheating system was originally included in the system. However, the system was not used because the electric heater proved to be ineffective. An alternate means of warming the system utilizing process air proved to be a more efficient and expedient.

The following paragraphs provide information on the major components in the system.

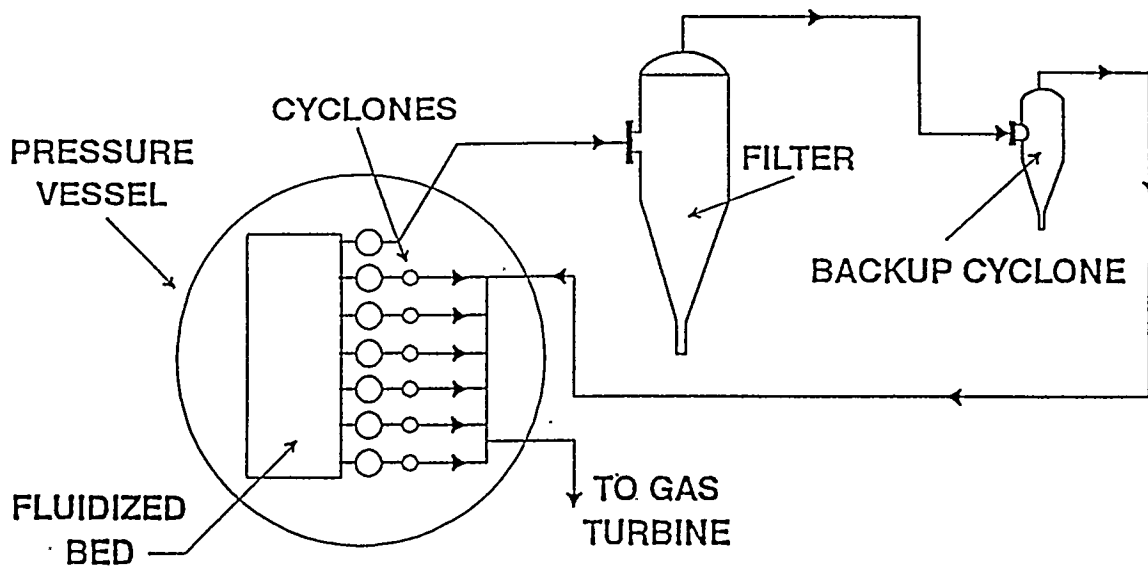


Figure 3.1.1 - HGCU Slipstream Schematic

# Project Description

---

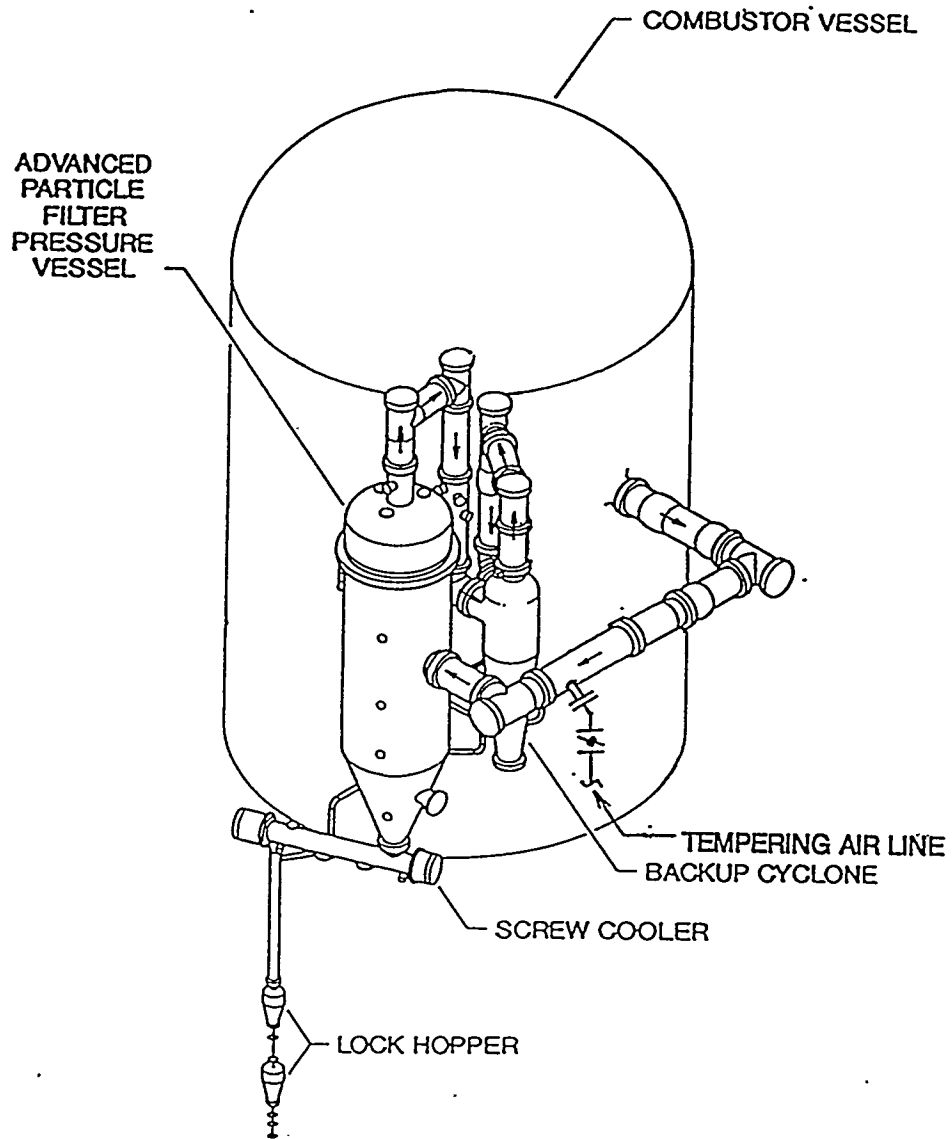


Figure 3.1.2 - Isometric View of HGCU System

## Project Description

---

### 3.2 Filter Vessel

The function of the filter vessel was to contain the filter elements in a pressurized environment. The vessel was comprised of two major parts, the body and the head. A tubesheet separated the dirty gas in the body from the clean gas in the head. The filter vessel was 10 feet in diameter and 44 feet high. The vessel was internally insulated with a 7 to 9-inch thick layer of alumina-silica ceramic fiber (Z-Block) insulation. The vessel was fabricated from carbon steel plate. A 310 stainless steel liner protected the insulation from gas impingement. A 310 stainless steel shroud inside of the vessel directed the dirty gas, which entered the side of the filter, toward the top of the filter. After flowing over the top of the shroud, the gas flowed in a downward direction past the filter elements. Hot gas entered the side of the body and exited from the top of the head.

The vessel was designed in accordance with ASME Section VIII for 185 psig, 1670F internal temperature and 650F external temperature.

The exterior of the vessel was coated with a temperature sensitive paint which changed colors at specific temperatures. The temperature sensitive paint provided a means of detecting hot spots on the vessel shell. No external insulation was applied to the filter vessel. A photograph of the filter vessel during erection is shown in Figure 3.2.

### 3.3 Filter Internals

The filter contained 384 filter elements which were referred to as candles because of their long cylindrical shape. The candles were arranged in three clusters spaced 120 degrees apart. Each cluster held three plenums arranged vertically. The upper and middle plenums each contained 38 candles, while the bottom plenums contained 52 candles each. (After Test Period III the inner rows of candles in the upper and middle plenums were removed, leaving 288 candles in the APF during Test Periods IV and V.) Each plenum bottom comprised a perforated plate similar to a tubesheet. Candle holders were welded to the plenum bottom plates, and the candles were held in the holders under the support plates by bolted collars and high temperature gaskets. Each candle was nominally 2.36 inches in outside diameter and 4.92 feet long. The candles were made of two layers of sintered silicon carbide. The outer layer was very thin and had much smaller porosity than the remainder of the candle. Essentially, all filtering was accomplished near the outer surface of the candle. Filter candles of different design were used in Test Periods IV and V.

## Project Description

---

The tubesheet and expansion cone performed three functions: (1) supported the filter clusters; (2) accommodated thermal stresses generated at its periphery; and (3) maintained a seal between the clean and dirty sides of the filter vessel. The 2" thick tubesheet and expansion cone were fabricated from RA-333 alloy. Thermal insulation protected the expansion cone from the hot gas temperature.

Figure 3.3.1 shows the arrangement of the filter internals. Figures 3.3.2, 3.3.3 and 3.3.4 are photographs of the filter internal assembly during initial installation into the vessel.

## Project Description

---

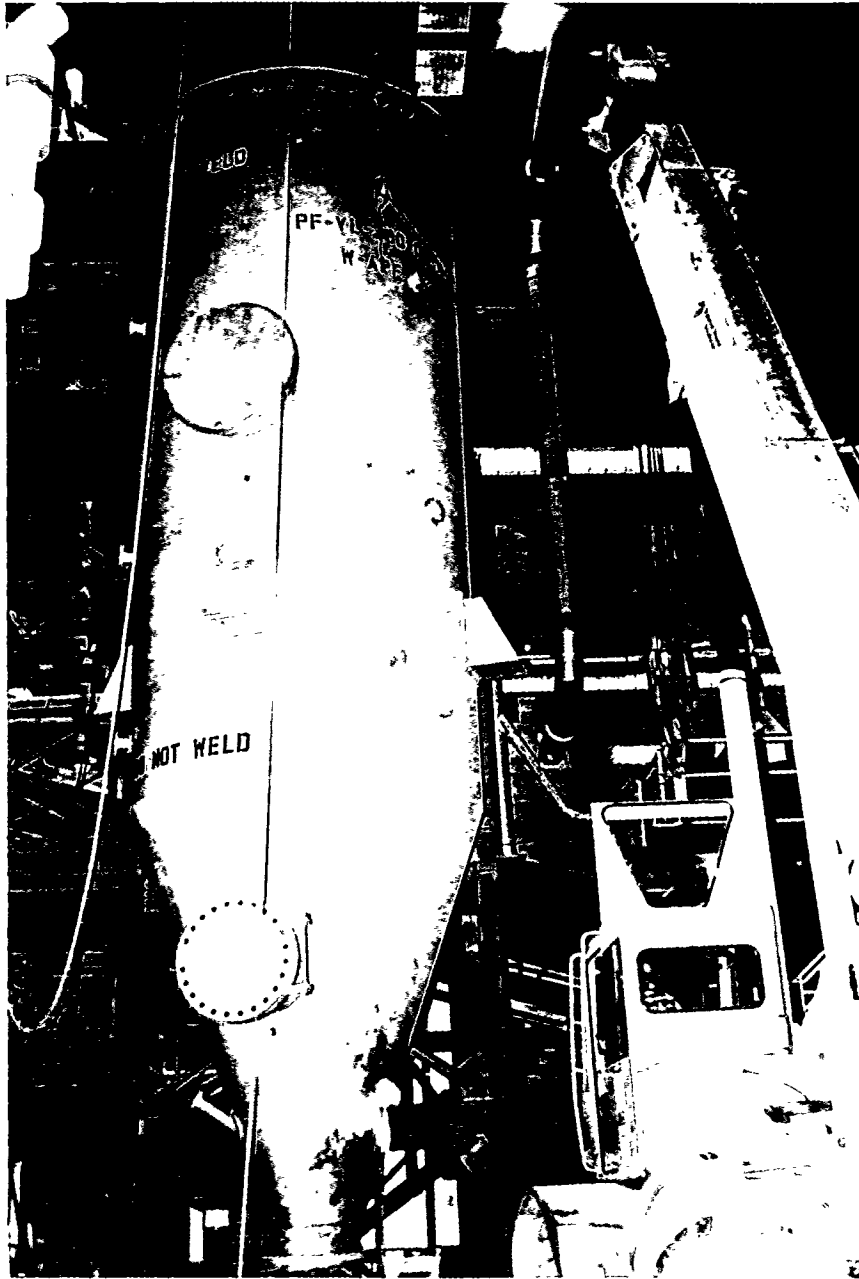


Figure 3.2 - Photograph of APF Vessel During Erection

# Project Description

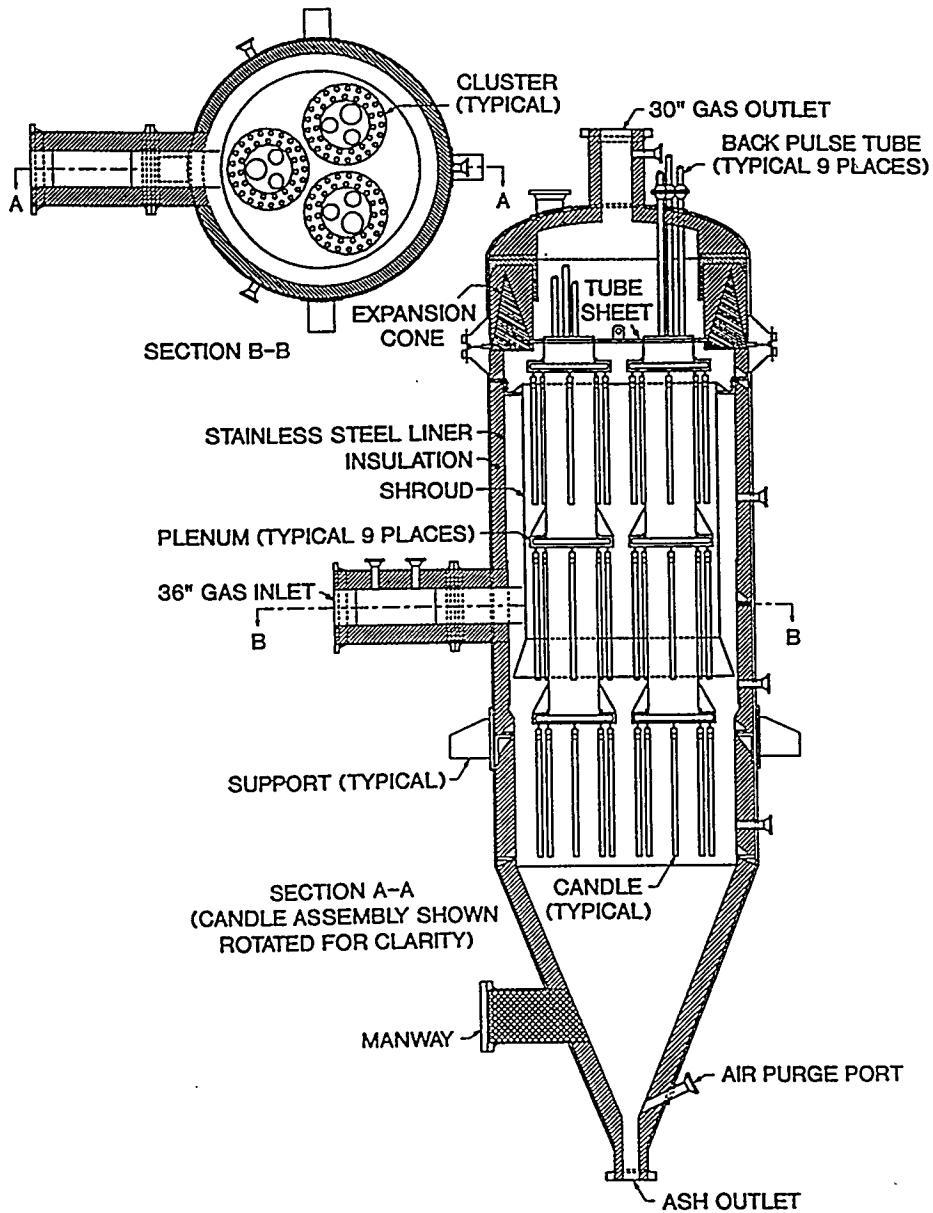


Figure 3.3.1 - APF Internal Arrangement

## Project Description

---

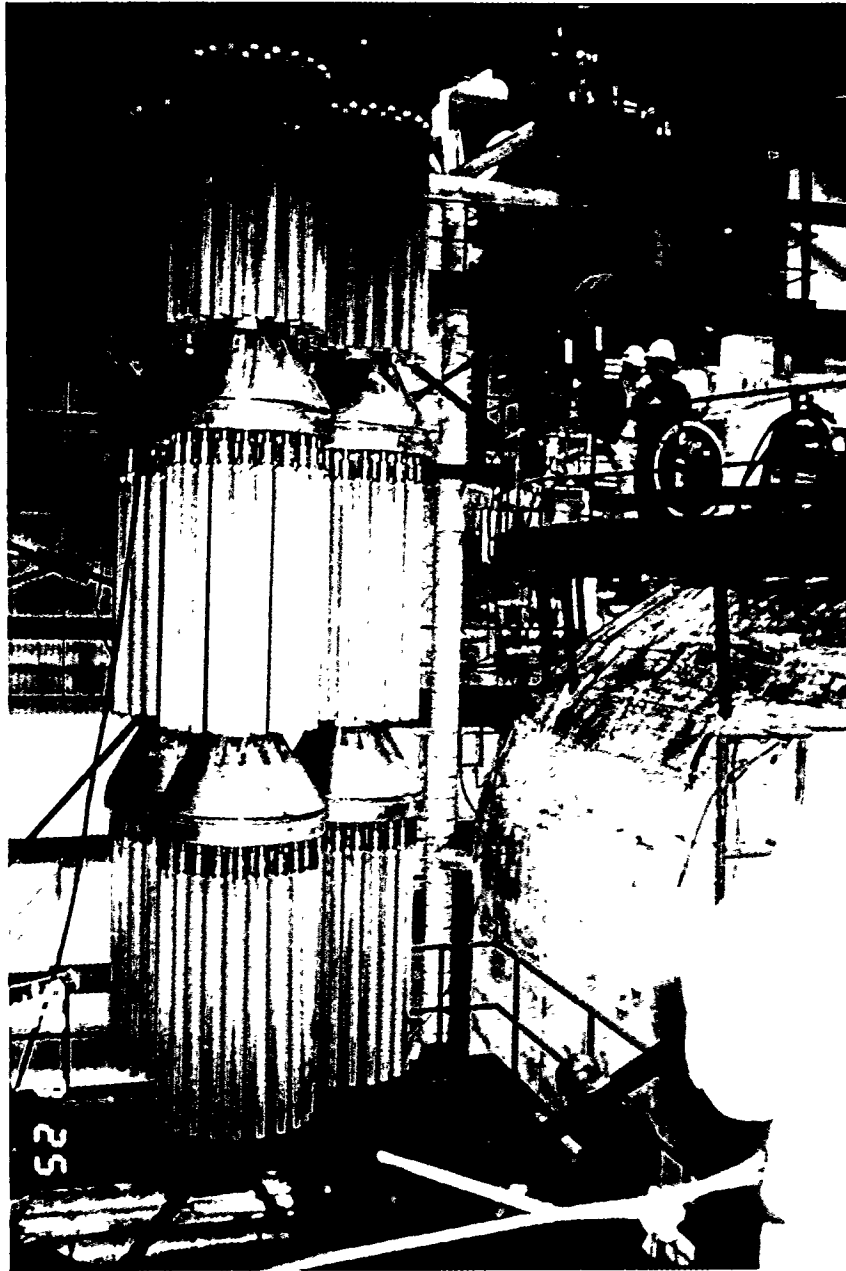
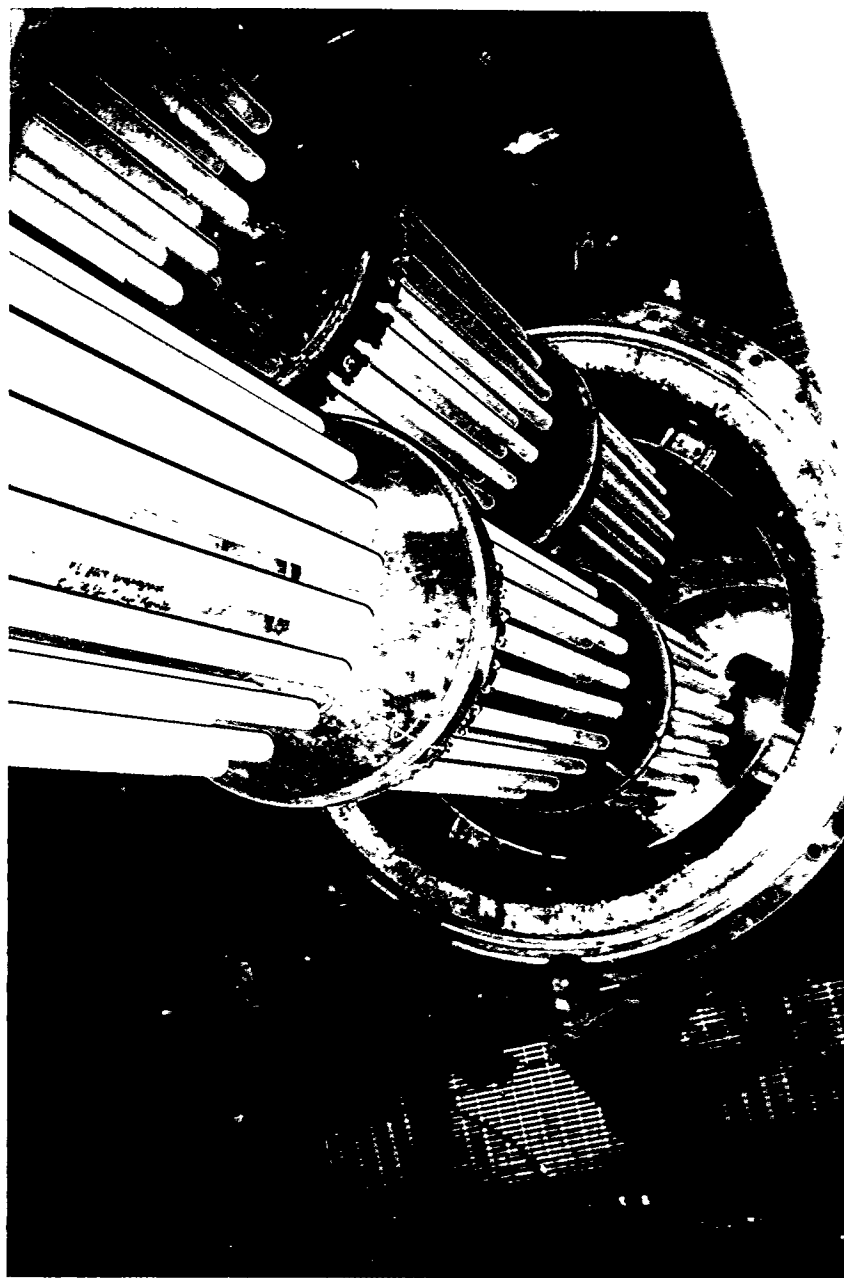


Figure 3.3.2 - Photograph of Filter Internals During Initial Installation

## Project Description

---



**Figure 3.3.3 - Photograph of Filter Internals During Initial Installation**

## Project Description

---

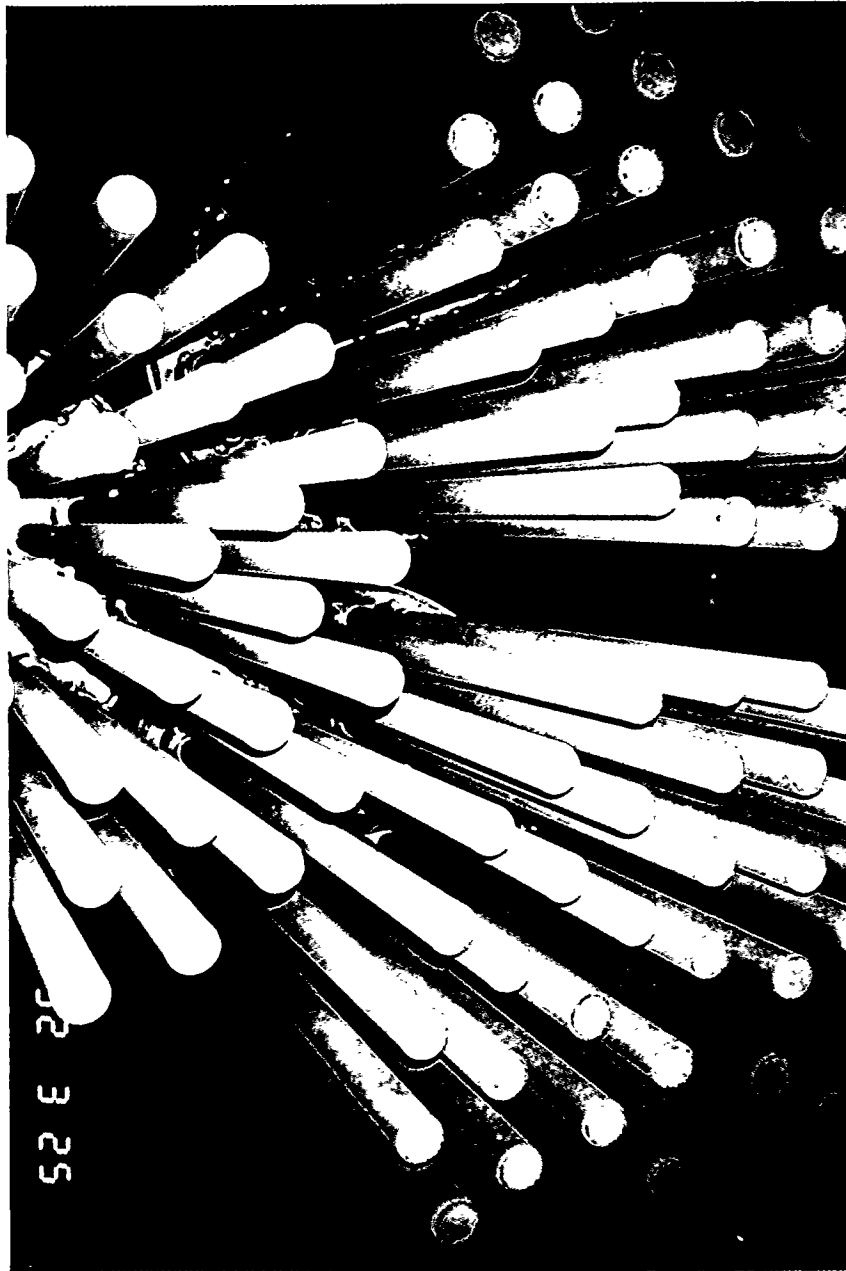


**Figure 3.3.4 - Photograph of Filter Internals During Initial Installation**

## Project Description

---

### 3.4 Backpulse System

The Backpulse System was comprised of a compressor skid, valve skid, and interconnecting piping. A schematic diagram of the system is shown in Figure 3.4.1, and photographs of the skid are shown in Figures 3.4.2 and 3.4.3.

The backpulse compressor was a heavy duty reciprocating compressor with four stages of compression. It was designed to compress 282 scfm of air up to 1500 psig. The compressor was built with balanced opposed cross heads which permitted operation over extended periods in an unloaded condition. The compressor skid included intercoolers, aftercooler, and moisture separators. It was a Norwalk Model Century 150-4.

The backpulse air dryer was mounted on the same skid as the compressor. The dryer was a refrigerant type which removed moisture from the air by cooling in a Freon gas heat exchanger. The air was warmed to about 80F before leaving the dryer by a regenerative heat exchanger. The dryer was designed to dry 300 scfm of air at 1500 psig to a dew point of 35F or below. It was a model UA100 made by Ultra Air Products, Inc.

The back pulse system included one large primary and five small secondary accumulators. The large accumulator was located on the same skid as the compressor and dryer. It received air from the dryer and supplied it to the five smaller accumulators.

The small accumulators were located on the backpulse valve skid located near the top of the filter vessel. One accumulator stored air for the pilot valves on the back pulse solenoid valves. A second accumulator stored air at nominal 250 psig for instrument purge. The other three accumulators stored air for pulsing at nominal 800 to 1200 psig.

The heart of the backpulse system was the backpulse solenoid valves manufactured by Atkomatic Valve Company. Downstream of each secondary accumulator there were two solenoid valves arranged in parallel. One of the two valves was a backup. The valves were fast-acting (200 to 700 msec stroke time) pilot operated solenoid valves which failed closed. A normally-closed automated ball valve downstream of each solenoid valve isolated the backpulse air system from the hot gas system and prevented excess air from entering the filter in case a solenoid valve failed to close. During Test Period V one of the Atkomatic valves was replaced with another type of valve manufactured by CO-AX Valves.

# Project Description

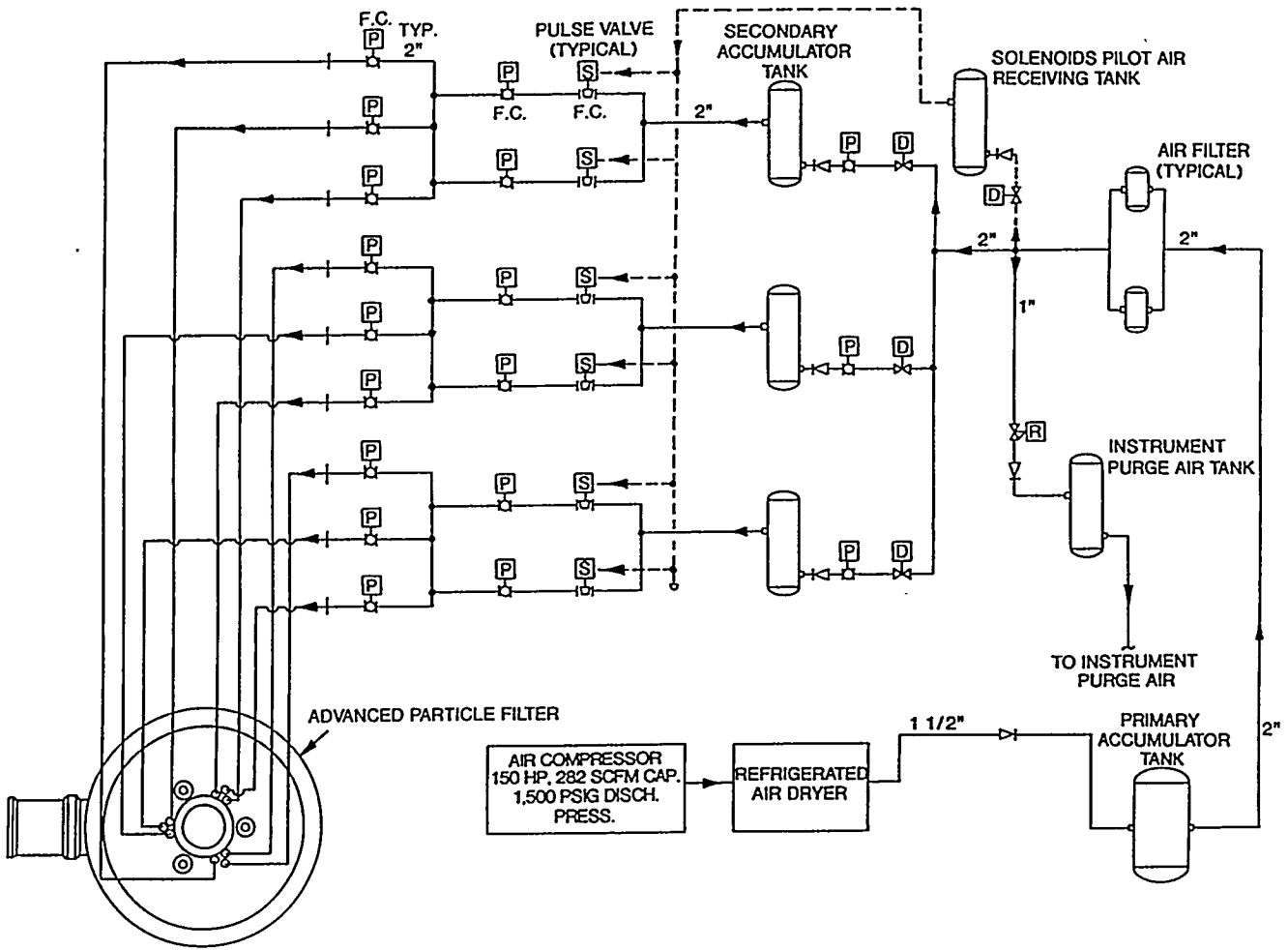
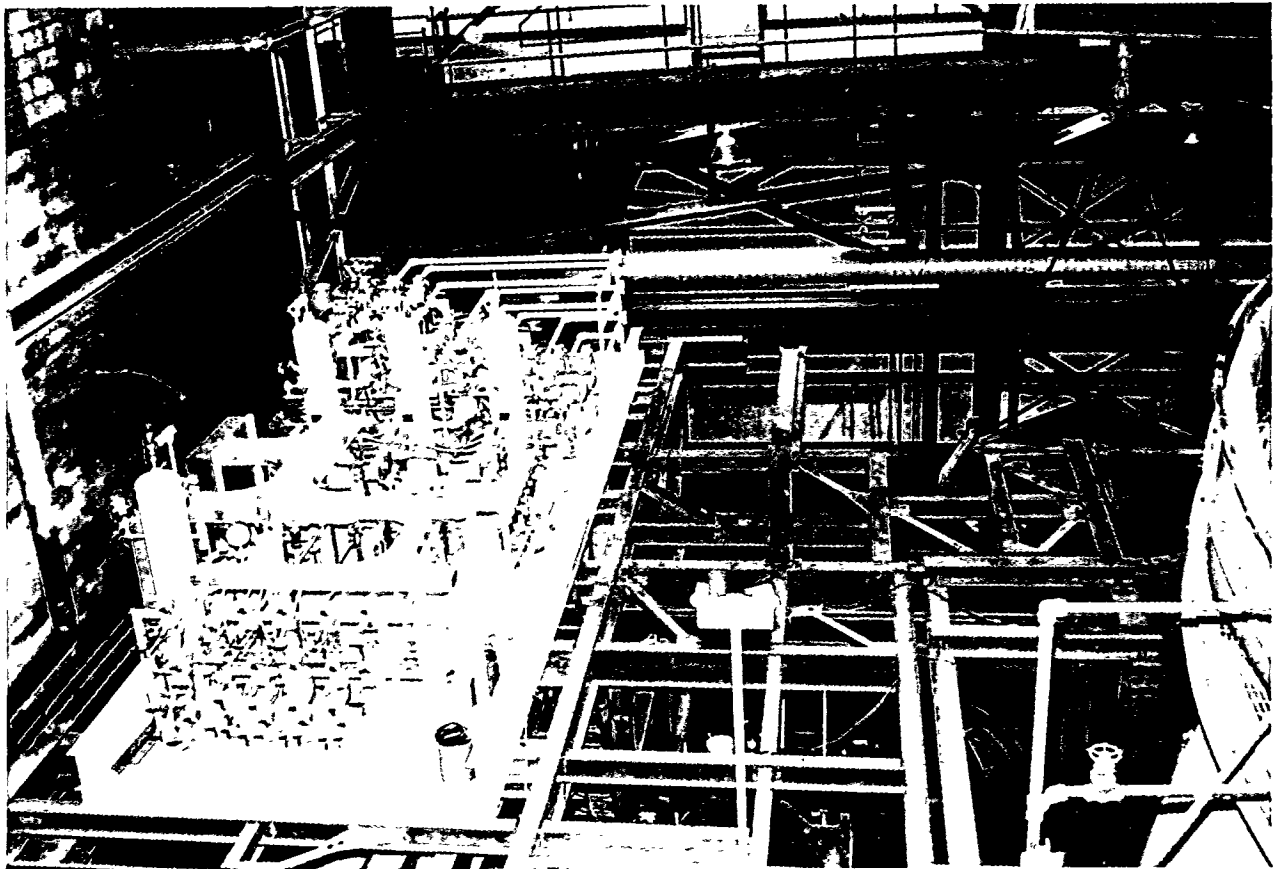


Figure 3.4.1 - Schematic Diagram of Backpulse System

## Project Description

---



**Figure 3.4.2 - Photograph of Backpulse Skid**

## Project Description

---

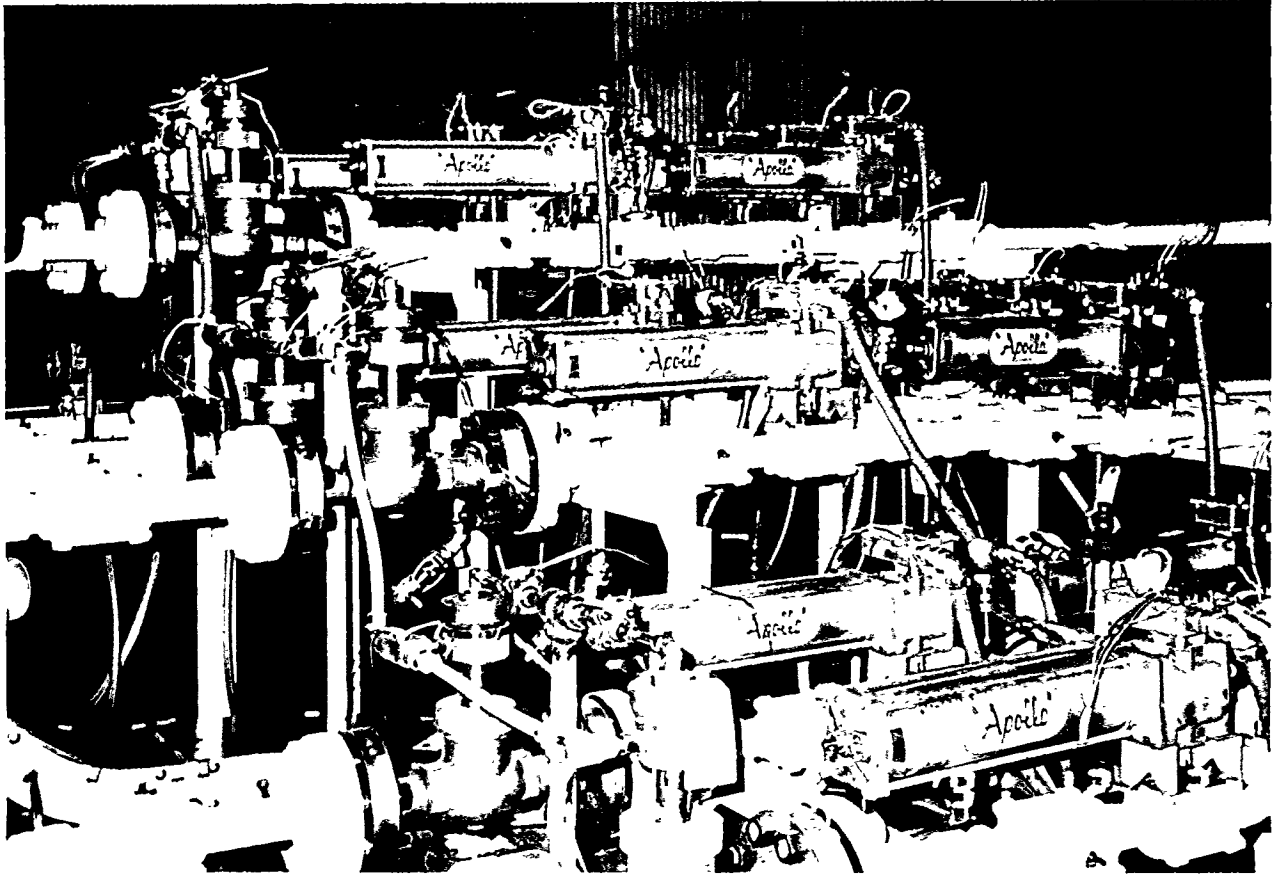


Figure 3.4.3 - Photograph of Backpulse Skid

## Project Description

---

### 3.5 Backup Cyclone

The original system design included a bypass cyclone as well as a backup cyclone. The purpose of the bypass cyclone was to clean the ash from the hot gas slipstream if the APF was not available for service and to allow the flow to be switched to bypass the APF if a problem developed during operation. However, following initial shakedown tests, it was decided not to connect the bypass cyclone to the system. It was noted following initial operation using the bypass cyclone that the stagnant flue gas in backup cyclone condensed resulting in corrosive condensation collecting on and corroding internal metal surfaces. It was concluded that the bypass cyclone would experience the same corrosive conditions when it was in the standby mode, i.e., pressurized with stagnant flue gas. Based on this observation, it was decided not to use the bypass cyclone.

The backup cyclone was sized to allow for the maximum particle removal efficiency given the available pressure drop. The available pressure drop across the backup cyclone was 2.4 psi with a corresponding inlet velocity of 95 fps at the design flowrate. A minimum of three inches of erosion resistant refractory was installed on surfaces exposed to hot gas. Insulating refractory approximately eight inches thick was installed between the vessel wall and erosion resistant refractory to limit the heat loss and outer wall temperature. During the first test run, problems were encountered with hot spots on the cyclone shell. Repair of cracks in the refractory and additional heat curing of the refractory were necessary to eliminate this problem. In order to monitor the steel shell of the cyclone for hot spots, no insulation was applied to its outside surface. The same temperature sensitive paint used on the APF vessel was also used on the cyclone. The vessel was designed in accordance with ASME Section VIII for 185 psig, 1670F internal temperature and 750F external temperature. Figure 3.5 is a cross section drawing of the backup cyclone.

# Project Description

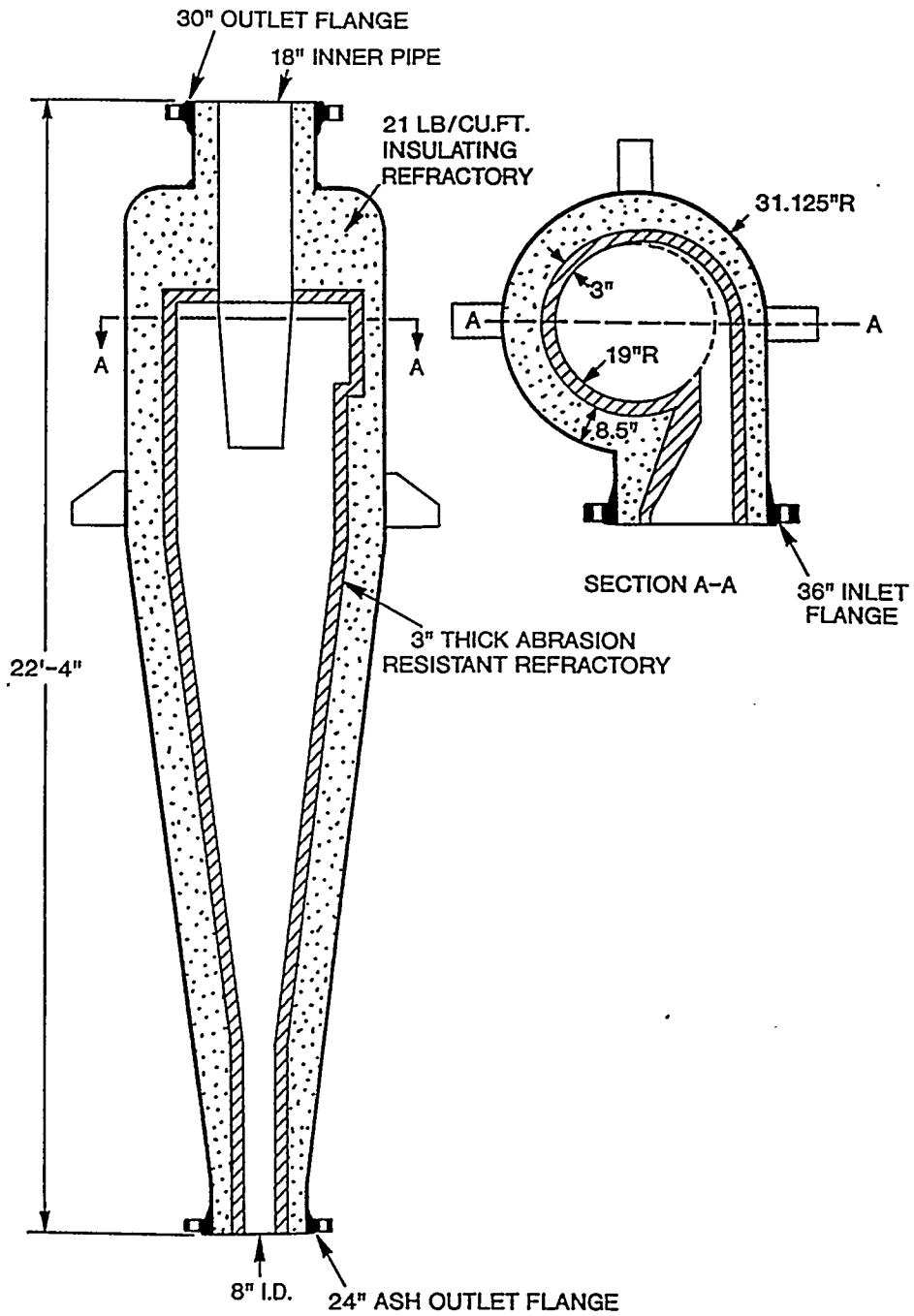


Figure 3.5 - Cross Section of Backup Cyclone

## Project Description

---

### 3.6 Ash Removal System

The function of the ash removal system was 1) to remove ash from the advanced particle filter vessel and cool, depressurize and convey the ash to an ash silo; and 2) to convey ash from the backup cyclone and cool, depressurize, and discharge the ash to the economizer outlet duct where it was collected by the precipitator.

A schematic diagram of the system is shown in Figure 3.6.

The system consisted of the following systems and components:

- Ash Screw Cooler
- Hydraulic Fluid System
- Gear Box Lubricating System
- HGCU Closed Cycle Cooling Water System
- Ash Surge Hopper
- Ash Lockhopper
- Lockhopper Isolation Valves
- Material Cycling Valve
- Lockhopper Pressure Equalizing Valves
- Ash Transport Piping and Valves
- Cyclone Ash Collection Vessels
- Cyclone Ash Transport Piping

Ash collected in the APF vessel was removed and cooled by the screw cooler, depressurized in the lockhopper assembly, and conveyed to an ash silo via a 4" vacuum ash transport line. A hydraulic fluid system was used to provide power to the screw cooler hydraulic drive unit. A closed cycle cooling water system was used to provide cooling water to the screw cooler.

Ash collected in the backup cyclone was conveyed to the economizer outlet duct using conveying air from the combustor vessel. The ash was cooled by mixing with conveying air in the cyclone ash collection vessel. The ash was depressurized in the cyclone ash transport line prior to being discharged into the economizer outlet duct. The ash then mixed with the flue gas and entered the precipitator where it was collected and discharged to an ash silo for disposal via truck.

## Project Description

---

An emergency pneumatic ash removal system was provided at the screw cooler outlet to facilitate ash removal in case the lockhopper system malfunctioned. Following bypassing of the primary cyclone in December 1994, an additional alternate ash transport line was installed to handle the heavy ash loading from the APF. The alternate ash line ran from the screw cooler outlet and tied into the ash line from the other primary cyclones. When the alternate ash line was in service, the lockhopper system was not used. The emergency and alternate ash lines used conveying air from the combustor (process air) in the same manner as the ash line from the backup cyclone.

The system was originally designed to handle an ash loading of 1000 lbm/hr from the APF vessel. The screw cooler was designed to cool ash from 1550F to 400F using closed cycle cooling water at 200 psig, 340F, and 36 gpm at the design ash loading. When the primary cyclone was bypassed in December 1994, the APF ash loading increased to about 2000 lbm/hr at full load. Consequently, the screw cooler outlet temperature was higher than design, typically in the range of 600-650F. However, this did not present a significant operating problem.

# Project Description

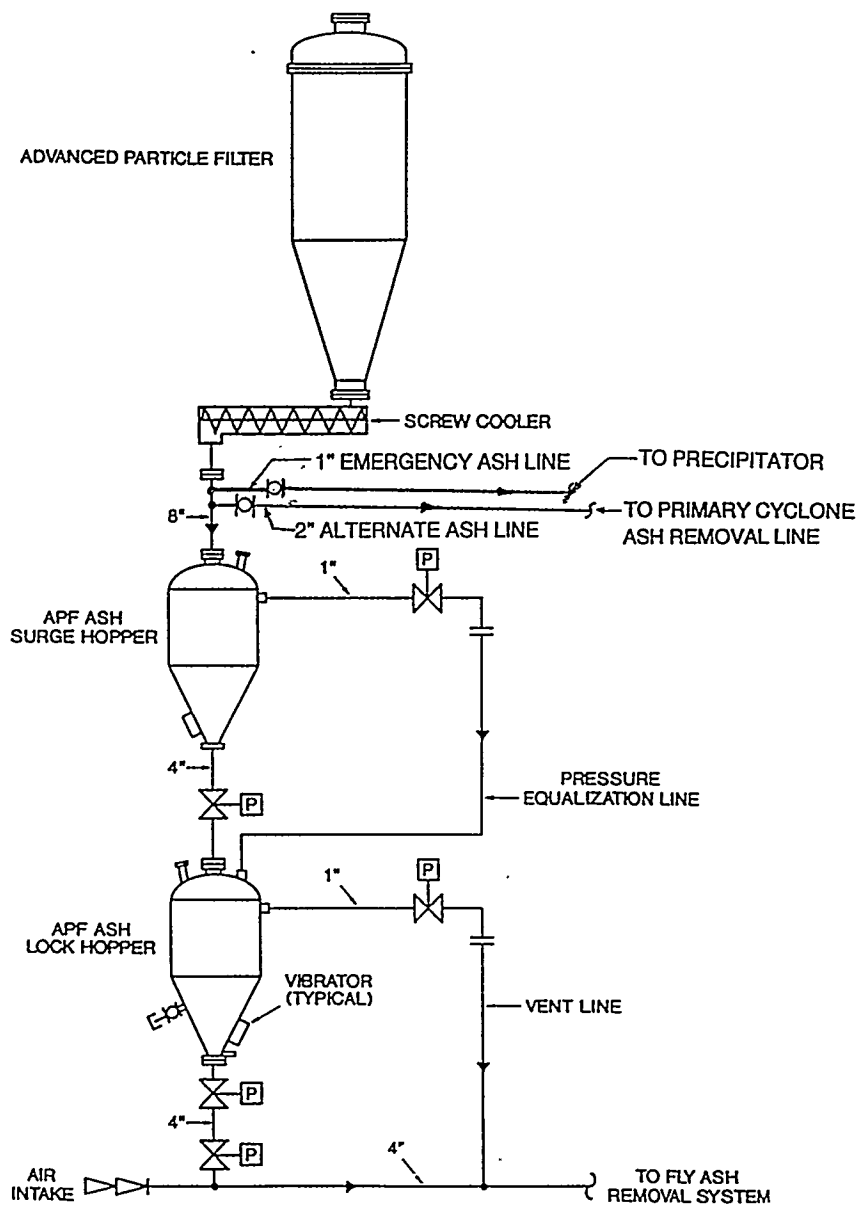


Figure 3.6 - Ash Removal System Schematic

## Project Description

---

### 3.6.1 Screw Cooler

The screw cooler was comprised of a cylindrical housing (trough), water-cooled screw, and a hydraulic drive unit. As ash was conveyed through the screw cooler, heat was transferred to the cooling water. There were three parallel cooling water circuits in the screw cooler. Figure 3.6.1 shows a schematic diagram of the screw cooler.

The screw cooler was supplied by Denver Equipment Company and was designed and stamped according to ASME pressure vessel standards.

The screw flights and stem pipe were hollow, and together they formed a cooling water loop. Most of the heat from the ash was transferred to the cooling water circuit in the screw. The screw pads and flights were made of 304 stainless steel and constructed of a "twin-pad" design to ensure a high structural integrity. This design consisted of a steel ribbon (or pads) wrapped around the stem pipe in a helical fashion and welded to the pipe at the ends only. The screw flights were positioned so they bridged the gap of the steel pads. This design offered free torsional movement of the pad and flights and room for longitudinal expansion under high temperature gradients.

The housing was a cylindrical pressurized water-cooled jacket with inspection ports. It allowed for pressurized ash operation and accounted for 10-15% of the total heat transferred. The housing diameter was larger than the screw diameter and the screw was offset from the housing centerline. This permitted relatively large objects to pass through the screw cooler without jamming. (When candles broke during operation, the screw cooler was able to continue to operate without jamming.) The housing contact surface was made of 304 stainless steel.

## Project Description

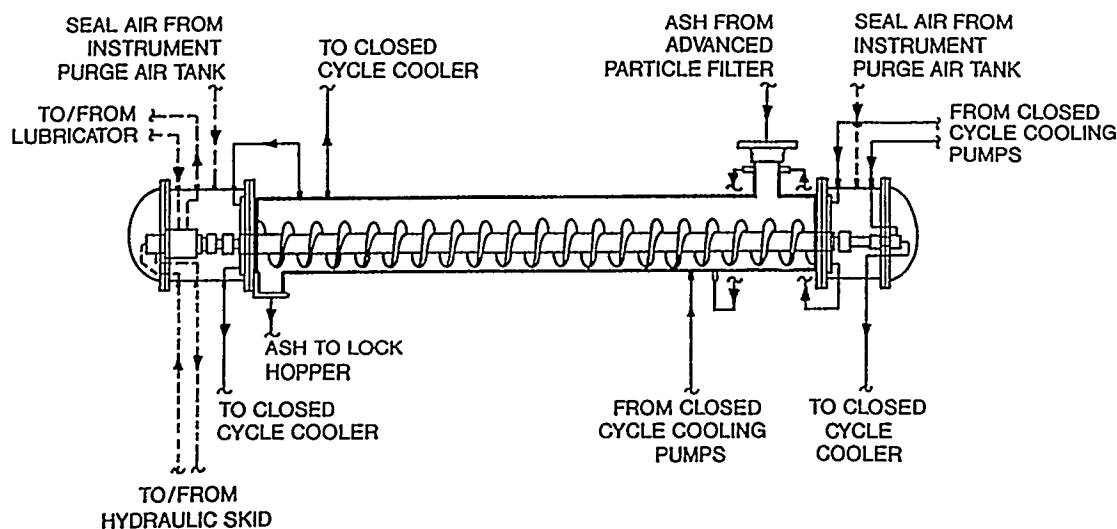


Figure 3.6.1 - Screw Cooler Schematic

The screw was driven through a reduction gear (36:1 gear reduction ratio) by a variable speed, 5 hp, hydraulic drive unit; both the reduction gear and drive unit were totally enclosed within the north end housing. The function of the reduction gear was to transfer power from the hydraulic motor to the screw at reduced speed and increased torque. Based on the maximum hydraulic fluid flow and pressure, the maximum output torque of the gear reducer was approximately 36,720 in.- lbf. If the screw became jammed, stalling occurred at the maximum torque value. The reduction gear was continuously lubricated by the gear box lubricating system located on the hydraulic skid. The hydraulic skid included the hydraulic fluid system, the gear box lubricating system, and the associated control circuitry and control panel for the screw cooler. Seal air was provided to each end housing to keep ash out of the shaft seals. The air pressure was maintained at 0.5 to 2 psi above the system gas pressure.

### 3.6.2 Surge Hopper and Lockhopper

The ash surge hopper had 3.34 cubic feet of net storage capacity and was used to store ash collected from the screw cooler during unloading of the ash lockhopper. The hopper was heat

## Project Description

---

traced and insulated. The hopper was provided with an electric vibrator to assist with hopper unloading and was fabricated of 304 stainless steel with 2B finish to ensure smooth surfaces. Steep hopper cone angles, 10 and 20 degrees (included), ensured good ash flowability.

The ash lockhopper had 12.25 cubic feet of net storage capacity and was used to collect ash from the screw cooler through the surge hopper. During unloading, the lockhopper was isolated from the surge hopper, depressurized, and the ash was emptied into the ash transport line through the two lower isolation valves. This hopper was provided with a compound pressure gauge, a level switch, an ash temperature indicator, heat tracing, insulation, an electric vibrator, and was fabricated of 304 stainless steel with 2B finish and similar cone angles as the surge hopper.

Two lockhopper isolation valves and one material cycling valve were provided on the lockhopper assembly. The upper isolation valve was used to isolate the lockhopper from the surge hopper during the unloading cycle. The two valves provided below the lockhopper were for pressure seal and material cycling. The valves were manufactured by the Everlasting Valve Co. and were 4" rotating disc type, ANSI Class 300, flanged, with a cast Stellite #6 disc and seat.

### 3.7 Hot Gas Piping

The hot gas piping was originally designed with an outer carbon steel pressure-retaining shell, an inner 316 stainless steel liner, and alumina-silica ceramic fiber blanket insulation between the liner and the shell. The inside of the carbon steel pipe shell was lined with an epoxy coating (Plasite 4300) for corrosion protection. Table 3.7 provides design parameters of the piping. Cast refractory rings were used at the ends of each pipe section to support the inner liners, which were designed to allow for thermal expansion at each connection. The system also required eight expansion joints to allow for thermal expansion and relative movement between the combustor vessel and the HGCU components. The expansion joint bellows were made of 321 stainless steel.

The piping and expansion joints were redesigned following initial system operation in May, 1992, as is discussed in Section 4.2.1.

## Project Description

---

**Table 3.7 - Hot Gas Piping Design**

	Upstream of Filter	Downstream of Filter
Gas Velocity	60 fps	75 fps
Outer Pipe	36 in. OD	30 in. OD
Inner Liner	20 in. OD	18 in. OD

### 3.8 Controls and Data Acquisition

There were three control modes available for the filter system, namely manual mode, automatic DP mode and automatic timer mode. The manual mode was generally only used after backpulse cleaning had been interrupted for some reason, and a large ash cake had accumulated on the candles. In this case it was advantageous to use the manual mode so the filter cleaning could be spread out over some time period to avoid overwhelming the ash removal system. During manual mode, the system internally checked the permissives for proper sequencing and operation of the solenoid valves and advised the operator of any malfunction.

The system was normally operated in the timer mode. In this mode, filter cleaning occurred at uniform time intervals, typically thirty minutes. In the timer mode, filter cleaning would be initiated by a DP override if the override setting was reached prior to the next timed cleaning. During test periods IV and V when ash loading to the filter was very heavy, the filter timer sequence was set up for continuous cleaning wherein all nine plenums were cleaned over a fifteen minute time period with backpulses occurring every 1.67 minutes. This was done to even out the ash flow to the ash removal system.

In the DP mode the filter was cleaned when the filter differential pressure reached a preset level. A timer override could be set to clean the filter if backpulsing had not occurred for a specified time period. This control mode was not used.

The cleaning sequence was programmable to allow the cleaning to occur by cluster or by level. For example, all upper level plenums could be cleaned first, then all middle level plenums, and finally all bottom level plenums. In the cluster mode, all plenums in a given cluster were cleaned before moving

## Project Description

---

to the next cluster. In this mode, the cleaning generally occurred in the sequence top, middle, bottom in a given cluster. The cluster mode of cleaning was normally used throughout the test program.

A Bailey Net 90 control system was used to monitor and control the system parameters and provide operator interfaces. System data and alarms were transmitted into the Net 90 system to allow continuous monitoring of the system. In addition, many of the important parameters were recorded in a POPS data system which provided digital and graphical displays of data which could be monitored in real time and printed out for specified time periods. The graphs shown later in this report were generated from data collected in the POPS system.

Data collected included pressure, temperature, flowrate, differential pressure, level, etc. throughout the system. POPS also displayed calculated parameters such as face velocity, gas viscosity, and filter permeability. Due to the huge volume of data collected during this program, it is not practical to summarize all of it in this report. Section 4 of this report presents the most important variables in graphical format.

## Results

---

### 4.0 RESULTS

#### 4.1 Proof-of-Concept Testing

During the design phase of the project, Westinghouse conducted proof-of-concept testing to verify the design basis of various system components. During this test phase, two types of filters were being considered for the Tidd APF, namely, candle and cross-flow. Proof-of-Concept tests were conducted on both types to determine the best choice for this program. Test results are as follows:

##### 4.1.1 Thermal Transient Tests

Both candle and cross-flow filter elements were subjected to thermal transient tests, which imposed a transient of 1550F to 1370F in 200 seconds, followed by a transient of 1370F to 1300F in 400 seconds. These transients simulated expected Tidd trip conditions. After 10 cycles, one cross-flow filter delaminated. Ninety start-up simulations were then conducted, and an additional filter failed. Three of the remaining cross-flow filters were subjected to a 600 hour durability test with no additional failures.

Three Schumacher SiC candles were subjected to 10 trips, 90 start ups, and 1000 blow back cycles with no visible degradation or failures.

##### 4.1.2 HTHP Array Backpulse Tests

Eleven candles were tested with PFBC ash for 368 hours at a face velocity of 3.4 fpm, for 47 cycles; cleaning was excellent. Five candles were tested for 51 hours at a face velocity of 5.7 fpm for 58 cycles; cleaning was also excellent. Three candles were tested with Tidd ash with a 1/2-inch back-pulse nozzle; the baseline pressure drop increased from 22 to 45 inches of water at 500 psig back pulse pressure. The nozzle size was increased to 3/4-inch. With the larger nozzle size, the baseline pressure drop remained below 35 inches of water at 500 psig back pulse pressure. Subsequent testing of the Tidd APF validated these test results by demonstrating the ability to clean up to 52 candles with a single backpulse.

## Results

---

### 4.1.3 Alkali Attack

The silicon carbide ceramic media was subjected to 400 hours of exposure to gas-phase alkali in the presence of steam at temperatures of 1550F to 1600F. No physical degradation of the material was observed, however, the hot strength of the material was reduced to less than 30% of its original design value. These results were confirmed during later testing at Tidd when the silicon carbide candles exposed to the PFBC flue gas exhibited a loss of strength of about 50%.

### 4.1.4 Pulse Valve Testing

An Atkomatic pulse valve was subjected to 101,000 cycles without any degradation in performance. The performance declined during the next 5000 pulses. This life well exceeded the cycle life specified for the Tidd APF system. In spite of these good results, galling problems in the valves were encountered later during system operation.

### 4.1.5 Cold Flow Modelling

Cold model tests were conducted on an 18-candle array to provide input to the APF vessel design. The cold flow testing also provided a verification of the selection of a radial inlet to the APF compared to a tangential inlet. Cold model testing of a 52 candle array showed less than 10% variation in the back pulse flow distribution. No evidence of flow maldistribution was seen during subsequent operation of the full scale Tidd APF, thus validating the cold flow modelling tests.

### 4.1.6 Gasket Tests

The fibrous ceramic material used for gaskets at the connection between the candles and the tube sheet were subjected to 15,000 cold-gas pulses at 1550F for 50 days, 1800F for 8 days, and cycled from ambient to 1800F for 15 days. No degradation was observed. In subsequent operation of the Tidd APF, the gaskets performed very well, again validating the proof-of-concept tests.

## Results

### 4.1.7 Filter Cake Properties

Filter cake properties were checked for three types of ash. Table 4.1.7 provides a summary of those results.

**Table 4.1.7 - PFBC Ash Properties**

Ash Source	Cake Density (gm/cc)	Mean Flow Resistance (Relative)	Mass Mean Particle Size ( $\mu\text{m}$ )	Backpulse Intensity Required (Relative)
Coarse PFB Ash	0.4	1.0	7.8	Lowest
Grimethorpe Ash <sup>(1)</sup>	0.6	1.8	5.3	Medium
Tidd Ash	0.3	2.7	3.5	High
Grimethorpe Ash <sup>(2)</sup>	0.2	6.8	4.0	Highest

(1) With Limestone as sorbent

(2) With Dolomite as sorbent

The actual Tidd PFBC ash cake proved much more difficult to remove from the filter candles than was expected based on the proof-of-concept tests. Therefore, these ash cake results were somewhat misleading.

### 4.1.8 Karhula Testing

While most of the testing of the Tidd APF utilized Schumacher silicon carbide candles, two other materials were tested during Test Periods IV and V, namely, Coors alumina/mullite and Refractron Vitropore silicon carbide filter candles. Proof-of-Concept testing for these two materials was conducted between the fall of 1992 and summer of 1994 at a 10 MWt PCFB test facility in Karhula Finland. This testing was conducted by A. Ahlstrom Corporation and funded by DOE as part of the Tidd HGCU Cooperative Agreement. The Coors candles underwent 716 hours of coal fire operation, and the Vitropore candles experienced 1340 hours of coal fire operation. Results of the Karhula testing increased the level of confidence for using the Coors and Vitropore filter candles in Test Periods IV and V of the Tidd HGCU program. Results of the Karhula test program are documented in a paper by T. E. Lippert, et al., published in the Proceedings of the 13th International Conference on Fluidized Bed Combustion, pp. 251-261, 1995.

## Results

---

### 4.2 Initial System Operation

Initial operation of the system using the bypass cyclone occurred during May 21-23, 1992. The APF was not connected to the system for this initial test. The performance of the bypass cyclone, and the operation of the ash removal system from the bypass cyclone was satisfactory. However, several hot spots developed on the piping system, expansion joints, and cyclone as unit load was increased.

On May 23, 1992, an expansion joint bellow ruptured, forcing the unit to be shut down after 35 hours of operation on coal. Another expansion joint bellows was found to have pinhole leaks on the bottom side of some convolutions. The failures were determined to be due to stress corrosion in the 321 stainless steel bellows due to chlorides in an aqueous solution of sulfuric acid. The solution formed from condensation of the moisture in the flue gas on the inside of the bellows.

Following the expansion joint failure, a complete engineering review of the system was undertaken. As a result of this review, several enhancements were made to the system.

From observations made during and after initial operation of the system, certain deficiencies became evident in the design of the hot gas piping system, as listed below:

- Hot spots appeared at various points in the system, indicating that the insulation was not packed tightly enough in those areas or that a gas leak path into the piping annulus had formed.
- Several expansion joint bellows exhibited elevated temperatures (250F to 670F) during operation, again indicating inadequate insulation or gas flow into the piping annulus.
- Corrosion of type 321 stainless steel expansion joint bellows was evident upon disassembly of the joints. The failure of one joint was attributed to stress corrosion cracking, while the pinholes found in another bellows was due to pitting corrosion. Chlorides were found in the condensed flue gas in the insulation material.

## Results

---

- Corrosion was also found on carbon steel surfaces that did not have the Plasite (epoxy) coating which was applied to the inside of the outer pipe. These areas included flange faces inside the gasket area, and various nozzles on the cyclones. This corrosion is believed to be from sulfuric acid formed from the flue gas condensation.
- The Plasite coating was burned off at locations where hot gas reached the carbon steel pipe.

### 4.2.1 System Modifications (5/92-10/92)

After reviewing the above problems and lengthy discussions with other users of hot gas piping systems, consultants, and others, the following piping modifications were undertaken:

- The expansion joint bellows material was changed from 321 SS to Hastelloy C-22. This is a high nickel alloy that has excellent resistance to pitting, crevice corrosion, and stress corrosion cracking in the presence of oxidizing agents and chlorides.
- A 2-ply expansion joint bellows was used with pressure monitoring capability between the plies. The inner ply was 0.038" thick and the outer ply was 0.062" thick. Failure of the inner ply would not result in failure of the joint and could be detected with local pressure gauges.
- The ceramic fiber insulation was replaced with a cast insulating refractory. It was concluded that a cast refractory would present a superior barrier to prevent gas from flowing behind the inner liner in the annulus compared to the ceramic fiber blanket insulation. (In order to retain freedom of movement in expansion joint spools, a small portion of fibrous insulation was used at the bellows location.) It was further decided to retain the inner liner (except in two instrument spools) to preclude the possibility of refractory spalling off and getting carried into the gas turbine. The liner also served as a form during the installation of the refractory. As additional enhancement, 1/4" thick ceramic fiber rollboard insulation was used on the ID of the cast refractory for expansion and cushioning. The refractory selected had a density of 50 lbs/ft<sup>3</sup> and a thermal conductivity which would keep the outer pipe temperature below 250F. The refractory was shop installed.
- The inside surfaces of all piping and flange faces were clad with Hastelloy C-22 material. The cladding was 16 gauge (1/16" thick) and was applied to the pipe ID by plug welding. The

## Results

---

function of this inner liner was to protect the inside of the outer pipe from the possibility of corrosion from condensed acid. Figure 4.2.1 is a photograph of a typical pipe spool following installation of the Hastelloy C-22 liner. The anchors used to secure the refractory in the pipe are also shown in the photograph.

- The liner end connection collars were modified where possible to minimize gas leaking behind the liner. One end of the collar was seal-welded to the liner where possible.
- The liners in the expansion joint assemblies were modified to include a bellows at the same location as the bellows in the outer pipe. This was necessary to allow the outer pipe, refractory, and liner to move together while still permitting freedom of movement at the bellows area. (Most of the expansion joints underwent angular rotation, not axial movement.) Figure 4.2.2 is a drawing of a typical expansion joint after the modifications.
- The flow liner tees were modified to function as 90° elbows where possible. The blind end of the tee was cut off and a curved plate was welded onto the tee to form an elbow. The end of the outer tee was filled with cast insulating refractory in order to better insulate the blind flange. This change reduced the possibility of ash collecting in the dead end of a tee and becoming dislodged and being carried into the gas turbine.

Figure 4.2.3 provides a comparison of the original and modified designs of the pipe internals.

The modifications described above proved successful, and the piping system performed very well during subsequent testing. However, corrosion of expansion joint bellows remained a problem until additional steps were taken later in the project as discussed in Section 4.3.5.

Following initial operation of the system, both cyclones were opened and inspected by the manufacturer, refractory supplier, and refractory installer. Some cracking of the refractory was apparent, but was not considered to be serious. Some corrosion was evident on the man way nozzle and flange. As a result, Plasite (epoxy) coating was applied to nozzles and flange faces on the cyclones and the APF vessel.

## Results

---



Figure 4.2.1 - Photograph of Hastelloy Liner in Hot Gas Pipe Spool

## Results

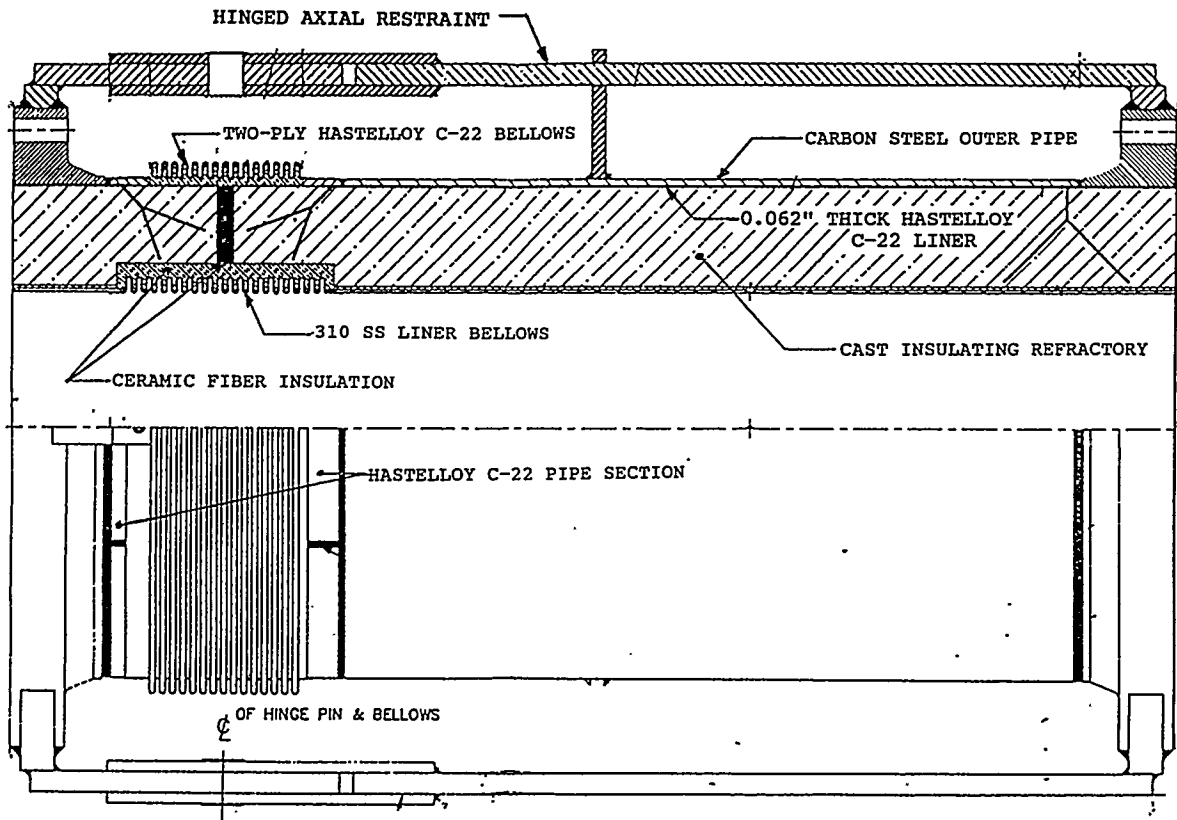
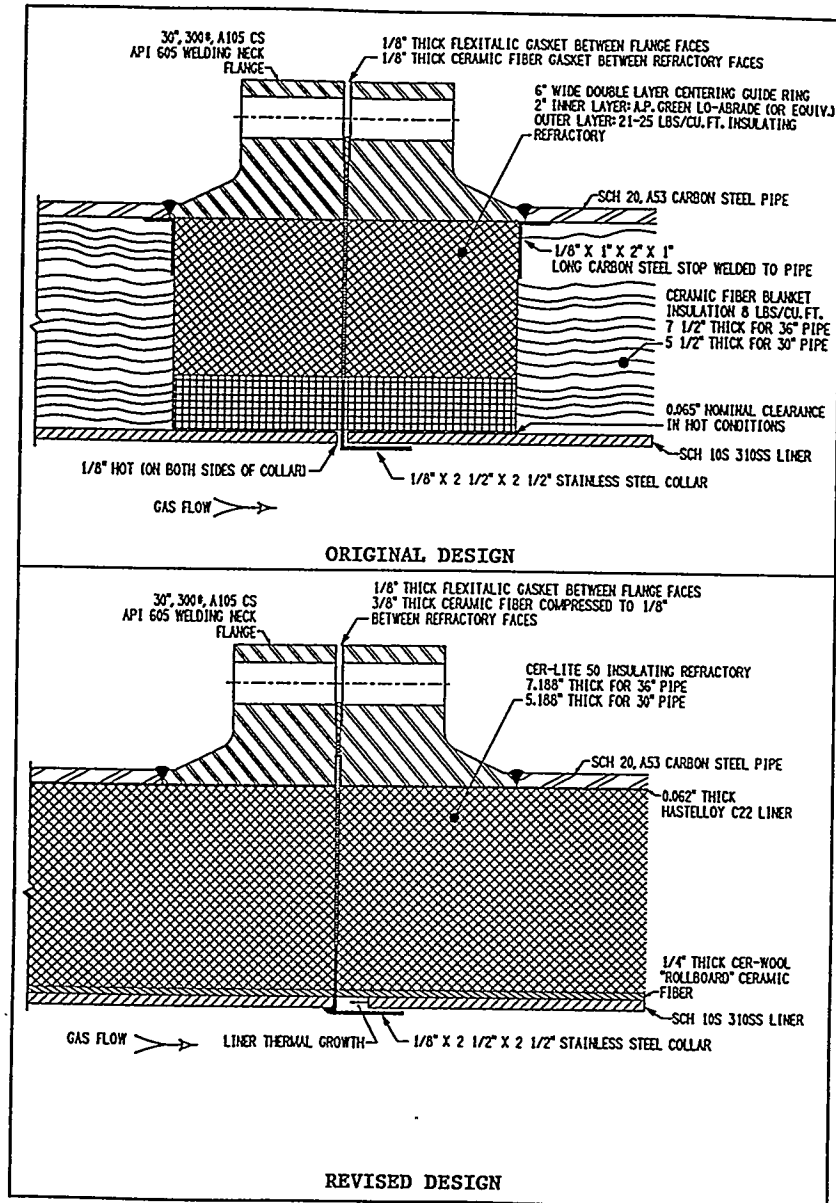


Figure 4.2.2 - Typical Expansion Joint After Modifications

## Results



**Figure 4.2.3 - Cross Section of Typical Hot Gas Piping Joint**

## Results

### 4.3 Test Period I: 10/92 - 12/92

Table 4.3 summarizes the operating conditions and observations from Test Period I.

**Table 4.3 - Summary of HGCU Operation - Test Period I**

	Operating Hours	Cumulative Hours	Operating Temp.	Pressure Drop	Inspection Observations
Run 1	101	101	1150°-1400°F	25-75 in. H <sub>2</sub> O Stable	● No filter issues
Runs 2 & 3	77	178	1000°-1450°F	40-180 in. H <sub>2</sub> O	_____
Run 4	286	464	1300°-1490°F	45-170 in. H <sub>2</sub> O	● 21 Broken candles in bottom plenums

#### 4.3.1 Test Run 1 - 10/28 to 11/1/92

First operation of the advanced particle filter on coal fire occurred on October 28, 1992. The first test of the APF included over 101 hours of operation on coal. During the initial operation, the APF exhibited a stable pressure drop over a range of plant conditions corresponding to the predicted values. Although the APF was operated to approximately 90 percent of the design flow with the PFBC at 80 to 85 percent of full load, full plant load was not achieved due to hot spots on the backup cyclone vessel and APF outlet nozzle. The plant was ultimately shut down due to ash pluggage of valves and instrument lines associated with the control of the APF ash removal system.

Following shutdown, the filter was visually inspected through access ports in the APF pressure vessel head and ash hopper. The inspection, while limited to the clean gas side of the tubesheet and the three bottom plenums of the three cluster assemblies, indicated the system to be in excellent condition with no evidence of filter failure or dust breach to the clean side of the filter. Furthermore, the filters appeared to be uniformly clean with no indication of ash buildup or bridging. Figure 4.3.1 shows a photograph of the bottom filter candles following Test Run 1.

Following repair and maintenance of the APF outlet nozzle and backup cyclone to eliminate local hot spots and to incorporate continuous instrumentation air purges, operation of the PFBC plant was resumed.

## Results

---

### 4.3.2 Test Run 2 - 11/17/92

This run was terminated after 1.3 hours of coal fire due to plugged primary cyclones, and will not be discussed.

### 4.3.3 Test Run 3 - 11/21 to 11/24/92

In Test Run 3, the APF was operated for approximately 76 hours on coal, reaching a maximum operating temperature of 1450F and 90 percent of the design flow. Again, stable filter pressure drops were demonstrated over a range of operating conditions.

Approximately 36 hours into this test, the fourth stage of the APF backpulse compressor failed, thus limiting the ability to clean the filter for 24 hours. During this period, the filter pressure drop reached a value of 180 inches of water. Once a pressurized nitrogen supply system was installed, a stable filter pressure drop was once again achieved. However, the original APF baseline pressure drop was never reestablished.

Following the compressor outage and reestablishment of stable filter operation, the performance of the APF was indirectly checked by briefly opening a vent valve on the backup cyclone ash discharge line. Visual inspection of the short burst of gas discharged from the vent valve showed no evidence of dust. This result, along with other operating data, supported the conclusion that no serious damage to the filter resulted from the compressor outage. In this test, the PFBC was shut down due to a paste feed pump issue unrelated to the APF. No visual inspection of the filter was made at this time.

## Results

---

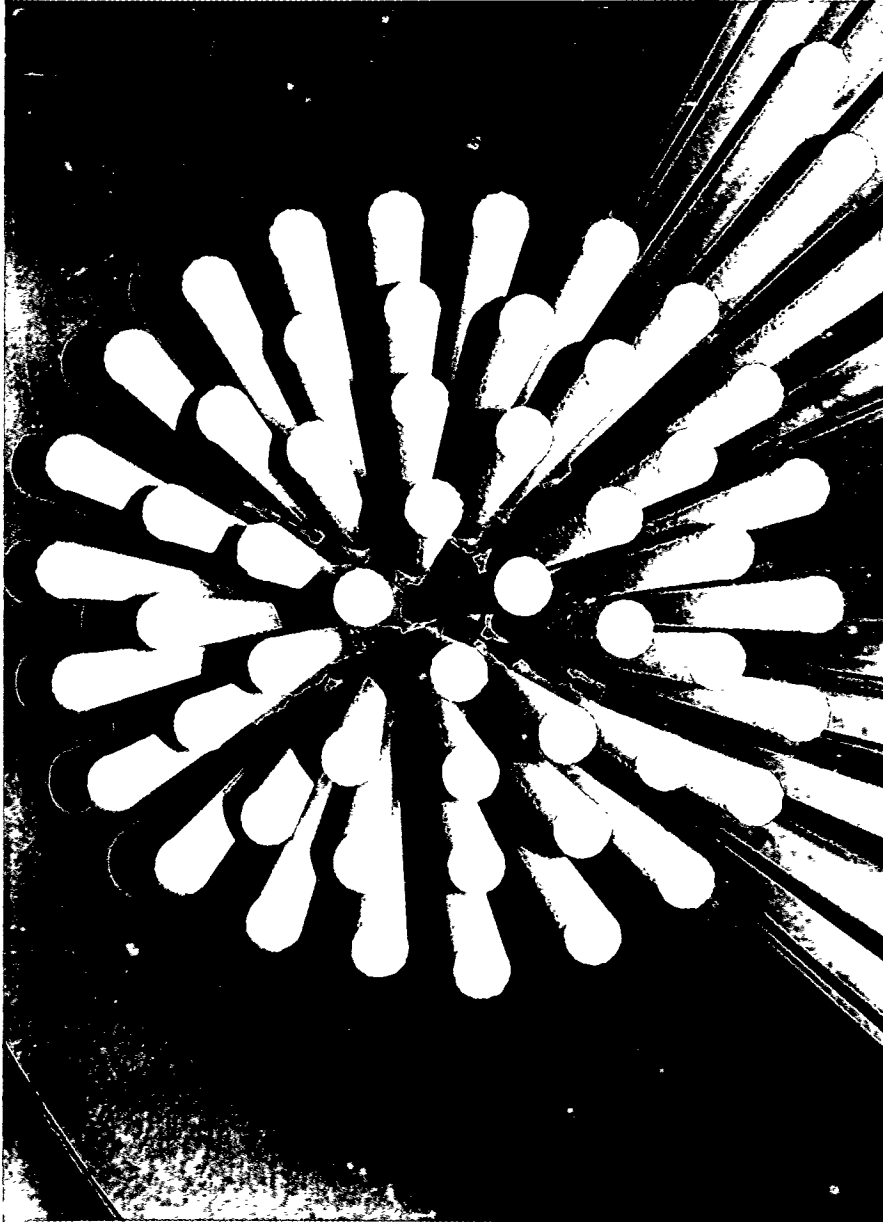


Figure 4.3.1 - Photograph of Bottom Filter Candles Following Test Run 1

## Results

---

### 4.3.4 Test Run 4 - 11/25 to 12/7/92

Test Run 4 was a hot restart of the plant following Test Run 3. Test Run 4 accumulated an additional 286 hours of operation on coal. At the start of this test, a nominally low baseline pressure drop was established, apparently due to pulse cleaning during the shutdown of Test Run 3 and prior to restart. During this test, several major events occurred, including high ash level alarm in the APF hopper, a second loss of the backpulse compressor, indications of an unstable pressure drop at temperatures above 1400F, first indications of dust breach, and the first identifiable change in pressure drop indicating a possible loss of filter elements. This test was eventually terminated due to a leak in a pipe expansion joint unrelated to the APF technology.

### 4.3.5 Posttest Inspection and Modifications (12/92-6/93)

Following the conclusion of Test Run 4 and a visual inspection of the filter internals, the tubesheet and cluster assemblies were removed from the pressure vessel. Figures 4.3.2 through 4.3.10 are photographs of the filter internals following Test Run 4. Based on a detailed inspection of the filter, the following observations were made:

- A total of 21 broken candle filters were identified occurring only on the bottom three plenums. Seventeen of the broken filters apparently failed near the transition from the dense-to-porous filter region. Plenum A had 15 failed elements, while Plenum B had 2 and Plenum C had 4.
- No broken candles were detected in the top or middle plenums. Some ash bridging was observed on the top and middle plenums between the inner ring of filters and the cluster support pipe.
- Bowing of filters was detected for some elements in the bottom plenums, as well as for broken filters removed from the ash hopper.

A possible failure scenario would conclude that ash, unable to properly discharge from the hopper, built up and reached the candle filters of the bottom plenums. Ash at this level then began to fill and pack the interstitial spacing, forming ash bridges between the candle filter elements. As cleaning continued, more ash was packed into the interstitial filter spacing with additional accumulation of ash in the hopper.

## Results

---

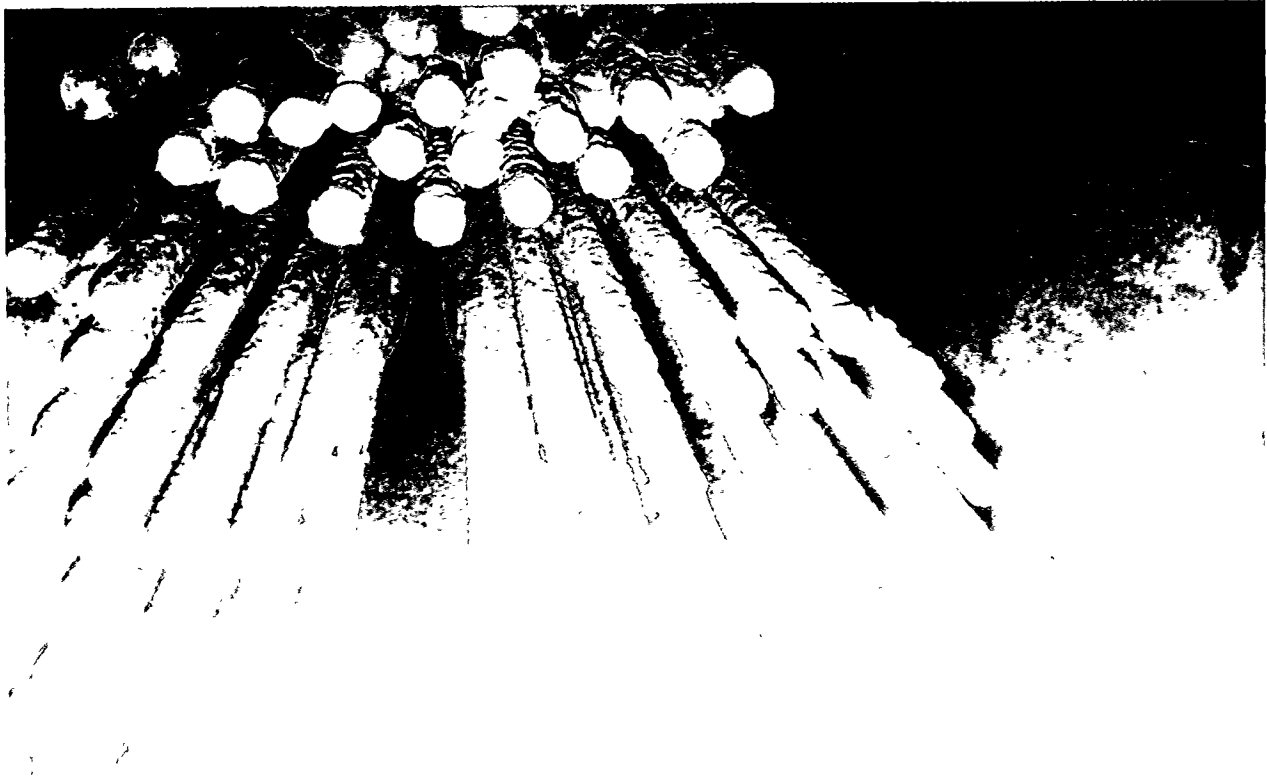


**Figure 4.3.2 - Photograph of Filter Internals Following Test Run 4**

## Results

---

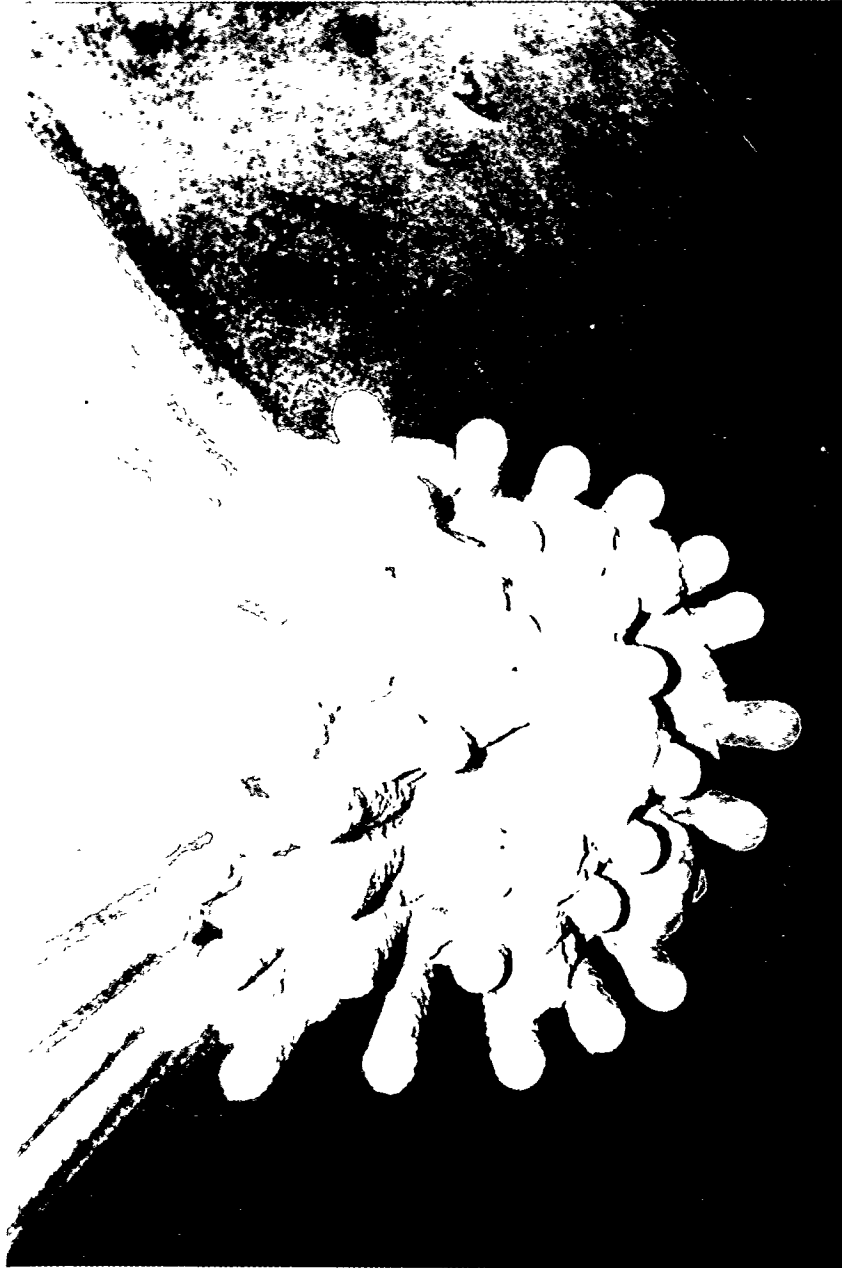


**Figure 4.3.3 - Photograph of Filter Internals Following Test Run 4**

## Results

---



**Figure 4.3.4 - Photograph of Filter Internals Following Test Run 4**

## Results

---

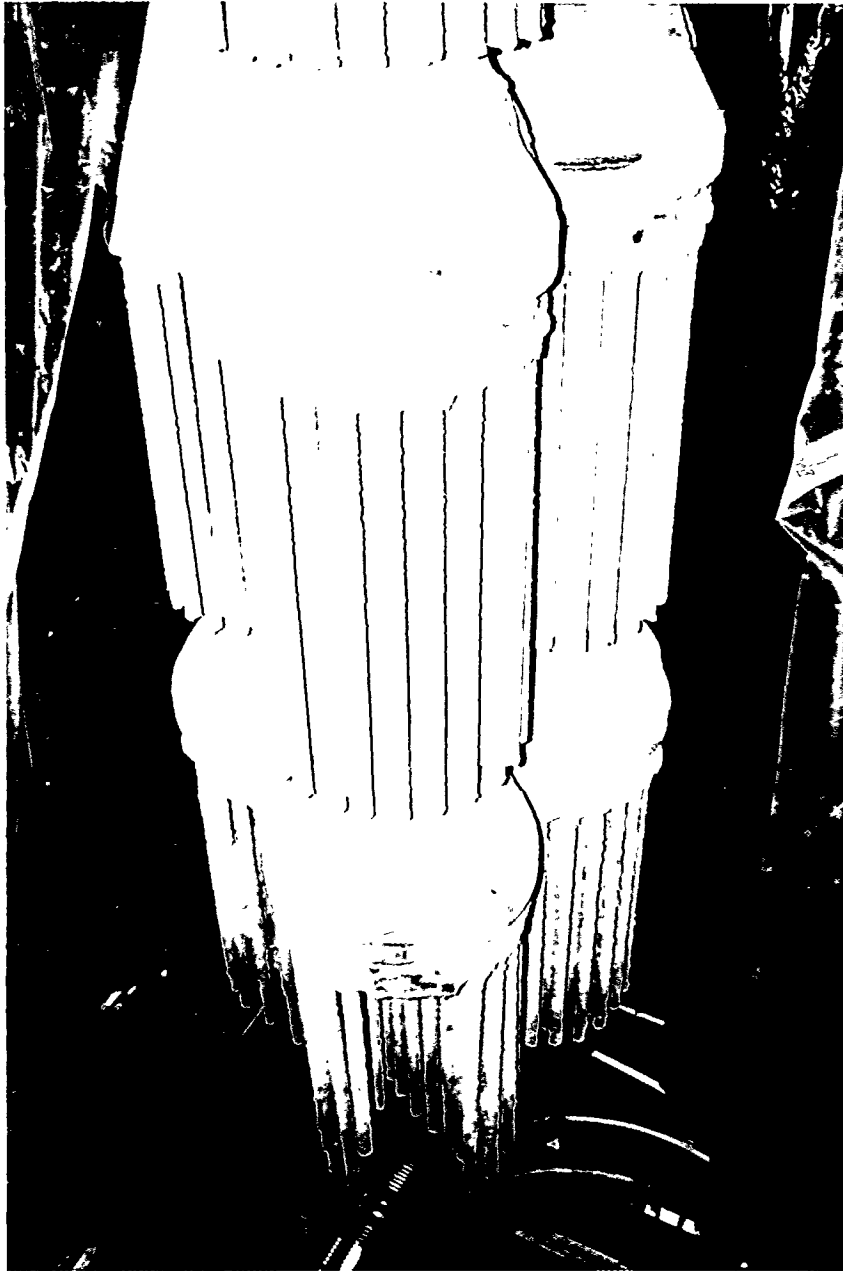


**Figure 4.3.5 - Photograph of Filter Internals Following Test Run 4**

## Results

---



**Figure 4.3.6 - Photograph of Filter Internals Following Test Run 4**

## Results

---



**Figure 4.3.7 - Photograph of Filter Internals Following Test Run 4**

## Results

---



**Figure 4.3.8 - Photograph of Filter Internals Following Test Run 4**

## Results

---

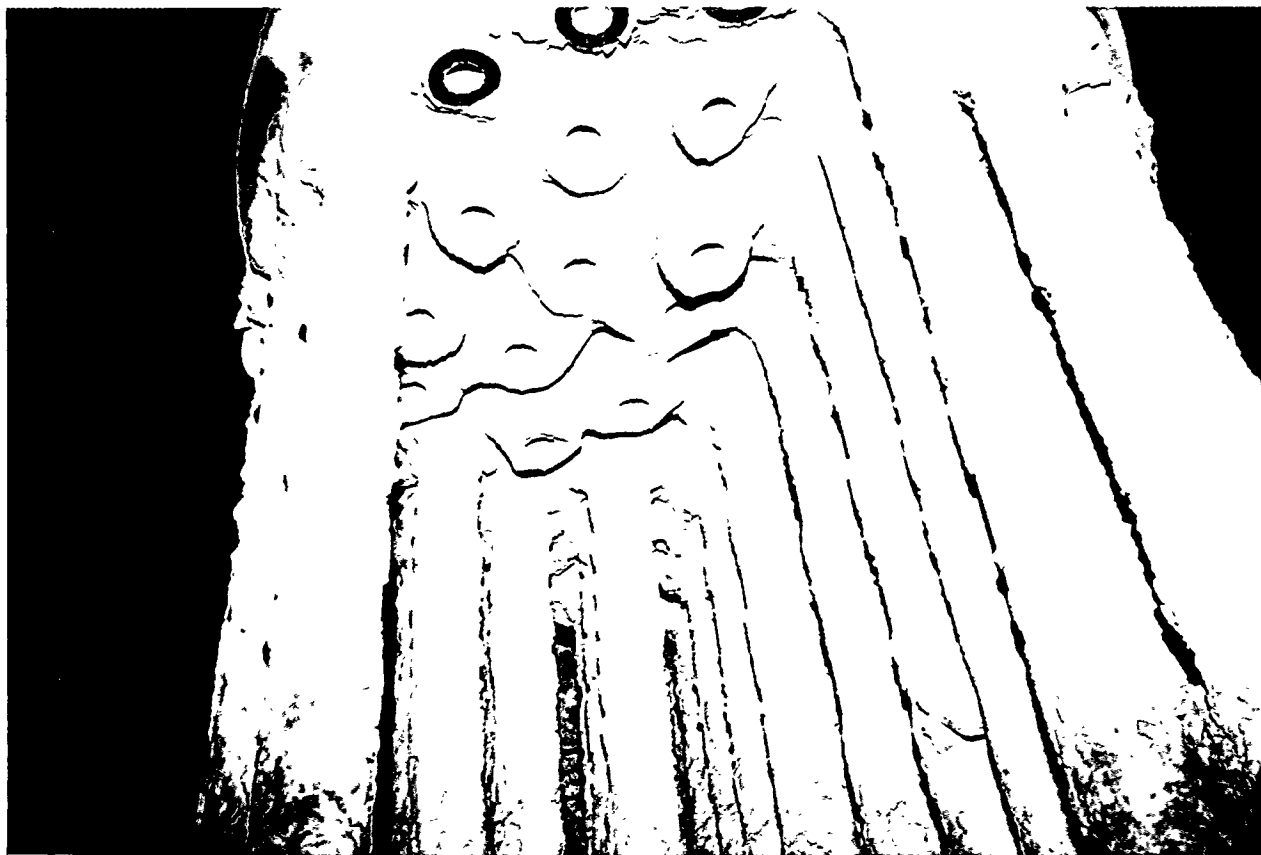


**Figure 4.3.9 - Photograph of Filter Internals Following Test Run 4**

## Results

---



**Figure 4.3.10 - Photograph of Filter Internals Following Test Run 4**

## Results

---

The high cohesive strength of this ash allowed lateral forces to develop on the filter elements. The lateral forces resulted in filter bowing and high shear loads. The concentration of stresses near the top of the filters resulted in a mechanical failure of the filter elements.

The initial operation of the HGCU system revealed some problems with the system. Since this was the first test of a large-scale hot gas clean up system, it is not surprising that problems arose. Most of the problems discussed below did not involve the APF. Other than the problems of hot spots on the shell of the APF and the ash accumulation in the hopper, the APF performed very well. It was necessary to overcome the problems associated with the balance of the system in order to achieve successful long-term operation. A summary of the problems encountered and corrective actions is discussed below.

**Hot Spots.** Hot spots were observed on the backup cyclone, APF vessel head and outlet nozzle, and several instrument nozzles on the hot gas piping. Following Test Run 1, the backup cyclone was heated internally and externally to remove any residual moisture from the refractory lining, and all refractory cracks were repaired. In subsequent tests, the cyclone skin temperature was much lower; however, it still exceeded the nameplate design rating of 200F at several locations. At our request, the cyclone manufacturer recertified the cyclone to 750F by resubmitting ASME code calculations based on this design temperature. Hot spots on the cyclone shell observed in subsequent testing remained well below the revised design temperature.

Also following Test Run 1, all instrument nozzles that exhibited hot spots were opened and inspected. In all cases, it was found that gaps between the refractory and insulation or instrument device allowed hot gas to reach the nozzle/pipe connection. Insulating caulking was added at these locations to seal the gaps. In subsequent tests, none of these hot spots, with one exception, reappeared. One nozzle reached about 400F, and it was reworked again prior to the resumption of testing.

The APF outlet nozzle and several locations on the top of the APF head exhibited high temperatures (up to 800F) during Test Run 1. Between Test Runs 1 and 2, the insulation in the outlet nozzle was revised to eliminate a likely gas flow path, and potential holes around head liner penetrations were repacked with insulation. The following test showed that the outlet nozzle had been successfully repaired, as well as most of the original hot spots on the top of the APF head. However, a new hot area appeared around the head knuckle. Upon disassembly following testing, this hot area was found to be caused by distortion of the brim of the dome liner which opened up a gap between it and the insulation. The brim was eliminated and the insulation repaired.

## Results

---

**Ash Accumulation in the APF Hopper.** Following Test Run 1, the APF hopper was inspected. Some ash was observed on the sides of the hopper near the outlet. However, it appeared to be less than one inch thick. It was cleaned out prior to Test Run 2. During Test Run 3, after approximately 19 hours on coal, the APF liner temperature began dropping, indicating ash buildup near the hopper outlet. Subsequent purging with air corrected the problem. Later in the test run, the backpulse air compressor failed and filter cleaning was abnormally low or completely interrupted for about 33 hours. Following resumption of cleaning, the high ash level annunciator alarmed, and the hopper liner temperatures decreased. During Test Run 4, several instances of low liner temperature and/or high ash level alarm occurred. Upon inspection of the APF hopper following the last test, the entire hopper was found to be full of ash. In some areas the ash level was higher than the bottom of the candles, leading to candle breakage.

Subsequent inspection revealed a solid plug of material in the 8-in. diameter APF hopper outlet pipe. It is unknown when this plug formed. Chemical analysis indicated that it was calcium sulfate and magnesium sulfate. Condensation of sulfuric acid from the flue gas in the relative cool outlet pipe is thought to have contributed to the formation of the plug. This was exacerbated by cool seal air from the screw cooler flowing upward into the filter ash outlet nozzle.

Several options were considered for improving ash flow through the hopper. These included installing purge air pipes or manifolds in the hopper, increasing the hopper angle, mounting the hopper liner supports on vibrators, and installing a pneumatic vibrator in the APF manway nozzle and linking it to the hopper. The purge air option was rejected since it was considered likely to move ash only in localized areas and cool the gas below the dew point causing the ash to become more sticky. Changing the hopper angle was rejected because laboratory flow tests indicated that the dimensional constraints of the APF vessel would make this impractical. The last alternative was chosen and preliminary testing at Tidd using a vibrator showed it to be effective in moving ash down the hopper wall. A detailed design was completed by Westinghouse and the vibrator and related hardware were installed prior to the next test. The screw cooler water temperature was increased in the next test series from 320 to 340F (the limit of the system) in order to increase the ash temperature at the screw cooler inlet.

**Ash Pluggage in the Lockhopper System.** Test Run 1 was terminated due to ash buildup in a lockhopper isolation valve and instrument lines. It was found that the valve purge air contained enough moisture to harden the ash in the valve body. The pressure sensing lines on the ash removal system became plugged with ash, causing erroneous pressure data which resulted in the logic

## Results

---

interrupting the sequence of operation. The lockhopper pressure equalization line also became plugged with ash. As a result, ash removal was sporadic during Test Run 1.

Several improvements were made to the ash removal system between Test Runs 1 and 2. The source of air for all valve purging was switched to a drier source. Blowdown valves were added to the purge air lines to remove any residual moisture accumulation. Constant flow regulators were installed to provide continuous instrument air purge to all pressure sensing lines. The lockhopper pressure equalizing line was revised to utilize clean process air instead of gas in the surge hopper for repressurization in order to keep ash from plugging the equalizing line. The ash removal system logic was revised to reduce the number of interruptions in the ash unloading sequence. Finally, as a backup, an emergency ash removal system was added downstream of the screw cooler. This system used process air to transport ash from the screw cooler discharge pipe in a manner similar to the method used for the backup cyclone ash removal. Ash removal during Test Runs 3 and 4 was much better than during Test Run 1. However, system logic enhancements continued to be made during and after Test Runs 3 and 4. Visual inspection of the system following Test Run 4 revealed that the lockhoppers were clean.

**Expansion Joint Bellows Leak.** The expansion joint bellows material was changed from 321 stainless steel to Hastelloy C22 (UNS N06022) following the failure of two expansion joints in May 1992, during initial operation of the system using only the bypass cyclone as previously discussed. The failures were attributed to stress corrosion and pitting corrosion due to sulfuric acid and chlorides. Hastelloy C22 was believed to be the best candidate material for the corrosive conditions created by condensation of the Tidd PFBC flue gas. Also, the revised expansion joints were made with a two-ply bellows, 0.038" (inner) and 0.062" (outer) in thickness. A pressure gauge was installed at each bellows to monitor the interply pressure and thereby detect a leak in the inner ply. A pinhole leak formed in the inner ply of one bellows during Test Run 4. A hot spot ( $\approx 540\text{F}$ ) was also observed at a localized area in the outer bellows. When the leak was confirmed, the plant was shut down. Subsequent failure analysis confirmed that a pinhole leak was formed by pitting corrosion from hydrochloric acid. The bellows was replaced. A second bellows was removed and examined as well. It also exhibited some pitting corrosion, but to a much lesser degree. It was not replaced. Thus, it was concluded that even Hastelloy C22 was not impervious to corrosion in this system, although it was far superior to stainless steel.

As a result of the failure, it was decided to heat trace and insulate all expansion joints in the hot gas piping system to maintain a temperature of 450F, well above the acid dew point ( $\approx 370\text{F}$ ) of the flue

## Results

---

gas. Necessary instrumentation and controls were installed prior to the next test series to monitor and control the temperature of the bellows.

**Loss of Backpulse Air Compressor.** The backpulse air compressor failed on two occasions, once during Test Run 3 and again during Test Run 4. Both failures were believed to be due to insufficient lubrication to the fourth stage cylinder. The manufacturer subsequently modified the fourth stage cylinder liner to relocate the oil port to eliminate the problem. However, excessive wear of fourth stage piston rings remained an intermittent problem for the remainder of the test program. The second failure also resulted in a broken crosshead which connected the second/third stage pistons to the crank shaft. The manufacturer suggested that this failure might have been due to excessive oil and moisture building up in the first stage moisture separator and carrying over into the second stage. Therefore, all four moisture separators were equipped with larger drain lines and drain valves, and the first stage separator drain valve was left open continuously in subsequent tests.

In addition, two spare compressors, each with approximately half the capacity of the original, were rented and placed on standby for use during the remainder of the program. They were used for brief periods when the main compressor had to be shut down for maintenance.

**Backpulse Valves.** Piston actuated ball valves were used on the backpulse valve skid to control flow paths during backpulsing. One valve failed during Test Run 4 due to excessive wear at the valve stem coupling. The valve was replaced during the test. Other ball valves also exhibited wear at the couplings. Between Test Runs 1 and 2, bracing was added to the valve operators to reduce misalignment of the stem and coupling during stroking. However, the couplings continued to wear. Following Test Run 4, all couplings, valve bodies, and actuator brackets were replaced with an improved design.

On several occasions backpulse valves failed to operate. In all cases, the parallel backup valve operated successfully. Post-test examination revealed some axial scratches and galling on the piston and cylinder wall. Atkomatic modified all of the solenoid valves in an effort to eliminate galling during valve actuation. However, additional modifications were required later in the program to overcome this problem.

**Unstable Filter DP Above 1400F.** Operating experience, both at Tidd and Westinghouse Test Facility, demonstrated that the filters are difficult to clean, particularly when the ash temperature

## Results

---

approaches 1500F. During Test Runs 1 and 3, filter pressure drop increased moderately (indicative of good cleaning). However, after failure of the backpulse compressor, baseline pressure drop increased considerably. After nitrogen was brought onto the site for backpulsing, the baseline pressure drop did not recover. Upon visual inspection, many candles had a "splotchy" appearance. Some intercandle and candle-to-plenum ash bridging was also observed.

Figure 4.3.11 shows the increase in filter baseline pressure differential over an 18-hour time period during Test Run 4. The temperature in the APF ranged from 1425 to 1450F during this time period. It is not clear whether the inability to clean effectively during this phase was due to a temperature effect on the ash or the result of a thick ash cake on the candles that had been partially cleaned by low pressure backpulsing. Once the candles became "splotched," subsequent cleaning may have been ineffective on the previously uncleaned areas. It should be noted that the filter pressure differential stabilized during portions of Test Runs 1 and 3 (prior to the backpulse compressor failure) at temperatures above 1400F, but below 1500F.

During Test Run 4, unit load was reduced to decrease gas temperature and flow to maintain the APF tubesheet pressure differential below the maximum limit. In order to increase the allowable pressure differential of the filter, stiffener bars were subsequently welded across the bottom filter plenums above the candle holders. The plenum bottoms were the limiting components of the maximum allowable pressure drop of the filter assembly. This modification increased the tubesheet allowable pressure differential from 7 to 9 psi.

In addition, a method of detuning the primary cyclone upstream of the APF was devised. The method involved injecting air from the sorbent system upwards into the cyclone dip leg, thereby reducing the cyclone efficiency. The purpose of cyclone detuning was to increase dust loading and the proportion of larger dust particles to the APF in order to improve filter cleaning and/or ash removal and transport. An analysis was performed to determine the proper air line size to obtain the required air velocity in the cyclone. The system included a manual globe valve and flow metering orifice outside the combustor to allow the detuning air flow to be adjusted or shut off. The system was installed prior to the next start-up, but was not tested until the latter part of Test Run 11.

## Results

---

Prior to the resumption of testing, all of the filter candles in the bottom plenums were replaced and all of the ash accumulation on the filter candles and metal surfaces in the upper and middle plenums was removed, as shown in Figures 4.3.12 through 4.3.15.

# Results

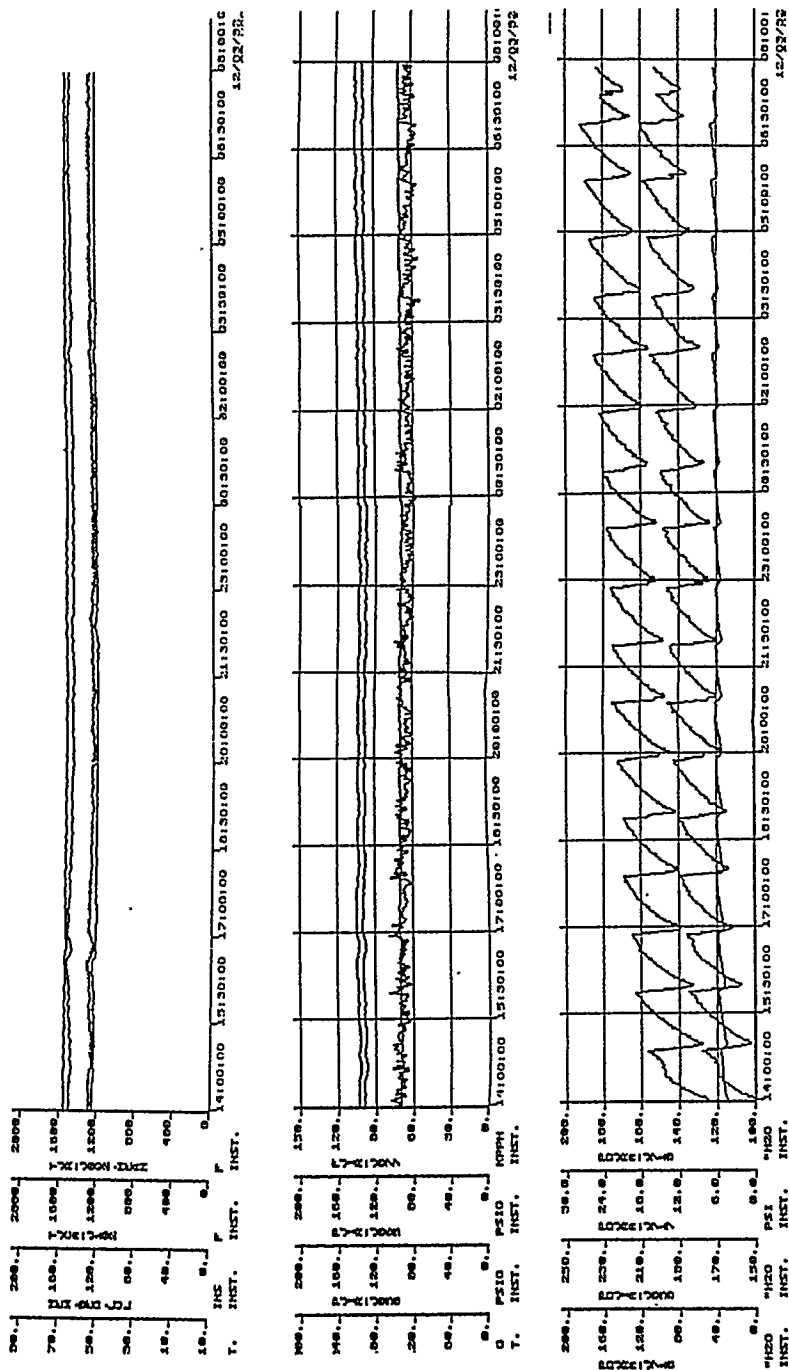


Figure 4.3.11 - Graphs of Filter Parameters During Test Run 4

**Top Set of Graphs:**

- Top Line: Mean Bed Temperature: 1540F
- Second Line: Freeboard Temperature: 1490F
- Third Line: Unit Load: 53 MW
- Bottom Line: Bed Level: 123"

**Second Set of Graphs:**

- Top Line: APF Inlet Pressure: 138 psig
- Second Line: APF Outlet Pressure: 130 psig
- Third Line: Freeboard Pressure: 139 psig
- Bottom Line: APF Gas Flow: 65,000 - 70,000 lb./hr.

**Bottom Set of Graphs:**

- Top Line: APF DP: Baseline Climbing from 125° H<sub>2</sub>O to 165° H<sub>2</sub>O
- Second Line: HGCU System DP: Baseline Climbing from 150° H<sub>2</sub>O to 190° H<sub>2</sub>O
- Bottom Line: APF Tubesheet DP: Climbing from 5 psi to 6 psi

**NOTE:** APF DP as measured between filter outlet nozzle and bottom of vessel cone.

Tubesheet DP as measured between filter outlet nozzle and lower cylindrical portion of vessel.

HGCU System DP as measured between inlet and outlet piping.

## Results

---

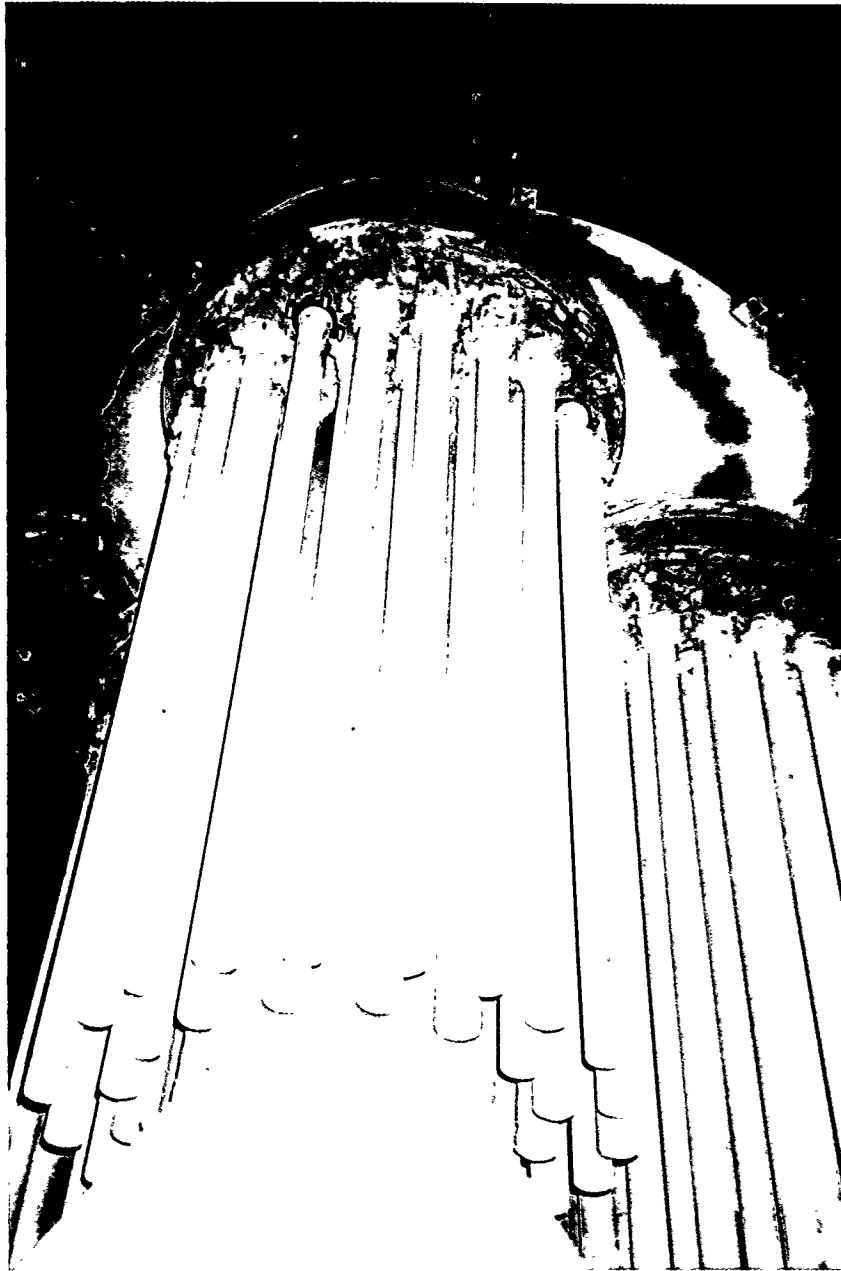


**Figure 4.3.12 - Photograph of Filter Internals Before Test Period II**

## Results

---

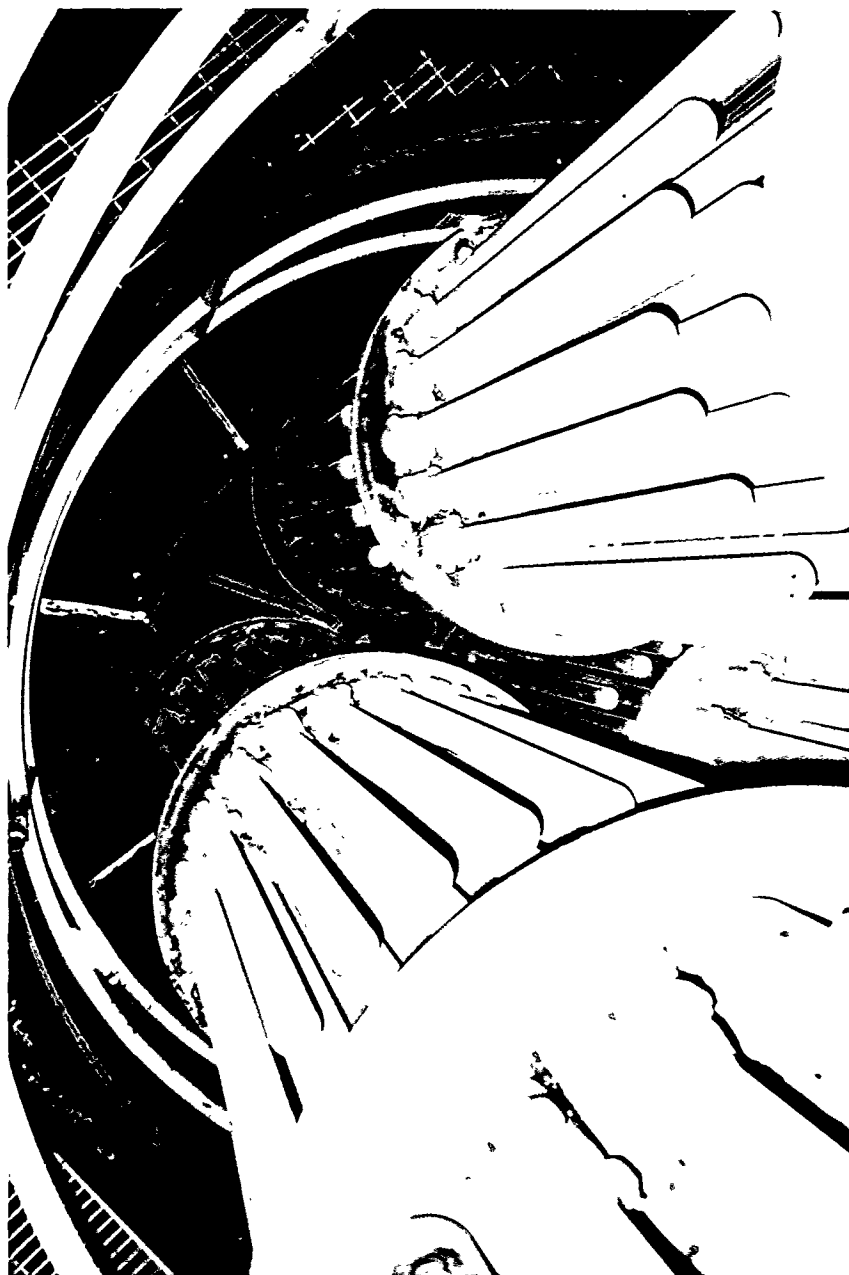


**Figure 4.3.13 - Photograph of Filter Internals Before Test Period II**

## Results

---

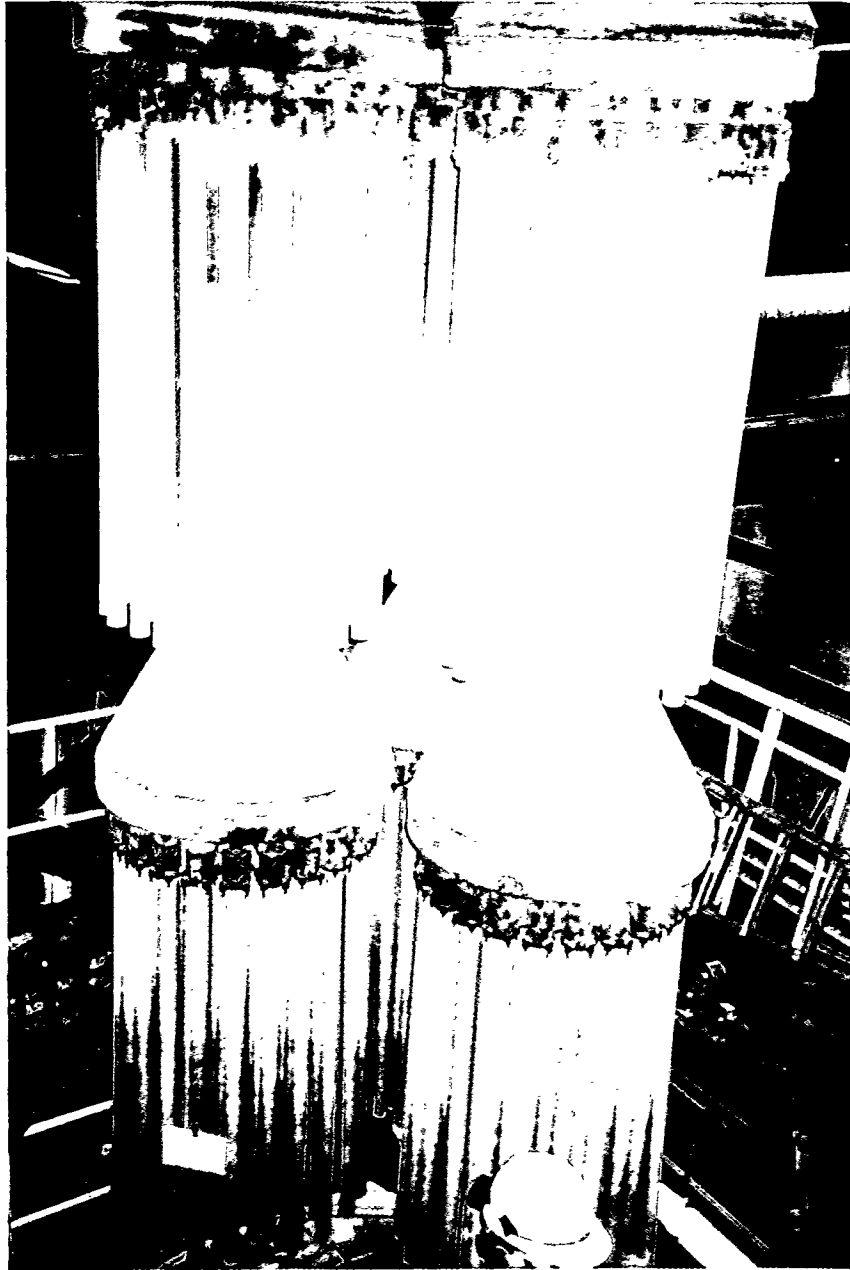


**Figure 4.3.14 - Photograph of Filter Internals Before Test Period II**

## Results

---

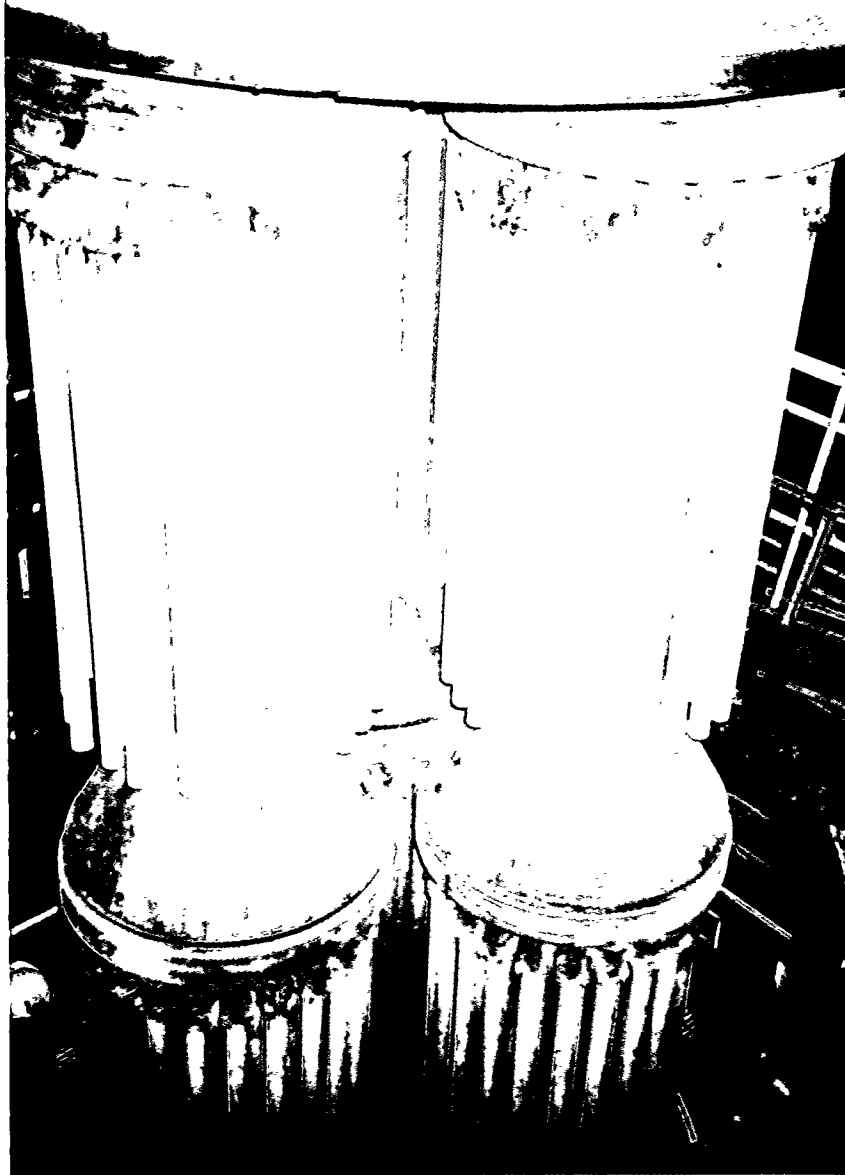


**Figure 4.3.15 - Photograph of Filter Internals Before Test Period II**

## Results

### 4.4 Test Period II: 6/93 - 9/93

Table 4.4 summarizes the operating conditions and observations from Test Period II.

**Table 4.4 - Summary of HGCU Operation - Test Period II**

	Operating Hours	Cumulative Hours	Operating Temp.	Pressure Drop	Inspection Observations
Run 5 & 6	77	541	<1400°F	Stable	● No filter issues
Run 7	426	967	1150°- 1350°F	Stable	● No filter issues
Run 8 & 9	80	1047	1450°F	Increasing $\Delta p$ , pulse pressure from 800 to 1000 to 1200 psig	● Patchy cleaning ● No ash bridging
Run 10	116	1163	1450°F	Slowly increasing $\Delta p$ , pulse pressure at 1200 psig	● Patchy cleaning ● No ash bridging
Run 11	596	1759	1450°F  1200°F	Increasing $\Delta p$ $\Delta p = 240$ in wg Stable $\Delta p$	● Outlet dust first detected (after 300 hours) ● Significant ash bridging, failed candles

#### 4.4.1 Test Runs 5 and 6 - 6/30 to 7/5/93

The unit was operated for 60 hours on coal fire during Run 5, and 17 hours during Run 6. While burning Pittsburgh No. 8 coal and Plum Run Greenfield dolomite, the unit achieved a maximum load during Run 5 of 53 MW and 116-inch bed level resulting in an APF gas temperature of approximately 1400F. The APF differential pressures remained stable during these runs and reached a maximum of 90 inches at 1400F gas temperature.

#### 4.4.2 Test Run 7 - 7/18 to 8/5/93

The unit was operated for 426 hours on coal fire burning Pittsburgh No. 8 coal and Plum Run Greenfield dolomite. PFBC performance tests were conducted at 95-inch and 80-inch bed levels and at 85%, 90%, and 95% sulfur retention. Due to problems with gas turbine vibration, the maximum unit load obtained was 46 MW at 110-inch bed level resulting in 1350F APF gas temperature.

## Results

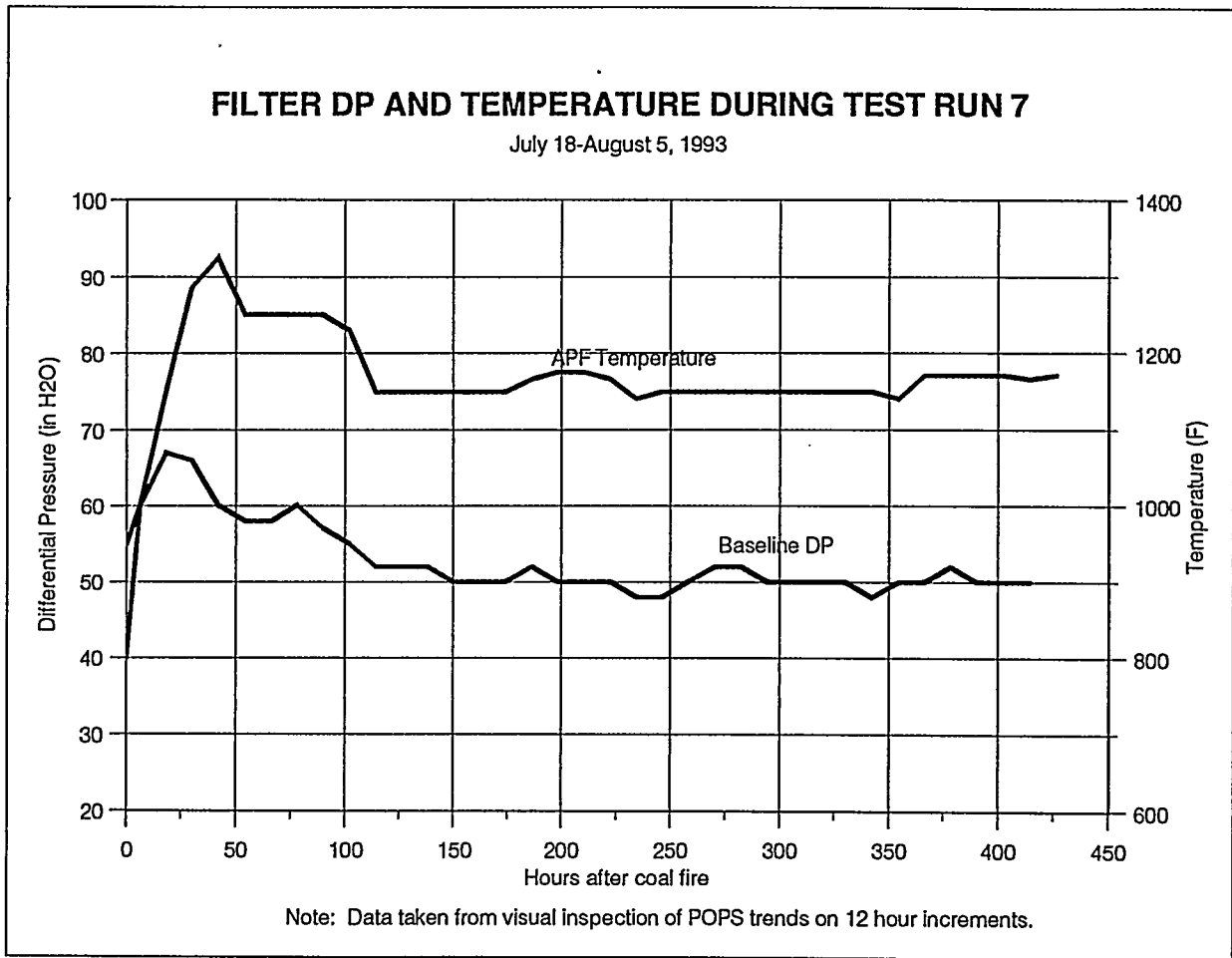


Figure 4.4.2 - Filter DP and Temperature During Test Run 7

## Results

---

Most of the operating time during this run was at 80-inch bed level and 1150F gas temperature. During these operating conditions, the APF DPs were stable at approximately 60-inches trigger and 50-inches baseline. The maximum DP obtained during this run was 105 inches during an excursion at 100-inch bed level and 1250F gas temperature. Figure 4.4.2 shows a graph of filter DP and temperature for the entire run.

The unit was shut down on 8/5 due to ash buildup in the APF hopper that was approaching levels up to the candles. Following shutdown, an inspection revealed three to four inches of ash buildup in areas on the hopper walls. Additionally, a large amount of ash fell off the hopper walls during unit shutdown. Prior to this test series, a pneumatic vibrator was installed in the APF vessel manway and linked to the hopper liner in an effort to keep ash from accumulating on the wall of the hopper. The vibrator, however, did not prove to be effective. Therefore, it was replaced with a larger single impactor-type pneumatic vibrator following this run.

Post-test inspection revealed a small amount of ash buildup on the candles; however, there was no splotching. In general, the candles appeared to be in good shape.

### 4.4.3 Test Runs 8 and 9 - 8/9 to 8/14/93

During most of the run the unit was operated at 115-inch bed level resulting in 1400 and 1450F APF gas temperatures. The APF DPs were unstable at this load. The trigger DP increased from 90 inches on the afternoon of 8/11 to 150 inches on the morning of 8/14. On 8/12, the backpulse pressure was increased from 800 to 1000 psig. On 8/13, the pressure was increased to 1200 psig and the backpulsing time interval was increased from 30 minutes to 60 minutes. Prior to the unit trip on 8/14, the APF DP reached 150 inches trigger and 115 inches baseline.

### 4.4.4 Test Run 10 - 8/19 to 8/24/93

The unit was operated for 116 hours burning Pittsburgh No. 8 coal. The unit was started up using Plum Run Greenfield dolomite, and on 8/24 sorbent feed was switched to Delaware limestone. The unit was shut down 13 hours later due to unstable bed and evaporator conditions experienced while burning limestone. Sulfur retention was maintained at 95% from start-up through the morning of 8/22 and then at 90% for the remainder of the run. The unit was operated at 115-inch bed level and 1450F APF gas temperature for most of the run. The maximum unit load was 52 MW at the conditions stated above.

## Results

---

During operation at 115-inch bed level and 1450F gas temperature, the APF DPs were somewhat unstable; however, not as severe as in Run 9. The trigger DP increased from 95 inches on 8/21 to 115-inches on 8/24, while backpulsing at 1200 psig. When sorbent feed was switched over to Delaware limestone, the baseline DP increased from 90 to 100 inches over a four-hour period while the trigger DP remained fairly constant.

Post-test inspection revealed splotchy areas of ash buildup on the candles. The candles were backpulsed during unit shutdown with little success in removing the ash buildup. The APF hopper walls also had areas of ash buildup.

### 4.4.5 Test Run 11 - 8/29 to 9/23/93

The unit was operated for 596 hours burning Pittsburgh No. 8 coal. The maximum unit load achieved during this run was 55 MW at 125-inch bed level, resulting in an APF gas temperature of 1500F. During start up while increasing load to 115-inch bed level and 1450F gas temperature, sorbent fines (Plum Run Greenfield dolomite, 100% less than 75 microns) were added to the coal water paste while reducing the pneumatic sorbent feed rate by approximately 50%. During this time period the APF DPs started to increase at a rate greater than had been experienced during previous load increases. While at temperatures over 1400F, the APF trigger DP increased from 100 to 168 inches over a period of two days. The baseline DP increased from 84 to 154 inches during this same time period. It is unknown whether this increase in DPs was due to the sorbent fines or whether it was a more aggressive deterioration of APF performance (due to some other phenomenon) than what had been experienced previously at temperatures above 1400F.

On 9/9, the APF trigger DP reached 250 inches, at which time it was decided to reduce unit load to 50-inch bed level, 1000F gas temperature to backpulse the APF. The APF DP was reduced to 145 inches by load reduction and dropped to 36 inches after minimum load backpulsing. However after unit load was brought back to 115-inch bed level, 1450F gas temperature, the APF trigger DP reached a level of 250 inches in less than two days. Load was reduced to 80-inch bed level, 1200F gas temperature to maintain DPs within acceptable limits.

On 9/12 and again on 9/13, indications of candle breaks were noticed by a sudden decrease in APF DP (by approximately 10 in. H<sub>2</sub>O) and a sudden increase in individual plenum gas flow which occurred simultaneously while backpulsing. Later on 9/13, fragments of broken candles were recovered from the

## Results

---

ash removal system. The total fragments recovered could not positively account for more than one candle. Figure 4.4.5 shows a graph of filter pressure drop and temperature for the entire run. On 9/17 the spoiling air to the primary cyclone was turned on to test the system. No problems arose during the initial operation of the system. On 9/21, the unit load was increased to 116-inch bed level and the spoiling air was put into service. The unit was removed from service on 9/23 due to a leak in the sorbent transport pipe caused by erosion. The effects of detuning were inconclusive due to the condition of the filter at the time it was used.

## Results

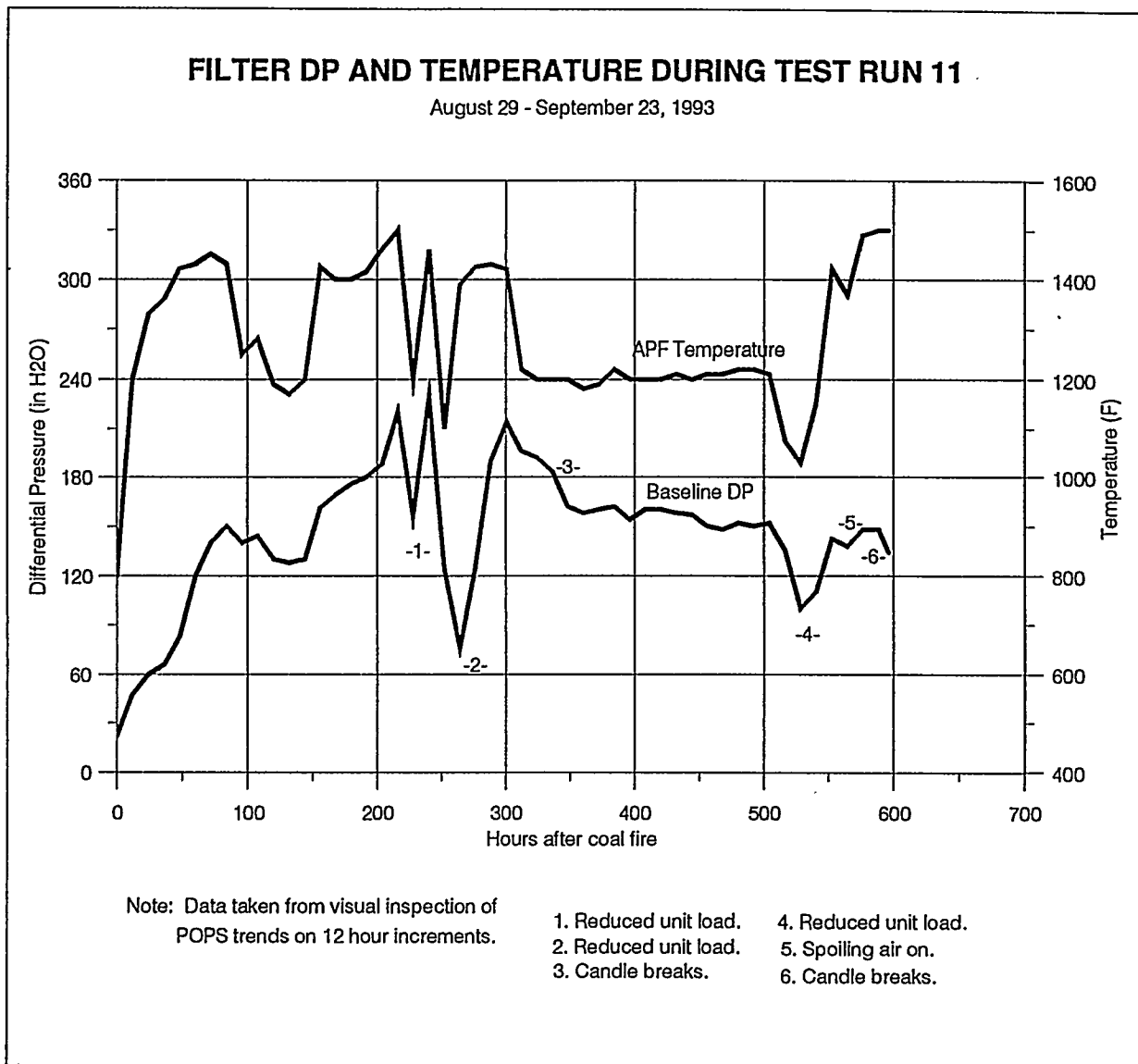


**Figure 4.4.5 - Filter DP and Temperature During Test Run 11**

## Results

### 4.4.6 Posttest Inspection and Modifications (9/93-1/94)

The APF internals were inspected through instrument nozzles and the manway nozzle on 9/27 and 9/28. During this inspection approximately 24 candles were observed to be broken. The ash hopper was filled with ash and broken candles to a level approximately 6 to 12 inches above the manway nozzle.

On 9/30, the APF internals were removed from the APF. Upon inspection, 62 candles were found to be broken. Approximately three candles were broken during removal from the APF vessel. The following table shows a summary of the location of the broken candles.

Location of Broken Candles  
September 1993

	Plenum A	Plenum B	Plenum C
Top	3	1	2
Middle	6	24	5
Bottom	0	1	20

Very heavy ash bridging was apparent between candles and between candles and support pipes. Figures 4.4.6 through 4.4.11 are photographs of the filter internals following Test Period II. The deposits were very hard and difficult to break into smaller pieces. Many candles were also found to be bowed. During subsequent cleaning of the ash deposits from the candles, approximately 40 more candles broke.

Two surveillance candles were recovered by Westinghouse and tested for remaining hot strength. One candle from the original set, which had been exposed to operating conditions for 1,759 hours, exhibited a 37 percent loss of its original strength. The second candle, which had been installed in December 1992 and had experienced 1,295 hours of operation, had lost 51 percent of its strength.

All filter candles were replaced with new silicon carbide candles between Test Series II and III, except for nine surveillance candles which were reused.

The backpulse solenoid valves exhibited random failures to actuate during these tests. In all cases, the backup valve functioned properly. Following Test Period II, the backpulse solenoid valves were

## Results

---

inspected and found to be galled on both the piston and cylinder walls. The valve pistons were stellite coated and the valve body bores were nickel-boron plated to improve resistance to galling. Following these modifications, the valves successfully underwent accelerated cycle testing to verify the design. Operation of the valves during Test Period III was much improved, and subsequent inspections revealed no galling.

At the end of Test Period II, one backpulse tube was cut up and examined for degradation. Microcracking was evident on the inside surface of the tube, with cracks as deep as 0.020". Based on this observation it was decided to replace the Incoloy 800HT material with Haynes 230 alloy, which has better resistance to thermal fatigue. The new backpulse tubes were fabricated and installed prior to the start of Test Period III. (As discussed in Section 4.6.8, two of the Haynes 230 backpulse tubes also cracked later in the test program.)

Between Test Series II and III, nine additional air purge nozzles were installed on the APF hopper to facilitate the removal of ash accumulation in the hopper. The hopper vibrator was moved from inside the APF nozzle to outside the nozzle because it proved to be unreliable inside the nozzle. It was mechanically linked to the hopper liner.

In an effort to improve the filter performance, it was decided to detune the primary cyclone upstream of the filter during the next test series. It was believed that the resulting coarser ash would be easier to remove from the filter candles and less likely to accumulate on the hopper walls. The system used to accomplish the detuning was described in Section 4.3.5. All testing during Test Period III was conducted with the cyclone detuned.

It was noted in previous runs that the filter DP sometimes became unstable at gas temperatures over 1400F. To prevent limiting the load on the unit because of the 1400F limit, a tempering air line was installed upstream of the filter which allowed 580F process air at a slightly higher pressure to be mixed with the gas to reduce the gas temperature by as much as 150F.

## Results

---

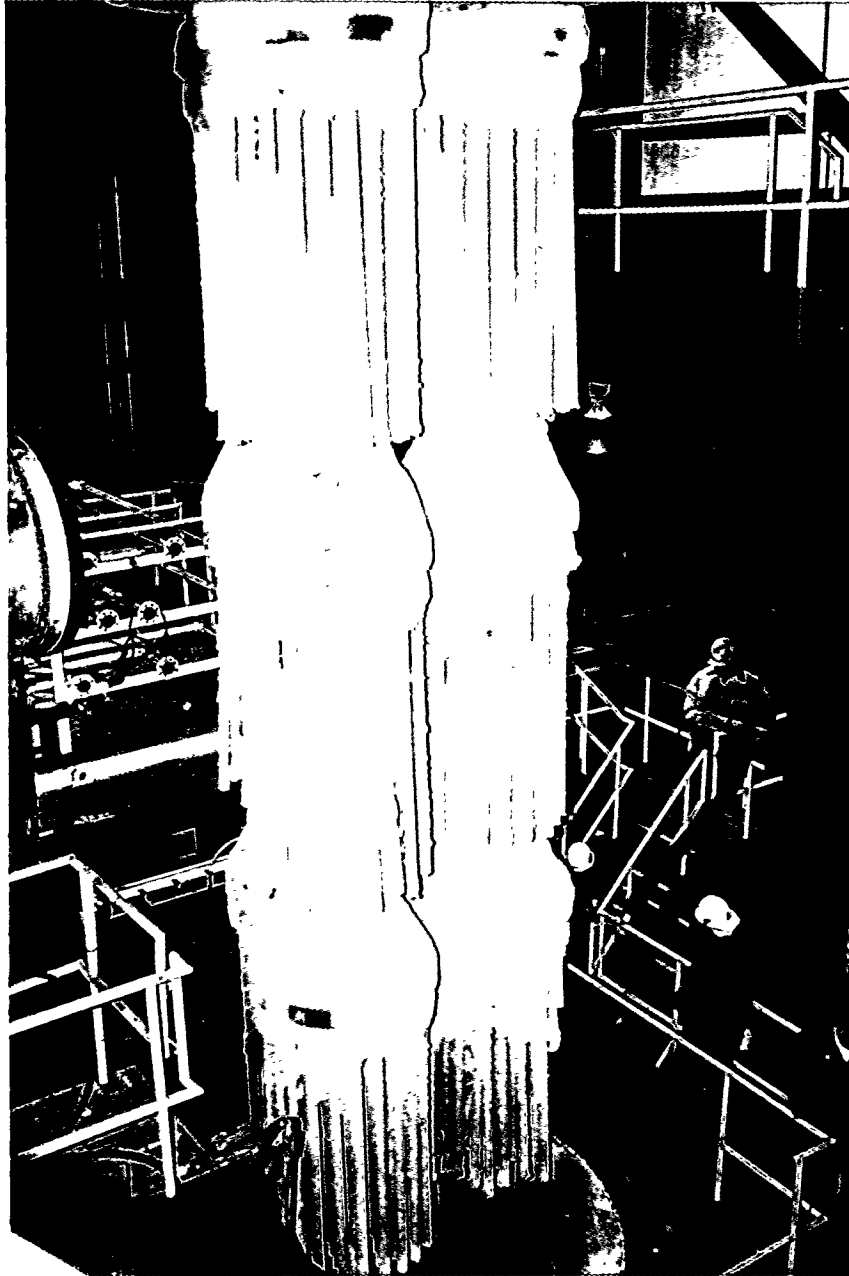


**Figure 4.4.6 - Photograph of Filter Internals Following Test Run 11**

## Results

---



**Figure 4.4.7 - Photograph of Filter Internals Following Test Run 11**

## Results

---

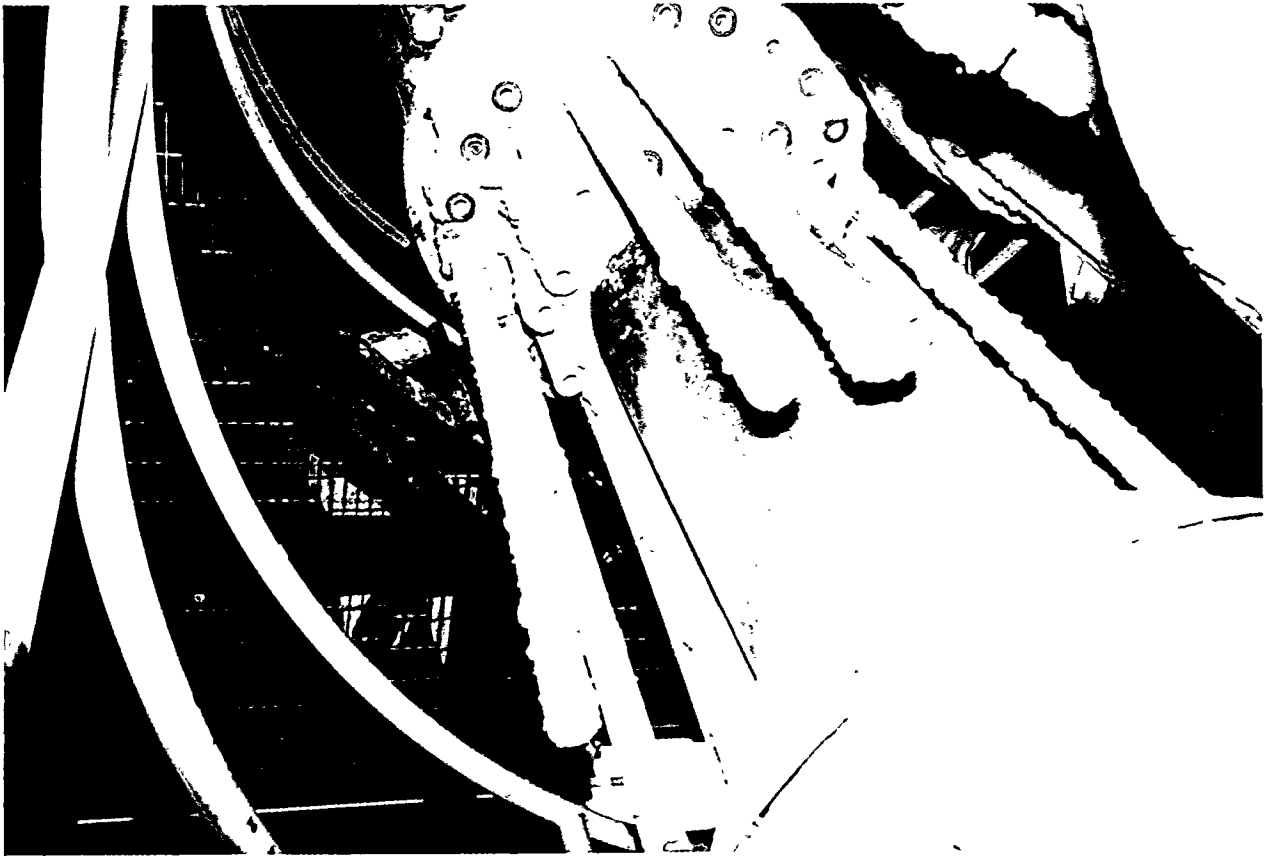


**Figure 4.4.8 - Photograph of Filter Internals Following Test Run 11**

## Results

---



**Figure 4.4.9 - Photograph of Filter Internals Following Test Run 11**

## Results

---



**Figure 4.4.10 - Photograph of Filter Internals Following Test Run 11**

## Results

---



**Figure 4.4.11 - Photograph of Filter Internals Following Test Run 11**

## Results

### 4.5 Test Period III: 1/94 - 4/94

Table 4.5 summarizes the operating conditions and observations from Test Period III.

**Table 4.5 - Summary of HGCU Operation - Test Period III**

	Operating Hours	Cumulative Hours	Operating Temp.	Pressure Drop	Inspection Observations
Run 12	19	1778	1300-1400 °F	Stable	_____
Run 13	333	2111	1300-1400 °F	Stable	<ul style="list-style-type: none"> <li>● Uniform residual ash cake</li> <li>● No failures</li> <li>● Ash accumulated on dust sheds</li> </ul>
Run 14	23	2134	1200-1300 °F	Stable	_____
Run 15	151	2285	1250-1370 °F	Stable	_____
Run 16	145	2430	1350-1400 °F	Stable	_____
Run 17	164	2594	1300-1425 °F	Gas flow rate decreased during run	<ul style="list-style-type: none"> <li>● Ash cake about ¼" thick</li> <li>● No failures</li> <li>● Ash accumulation on sheds</li> </ul>
Run 18	444	3038	1350-1450 °F	Baseline $\Delta p$ increased $\approx$ 20 in. wg	<ul style="list-style-type: none"> <li>● 28 broken candles</li> <li>● Inner rows of top and middle plenums heavily bridged</li> </ul>

#### 4.5.1 Test Run 12 - 1/10 to 1/11/94

This test run was terminated after 19 hours of coal fire when several primary cyclones became plugged. Due to the brevity of this run and lack of steady state operation near design conditions, it will not be discussed further.

## Results

---

### 4.5.2 Test Run 13 - 1/15 to 1/29/94

The unit was operated for 333 hours on coal fire burning Pittsburgh No. 8 coal and Plum Run Greenfield dolomite. The primary objective of this run was to assess the performance of the APF while operating with the primary cyclone ahead of the filter detuned to produce a coarser ash and higher ash loading. The tempering air system was commissioned during this run and functioned without any problems.

During the run ash sampling was performed upstream and downstream of the APF using specially designed sampling probes. The results showed that by detuning the primary cyclone, the ash loading to the filter increased from a design value of 600 ppmw to about 3400 ppmw, and the mass mean particle size of the ash increased from about 3 to 7 microns. The higher ash concentration resulted in significantly higher ash loading. Despite the higher ash loading, the filter performed very well.

Figure 4.5.2 shows a graph of filter pressure drop and temperature for Run 13. The unit load was reduced at about 200 and 250 hours into the run due to bed sintering problems, which accounts for the dips in temperature and DP during these periods. During the remaining periods of this run, the filter pressure drop remained stable and exhibited the usual trend of following gas temperature. During the last 50 to 75 hours of the run, the unit bed height was increased to the maximum (142 inches), and the filter DP increased somewhat due to higher gas flow and dust loading.

Following shutdown of the unit, the filter was inspected via nine 3-in. nozzles on the side of the vessel. In general the candles looked in good condition with very little residual ash accumulation. However, some ash bridging was seen between the bottoms of the inner rows of candles and the dust sheds on the plenum support pipes.

### 4.5.3 Test Run 14 - 2/17 to 2/18/94

This test run was terminated after 23 hours of coal fire when a 1" nipple on the HGCU piping developed a leak that could not be repaired in service. Although the nipple was made from Hastelloy C-276 material, it experienced corrosion because it was used for gas sampling which exposed it to flowing flue gas and it operated below the acid dew point. The nipple was replaced with thicker wall Hastelloy C-22 material and was heat traced and insulated in subsequent operation. Following these modifications, no further problems were encountered with the nipple.

## Results

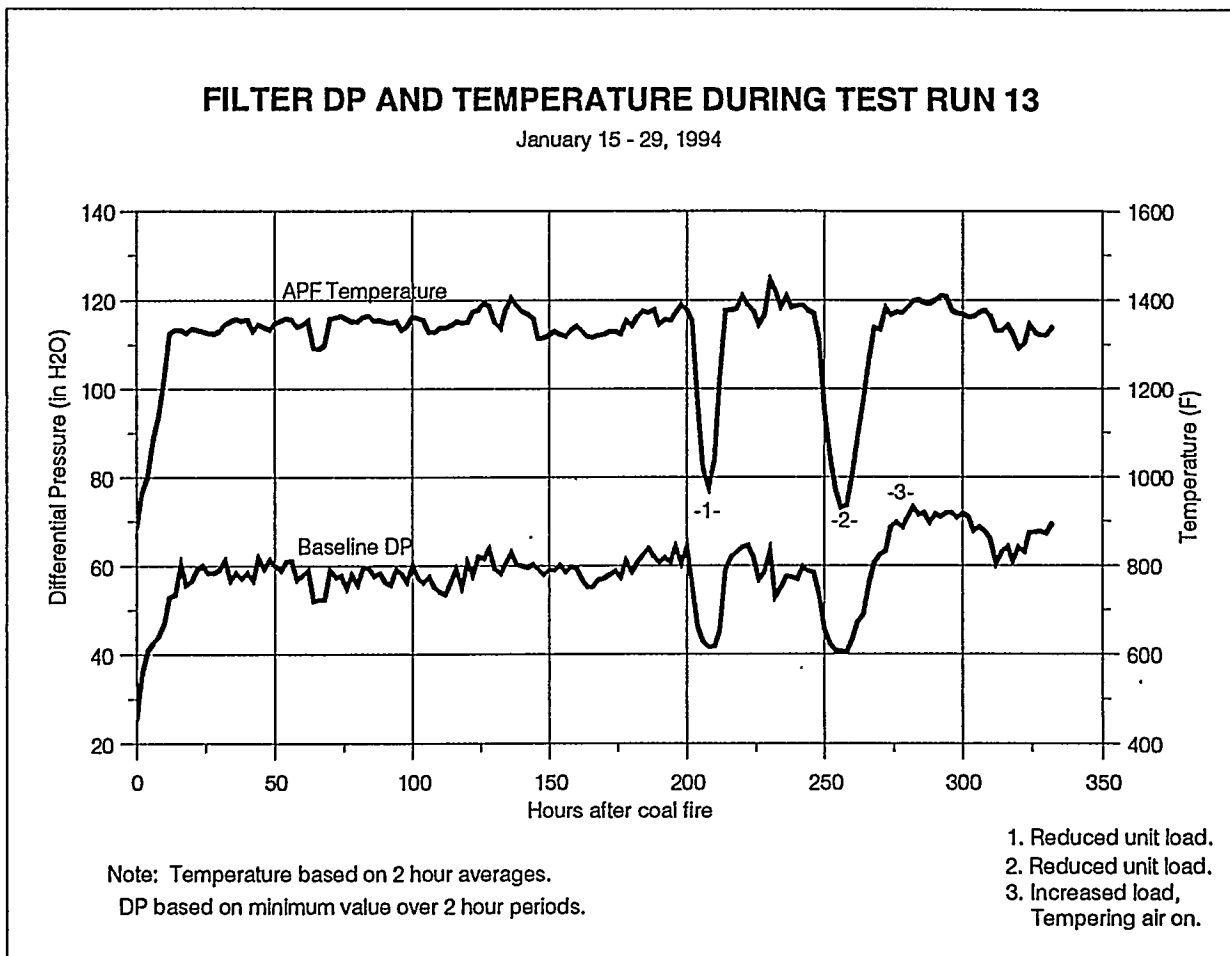


Figure 4.5.2 - Filter DP and Temperature During Test Run 13

## Results

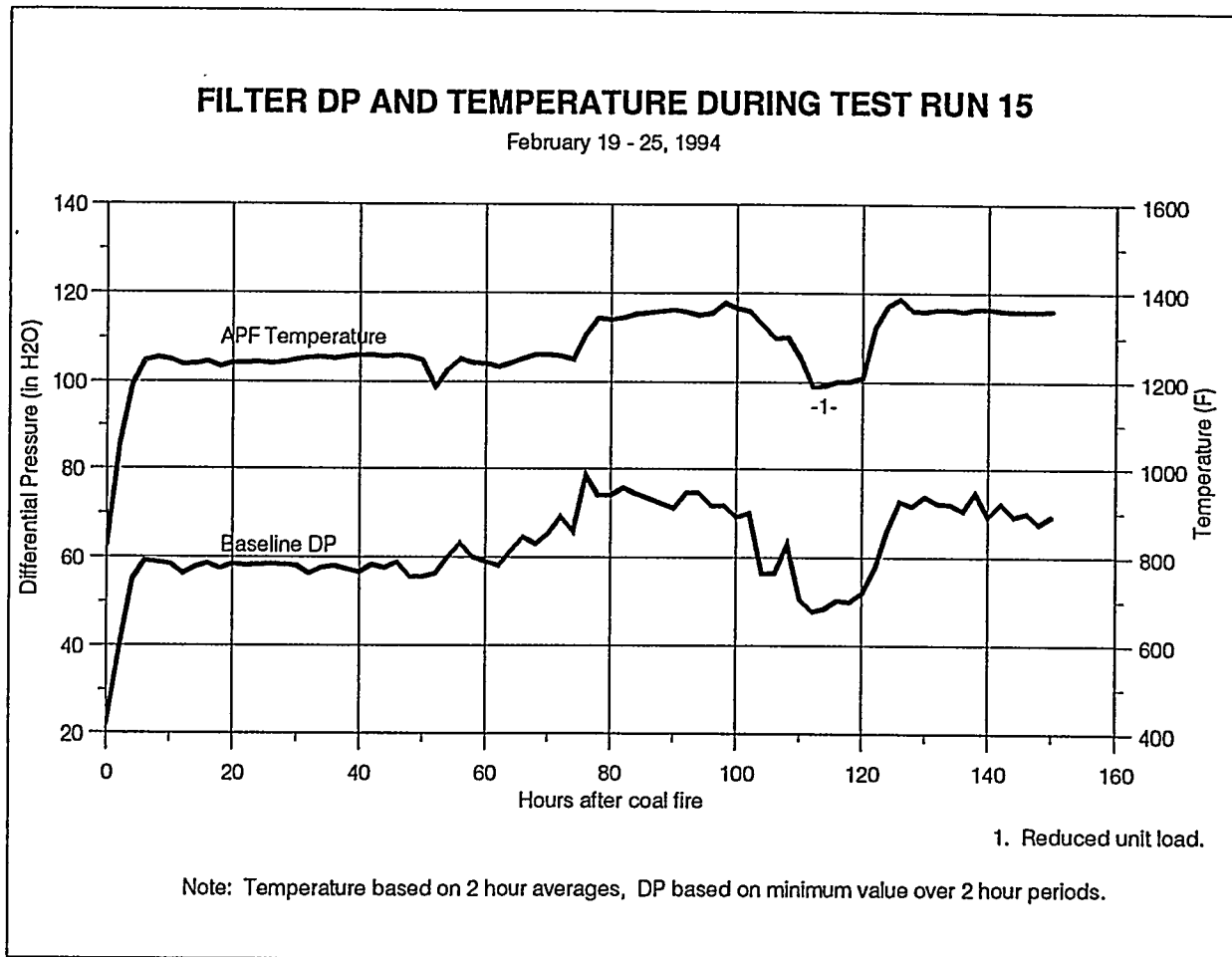


Figure 4.5.4 - Filter DP and Temperature During Test Run 15

## Results

---

### 4.5.4 Test Run 15 - 2/19 to 2/25/94

This run was a hot restart of the previous run. The APF performed without any major problems during this run. Some minor problems, however, arose. Shortly after start-up, the APF head exhibited elevated temperatures (up to 730F) near the gas outlet nozzle. The gas temperature was held to the 1250F range in order to keep the hot areas below 750F. On 2/21 an on-line repair was successfully made which reduced the hot areas to below 300F in some areas and to below 400F in others. The repair involved drilling and tapping three 1/4" holes in the outlet nozzle near the head and pumping in 45 gallons of pumpable insulation. Following this repair, the unit was brought up to full bed height (142 inches).

Tempering air was again used to limit the gas temperature in the APF to 1400F. Figure 4.5.4 shows a graph of APF DP and temperature versus time for this run. The unit load was reduced about 110 hours into the run when a coal paste pump stopped working. After the bed again stabilized, the unit was returned to full load. The HGCU system functioned without further problems from this point until the unit tripped due to loss of the sorbent booster compressor.

### 4.5.5 Test Run 16 - 3/3 to 3/9/94

Most of this test run was conducted at 142 and 150-inch bed levels. As in the previous run, tempering air was used to limit the filter gas temperature to 1400F. This run was the smoothest so far the HGCU system. The system operated for over 145 hours without any major problems. Figure 4.5.5 shows a plot of APF DP and temperature during Run 16. Figure 4.5.6 shows DP and flowrate. The APF DP exhibited a gradual decline throughout this run. The reason for this is unknown. The test conditions throughout Run 16 were the most steady of all the runs. Therefore, data from this run should be considered a good baseline reference for APF operation at 1400F. This run was terminated when the unit tripped due to the loss of two coal paste pumps.

### 4.5.6 Test Run 17 - 3/16 to 3/23/94

This was another relatively uneventful run on the HGCU system. The unit operated for approximately 164 hours on coal fire. Most of the run was conducted at 128-inch bed level, with portions at 142-inch and 115-inch. Due to bed sintering problems, the bed level could not be maintained at 142 inches. The tempering air was turned off during this run which allowed the APF to operate up to 1450F. The filter pressure differential was relatively stable throughout the run as shown in Figures 4.5.7 and 4.5.8.

## Results

---

However, the gas flowrate through the filter decreased throughout the run. During this run additional insulation was pumped into the APF head to lower the surface temperature in one area from 550F to 400F. The unit tripped due to a low oil pressure indication on the gas turbine.

The APF internals were inspected through the nine instrument nozzles following Test Run 17. No broken candles were observed. The residual ash layer on the candles was somewhat thicker than seen following Test Run 13 and appeared to be about 1/8" to 1/4" thick. The ash coating was uniform from candle to candle but also very rough looking on all the candles. The ash bridging previously seen between the dust sheds and the inner rows of candles was still evident, but not obviously worse than before. The amount of ash accumulation on the dust sheds varied considerably (1/2" to 4") among the six dust sheds. No candle-to-candle bridging was seen.

### 4.5.7 Test Run 18 - 3/31 to 4/18/94

This was the longest run of this test period with almost 444 hours of coal fire. The bed height during most of the run was 115 inches and the APF temperature was generally in the 1350 to 1400F range. The temperature was approximately 1450F for about 30 hours of the run. Due to a corroded instrument tube, flowrate data were not obtained during this run. Hazardous air pollutant sampling was conducted during this run. No major problems arose with the APF during this test. The baseline pressure differential increased during this run from about 70 to 90 inches as shown in Figure 4.5.9. This was the first run of this test series in which the DP increased noticeably from the beginning to the end of the run.

Hazardous Air Pollutant sampling was performed by Radian Corporation during Test Run 18. The results of the testing are documented in Radian Report Number DCN 94-633-021-03, dated October, 1994. As part of Hazardous Air Pollutant testing, SO<sub>2</sub> data were obtained upstream and downstream of the APF. Preliminary results indicated that the SO<sub>2</sub> level in the gas was reduced approximately 40% by the APF. Post-test analysis of ash samples retrieved from the APF and precipitator hoppers confirmed this observation. The percent sulfation (calculated as moles of SO<sub>3</sub>/moles of CaO) of the APF hopper ash was 78.6% as compared to 50.0% for ash that did not pass through to APF sampled from the precipitator hopper.

## Results

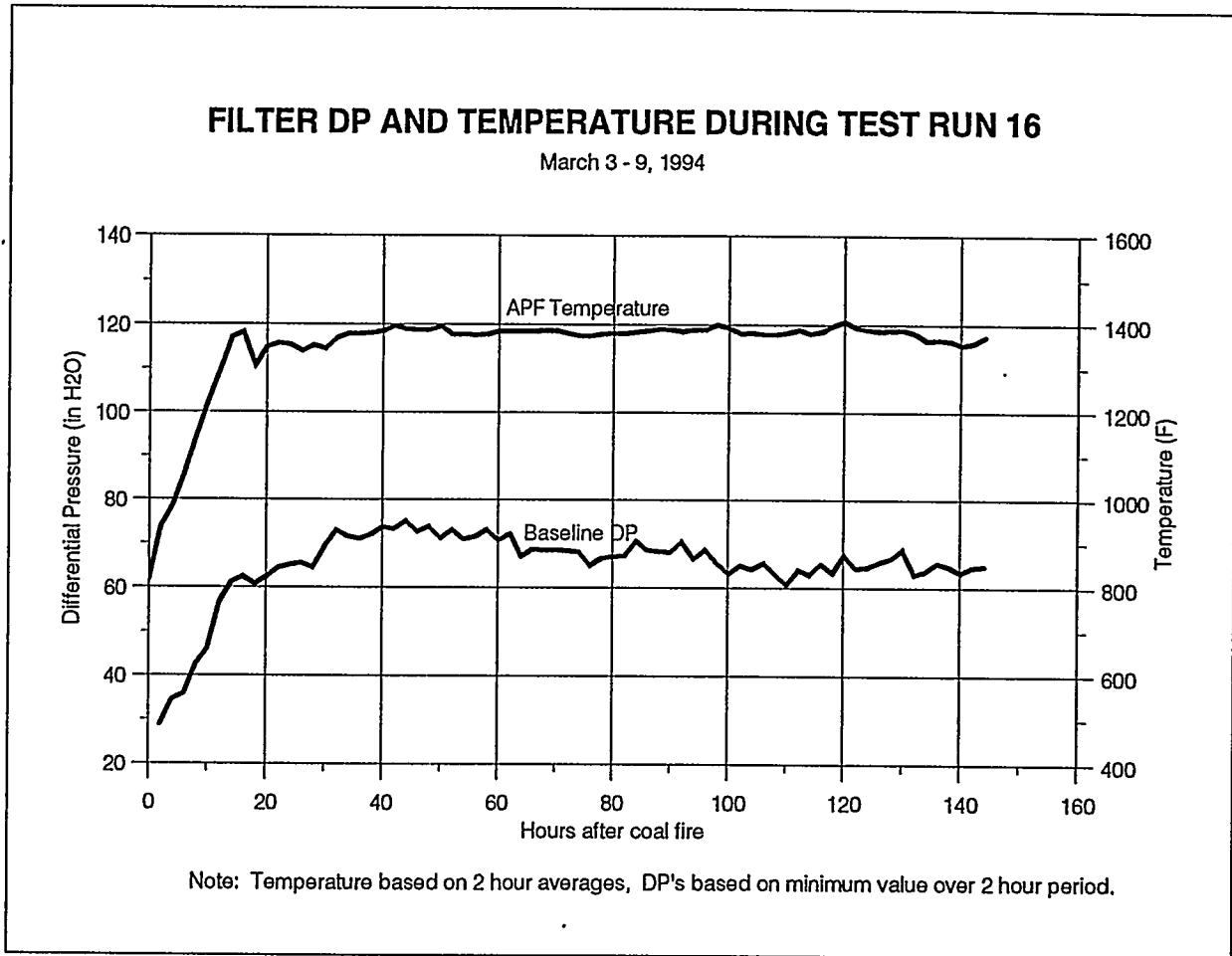


Figure 4.5.5 - Filter DP and Temperature During Test Run 16

## Results

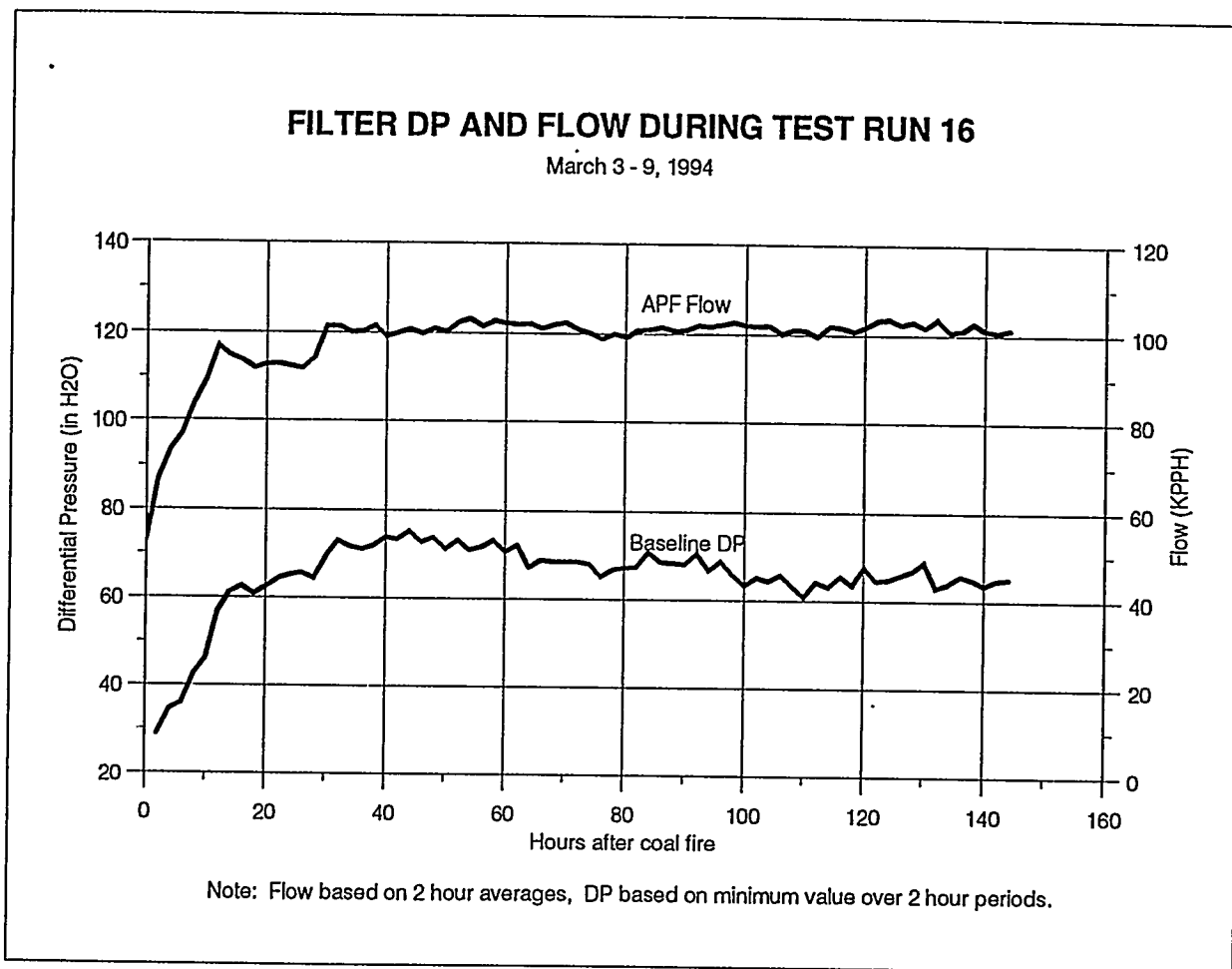
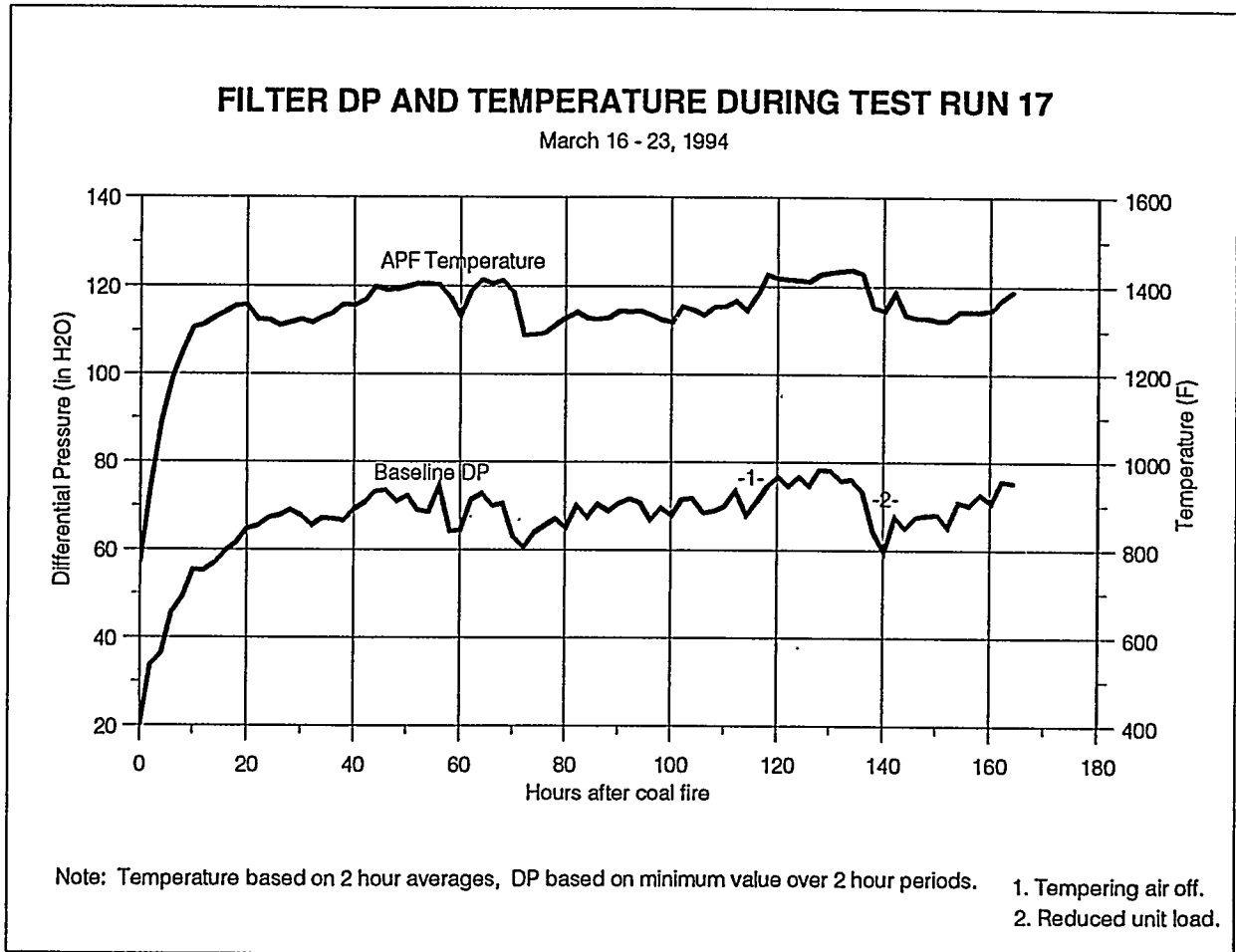


Figure 4.5.6 - Filter DP and Flow During Test Run 16

## Results



**Figure 4.5.7 - Filter DP and Temperature During Test Run 17**

## Results

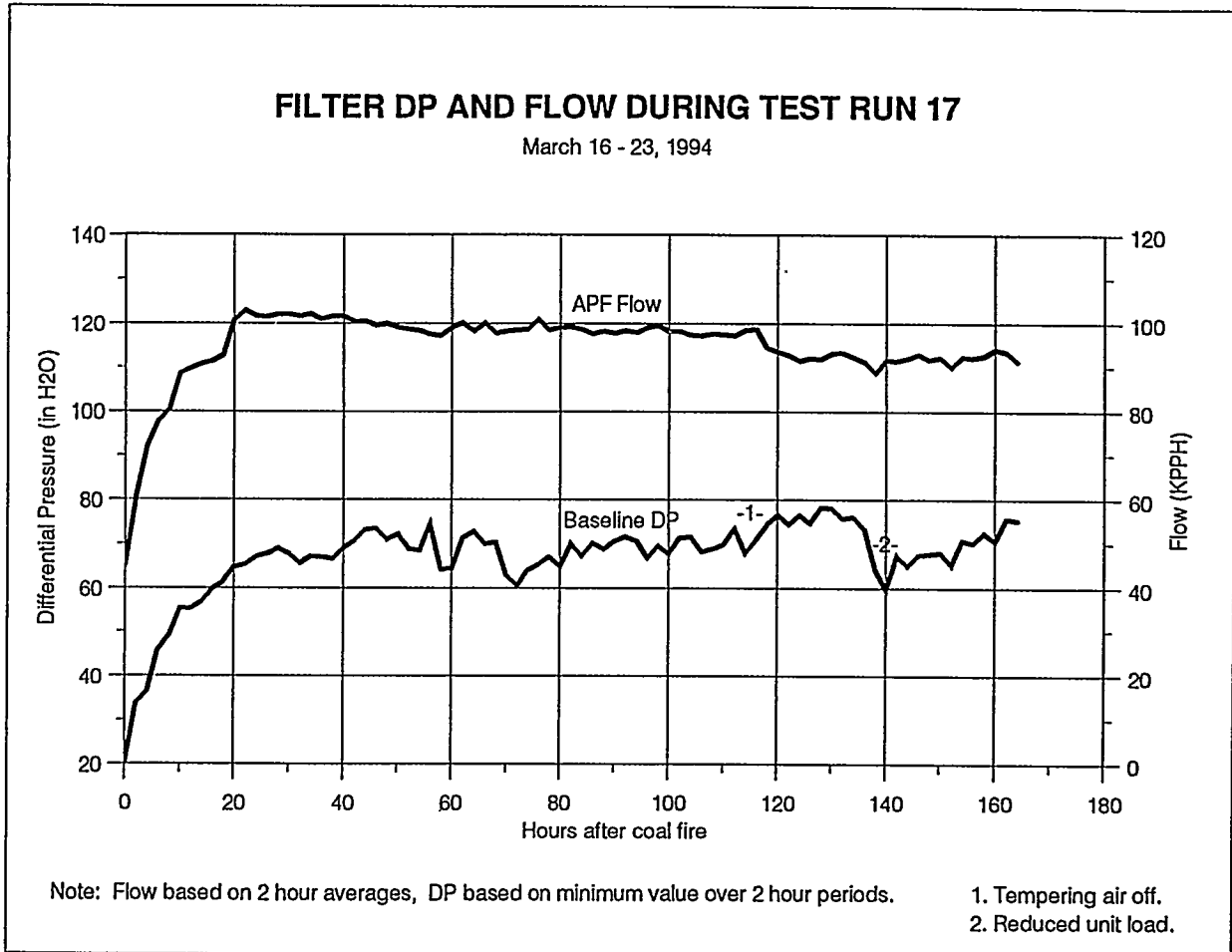


Figure 4.5.8 - Filter DP and Flow During Test Run 17

## Results

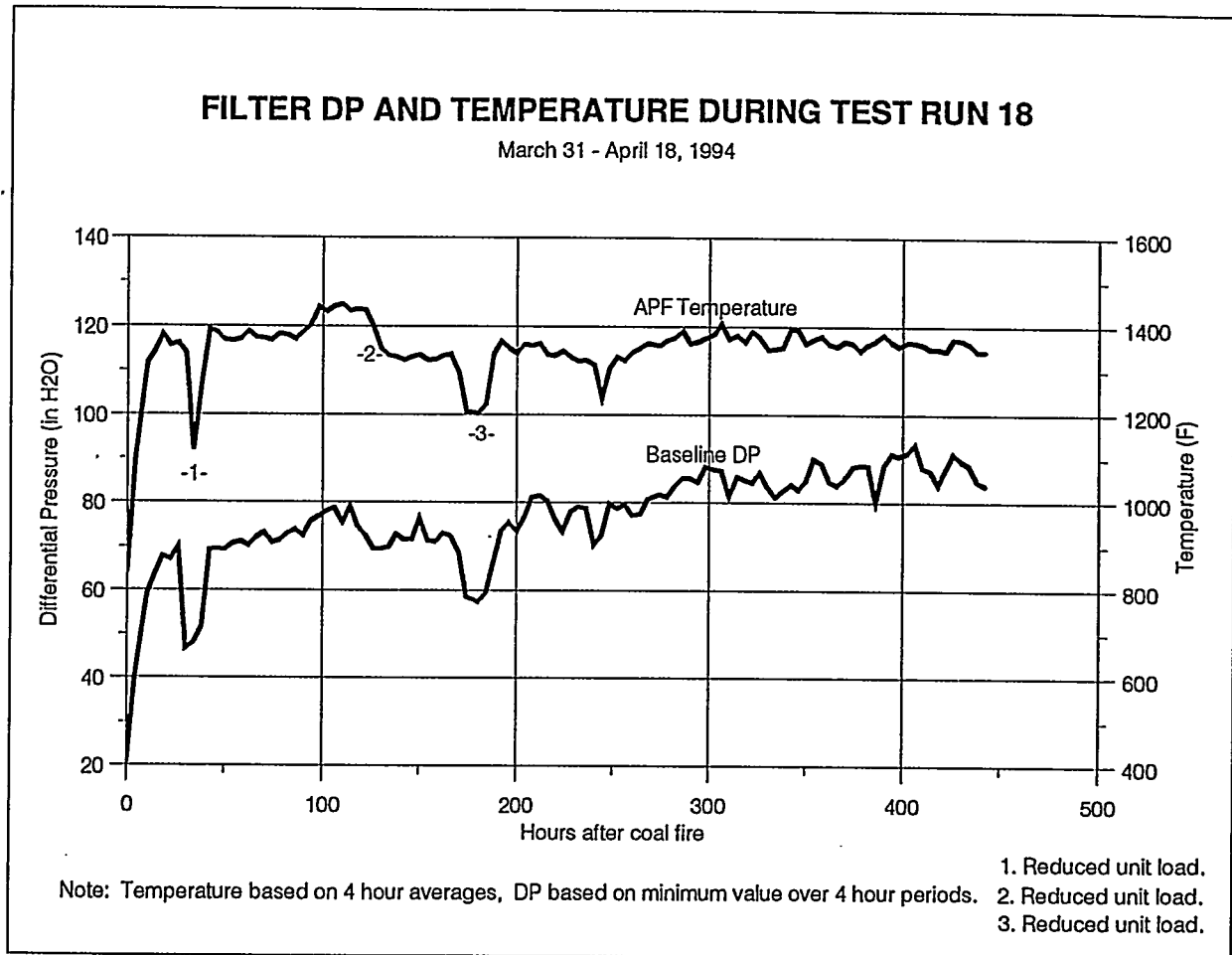


Figure 4.5.9 - Filter DP and Temperature During Test Run 18

## Results

### 4.5.8 Posttest Inspection and Modifications (4/94-7/94)

The APF internals were inspected via the instrument ports after this run. The filter candles had a thin layer (about 1/8") of residual ash, however broken candles were observed during this inspection. The filter internals were removed from the APF vessel on 5/5/94 and a more detailed inspection was performed. A total of 28 broken candles were found at the following locations:

Location of Broken Candles  
May 1994

	Plenum A	Plenum B	Plenum C
Top	7	7	2
Middle	0	2	8
Bottom	0	2	0

The two breaks in the bottom plenum are believed to have occurred during removal of the filter internals from the filter housing. Very heavy ash bridging was observed between the inner rows of candles and the support pipe on the top and middle plenums. Figures 4.5.10 through 4.5.18 are photographs of the candle clusters following Test Period III. The ash build-up extended over the entire length of the inner candles. In some cases the ash bridging extended into the outer rows of candles. Many of the inner candles were bowed outward and in some cases almost contacted the candles in the outer row. All of the candle breaks except one appeared to be fresh breaks judging from the clean fracture surfaces. All of the breaks occurred at the top of the candle just below the candle holder. The breaks appeared to result from bending forces from ash bridging from the inner candles to the outer candles. Only one break was in an inner row; the remainder were in outer rows.

The outlet side of the filter was very clean with virtually no ash deposits. This is further indication that the failures occurred during or after plant shutdown, and that the filter was not leaking ash to the clean side during operation.

All of the candles in the upper and middle plenums were removed, cleaned, and inspected. The bottom plenum candles were not removed and cleaned since they did not exhibit significant bridging. There was, however, about 1/8 in. thick ash layer remaining on these candles. The upper and middle plenums

## Results

---

were reassembled with an assortment of new and used candles. In an effort to expand the knowledge base of candle materials, 30 of the candles installed following this test series were second generation materials and included 8 Coors alumina/ mullite, 8 Schumacher FT 20 second generation clay bonded silicon carbide, 8 Pall Vitropore clay bonded silicon carbide, 3 3M silicon carbide composite, and 3 Dupont filament wound mullite structure candles.

In an effort to overcome the ash bridging problem between the support pipe and inner row of candles, it was decided to remove the inner row of candles from the six upper and middle plenums. This reduced the number of candles from 384 to 288 and increased the face velocity from 7.1 ft/min to 8.9 ft/min. In addition, provisions were added to totally spoil the primary cyclone ahead of the filter to evaluate operation with a higher mean particle size.

Figures 4.5.19 through 4.5.24 are photographs of the filter internals prior to Test Period IV.

## Results

---

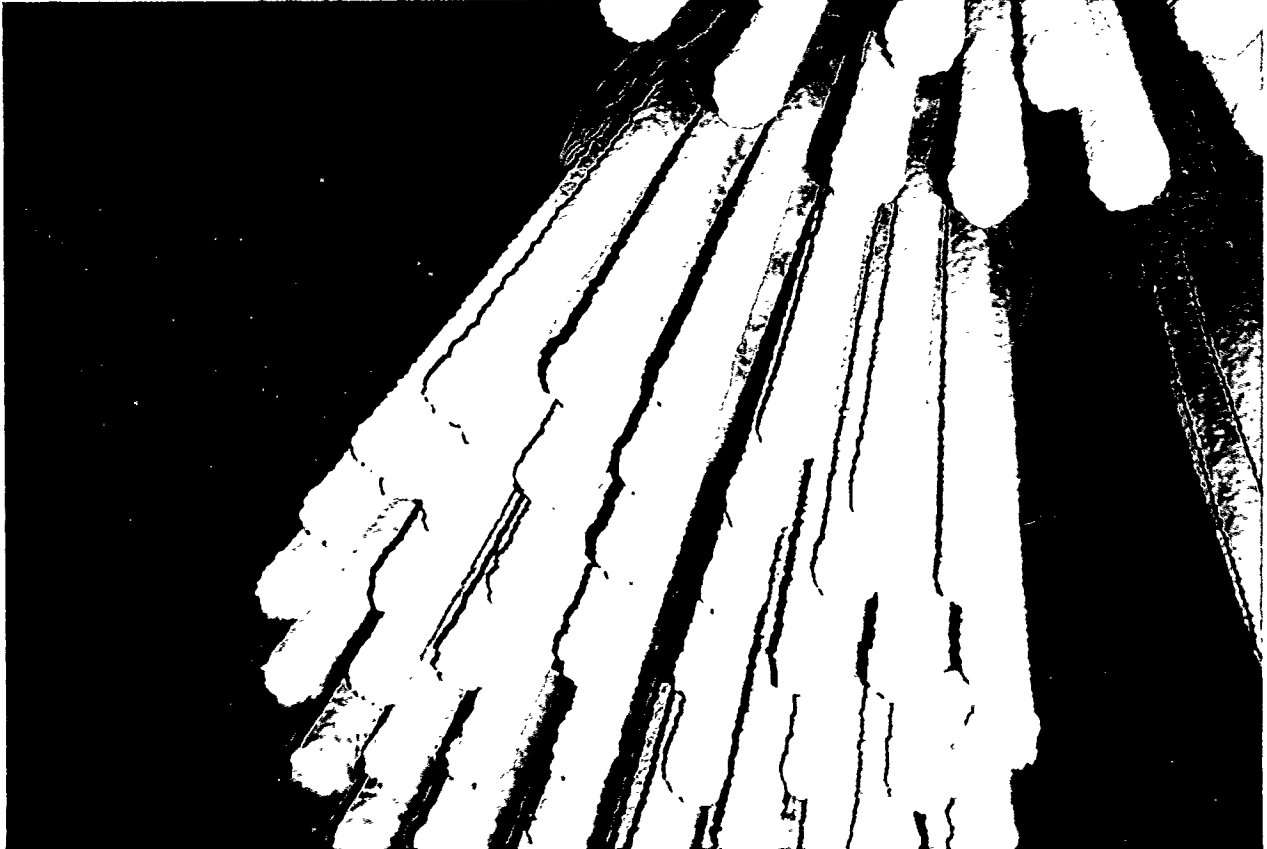


**Figure 4.5.10 - Photograph of Filter Internals Following Test Run 18**

## Results

---



**Figure 4.5.11 - Photograph of Filter Internals Following Test Run 18**

## Results

---

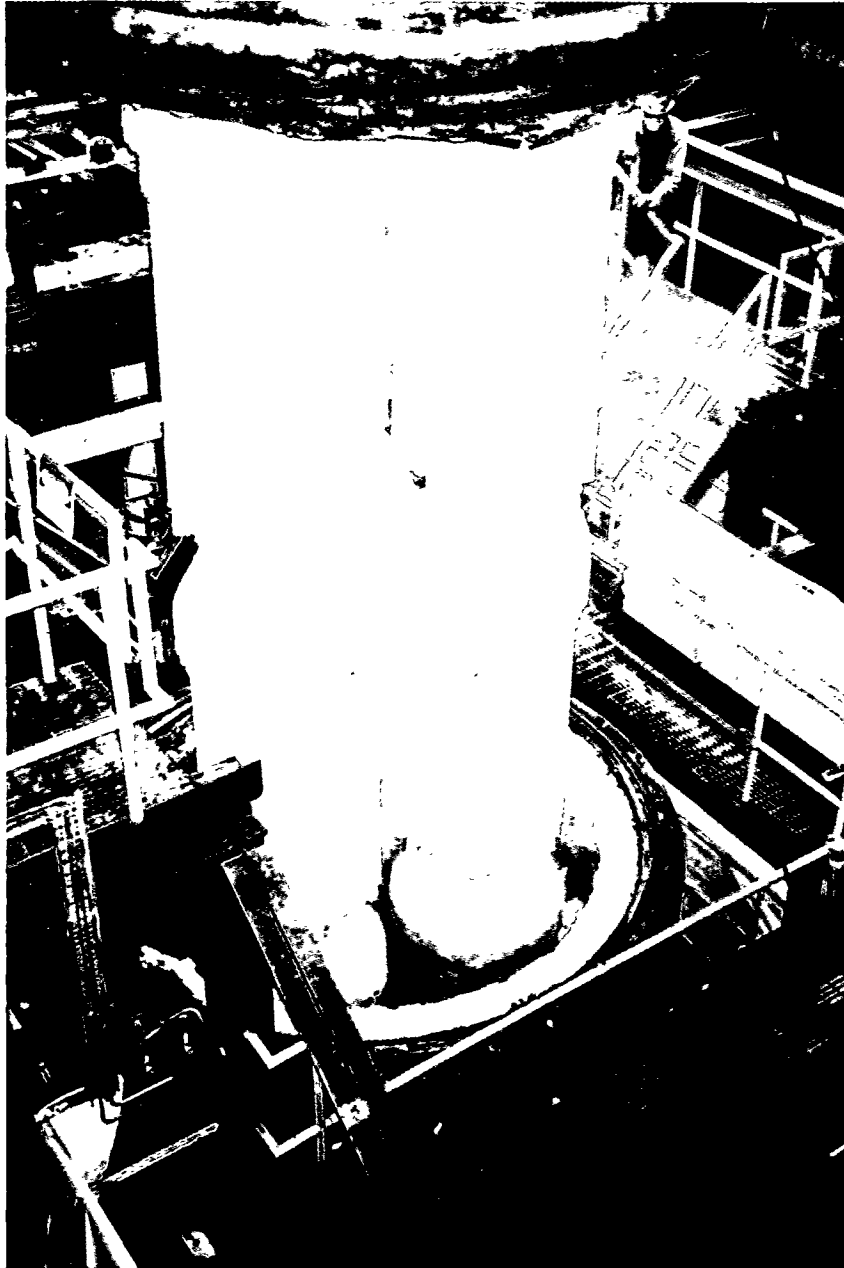


**Figure 4.5.12 - Photograph of Filter Internals Following Test Run 18**

## Results

---



**Figure 4.5.13 - Photograph of Filter Internals Following Test Run 18**

## Results

---



**Figure 4.5.14 - Photograph of Filter Internals Following Test Run 18**

## Results

---



**Figure 4.5.15 - Photograph of Filter Internals Following Test Run 18**

## Results

---

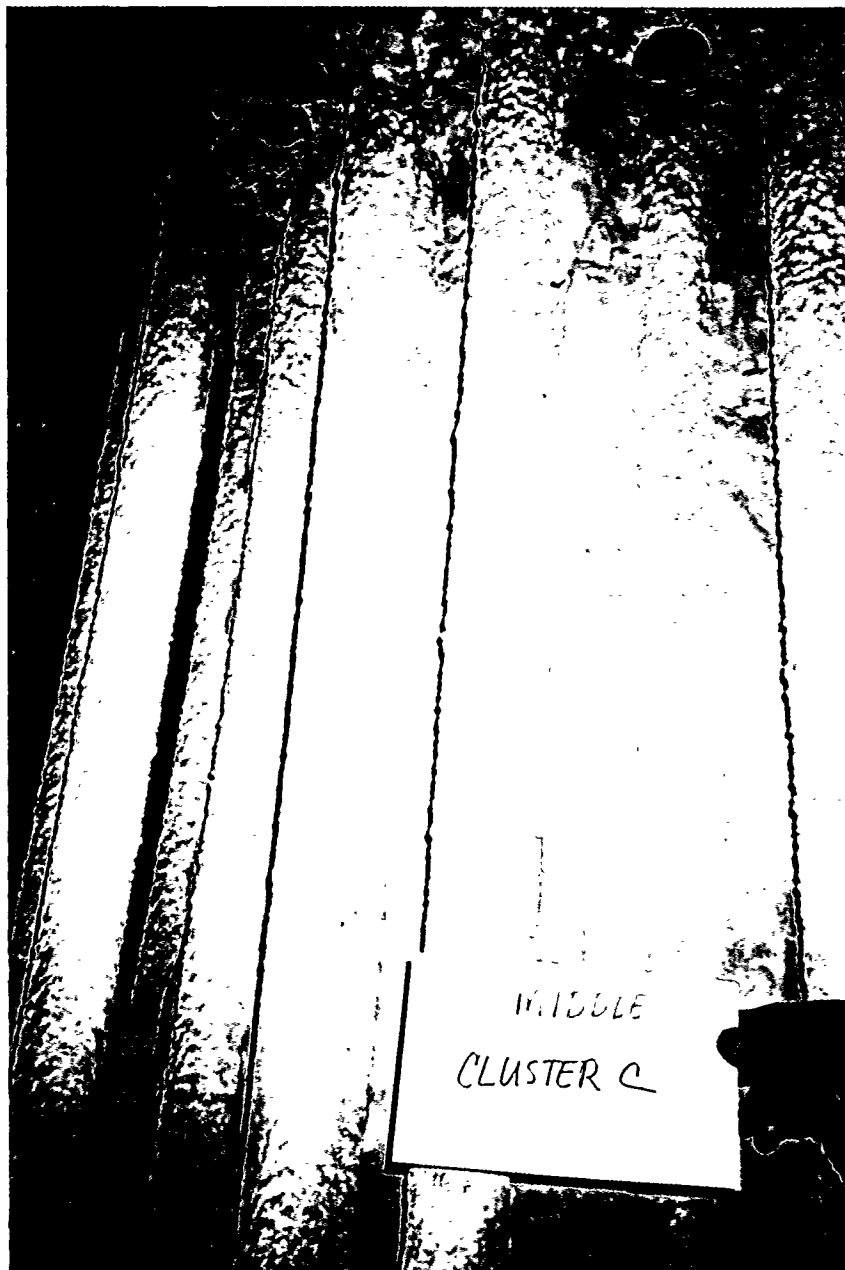


**Figure 4.5.16 - Photograph of Filter Internals Following Test Run 18**

## Results

---



**Figure 4.5.17 - Photograph of Filter Internals Following Test Run 18**

## Results

---



**Figure 4.5.18 - Photograph of Filter Internals Following Test Run 18**

## Results

---



**Figure 4.5.19 - Photograph of Filter Internals Before Test Period IV**

## Results

---



Figure 4.5.20 - Photograph of Filter Internals Before Test Period IV

## Results

---



**Figure 4.5.21 - Photograph of Filter Internals Before Test Period IV**

## Results

---



**Figure 4.5.22 - Photograph of Filter Internals Before Test Period IV**

## Results

---



**Figure 4.5.23 - Photograph of Filter Internals Before Test Period IV**

## Results

---

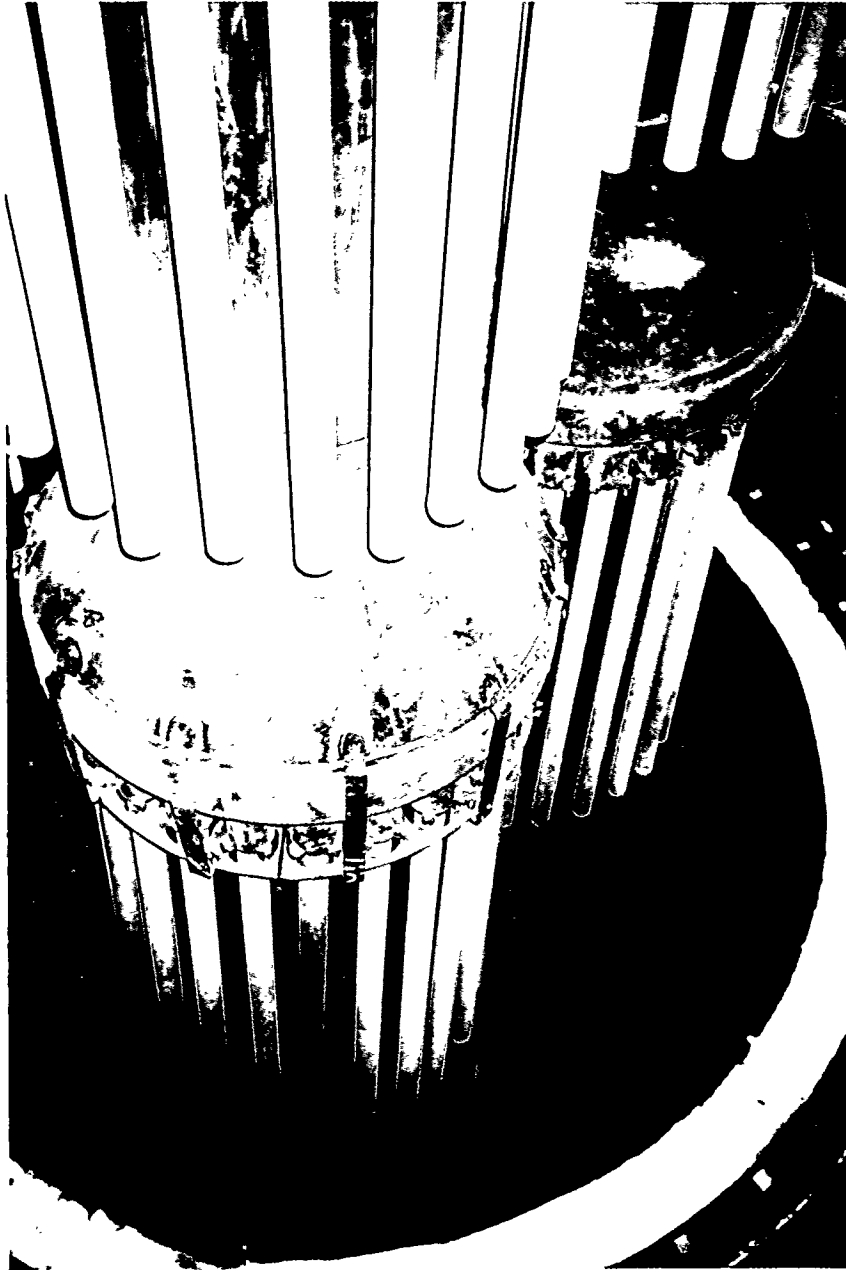


**Figure 4.5.24 - Photograph of Filter Internals Before Test Period IV**

## Results

### 4.6 Test Period IV: 7/94 - 10/94

Table 4.6 summarizes the operating conditions and observations from Test Period IV.

**Table 4.6 - Summary of HGCU Operation - Test Period IV**

	Operating Hours	Cumulative Hours	Operating Temp.	Pressure Drop	Inspection Observations
Run 19 & 20	3	3041	_____	_____	_____
Run 21	161	3202	1125-1150 °F	Stable	
Run 22	680	3882	1200-1400 °F	Baseline $\Delta p$ increased $\approx$ 40 in. wg	<ul style="list-style-type: none"> <li>● Bridging from dust shields</li> <li>● 14 candles broken 3 days after shutdown (not replaced)</li> </ul>
Run 23	171	4053	1170-1400 °F	Stable $\Delta p$ with cyclone spoiled	<ul style="list-style-type: none"> <li>● Ash bridging much less than at start of run</li> </ul>
Run 24	691	4744	1300-1450 °F	Baseline $\Delta p$ increased $\approx$ 60 in. wg without cyclone spoiled	<ul style="list-style-type: none"> <li>● 30 broken candles (including previous 14)</li> <li>● Some ash bridging from dust sheds</li> </ul>

#### 4.6.1 Test Runs 19 and 20 - 7/16/94

These two runs together totaled only three hours and therefore will not be discussed.

#### 4.6.2 Test Run 21 - 7/20/94 to 7/27/94

This 161-hour run was terminated to repair a vibration problem on the gas turbine. Because of the turbine limitation, the APF temperature was in the 1125-1150F range during most of this run. The APF differential pressure remained stable during the run, as shown in Figure 4.6.2.

Between Test Runs 21 and 22 a second nuclear level device was installed on the APF hopper at a higher level than the first level detector, and served as an extreme high alarm. The detector at the lower elevation was revised to produce a digital signal indicative of the ash thickness on the APF hopper wall. The signal from this detector which was trended on POPS provided early indication of ash buildup in the hopper and was useful in alerting the plant operators when to use the air purges and air cannon.

## Results

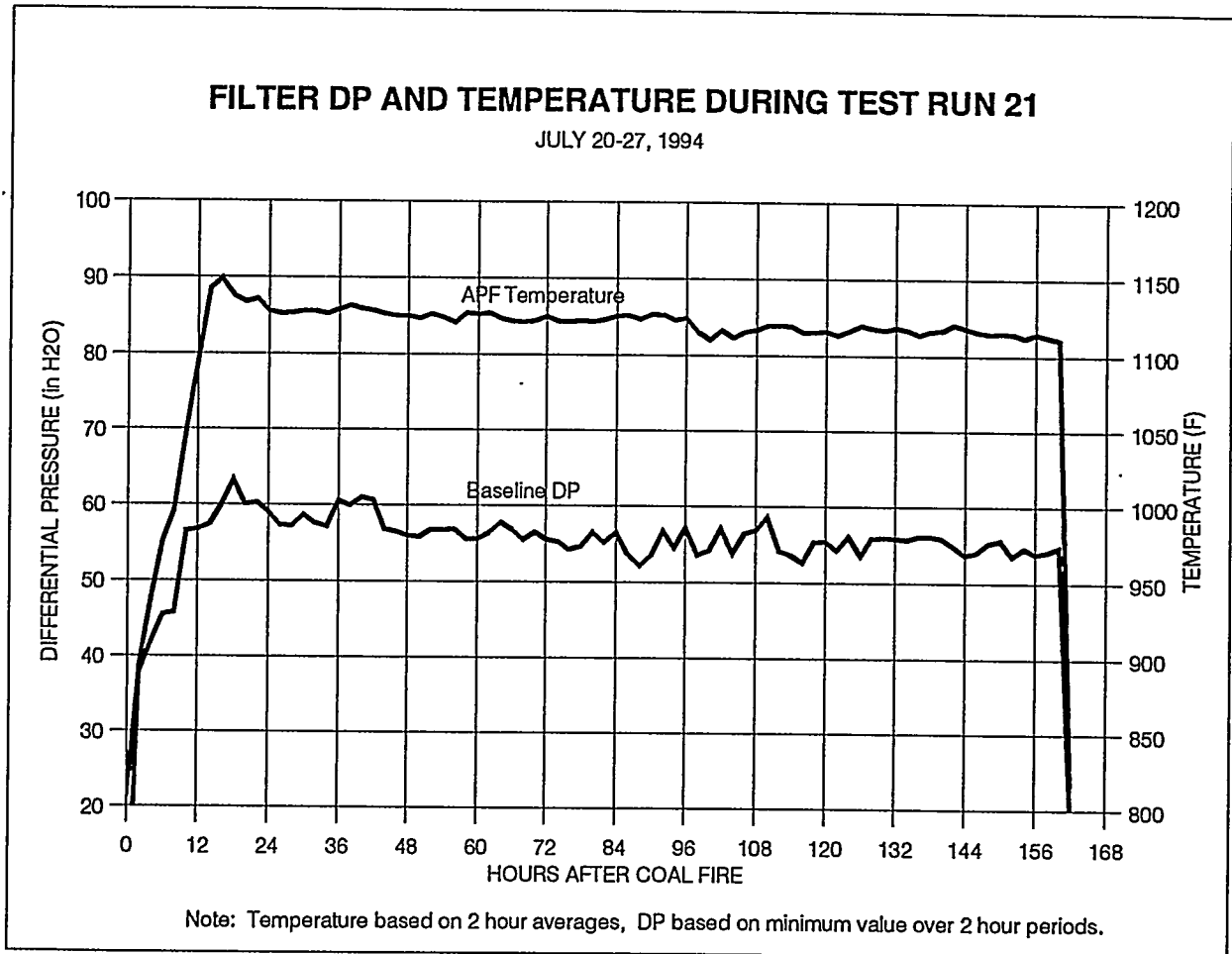


Figure 4.6.2 - Filter DP and Temperature During Test Run 21

## Results

### 4.6.3 Test Run 22 - 7/28/94 to 8/25/94

This was hot restart from the previous run. This was the longest run to date for the HGCU system at just under 680 hours. Unit load was reduced on 8/1 to limit hot spots on the APF head. After insulation was pumped in, the hot spots were reduced to below 500F. Several performance tests were conducted during this run using Pittsburgh #8 coal and various sorbents as shown in Figure 4.6.3 which is a plot of the APF DP, temperature, and flowrate for this run. The DP exhibited periods of instability during this run. On 8/5 the ash removal system became plugged and several candles fragments were removed from the ash line. On 8/6 hot spots again appeared on the APF head and tempering air was used to control the hot spot temperatures. On 8/9 the hot spots were pumped with insulation.

### 4.6.4 Posttest Inspection (8/94)

At the end of Run 22 the APF had logged 844 hours of operation since it was reconfigured with 288 candles. The objective of this test series was to determine if removal of the inner rows of candles from the upper and middle plenums would eliminate ash from accumulating on the ash sheds and bridging over to the candles. An inspection on 8/29 revealed that ash bridging, while less than before, had still occurred. The APF hopper was clean two days following shutdown, but when inspected again four days following shutdown, ash was found in the hopper. During the inspection with a boroscope, 14 broken filter candles were seen, and candle pieces were later removed from the hopper. A total of nine candle bottoms were recovered in the hopper. A possible explanation for the candle breakage would be that ash, bridged between the ash sheds and candles, expanded slightly during cooling and absorbed moisture from the air, thereby inducing bending moments on the candles which all failed near the top. Another possible explanation is that the metal support pipe contracted more than the ceramic candles upon cooling and thereby induced bending stresses in the candles due to ash that was wedged between the candle bottoms and sloping dust shed surfaces.

Location of Broken Candles  
August 1994

	Plenum A	Plenum B	Plenum C
Top	4	0	0
Middle	4	0	6
Bottom	0	0	0

# Results

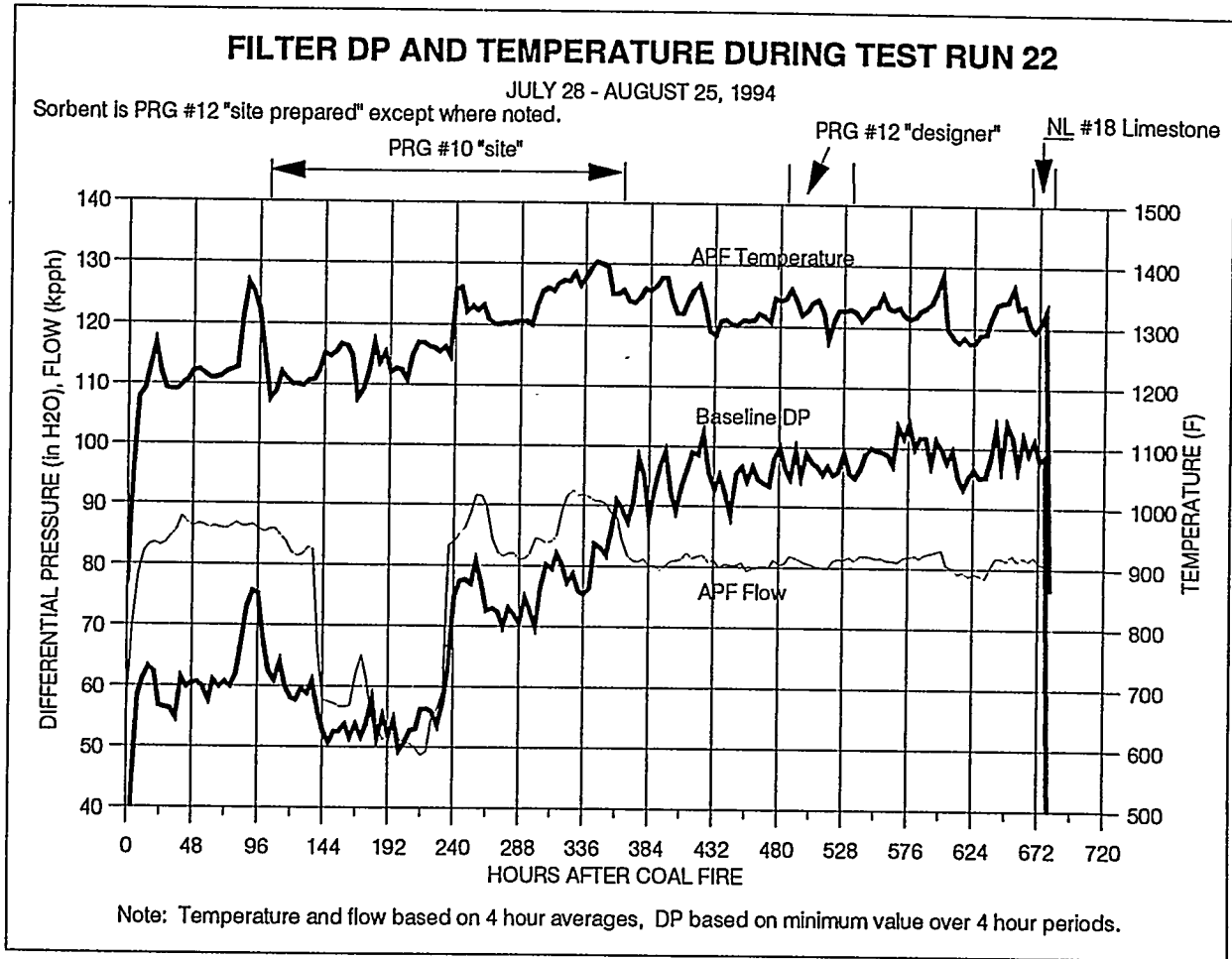


Figure 4.6.3 - Filter DP and Temperature During Test Run 22

## Results

---

It was decided to continue this test series with 14 broken candles rather than take the system out of service at this time to replace them. It was planned to replace all of the candles in the fall of 1994.

### 4.6.5 Test Run 23 - 9/3/94 to 9/10/94

During the last 90 hours of this 171-hour run, the primary cyclone was spoiled by injecting air into the ash pickup nozzle to reduce the ash transport ability and force the ash to build up in the dip leg of the cyclone. In order to even out the ash discharge from the APF, the backpulsing sequence was changed to produce uniform cleaning. Each plenum was backpulsed every 15 minutes with backpulses occurring every 1.67 minutes. During this period the APF temperature was in the 1300F to 1400F range and the DP was stable as shown in Figure 4.6.5. Ash removal during this run was difficult since the lockhopper system could not keep up with the approximately 1700 lb/hour of ash flow. A new alternate ash removal line was successfully used to overcome this problem.

### 4.6.6 Posttest Inspection (9/94)

The APF was inspected using a boroscope on 9/14. This inspection revealed that most of the ash bridges seen in the previous inspection had disappeared, and the few that remained appeared smaller. This indicated that the coarser ash was cleaning the ash accumulation from the ash sheds. The liner and hopper also were very clean of ash deposits. No additional broken candles were observed. The backup cyclone ash removal line was found to be eroded near the first two bends as a result of coarser ash and missing candles. A new line was designed with lower velocities and installed following this test series.

### 4.6.7 Test Run 24 - 9/22/94 to 10/21/94

Due to the problem with the erosion of the BUC ash line, it was decided to operate the unit with the primary cyclone only partially detuned for the first three weeks of this scheduled four-week run, and the cyclone was totally spoiled during the last four days of the run. Figure 4.6.7 shows the trend of filter DP and temperature throughout this longest run of 691 hours. The DP increased significantly during the first 300 hours, increased gradually over the next 300 hours, and increased dramatically when the cyclone was spoiled due to the increased ash loading. Unit performance tests were conducted during this run at various bed levels and sulfur retention, using various sorbents as shown in Figure 4.6.7.

## Results

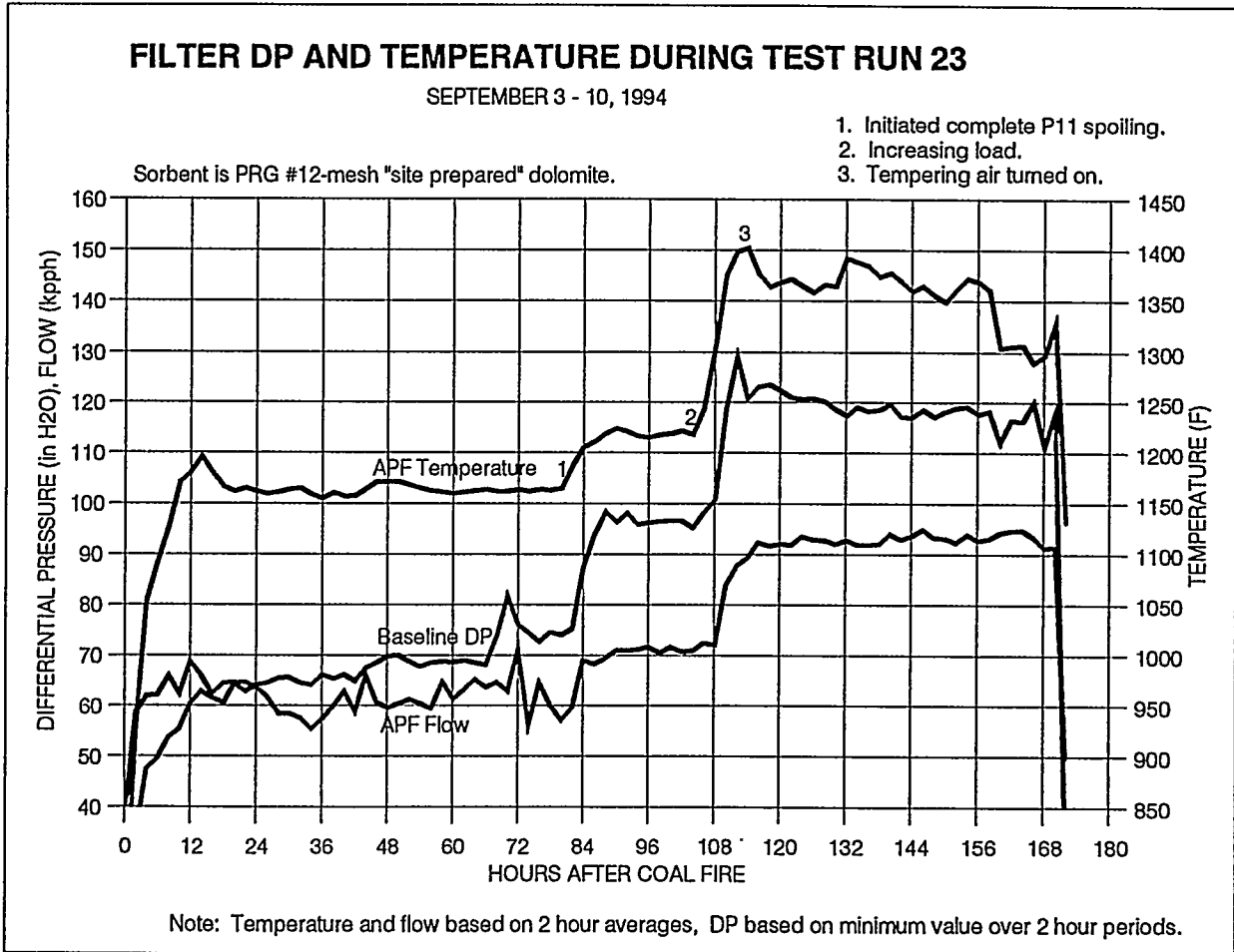


Figure 4.6.5 - Filter DP and Temperature During Test Run 23

## Results

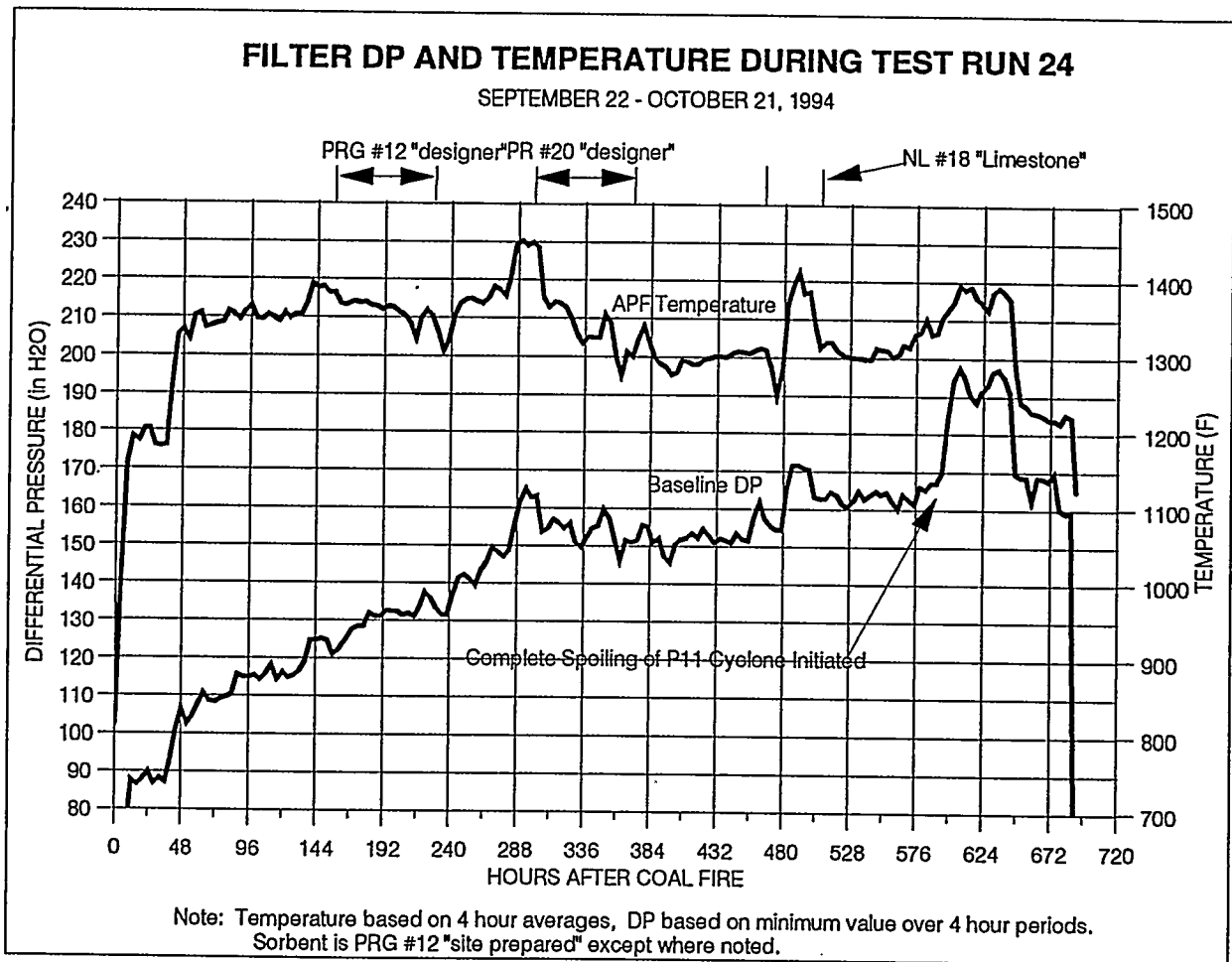


Figure 4.6.7 - Filter DP and Temperature During Test Run 24

## Results

### 4.6.8 Posttest Inspection (10/94)

On 10/27/94 the APF internals were removed from the vessel for inspection and candle replacement. A total of 30 candles were observed to be broken, as listed below.

Location of Broken Candles  
October 1994

	Plenum A	Plenum B	Plenum C
Top	6	1	7
Middle	4	2	6
Bottom	2	1	1

Ten of the 30 breaks had clean fracture surfaces indicating that the breaks occurred after shutdown or during removal from the vessel. Heavy ash bridging was apparent near the bottoms of candles in clusters B Top and B Middle, while light to moderate ash bridging was seen in clusters C Top, A Bottom, and B Bottom. Figure 4.6.8 through 4.6.16 are photos of the candle clusters following Test Period IV. It was evident that the ash accumulation that occurred during the first 600 hours of this run was not removed during the last 90 hours of operation with the cyclone spoiled.

Two of the nine backpulse tubes were found to have longitudinal cracks through the wall about 12 to 16 inches long (see Figure 4.6.17). The cracks occurred only on two of the bottom plenum tubes which were backpulsed at a higher pressure (1300 psig) than the upper and middle plenums (1000 psig). The cracks were believed to be due to thermal fatigue. All nine tubes were replaced in kind following Run 24. The tube material was Haynes Alloy 230.

All of the filter candles in the APF were replaced between Test Periods IV and V. In order to broaden the base of candle filter material testing, the filter was fitted with a combination of silicon carbide, alumina mullite, and two other second generation materials, namely, Dupont PRD66 and 3M CVI-SiC. Figure 4.6.18 shows the location of the various candle materials as installed for the last test period. The inner rows of candles in the upper and middle plenums were left out, the same as in the prior test series. Figures 4.6.19 and 4.6.20 are photos of the candle clusters showing the different candle materials installed prior to the start of Test Period V.

## Results

---

In order to protect the gas turbine from erosion by the coarse ash in case the filter leaked during the next test series, fail-safe devices were installed above each filter candle. The devices were designed to plug up when exposed to ash, but not impose a significant restriction to the normal flow of gas and backpulse air. These devices also functioned as heat regenerators for the backpulse air in order to mitigate the thermal shock of the backpulse air on the filter candles. Appendix II is a discussion of the performance of the fail safe devices prepared by Westinghouse STC.

During removal of the filter internals on 10/27/94, it was noted that the top of the shroud inside the APF was distorted inward at its four support brackets (Figure 4.6.21) which made removal of the clusters difficult due to interference between the shroud and the plenums. There was concern over the ability to reinstall the candle clusters due to this interference. Consequently, prior to the next test series, the upper 26" of the shroud was replaced with thicker material with stiffener rings at top and bottom (Figure 4.6.22). The four shroud support brackets were also replaced as they were found to be distorted. The distortion was attributed to thermal creep.

The primary cyclone upstream of the APF was modified between Test Periods IV and V to force all the gas and ash to flow through it and not collect any ash. This was done to demonstrate that the APF would operate at full load gas temperature (1550F) without ash bridging and without the formation of hard ash cake deposits on the filter candles which had caused the filter DP to become unstable in prior tests runs.

## Results

---

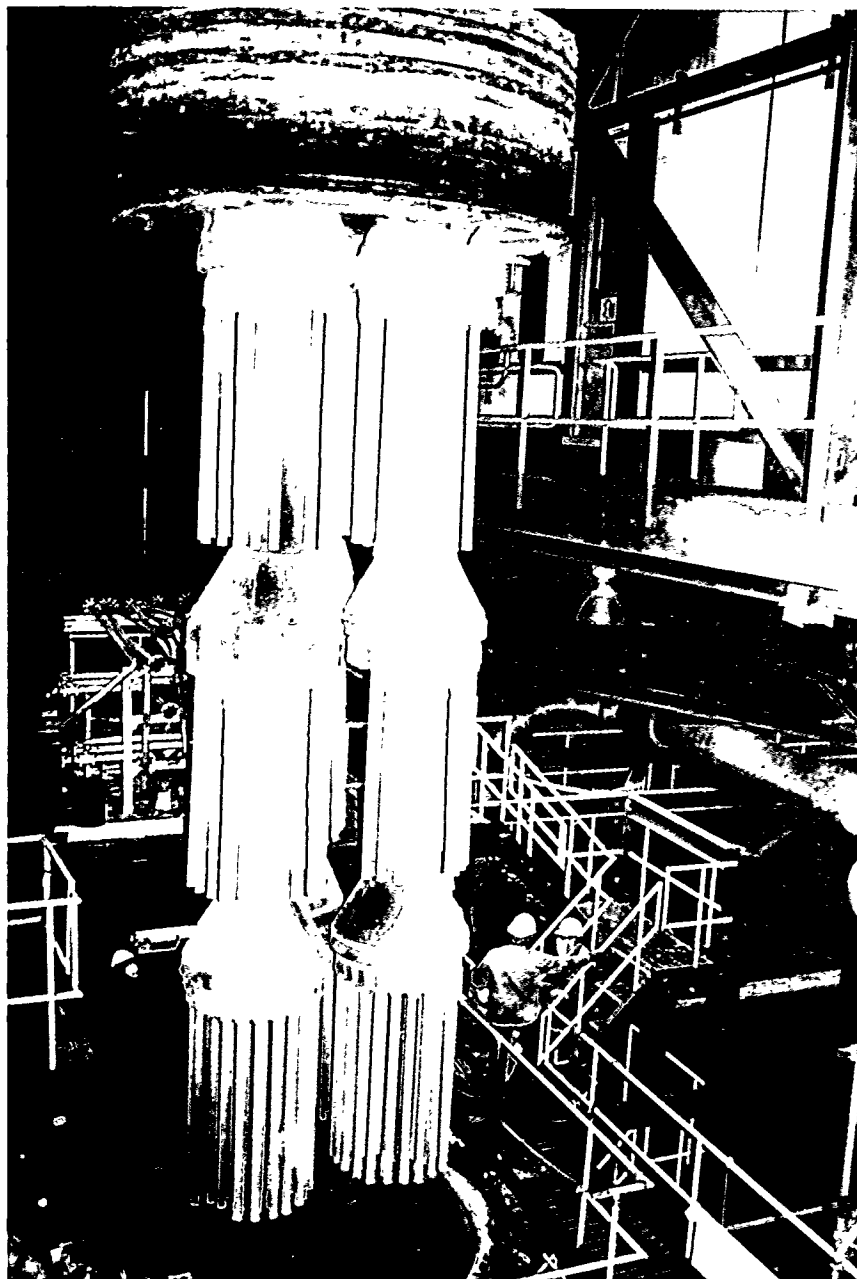


**Figure 4.6.8 - Photograph of Filter Internals Following Test Run 24**

## Results

---

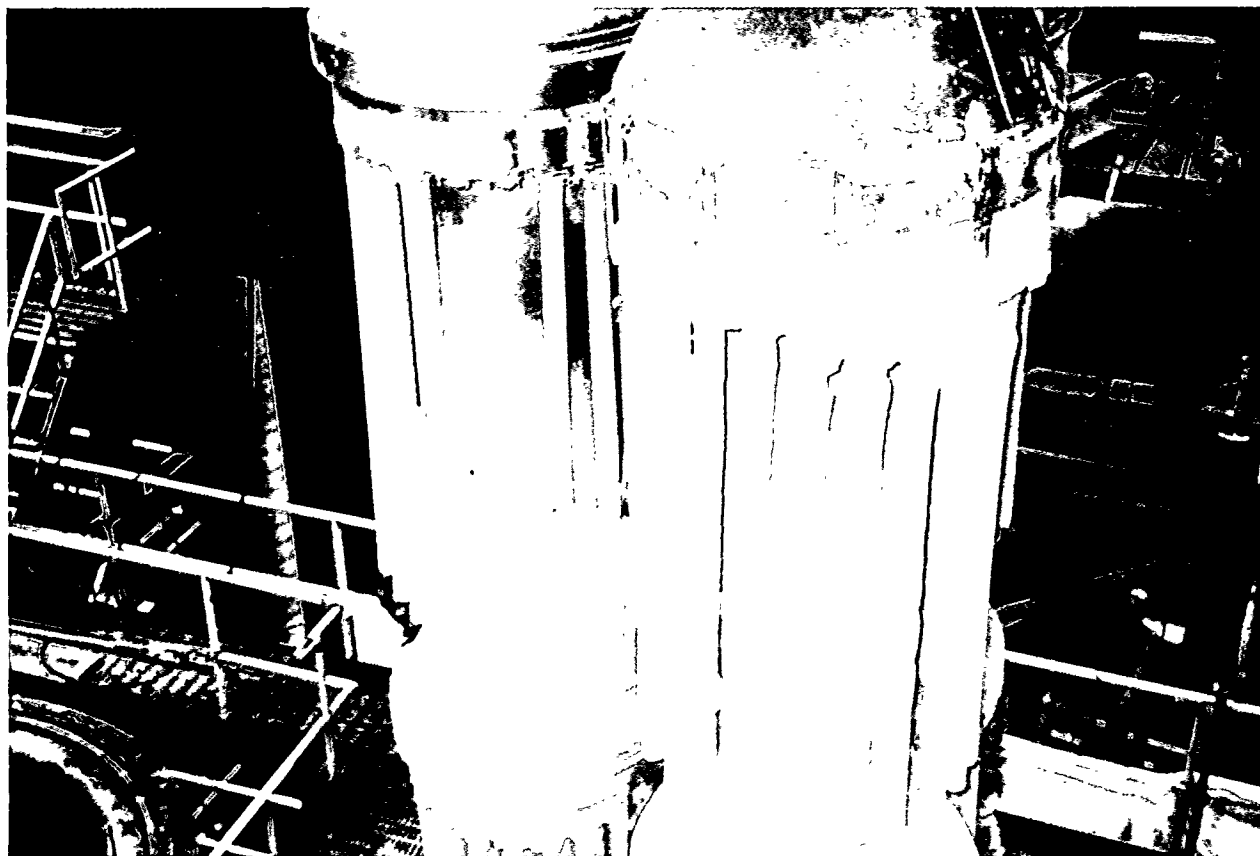


**Figure 4.6.9 - Photograph of Filter Internals Following Test Run 24**

## Results

---



**Figure 4.6.10 - Photograph of Filter Internals Following Test Run 24**

## Results

---



**Figure 4.6.11 - Photograph of Filter Internals Following Test Run 24**

## Results

---



**Figure 4.6.12 - Photograph of Filter Internals Following Test Run 24**

## Results

---



**Figure 4.6.13 - Photograph of Filter Internals Following Test Run 24**

## Results

---



**Figure 4.6.14 - Photograph of Filter Internals Following Test Run 24**

## Results

---



**Figure 4.6.15 - Photograph of Filter Internals Following Test Run 24**

## Results

---



**Figure 4.6.16 - Photograph of Filter Internals Following Test Run 24**

## Results

---



**Figure 4.6.17 - Photograph of Crack in Back Pulse Tube**

## Results

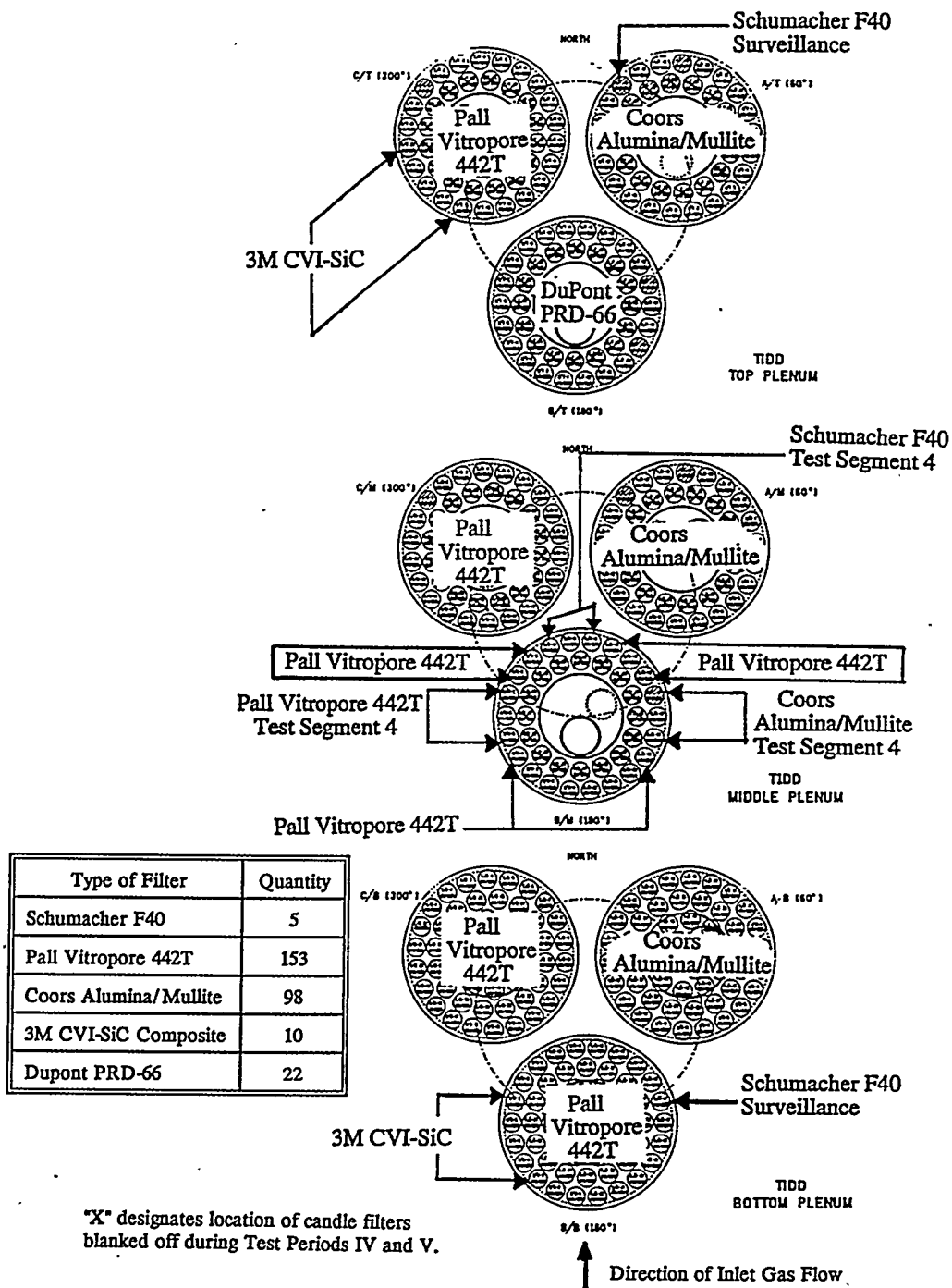


**Figure 4.6.18 - Location of Filter Candle Materials Before Test Period V**

## Results

---

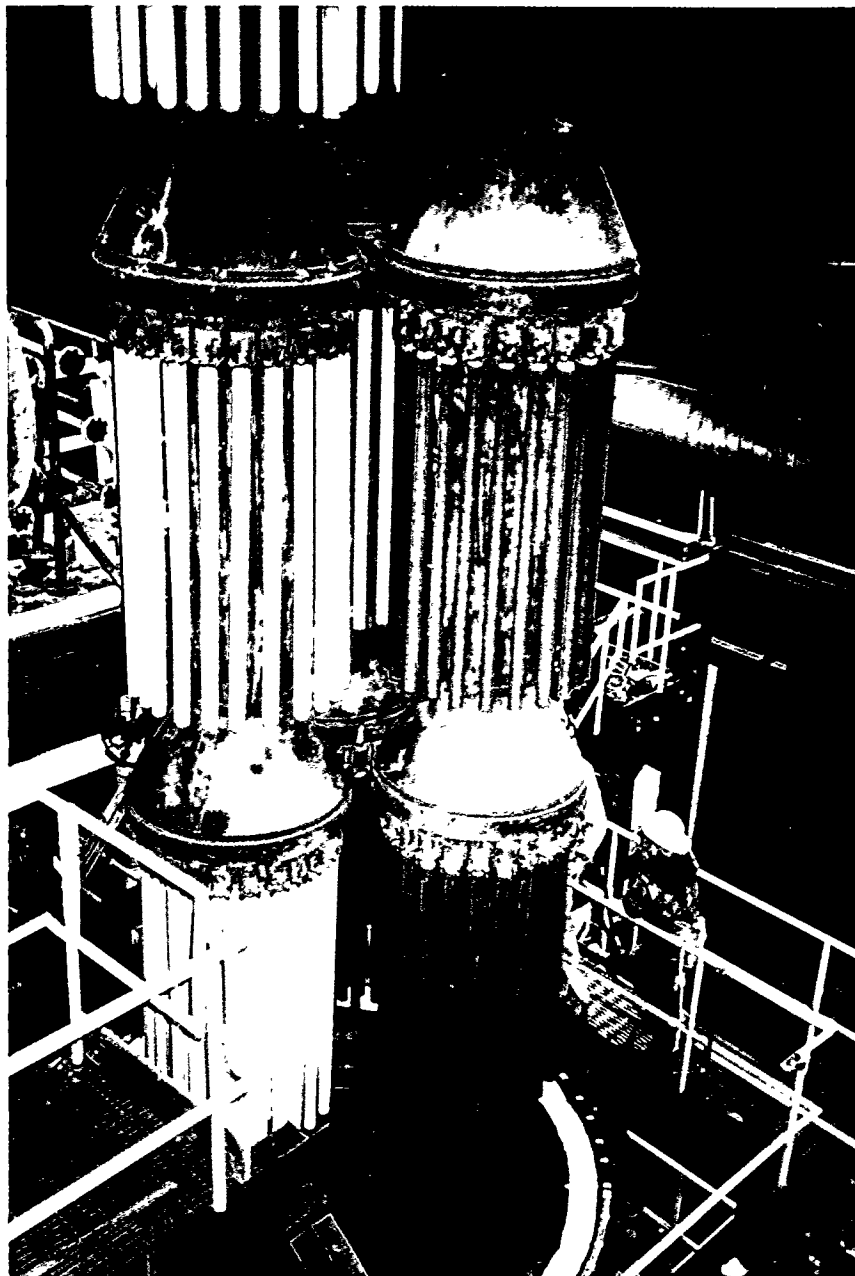


Figure 4.6.19 - Photograph of Filter Internals Before Test Period V

## Results

---



**Figure 4.6.20 - Photograph of Filter Internals Before Test Period V**

## Results

---



**Figure 4.6.21 - Photograph of APF Shroud Following Test Run 24**

## Results

---

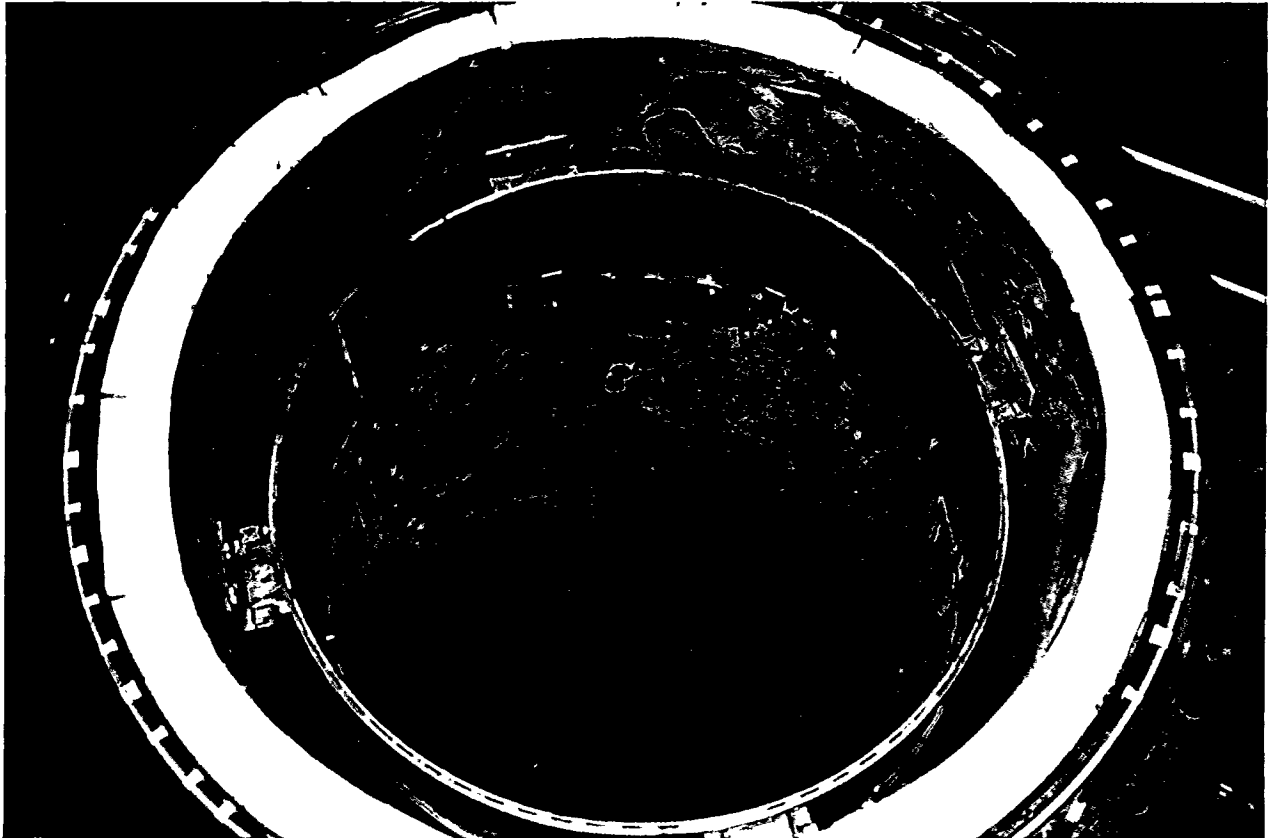


**Figure 4.6.22 - Photograph of APF Shroud After Replacement of Upper Portion**

## Results

### 4.7 Test Period V: 1/95-3/95

Table 4.7 summarizes the operating conditions and observations from Test Period V, the final test period.

**Table 4.7 - Summary of HGCU Operation - Test Period V**

	Operating Hours	Cumulative Hours	Operating Temp.	Pressure Drop	Inspection Observations
Run 25, 26, and 27	28	4772	_____	_____	_____
Run 28	145	4917	1350-1525 °F	Stable	● Filter internals very clean
Run 29 and 30	29	4946	_____	_____	_____
Run 31	32	4978	1420-1540 °F	Stable	_____
Run 32	73	5051	1240-1540 °F	Stable	_____
Run 33	427	5478	1275-1560 °F	Slight increase	_____
Run 34	375	5854	1275-1425 °F	Slight increase near end of run	● No ash bridging ● 22 Broken candles

#### 4.7.1 Test Runs 25, 26, and 27 - 1/13/95 to 1/21/95

These test run durations were 4.4, 16.8, and 7.1 hours, respectively. In each case the unit was shut down due to a problem not related to the HGCU system. Due to the brevity of these runs, they will not be discussed.

#### 4.7.2 Test Run 28 - 1/27/95 to 2/2/95

This run lasted 145 hours and was terminated when insulation came off the surface of a blind flange and the flange temperature exceeded 1350F at one point. It was found upon inspection that the anchor pins

## Results

---

which held a stainless steel cover plate over the insulation boards corroded which allowed the plate to fall away from the insulation. The gas flow entrained the insulation and carried it through the gas turbine. Portions of four anchor pins also were carried into the turbine and one of them passed through the turbine causing minor blade damage. (The blind flange was downstream of the backup cyclone.) During the early part of this run, problems with ball valves and pressure regulators on the backpulse skid interrupted filter cleaning for some periods which resulted in abnormally high DP as shown in Figure 4.7.2. During the last half of the run, the filter DP was stable with the gas temperature at 1500F. The drop in DP and flow late in the run is due to the effects of the restriction in flow downstream of the APF caused by the blind flange insulation cover plate falling partially into the gas steam. During the run approximately 11 gallons of Fiberfrax insulation were pumped into the APF head to control three hot spots.

## Results

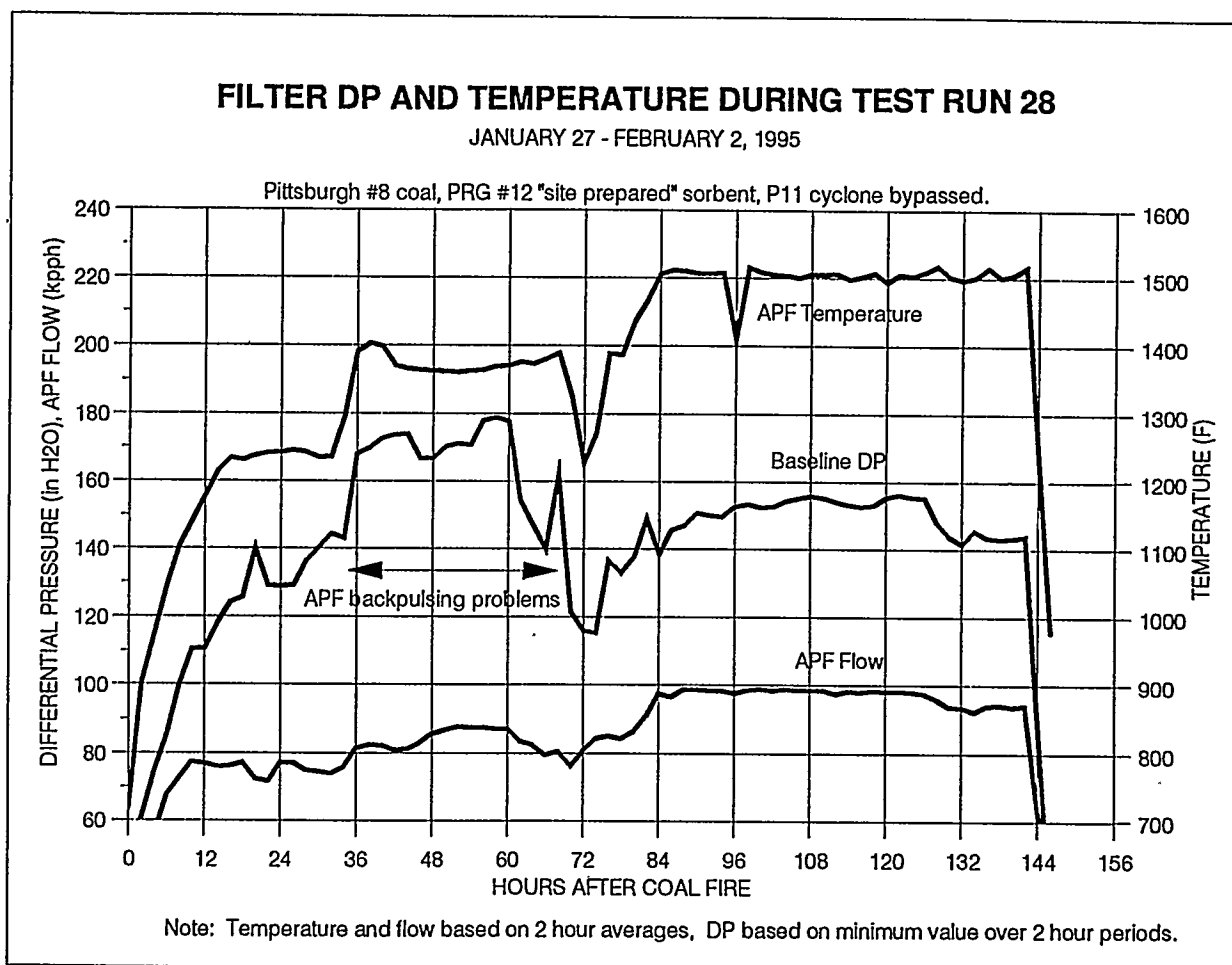


Figure 4.7.2 - Filter DP and Temperature During Test Run 28

## Results

---

### 4.7.3 Posttest Inspection (2/95)

Following Run 28 the APF was inspected using a boroscope passed through three instrument nozzles on the side of the filter vessel. The filter internals were found to be very clean with no ash bridging seen between the candles and the ash sheds. One very minor ash accumulation was seen between two candles in a bottom plenum, but overall, the filter looked cleaner than it had since the inspection following Test Run 1. The bottom of the APF hopper was also without significant ash deposits. Very little (less than 1/8") ash coating was observed on the candles. It was obvious that the coarser ash resulting from bypassing the primary cyclone was much easier to remove from the candles and did not tend to stick to the sides of the hopper, thereby making ash removal a non-issue.

### 4.7.4 Test Runs 29 and 30 - 2/9/95 to 2/10/95

These test run durations were 14.7 and 14.4 hours, respectively. Run 29 was terminated due to a failure unrelated to HGCU, and Run 30 was terminated to repair a gasket leak at the inlet of the ash surge hopper. Due to their brevity, they will not be discussed.

### 4.7.5 Test Run 31 - 2/11/95 to 2/12/95

This 32-hour run was terminated when the alternate ash line became plugged and the APF hopper began filling with ash. During the run candle fragments were found in the ash line from the lockhopper. Additional fragments were found upon shutdown in the alternate ash line while it was being cleaned. It is believed that a candle fragment became lodged in the orifice in the alternate ash line causing it to plug. The candle was a second generation Dupont PRD66 candle.

### 4.7.6 Test Run 32 - 2/13/95 to 2/16/95

Run 32 was a hot restart of the previous run. This test duration was 73 hours and was terminated due to plugged coal paste pumps. Early in the run the APF head exhibited additional hot spots and another 50 gallons of Fiberfrax insulation were pumped in to correct the problem. Once the gas temperature reached 1450-1500F, the APF DP remained fairly stable as shown in Figure 4.7.6.

# Results

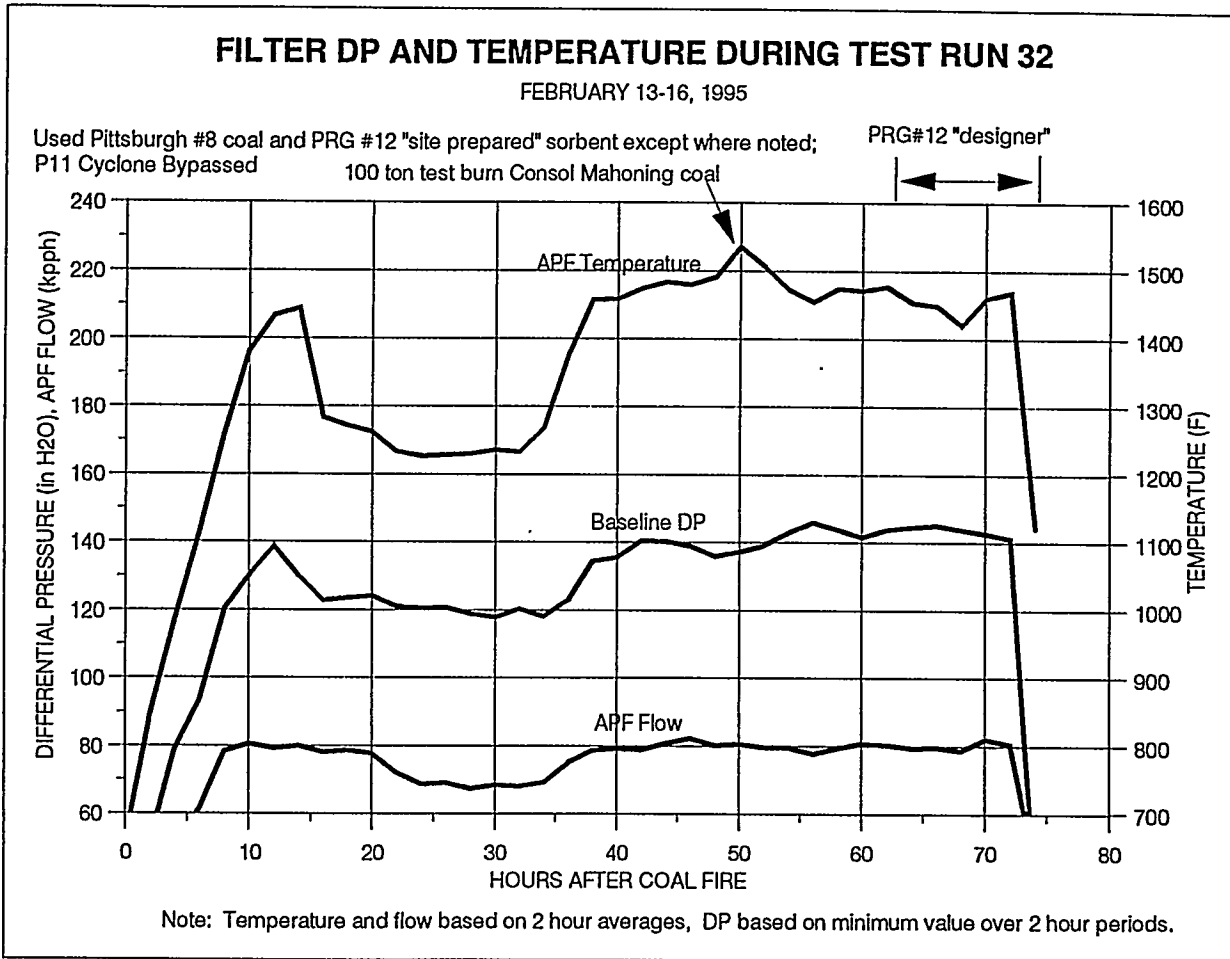


Figure 4.7.6 - Filter DP and Temperature During Test Run 32

## Results

---

### 4.7.7 Posttest Modifications (2/95)

Following shutdown another candle fragment was found in the lockhopper isolation valve. This fragment was the same material as the earlier fragments, and is believed to be from the same broken candle. In order to prevent the alternate ash line from becoming plugged by a candle fragment, a perforated plate was added at the inlet of the ash line between Run 32 and 33.

### 4.7.8 Test Run 33 - 2/18/95 to 3/8/95

Test Run 33 was one of the longest runs of the program at 427 hours. It was also the first run during which the filter operated at or above 1550F for significant time periods. Figure 4.7.8 shows the filter performance trends for this run. The Tidd unit reached its maximum output during this run, and the APF operated above 1550F during three separate time periods as shown by the temperature data in Figure 4.7.8. Portions of this run were conducted using two different coals, namely Minnehaha (from Indiana) and Consol coal. The remainder of the run used Pittsburgh 8, the same coal as in all other runs. The dolomite was also changed from Plum Run to Mulzer during part of the run. These periods are noted in Figure 4.7.8. The APF DP remained relatively stable during this run, but there was a noticeable increase in the DP following the last test at 1550F. The plant did not operate at full load for longer than about 20 hours at a time, so it is not known if the filter DP would have become unstable at 1550F for longer time periods.

During this run the APF head had to be pumped again with 20 additional gallons of insulation to control hot spots. On 2/24 the ash line from the Backup Cyclone became plugged, and for the remaining twelve days of the run no ash could be removed from the cyclone.

The run ended when the coal paste pumps plugged. Following shutdown, the Backup Cyclone was opened and found to be nearly full of ash. The ash was removed with a vacuum truck.

### 4.7.9 Test Run 34 - 3/14/95 to 3/30/95

This was the final test run of the HGCU system as the Tidd Plant was shut down permanently at the end of this run. The run time exceeded 375 hours which was the second longest of the test period. Two days after the start of this test run, APF candle fragments were removed from the lockhopper system.

## Results

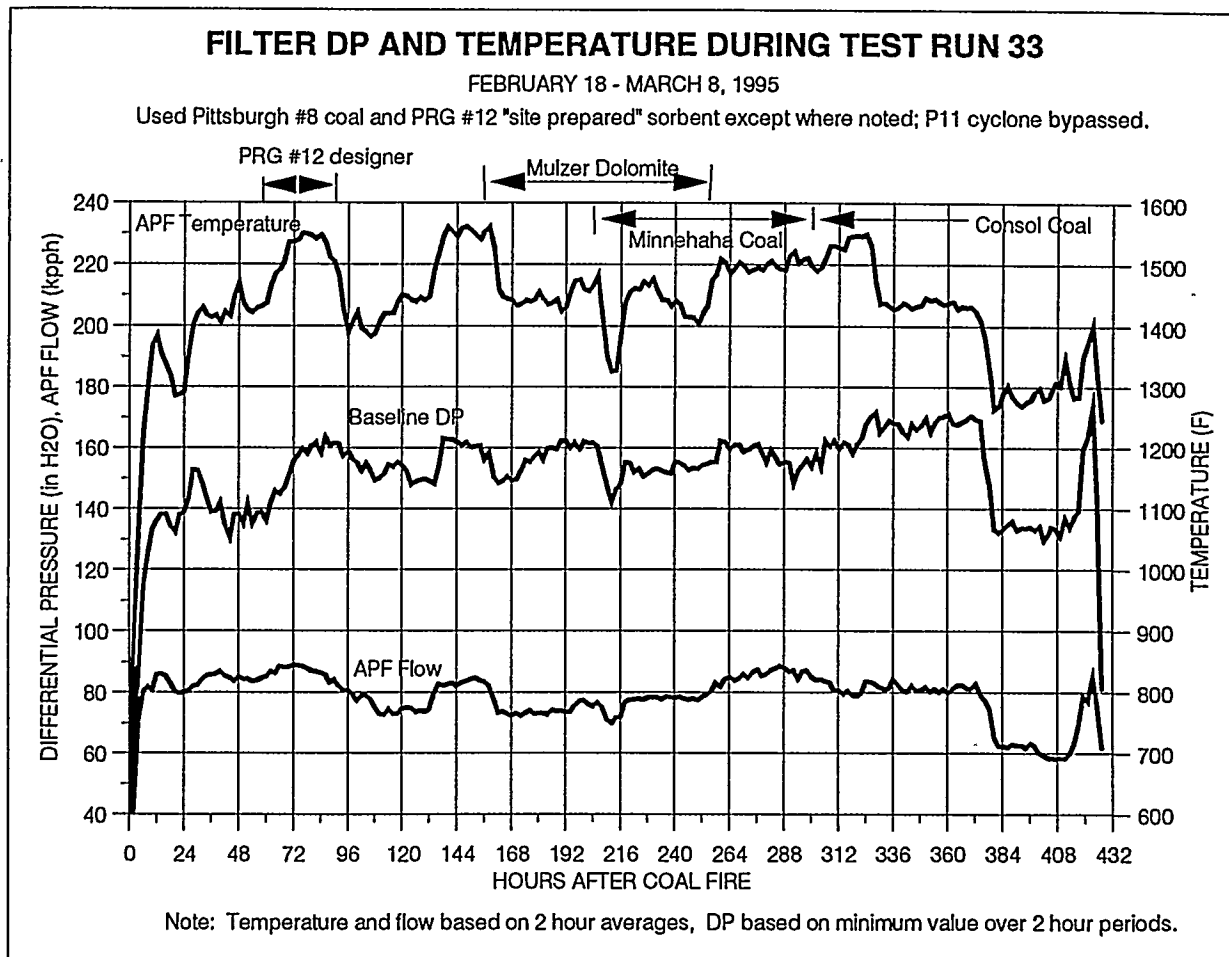


**Figure 4.7.8 - Filter DP and Temperature During Test Run 33**

## Results

---

The fragments were examined, and it was determined that they came from one Coors alumina-mullite and two Dupont PRD66 candles. The candle breaks apparently occurred during the first two days of this run. No other candle fragments were found for the remaining 13 days of the run. Most of this run was conducted at 90" and 115" bed level, and as a result, the APF temperatures ranged from 1250 to 1400F during most of the run. Figure 4.7.9 shows APF DP and temperature for this run. The DP was constant at a given temperature, but showed a slight increase during the last two days of the run. During the final week of operation, limestone was used as the sorbent instead of dolomite.

### 4.7.10 Posttest Inspection (4/95-5/95)

On 4/26 the internals of the APF were inspected with a boroscope. The internals were very clean with no ash bridges observed. All but two of the 22 Dupont PRD66 experimental filter candles appeared to be missing or were partially broken off. In addition, one Coors alumina-mullite candle was observed partially broken off. The remaining candles appeared in good condition.

On 5/11 the APF internals were removed from the filter vessel. Figures 4.7.10 through 4.7.18 are photographs of the filter internals after removal. As observed by the boroscopic inspection, 20 of 22 of the Dupont PRD66 candles were broken, all in plenum B Top. In addition, two Coors alumina-mullite candles were broken (rather than one), one near the top in plenum A Top and the other about 2/3 down from the top in plenum A Middle. No ash bridging was seen. The residual ash cake layer thickness on the candles ranged from about 1/8" on the Coors alumina-mullite candles to about 3/8" on the Vitropore silicon carbide candles. During removal, cracks were seen in two candles (Figure 4.7.18), one alumina-mullite the other an original Schumacher silicon carbide surveillance candle. Both candles broke during removal and handling. Hard ash deposits were found in the bottom 6 to 12 inches of these cracked candles. In addition, a 3M candle was found to be cracked near the bottom after it was removed. No indication of an ash leak path was seen at the gasket area of any of these candles, but it appeared that ash accumulated in the bottom portion of these candles which resulted in cracking of the candles.

# Results

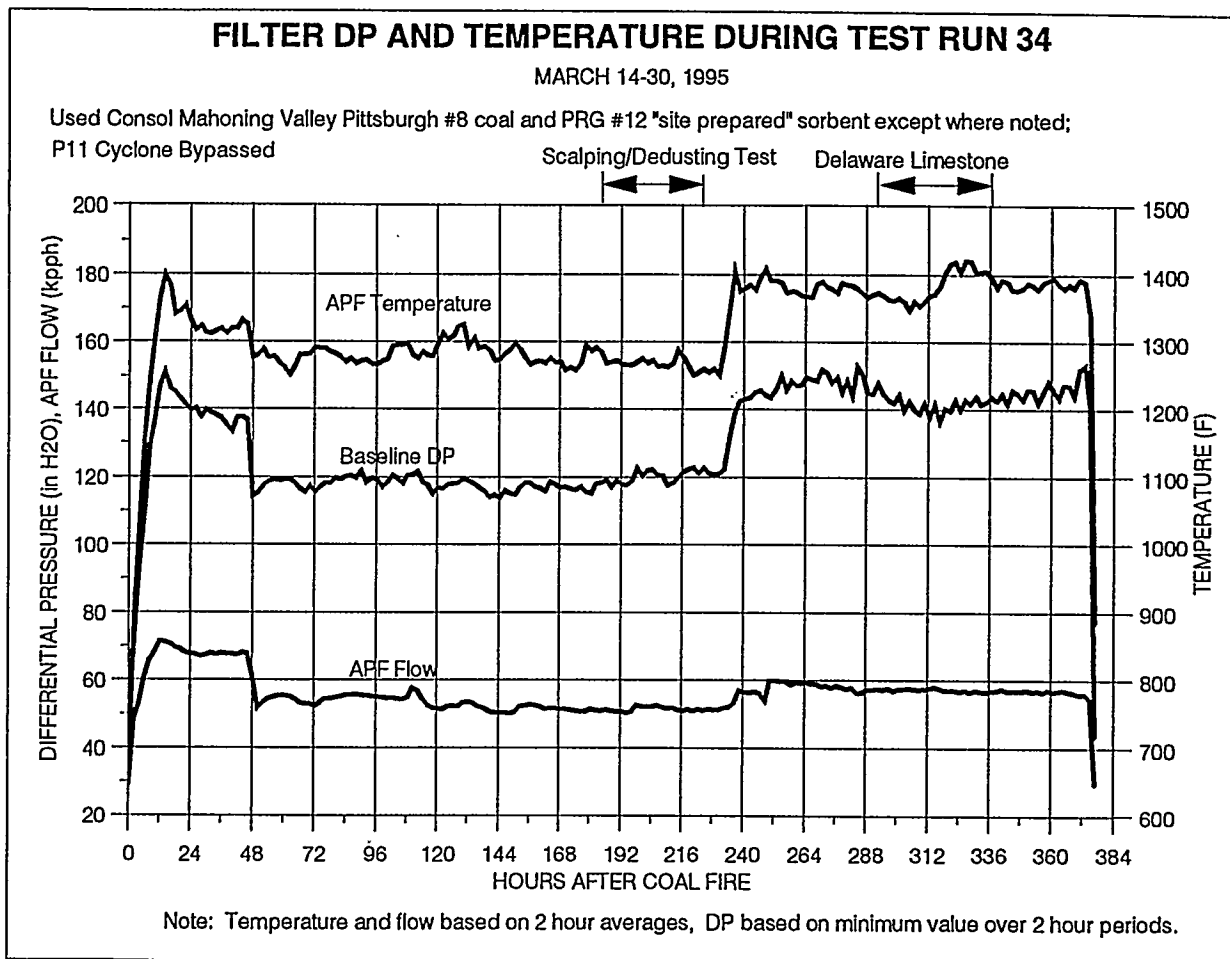


Figure 4.7.9 - Filter DP and Temperature During Test Run 34

## Results

---

The outlet side of the filter was inspected and about 1/16" of ash was found on the top of the tubesheet. The vertical surfaces in the outlet side did not have ash accumulations. Some ash dust was found in the venturi outlet pipes. If ash which leaked into the outlet side of the filter due to the broken Dupont candles became entrained by the backpulse air, it could explain how ash accumulated in the bottom of the other candles. However, the fail-safe devices removed from the candles did not show signs of ash on the outlet side.

## Results

---

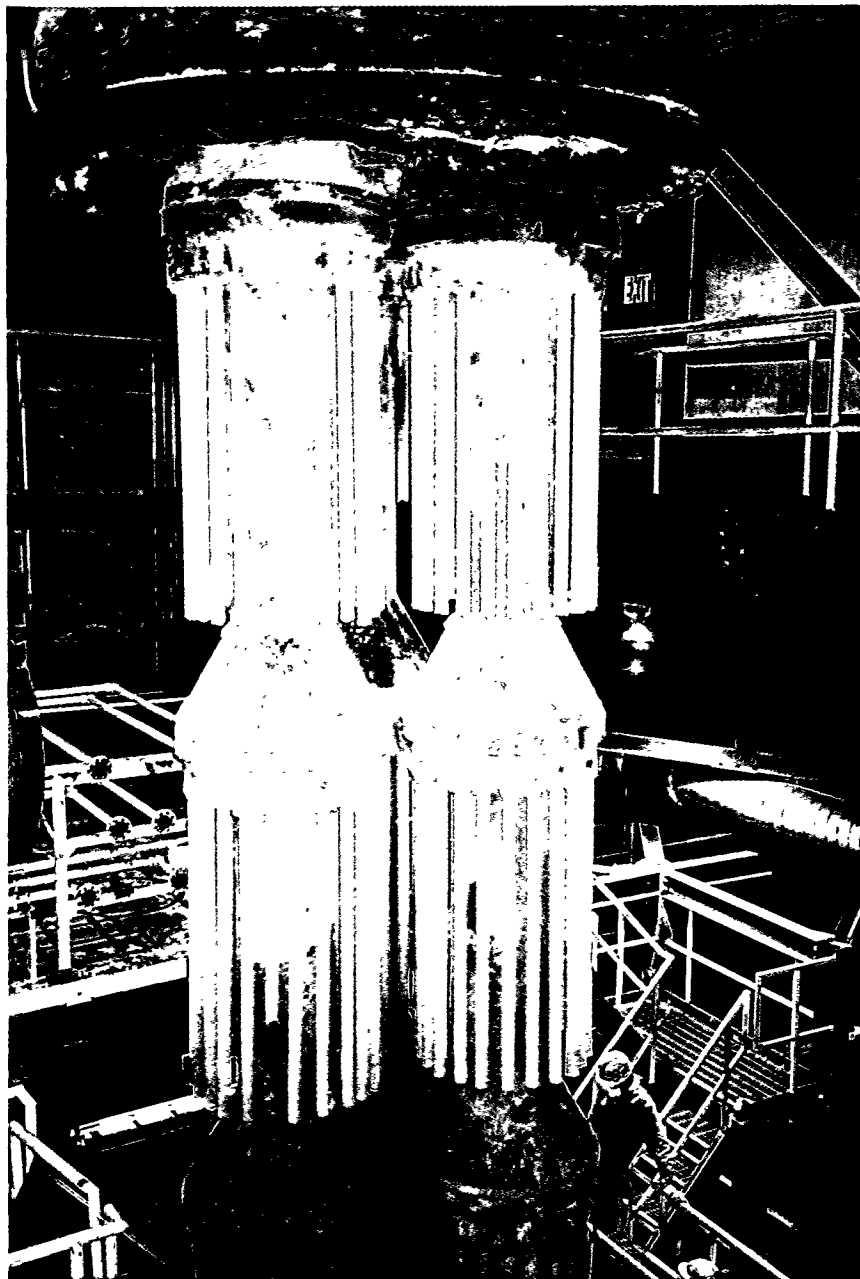


**Figure 4.7.10 - Photograph of Filter Internals Following Test Run 34**

## Results

---

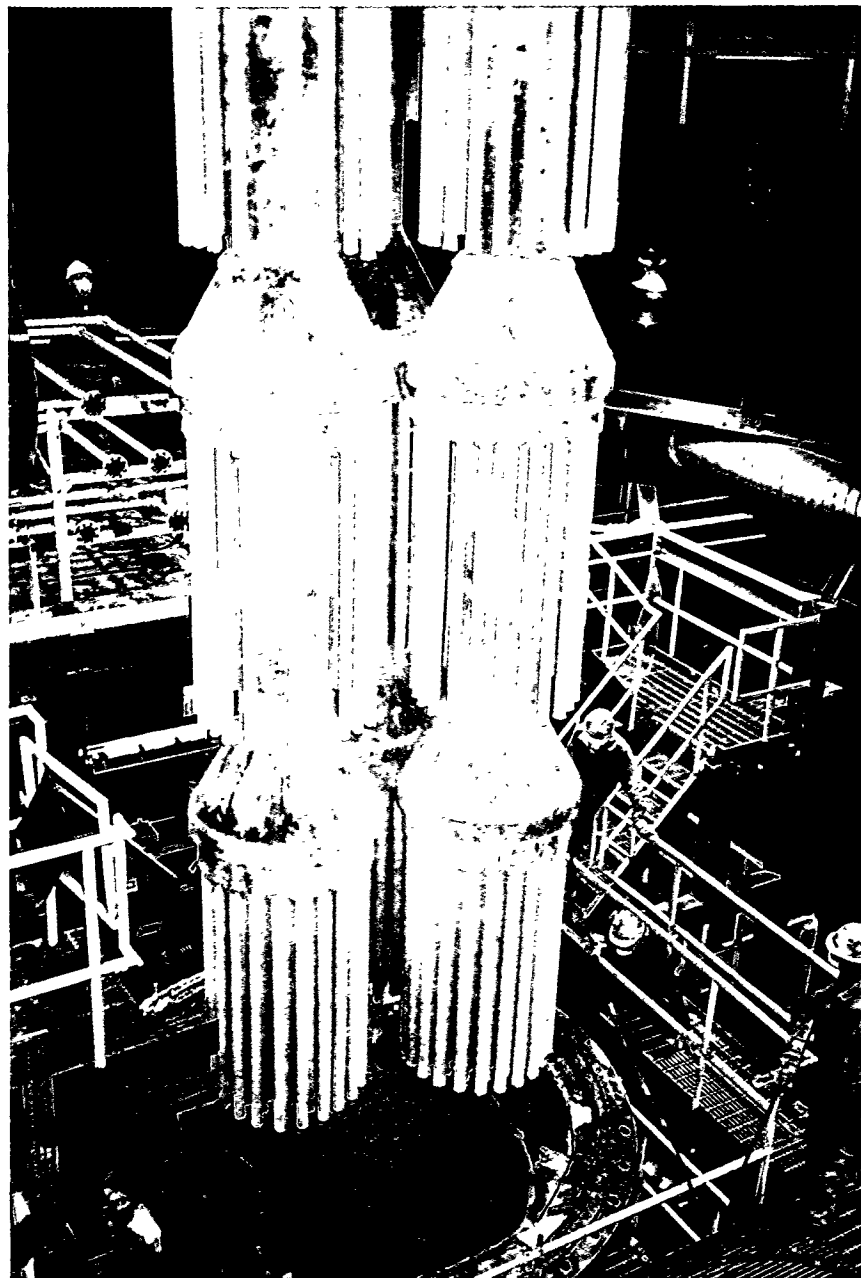


**Figure 4.7.11 - Photograph of Filter Internals Following Test Run 34**

## Results

---

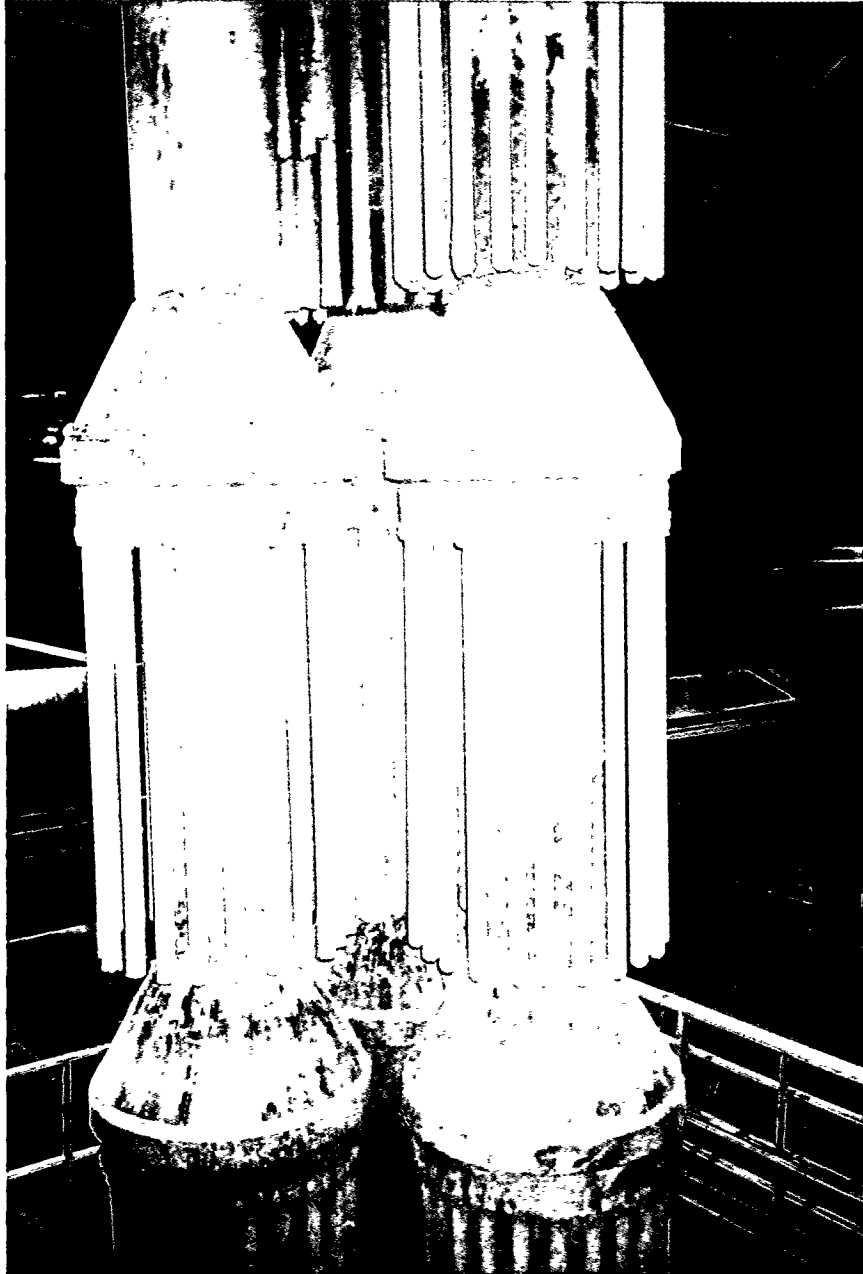


**Figure 4.7.12 - Photograph of Filter Internals Following Test Run 34**

## Results

---

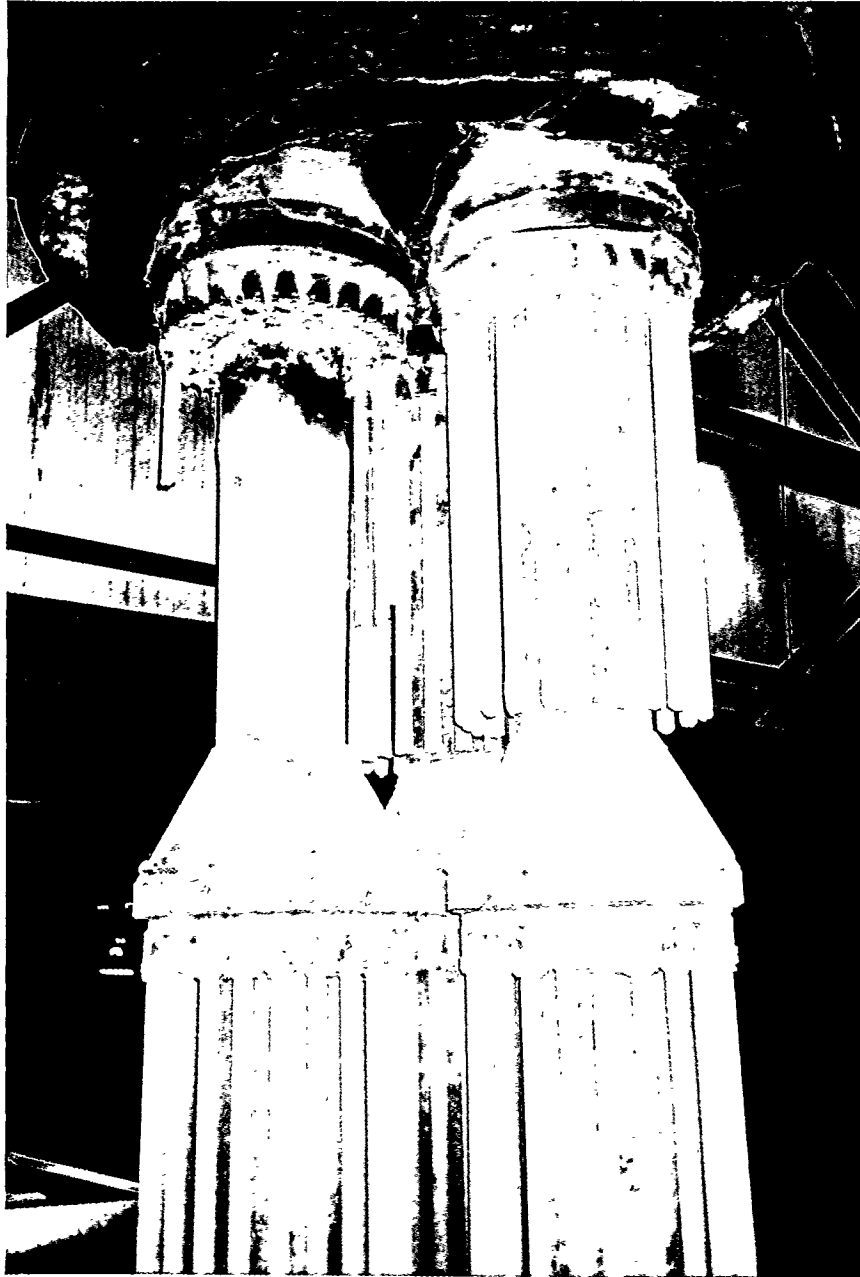


**Figure 4.7.13 - Photograph of Filter Internals Following Test Run 34**

## Results

---

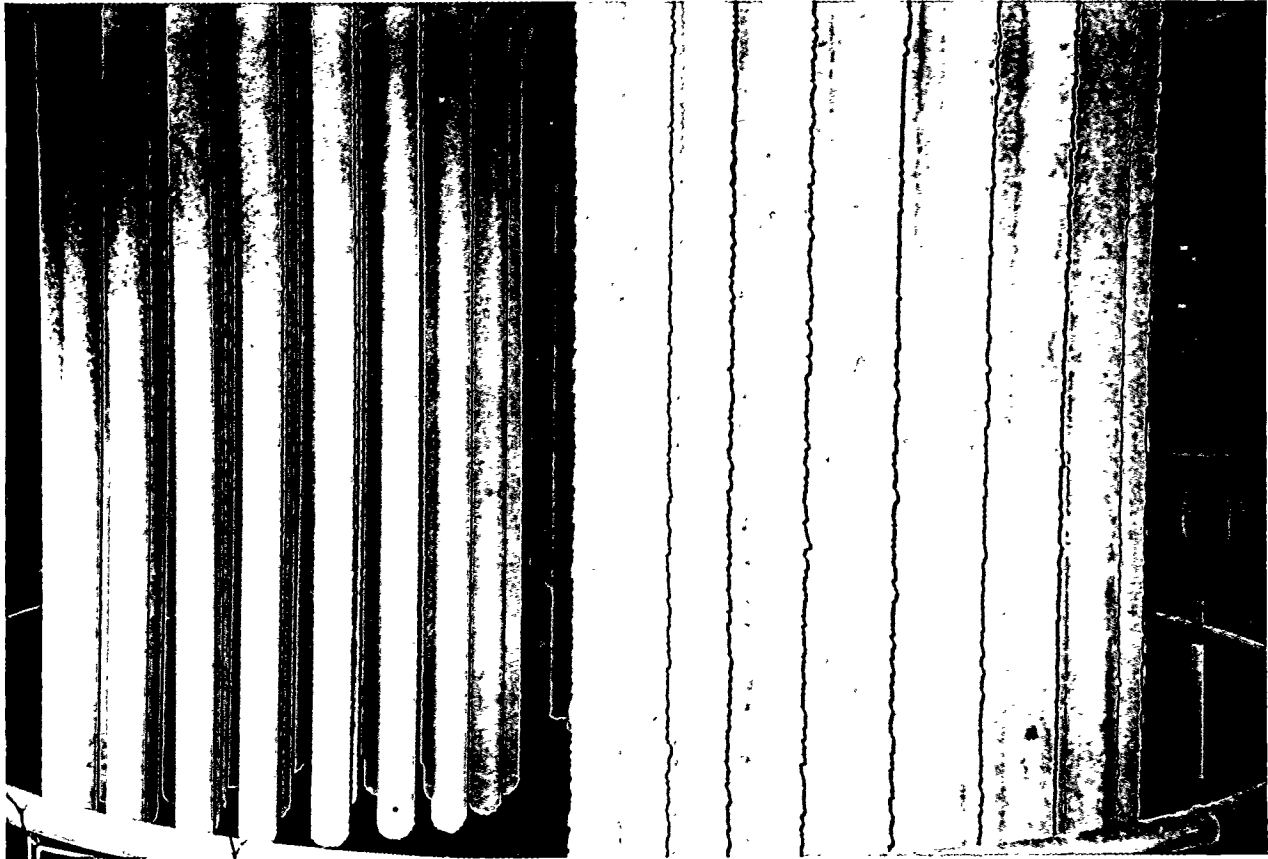


**Figure 4.7.14 - Photograph of Filter Internals Following Test Run 34**

## Results

---



**Figure 4.7.15 - Photograph of Filter Internals Following Test Run 34**

## Results

---



**Figure 4.7.16 - Photograph of Filter Internals Following Test Run 34**

## Results

---



**Figure 4.7.17 - Photograph of Filter Internals Following Test Run 34**

## Results

---



**Figure 4.7.18 - Photograph of Filter Internals Following Test Run 34**

## Results

---

### 4.8 Final Equipment Inspections

Following completion of the test program, inspections were conducted on system components to assess their condition. This section of the report describes the results of those inspections.

#### 4.8.1 Filter Vessel

During much of the test program, the APF head exhibited hot spots near the outlet nozzle and the backpulse piping nozzles. The hot spots were corrected by drilling small holes through the head and pumping in insulation. Experience has shown that hot gas flowing against a cold metal surface promotes rapid corrosion. Therefore, the inside surface of the APF head was inspected following completion of the test program. A section of the head liner and Z-Block insulation was removed to expose the inside surface of the head. Heavy corrosion was apparent, as shown in Figure 4.8.1. Portions of the metal were so corroded that large (3 to 4 inch) pieces of corroded metal about 1/16 to 1/8-inch thick would flake off the surface by pulling with one finger. Following this observation, shell thickness data were obtained using an ultrasonic instrument. It was found that thickness of the top portion of the head averaged 7.6% below the nominal 1.50 inches, and was 12.2% below nominal at the thinnest point measured. The thickness of the bottom portion of the outlet nozzle near the nozzle-to-head weld was found to be 4.5% to 7.8% below the nominal 7/8 inch. It was evident that the carbon steel exposed to the flowing hot gas experienced significant corrosion. The remainder of the APF head which did not exhibit hot spots due to flowing hot gas was in excellent condition with the epoxy surface coating still intact.

#### 4.8.2 Filter Internals

The shroud was removed from the vessel for inspection. It appeared to be in generally good condition as shown in Figure 4.8.2. No erosion was seen on the impingement plate opposite the inlet nozzle. This was of concern after the ash loading and particle size were increased during the last test period. The ash tended to form a deposit and flake off on the impingement plate as shown in Figure 4.8.3. One problem was noted with the shroud. The four support brackets were bent upward due to deformation of the shroud. This occurred even after the shroud material thickness was increased to 1/4 inch and a stiffening ring was added at the top of the shroud to mitigate this problem prior to the last test period. It was apparent that the shroud thickness was still insufficient to prevent distortion.

## Results

---

Upon removal of the shroud, the filter liner was exposed for better inspection. The upper portion of the liner was in generally good condition, except near the very top where it had been distorted by the weight of the shroud support brackets. However, severe distortion and warpage was apparent in the lower half of the liner as shown in Figure 4.8.4. This distortion was much worse than observed in previous inspections and probably resulted from operating the APF at very high temperatures (above 1550F) during the last test period. It appeared that the liner could not expand properly and buckled inward as a result. The hopper cone appeared to be in good condition; only the cylindrical sections were warped. Ash had accumulated behind the liner at points where it had buckled inward and this may have prevented the liner from returning to its original position upon cooling.

The tubesheet support cone was inspected by removing some of the insulation from the upper side of the cone. The expansion cone and tubesheet appeared in excellent condition, as shown in Figures 4.8.5 and 4.8.6. Dye penetrant tests were conducted on the seam and circumferential welds on the inner cone, and no indications were noted.

The insulating plug used in the APF manway deteriorated severely. The 310 stainless steel metal used to contain the insulation corroded to such a degree that it essentially fell apart upon removal. The plug was exposed to flue gas below the dew point which aggressively attacked the stainless steel in the plug. However, the manway nozzle which had been coated with epoxy was in good condition.

### 4.8.3 Backpulse System

Two of the Atkomatic solenoid valves and the COAX valve (used in the last test period) were disassembled for inspection. The COAX valve did not show any signs of degradation. The two Atkomatic valves appeared to be in excellent condition. Some very minor surface scratches were seen in localized areas on the pistons indicating that the Stellite coating held up very well. The valve body bores showed very minor surface pitting, but felt very smooth. Figures 4.8.7 and 4.8.8 are photographs of the valve internals.

## Results

---

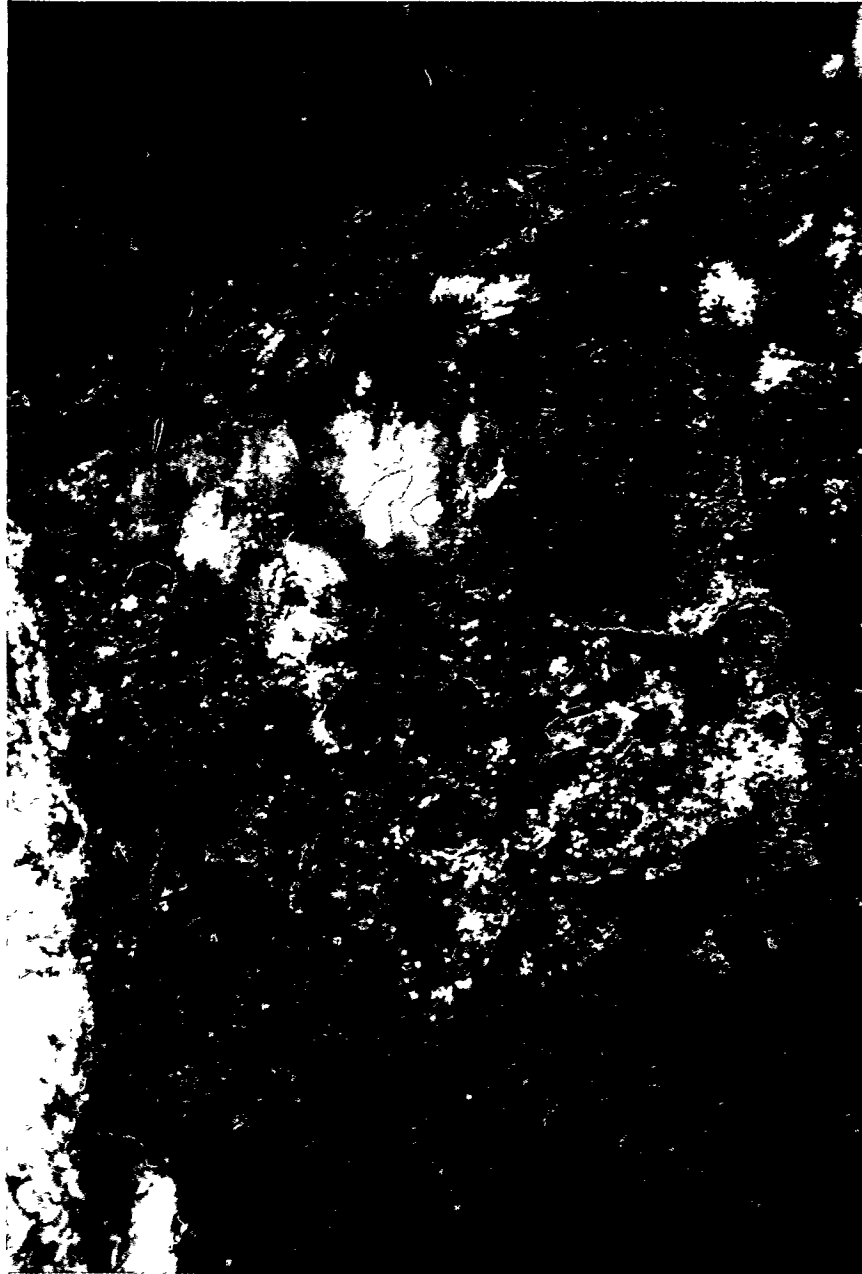


**Figure 4.8.1 - Photograph of Corrosion of APF Head Under Insulation Near Outlet Nozzle**

## Results

---



**Figure 4.8.2 - Photograph of APF Shroud During Final Removal**

## Results

---



**Figure 4.8.3 - Photograph of Shroud Impingement Plate**

## Results

---

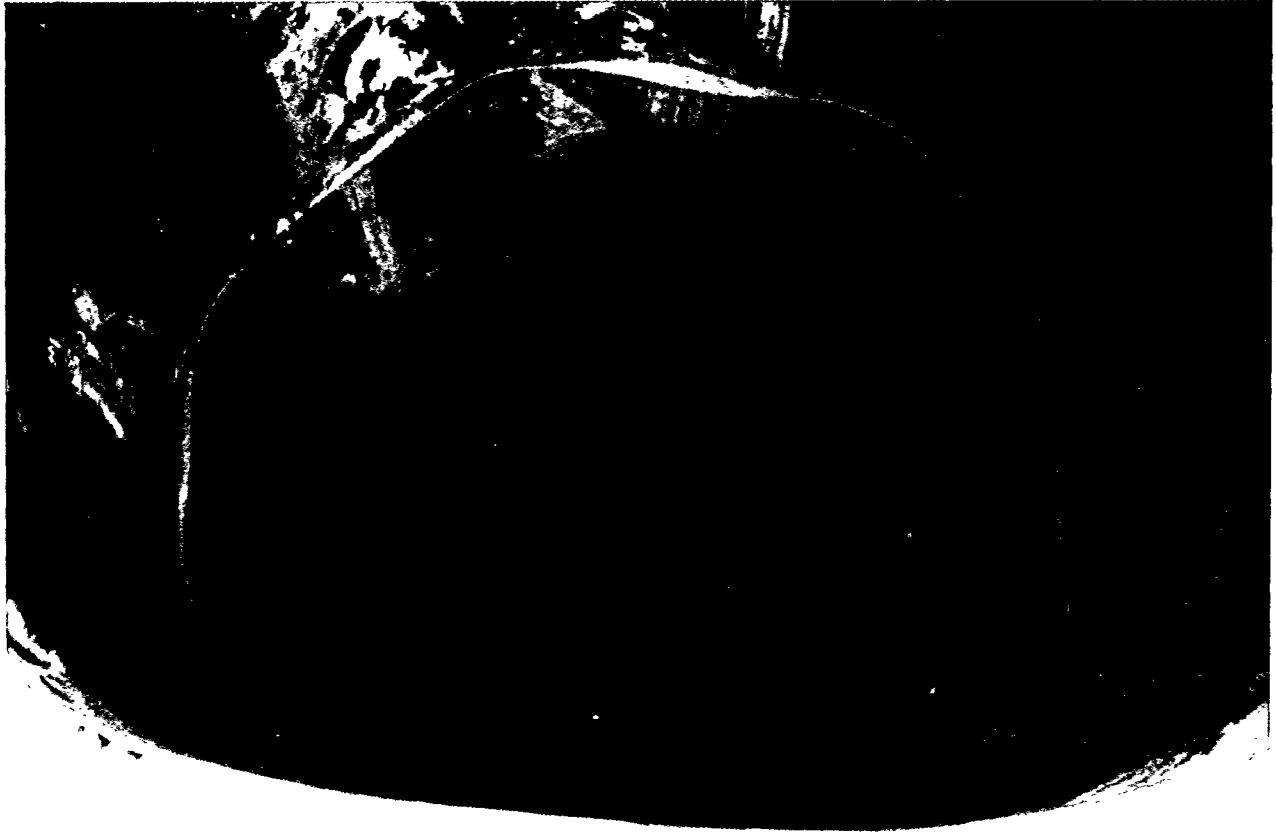


Figure 4.8.4 - Photograph of APF Liner

## Results

---



**Figure 4.8.5 - Photograph of Tubesheet Cone**

## Results

---



Figure 4.8.6 - Photograph of Tubesheet Cone

## Results

---

### 4.8.4 Backup Cyclone

The backup cyclone was inspected through the manway nozzle and found in good condition. Figures 4.8.9 - 4.8.11 are photographs of the internals of the cyclone. Cracks in the refractory noted after the first test period did not appear to be much worse. However, a portion of the refractory liner used at the level detector location appeared to be eroded away as shown in Figure 4.8.10. The stainless steel sheet metal used to contain the refractory on the manway door was pitted but still in one piece. The ash line outlet and air nozzles at the bottom of the cyclone were in good condition. A solid plug of ash about 4 inches deep was found in the bottom of the ash removal vessel as seen in Figure 4.8.12.

### 4.8.5 Ash Removal System

A section of the alternate ash line was removed and sectioned to determine if it had experienced erosion. No erosion was noted. This indicated that ash conveying lines can be properly sized to handle heavy ash loading with coarse particles without experiencing erosion. The restrictive orifice in the alternate ash line was removed and inspected. The orifice, which was a tungsten carbide nozzle, appeared in excellent condition, as shown in Figures 4.8.13 and 4.8.14. Also, the tee downstream of the orifice was inspected and it also was undamaged.

The screw cooler internals were inspected using a boroscope. No problems were noted, however, fibrous material apparently from broken second generation filter candles was wrapped around the screw in several locations. The screw cooler end housings were removed to expose the hydraulic motor and bearings. No problems were apparent. However, ash was seen in both end housings indicating that the pressure sealing system had not been totally effective in keeping ash out of the housings.

### 4.8.6 Hot Gas Piping

Corrosion of the hot gas piping system was a concern following the failure of the expansion joint during initial system operation. Major effort was made to improve the design of the piping system to overcome this problem as previously discussed. In order to determine how successful these modifications were, a section of a pipe spool including a portion of an expansion joint bellows was cut out for inspection. The Hastelloy liner between the refractory and the outer pipe was in excellent condition as shown in Figure 4.8.15. The outer bellows was also in excellent condition. The carbon steel surface under the Hastelloy was not corroded at all (Figure 4.8.16). The refractory was not cracked and was intact. In

## Results

---

fact, it was very difficult to remove from the pipe. Figures 4.8.17 - 4.8.20 are photographs of the inside of the pipe spool after removal of the section. This expansion joint had been pumped with insulation which could be seen in the expansion joint convolutions.

## Results

---

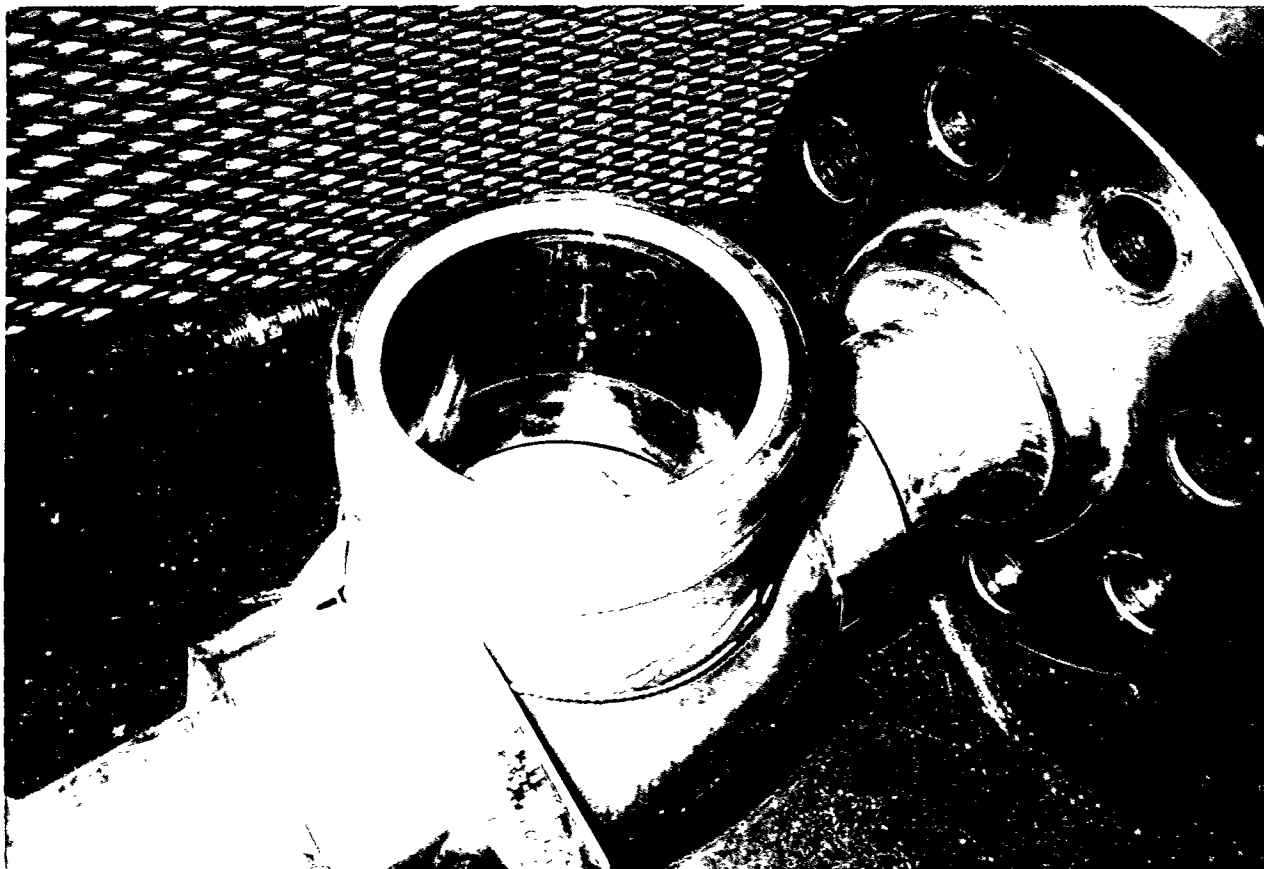


**Figure 4.8.7 - Photograph of Backpulse Valve Internals**

## Results

---

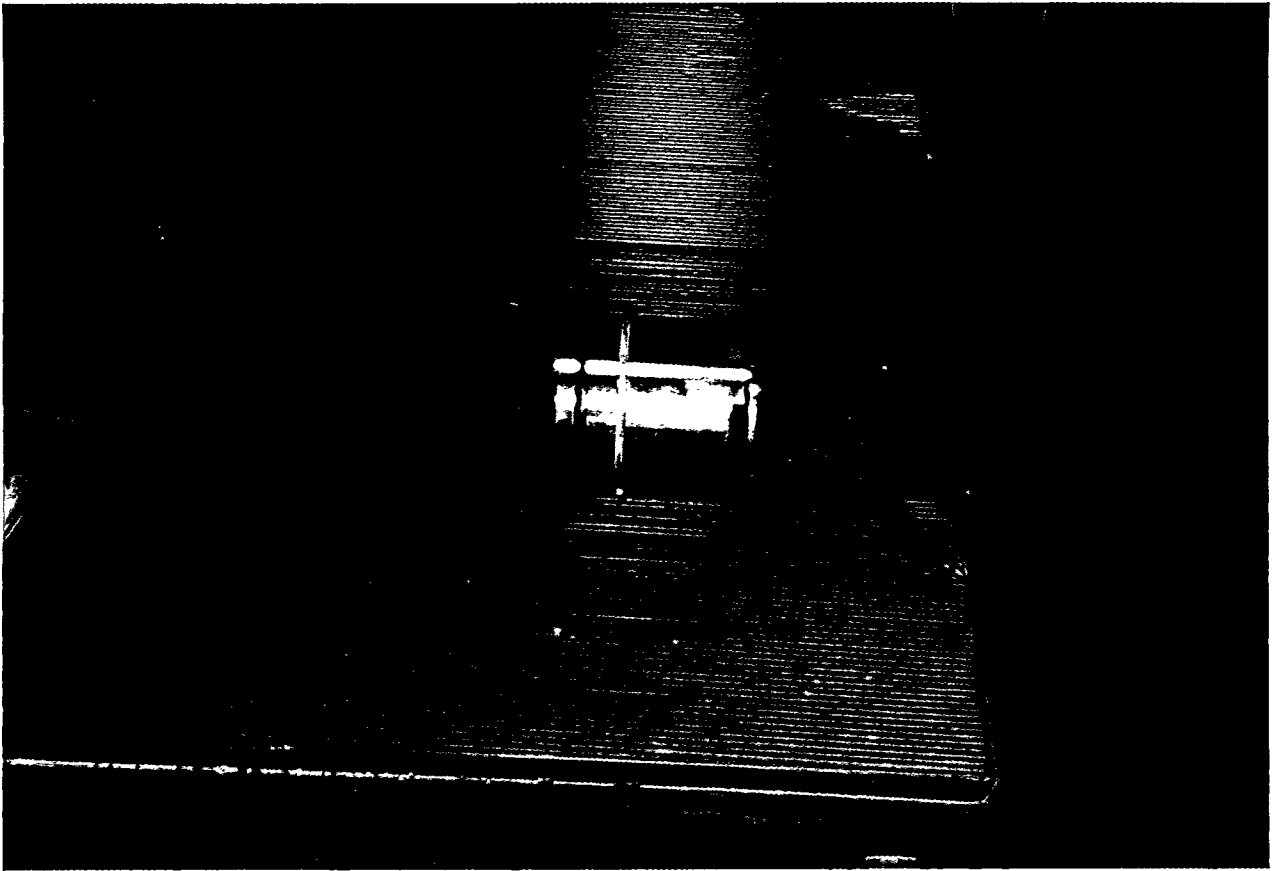


**Figure 4.8.8 - Photograph of Backpulse Valve Internals**

## Results

---

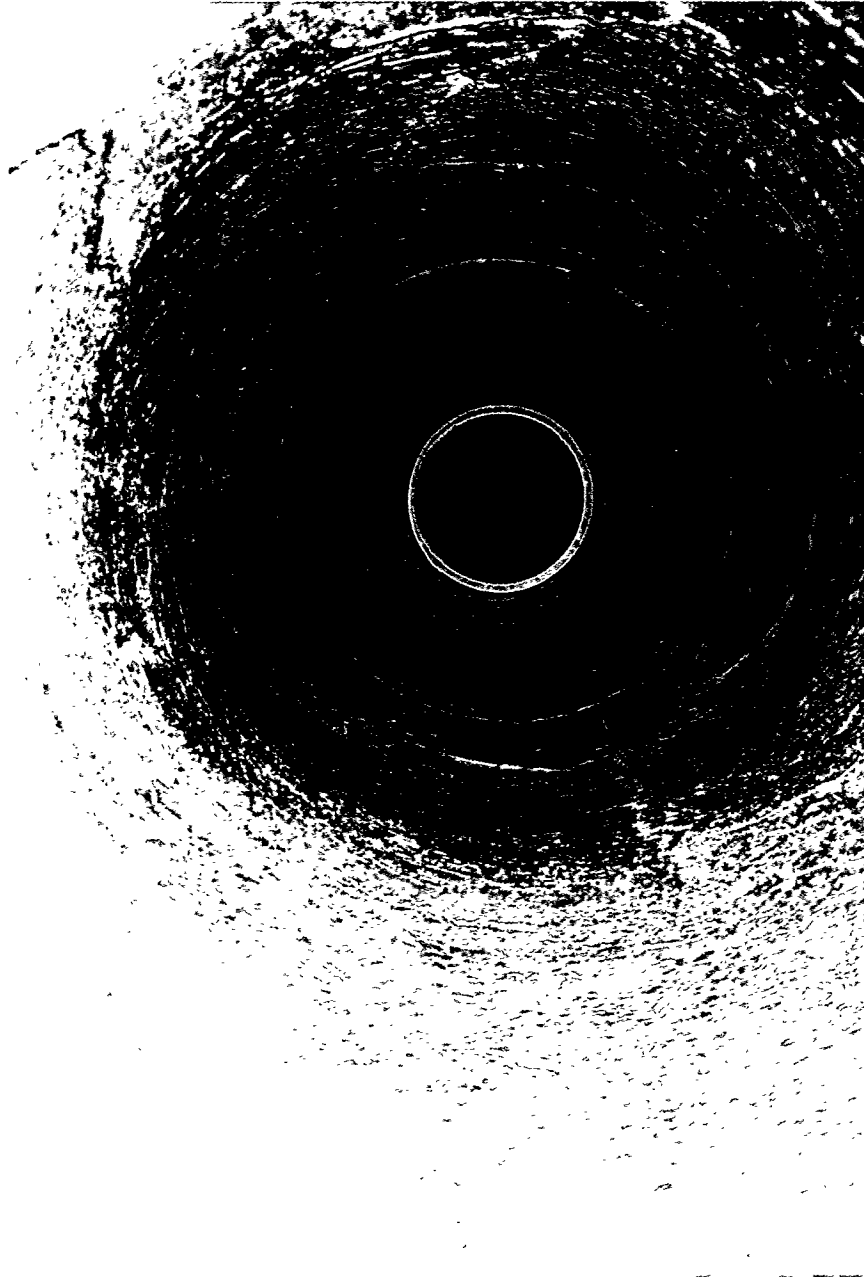


**Figure 4.8.9 - Photograph of Backup Cyclone Internals**

## Results

---

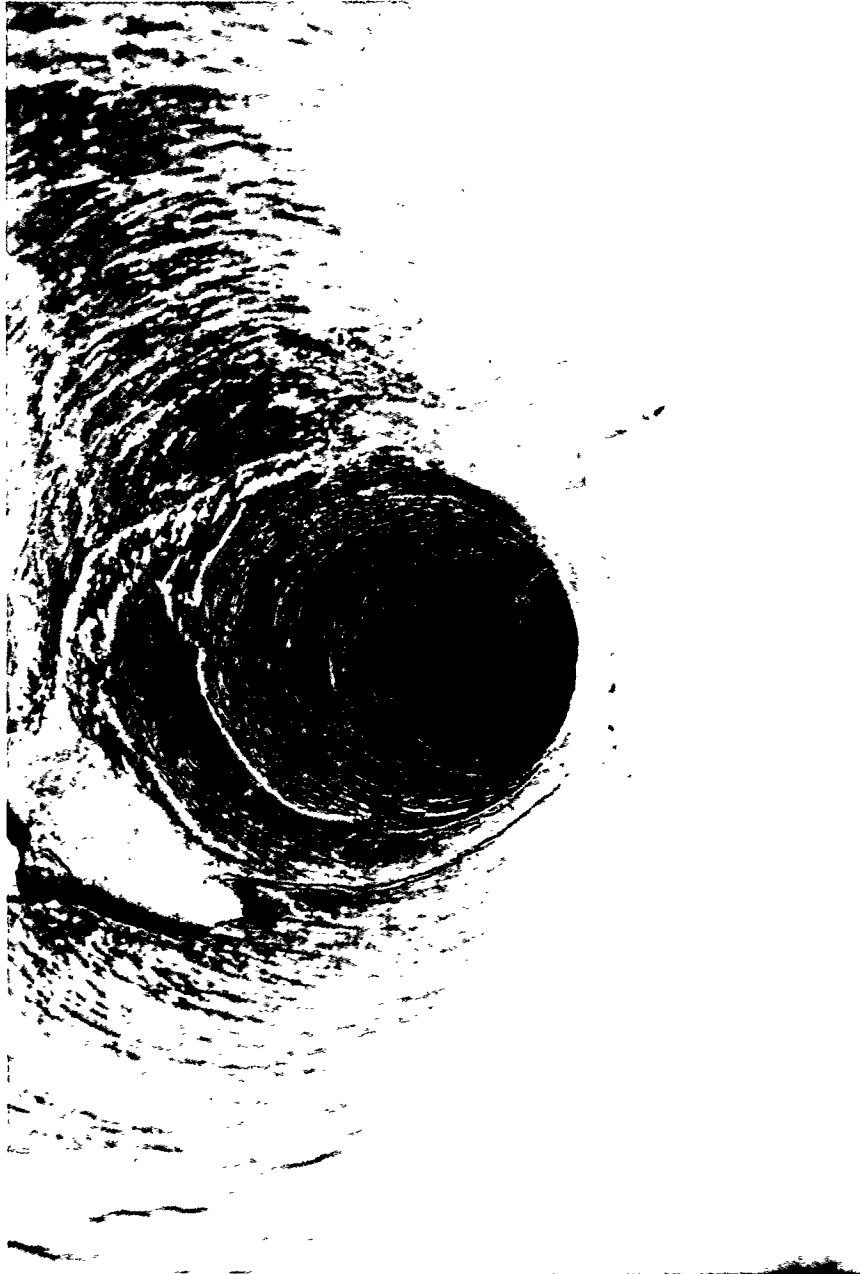


**Figure 4.8.10 - Photograph of Backup Cyclone Internals**

## Results

---

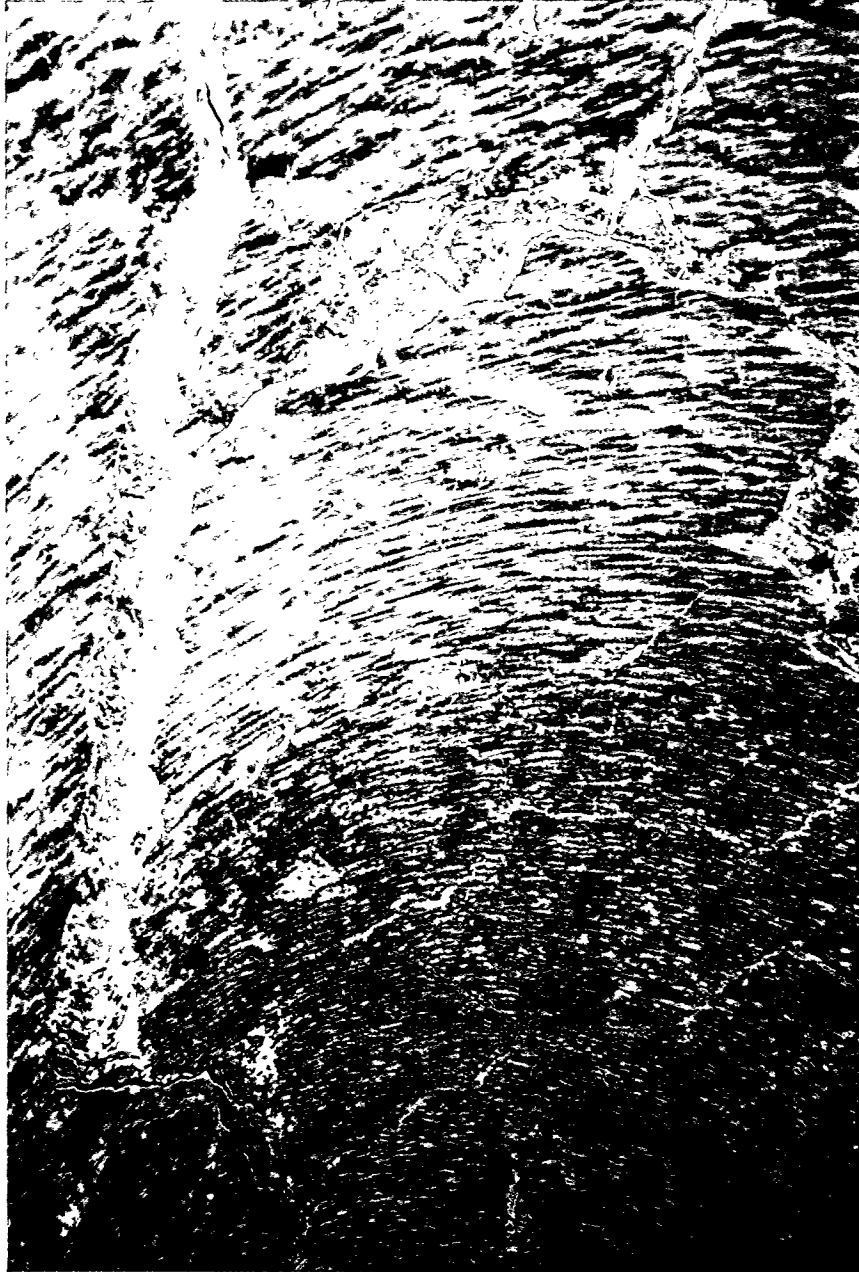


**Figure 4.8.11 - Photograph of Backup Cyclone Internals**

## Results

---

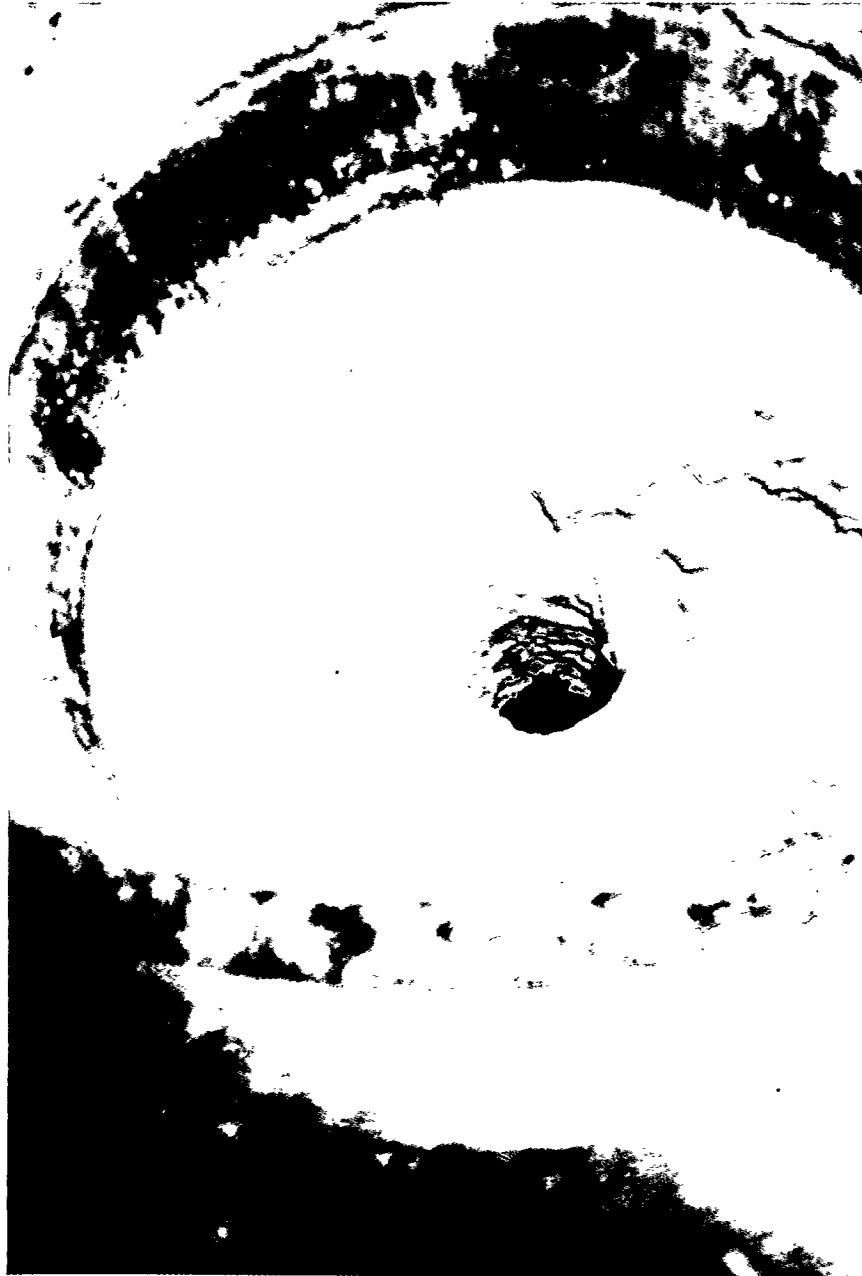


**Figure 4.8.12 - Photograph of Backup Cyclone Internals**

## Results

---

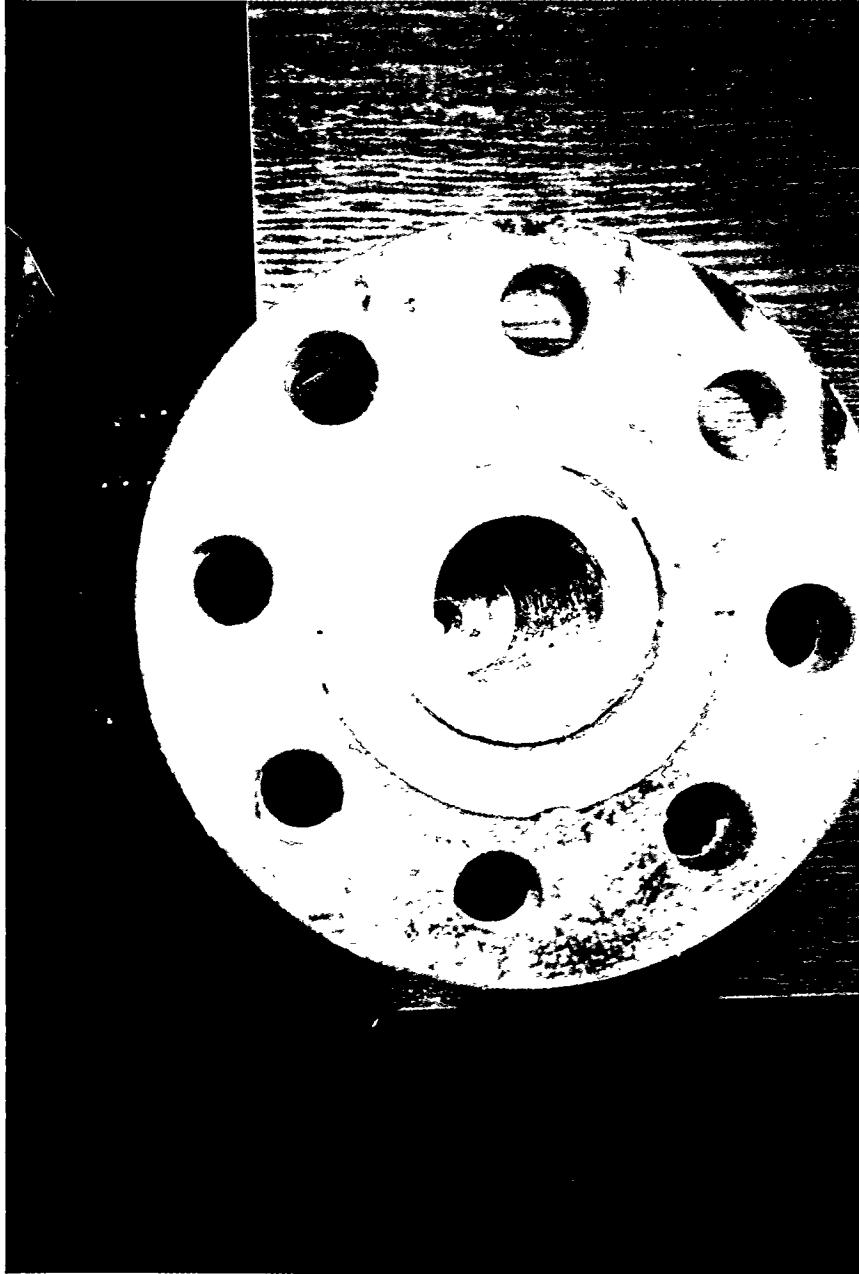


**Figure 4.8.13 - Photograph of Alternate Ash Line Restrictive Orifice**

## Results

---

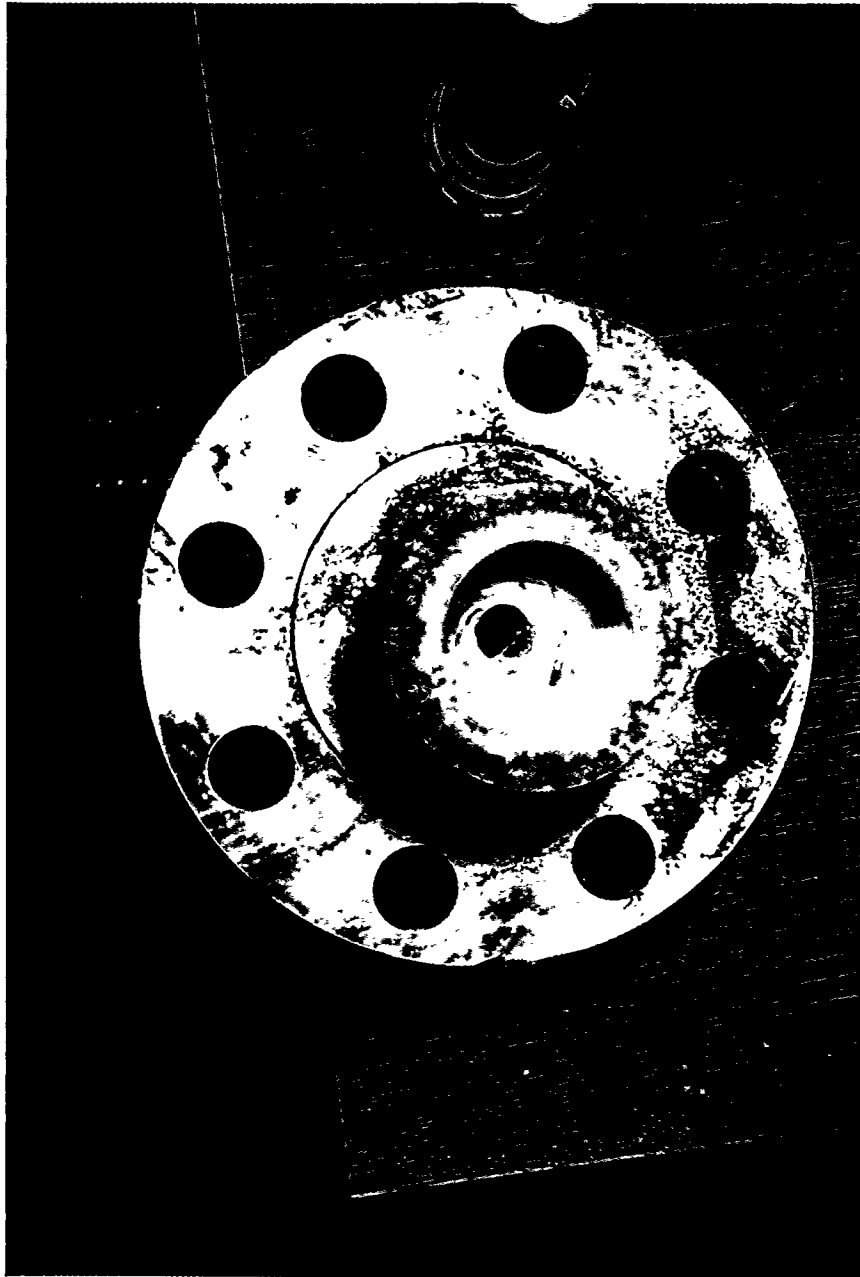


Figure 4.8.14 - Photograph of Alternate Ash Line Restrictive Orifice

## Results

---



**Figure 4.8.15 - Photograph of Hastelloy Liner After Removal From Pipe Section**

## Results

---

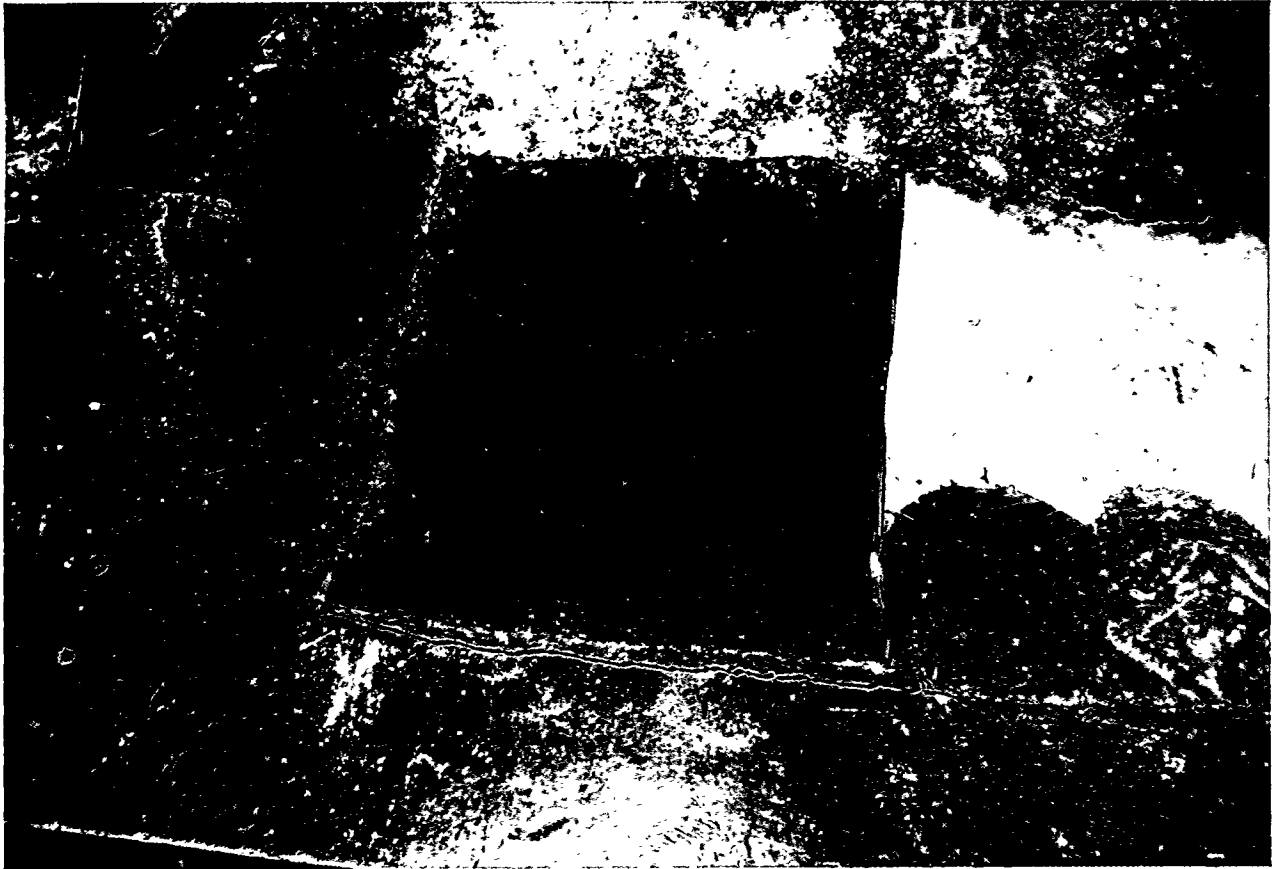


**Figure 4.8.16 - Photograph of Inside Surface of Carbon Steel Pipe Under Hastelloy Liner**

## Results

---



**Figure 4.8.17 - Photograph of Inside of Pipe Spool Following Removal of Section**

## Results

---



**Figure 4.8.18 - Photograph of Inside of Pipe Spool Following Removal of Section**

## Results

---



**Figure 4.8.20 - Photograph of Inside of Pipe Spool Following Removal of Section**

## Results

---

### 4.9 Materials Surveillance Test Results

In order to put the results of the material surveillance tests in the proper perspective, the operating temperature history of the Tidd APF is presented below.

Figure 4.9 is a bar graph which depicts the operating temperature history of the APF. It can be seen that two-thirds of the operating time was in the 1250-1500F range, and about one-fourth of the operating time was in the 1000-1250F range. A comparatively small percentage of the operating time was above 1500F. At the beginning of the project it was planned to operate the APF at full load conditions (1550F) as much as possible during the test program. However, a number of factors limited the operating time at full load conditions. First, Tidd PFBC could not achieve full load except during cold ambient air conditions due to the gas turbine/compressor limitations. Second, much of the operating time, the fluidized bed experienced sintering and/or fluidizing problems which precluded reaching full bed height and load. Third, hot spots on the APF limited unit load on some occasions. Two other factors caused the APF temperature to be lower than the freeboard temperature during much of the test program. Spoiling air supplied from the sorbent air system injected into the dip leg of the primary cyclone for detuning purposes lowered the gas temperature to the APF about 70 to 90F. Tempering (cooling) air was injected upstream of the APF to limit the gas temperature to 1400F during some test periods to mitigate the problem of filter pressure drop instability above this temperature. Only during the final test period when the primary cyclone was bypassed and the ash particle size was much larger did the APF operate above 1550F for sustained periods. It should be recognized that the limited operating time near the full load temperature of 1550F reduced the opportunity to observe long-term high-temperature effects on both ceramic filter elements and the metallic components inside the APF.

## Results

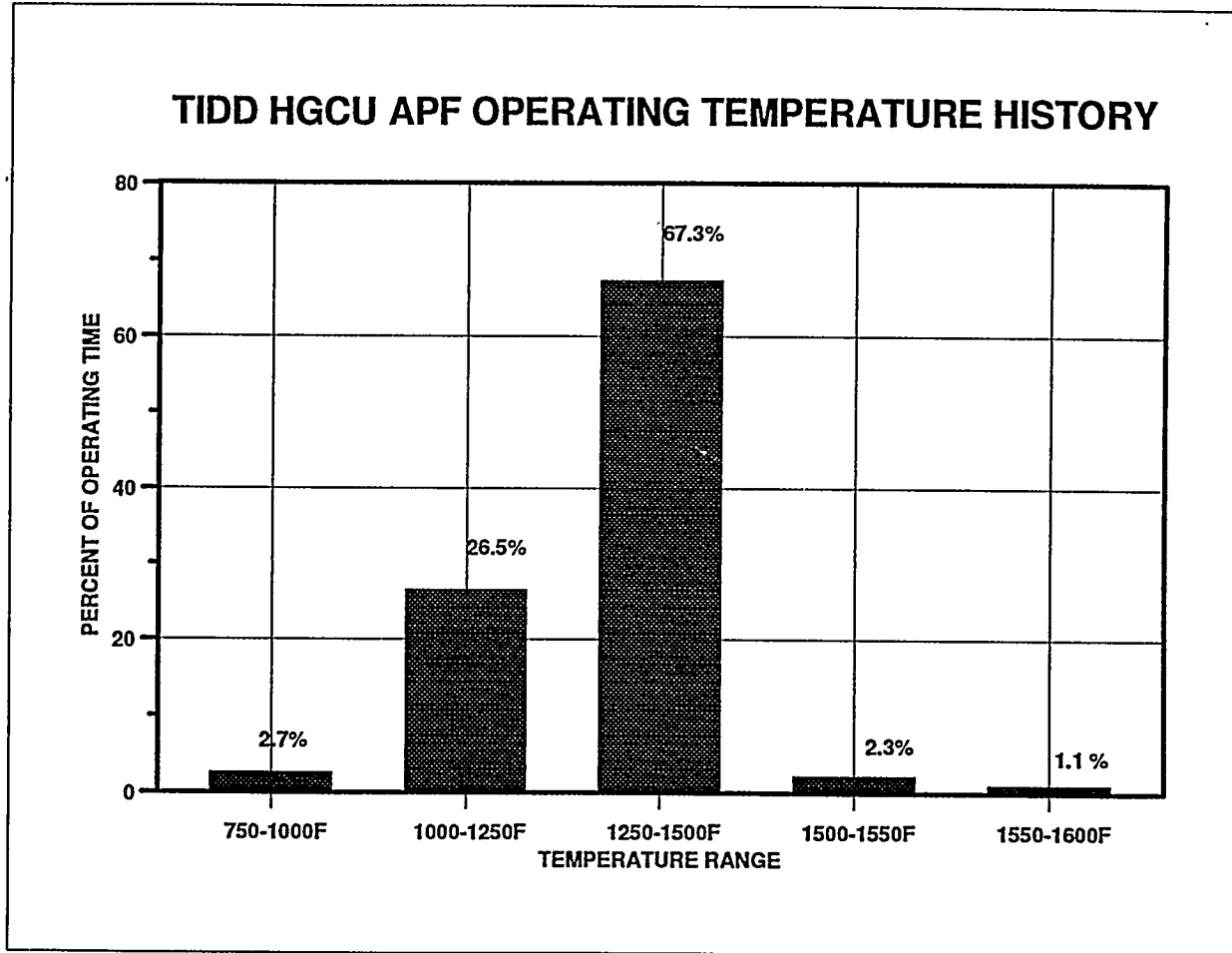


Figure 4.9 - Tidd HGCU APF Operating Temperature History

## Results

---

### 4.9.1 Metal Structures and Test Coupons

Internal structural components of the APF were inspected during a number of plant outages. The key results of these inspections are summarized in Table 4.9.1. This section provides a summary of findings observed during the test program and description of final inspections on an individual component basis. A metallurgical evaluation is described for the critical fine wire mesh used in the fail-safe regenerators. Finally, additional tests, observations and resulting conclusions are summarized for final evaluation of surveillance coupons.

**Cluster.** Type 310S stainless steel was chosen for the Tidd cluster fabrication because of the alloy's good high temperature mechanical properties and resistance to oxidation. On the other hand, it is recognized that type 310S embrittles and hardens due to sigma formation over a range of temperatures encompassing the temperature of Tidd operation.

The principal concern with respect to the expected cluster property changes was the ability to retrofit and/or repair the cluster after operation. For example, during recandling of the filter, it was found desirable to enlarge holes in the filter holder lower cast nuts. (Larger holes enhanced alignment of bolting during assembly.) Redrilling of exposed nuts (1760 hours of operation) was accomplished at Westinghouse with the use of cobalt drill bits. Other evidence of such hardening was encountered after final shutdown (5854 hours of operation) when a few filter holders were removed. Removal of the holders by grinding was found more practical than by sawing because of the hardening that had occurred.

An opportunity to retrofit the cluster was encountered in December 1992 (465 hours of operation) when it was deemed desirable to weld bars across the bottom plates of the bottom plenums to stiffen them and thereby to effect the ability to run a higher differential pressures. Prior to such retrofit, weldability testing was conducted using surveillance coupon material that had been stored in the head of the APF. Simulation welds with significant imposed restraint were prepared, metallographically examined and penetrant tested. The welds were found to be acceptable and successful retrofit was subsequently achieved.

An opportunity for cluster repair was encountered in October 1993 (1760 hours of operation). Several filter holders were found to be out of plumb and an attempt was made to mechanically straighten one at room temperature. The filter holder neck cracked in a circumferential orientation for a length of

## Results

---

approximately one inch. The type 310S (cast HK) material had evidently embrittled during exposure. Again, surveillance material that had been stored in the APF head was weldability tested. Visual and penetrant examination confirmed soundness of the test weld and heat affected zone. The filter holder crack was then repair welded.

Cluster A was chosen for visual and penetrant inspection of welds. No relevant indications were detected after 3039 hours of operation. Also no evidence of creep elongation could be detected. Cluster A was again chosen to verify the post service integrity of critical structural welds. Approximately three feet of top plenum circumferential weld joining top plate to side plate were penetrant tested. No relevant indications were found. Approximately three feet of support pipe joining top plenum to middle plenum were also penetrant tested. Again no relevant indications were found.

**Tubesheet.** Permanent distortion after prolonged high temperature exposure was possible in the thin member (1/4 inch) inner cone near to its juncture with the tubesheet inner disk. Alloy 333 was chosen for this application and analytically judged to have appropriate resistance to such creep.

Surveillance verification of creep effects was provided in the following manner. At the time of manufacture rows of fiducial marks (1/2 inch spacing) were placed parallel and perpendicular to the tubesheet inner disk-to-inner cone circumferential weld at the locations where inner cone to inner cone radial welds intersect the circumferential weld. Then three dimensional as-manufactured Silastic replicas were made at these junctures. Following shutdown, another replica was made at one of the junctures.

## Results

**Table 4.9.1 -Summary of Internal Structural Component Performance Issues and Corrective Actions**

Aberrant Component Condition	Corrective Action and Result
<p><b>Filter Holder Embrittlement</b> Attempt to straighten a filter holder at room temperature caused cracking of the neck of the holder. The 1760 hours of operation are speculated to have precipitated sigma phase and embrittled the type 310 stainless steel.</p>	<p>Performed Weldability Test on Surveillance Coupon. Repaired (Welded) Crack. While the repair was successful, subsequent straightening operations were avoided.</p>
<p><b>Pulse Pipe Cracking</b> Longitudinal cracks were noted in Incoloy 800HT pulse pipes after approximately 1760 hours. The problem is attributable to thermal fatigue.</p>	<p>Replaced Pipes using Haynes 230 NOTE: Alternate thermally sleeved design performed without incident at Karhula.</p>
<p><b>Thermocouple Sheath Degradation</b> Embrittlement and/or corrosion of type 310 stainless steel sheathing caused thermocouple failure in times less than 3039 hours.</p>	<p>Performed Service Exposure of Matrix of Alloys: 1. Incoloy 825 2. Hastelloy C276 3. Inconel 600 Subsequent operation for approximately 2815 hours showed best performance for Inconel 600.</p>
<p><b>Linear Indication in Tubesheet Lift Lug Weld (3039 hours)</b></p>	<p>Ground Out and PT. It is speculated that this indication is not service related because the lug is not stressed during operation.</p>
<p><b>Corrosion Under Tubesheet Outer Ring</b> Significant corrosion of the type 310 stainless steel liner and more shallow corrosion of the Alloy 330 outer ring was noted after 3039 hours.</p>	<p>None. Acid resistant coating is recommended in areas of condensate formation for prolonged operation.</p>
<p><b>Pulse Pipe Centering Device Broke</b> Vibrations and fatigue may have caused welds to break (3039 hours).</p>	<p>Replaced Component. NOTE: Alternate spring-loaded fixture used at Karhula has performed relatively well.</p>
<p><b>Venturi Broke</b> Tack welds and cap screws holding venturi in place broke causing dislodging of venturi (3039 hours).</p>	<p>Replaced Venturi and Seal Welded the Entire Circumference of all Venturis. Venturis remained intact and in place during subsequent operation for 2815 hours.</p>
<p><b>Shroud Rotation</b> After approximately 3039 hours of operation, significant shroud rotation was noticed. Further rotation could cause shroud to drop.</p>	<p>Welded angle Stops to Shroud Bracket. Subsequent operation showed rotation was effectively limited.</p>
<p><b>Shroud Distortion</b> After approximately 4745 hours of operation, distortion near the shroud top encumbered removal of internals.</p>	<p>Reinforced Top Section. Additional operation for approximately 1109 hours showed the newly reinforced shroud to reduce distortion.</p>

## Results

---

Careful measurements were taken to compare fiducial mark spacing as manufactured and after shutdown. No evidence of creep could be detected. In fact, purely due to limitations in measurement accuracy/precision, it can be concluded that creep was no more than one tenth of one percent. The replicas were also used to compare inner cone to inner disk angles. Using an optical comparator, as manufactured and post service angles were both measured to be 13°-50'. The tubesheet may therefore be judged to have resisted detectable creep during its 5854 hours operation at Tidd.

Following final shutdown the tubesheet top liner and localized Fiberfrax insulation were removed to expose: (1) the entire inner cone-to-tubesheet inner disk circumferential weld, (2) one (of three) inner cone-to-inner cone radial welds, (3) one (of three) outer cone-to-outer cone radial welds, and (4) a limited length (about one foot each) of top cap-to-cone and outer cone-to-outer ring welds. Penetrant examination of the aforementioned welds revealed no relevant indications.

**Pulse Pipes.** The performance of pulse pipes was considered a particularly relevant issue of metal ally performance for the Tidd APF. Incoloy 800 HT was chosen for Tidd's original pulse pipe fabrication because of its superior performance relative to type 310S stainless steel at Grimethorpe.

All nine of the Tidd pulse pipes were 100% dye penetrant inspected on their outside surface at site and prior to installation in the APF head. No relevant indications were detected. In December 1992 (465 hours of operation) one Incoloy 800 HT pulse pipe was inspected by dye penetrant examination and radiography. While dye penetrant examination was found to be inconclusive, radiography indicated satisfactory pulse pipe performance.

In December 1993 (1760 hours of operation) one Incoloy 800 HT pulse pie was removed from Tidd and examined by multiple destructive sectioning and metallography. Cracking was noted to have initiated on the pipe's inside surface similar to cracking found in Incoloy 800 HT in the APF at Karhula. The Karhula pulse pipe cracking was attributed to thermal fatigue arising from repetitive "cold" pulsing of this normally hot structure. All nine pipes were replaced with pipes made of a potentially more fatigue resistant material -Haynes Alloy 230.

The Haynes 230 pulse pipes were examined by borescopic, visual and penetrant examination in October 1994 (2985 hours of operation for these pipes). Two of the three bottom plenum pulse pipes showed through-wall longitudinal cracks. While exposed to more hours of operation than the Incoloy 800 HT pulse pipes, the Haynes 230 material was evidently not sufficiently resistant to fatigue for prolonged

## Results

---

service at Tidd operating conditions. The pipes were again replaced with Haynes 230 and performed without macroscopic cracking for the balance of Tidd operation (1109 hours of additional operation).

Geometric constraints and issues of material availability were key elements in the decisions at Tidd to utilize relatively fatigue resistant materials for the back pulse pipes. In contrast, the larger pulse pipe size at Karhula permitted a design alternative, i.e., use of a sacrificial thermal barrier sleeve inserted inside of the primary pulse pipe. This design, consisting of a thin Alloy 333 sleeve within an Alloy RA 253MA pulse pipe, has thus far performed without visually detectable problems in the APF at Karhula.

**Fail-Safe Regenerators.** The fail-safe regenerators used at Tidd were comprised of type 310 stainless steel Raschig rings sandwiched between two Haynes Alloy 25 (Alloy L 605) fine mesh screens using a type 310 stainless steel body. The fine mesh was the most delicate member of this package. Degradation of the 0.0055 inch diameter wire used for this mesh may result from high temperature corrosion (e.g., oxidation) and/or thermal shock during back pulsing. Appendix II presents additional discussion of the performance of the fail-safe regenerators.

Fine mesh used at both Karhula and Tidd was compared to as manufactured mesh. Samples of these three conditions were silver flash coated and nickel electroplated (to preserve edge and/or oxide), mounted in cross section and prepared metallographically. Photo micrographs of unetched cross sections of individual wires are shown in Figure 4.9.1, 4.9.2 and 4.9.3. A thin (0.0001 to 0.0008 inch) layer speculated to be oxide developed on the surface and/or into the substrate of the exposed wires. In addition, reaction is evident in a zone within approximately 0.0015 inches of the surface. Both Karhula and Tidd samples appeared to be of similar condition even though the times and temperatures of exposure were somewhat different. Protracted exposure would need to be conducted to verify if the oxidation/precipitation has stabilized and reached a steady state.

**Coupon Examinations.** High temperature oxidation/corrosion of alloys chosen for Tidd structures (Alloy 333 and Type 310 stainless steel) and of candidate alloys for retrofit and/or future filter applications (Alloys 617, 556, 188 and 253 MA), was monitored using a surveillance tree which suspended such alloy coupons on the top side of the tubesheet inner disk during the entire 5854 hours of Tidd operation.

## Results

Nominal compositions and weight comparisons of the samples are shown in Table 4.9.2. All alloys showed slight weight loss except for Alloy 556 which showed a slight weight gain.

Samples of all coupons were silver flash coated and nickel electroplated (to preserve edge and/or oxide), mounted in cross section and prepared metallographically. Photo micrographs comparing unetched cross sections are provided in Figures 4.9.4 through 4.9.9. The nickel based alloys 333 and 617, cobalt based alloy 188 and type 310 stainless steel all showed surface reaction (0.0005 to 0.001 inch thick) and near surface grain boundary reaction up to 0.004 inch deep. Alloy 253 MA showed no grain boundary reaction but developed approximately 0.001 inch thick surface product. Alloy 556 showed a relatively thick (0.003 inch) surface layer and approximately 0.006 inch deep grain boundary reaction.

The reaction of all alloys studied is considered to be modest in the context of their thick section structural applications. Several mils of affected substrate represents a percentage of the substrate of the order of only 1%. Furthermore, the slight weight changes suggest that the reaction is relatively stable after 5854 hours.

**Table 4.9.2 - Surveillance Tree Coupon Weight Comparisons**

Alloy	Nominal Composition							Weight			
	Ni	Cr	Fe	Si	Mo	Co	W	Original, gm	Final, gm	Change, gm	% Change
333	45	25	18	1.0	3	3	3	32.76	32.67	-.09	-0.3
617	45	22	3	1	9	12		33.22	33.12	-.10	-0.3
556	21	22	31	0.5	3	18	3	32.49	32.54	+.05	+0.2
188	22	22	3	0.35		37	14	35.81	35.68	-.13	-0.4
253MA	11	21	65	1.7				31.02	30.92	-.10	-0.3
310	20	25	52	0.5				30.77	30.70	-.07	-0.2

## Results

---

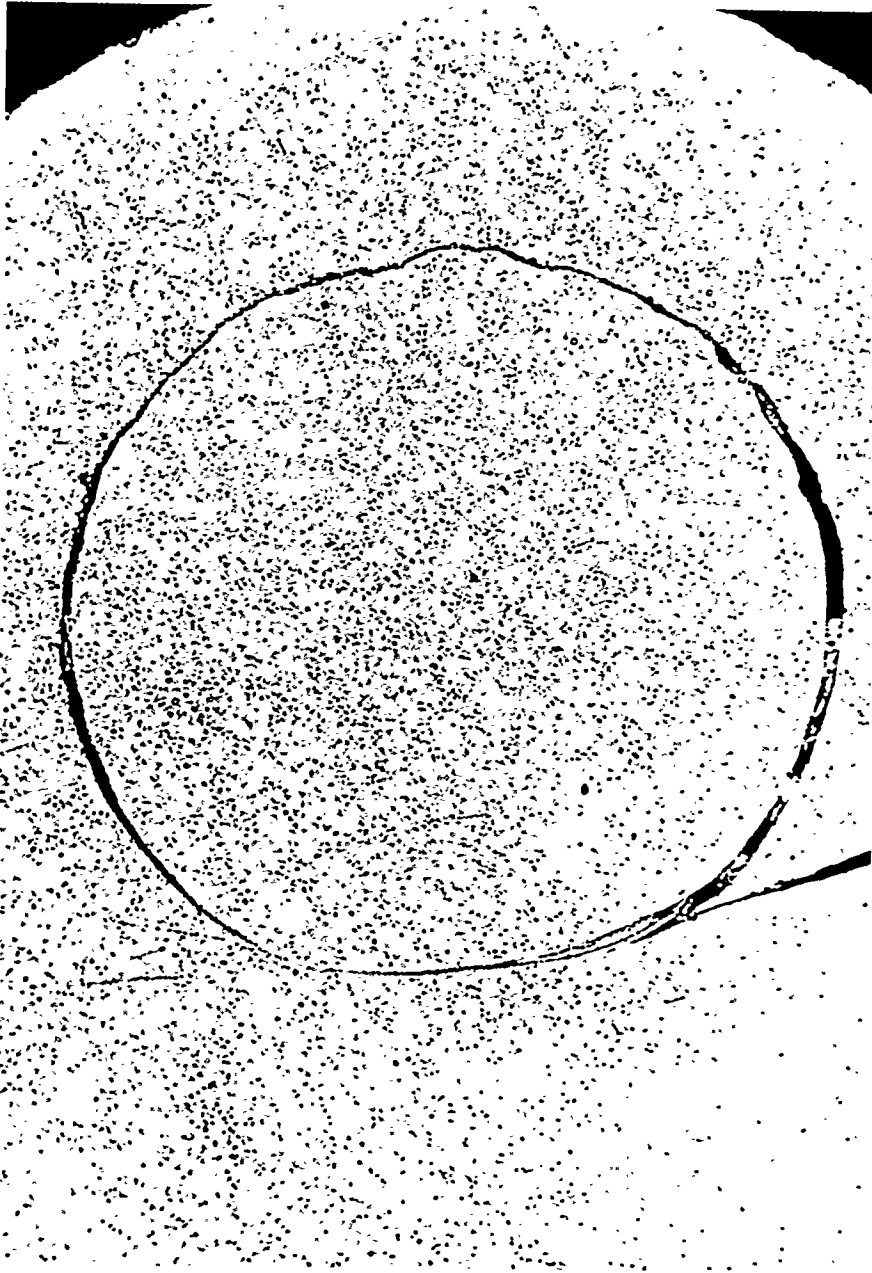


**Figure 4.9.1 - Cross Section of 0.005-inch Wire from Fine Fail-safe Mesh As New-700X**

## Results

---

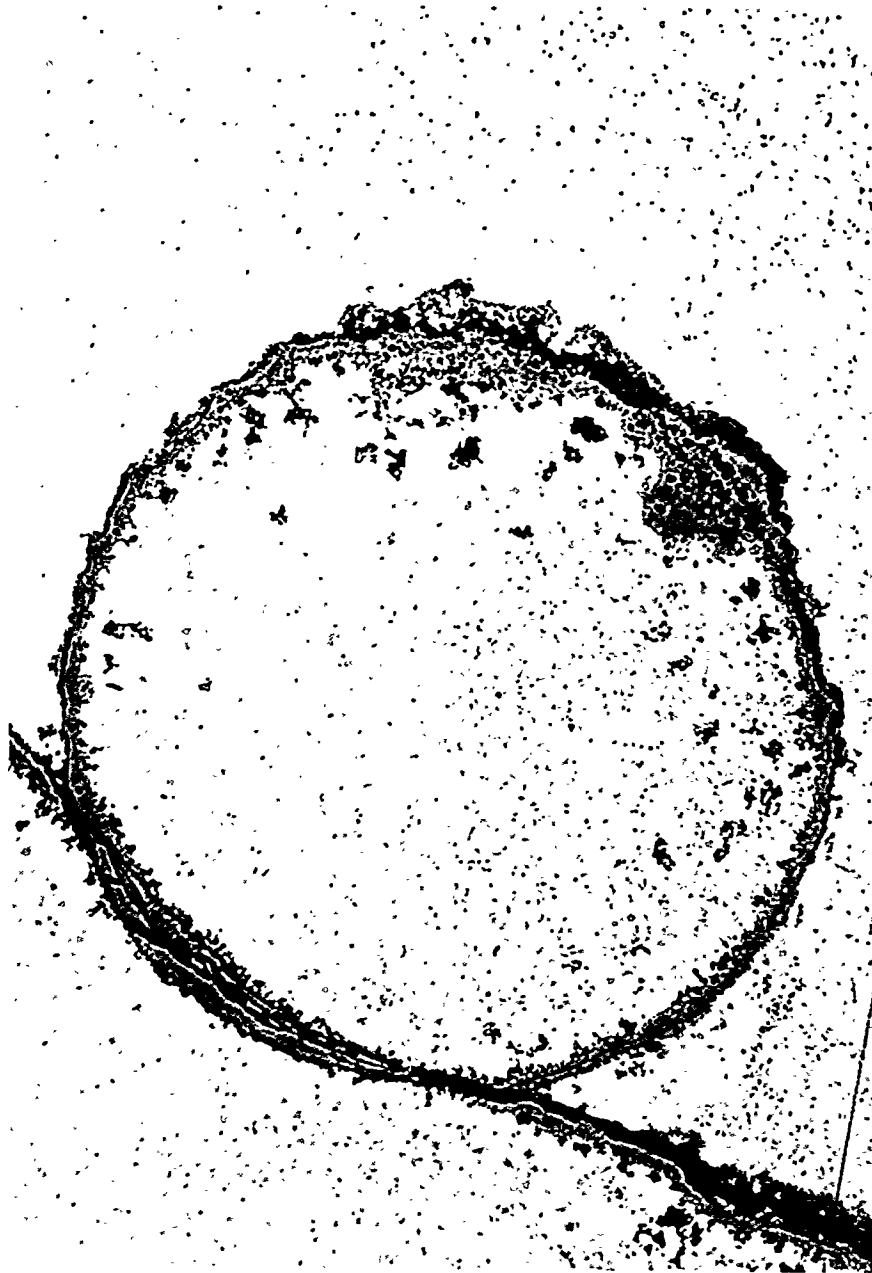


**Figure 4.9.2 - Cross Section of 0.005-inch Wire from Fine Fail-safe Mesh After 1329 hours at Karhula-700X**

## Results

---

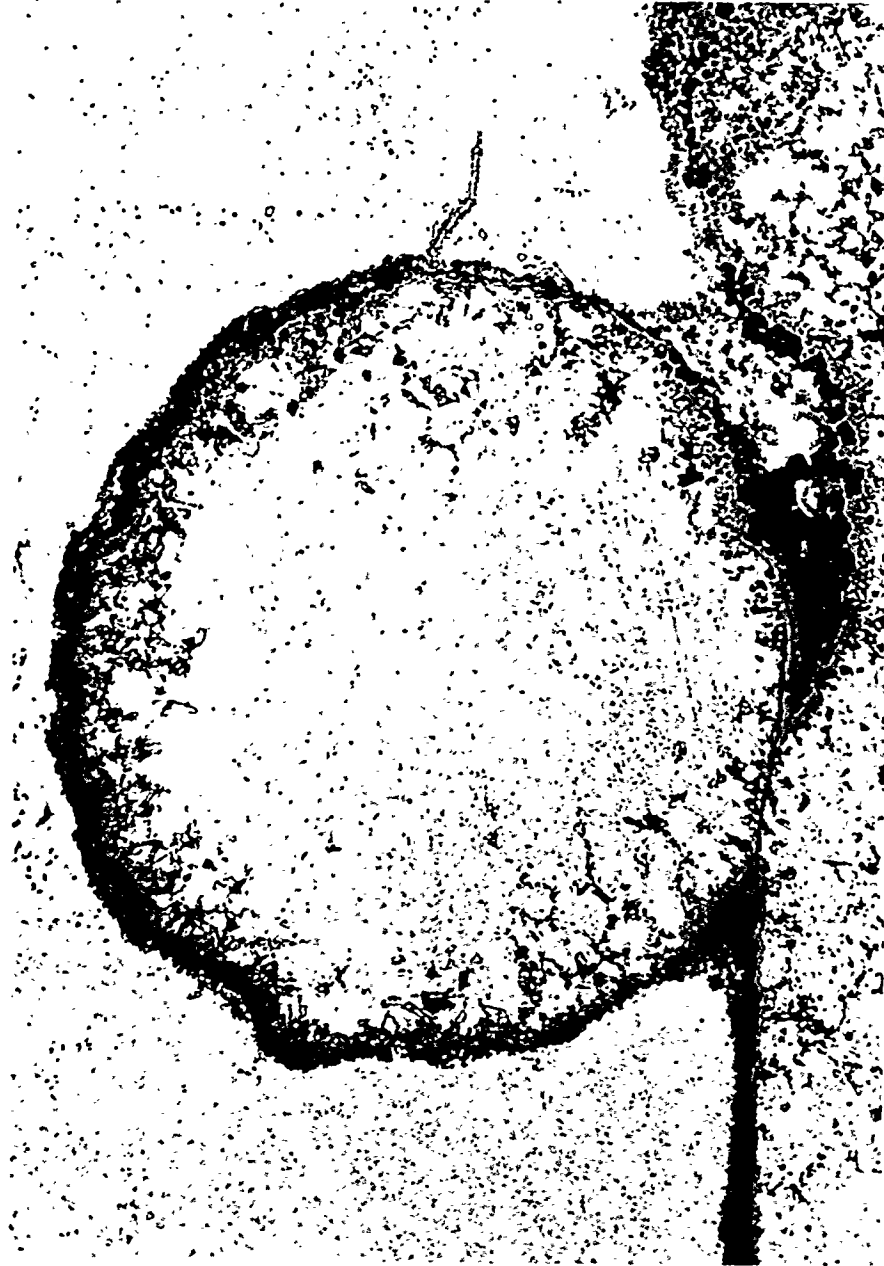


**Figure 4.9.3 - Cross Section of 0.005-inch Wire from Fine Fail-safe Mesh After 1110 hours at Tidd-700X**

## Results

---

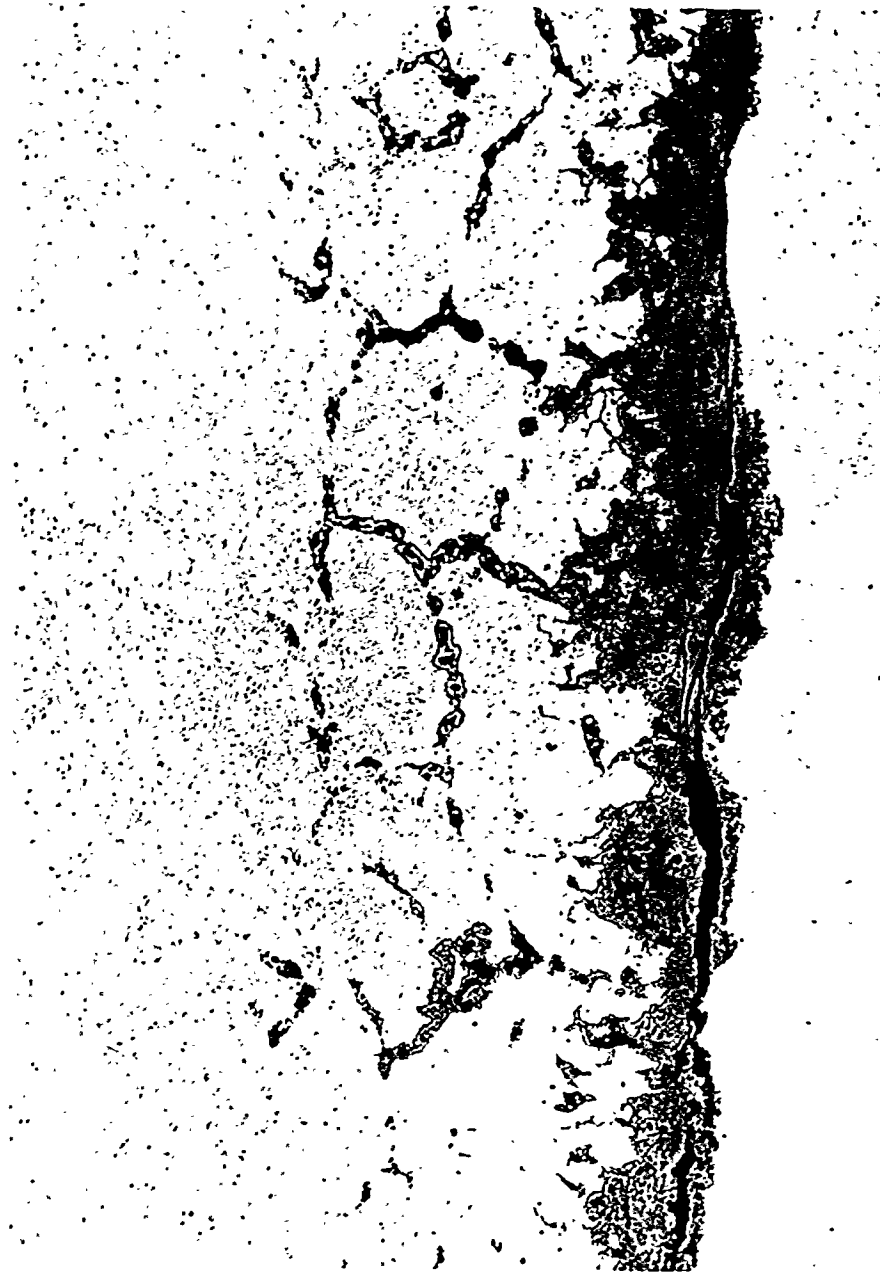


**Figure 4.9.4 - Cross Section of Alloy 333 Coupon-700X**

## Results

---

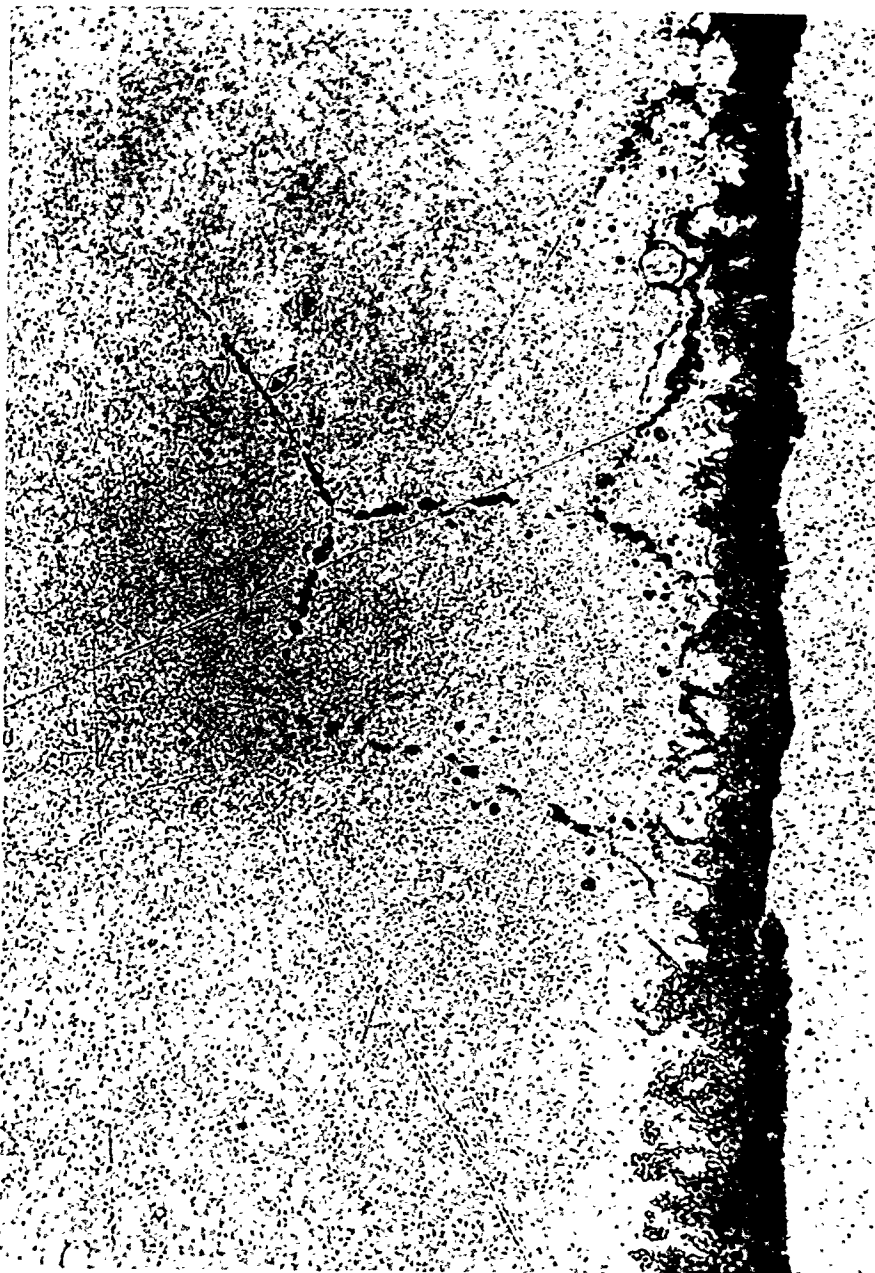


**Figure 4.9.5 - Cross Section of Alloy 617 Coupon-700X**

## Results

---



Figure 4.9.6 - Cross Section of Alloy 556 Coupon-700X

## Results

---



**Figure 4.9.7 - Cross Section of Alloy 188 Coupon-700X**

## Results

---



**Figure 4.9.8 - Cross Section of Alloy 253MA Coupon-700X**

## Results

---

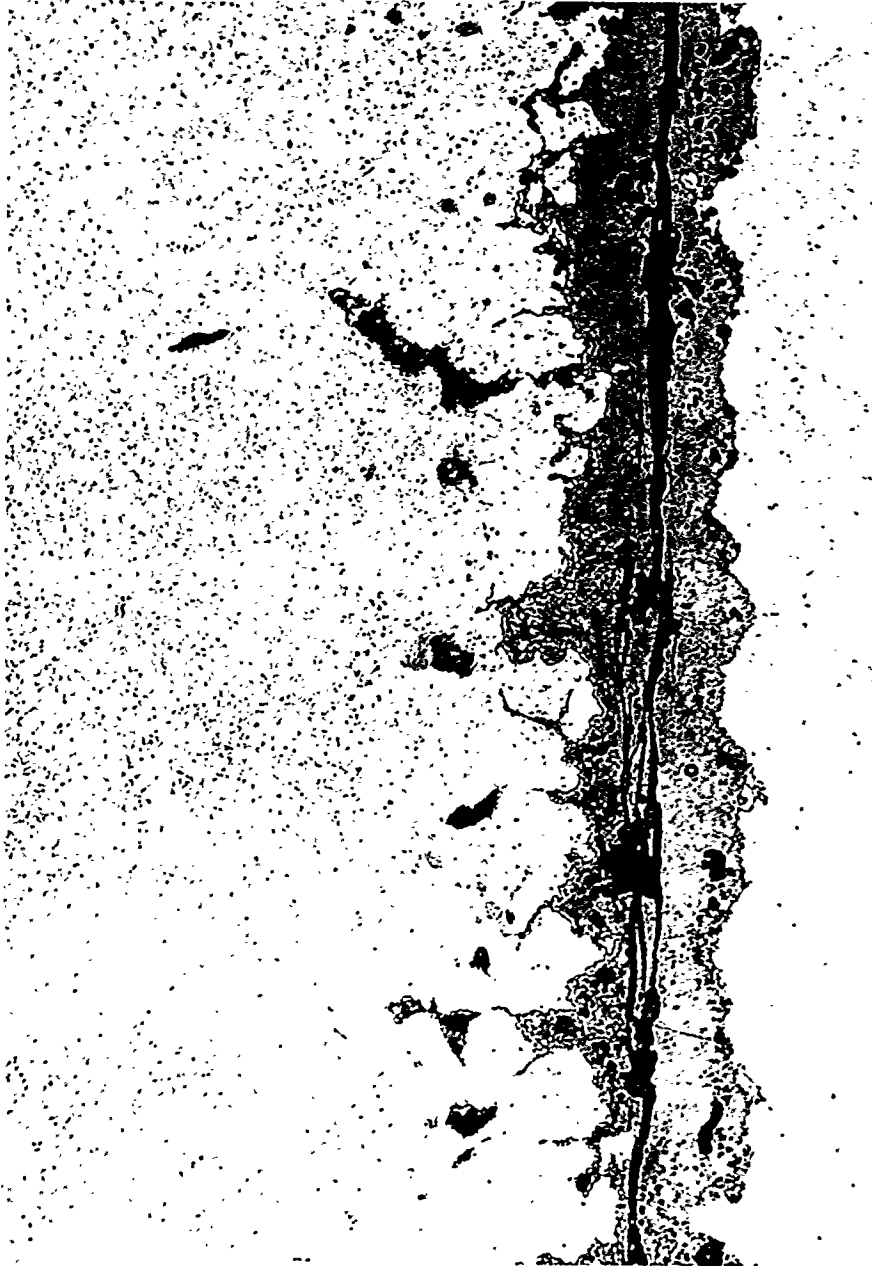


**Figure 4.9.9 - Cross Section of Alloy 310 Coupon-700X**

## Results

---

### 4.9.2 Candle Filters

Westinghouse conducted material surveillance tests on selected candle filters throughout the HGCU program. This section presents a discussion of candle surveillance testing and summarizes the conclusions reached during the surveillance program.

All filter candles were subjected to a formal QA/QC program both at the supplier sites and at Westinghouse or Tidd Plant. The surveillance program included post-test non-destructive inspection and characterization of selected filter candle properties, such as gas flow resistance, measurements of creep and bow, and time-of-flight measurements. Destructive testing to determine residual bulk strength and morphological changes was also performed.

### Filter Selection and Qualification

Throughout this program, it was the responsibility of the filter suppliers to meet defined material tolerance specifications for filter length, outer body diameter, flange diameter and length, concentricity, perpendicularity, gas flow resistance, and particle collection efficiency. Generally, re-inspection of filter elements either on an entire production batch or on a randomly selected basis was conducted prior to final selection and installation within the filter in order to confirm production quality and uniformity.

The material properties of the filter matrix defined the required composition, construction, porosity, membrane thickness and manner of its application in order to achieve a desired gas flow resistance, particle collection efficiency and bulk matrix strength. Similarly, the specific manufacturing process defined the component wall thickness, flange and end cap assembly, and final weight of an individual filter element. Post-manufacturing QA/QC testing frequently included a final visual inspection to screen for not only unwanted cracks, chips, voids and/or bumps, but also a smooth and uniform texture of the outer filter wall surface. Both bubble and/or burst testing were conducted by the suppliers to ensure the as-manufactured integrity of the filter element, and ultimately to identify and reject elements which had inherent cracks, flaws or an inadequately coated membrane surface, prior to shipment and installation.

As shown in Figure 4.9.10, current monolithic and advanced second generation candle filters have achieved acceptable gas permeability tolerances (i.e., 1 in. H<sub>2</sub>O / fpm at 70°F) for use in advanced coal-fired applications. Pre-qualification testing was frequently conducted at Westinghouse to assure that a

## Results

>99.99% particle collection efficiency was achieved by the filter elements at simulated steady-state PFBC process operating conditions, prior to acceptance for field use. Pre-qualification testing was designed to qualify the performance and integrity of filter elements under extreme conditions such as accelerated pulse cycling which monitors the performance of the matrix with respect to thermal fatigue, or exposure to thermal transient events which simulated rapid start-up or shut-down ramps experienced during process upset conditions. During pre-qualification testing, the as-manufactured strength of the flange was evaluated, and mechanical sealing and mounting of the element within the filter holder were assessed. Candle filters were required to have an as-manufactured bulk material strength of >1800 psi. During conduct of this program, residual or conditioned strengths of 800-1200 psi were observed after 3000-6000 hours of operation of the Schumacher Dia Schumalith F40 filters. The conditioned strength of the Schumacher filters was adequate to permit retention of the candle's physical integrity, and continued process operation of the filter elements.

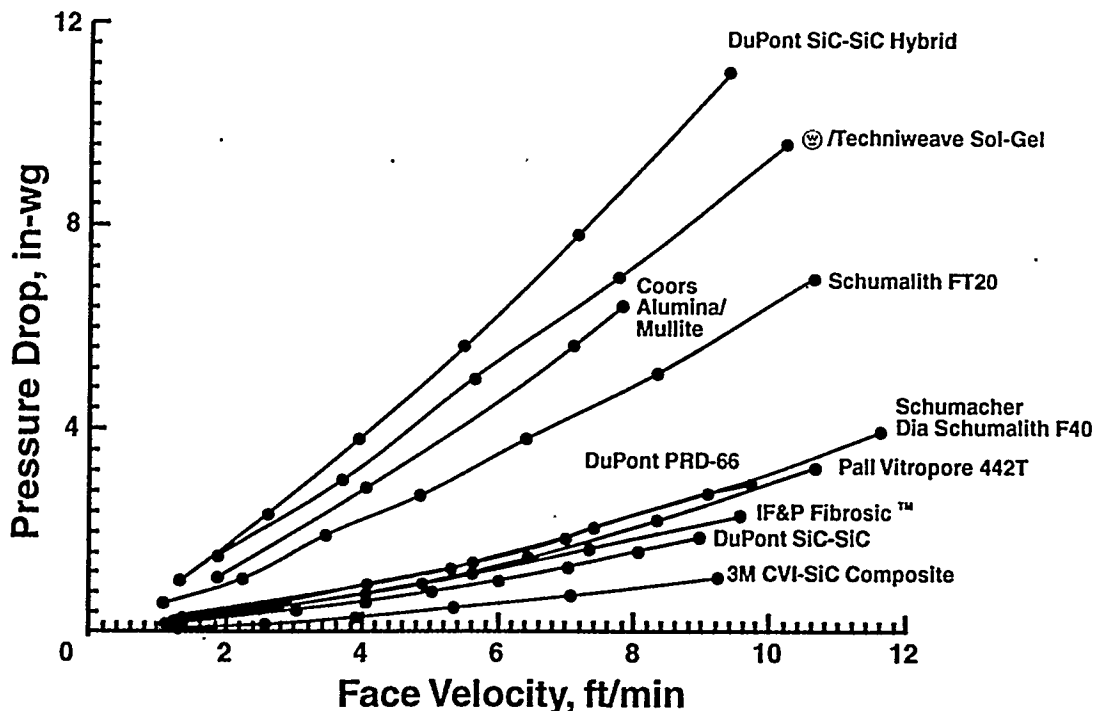


Figure 4.9.10 - Room Temperature Gas Flow Resistance of the First Generation Monolithic and Advanced Second Generation Candle Filters

## Results

---

### Posttest Inspection And Characterization

Filter elements were randomly subjected to posttest gas flow resistance measurements, overall length measurements to detect creep within the matrix, bow and/or perpendicularity measurements prior to conducting destructive testing which determined the residual bulk matrix strength, and phase and morphological changes that resulted within the filter matrix.

**Gas Flow Resistance Measurements.** During operation, fines accumulated along the surface of the candles which increased the pressure drop across the porous ceramic filter elements. In order to remove the collected dust cake layer, pulse gas was delivered to the ID of the candles, which permeated through the filter wall, releasing the deposited fines from the filter element surface. After each pulse cycle event, a conditioned layer of fines was expected to remain along the element, while the majority of the deposited ash was collected in the ash hopper.

Frequently, ash nodules 1 cm diameter x 0.5-1.0 cm high formed along the filter surface during operation. Similarly, continuous dust cake layers formed which ranged from 1-2 mm to 1-1.5 cm. When ash bridging events resulted within the filter array prior to detuning or bypassing of the primary cyclone, the nodules or dust cake layer were observed to be separated from the bridged mass of ash which formed between adjacent candles, or between candles and the plenum pipes or dust sheds.

As shown in Figure 4.9.11, the pressure drop or gas flow resistance through the filter element increased as fines collected and remained along the outer surface of the filter elements. Following normal operating conditions, the as-manufactured gas flow resistance was regenerated by simply washing the elements with water and drying. In the event that candles failed and process operation continued, fines released into the clean gas stream were pulsed back into the inner wall of the remaining intact filter elements. Posttest washing of these elements generally did not permit regeneration of the as-manufactured gas flow resistance, since the fines typically blinded the inner wall of the coarse support matrix. Since the ID fines generally could not be removed, the elements were eliminated for continued use.

## Results

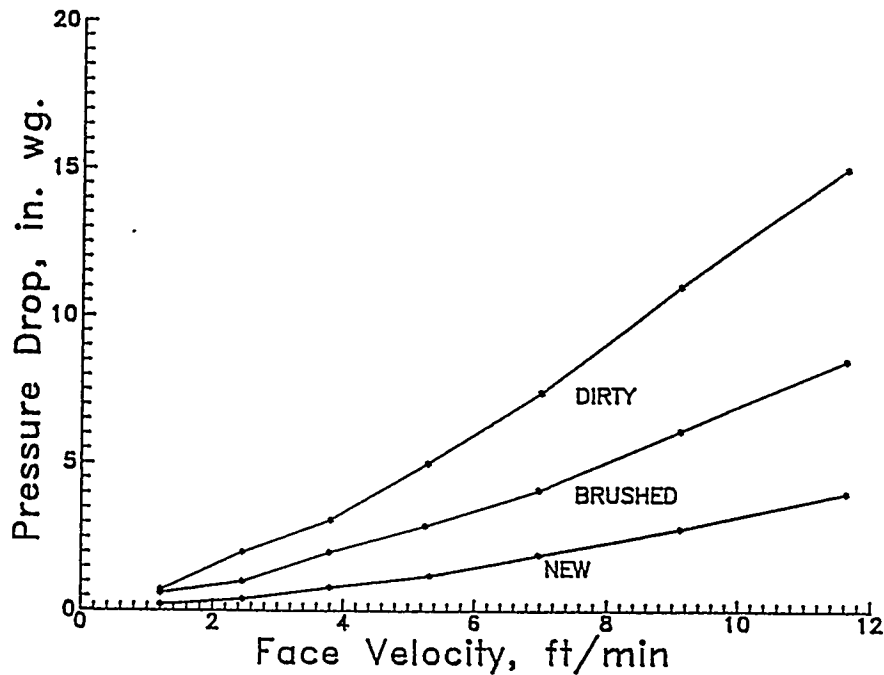


Figure 4.9.11 - Room Temperature Gas Flow Resistance Measurements Across As-Manufactured Clay Bonded Silicon Carbide Filter Elements. Measurements Were Repeated After Operation at Tidd.

**Bow and Creep Measurements.** During normal operation, overall straightness of the candle filters was maintained. When ash bridging events occurred within the filter, bowing of the clay bonded silicon carbide elements resulted (see Figure 4.3.8). Following 464 hours of operation in Test Period I, a maximum bow of 17 mm was observed along the length of the Schumacher Dia Schumalith F40 candle filter body. This significantly exceeded the 3 mm as-manufactured Westinghouse tolerance for allowable bow.

Bowing which occurred in the clay bonded silicon carbide filters resulted from softening or plastic deformation of the binder in the Schumacher Dia Schumalith F40 filter matrix when it was subjected to an applied load. In addition to bowing, softening of the binder phase resulted in the elongation of the filters during operation as shown in Table 4.9.3. The extent of elongation of either the Schumacher Dia

## Results

Schumalith F40 or Pall Vitropore 442T clay bonded silicon carbide candles was not sufficient to fail the elements through the creep crack growth mechanism that had been identified for the Pall Vitropore 442T elements during operation in Ahlstrom's pressurized circulating fluidized-bed combustion test facility.

**Time-Of-Flight and Burst Strength Measurements.** During this program, Westinghouse focused its efforts on conducting a filter material surveillance program which monitored the residual bulk strength and phases present within the various elements after each Test Period. After Test Period I, time-of-flight (TOF) measurements were also performed on 32 filters prior to subjecting select filter elements to destructive materials characterization. As shown in Table 4.9.4, with the exception of two candles, each filter element experienced an increase in its TOF measurement after exposure to the Tidd operating conditions. Although ash and sorbent fines remained along the surface of the candles (i.e., a portion of the non-removable conditioned layer) and through the filter wall (i.e., ID wall pulse cycled fines) after each element had been vacuumed brushed, the presence of fines did not appreciably impact the resulting TOF measurements.

**Table 4.9.3 - Elongation of Clay Bonded Silicon Carbide Candle Filters**

Filter Type	Test Period	Operating Time, Hours	Elongation, mm
Schumacher F40	I	464	1
	I, II, III, IV	4744	3
	I, II, III, IV, V	5854	5-7
Pall Vitropore 442T	IV	1706	ND
	IV, V	2816	17-20
	V	1110	0-4

ND: Not Determined.

## Results

**Table 4.9.4 - Posttest Candle Filter Time-Of-Flight Measurements**

Candle	Position	Tag Number	TOF, $\mu$ sec				
			Initial	Vacuumed Brushed	$\Delta$ TOF	Vacuumed Brushed Washed/Dried	$\Delta$ TOF
1	A/T-1 *	492	330	337	7	337	7
2	B/T-1 *	504	332	339	7	331	-1
3	B/T-23	459		338		333	
4	A/M-1 *	367	332	340	8	339	7
5	B/M-1 *	436	336	343	7	343	7
6	B/M-23	244		344		334	
7	A/B-5 *	028	343	353	10		
8	A/B-6 *	065	348	362	14		
9	A/B-7 *	019	340	356	16		
10	A/B-8 *	083	339	342	3		
11	A/B-16 *	075	343	351	8		
12	A/B-17 *	172	342	349	7		
13	A/B-18 *	164	338	347	9	346	8
14	A/B-19 *	002	339	353	14		
15	A/B-35 *	056	346	357	11		
16	A/B-36 *	071		352		351	
17	B/B-1 *	193	323	335	12	334	11
18	B/B-5 *	343	345	356	11		
19	B/B-6 *	297	334	341	7		
20	B/B-7 *	115	335	340	5		
21	B/B-8 *	238	331	339	8		
22	B/B-16 *	089	350	342	-8		
23	B/B-17 *	328	339	344	5		
24	B/B-18 *	253	335	344	9	346	11
25	B/B-19 *	213	323	342	19		
26	B/B-34	127		340			
27	B/B-45	106		348			
28	C/B-5	187		347			
29	C/B-6 *	178	333	344	11		
30	C/B-7 *	129	347	356	9		
31	C/B-17 *	314	332	338	6		
32	C/B-18 *	097	351	345	-6	347	-4

\* Initial Surveillance Candles.

## Results

As shown in Figure 4.9.12, a direct correlation between room temperature C-ring compressive and burst strength of the 464 hr PFBC-exposed clay bonded silicon carbide filter matrix resulted particularly for candles that were located in a common cluster or location within the system. As the TOF value for a given filter element increased, the room temperature C-ring compressive strength of the clay bonded silicon carbide filter matrix decreased, again for candle filters that were located in a common cluster. Cluster A candles and the bowed Cluster B candles tended to deviate from the TOF/C-ring compressive and burst strength/C-ring compressive relationship.

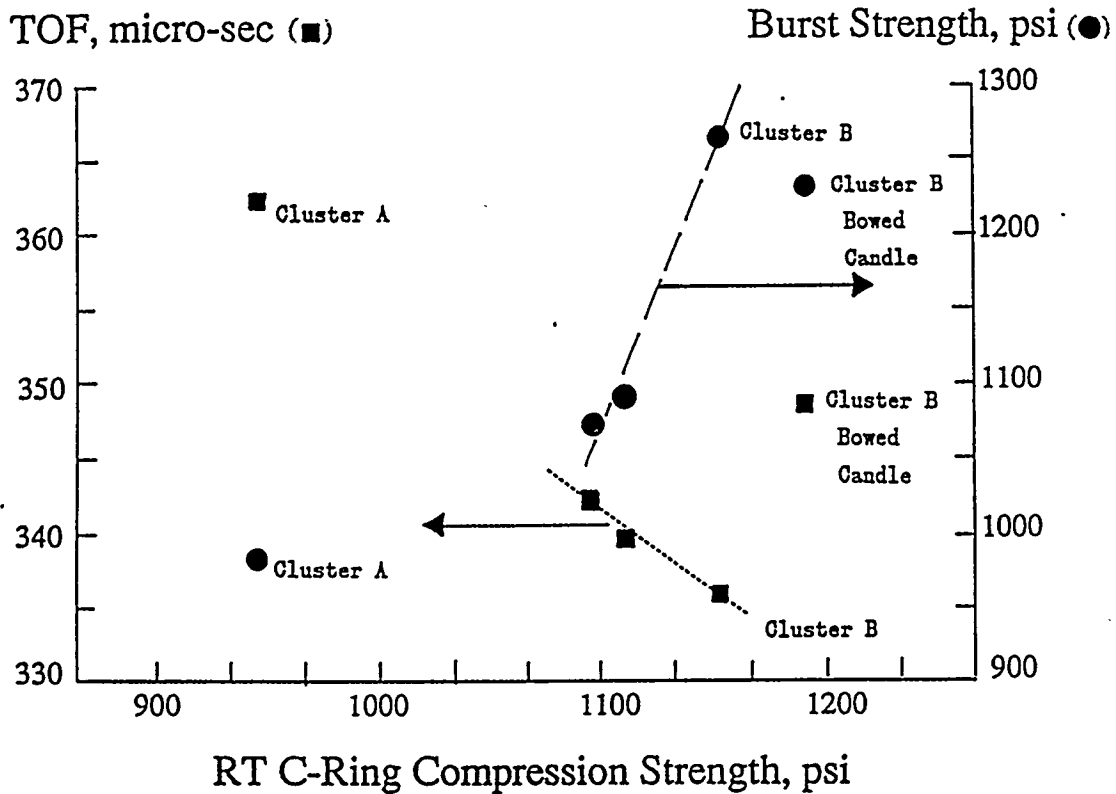


Figure 4.9.12 - Correlation of Time-of-Flight and Burst Strength with Room Temperature C-Ring Compressive Strength for Candle Filters Exposed for 464 Hours of PFBC Operating Conditions in Test Period I.

## Results

Table 4.9.5 lists the number of each type of candle filter used in the five test periods. First generation, monolithic, Schumacher Dia Schumalith F40 clay bonded silicon carbide candle filters were primarily used during the first four test periods. During the last two test periods, advanced, second generation candle filter elements were used.

With the exception of ash bridging which failed the filter elements, the stability and long-term viability of the "aged" or "conditioned" candle filter materials were demonstrated during operation in the PFBC gas environment. A summary of the residual strength, microstructural and phase changes which occurred during operation of the first and second generation candle filter materials is presented in this section. Table 4.9.6 presents a summary of the candle filter failure mechanisms experienced during operation at Tidd.

**Schumacher Dia Schumalith F40.** The Schumacher Dia Schumalith F40 filter matrix consists of an aluminosilicate binder phase that encapsulates and bonds together silicon carbide grains, forming 40-50  $\mu\text{m}$  pores within a 15-mm thick support wall. An  $\sim 100 \mu\text{m}$  thick, aluminosilicate fibrous membrane is applied to the outer surface of the filter body, in order to prevent fines penetration into and/or through the porous ceramic filter wall. During test operation, the integrity of the membrane was retained, imparting complete barrier filtration characteristics to the Schumacher Dia Schumalith 40 filter matrix.

**Table 4.9.5 - Filter Candle Materials**

Test Period	I	II	III	IV	V
Type of Filter	Number of Filter Elements				
Schumacher F40	384	384	384	258	5
Schumacher FT20	—	—	—	8	—
Pall Vitropore 442T	—	—	—	8	153
Coors Alumina/Mullite	—	—	—	8	98
3M CVI-SiC Composite	—	—	—	3	10
DuPont PRD-66	—	—	—	3	22

## Results

**Table 4.9.6 - Candle Filter Failure Mechanisms Experienced During Operation at Tidd**

Filter Element	Maximum Hours of Operation/ (Test Period)	Failure Mechanism	Comments
Schumacher Dia Schumalith F40	5854 (I, II, III, IV, V)	Ash Bridging	Maximum elongation of 5-7 mm; Reduction of strength; Conditioned strength of 800-1200 psi; Binder crystallization; Bowing under load; Failure at base of the flange during bridging; Failure along end cap when ID filled with ash
Schumacher Dia Schumalith FT20	1706 (IV)	None-Experienced	Improved high temp. creep resistant binder; No loss of strength identified
Pall Vitropore 442T	2816 (IV, V)	None-Experienced	Maximum elongation of 17-20 mm; Strength reduction
Coors Alumina/Mullite	2816 (IV, V)	Possible Thermal Fatigue	Mid-body or failure at the base of the flange for isolated elements; End cap failure when ID filled with ash; Loss of strength experienced at elevated operating temperatures
3M CVI-SiC	1706 (IV)	Ash Bridging	Failure at the base of flange during bridging; Failure along end cap when ID filled with ash; Apparent strength increase due to fines filling matrix wall
DuPont PRD-66	1706 (IV)	Divot Formations Mid-Body Failure	Failure occurred at the base of the flange when ash encapsulated the filter holder mount; Body thinned where divots formed; Divots may be responsible for mid-body fracture; Apparent strength increase due to fines filling matrix wall; Minimal adherence of ash along outer filtration surface; Bridging and ash ID bore filling did not cause failure

## Results

Within the entire candle filter assembly, generally 5-16% of the Schumacher Dia Schumalith F40 filter elements failed during operation in Test Periods I through IV, primarily as a result of ash bridging. After removal of the primary cyclone from service in Period V, ash bridging, as well as candle failure were mitigated. Schumacher Dia Schumalith F40 surveillance candles, however, successfully achieved 5854 hours of operation. The residual bulk strength of the Schumacher Dia Schumalith F40 matrix was determined via room temperature and process temperature C-ring compressive and tensile testing. As shown in Figure 4.9.13, the process temperature bulk strength of the Schumacher Dia Schumalith F40 matrix decreased during the initial 1000-2000 hours of PFBC operation. With continued operation, however, the bulk strength of the Schumacher Dia Schumalith F40 matrix remained constant. The residual or "conditioned" strength was considered to result from the complete or nearly complete crystallization of the binder phase that encapsulated the silicon carbide grains, as well as the bond posts or ligament surfaces as shown in the photo micrograph in Figure 4.9.14.

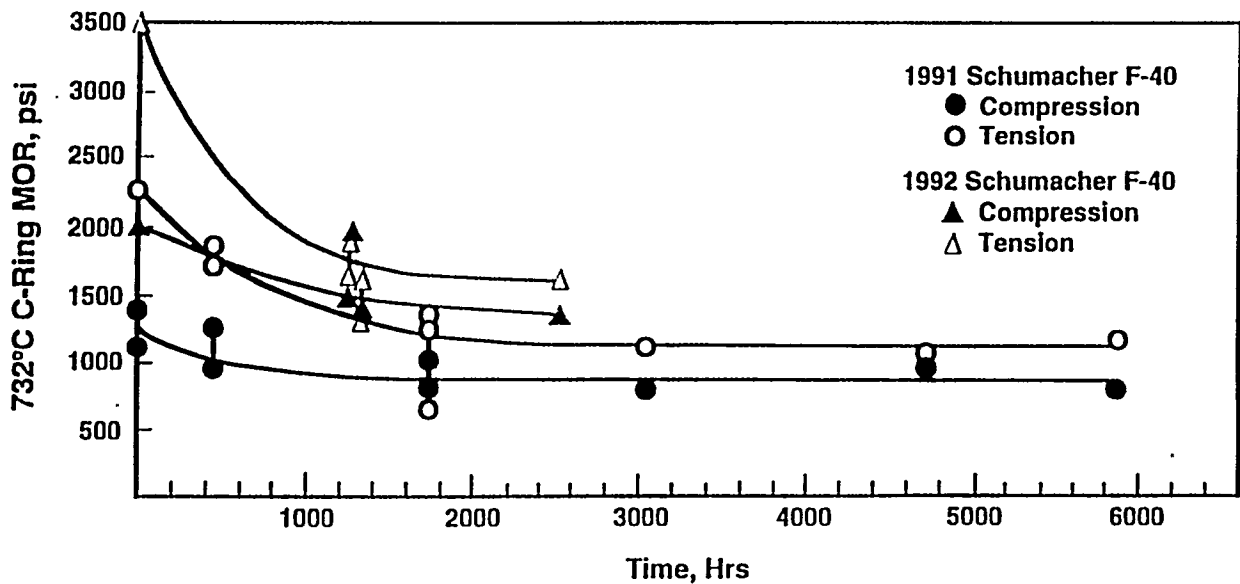


Figure 4.9.13 - Schumacher Strength Profile

## Results

---

Previous use of alternate clay bonded silicon carbide candle filters indicated that creep crack growth occurred primarily at the base of the flange, and failure of the elements resulted after 500-1000 hours of operation in ~ 1525F, circulating pressurized fluidized-bed combustion environment. In order to ascertain whether the Schumacher Dia Schumalith F40 filter matrix experienced creep during operation, the overall lengths of the surveillance filter elements were measured after the various test campaigns, and compared to their initial, as-manufactured lengths. After 5854 hours of operation, two surveillance filters were observed to have elongated by 5-7 mm. Cracks as a result of high temperature creep were not evident along the external surface of the filter elements, particularly within and/or below the densified section of the flange.

**Pall Vitropore 442T.** The Pall Vitropore 442T matrix also consists of silicon carbide grains that are bonded together via an oxide-based binder to form the 10 mm filter support wall. A finer grit silicon carbide layer is applied to the outer surface of the filter element, forming the barrier filter's membrane. During Test Period IV, eight Pall Vitropore 442T, clay bonded silicon carbide candle filters were installed and operated in the system. Similar to the "conditioning" experienced by the Schumacher Dia Schumalith F40 filters, the Pall Vitropore 442T clay bonded silicon carbide filters experienced a loss of bulk material strength after 1706 hours of operation in the PFBC gas environment as shown in Table 4.9.7.

Three of the Pall Vitropore 442T filter elements which had been used during Test Period IV were reinstalled and acquired an additional 1110 hours of operating life in Test Period V. Post-test inspection indicated that the 2816 hour PFBC-exposed Pall Vitropore 442T filters elongated by 17-20 mm. Cracks which are an indication of high temperature creep were not evident along the external surface of the filter elements, particularly in the area of the filter directly below the flange.

During Test Period V, 150 new Pall Vitropore 442T candle filter elements were installed in the APF. All candles remained intact after 1110 hours of operation. Posttest characterization of seventeen elements indicated that the filters elongated by 0-4 mm. Since all of the Pall Vitropore 442T filter elements had been identically manufactured, the difference in elongation which resulted between the two test periods was considered to reflect "aging" or the time lag required to initiate high temperature creep in the Vitropore 442T clay bonded silicon carbide candle filter matrix.

## Results

### Table 4.9.7 - Candle Filter Bulk Matrix Strength

Filter ID No.	Filter Location	Test Period No.	Operating Time, Hrs.	Room Temperature Strength, psi C-Ring Testing		High Temperature (732 °C) Strength, psi C-Ring Testing	
				Compression	Tension	Compression	Tension
Schumacher Dia Schumalith F40 - 1991 Production Lot				Compression	Tension	Compression	Tension
S153/317B	---	---	---	1300±213	1907±111	1416±127	2328±228
S504/322B	B/T-1	I	464	1120±123		1226±116	
S436/321B	B/M-1	I	464	1096±116		1172±134	
S193/318B	B/B-1	I	464	1147±119		1245±108	
S065/314B	A/B-6	I	464	940±60		1056±131	
S106/317B	B/B-45	I	464	1180±98		1230±127	
S324/319B	B/B-9	I	464	1083±148	1438±108	1137±101	1778±246
S109/317B	B/B-41	I	464	1140±120	1424±162	1132±112	1873±174
S215/378B	B/M-22	I, II	1760	908±72	1117±91	1064±72	1418±122
S447/322B	A/T-22	I, II	1760	794±50	709±71	1028±94	973±121
S455/322B	B/T-22	I, II	1760	793±58	711±89	989±77	885±54
S523/322B	C/T-22	I, II	1760	793±39	1016±134	968±96	1252±241
S418/321B	B/T-16	I, II, III	3038	720±57	944±172	890±65	1284±199
S422/322B	B/B-16	I, II, III, IV	4734	870±145	816±112	1031±105	1139±160
S228/318B	A/T-16	I, II, III, IV, V	5854	592±56	763±87	777±57	1208±99
						891±52(a)	966±47(a)
Schumacher Dia Schumalith FT20							
S199/315E	---	---	---	2296±261	2268±167	3034±148	2708±360
S039/312E	C/M-15	IV	1706	2283±184	2370±238	3041±238	3102±272
Pall Vitropore 442T							
R2-325	---	---	---	2857±186	2574±177	3430±221	3029±149
R5-325	B/M-20	IV	1706	2311±231	2034±139	2453±187	2138±180
R2-360	C/T-1	V	1110	2569±132	2277±156	2721±138	2201±212
						2454±214(a)	2115±238(a)

## Results

### Table 4.9.7 - Candle Filter Bulk Matrix Strength (Cont'd.)

Filter ID No.	Filter Location	Test Period No.	Operating Time, Hrs.	Room Temperature Strength, psi C-Ring Testing		High Temperature (732°C) Strength, psi C-Ring Testing	
				Compression	Tension	Compression	Tension
<b>Coors Alumina/Mullite</b>				Compression	Tension	Compression	Tension
DC-013	—	—	—	2575 ± 182	2721 ± 415	3107 ± 276	3353 ± 231
DC-003	B/M-16	IV	1706	2475 ± 189	2903 ± 289	2738 ± 161	3291 ± 246
DC-056	A/T-17	V	1110	2079 ± 140	2392 ± 130	2368 ± 93	2636 ± 238
						2512 ± 107(a)	2717 ± 167(a)
DC-068	A/T-1	V	1110	1958 ± 68	2544 ± 214	1800 ± 135	2542 ± 196
						2079 ± 85(a)	2659 ± 109(a)
DC-002	B/M-17	IV, V	2816	2097 ± 119	2063 ± 178	2200 ± 141	2146 ± 362
						2360 ± 116(a)	2287 ± 251(a)
<b>DuPont PRD-66</b>							
D-99	—	—	—	1219 ± 162	1265 ± 188	1277 ± 178	1304 ± 327
D-132	B/M-7	IV	1706	1830 ± 238	1725 ± 320	1884 ± 142	1642 ± 401
D-237	B/M-8	V	1110	1533 ± 202	1380 ± 188	1897 ± 256	1356 ± 104
						1872 ± 230(a)	1460 ± 197(a)
<b>Diametral O-Ring Testing</b>							
Filter ID No.	Filter Location	Test Period No.	Operating Time, Hrs.	Room Temperature Strength, psi		High Temperature (732°C) Strength, psi	
				Composite	Triaxial Braid	Composite	Triaxial Braid
<b>3M CVI-SiC Composite</b>							
43-1-2	—	—	—	1341 ± 254	14026 ± 2012	1060 ± 219	11012 ± 1795
43-1-6	B/M-15	IV	1706	1696 ± 195	18220 ± 1356	1429 ± 159	15599 ± 2246
45-18-02	C/T-18	V	1110	2333 ± 415	18975 ± 3117	2225 ± 361	18001 ± 3745
						1850 ± 299(a)	16173 ± 2245(a)

(a) High Temperature Strength Testing Conducted at 843°C

## Results

---



**Figure 4.9.14 - Photo Micrograph Showing Crystallization of the Schumacher Dia Schumalith F40 Filter Matrix**

## Results

---

**Schumacher Dia Schumalith FT20.** Eight improved, high temperature, creep resistant Schumacher Dia Schumalith FT20 clay bonded silicon carbide candles were installed and operated during Test Period IV. The initial bulk strength of the 10-mm wall Schumacher Dia Schumalith FT20 matrix was comparable to the higher strength, 15-mm wall, Schumacher Dia Schumalith F40 filters which had been manufactured in 1992. As shown in Table 4.9.7, the residual bulk strength of the Schumacher Dia Schumalith FT20 matrix after 1706 hours of operation was comparable to that of the initial bulk strength of the filter matrix.

**Coors Alumina/Mullite.** In contrast to the clay bonded silicon carbide candle filters, the alumina/mullite matrix consists of mullite rods that are embedded within an amorphous phase that contains corundum ( $\text{Al}_2\text{O}_3$ ) and anorthite ( $\text{CaAl}_2\text{Si}_2\text{O}_8$ ). Eight Coors filters were used during Test Period IV. All Coors filter elements remained intact after 1706 hours of operation. The residual bulk strength of the 1706 hour PFBC-exposed Coors filter matrix was comparable to that of the as-manufactured filter matrix as shown in Table 4.9.7.

Three of the Test Period IV Coors filters were reused during test Period V. Post-test inspection indicated that all three of the Coors filters remained intact, achieving 2816 hours of successful operation. In addition, 95 newly manufactured Coors filters were installed for Test Period V. After 1110 hours of operation, two filters failed, while the remaining Coors filters remained intact. One of the Coors filters failed directly below the flange, while the second filter fractured at approximately 1000 mm below the flange.

Characterization of the residual bulk strength of the 1110 hour, PFBC-exposed, Coors alumina/mullite filter elements indicated that they lost strength during operation in the 1400-1550F, oxidizing environment. This implied a sensitivity of the alumina/mullite matrix to higher process operating temperatures which may either induce or accelerate phase changes, or enhance crack propagation properties along the ID surface and/or through the 10 mm filter wall. A further reduction of residual bulk strength along the ID surface and/or through the filter wall was exhibited within the Coors filter matrix after 2816 hours of operation (Test Periods IV and V).

As shown in Figures 4.9.15 and 4.9.16, extensive mullitization resulted along the pore cavity wall of the Coors alumina/mullite filter matrix as both operating time and process temperature increased. As determined by qualitative x-ray diffraction analysis, minor dissociation of mullite that was present in the as-manufactured Coors filter matrix was initiated early during process operation. Simultaneously a

## Results

---

reduction and/or depletion of the as-manufactured anorthite and glass phases resulted, leading to the production of trace and minor concentrations of alumina, cordierite and cristobalite within the bulk matrix. Retention of the bulk matrix strength with time will largely depend on the rate of cristobalite and cordierite grain growth, which could ultimately lead to the formation of microcracks and loss of material strength. Since phase conversion appears to have stabilized within the first 1100 hours of operation, additional microcrack formation and/or loss of bulk material strength would be attributed to thermal fatigue (i.e., increased pulse intensity or duration) and/or thermal shock of the Coors alumina/mullite filter matrix during high temperature PFBC process operation.

**3M CVI-SiC Composite.** The 3M Chemical Vapor Infiltration-Silicon Carbide (CVI-SiC) composite filter consists of three layers – an outer open mesh confinement layer, a middle filtration mat, and an inner triaxial braided fabric layer which forms the structural support matrix of the filter element. Within the confinement and filtration mat layers, an 1-2  $\mu\text{m}$  layer of silicon carbide encapsulates Nextel 312 or alumina-based fibers, while an 100  $\mu\text{m}$  layer of silicon carbide is deposited along the Nextel 312 triaxial braid in the support matrix.

Three 3M CVI-SiC composite filters were used during Test Period IV, and after 1015 hours of operation, two of the elements failed at the base of their flange due to ash bridging. The third 3M filter element, which remained intact, achieved 1706 hours of operation prior to termination of Test Period IV. Post-test, room temperature, gas flow resistance measurements of the intact 3M filter indicated that the pressure drop across the element was 220 in-wg at a gas face velocity of 10 ft/min. The room temperature pressure drop across the ash coated 3M filter was relatively high in comparison to alternate filter elements which were exposed to similar PFBC test conditions. The high pressure drop across the candle filter was attributed to the adherence of the dust cake layer along and within the confinement layer, as well as through the filtration mat, and triaxial support braid.

Characterization of the 3M CVI-SiC matrix via scanning electron microscopy/energy dispersive x-ray analysis indicated that minor changes in the morphology of the filter matrix had occurred after 1705 hours of operation in the 1225-1400F temperature range. Due to deposition of the thin  $<1 \mu\text{m}$  interface coating, it was frequently difficult to discern whether the interface coating had remained intact. A gap or separation was considered to exist between the CVI-SiC coating and the underlying Nextel 312 fibers in several areas of the PFBC-exposed 3M composite filter matrix. In the high temperature PFBC environment, oxidation of the interface coating is expected to occur.

## Results

---

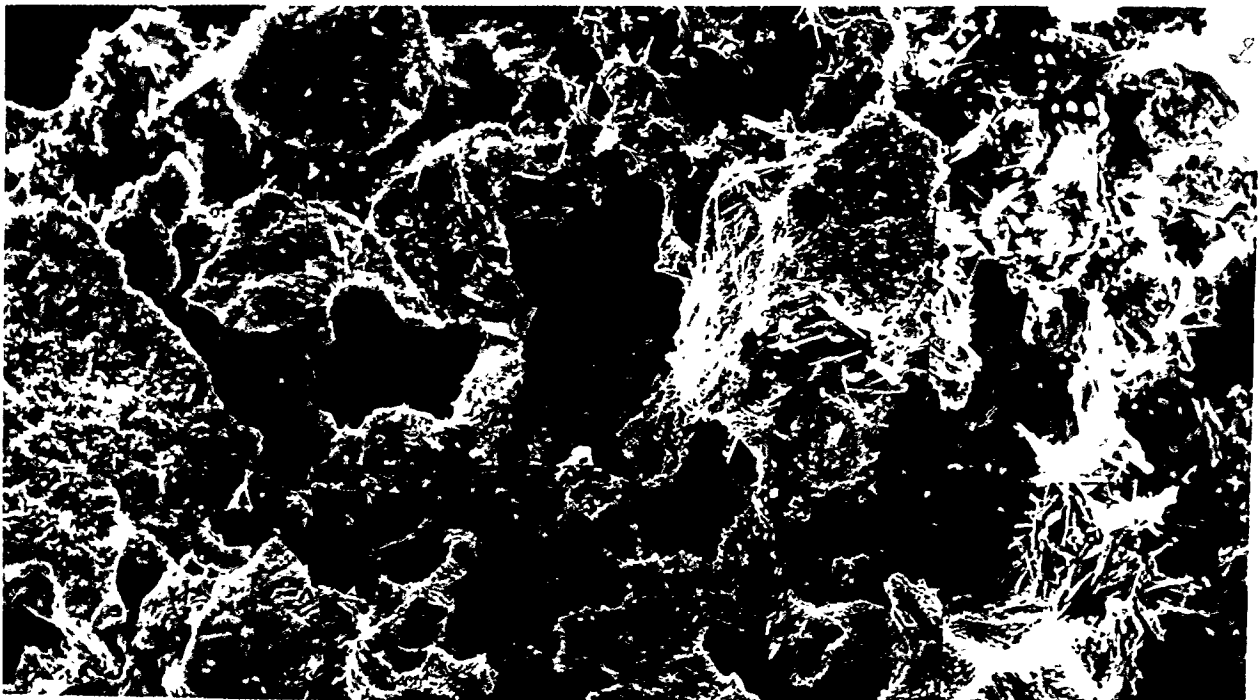


**Figure 4.9.15 - Crystallization of the Coors Alumina/Mullite Filter Matrix after  
1110 hrs of Operation in Test Period IV**

## Results

---

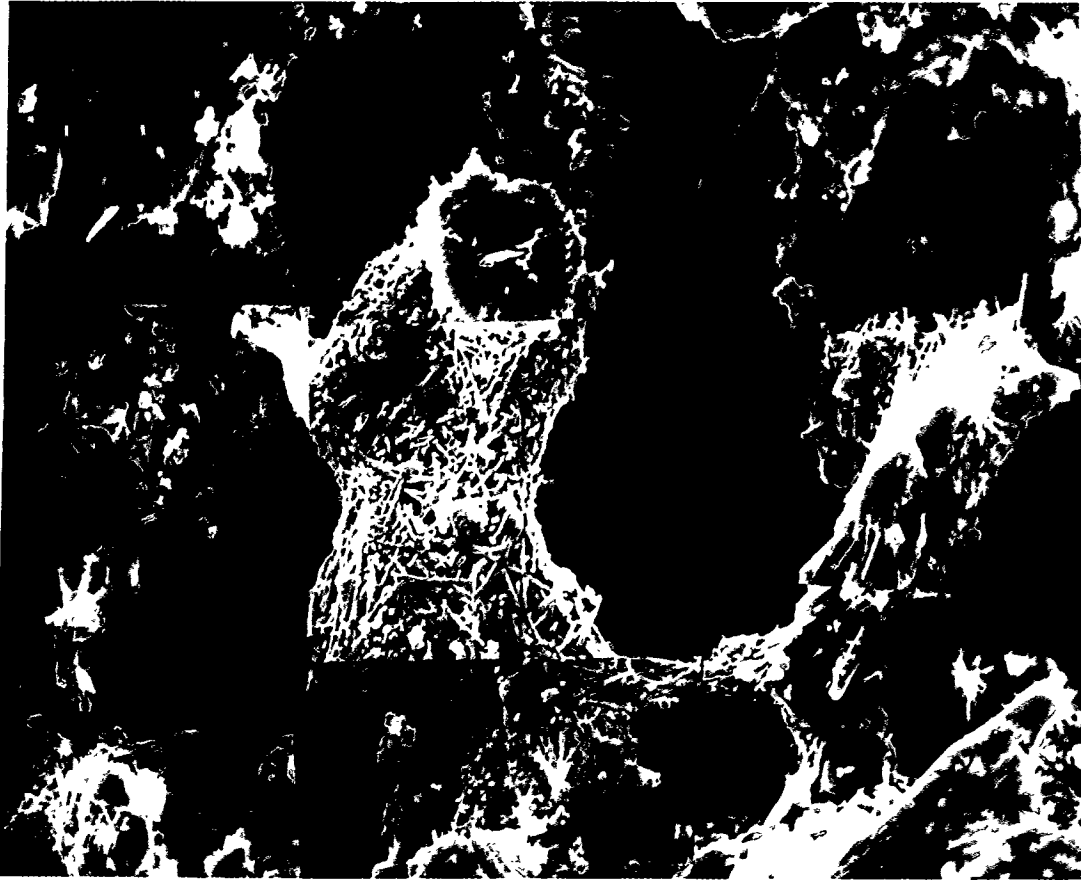


**Figure 4.9.16 - Crystallization of the Coors Alumina/Mullite Filter Matrix after 2816 hrs of Operation in Test Period IV and V**

## Results

---

Post-test O-ring diametral compressive strength testing indicated that the strength of the 3M CVI-SiC composite matrix was greater than that of the as-manufactured filter matrix. Due to the accumulation of fines within the PFBC-exposed matrix, "wedging" of fines in between the SiC coated fibers may require a higher load to be applied to the matrix prior to failure, thus generating what appeared to be a strengthened composite matrix. Alternate secondary mechanisms have been considered which include phases changes within the matrix which provide additional strength during process operation. During diametral compressive strength testing, the relatively low load bearing, PFBC-exposed, 3M CVI-SiC matrix generally retained the graceful fiber "pull-out" characteristics of the fracture toughened, as-manufactured matrix.

Ten newly manufactured CVI-SiC composite filters were used during Test Period V. After 1110 hours of operation, post-test inspection of the filter cluster indicated that all ten of the 3M CVI-SiC composite filter elements were intact. Assuming that the strength of the as-manufactured 3M filters which were used for testing in Test Period V was equivalent to the strength of the as-manufactured filter elements which were used in Test Period IV, characterization of the 1110 hour, 3M CVI-SiC composite filter elements indicated that the strength of the ash-filled matrix once again appeared to increase.

**DuPont PRD-66 Filament Wound Filters.** The oxide-based, filament wound, DuPont PRD-66 matrix consists of a layered cordierite ( $M_{32}Al_4Al_5O_{18}$ ), mullite ( $3Al_2O_3 \cdot 2SiO_2$ ), cristobalite ( $SiO_2$ ), and corundum ( $Al_2O_3$ ) microstructure. An amorphous phase is also present in the as-manufactured PRD-66 filter matrix. Due to the differences in the thermal coefficient of expansion for mullite, cordierite, and corundum which are present in the PRD-66 matrix, a microcracked structure is formed after firing.

The "diamond" pattern weave of the polycrystalline refractory oxide-based fibers forms the ~7 mm structural support layer of the DuPont PRD-66 filter matrix. A thin membrane layer is wrapped along the outer surface of the support matrix, producing a light weight, bulk filter element.

During Test Period IV, three DuPont PRD-66 filter elements were installed in a middle array. After 1706 hours of operation, all three filters remained intact. During C-ring preparation of the Tidd-exposed PRD-66 filter element, magnesium sulfate crystallized along the outer surface of the filter, as a result of leaching of the ash that was contained within the filter ID bore and wall during wet cutting with a diamond wheel. Posttest strength characterization of the PRD-66 matrix indicated that the bulk strength of the ash filled matrix tended to increase after 1706 hours of operation.

## Results

---

Twenty-two DuPont PRD-66 candle filters were installed in a top array for operation in Test Period V. After 232 hours of operation, sections of the PRD-66 matrix were identified in the ash hopper discharge, implying that failure had occurred. Testing continued, and after ~775 hours of operation, additional sections of the PRD-66 filter matrix were evident in the ash hopper discharge.

Testing was terminated after 1110 hours of operation. Only two of the DuPont PRD-66 filter elements remained intact, four had suffered either mid-body fracture or failure at a location that was approximately three-quarters of the candle length below the flange, and sixteen filters had fractured at the base of the flange. The outer surface of the intact and fractured filters was generally "ash free", particularly along the portion of the body that was adjacent to the plenum pipe, and to approximately mid-way down the length of the filter element. Alternately 1-2 mm of ash was deposited along the outer surface of the PRD-66 candles, near the bottom end cap. "Divot-like" formations resulted in lines which ran parallel down both sides of the remaining intact and fractured filter elements. Localized "divoting" was also observed underneath the outer protected gasket sleeve, as well as in alternate, isolated areas along the filter body. The mechanisms leading to "divoting", flange fracture, and mid-body failure of the DuPont PRD-66 filter elements are under investigation. The formation of divots is believed to be either thermal and/or mechanical in nature, as opposed to a response of the DuPont PRD-66 filter matrix to the process gas chemistry and/or particulate fines. Since the PRD-66 filter array had suffered failure after 232 hours of operation, ash filled the inside bore of the remaining PRD-66 candles (i.e., 120 mm and 350 mm) during pulse cycling. Unlike the 3M CVI-SiC matrix and alternate filter elements, failure of the ash-filled PRD-66 end cap region was not observed.

Assuming that the strength of the PRD-66 elements used in Test Period V was equivalent to the strength of the PRD-66 elements used in Test Period IV, post-test strength characterization of the 1110-hour Tidd-exposed PRD-66 filter matrix indicated that an increase in strength appeared to have occurred along the ash-filled OD surface, while virtually no change in strength was detected along the ID or pulse cycled surface of the filament wound matrix.

With the exception of ash bridging which failed the filter elements, the stability and long-term viability of the "aged" or "conditioned" candle filter materials were generally demonstrated during operation in the pressurized fluidized-bed combustion gas environment. Due to the differences in the thermal coefficient of expansion of the PFBC ash and ceramic filter matrices, as shown in Figure 4.9.17, the clay bonded silicon carbide Schumacher Dia Schumalith F40, Coors alumina/mullite, and 3M CVI-SiC

## Results

composite filters frequently failed due to ash bridging. Failure of the filters also occurred when a densified plug of fines was embedded within the ID bore of the filter elements.

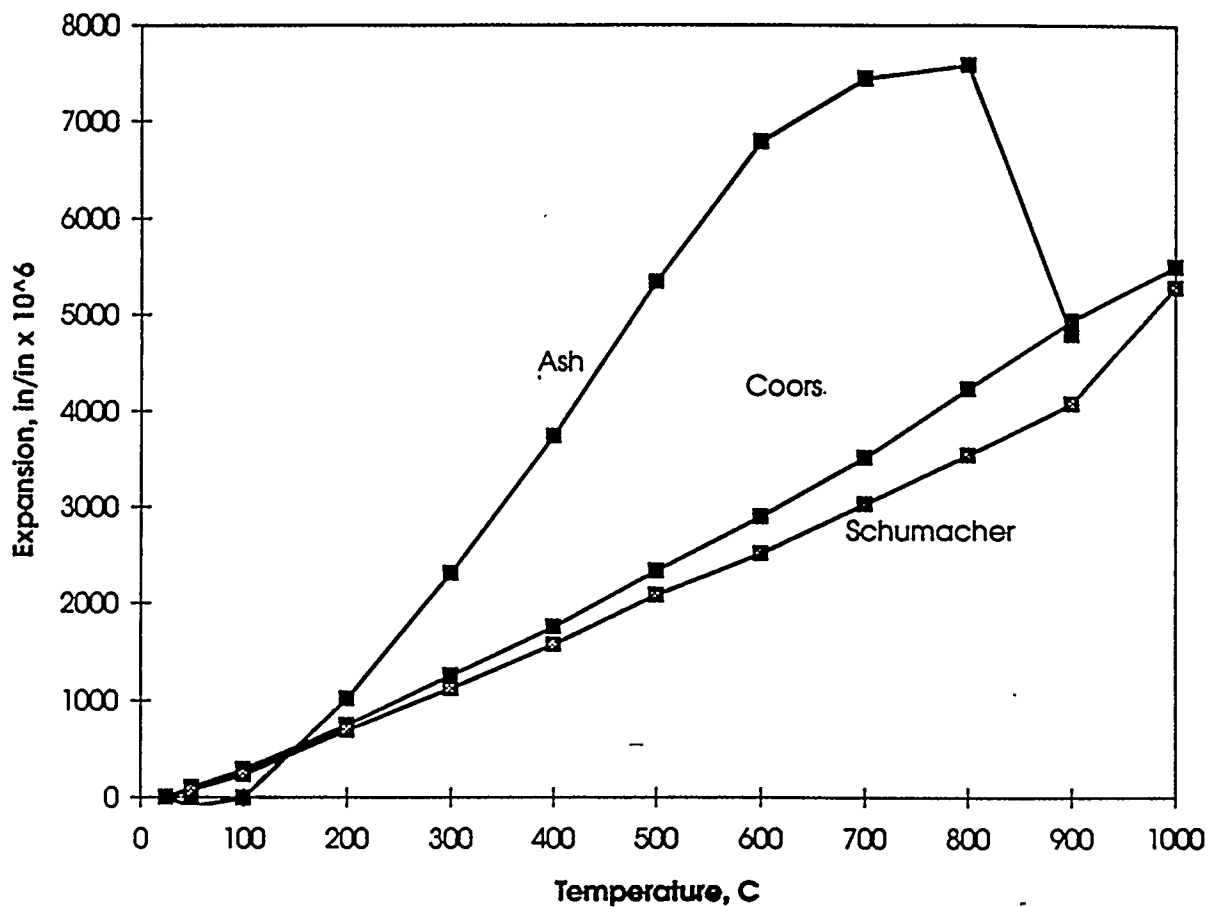


Figure 4.9.17 - Thermal Coefficient of Expansion of the Tidd PFBC Ash and Select Porous Ceramic Filter Materials

## Conclusions

---

### 5.0 CONCLUSIONS

The Tidd Hot Gas Clean Up Program provided valuable information for the future design and operation of ceramic barrier filters in a PFBC flue gas environment. The most important conclusions reached from this program are listed below.

1. The basic design of the candle-based APF was structurally adequate. The hot metal structure of tubesheet, plenums, and candle holders operated without problems.
2. Clay-bonded silicon carbide candle material exhibited an approximately 50% loss of strength after 1000-2000 hours of exposure to the PFBC environment. The strength level stabilized upon further exposure time. The candles maintained their functionality after undergoing the loss of strength.
3. Nearly all of the silicon carbide candle breakage observed in this program was attributed to ash bridging in the APF. Ash bridging was strongly affected by the size and temperature of the ash entering the filter. Very small ash (1 to 3 microns) passing through a well-tuned cyclone formed an ash cake on the filter candles that was extremely difficult to remove at operating temperatures over 1400F. Ash from a partially detuned cyclone (about 7 microns) was more easily removed than the smaller ash, but still difficult to remove at operating temperatures over 1450F. Ash from a completely spoiled cyclone (above 27 microns) was easily removed and did not tend to bridge. The coarse ash was also much easier to handle in the ash removal system.
4. It is important to prevent ash from contaminating the inside of filter candles to avoid blinding them on the inside surfaces which have larger pore size than the outside surfaces. Also, ash accumulation in the bottom of candles can induce candle cracking.
5. The design of hot gas piping is critical. Cast refractory thermal insulation was required to protect the pipe from the hot gas. Ceramic fiber insulation proved unsatisfactory as internal thermal insulation in the hot gas piping.
6. Flue gas which contacts metal surfaces below the acid dew point forms a very corrosive liquid. Metal surfaces that were not protected from contact with the gas experienced corrosion. Stainless steel and Hastelloy C-22 experienced pitting attack while carbon steel exhibited

## Conclusions

---

generalized corrosion. Carbon steel exposed to flowing gas exhibited up to 12% loss of wall thickness over the duration of the test program. Expansion joint bellows proved to be the most troublesome elements in the piping system.

7. The head of the Tidd APF was plagued by hot spots throughout the program due to hot gas flowing behind the ceramic fiber insulation. On-line pumping of insulating refractory was demonstrated to be effective in controlling these hot spots. Temperature sensitive paint used on the filter vessel and piping system proved useful in detecting hot spots.
8. It is important to have reliable continuous ash removal from the filter. Ash buildup in the APF hopper resulted in candle breakage. High level alarms in the hopper were important in preventing additional failures. Continuous discharge of ash with gas and cooling air through carefully sized lines proved more reliable than a lockhopper system.
9. Based on very limited data, the APF reduced the SO<sub>2</sub> concentration in the gas passing through it approximately 45%. This is believed to result from the gas reacting with ash cake on the filter candles as evidenced by a higher degree of sulfation of the APF ash than the precipitator ash.

## Recommendations

---

### 6.0 RECOMMENDATIONS

1. In future HGCU applications on PFBC flue gas, it is recommended to not utilize a cyclone upstream of the filter to reduce the filter inlet dust loading. The advantage of coarse ash in improving filter cleaning and ash removal outweighs the disadvantage of higher ash loading to the filter and higher backpulse frequency.
2. The Tidd PFBC plant design utilized a combustor vessel different from the vessel for the fluidized bed to separate the thermal boundary from the pressure boundary. When this approach is used for the system, it is recommended that the APF be installed inside the combustor vessel. Such an arrangement would eliminate most of the hot gas piping and many of the corrosion problems which were experienced in the HGCU slipstream but not experienced in the Tidd PFBC system. The disadvantage of this arrangement is reduced access to the filter for inspection and servicing.
3. It is recommended that fail-safe devices be included in the APF design to minimize ash penetration in the event of broken elements. Fail-safes will protect the gas turbine from erosion by coarse ash in case of candle breakage and ensure that particulate emission limits can be maintained. Fail-safe devices need to be improved to reduce the amount of ash entering the filter outlet under a broken candle scenario to prevent ash from being entrained with back pulse air and accumulating in other candles which could result in candle failures.
4. A means to detect filter leakage on line should be developed. At Tidd the only method available for this purpose was to briefly open a valve downstream of the filter and look for dust in the gas. However, this method was crude and unreliable unless the filter leakage was large.
5. The APF vessel should include a sufficient quantity of adequately sized nozzles for inspection of all filter clusters. A means to safely enter the filter vessel to replace broken filter elements should be developed. Removing the filter internals for this purpose was costly and time consuming.
6. In future filter designs with plenums arranged vertically, ash sheds below the filter candles should include provisions for pneumatically removing ash accumulations from them. The

## Recommendations

---

distance between ash sheds and candle bottoms should be increased to minimize the possibility of ash bridging between them.

7. The filter vessel ash hopper angle should be steep enough to ensure good ash flow. Flow testing with the ash is recommended to confirm the design prior to fabrication. The hopper should contain an adequate number of nozzles for air purging.
8. A minimum of two level detectors (high and extreme high) should be installed at the filter hopper to detect ash build up.
9. Continuous pneumatic ash removal is recommended in lieu of a screw cooler and lockhopper arrangement. This type of system was found to be reliable in removing ash from the primary and secondary cyclones in the PFBC combustor and was effectively used as an alternate means of ash discharge from the Tidd APF.
10. Cast refractory is recommended as the internal insulating material for the filter vessel head and piping. Fibrous (Z-Block) insulation is suitable for the body of the filter vessel. Expansion joints in the piping system should be avoided or at least minimized.
11. If a hot gas filter system is installed external to the combustor and the piping system operates below the acid dew point of the flue gas, it is imperative that internal corrosion protection be addressed in the design.
12. Conduct additional long-term high temperature testing of clay bonded silicon carbide candles to confirm that their loss of strength is not a serious disadvantage for commercial applications. Alumina-mullite material also merits additional testing.
13. All pressure sensing lines in the HGCU system should have continuous air purge to prevent pluggage.
14. Conduct further investigations into the chemistry of high temperature ash agglomeration.
15. Conduct additional research into the phenomenon of SO<sub>2</sub> removal through ash cakes.

## Appendix I

---

### APPENDIX I (Prepared by Southern Research Institute)

#### ANALYSES OF ASH SAMPLES FROM THE TIDD ADVANCED PARTICLE FILTER

##### Background

The Tidd Advanced Particle Filter (APF) was designed to perform as a barrier filter with periodic reverse pulses of high pressure air used to remove ash from the filtering surface of the ceramic candle filter elements. In its initial configuration, the APF was preceded by a cyclone designed to capture most of the entrained particulate matter. As operating experience with the APF accumulated, this cyclone was first derated, and then completely bypassed in order to alter the characteristics of the ash entering the filter vessel.

The operating history of the Tidd APF has demonstrated the importance of ash characteristics in determining the overall performance of the filter. Although the performance of the different types of candle filter elements that were tested varied considerably, the ash deposits that formed in the APF were the primary factor that determined the integrity of the barrier filter. Almost all of the ashes removed from the filter vessel comprise relatively fine particles, and are highly cohesive. Observations of the APF made throughout its operating history, coupled with laboratory analyses of the bulk ash and ash deposits collected in the filter assembly, have shown how strong, tenacious ash deposits form in the APF, and how these deposits often led directly to bent and broken candle filter elements. Analyses of various Tidd ashes indicate that after the ash particles are initially deposited, the ash deposit undergoes a physical restructuring or consolidation that significantly reduces the overall porosity of the ash deposit.

Although the filtration of particulate matter from flue gas streams is an established technology for conventional pulverized-coal-fired plants, the environment within the APF and the specific characteristics of the PFBC ash being collected presented unique challenges for this installation. The high temperatures in the filter vessel combined with the chemistry and morphology of the ash entering the filter vessel to form ash deposits that severely limited APF operation.

##### On-Site Observations

Southern Research Institute personnel made four site visits to the Tidd APF to inspect and document the condition of the filter vessel and to collect representative samples of the various deposits of ash found in the APF

## Appendix I

---

for analysis. When the filter assembly was opened during the first of these site visits on September 30, 1993, extensive deposits of ash were found on candle surfaces, bridged between candles, and on non-filtering surfaces. The deposits found on non-filtering surfaces formed by the gradual deposition of particles as a result of turbulent diffusion. Some of these passive deposits were up to six inches thick with high mechanical strength. Many of the candle filter elements were covered by filter cakes up to one inch thick. Like the passively deposited agglomerates of ash, these filter cakes also had high mechanical strength.

The filter vessel was again opened for inspection and refitting on May 5, 1994. Despite the relative cleanliness of the candles, significant deposits of ash were observed at several other locations in the assembly. For each of the nine clusters, the underside of the tube sheet was coated with a deposit of ash about eight inches thick. Although the outer (presumably the most recently deposited) portions of these deposits were fairly fluffy, the inner regions were hard, strong, and well consolidated. Similar deposits were apparent on the ash sheds above the middle and bottom plenums. These deposits were about three inches thick, and were also strong and well consolidated. Strong, thick deposits were present on the center support conduits that are part of the top and middle plenum assemblies. These deposits were thick enough (over four inches) in most areas to envelop the inner ring of candles in these plenum assemblies. Many of the innermost candles in the top two plenums were bent away from the center plenum support conduits. The region between these candles and the center support conduits was almost completely filled with ash.

Observations of the APF during this refitting indicated that severe bridging of ash between adjacent candles was still a serious problem. Many ash bridges were present, some of which extended from the deposit on the underside of the tube sheet all the way down to the conical surface of the ash shed below the bottom ends of the candles. Ash bridges were identified in many different stages of formation. Most ash bridges were found in the top and middle plenums, which are also the locations where most of the severely bent candles were found. The bottom plenum had the fewest ash bridges, and the fewest bent or broken candles. As was observed previously, the ash deposits throughout the APF had high mechanical strength. However, the filter cakes observed during this second site visit were only about 0.4 inch thick, compared with the one inch thick cakes present in September 1993.

From May 1994 until the shutdown of the facility in the spring of 1995, operation of the APF focused on two separate approaches to eliminating the ash bridges previously formed between candle filter elements and nearby surfaces. The first approach involved increasing the mean size of the entrained particles entering the filter vessel by derating the cyclone located just upstream of the filter. The other approach was to remove the inner ring of candle filter elements from the top two plenum assemblies. Although this latter approach involved removing

## Appendix I

---

25 % of the ceramic candle filter elements, and consequently 25 % of the active surface area, it was implemented to increase the separation between the candle filter elements and the ash sheds and center support conduits, reducing the likelihood that ash bridges would form at this location.

When the APF was opened on October 27, 1994 a significant number of candle filter elements were broken, and ash deposits were present at various locations throughout the filter assembly. As observed in two previous site visits, the region under each tube sheet where the candle filter elements are mounted to the tube sheet was completely packed with ash deposits. Although the number of ash bridges adjacent to the filter elements was reduced compared to the two prior observations, there were still a few large ash bridges formed between the lower portion of filter elements in the top two plenums and the ash sheds and/or the plenum support conduits. In general, the filtering surfaces of the intact filter elements were relatively clean, except for regions of the candles just below the tube sheet deposits mentioned above. The surfaces of the center support conduits and the ash sheds were cleaner than previously observed; however, several thick ash deposits were present on portions of these surfaces. Bridging of ash between filter elements in the bottom plenum did not seem to be a serious problem.

The APF was opened once more on May 11, 1995 after the final shutdown of the Tidd Demonstration Plant. During this last operating period, the cyclone upstream of the APF was entirely bypassed in order to get as many relatively large particles into the filter vessel as possible. In general, the filter assembly was quite clean. The only significant deposits of ash were on the underside of the tube sheets, much like the deposits found in these locations during prior inspections. Most of the broken candle filter elements were of a particular experimental design. Most of the other filter elements were intact.

Early observations of the Tidd APF led to the conclusion that tenacious ash deposits can form in the filter vessel and induce stresses that result in bent and/or broken ceramic candle filter elements. The proximity of these bent and broken candle filter elements to large, strong ash deposits emphasized the need to prevent or control the growth of these deposits, facilitate their on-line removal, and/or to redesign the filter to lessen their effects on individual filter elements. The approach that proved most successful in eliminating the deposits was the total bypassing of the cyclone upstream of the APF.

### Laboratory Analyses

During each of the four site visits described above, Southern Research Institute personnel collected a suite of ash samples from various locations in the APF for analysis. These samples included large pieces of the various

## Appendix I

---

types of deposits present throughout the filter vessel, as well as samples of loose ash that were found at several places in the APF. Analyses performed on the ash deposits included SEM examinations of their structure and chemical composition, as well as measurements of their porosity and strength. Measurements on loose bulk ash or deagglomerated (broken up) deposits included size distribution, chemical composition, specific surface area, uncompacted bulk porosity, tensile strength, solubility studies, and SEM photographs to assess particle morphology.

In general, analyses of the ash samples from the Tidd APF showed that the ash that collects at various places throughout the filter vessel initially forms loose, weak, uncompacted deposits that are 85 to 90 % porous. (After the cyclone was completely bypassed, the ash formed deposits that were initially around 80 % porous.) In almost all cases, when these deposits were exposed to temperatures like those in the APF (1200-1550 °F), they gradually consolidated, transforming into much stronger structures having porosities as low as 69 %. Various analyses and reviews of pertinent literature indicate that the mechanism responsible for the extreme consolidation of these agglomerates of ash was a physical rearrangement of the ash particles due to the surface tension of melted or partially melted alkali-aluminosilicate eutectic mixture(s) formed at the contact points between adjacent particles after long-term exposure to the temperatures in the APF.

Because the most freshly deposited portions of the filter cakes and passively deposited ash deposits collected during the site visits were so fragile, a number of these samples were encapsulated in low-viscosity epoxy at the plant. This procedure allowed more detailed measurements of the porosity of these deposits as well as preservation of the samples for further analyses. When thick filter cakes were allowed to form on the candle surfaces, they consolidated as a result of eutectic formation, and they also tended to compact under the force of filtering pressure drop. The compaction was greatest in the layer closest to the filtering surface and progressively less pronounced in the outer layers. Measurements of the porosity of filter cakes removed from Tidd in September 1993 verified the existence of a gradient in the porosity of the filter cake. Porosity gradually increased from about 72 % in the 0.1 inch of cake closest to the candle, to about 85 % for the 30 to 40 % of the cake most recently deposited. These compacted filter cakes had comparatively high mechanical strength and high resistance to gas flow. Laboratory data showed that the tensile strength of a fully consolidated filter cake nodule can exceed 12.5 psi.

Stereographic SEM photographs were made of a fresh fracture surface of a nodule taken from an ash shed in October 1994. The stereographic image was very enlightening as to the structure of the nodule. (One of the pair of SEM photographs used to create the stereographic image is shown in Figure I-1.) The nodule appeared to be a concretion composed of discrete fine particles almost completely embedded in a pervasive amorphous

## Appendix I

mass which apparently formed in the APF after the particles were initially collected. The origin of this amorphous mass is discussed in more detail later in this appendix. Passively deposited agglomerates of ash like the one shown in Figure I-1 were found to have porosities around 74 %.

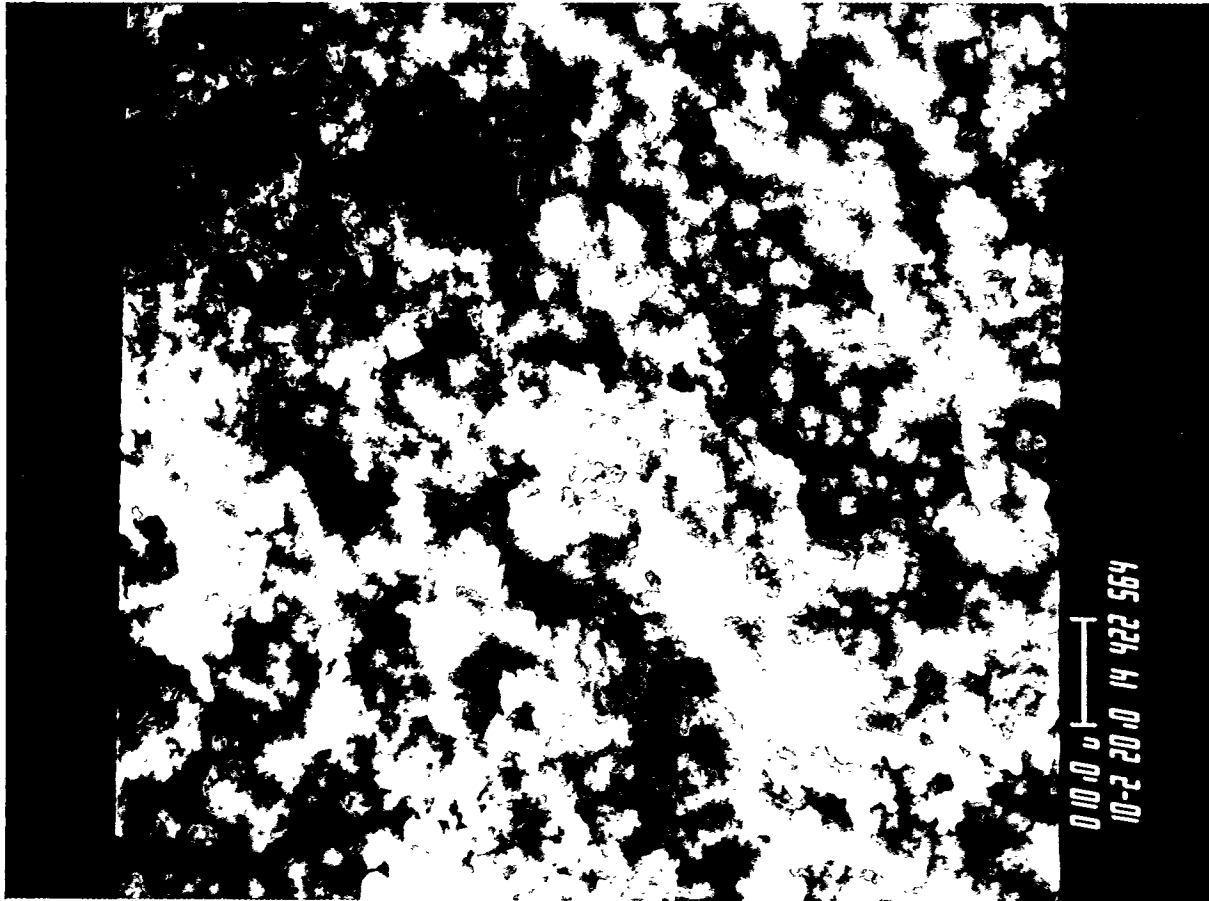


**Figure I-1 - SEM Photograph of a Fresh Fracture Surface of an Ash Agglomerate  
Taken from an Ash Shed in the Tidd APF in October 1994**

## Appendix I

---

An SEM microprobe was used to examine agglomerates of ash obtained from the filter vessel in May 1994. The device performs elemental analyses on selected 1  $\mu\text{m}$  diameter hemispherical regions. There was little consistency from region to region in the various specimens that were examined. Each particle observed was a special case. Some particles were almost completely iron, others were very high in calcium or magnesium. Aluminosilicate particles were also common. The shapes and sizes of the particles also varied considerably. Some particles showed evidence of having been melted and resolidified. Such particles, to the extent that it was possible to determine, were enriched in magnesium because of the formation of  $\text{MgSO}_4$ . The bonds between particles showed some enhanced levels of Mg, accompanied by such other species as Ti, Al, Ca, and S. Although conclusions are hard to verify because of the limitations of the technique and the heterogeneity of the samples, particles rich in Mg and S apparently softened during combustion and/or collection and residence in the filter vessel. The presence of significant amounts of Mg and S in the ash particles may have enhanced the chances for eutectic formation between particles.

Tidd ash nodules that were slowly covered with water rapidly disintegrated. When this same procedure was performed with ethanol, the nodules maintained their shape, and when they dried, they seemed to recover all of their initial strength. Apparently the hydration of various compound(s) in the ash or the dissolution of soluble compounds into the water broke apart the interparticle bonds in the nodules.

The most useful information describing the bulk ash samples was derived from determinations of size distribution, chemical analyses, and uncompacted bulk porosity measurements. Size distributions were measured by sieving and sedigraphic analysis. Prior to derating and eventually bypassing the cyclone upstream of the APF, the ash particles collected in the filter vessel were very fine, with MMD's around 3 to 5  $\mu\text{m}$ . As efforts to increase the size of the ash entering the APF by derating the cyclone progressed, somewhat larger MMD's were observed. However, the major changes in the size distributions of the ashes collected in the APF did not occur until the last period of operation, during which the cyclone was completely bypassed.

Sedigraphic and sieve analyses were performed on ashes collected in October 1994, after derated cyclone operation, and May 1995, after operation with the cyclone completely bypassed. These data, which are summarized in Tables I-1 and I-2, show that bypassing the cyclone between October 1994 and May 1995 significantly increased the size distributions of ash collected in the APF. The sieving process used on these five ashes separated a portion of the original ashes into three size fractions: particle diameters  $> 45 \mu\text{m}$ , particle diameters  $> 15 \mu\text{m}$ , but smaller than  $45 \mu\text{m}$ , and ash particles with diameters  $< 15 \mu\text{m}$ . (The sieving process caused this last, smallest fraction to be discarded along with the isopropanol used to wash the particles through the  $45 \mu\text{m}$  and  $15 \mu\text{m}$  sieves.)

## Appendix I

### Table I-1 - Sedigraphic Analyses of Tidd Ashes

Location, Date	Size Range Measured, $\mu\text{m}$	Stokes' MMD, $\mu\text{m}$
Bottom Plenum Tube Sheet, Oct. 1994	1.0 - 40	7.0
Middle Plenum Ash Shed, Oct. 1994	1.0 - 40	3.6
Top Plenum Tube Sheet, May 1995	0.4 - 40	17
Top Plenum Filter Cake, May 1995	0.6 - 40	11
Middle Plenum Tube Sheet, May 1995	0.6 - 40	16

### Table I-2 - Sieve Analyses of Tidd Ashes

Location, Date	% weight		
	dia > 45 $\mu\text{m}$	45 $\mu\text{m}$ >diam>15 $\mu\text{m}$	diam < 15 $\mu\text{m}$
Bottom Plenum Tube Sheet, Oct. 1994	4.03	17.3	78.6
Middle Plenum Ash Shed, Oct. 1994	0.64	3.84	95.5
Top Plenum Tube Sheet, May 1995	28.9	50.7	20.4
Top Plenum Filter Cake, May 1995	30.1	34.3	35.6
Middle Plenum Tube Sheet, May 1995	44.8	33.3	21.9

In Figure I-2, the size distribution data for these five samples obtained with the sieves have been combined with size distribution data obtained with the sedigraph. These data clearly show the increase in particle size induced by bypassing the cyclone. The ash corresponding to the last row in Tables I-1 and I-2 behaved much more like a free flowing powder than the other samples collected on the same site visit. Based on our sieving measurements, this free flowing ash exhibited the largest particle size distribution of those ashes that were analyzed. When this ash was removed from the tube sheet, it was loose and fluffy, unlike the other ash samples that were consolidated into nodules and strong deposits. This type of difference is common with fine powders. All other conditions the same, powders tend to become more free flowing as their particle size distribution becomes coarser.

## Appendix I

Chemical analyses of this free flowing ash and one of the nodular ashes were performed to determine if differences other than particle size might account for the tendency of the coarser ash to behave like a free flowing powder. Chemical analyses of these two ashes and the size-separated portions generated from them during sieving are summarized in Table I-3.

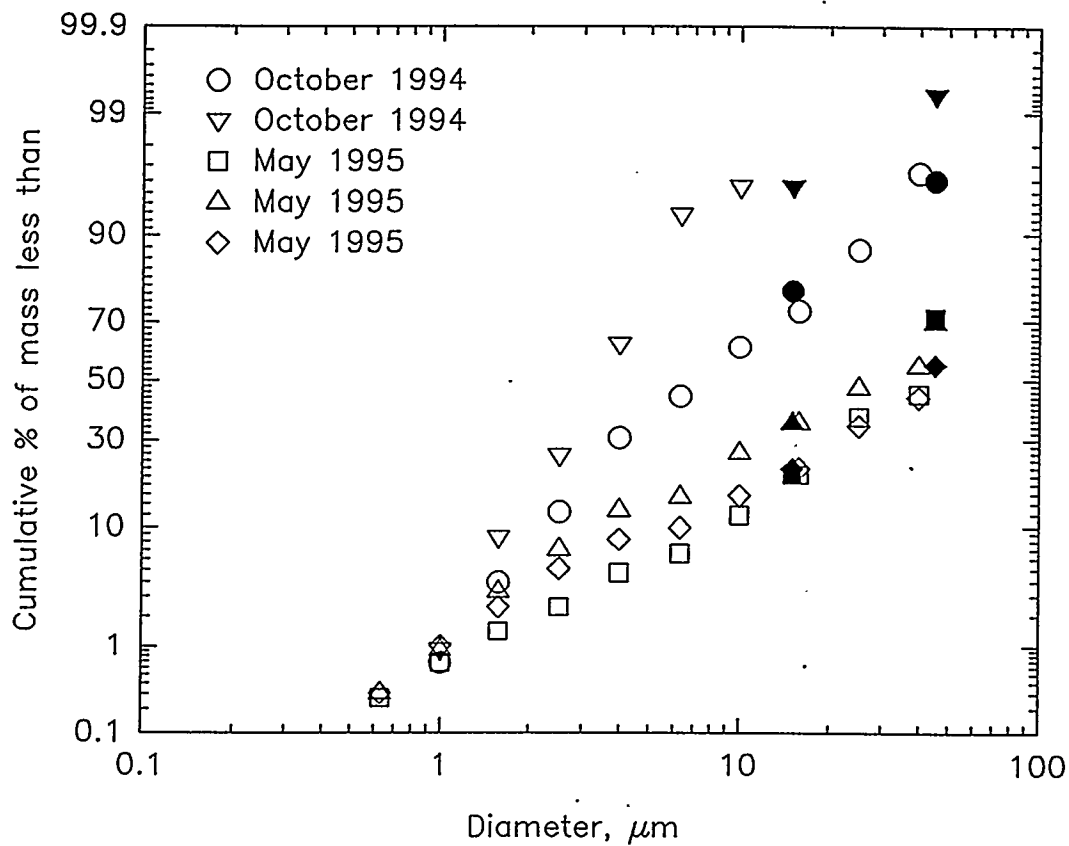


**Figure I-2 - Cumulative Size Distribution Data Measured with a Sedigraph and Sieves for Five Ashes Collected from the Tidd APF**

The hollow data points represent sedigraphically obtained Stokes' diameters. The filled data points represent data obtained in the sieve analyses.

## Appendix I

**Table I-3 - Chemical Analyses of Tidd Ashes Collected in May 1995, % wt.**

Constituent	Nodular Ash (Filter Cake)			Free Flowing Ash (Tube Sheet)		
	all diameters	d > 45 $\mu\text{m}$	15 $\mu\text{m}$ < d, d < 45 $\mu\text{m}$	all diameters	d > 45 $\mu\text{m}$	15 $\mu\text{m}$ < d, d < 45 $\mu\text{m}$
Li <sub>2</sub> O	0.01	0.01	0.01	0.01	0.01	0.01
Na <sub>2</sub> O	0.29	0.16	0.23	0.27	0.13	0.20
K <sub>2</sub> O	1.3	0.83	1.3	1.2	0.77	1.1
MgO	8.3	11.3	8.5	13.2	16.5	13.5
CaO	14.1	18.1	15.0	20.5	24.7	21.0
Fe <sub>2</sub> O <sub>3</sub>	7.1	4.8	7.5	8.0	6.2	9.9
Al <sub>2</sub> O <sub>3</sub>	11.7	7.5	10.8	10.8	7.2	9.5
SiO <sub>2</sub>	26.1	17.6	26.0	25.1	19.6	25.6
TiO <sub>2</sub>	1.2	0.41	0.46	1.1	0.33	0.49
P <sub>2</sub> O <sub>5</sub>	0.15	0.12	0.14	0.14	0.10	0.14
SO <sub>3</sub>	30.1	38.5	28.5	19.5	22.9	17.4
LOI	13.5	19.6	15.3	1.5	2.4	1.1
soluble SO <sub>4</sub> <sup>=</sup>	29.7	36.0	29.8	22.4	26.3	20.6

These analyses demonstrated that the larger ash particles in both samples contain more Mg, Ca, SO<sub>3</sub>, and have higher LOI values than the smaller particles. The smaller particles are richer in Al, Na, K, Fe, Ti, and Si. These results suggest that the larger ash particles are derived mainly from the sorbent used in the combustion process, while the smaller particles are derived mainly from the coal. This is supported by comparisons of the concentrations of calcium and magnesium in the two parent samples and their corresponding size fractions. The coarser ash contains about 50% more calcium and magnesium than the finer filter cake ash. These differences suggest that the sorbent-derived ash particles are somewhat larger than the coal-derived ash particles in these samples.

Another difference in these two samples is evident in the acid/base ratios as defined in Table I-4.

## Appendix I

**Table I-4 - Acid/ Base Ratios of Ashes Collected at Tidd on May 11, 1995**

Location	SO <sub>3</sub> /(Ca+Mg)	Soluble SO <sub>4</sub> <sup>=</sup> /(Ca+Mg)
Top Plenum Filter Cake	1.3	1.3
Middle Plenum Tube Sheet	0.58	0.66

The differences in these ratios are due to the exposure of the filter cake ash to much more flue gas than the ash obtained from the passive deposit under the tube sheet. As flue gas is filtered through the filter cake, additional SO<sub>2</sub> in the flue gas is captured by calcium and/or magnesium still remaining in the ash. Although unreacted sorbent present in the passive ash deposits can still react with SO<sub>2</sub> in the flue gas, the reaction is diminished because the flue gas in direct contact with the ash particles in the deposit is exchanged or refreshed relatively slowly. The higher LOI of the filter cake ash is attributed to the presence of the increased amounts of sulfur captured by chemical absorption in the filter cake. The comparisons discussed above suggest that it is possible that the increased flowability of the tube sheet ash may be partially due to chemical differences as well as differences in size distribution.

Standard mineral analyses of two bulk hopper ash samples and two filter cake ash samples (Table I-5) found that, like other Tidd ashes that have been analyzed, the primary elemental constituents of these ash samples were calcium, magnesium, aluminum, silicon and sulfur. Most of the calcium and magnesium in the ash in these samples is derived from use of limestone and/or dolomite in the fluidized bed. The other major constituents of the ash are derived from the coal. These chemical comparisons of hopper ashes and filter cake ashes have also helped to identify the mechanism controlling the consolidation of ash deposits in the APF, as discussed below.

## Appendix I

**Table I-5 - Chemical Analyses of Tidd Ashes Collected in 1993, % wt.**

Constituent	Hopper Ashes		Filter Cake Ashes	
Na <sub>2</sub> O	0.30	0.31	0.30	0.27
K <sub>2</sub> O	1.6	1.42	1.73	1.77
MgO	9.9	9.63	8.77	7.96
CaO	15.3	15.48	14.16	13.67
Fe <sub>2</sub> O <sub>3</sub>	5.3	6.49	4.79	5.63
Al <sub>2</sub> O <sub>3</sub>	13.4	11.80	13.01	13.63
SiO <sub>2</sub>	19.2	21.29	23.03	22.89
TiO <sub>2</sub>	0.50	0.56	0.61	0.07
P <sub>2</sub> O <sub>5</sub>	0.08	0.12	0.11	0.10
SO <sub>3</sub>	33.6	31.10	31.06	31.38
LOI	1.5	2.96	1.45	1.84
Soluble SO <sub>4</sub> <sup>=</sup>	48.3	—	—	40.2

In other chemical analyses, a sample of Tidd ash was leached with water. These analyses indicated that large proportions, but not all, of the Mg, Ca, K, Na, and SO<sub>4</sub> were leached out of the ash in this procedure. Analyses of the leachate showed that the leachable sulfate ions were almost totally bound up as magnesium sulfate and calcium sulfate. At least 30% by weight of the ash was soluble in water.

A variety of physical analyses were also performed on several of the ashes collected in May, 1995. The results of these analyses are presented in Table I-6.

## Appendix I

**Table I-6 - Physical Analyses of Ashes Collected at Tidd on May 11, 1995**

Location (Size Range)	Nodule Porosity, %	Uncompacted Bulk Porosity, %	Specific Surface Area, m <sup>2</sup> /g
Top Plenum Tube Sheet, (all diameters)	73	80	—
Top Plenum Filter Cake (all diameters)	70	84	—
Middle Plenum Tube Sheet, (all diameters)	—	81	—
Top Plenum Filter Cake (diameter >45 μm)	—	—	6.9
Top Plenum Filter Cake 15 μm < diameter < 45 μm	—	—	5.1
Middle Plenum Tube Sheet (diameter > 45 μm)	—	—	1.7
Middle Plenum Tube Sheet 15 μm < diameter < 45 μm	—	—	1.8

The relative coarseness of ash removed from the middle plenum tube sheet, as indicated by the sieve analyses, is evident in the values of specific surface area data measured for the two samples comprising particles with diameters larger than 45 μm.

### Mechanisms Controlling the Consolidation of Ash Deposits

Studies of the buildup of boiler tube deposits in conventional pulverized-coal fired boilers describe a mechanism which may account for the apparent consolidation of the Tidd ash deposits. Many of the ash particles collected in HGCU filter assemblies are derived directly from coal particles. These ash particles often contain a large percentage of aluminosilicate compounds. The other main source of ash particles is the sorbent used in the PFBC process. Sorbent-derived ash particles contain relatively large amounts of magnesium and/or calcium.

## Appendix I

---

Once these two types of ash particles come in contact with each other in the agglomerates formed in the filter vessel, the aluminosilicate compounds in the coal fly ash tend to react with alkali and alkaline metals in the sorbent ash particles to form eutectics that melt at relatively low temperatures<sup>1</sup>. The progress of these reactions is supported by the intimate contact of the ash particles in the agglomerate and by long-term exposure of the ash particles to the temperatures in the filter vessel.

Most of the research into the formation of these eutectics has examined the formation of calcium aluminosilicate compounds (e.g.  $2\text{Ca}\cdot\text{Al}_2\text{O}_3\cdot\text{SiO}_2$  or  $\text{CaO}\cdot\text{Al}_2\text{O}_3\cdot 2\text{SiO}_2$ ). Although pure forms of these compounds do not melt at the temperatures encountered in HGCU filter vessels (pure  $2\text{Ca}\cdot\text{Al}_2\text{O}_3\cdot\text{SiO}_2$  and  $\text{CaO}\cdot\text{Al}_2\text{O}_3\cdot 2\text{SiO}_2$  melt at around 2800 °F), impurities that would almost certainly be present in these compounds because of the heterogeneous nature of coal fly ash particles would lower their melting points. It is likely that this reduction in melting points could combine with long-term exposure to the temperatures in the filter vessel to create relatively soft, sticky layers on the surfaces of the ash particles<sup>2,3</sup>. As the viscosity of the outer layer of the ash particles decreases, the bonds between the particles become stronger. Also, the surface tension of the near-liquid layer on the particles tends to pull adjacent ash particles closer together, thereby eventually consolidating the structure of the entire ash agglomerate. This mechanism may be further enhanced by the relatively small size of the ash particles in the agglomerate.

Chemical reactions, such as the formation of calcium sulfate and/or magnesium sulfate on the surfaces of incompletely reacted sorbent particles in the agglomerate, may increase the strength of interparticle bonds and contribute to another mechanism for eutectic formation. Sulfate salts which form on the surfaces of the ash and sorbent particles result primarily from the reaction of gaseous  $\text{SO}_2$  with solid calcium oxide and/or magnesium oxide. Pure calcium sulfate melts at around 2600 °F, and pure magnesium sulfate decomposes at around 2000 °F. Therefore, it is possible, even with the effects that impurities have on melting points, that these salts do not melt in the filter vessel. Because these sulfate salts may remain in the solid state, they could act as solid bridges between adjacent particles. Such salt bridges can increase particle bonding strengths by several orders of magnitude<sup>4</sup>. Because filter cake ash contacts much more flue gas than passively deposited ash, this type of reaction would be accentuated in the filter cake. However, passive ash deposits can remain in the filter vessel for extended periods since there is no effective means for their periodic on-line removal. Therefore this type of reaction may also occur to a significant extent in these passive deposits.

Additionally sodium, although present in only small amounts in the sorbent and coal fly ash particles, may react with sulfur compounds in the flue gas to form sodium sulfate. Although the melting point of sodium sulfate is over 1600 °F, it may form eutectic mixtures with calcium sulfate, thereby lowering the melting point of the

## Appendix I

---

eutectic mixture into the range of temperatures encountered in barrier filters. (A parallel reaction may also occur with sodium sulfate and magnesium sulfate.) Once this eutectic mixture is formed, it could then act to consolidate the ash agglomerate in the same way as does the calcium aluminosilicate eutectic mixture described above. The same consolidating mechanism would apply to any other eutectic mixture that melted or significantly softened at the temperatures within the filter vessel.

A review of the chemical analyses of hopper and filter cake ashes from Tidd was performed to assess whether additional material that might be condensed out of the flue gas or adsorbed onto the collected particles could account for the apparent consolidation of the various agglomerates of ash present in the filter vessel. The data show that the degree of consolidation of these agglomerates can not be accounted for by condensation and/or adsorption of materials from the flue gas. The mechanism responsible for the extreme consolidation of these agglomerates of ash is most likely a physical rearrangement of the ash particles due to the surface tension of melted or partially melted alkali-aluminosilicate eutectic mixture(s) that form at the contact points between adjacent particles after long-term exposure to the temperatures in the APF.

As can be seen in the SEM photograph of an aggregate of ash removed from the Tidd APF in October 1994 (Figure I-1), the primary ash particles are nearly completely imbedded in a pervasive amorphous mass. Based on various observations of the behavior of these aggregates, it is apparent that the amorphous mass in which the particles are embedded is derived directly from the primary coal ash particles and sorbent particles originally deposited on the surface of the aggregate. The first observation that supports this contention is based on the difference between the porosity of newly-deposited regions of ash aggregates (85 % or higher) and the porosity of portions of the aggregates that have been exposed to the temperatures in the APF for extended periods (around 74 %). In other words, the newly-deposited regions of the agglomerates are no more than 15 % solid, whereas the solid content of older portions is at least 26 %. This means that as the aggregates age in the APF, either the amount of mass has been nearly doubled from some source other than the primary particles (condensation or adsorption from the flue gas), or the primary particles have rearranged themselves to occupy about 58 % of their original total volume.

If the flue gas contributed large amounts of mass to the aggregate through condensation or adsorption, the chemical constituents of this added mass would be limited to compounds that could exist as a vapor at the normal operating conditions of the APF. Although many compounds could satisfy these requirements, some of the major constituents found in the fly ash do not. Three major constituents that will not be found in a gaseous state in the APF are iron, aluminum and silicon. When we compare the mineral analyses of Tidd APF hopper ashes with mineral analyses of aged Tidd filter cake ashes (see Table I-5), the iron, aluminum, and silicon

## Appendix I

---

contents of the two types of samples are very similar. Since the amounts of these three non-volatile elements are not significantly lower in filter cake ash than in hopper ash, it is apparent that essentially all of the mass of the filter cake is due to the original ash particles, and not to any significant deposition of gas-phase constituents from the flue gas.

By examining the SEM photograph of an aggregate of ash taken from the ash shedding cone below the middle plenum at Tidd (Figure I-1), it is apparent that a significant portion of the mass of the ash particles has been transformed into the amorphous material mentioned above. The physical appearance of the amorphous mass is clearly distinct from the appearance of the small ash particles. The appearance of the amorphous mass can best be described as concretion formed from individual ash particles embedded in what appears to be a large, interconnected molten mass. This appearance also supports the contention that eutectics have formed in the ash aggregate.

### Modification of Ash Characteristics

It is doubtful that process changes such as slightly lowering the temperature in the APF, sorbent switching, or addition of a conditioning agent will be able to significantly affect the formation of these eutectics and the subsequent consolidation and strengthening of the ash aggregates. The minimum operating temperature of the APF is strictly limited by the economics of the PFBC process. Past operation at reduced temperatures around 1250 °F have not been able to prevent the formation of consolidated ash aggregates. Since magnesium and calcium are both excellent fluxing agents, altering the type of sorbent used in the PFBC process is not likely to alter the tendency for eutectic formation. Finally, the addition of any conditioning agent to the eutectic system is only likely to lower its melting point even further.

In an attempt to prevent the development of excessive pressure drop at Tidd, efforts have recently been made to alter the characteristics of the filter cake. The approach used has been to decrease the efficiency of the cyclone upstream of the filter assembly. This method, known as derating, can be used to increase the mean diameter of particles exiting the cyclone. For this approach to be effective the size distribution of the entrained ash at the inlet to the filter vessel must be shifted toward larger particle sizes, and this altered size distribution entering the vessel must result in an altered size distribution of particles being deposited on the filter cake and in other locations where tenacious ash deposits have been observed to form. The extent to which relatively large particles entering the APF are actually transported to these locations could not be accurately assessed until samples of actual filter cake ash from derated-cyclone operation had been obtained and analyzed.

## Appendix I

---

### Conclusions

Operation of the Tidd APF has demonstrated the importance of ash characteristics in determining overall filter performance. Ash deposits that formed in the APF were the primary factor that determined the integrity of the barrier filter. The high temperatures in the filter vessel combined with the chemistry and morphology of the ash to form strong, tenacious deposits that often led directly to bent and broken candle filter elements.

The optimum solution to the problems in the Tidd APF caused by the ash aggregates that have been consolidated and strengthened by pervasive eutectic formation is the removal of these aggregates from the APF before the eutectics have had enough time to develop. A large measure of success has been achieved by bypassing the cyclone upstream of the APF. This increases the size distribution of the particles forming the various ash deposits (filter cakes and passive deposits), thereby decreasing their inherent cohesivity. Although particle size is probably the primary reason for these decreases in cohesivity, the somewhat different chemical composition of these larger particles may also influence cohesivity. These agglomerates of lower cohesivity do not have sufficient strength to remain in the APF long enough to undergo consolidation. Gravity and/or vibration cause them to fall off the surface on which they initially formed.

### References

1. O'Gorman, J.V. and P.L. Walker, Jr. "Thermal behavior of mineral fractions separated from selected American coals," Fuel **52**, 71 (1973).
2. Wibberley, L.J. and T.F. Wall. "Alkali-ash reactions and deposit formation in pulverized-coal-fired boilers: experimental aspects of sodium silicate formation and the formation of deposits," Fuel **61**, 93 (1982).
3. Helble, J.J., S. Srinivasachar, and A.A. Boni. "Factors influencing the transformation of minerals during pulverized coal combustion," Prog. Energy Combust. Sci. **16**, 267 (1990).
4. Williams, R. and R.W. Nosker. "Adherent dust particles," RCA Engineer **28**, 76 (1983).

## Appendix II

---

### APPENDIX II (Prepared by Westinghouse STC)

#### FAIL-SAFE DEVICE PERFORMANCE

##### Background

Westinghouse has developed and tested a patented fail-safe regenerator device (FSRD). The device, one of which is installed in the filter holder above each ceramic candle filter, is intended to both minimize thermal shock of the ceramic during pulse cleaning, and minimize penetration of dust when the ceramic filter has failed. When an intact filter is present, the FSRD should not have a high pressure drop nor interfere with pulse gas delivery, but it should heat the pulse gas. In the event of a filter failure the FSRD should restrict flow so as to minimize dust penetration, eventually plug so that penetration stops, and retain the dust plug when its plenum is back pulsed.

Prior developments featured testing of various candidate components, including porous ceramic foam plugs, wire mesh screens, and metal particle beds. Of these, only the fine mesh screen was demonstrated to plug with dust during high-pressure, high-temperature test facility operation. Consequently, the current design evolved, which includes a layered arrangement of fine mesh screen (dust collection barrier), Raschig Rings (heat storage medium), and coarse screens or perforated plates (layer separation and support). Recommended correlations for heat transfer, pressure drop, and dust collection performance were established from Westinghouse STC in-house testing. Rather than correlating these performance parameters in terms of the devices as a whole, the correlations were established for each component layer. Subsequent to these developments, prototype components were built and installed in the Westinghouse filter units operating at Tidd and at Karhula. Results of this testing are reported in this Appendix.

##### Testing at Tidd

In October of 1993, nine FSRDs were installed, one on each plenum in position number 16. This original design (Design A) had the fine mesh screens close together at the bottom of the device. These ran for 1279 hours from January to April 1994. The devices were examined and found to be in good condition. Those above broken candles and in plenums with broken candles had substantial dust in them. No additional data were collected.

## Appendix II

---

In May of 1994 the nine FSRDs were removed and new FSRDs were installed above each candle in the middle plenum of cluster B (twenty-two total). The new FSRDs were of a design which had been improved by separating the fine screens by the width of the Raschig ring bed, to allow trapping of a thick dust cake in event of function as a fail-safe device (Design B). This plenum was the one fitted with prototype developmental candles from a variety of manufacturers, as discussed in Section 4.6.8. These FSRDs were used for 1706 hours from July to October 1994. FSRDs operating above broken candles were recovered, inspected and observed to have been effectively plugged. The pressure drop across a plugged FSRD and across a clean used FSRD were measured at Westinghouse STC.

In November 1994 FSRDs of the B Design were installed at all 288 positions and were subsequently in place for 1110 hours of testing between January and March of 1995. Physical appearance of the intact devices, and in particular of the fine mesh screen elements, is described in Section 4.7.10 and 4.9.1. Again, some of the plugged (broken filter) and still-clean FSRD devices were returned for pressure drop measurement.

### Testing at Karhula

FSRDs of the A Design were installed at Karhula and tested for 1329 hours from November 1993 until June 1994. Upon removal, the FSRDs corresponding to broken candles were plugged. Upper coarse screens had some broken wires, presumably due to a combination of corrosion and thermal shock. The fine mesh screens were torn in some instances. The pressure drop across several used, clean FSRD devices was again measured at Westinghouse. The pressure drop across a plugged device was also measured by Ahlstrom.

### Pressure Drop Assessment

Pressure drop is important because it must be minimal when an intact filter is in place and very high when a filter is broken. Pressure drop may be characterized in terms of flow resistance, i.e., a number of velocity head (N) lost by gas flowing through the device, based on superficial velocity of gas through the 2.62 inch ID internal channel of the FSRD. The pressure drop  $\Delta P$  is related to number of velocity heads N by:

$$\Delta P = \frac{1}{2} N \rho V^2$$

where  $\rho$  is gas density and  $V$  is gas velocity.

## Appendix II

Table II-1 summarizes pressure drop measurements. The number 36 listed for the "Broken Candle" is the flow resistance from the head of a candle with a 30 mm orifice at the center of the candle head, which is assumed to be still in place. It should be added to any of the other numbers in the Table for a final head loss. The data indicates a maintenance of clean permeability with exposure, as well as a substantial decrease in permeability upon plugging. The actual measured decrease in permeability may be low due to loss of dust during handling.

Figure II-1 shows projected gas flow split that occurs with large numbers of candle failures. The top line, developed from pressure drop modeling, shows what would occur with no FSRDs in place. This curve predicts, for example, that approximately 82% of the total gas flow would pass through the open area left by the 25% broken candle elements. The gas passing through this area carries the inlet dust concentration. The lower line shows the projected gas flow split with the FSRDs in place. The curve is based on dust sampling from the controlled four candle element (3 candles intact, 1 broken) laboratory test run. In this case the flow split is assumed proportional to the ratio of the outlet to inlet dust loading. It is also assumed in this testing that only 50% of the dust feed reaches the test unit. This provides, perhaps by a factor of two, a very conservative basis for predicting the performance of the FSRD device.

**Table II-1 - Head Loss Across Fail-Safe Regenerator Devices**

Design	Where Used	Condition After Use	No. Velocity Heads
Broken candle, no FSRD			36
Design A	Laboratory STC	Unused	110
Design B	Laboratory STC	Unused	150
Design A	Laboratory STC	Used/ Broken Candle	4000
Design A	Tidd	Used/ Intact Candle	190
Design A	Tidd	Used/ Broken Candle	2,000,000
Design B	Tidd	Used/ Intact Candle	122
Design B	Tidd	Used/ Broken Candle	1700
Design A	Karhula	Used/ Intact Candle	100
Design A	Karhula	Used/ Broken Candle	5000*

\* Based on measurement by Ahlstrom

## Appendix II

The field test data, Table II-1, show comparable or better performance levels based on flow resistance measurements than that of the reference laboratory test. It is uncertain as to how the dismantling, handling and transporting of the field tested units may have compromised the flow resistance measurements.

Operating the hot gas filter unit with the FSRD devices in place provides considerable margin for failed candle elements. For example, assuming 1000 ppm inlet dust concentration and the conditions given in Figure II-1, the predicted outlet dust loading from the filter unit with 5% failed elements would be expected to be less than 20 ppm based on the conservative laboratory test and perhaps as low as less than 1 ppm based on the most optimistic field test data.

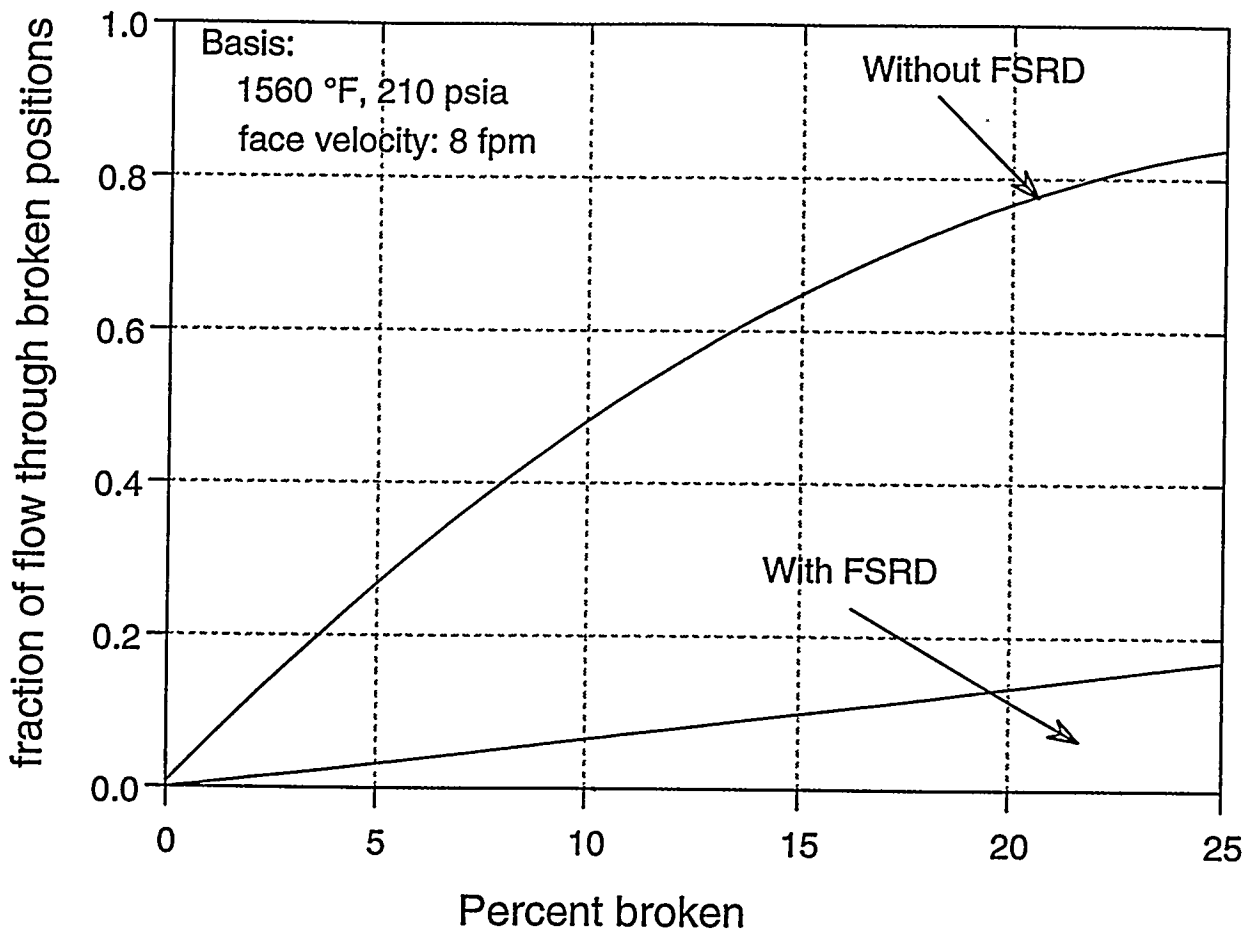


Figure II-1 - Fraction of Flow Through Broken Positions Versus Percent Broken

# **Tidd Hot Gas Clean Up Program**

## **Final Report**

October 1995

Work Performed Under Contract No.: DE-FC21-89MC26042

For  
U.S. Department of Energy  
Office of Fossil Energy  
Morgantown Energy Technology Center  
Morgantown, West Virginia

By  
Ohio Power Company  
Columbus, Ohio

**MASTER**

## **DISCLAIMER**

This report was prepared as an account of work sponsored by an agency of the United States Government. Neither the United States Government nor any agency thereof, nor any of their employees, makes any warranty, express or implied, or assumes any legal liability or responsibility for the accuracy, completeness, or usefulness of any information, apparatus, product, or process disclosed, or represents that its use would not infringe privately owned rights. Reference herein to any specific commercial product, process, or service by trade name, trademark, manufacturer, or otherwise does not necessarily constitute or imply its endorsement, recommendation, or favoring by the United States Government or any agency thereof. The views and opinions of authors expressed herein do not necessarily state or reflect those of the United States Government or any agency thereof.

This report has been reproduced directly from the best available copy.

Available to DOE and DOE contractors from the Office of Scientific and Technical Information, 175 Oak Ridge Turnpike, Oak Ridge, TN 37831; prices available at (615) 576-8401.

Available to the public from the National Technical Information Service, U.S. Department of Commerce, 5285 Port Royal Road, Springfield, VA 22161; phone orders accepted at (703) 487-4650.



This cover stock is 30% post-consumer waste  
and 30% pre-consumer waste, and is recyclable.



# **Tidd Hot Gas Clean Up Program**

## **Final Report**

Work Performed Under Contract No.: DE-FC21-89MC26042

For  
U.S. Department of Energy  
Office of Fossil Energy  
Morgantown Energy Technology Center  
P.O. Box 880  
Morgantown, West Virginia 26507-0880

By  
Ohio Power Company  
1 Riverside Plaza  
Columbus, Ohio 43216-6631

October 1994



## Forward

---

This Final Report on the Tidd Hot Gas Clean Up Program covers the period from initial Proof-of-Concept testing in August, 1990, through final equipment inspections in May, 1995.

The Tidd Hot Gas Clean Up (HGCU) system was installed in the Tidd Pressurized Fluidized Bed Combustion (PFBC) Demonstration Plant, which is the first utility-scale PFBC plant in the United States. The plant is owned and operated by Ohio Power Company and is located on the banks of the Ohio River, approximately 75 miles downstream of Pittsburgh, Pennsylvania.

This project was funded by the U. S. Department of Energy (DOE), administered by the Morgantown Energy Technology Center (METC) in accordance with DOE Cooperative Agreement No. DE-FC21-89MC26042. Westinghouse Science and Technology Center (STC) of Pittsburgh, Pennsylvania, also contributed 20% cost share for their portion of the project.

The METC Project Manager was Richard A. Dennis. The Contractor Project Manager was Michael J. Mudd and the Principal Investigator was John D. Hoffman. The Westinghouse Project Manager was Thomas E. Lippert.

Detailed design work on the project began in July, 1990, and site construction began in December, 1991. Initial operation of the system occurred in May, 1992, and the hot gas filter was commissioned in October, 1992. The test program ended in March, 1995, when the Tidd Plant was shut down following its four-year test program.

Section 1.0 of this report is an executive summary of the project covering the project background, system description, test results and conclusions. Section 2.0 is an introduction covering the program objectives and schedule. Section 3.0 provides detailed descriptions of the system and its major components. Section 4.0 provides detailed results of all testing including observations and posttest inspection results. Sections 5.0 and 6.0 list the program conclusions and recommendations, respectively. Appendix I is a report prepared by Southern Research Institute on the properties of Tidd PFBC ash sampled during the test program. Appendix II is a report prepared by Westinghouse STC on the performance of candle filter fail-safe regenerator devices.

This report was prepared by American Electric Power Service Corporation (AEPSC) as agent for Ohio Power Company. The portions of the report covering material surveillance test results (Sections 4.9.1 and 4.9.2) were prepared by Westinghouse STC. The following individuals prepared this report:

American Electric Power Service Corporation, Columbus, Ohio:

John D. Hoffman  
Michael J. Mudd  
William P. Reinhart

Westinghouse Science and Technology Center, Pittsburgh, Pennsylvania:

Gerald J. Bruck  
Mary Ann Alvin  
Dennis M. Bachovchin

Southern Research Institute, Birmingham, Alabama:

Todd R. Snyder



## Table of Contents

---

1.0 EXECUTIVE SUMMARY .....	1
1.1 Background .....	1
1.2 Project Description .....	1
1.3 Results .....	2
1.4 Conclusions .....	7
2.0 INTRODUCTION .....	9
2.1 Program Objectives .....	9
2.2 Program Schedule and Milestones .....	9
3.0 PROJECT DESCRIPTION .....	13
3.1 System Description .....	13
3.2 Filter Vessel .....	17
3.3 Filter Internals .....	17
3.4 Backpulse System .....	24
3.5 Backup Cyclone .....	28
3.6 Ash Removal System .....	30
3.6.1 Screw Cooler .....	33
3.6.2 Surge Hopper and Lockhopper .....	34
3.7 Hot Gas Piping .....	35
3.8 Controls and Data Acquisition .....	36
4.0 RESULTS .....	38
4.1 Proof-of-Concept Testing .....	38
4.1.1 Thermal Transient Tests .....	38
4.1.2 HTHP Array Backpulse Tests .....	38
4.1.3 Alkali Attack .....	39
4.1.4 Pulse Valve Testing .....	39
4.1.5 Cold Flow Modelling .....	39
4.1.6 Gasket Tests .....	39
4.1.7 Filter Cake Properties .....	40
4.1.8 Karhula Testing .....	40
4.2 Initial System Operation .....	41
4.2.1 System Modifications (5/92-10/92) .....	42
4.3 Test Period I: 10/92 - 12/92 .....	47
4.3.1 Test Run 1 - 10/28 to 11/1/92 .....	47
4.3.2 Test Run 2 - 11/17/92 .....	48
4.3.3 Test Run 3 - 11/21 to 11/24/92 .....	48
4.3.4 Test Run 4 - 11/25 to 12/7/92 .....	50
4.3.5 Posttest Inspection and Modifications (12/92-6/93) .....	50
4.4 Test Period II: 6/93 - 9/93 .....	71
4.4.1 Test Runs 5 and 6 - 6/30 to 7/5/93 .....	71
4.4.2 Test Run 7 - 7/18 to 8/5/93 .....	71
4.4.3 Test Runs 8 and 9 - 8/9 to 8/14/93 .....	73
4.4.4 Test Run 10 - 8/19 to 8/24/93 .....	73
4.4.5 Test Run 11 - 8/29 to 9/23/93 .....	74

## Table of Contents

---

4.4.6	Posttest Inspection and Modifications (9/93-1/94)	77
4.5	Test Period III: 1/94 - 4/94	85
4.5.1	Test Run 12 - 1/10 to 1/11/94	85
4.5.2	Test Run 13 - 1/15 to 1/29/94	86
4.5.3	Test Run 14 - 2/17 to 2/18/94	86
4.5.4	Test Run 15 - 2/19 to 2/25/94	89
4.5.5	Test Run 16 - 3/3 to 3/9/94	89
4.5.6	Test Run 17 - 3/16 to 3/23/94	89
4.5.7	Test Run 18 - 3/31 to 4/18/94	90
4.5.8	Posttest Inspection and Modifications (4/94-7/94)	96
4.6	Test Period IV: 7/94 - 10/94	113
4.6.1	Test Runs 19 and 20 - 7/16/94	113
4.6.2	Test Run 21 - 7/20/94 to 7/27/94	113
4.6.3	Test Run 22 - 7/28/94 to 8/25/94	115
4.6.4	Posttest Inspection (8/94)	115
4.6.5	Test Run 23 - 9/3/94 to 9/10/94	117
4.6.6	Posttest Inspection (9/94)	117
4.6.7	Test Run 24 - 9/22/94 to 10/21/94	117
4.6.8	Posttest Inspection (10/94)	120
4.7	Test Period V: 1/95-3/95	137
4.7.1	Test Runs 25, 26, and 27 - 1/13/95 to 1/21/95	137
4.7.2	Test Run 28 - 1/27/95 to 2/2/95	137
4.7.3	Posttest Inspection (2/95)	140
4.7.4	Test Runs 29 and 30 - 2/9/95 to 2/10/95	140
4.7.5	Test Run 31 - 2/11/95 to 2/12/95	140
4.7.6	Test Run 32 - 2/13/95 to 2/16/95	140
4.7.7	Posttest Modifications (2/95)	142
4.7.8	Test Run 33 - 2/18/95 to 3/8/95	142
4.7.9	Test Run 34 - 3/14/95 to 3/30/95	142
4.7.10	Posttest Inspection (4/95-5/95)	144
4.8	Final Equipment Inspections	156
4.8.1	Filter Vessel	156
4.8.2	Filter Internals	156
4.8.3	Backpulse System	157
4.8.4	Backup Cyclone	164
4.8.5	Ash Removal System	164
4.8.6	Hot Gas Piping	164
4.9	Materials Surveillance Test Results	180
4.9.1	Metal Structures and Test Coupons	182
4.9.2	Candle Filters	197
5.0	CONCLUSIONS	218
6.0	RECOMMENDATIONS	220

## Table of Contents

---

APPENDIX I (Prepared by Southern Research Institute) .....	222
APPENDIX II (Prepared by Westinghouse STC) .....	238

## Table of Contents

---

### List of Tables

Table 2.2.1 - Tidd HGCU Test Periods .....	10
Table 2.2.2 - Tidd HGCU Runs Summary .....	11
Table 3.1 - APF Design Basis .....	14
Table 3.7 - Hot Gas Piping Design .....	36
Table 4.1.7 - PFBC Ash Properties .....	40
Table 4.3 - Summary of HGCU Operation - Test Period I .....	47
Table 4.4 - Summary of HGCU Operation - Test Period II .....	71
Table 4.5 - Summary of HGCU Operation - Test Period III .....	85
Table 4.6 - Summary of HGCU Operation - Test Period IV .....	113
Table 4.7 - Summary of HGCU Operation - Test Period V .....	137
Table 4.9.1 - Summary of Internal Structural Component Performance Issues and Corrective Actions .....	184
Table 4.9.2 - Surveillance Tree Coupon Weight Comparisons .....	187
Table 4.9.3 - Elongation of Clay Bonded Silicon Carbide Candle Filters .....	201
Table 4.9.4 - Posttest Candle Filter Time-Of-Flight Measurements .....	202
Table 4.9.5 - Filter Candle Materials .....	204
Table 4.9.6 - Candle Filter Failure Mechanisms Experienced During Operation at Tidd .....	205
Table 4.9.7 - Candle Filter Bulk Matrix Strength .....	208
Table I-1 - Sedigraphic Analyses of Tidd Ashes .....	228
Table I-2 - Sieve Analyses of Tidd Ashes .....	228
Table I-3 - Chemical Analyses of Tidd Ashes Collected in May 1995, % wt. ....	230
Table I-4 - Acid/Base Ratios of Ashes Collected at Tidd on May 11, 1995 .....	231
Table I-5 - Chemical Analyses of Tidd Ashes Collected in 1993, % wt. ....	232
Table I-6 - Physical Analyses of Ashes Collected at Tidd on May 11, 1995 .....	233
Table II-1 - Head Loss Across Fail-Safe Regenerator Devices .....	240

## Table of Contents

### List of Figures

Figure 2.2 - Program Schedule .....	10
Figure 3.1.1 - HGCU Slipstream Schematic .....	15
Figure 3.1.2 - Isometric View of HGCU System .....	16
Figure 3.2 - Photograph of APF Vessel During Erection .....	19
Figure 3.3.1 - APF Internal Arrangement .....	20
Figure 3.3.2 - Photograph of Filter Internals During Initial Installation .....	21
Figure 3.3.3 - Photograph of Filter Internals During Initial Installation .....	22
Figure 3.3.4 - Photograph of Filter Internals During Initial Installation .....	23
Figure 3.4.1 - Schematic Diagram of Backpulse System .....	25
Figure 3.4.2 - Photograph of Backpulse Skid .....	26
Figure 3.4.3 - Photograph of Backpulse Skid .....	27
Figure 3.5 - Cross Section of Backup Cyclone .....	29
Figure 3.6 - Ash Removal System Schematic .....	32
Figure 3.6.1 - Screw Cooler Schematic .....	34
Figure 4.2.1 - Photograph of Hastelloy Liner in Hot Gas Pipe Spool .....	44
Figure 4.2.2 - Typical Expansion Joint After Modifications .....	45
Figure 4.2.3 - Cross Section of Typical Hot Gas Piping Joint .....	46
Figure 4.3.1 - Photograph of Bottom Filter Candles Following Test Run 1 .....	49
Figure 4.3.2 - Photograph of Filter Internals Following Test Run 4 .....	51
Figure 4.3.3 - Photograph of Filter Internals Following Test Run 4 .....	52
Figure 4.3.4 - Photograph of Filter Internals Following Test Run 4 .....	53
Figure 4.3.5 - Photograph of Filter Internals Following Test Run 4 .....	54
Figure 4.3.6 - Photograph of Filter Internals Following Test Run 4 .....	55
Figure 4.3.7 - Photograph of Filter Internals Following Test Run 4 .....	56
Figure 4.3.8 - Photograph of Filter Internals Following Test Run 4 .....	57
Figure 4.3.9 - Photograph of Filter Internals Following Test Run 4 .....	58
Figure 4.3.10 - Photograph of Filter Internals Following Test Run 4 .....	59
Figure 4.3.11 - Graphs of Filter Parameters During Test Run 4 .....	66
Figure 4.3.12 - Photograph of Filter Internals Before Test Period II .....	67
Figure 4.3.13 - Photograph of Filter Internals Before Test Period II .....	68
Figure 4.3.14 - Photograph of Filter Internals Before Test Period II .....	69
Figure 4.3.15 - Photograph of Filter Internals Before Test Period II .....	70
Figure 4.4.2 - Filter DP and Temperature During Test Run 7 .....	72
Figure 4.4.5 - Filter DP and Temperature During Test Run 11 .....	76
Figure 4.4.6 - Photograph of Filter Internals Following Test Run 11 .....	79
Figure 4.4.7 - Photograph of Filter Internals Following Test Run 11 .....	80
Figure 4.4.8 - Photograph of Filter Internals Following Test Run 11 .....	81
Figure 4.4.9 - Photograph of Filter Internals Following Test Run 11 .....	82
Figure 4.4.10 - Photograph of Filter Internals Following Test Run 11 .....	83
Figure 4.4.11 - Photograph of Filter Internals Following Test Run 11 .....	84
Figure 4.5.2 - Filter DP and Temperature During Test Run 13 .....	87
Figure 4.5.4 - Filter DP and Temperature During Test Run 15 .....	88

## Table of Contents

---

Figure 4.5.5 - Filter DP and Temperature During Test Run 16 .....	91
Figure 4.5.6 - Filter DP and Flow During Test Run 16 .....	92
Figure 4.5.7 - Filter DP and Temperature During Test Run 17 .....	93
Figure 4.5.8 - Filter DP and Flow During Test Run 17 .....	94
Figure 4.5.9 - Filter DP and Temperature During Test Run 18 .....	95
Figure 4.5.10 - Photograph of Filter Internals Following Test Run 18 .....	98
Figure 4.5.11 - Photograph of Filter Internals Following Test Run 18 .....	99
Figure 4.5.12 - Photograph of Filter Internals Following Test Run 18 .....	100
Figure 4.5.13 - Photograph of Filter Internals Following Test Run 18 .....	101
Figure 4.5.14 - Photograph of Filter Internals Following Test Run 18 .....	102
Figure 4.5.15 - Photograph of Filter Internals Following Test Run 18 .....	103
Figure 4.5.16 - Photograph of Filter Internals Following Test Run 18 .....	104
Figure 4.5.17 - Photograph of Filter Internals Following Test Run 18 .....	105
Figure 4.5.18 - Photograph of Filter Internals Following Test Run 18 .....	106
Figure 4.5.19 - Photograph of Filter Internals Before Test Period IV .....	107
Figure 4.5.20 - Photograph of Filter Internals Before Test Period IV .....	108
Figure 4.5.21 - Photograph of Filter Internals Before Test Period IV .....	109
Figure 4.5.22 - Photograph of Filter Internals Before Test Period IV .....	110
Figure 4.5.23 - Photograph of Filter Internals Before Test Period IV .....	111
Figure 4.5.24 - Photograph of Filter Internals Before Test Period IV .....	112
Figure 4.6.2 - Filter DP and Temperature During Test Run 21 .....	114
Figure 4.6.3 - Filter DP and Temperature During Test Run 22 .....	116
Figure 4.6.5 - Filter DP and Temperature During Test Run 23 .....	118
Figure 4.6.7 - Filter DP and Temperature During Test Run 24 .....	119
Figure 4.6.8 - Photograph of Filter Internals Following Test Run 24 .....	122
Figure 4.6.9 - Photograph of Filter Internals Following Test Run 24 .....	123
Figure 4.6.10 - Photograph of Filter Internals Following Test Run 24 .....	124
Figure 4.6.11 - Photograph of Filter Internals Following Test Run 24 .....	125
Figure 4.6.12 - Photograph of Filter Internals Following Test Run 24 .....	126
Figure 4.6.13 - Photograph of Filter Internals Following Test Run 24 .....	127
Figure 4.6.14 - Photograph of Filter Internals Following Test Run 24 .....	128
Figure 4.6.15 - Photograph of Filter Internals Following Test Run 24 .....	129
Figure 4.6.16 - Photograph of Filter Internals Following Test Run 24 .....	130
Figure 4.6.17 - Photograph of Crack in Back Pulse Tube .....	131
Figure 4.6.18 - Location of Filter Candle Materials Before Test Period V .....	132
Figure 4.6.19 - Photograph of Filter Internals Before Test Period V .....	133
Figure 4.6.20 - Photograph of Filter Internals Before Test Period V .....	134
Figure 4.6.21 - Photograph of APF Shroud Following Test Run 24 .....	135
Figure 4.6.22 - Photograph of APF Shroud After Replacement of Upper Portion .....	136
Figure 4.7.2 - Filter DP and Temperature During Test Run 28 .....	139
Figure 4.7.6 - Filter DP and Temperature During Test Run 32 .....	141
Figure 4.7.8 - Filter DP and Temperature During Test Run 33 .....	143
Figure 4.7.9 - Filter DP and Temperature During Test Run 34 .....	145
Figure 4.7.10 - Photograph of Filter Internals Following Test Run 34 .....	147
Figure 4.7.11 - Photograph of Filter Internals Following Test Run 34 .....	148
Figure 4.7.12 - Photograph of Filter Internals Following Test Run 34 .....	149

## Table of Contents

Figure 4.7.13 - Photograph of Filter Internals Following Test Run 34 .....	150
Figure 4.7.14 - Photograph of Filter Internals Following Test Run 34 .....	151
Figure 4.7.15 - Photograph of Filter Internals Following Test Run 34 .....	152
Figure 4.7.16 - Photograph of Filter Internals Following Test Run 34 .....	153
Figure 4.7.17 - Photograph of Filter Internals Following Test Run 34 .....	154
Figure 4.7.18 - Photograph of Filter Internals Following Test Run 34 .....	155
Figure 4.8.1 - Photograph of Corrosion of APF Head Under Insulation Near Outlet Nozzle .....	158
Figure 4.8.2 - Photograph of APF Shroud During Final Removal .....	159
Figure 4.8.3 - Photograph of Shroud Impingement Plate .....	160
Figure 4.8.4 - Photograph of APF Liner .....	161
Figure 4.8.5 - Photograph of Tubesheet Cone .....	162
Figure 4.8.6 - Photograph of Tubesheet Cone .....	163
Figure 4.8.7 - Photograph of Backpulse Valve Internals .....	166
Figure 4.8.8 - Photograph of Backpulse Valve Internals .....	167
Figure 4.8.9 - Photograph of Backup Cyclone Internals .....	168
Figure 4.8.10 - Photograph of Backup Cyclone Internals .....	169
Figure 4.8.11 - Photograph of Backup Cyclone Internals .....	170
Figure 4.8.12 - Photograph of Backup Cyclone Internals .....	171
Figure 4.8.13 - Photograph of Alternate Ash Line Restrictive Orifice .....	172
Figure 4.8.14 - Photograph of Alternate Ash Line Restrictive Orifice .....	173
Figure 4.8.15 - Photograph of Hastelloy Liner After Removal From Pipe Section .....	174
Figure 4.8.16 - Photograph of Inside Surface of Carbon Steel Pipe Under Hastelloy Liner .....	175
Figure 4.8.17 - Photograph of Inside of Pipe Spool Following Removal of Section .....	176
Figure 4.8.18 - Photograph of Inside of Pipe Spool Following Removal of Section .....	177
Figure 4.8.19 - Photograph of Inside of Pipe Spool Following Removal of Section .....	178
Figure 4.8.20 - Photograph of Inside of Pipe Spool Following Removal of Section .....	179
Figure 4.9 - Tidd HGCU APF Operating Temperature History .....	181
Figure 4.9.1 - Cross Section of 0.005-inch Wire from Fine Fail-safe Mesh As New-700X .....	188
Figure 4.9.2 - Cross Section of 0.005-inch Wire from Fine Fail-safe Mesh After 1329 hours at Karhula-700X .....	189
Figure 4.9.3 - Cross Section of 0.005-inch Wire from Fine Fail-safe Mesh After 1110 hours at Tidd-700X .....	190
Figure 4.9.4 - Cross Section of Alloy 333 Coupon-700X .....	191
Figure 4.9.5 - Cross Section of Alloy 617 Coupon-700X .....	192
Figure 4.9.6 - Cross Section of Alloy 556 Coupon-700X .....	193
Figure 4.9.7 - Cross Section of Alloy 188 Coupon-700X .....	194
Figure 4.9.8 - Cross Section of Alloy 253MA Coupon-700X .....	195
Figure 4.9.9 - Cross Section of Alloy 310 Coupon-700X .....	196
Figure 4.9.10 - Room Temperature Gas Flow Resistance of the First Generation Monolithic and Advanced Second Generation Candle Filters .....	198
Figure 4.9.11 - Room Temperature Gas Flow Resistance Measurements Across As-Manufactured Clay Bonded Silicon Carbide Filter Elements. Measurements Were Repeated After Operation at Tidd. ....	200
Figure 4.9.12 - Correlation of Time-of-Flight and Burst Strength with Room Temperature C-Ring Compressive Strength for Candle Filters Exposed for 464 Hours of PFBC Operating Conditions in Test Period I. ....	203

## Table of Contents

---

Figure 4.9.13 - Schumacher Strength Profile .....	206
Figure 4.9.14 - Photo Micrograph Showing Crystallization of the Schumacher Dia Schumalith F40 Filter Matrix .....	210
Figure 4.9.15 - Crystallization of the Coors Alumina/Mullite Filter Matrix after 1110 hrs of Operation in Test Period IV .....	213
Figure 4.9.16 - Crystallization of the Coors Alumina/Mullite Filter Matrix after 2816 hrs of Operation in Test Period IV and V .....	214
Figure 4.9.17 - Thermal Coefficient of Expansion of the Tidd PFBC Ash and Select Porous Ceramic Filter Materials .....	217
Figure I-1 - SEM Photograph of a Fresh Fracture Surface of an Ash Agglomerate Taken from an Ash Shed in the Tidd APF in October 1994 .....	226
Figure I-2 - Cumulative Size Distribution Data Measured with a Sedigraph and Sieves for Five Ashes Collected from the Tidd APF .....	229
Figure II-1 - Fraction of Flow Through Broken Positions Versus Percent Broken .....	241

## Acronyms and Abbreviations

---

<b>acfm</b>	Actual Cubic Feet Per Minute
<b>AEP</b>	American Electric Power Company, Inc.
<b>APF</b>	Advanced Particle Filter
<b>ANSI</b>	American National Standards Institute
<b>ASME</b>	American Society of Mechanical Engineers
<b>BUC</b>	Backup Cyclone
<b>CaO</b>	Calcium Oxide
<b>cm</b>	Centimeter
<b>CVI-SiC</b>	Chemical Vapor Infiltration-Silicon Carbide
<b>Δ</b>	Delta
<b>DP</b>	Differential Pressure
<b>EDAX</b>	Energy Dispersive X-Ray Analyses
<b>F</b>	Degrees Fahrenheit
<b>FSRD</b>	Fail-Safe Regenerator Device
<b>fps</b>	Feet Per Second
<b>gm/cc</b>	Grams Per Cubic Centimeter
<b>gpm</b>	Gallons Per Minute
<b>GT</b>	Gas Turbine
<b>HGCU</b>	Hot Gas Clean Up
<b>hp</b>	Horsepower
<b>hr</b>	Hour

## Acronyms and Abbreviations

---

<b>HTHP</b>	High Temperature High Pressure
<b>ID</b>	Inside Diameter
<b>in.</b>	Inches
<b>in. H<sub>2</sub>O</b>	Inches of Water
<b>in.-lbf.</b>	Inch-Pounds of Torque
<b>lbm</b>	Pounds Mass
<b>mm</b>	Millimeter
<b>MWe</b>	Megawatt Electric
<b>MWt</b>	Megawatt Thermal
<b>OD</b>	Outside Diameter
<b>PCFB</b>	Pressurized Circulating Fluidized Bed
<b>PFBC</b>	Pressurized Fluidized Bed Combustion
<b>POPS</b>	Plant Operations and Performance System
<b>ppmw</b>	Parts Per Million by Weight
<b>psi</b>	Pounds Per Square Inch
<b>psig</b>	Pounds Per Square Inch Gauge
<b>PT</b>	Penetrant Test
<b>QA/QC</b>	Quality Assurance/Quality Control
<b>scfm</b>	Standard Cubic Feet Per Minute
<b>SEM</b>	Scanning Electron Microscopy
<b>SSH</b>	Secondary Superheater

## Acronyms and Abbreviations

---

<b>ST</b>	Steam Turbine
<b>TOF</b>	Time of Flight
<b><math>\mu\text{m}</math></b>	Microns
<b>UNS</b>	Unified Numbering System
<b>XJ</b>	Expansion Joint
<b>XRD</b>	X-Ray Diffraction



## Executive Summary

---

### 1.0 EXECUTIVE SUMMARY

#### 1.1 Background

The objective of this program was to evaluate the design and obtain operating experience for a commercial size Advanced Particle Filter (APF) through long-term testing on a slipstream at Ohio Power Company's Tidd Pressurized Fluidized Bed Combustion (PFBC) Demonstration Plant. The 70 MWe Tidd PFBC Demonstration Plant in Brilliant, Ohio was completed in late 1990, and operated through March 1995 as part of the Department of Energy's Clean Coal Technology Program. Provisions were included as part of the original design to install a one-seventh slipstream on the PFBC exhaust gases between the fluidized bed and the gas turbine to test an APF system. In July 1990, AEP awarded a contract to Westinghouse Science and Technology Center to provide a candle-based APF. Detailed engineering and material procurement were completed by the end of 1991 when installation began. Initial operation of the system occurred in May, 1992, and the APF was commissioned in October, 1992. The HGCU system operated during five separate test periods between October, 1992, and March, 1995, compiling a total of 5854 hours of operation on coal fire.

#### 1.2 Project Description

In the original design, the Tidd PFBC Demonstration Plant utilized seven strings of primary and secondary cyclones to remove 98% of the particulate matter from the gases between the fluidized bed and the gas turbine. The HGCU slipstream replaced one of the seven secondary cyclones by taking the discharge gas of one of the primary cyclones to outside of the combustor vessel and into the APF. After passing through the APF, the gas flowed through a backup cyclone and then returned to the combustor vessel, where the slipstream flow rejoined the combustor gas at the discharge of the other six cyclone strings.

Under the original maximum load design conditions, gas at approximately 150 psig, 1550F flowed into the filter at 7600 acfm with a dust loading of approximately 600 ppmw. In January 1994, the dust loading to the filter was increased from approximately 600 ppmw to 3400 ppmw by detuning the primary cyclone upstream of the APF. In January 1995, the primary cyclone was bypassed which increased the ash loading to approximately 20,000 ppmw. Ash collected in the APF was discharged to a screw cooler and into a lockhopper system which fed a vacuum pneumatic ash transport system. A backup cyclone

## Executive Summary

---

downstream of the filter was included to clean the gas in case of a filter malfunction, and to balance the pressure drop of the slipstream with the other six cyclone strings.

The system was designed to remove virtually all entrained particulates discharged from one of the seven parallel primary cyclones on the outlet of the PFBC combustor. Ash collected on the outside surface of ceramic filter elements (candles), resulting in a gradual increase in the overall flow resistance of the slipstream. The filter cake was periodically dislodged by injecting a high pressure air pulse to the clean side of the candles. The ash cake on the candles then fell to the conical discharge hopper where it was removed from the filter vessel and cooled by an ash screw cooler which discharged into a lockhopper system.

The main elements of the system included the filter vessel and its internals; back pulse skid, including secondary accumulators and valves; back pulse air supply skid, including compressor, dryer and primary accumulator; backup cyclone; ash screw cooler, surge hopper, lockhopper, piping, and instrumentation.

The filter vessel was 10 feet in diameter and 44 feet high. The vessel was internally insulated with a 7 to 9-inch thick layer of alumina-silica ceramic fiber insulation to keep the vessel shell temperature below 250F. The filter contained 384 filter elements which were referred to as candles because of their long cylindrical shape. Each candle was nominally 2.36 inches in outside diameter and 4.92 feet long. The candles were made of two layers of sintered silicon carbide.

The Backpulse System was comprised of a compressor skid, valve skid, and interconnecting piping.

There were three control modes available for the filter system, namely manual mode, automatic differential pressure (DP) mode and automatic timer mode. The system was normally operated in the timer mode. In this mode, filter cleaning occurred at uniform time intervals, typically thirty minutes. A Bailey Net 90 control system was used to monitor and control the system parameters and provide operator interfaces. Data collected included pressure, temperature, flowrate, differential pressure, level, etc. throughout the system.

### 1.3 Results

During the design phase of the project, Westinghouse conducted proof-of-concept testing to verify the design basis of various system components. The tests included thermal transient tests of filter elements,

## Executive Summary

---

high temperature high pressure tests of an eleven candle array, cold flow modeling, pulse valve tests, gasket tests, alkali attack tests on silicon carbide, and ash characterization.

During initial operation of the system in May, 1992, using a bypass cyclone with the APF not in service, an expansion joint in the hot gas piping system ruptured due to stress corrosion from chemical attack by condensed flue gas. Hot spots also were detected in the piping system during this test. As a result of the problems noted during initial testing, several modifications were made to the piping system before the APF was commissioned. The stainless steel expansion joint bellows were replaced with two-ply Hastelloy C-22 material which had much better corrosion resistance to condensed flue gas. The ceramic fiber material used to internally insulate the hot gas piping and expansion joints was replaced with cast refractory to prevent hot gas from flowing to the outer pipe and creating hot spots. Hastelloy cladding was added to the inside surface of the hot gas pipe to protect it from corrosion. The modifications described above proved successful, and the piping system performed very well during subsequent testing. However, corrosion of expansion joint bellows remained a problem until additional steps were taken later in the project.

The filter was commissioned on coal fire on October 28, 1992. During the first test period from October to December, 1992, the system operated 464 hours during four test runs, with the longest run of 286 hours. The major problem during this test period was unreliable ash removal from the APF and lockhopper system. In addition, another expansion joint bellows (inner ply only) developed a pinhole leak due to corrosion, the backpulse air compressor failed resulting in a 17-hour interruption in filter cleaning, and the APF pressure drop was unstable at operating temperatures above 1400F. Upon shutdown, the APF hopper was full of ash above the level of the lower candles which resulted in the breakage of 21 bottom candles. The HGCU system was bypassed and Tidd continued to operate on six cyclone strings until the next test period.

Prior to the next test period, several modifications were made to address the problems encountered during the first test period. All of the bottom filter candles were replaced. The ash removal system was modified to improve the operation of the lockhopper system, a vibrator was added to the APF hopper liner to aid in ash removal, the expansion joints were heat traced and insulated to maintain them above the flue gas acid dew point, and backup compressors were added to ensure continuous filter cleaning in case a future compressor failures.

## Executive Summary

---

The second test series began in June, 1993, and lasted until September, 1993. During this period, the system operated for 1295 hours on coal fire over seven separate runs with the longest run of 597 hours. During this period problems with ash removal from the APF hopper persisted and the filter pressure drop was unstable during some of the runs. It was possible to clean the ash from the filter candles at reduced load (temperature) and thereby lower the filter pressure drop; however, the high filter pressure drop recurred after two days of operation at higher temperatures.

Posttest inspection revealed 62 broken candles and very heavy ash bridging between candles and support pipes. Microcracking was detected in the high temperature portion of the backpulse tubes. Galling was found on the backpulse valve internals. Modifications made to the system prior to the next test series included replacing all of the filter candles, replacing the backpulse tubes with a different material, adding hardened surfaces to the backpulse valve internals, and adding nine purge air nozzles to the APF hopper to aid in ash removal.

In an effort to overcome the ash bridging problem, it was decided to detune the primary cyclone upstream of the filter during the next test series. It was believed that the resulting coarser ash would be easier to remove from the filter candles and less likely to accumulate on the hopper walls. All testing during the next test period was conducted with the cyclone detuned.

The third test period was from January to April, 1994, and covered 1279 hours of operation with seven runs, the longest being 444 hours. Ash sampling was performed upstream and downstream of the APF using specially designed sampling probes. The results showed that by detuning the primary cyclone, the ash loading to the filter increased from a design value of 600 ppmw to about 3400 ppmw, and the mass mean particle size of the ash increased from about 3 to 7 microns. The higher ash concentration resulted in significantly higher ash loading. Despite the higher ash loading, the filter pressure drop was stable during this period up to 1450F operating temperature.

Hazardous Air Pollutant testing was conducted by Radian Corporation in April, 1994, and the results of the testing are documented in Report Number DCN 94-633-021-03, dated October, 1994. As part of Hazardous Air Pollutant testing, SO<sub>2</sub> data were obtained upstream and downstream of the APF. Results indicated that the SO<sub>2</sub> level in the gas was reduced approximately 40% by the APF. Post-test analysis of ash samples retrieved from the APF and precipitator hoppers confirmed this observation.

## Executive Summary

---

The filter internals were removed from the APF vessel following this test series, and 28 broken candles were found. Very heavy ash bridging was observed between the inner rows of candles and the support pipe on the top and middle plenums. All of the candle breaks except one appeared to be fresh breaks judging from the clean fracture surfaces. All of the breaks occurred at the top of the candles just below the candle holders. The breaks appeared to result from bending forces from ash bridging from the inner candles to the outer candles. The outlet side of the filter was very clean with virtually no ash deposits. This indicated that the failures occurred during or after plant shutdown, and that the filter was not leaking ash to the clean side during operation.

All of the candles in the upper and middle plenums were removed, cleaned, and inspected. The bottom plenum candles were not removed and cleaned since they did not exhibit significant bridging. The upper and middle plenums were reassembled with an assortment of new and used candles. Thirty of the new replacement candles were second generation materials.

Since ash bridging between the support pipes and inner rows of candles remained a problem, it was decided to remove the inner row of candles from the six upper and middle plenums to determine if this would eliminate the ash bridging. Removal of the inner rows reduced the number of candles from 384 to 288 and increased the face velocity from 7.1 ft/min to 8.9 ft/min. In addition, provisions were added to totally spoil the primary cyclone ahead of the filter to evaluate operation with a higher mean particle size.

The fourth test period began in July, 1994 and ended in October, 1994. Operation totaled 1706 hours of coal fire over six runs, the longest being 691 hours. After operating for 844 hours, the filter was inspected using a boroscope to determine if removal of the inner rows of candles from the upper and middle plenums had eliminated ash from accumulating on the ash sheds and bridging over to the candles. This was believed to be the root cause of the candle failures in the previous tests. Ash bridging, while less than before, had still occurred. The APF hopper was clean two days following shutdown, but when inspected again four days following shutdown, ash was found in the hopper. During the inspection with a boroscope, 14 broken filter candles were seen, and candle pieces were later removed from the hopper. It was decided to continue this test series with 14 broken candles.

During the following test run, the primary cyclone was completely spoiled for 90 hours causing all of the ash entering it to flow into the APF. The APF was again inspected using a boroscope following this run, and it was found that most of the ash bridges seen in the previous inspection had disappeared, and

## Executive Summary

---

the few that remained appeared smaller. This indicated that the coarser ash was cleaning the ash accumulation from the ash sheds. The liner and hopper also were very clean of ash deposits. No additional broken candles were observed.

At the end of this test series the APF internals were removed from the vessel for inspection and candle replacement. A total of 30 candles were observed to be broken. Ten of the 30 breaks had clean fracture surfaces indicating that the breaks occurred after shutdown or during removal from the vessel. Heavy ash bridging was apparent near the bottoms of some of the candles. It was evident that the ash accumulation that occurred during the first 600 hours of this run was not removed during the last 90 hours of operation with the cyclone spoiled.

Two of the nine backpulse tubes were found to have longitudinal cracks, believed to be due to thermal fatigue. All nine tubes were replaced in kind following this test series.

All of the filter candles in the APF were replaced prior to the next (and final) test series. In order to broaden the base of candle filter material testing, the filter was fitted with a combination of silicon carbide, alumina mullite, and two other second generation materials. The inner rows of candles in the upper and middle plenums were left out, the same as in the prior test series. The primary cyclone upstream of the APF was modified to force all the gas and ash to flow through it and not collect any ash. This was done to determine whether the APF would operate at full load gas temperature (1550F) without ash bridging and without unstable pressure drop. As a precautionary measure to protect the gas turbine from erosion by the coarse ash if a candle broke, fail-safe devices were installed above each candle. The devices were designed to plug when exposed to ash, but otherwise not interfere with the normal flow of gas and backpulse cleaning air.

The final test series ran from January through March, 1995, and totaled 1110 hours over 10 runs, the longest being 427 hours. All tests during this period were conducted with the primary cyclone bypassed resulting in heavy, coarse ash loading to the APF. This was the first test series in which the APF operated above 1500F for sustained periods. Filter pressure drop was stable during most of this period, with indications of a slight increase near the end of the period. Inspection after 173 hours of operation revealed no ash bridging and very clean filter internals. Later in the test period fragments from one type of second generation filter candle were removed from the ash removal system. Posttest inspection revealed that 20 of 22 Dupont PRD66 second generation candles and two Coors alumina-mullite candles

## Executive Summary

---

were broken. No ash bridging was seen. Some of the candles were found to have internal ash accumulation in the bottom. Three candles were found to be cracked in the bottom portion.

Following completion of the test program, equipment inspections were performed to assess the condition of the hardware. The APF vessel was in good condition except for significant corrosion in the top of the head where hot gas had contacted the metal surface. The shroud was in good condition, but the liner appeared warped in some locations. The tubesheet and support cone were in excellent condition. The backpulse valves, backup cyclone, ash removal system, and hot gas piping were all found to be in good to excellent condition.

Westinghouse conducted a materials surveillance program during the project. This program included both metal structures (and coupons) and filter candle material monitoring. The metal structures in general exhibited few problems. Creep data and penetrant testing of welds did not reveal problems. Some embrittlement of 310 stainless steel was noted. Candle surveillance data included pretest dimensional checks, gas flow resistance, burst testing, time-of-flight testing, and visual examination. Posttest data included dimensional checks for creep and bowing, bulk strength measurements by C-ring testing, and photo micrograph examination for phase changes in the material.

The bulk strength of Schumacher Dia Schumalith F40 filter surveillance candles was measured at various points during the program. The bulk strength decreased approximately 50% during the initial 1000-2000 hours of operation, but remained relatively stable during remaining operation. Two of the surveillance candles remained in service for the full test duration of 5854 hours.

### 1.4 Conclusions

The Tidd Hot Gas Clean Up Program provided valuable information for the future design and operation of ceramic barrier filters in a PFBC flue gas environment. The most important conclusions reached from this program are listed below.

1. The basic design of the candle-based APF was structurally adequate. The hot metal structures of tubesheet, plenums, and candle holders operated without problems.

## Executive Summary

---

2. Clay-bonded silicon carbide candle material exhibited approximately 50% loss of strength after 1000-2000 hours of exposure to the PFBC environment. The strength level stabilized upon further exposure time.
3. Nearly all of the silicon carbide candle breakage observed in this program was attributed to ash bridging in the APF. Ash bridging was strongly affected by the size and temperature of the ash entering the filter. Very small ash (mass mean particle size 1 to 3 microns) passing through from a well-tuned cyclone formed an ash cake on the filter candles that was extremely difficult to remove at operating temperatures over 1400F. Ash from a partially detuned cyclone (about 7 microns) was more easily removed than the smaller ash, but still difficult to remove at operating temperatures over 1450F. Ash from a completely spoiled cyclone (above 27 microns) was easily removed and did not tend to bridge.
4. It is important to prevent ash from entering the inside of the filter candles to avoid blinding them on the inside surfaces which have larger pore size than the outer surfaces. Also, ash accumulation in the inside bottom of candles can induce cracking in the candles.
5. The design of hot gas piping is critical. Cast refractory thermal insulation was required to protect the pipe from the hot gas. Ceramic fiber insulation proved unsatisfactory as internal thermal insulation in the hot gas piping.
6. Flue gas which contacts metal surfaces below the acid dew point forms a very corrosive liquid. Metal surfaces that were not protected from contact with the gas experienced corrosion.
7. It is important to have reliable continuous ash removal from the filter. Ash buildup in the APF hopper resulted in candle breakage.
8. Based on very limited data, the APF reduced the SO<sub>2</sub> concentration in the gas passing through it approximately 40%. This is believed to result from the gas reacting with ash cake on the filter candles as evidenced by a higher degree of sulfation of the APF ash than the precipitator ash.

## Introduction

---

### 2.0 INTRODUCTION

#### 2.1 Program Objectives

The objective of this program was to evaluate the design and obtain operating experience for a commercial size Advanced Particle Filter (APF) through long-term testing on a slipstream at Ohio Power Company's Tidd Pressurized Fluidized Bed Combustion (PFBC) Demonstration Plant. Performance and reliability of commercial-scale filter modules were monitored to assess of the readiness and economic viability of this technology for commercial PFBC applications.

At the beginning of the program, it was intended to test two different filters. However, the program scope was narrowed to evaluate different filter candle materials in the same filter vessel. It was not feasible within the cost and time constraints of the program to completely replace the filter with another of a different configuration.

#### 2.2 Program Schedule and Milestones

The 70 MWe Tidd PFBC Demonstration Plant in Brilliant, Ohio was completed in late 1990, and operated through March 1995 as part of the Department of Energy's Clean Coal Technology Program. Provisions were included as part of the original design to install a one-seventh slipstream on the PFBC exhaust gases between the fluidized bed and the gas turbine to test an APF system. In November 1988, AEP submitted a proposal to the DOE for the Hot Gas Clean Up (HGCU) Program, and in August 1989, a cooperative agreement was signed. In July 1990, AEP awarded a contract to Westinghouse Science and Technology Center to provide a candle-based APF. Detailed engineering and material procurement were completed by the end of 1991 when installation began. Initial operation of the system occurred in May, 1992, and the APF was commissioned in October, 1992.

## Introduction

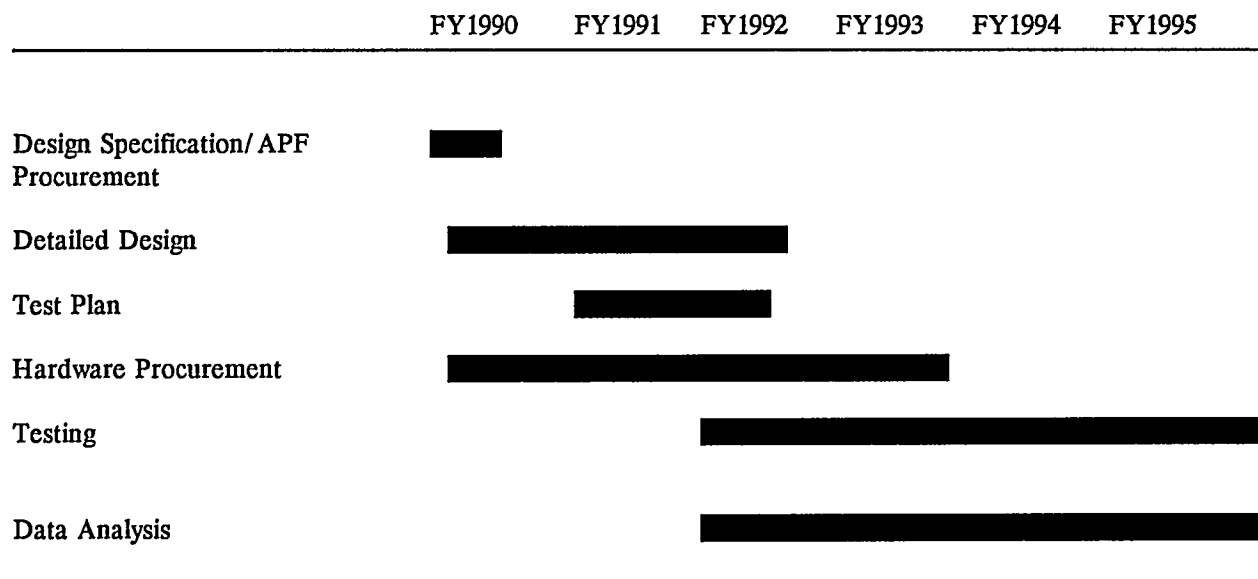


**Figure 2.2 - Program Schedule**

The HGCU system was operated during five separate test periods between October, 1992, and March, 1995, as listed in Table 2.2.1. Table 2.2.2 presents a summary of all HGCU test runs for the entire program. Figure 2.2 shows the duration of each of the program's major activities.

**Table 2.2.1 - Tidd HGCU Test Periods**

Test Period	I	II	III	IV	V
Date	10/92-12/92	6/93-9/93	1/94-4/94	7/94-10/94	1/95-3/95
Run No.	1-4	5-11	12-18	19-24	25-34
Test Period Total Hours	464	1295	1279	1706	1110
Longest Run, Hours	286	597	444	691	427

## Introduction

### Table 2.2.2 - Tidd HGCU Runs Summary

RUN NO.	COAL FIRE		UNIT TRIP		COAL FIRE HOURS	NOTES
	DATE	TIME	DATE	TIME		
0	05/21/92	20:26	05/23/92	07:41	35.3	Bypass mode. Coal fire hours not included in totals. Unit trip due to XJ-4 failure.
1	10/28/92	18:10	11/01/92	23:32	101.4	Unit trip due to HGCU ash lockhopper pluggage.
2	11/17/92	09:33	11/17/92	10:50	1.3	Unit trip due to plugged primary cyclones.
3	11/21/92	18:41	11/24/92	22:50	76.2	Unit trip due to coal paste problems.
4	11/25/92	12:11	12/07/92	09:56	285.8	Warm startup. Unit trip due to XJ7 failure. 21 candles found broken during outage.
<b>TOTAL FOR RUNS 1 - 4</b>					<b>464.6</b>	
5	06/30/93	17:28	07/03/93	05:04	59.6	Shutdown to change GT telemetry instrumentation.
6	07/05/93	00:35	07/05/93	17:17	16.7	Completed GT testing.
7	07/18/93	18:20	08/05/93	12:22	426.0	Shutdown due to ash buildup in APF hopper.
8	08/09/93	10:18	08/09/93	11:37	1.3	GT trip due to bearing vibration.
9	08/10/93	22:29	08/14/93	05:27	79.0	Warm startup. Shutdown due to low O2 resulting from high coal paste excursion.
10	08/19/93	17:48	08/24/93	13:28	115.7	Manual combustor trip due to unstable bed conditions after switching to limestone.
11	08/29/93	23:31	09/23/93	20:12	596.7	Combustor trip due to leak in sorbent transport pipe. 62 candles found broken during outage.
<b>TOTAL FOR RUNS 5 - 11</b>					<b>1295.0</b>	
12	01/10/94	06:41	01/11/94	01:36	18.9	Manual combustor trip due to plugged primary cyclone.
13	01/15/94	23:42	01/29/94	20:31	332.8	Manual combustor trip due to boiler tube leak.
14	02/17/94	14:58	02/18/94	14:14	23.3	Manual combustor trip due to leak in HGCU gas sample connection.
15	02/19/94	06:12	02/25/94	13:09	151.0	Manual combustor trip due to loss of sorbent air compr.
16	03/03/94	10:22	03/09/94	11:30	145.1	Manual combustor trip due to loss of two paste pumps.
17	03/16/94	14:48	03/23/94	10:50	164.0	GT trip due to low lube oil pressure.
18	03/31/94	09:04	04/18/94	20:43	443.7	Manual combustor trip due to internal sorbent injection pipe leak. 28 candles found broken during outage.
<b>TOTAL FOR RUNS 12 - 18</b>					<b>1278.8</b>	

## Introduction

RUN NO.	COAL FIRE		UNIT TRIP		COAL FIRE HOURS	NOTES
	DATE	TIME	DATE	TIME		
19	07/16/94	01:56	07/16/94	04:27	2.5	Manual combustor trip due to loss of three paste pumps.
20	07/16/94	12:59	07/16/94	13:55	0.9	Manual combustor trip due to plugged primary cyclones.
21	07/20/94	19:18	07/27/94	12:08	160.8	Shutdown due to GT vibration.
22	07/28/94	09:59	08/25/94	17:47	679.8	Manual combustor trip due to bad signal relay from the ST generator. 14 candles found broken during outage.
23	09/03/94	01:01	09/10/94	04:07	171.1	Manual combustor trip due to sorbent pipe leak. Operated part-time with P11 cyclone totally spoiled.
24	09/22/94	17:02	10/21/94	11:39	690.6	Operated part-time with P11 cyclone totally spoiled. Planned outage. 30 candles found broken during outage.
<b>TOTAL FOR RUNS 19 - 24</b>					<b>1705.8</b>	
25	01/13/95	13:24	01/13/95	17:47	4.4	Manual combustor trip due to plugged primary cyclone
26	01/18/95	15:53	01/19/95	08:39	16.8	GT trip due to low control fluid pressure.
27	01/20/95	17:35	01/21/95	00:44	7.2	Manual combustor trip due to unstable bed conditions.
28	01/27/95	00:58	02/02/95	02:05	145.1	Manual comb. trip due to hot spot on HGCU pipe flange.
29	02/09/95	00:30	02/09/95	15:09	14.7	Combustor trip due to high SSH outlet temperature.
30	02/10/95	04:05	02/10/95	18:34	14.5	Hot restart. Manual combustor trip due to gasket leak on HGCU surge hopper.
31	02/11/95	09:26	02/12/95	17:51	32.4	Hot restart. Manual combustor trip due to plugged HGCU alternate ash removal line.
32	02/13/95	11:40	02/16/95	12:43	73.1	Hot restart. Combustor trip due to plugged paste nozzles.
33	02/18/95	19:29	03/08/95	14:40	427.2	Manual combustor trip due to loss of two paste pumps.
34	03/14/95	17:15	03/30/95	08:27	375.2	Planned final shutdown.
<b>TOTAL FOR RUNS 25 - 34</b>					<b>1110.4</b>	
<b>TOTAL FOR RUNS 1 - 34</b>					<b>5854.5</b>	

## Project Description

---

### 3.0 PROJECT DESCRIPTION

#### 3.1 System Description

In the original design, the Tidd PFBC Demonstration Plant utilized seven strings of primary and secondary cyclones to remove 98% of the particulate matter from the gases between the fluidized bed and the gas turbine. The HGCU slipstream replaced one of the seven secondary cyclones by taking the discharge gas of one of the primary cyclones to outside of the combustor vessel and into the APF. After passing through the APF, the gas flowed through a backup cyclone and then returned to the combustor vessel, where the slipstream flow rejoined the combustor gas at the discharge of the other six cyclone strings.

Figure 3.1.1 provides a simplified schematic of the HGCU system, and Figure 3.1.2 shows an isometric view of the system.

Under the original maximum load design conditions, gas at approximately 150 psig, 1550F flowed into the filter at 7600 acfm with a dust loading of approximately 600 ppmw. In January 1994, the dust loading to the filter was increased from approximately 600 ppmw to 3400 ppmw by detuning the primary cyclone upstream of the APF. In January 1995, the primary cyclone was bypassed which increased the ash loading to approximately 20,000 ppmw. Ash collected in the APF was discharged to a screw cooler and into a lockhopper system which fed a vacuum ash transport system. In December, 1994, an alternate ash line was installed at the screw cooler outlet to handle the heavy ash loading resulting from bypassing the primary cyclone.

## Project Description

Table 3.1 provides the design basis of the APF system.

**Table 3.1 - APF Design Basis**

Maximum Temperature	1670 F
Operating Temperature	1550 F
Maximum Pressure	185 psig
Operating Pressure	150 psig
Gas Flow Rate	100,700 lb/hr
Inlet Dust Loading	5000-500 ppm
Outlet Dust Loading	<15 ppm
Mass Mean Particle Size	1.5 microns
Temperature Drop	5 F
Pressure Drop	3 psi
Face Velocity	7.1 ft/min

The main elements of the system included the filter vessel and its internals; back pulse skid, including secondary accumulators and valves; back pulse air supply skid, including compressor, dryer and primary accumulator; backup cyclone; ash screw cooler, surge hopper, lockhopper, piping, and instrumentation.

The system was designed to remove virtually all entrained particulates discharged from one of the seven parallel primary cyclones on the outlet of the PFBC combustor. Ash collected on the outside surface of ceramic filter elements (candles), resulting in a gradual increase in the overall flow resistance of the slipstream. The filter cake was periodically dislodged by injecting a high-pressure air pulse to the clean side of the candles. The ash cake on the candles then fell to the conical discharge hopper. Back pulse air was routed individually to nine plenums (3 clusters, each with 3 plenum levels), via injection tubes mounted on the top head of the filter vessel. Back pulsing was controlled by means of high-speed pilot-assisted solenoid valves and air-actuated isolation valves. The pressure in the secondary accumulator tanks typically ranged from 800 to 1200 psig. The electrical pulse duration was 0.2 to 0.7 second, and the corresponding air pressure pulse duration was 0.5 to 1.0 second. The pulse air supply system, located in the combustor building basement, provided high pressure dried and filtered air on as-needed basis to five secondary accumulators, via a primary accumulator on the discharge side of the compressor.

## Project Description

---

An air preheating system was originally included in the system. However, the system was not used because the electric heater proved to be ineffective. An alternate means of warming the system utilizing process air proved to be a more efficient and expedient.

The following paragraphs provide information on the major components in the system.

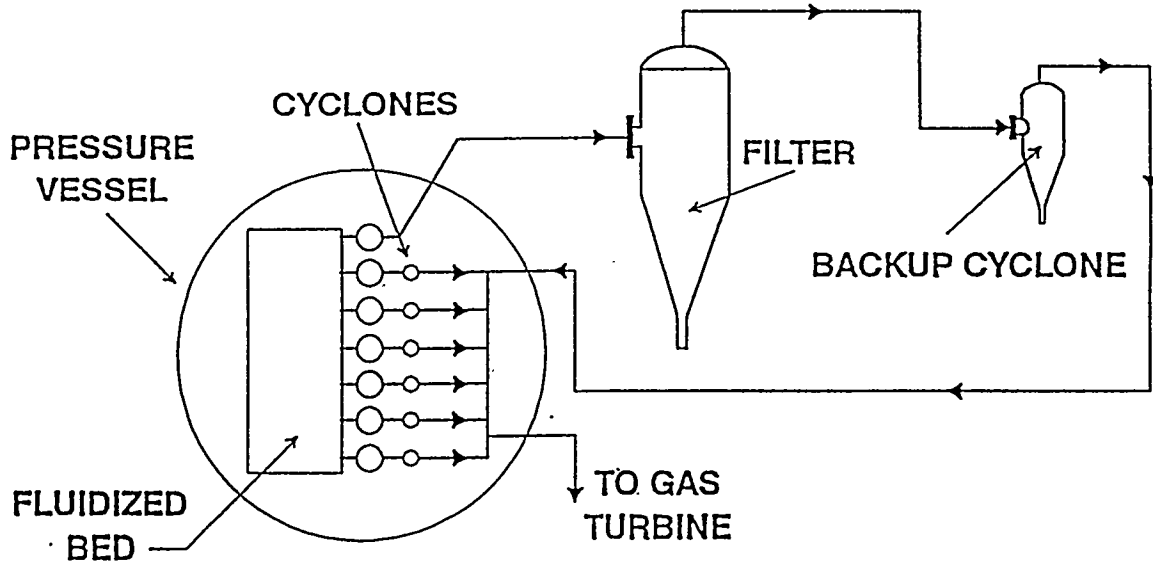


Figure 3.1.1 - HGCU Slipstream Schematic

# Project Description

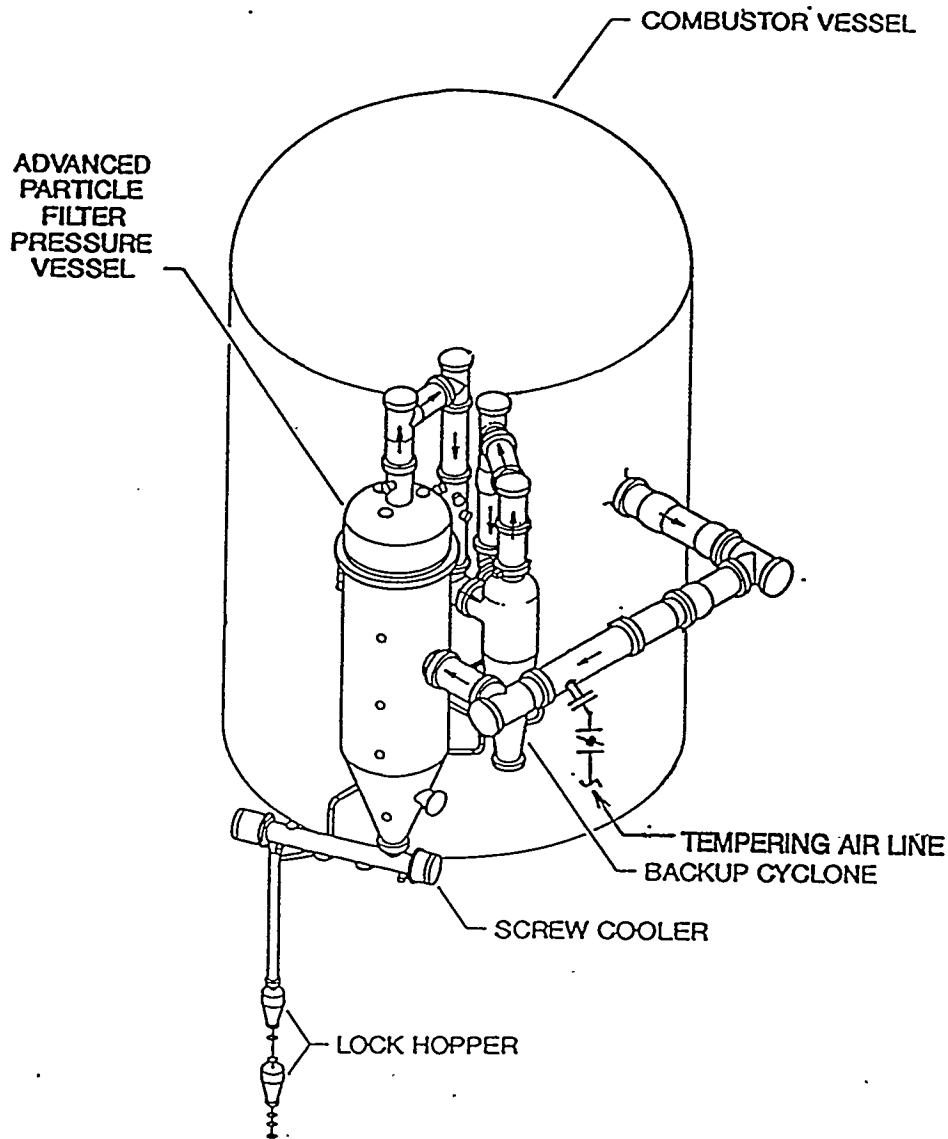


Figure 3.1.2 - Isometric View of HGCU System

## Project Description

---

### 3.2 Filter Vessel

The function of the filter vessel was to contain the filter elements in a pressurized environment. The vessel was comprised of two major parts, the body and the head. A tubesheet separated the dirty gas in the body from the clean gas in the head. The filter vessel was 10 feet in diameter and 44 feet high. The vessel was internally insulated with a 7 to 9-inch thick layer of alumina-silica ceramic fiber (Z-Block) insulation. The vessel was fabricated from carbon steel plate. A 310 stainless steel liner protected the insulation from gas impingement. A 310 stainless steel shroud inside of the vessel directed the dirty gas, which entered the side of the filter, toward the top of the filter. After flowing over the top of the shroud, the gas flowed in a downward direction past the filter elements. Hot gas entered the side of the body and exited from the top of the head.

The vessel was designed in accordance with ASME Section VIII for 185 psig, 1670F internal temperature and 650F external temperature.

The exterior of the vessel was coated with a temperature sensitive paint which changed colors at specific temperatures. The temperature sensitive paint provided a means of detecting hot spots on the vessel shell. No external insulation was applied to the filter vessel. A photograph of the filter vessel during erection is shown in Figure 3.2.

### 3.3 Filter Internals

The filter contained 384 filter elements which were referred to as candles because of their long cylindrical shape. The candles were arranged in three clusters spaced 120 degrees apart. Each cluster held three plenums arranged vertically. The upper and middle plenums each contained 38 candles, while the bottom plenums contained 52 candles each. (After Test Period III the inner rows of candles in the upper and middle plenums were removed, leaving 288 candles in the APF during Test Periods IV and V.) Each plenum bottom comprised a perforated plate similar to a tubesheet. Candle holders were welded to the plenum bottom plates, and the candles were held in the holders under the support plates by bolted collars and high temperature gaskets. Each candle was nominally 2.36 inches in outside diameter and 4.92 feet long. The candles were made of two layers of sintered silicon carbide. The outer layer was very thin and had much smaller porosity than the remainder of the candle. Essentially, all filtering was accomplished near the outer surface of the candle. Filter candles of different design were used in Test Periods IV and V.

## Project Description

---

The tubesheet and expansion cone performed three functions: (1) supported the filter clusters; (2) accommodated thermal stresses generated at its periphery; and (3) maintained a seal between the clean and dirty sides of the filter vessel. The 2" thick tubesheet and expansion cone were fabricated from RA-333 alloy. Thermal insulation protected the expansion cone from the hot gas temperature.

Figure 3.3.1 shows the arrangement of the filter internals. Figures 3.3.2, 3.3.3 and 3.3.4 are photographs of the filter internal assembly during initial installation into the vessel.

## Project Description

---



**Figure 3.2 - Photograph of APF Vessel During Erection**

# Project Description

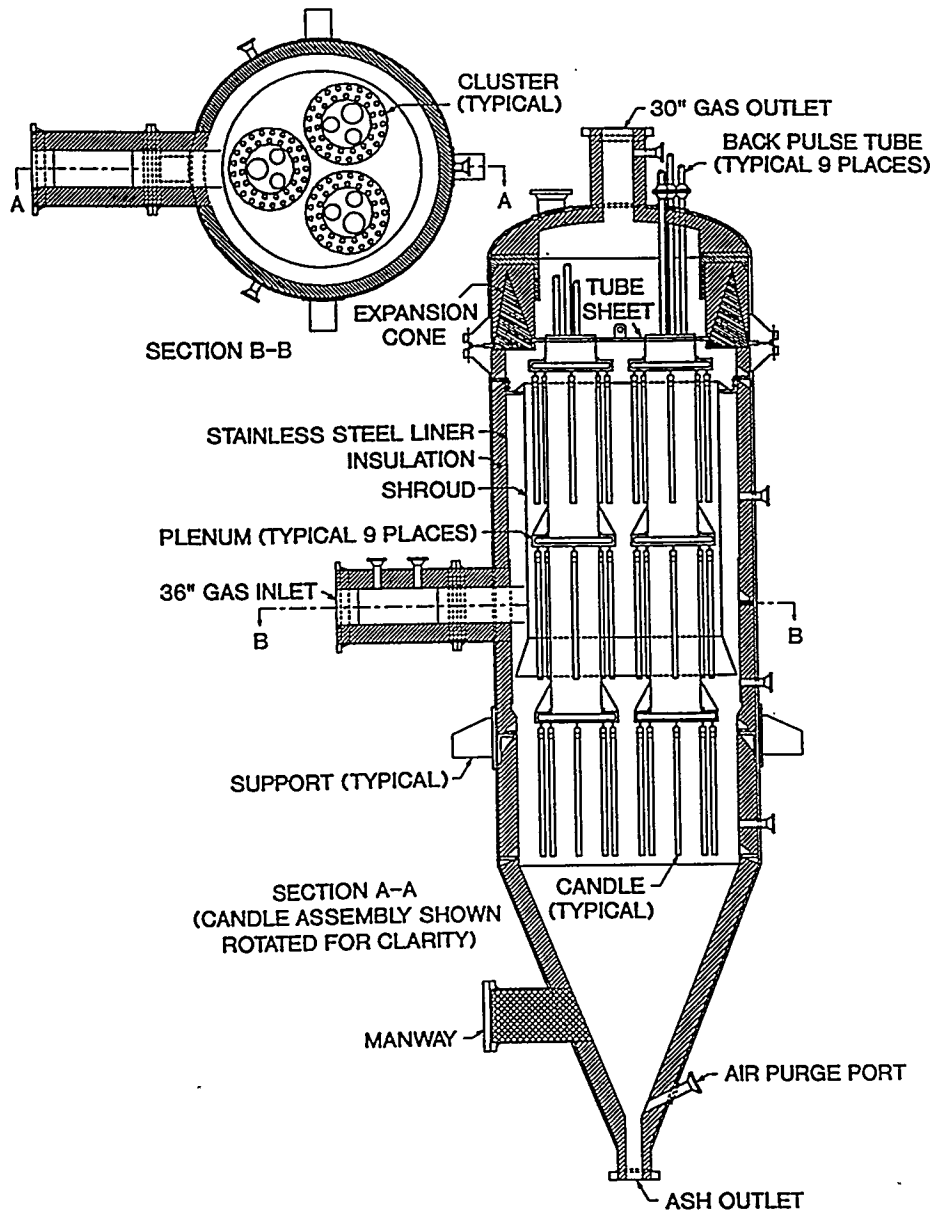
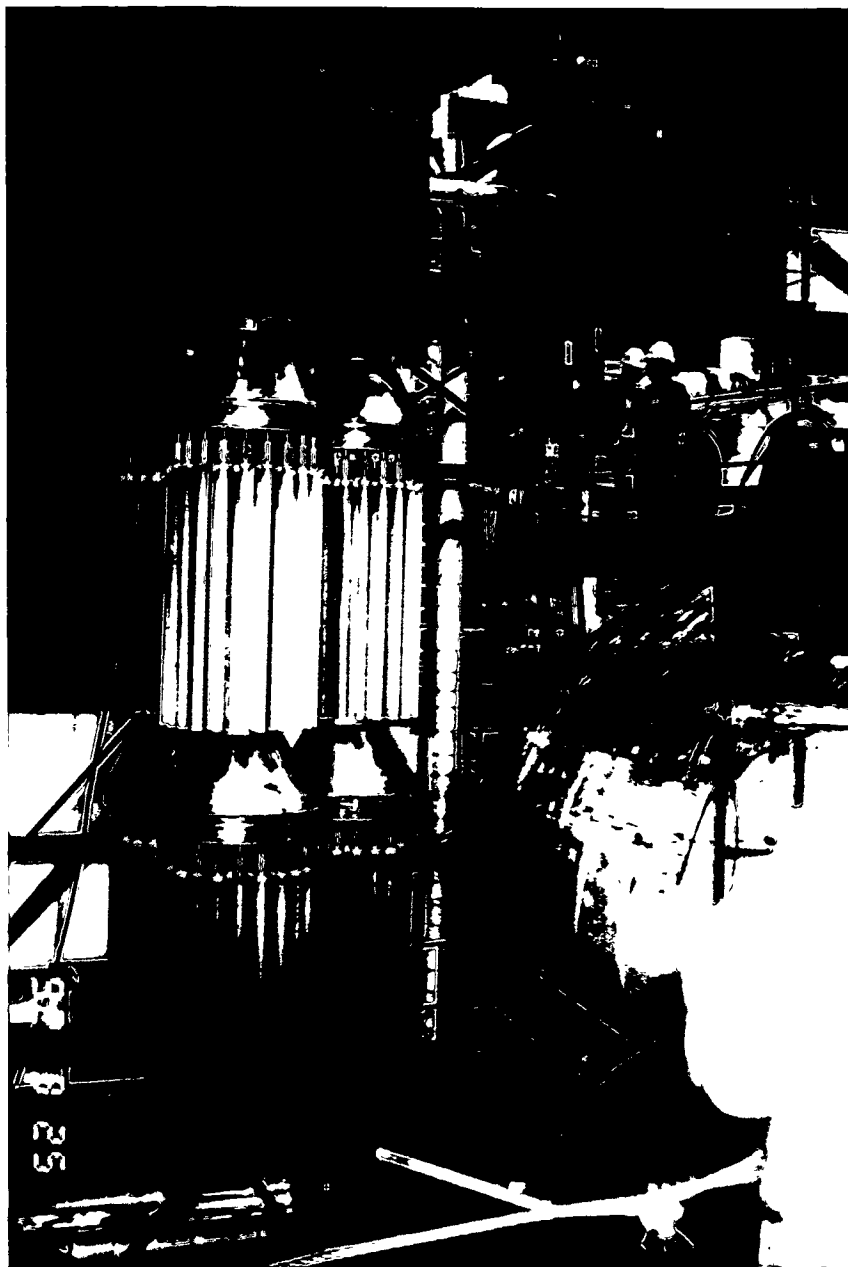


Figure 3.3.1 - APF Internal Arrangement

## Project Description

---



**Figure 3.3.2 - Photograph of Filter Internals During Initial Installation**

## Project Description

---



**Figure 3.3.3 - Photograph of Filter Internals During Initial Installation**

## Project Description

---

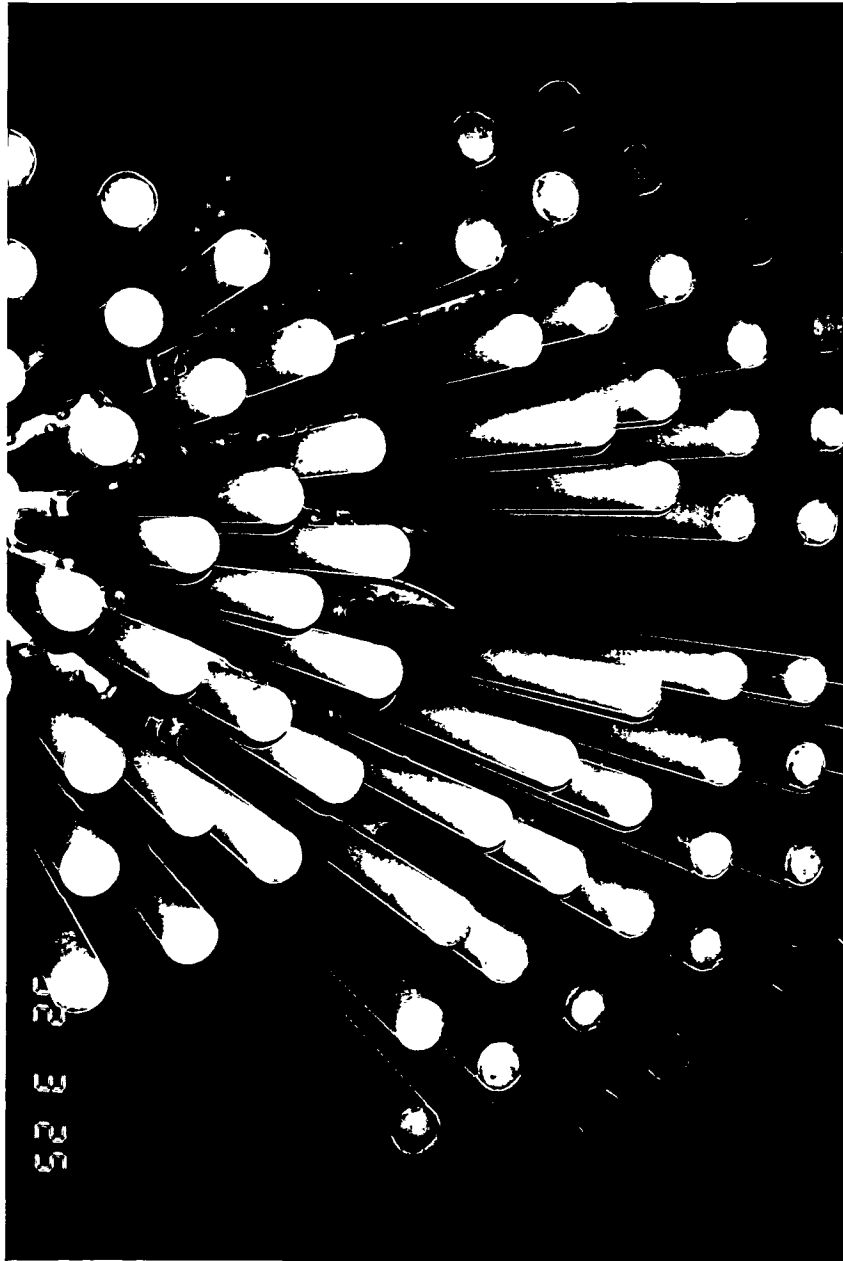


**Figure 3.3.4 - Photograph of Filter Internals During Initial Installation**

## Project Description

---

### 3.4 Backpulse System

The Backpulse System was comprised of a compressor skid, valve skid, and interconnecting piping. A schematic diagram of the system is shown in Figure 3.4.1, and photographs of the skid are shown in Figures 3.4.2 and 3.4.3.

The backpulse compressor was a heavy duty reciprocating compressor with four stages of compression. It was designed to compress 282 scfm of air up to 1500 psig. The compressor was built with balanced opposed cross heads which permitted operation over extended periods in an unloaded condition. The compressor skid included intercoolers, aftercooler, and moisture separators. It was a Norwalk Model Century 150-4.

The backpulse air dryer was mounted on the same skid as the compressor. The dryer was a refrigerant type which removed moisture from the air by cooling in a Freon gas heat exchanger. The air was warmed to about 80F before leaving the dryer by a regenerative heat exchanger. The dryer was designed to dry 300 scfm of air at 1500 psig to a dew point of 35F or below. It was a model UA100 made by Ultra Air Products, Inc.

The back pulse system included one large primary and five small secondary accumulators. The large accumulator was located on the same skid as the compressor and dryer. It received air from the dryer and supplied it to the five smaller accumulators.

The small accumulators were located on the backpulse valve skid located near the top of the filter vessel. One accumulator stored air for the pilot valves on the back pulse solenoid valves. A second accumulator stored air at nominal 250 psig for instrument purge. The other three accumulators stored air for pulsing at nominal 800 to 1200 psig.

The heart of the backpulse system was the backpulse solenoid valves manufactured by Atkomatic Valve Company. Downstream of each secondary accumulator there were two solenoid valves arranged in parallel. One of the two valves was a backup. The valves were fast-acting (200 to 700 msec stroke time) pilot operated solenoid valves which failed closed. A normally-closed automated ball valve downstream of each solenoid valve isolated the backpulse air system from the hot gas system and prevented excess air from entering the filter in case a solenoid valve failed to close. During Test Period V one of the Atkomatic valves was replaced with another type of valve manufactured by CO-AX Valves.

# Project Description

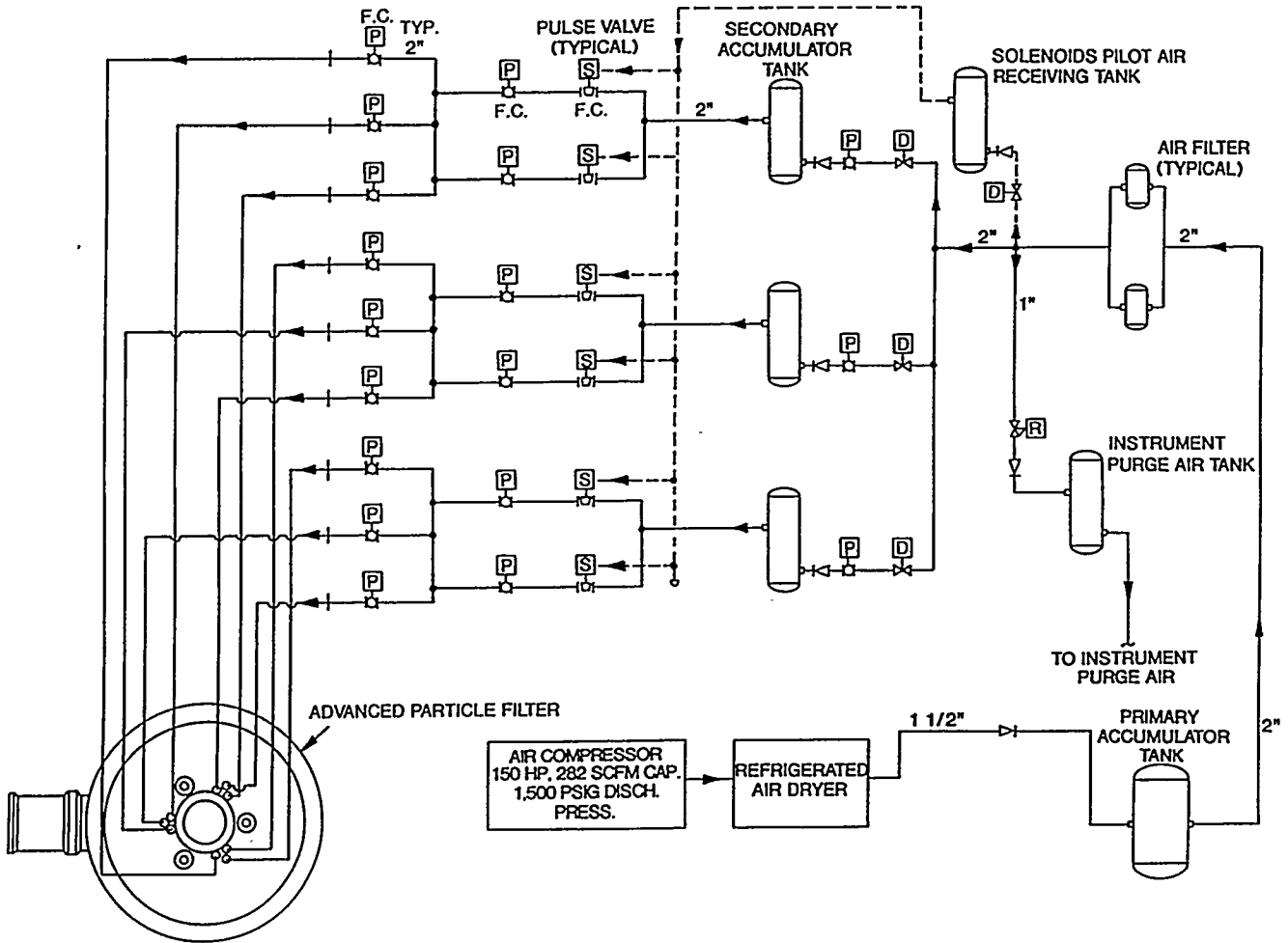


Figure 3.4.1 - Schematic Diagram of Backpulse System

## Project Description

---

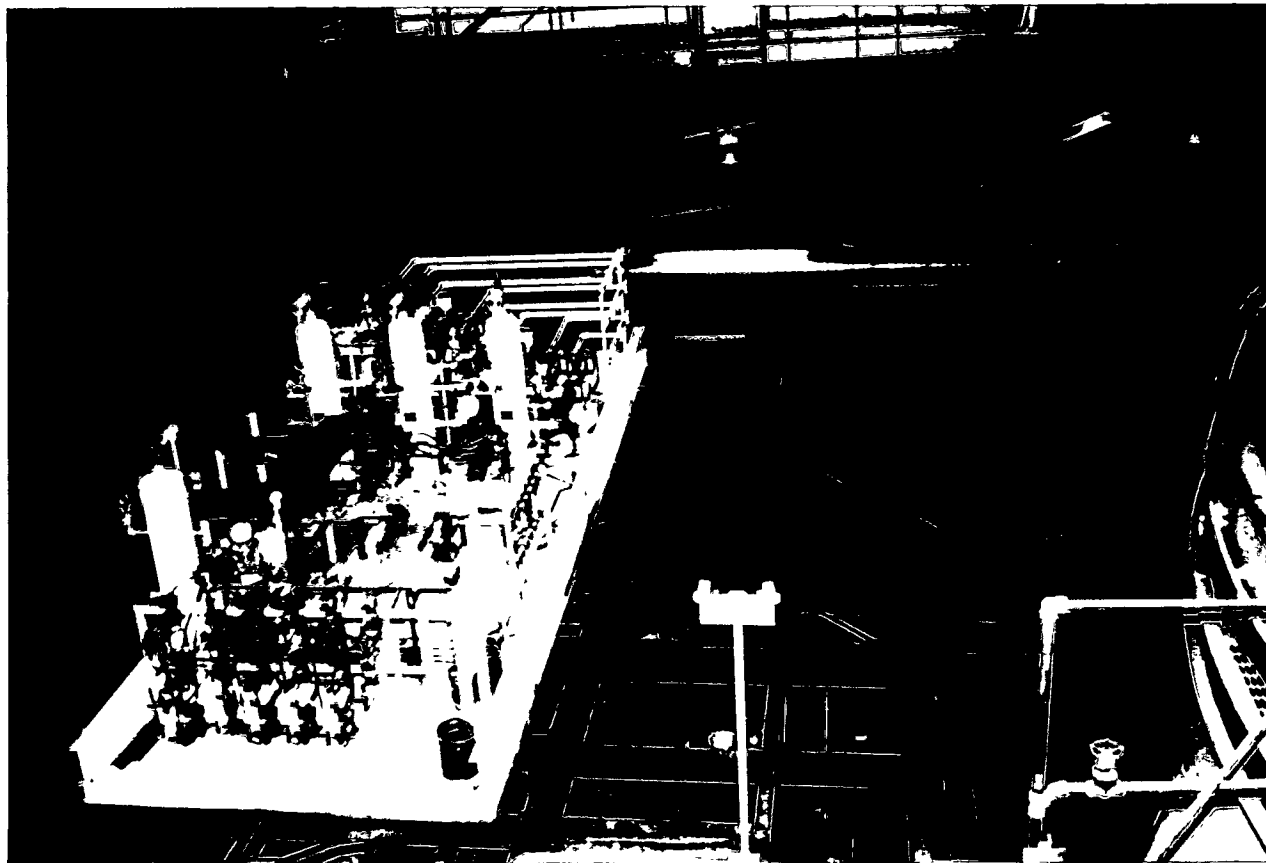
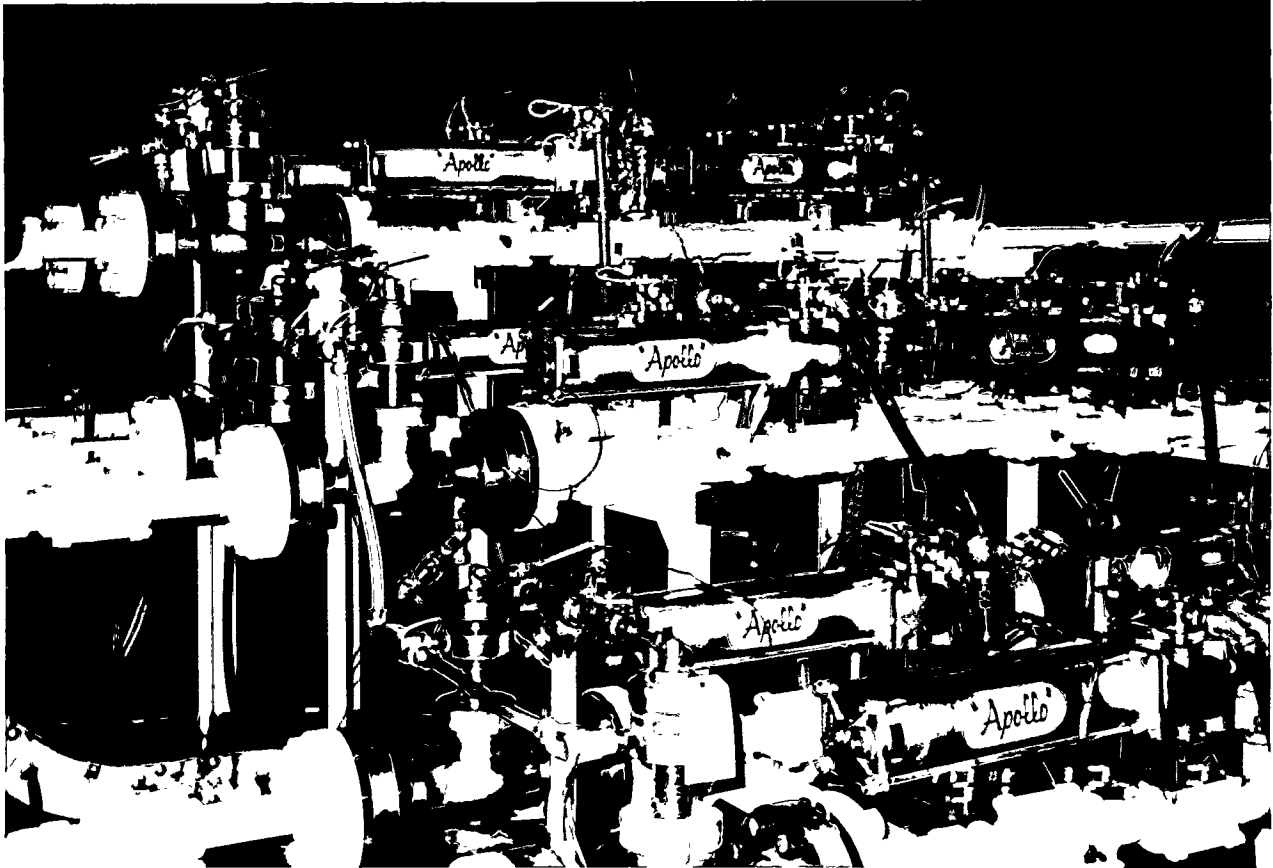


Figure 3.4.2 - Photograph of Backpulse Skid

## Project Description

---



**Figure 3.4.3 - Photograph of Backpulse Skid**

## Project Description

---

### 3.5 Backup Cyclone

The original system design included a bypass cyclone as well as a backup cyclone. The purpose of the bypass cyclone was to clean the ash from the hot gas slipstream if the APF was not available for service and to allow the flow to be switched to bypass the APF if a problem developed during operation. However, following initial shakedown tests, it was decided not to connect the bypass cyclone to the system. It was noted following initial operation using the bypass cyclone that the stagnant flue gas in backup cyclone condensed resulting in corrosive condensation collecting on and corroding internal metal surfaces. It was concluded that the bypass cyclone would experience the same corrosive conditions when it was in the standby mode, i.e., pressurized with stagnant flue gas. Based on this observation, it was decided not to use the bypass cyclone.

The backup cyclone was sized to allow for the maximum particle removal efficiency given the available pressure drop. The available pressure drop across the backup cyclone was 2.4 psi with a corresponding inlet velocity of 95 fps at the design flowrate. A minimum of three inches of erosion resistant refractory was installed on surfaces exposed to hot gas. Insulating refractory approximately eight inches thick was installed between the vessel wall and erosion resistant refractory to limit the heat loss and outer wall temperature. During the first test run, problems were encountered with hot spots on the cyclone shell. Repair of cracks in the refractory and additional heat curing of the refractory were necessary to eliminate this problem. In order to monitor the steel shell of the cyclone for hot spots, no insulation was applied to its outside surface. The same temperature sensitive paint used on the APF vessel was also used on the cyclone. The vessel was designed in accordance with ASME Section VIII for 185 psig, 1670F internal temperature and 750F external temperature. Figure 3.5 is a cross section drawing of the backup cyclone.

# Project Description

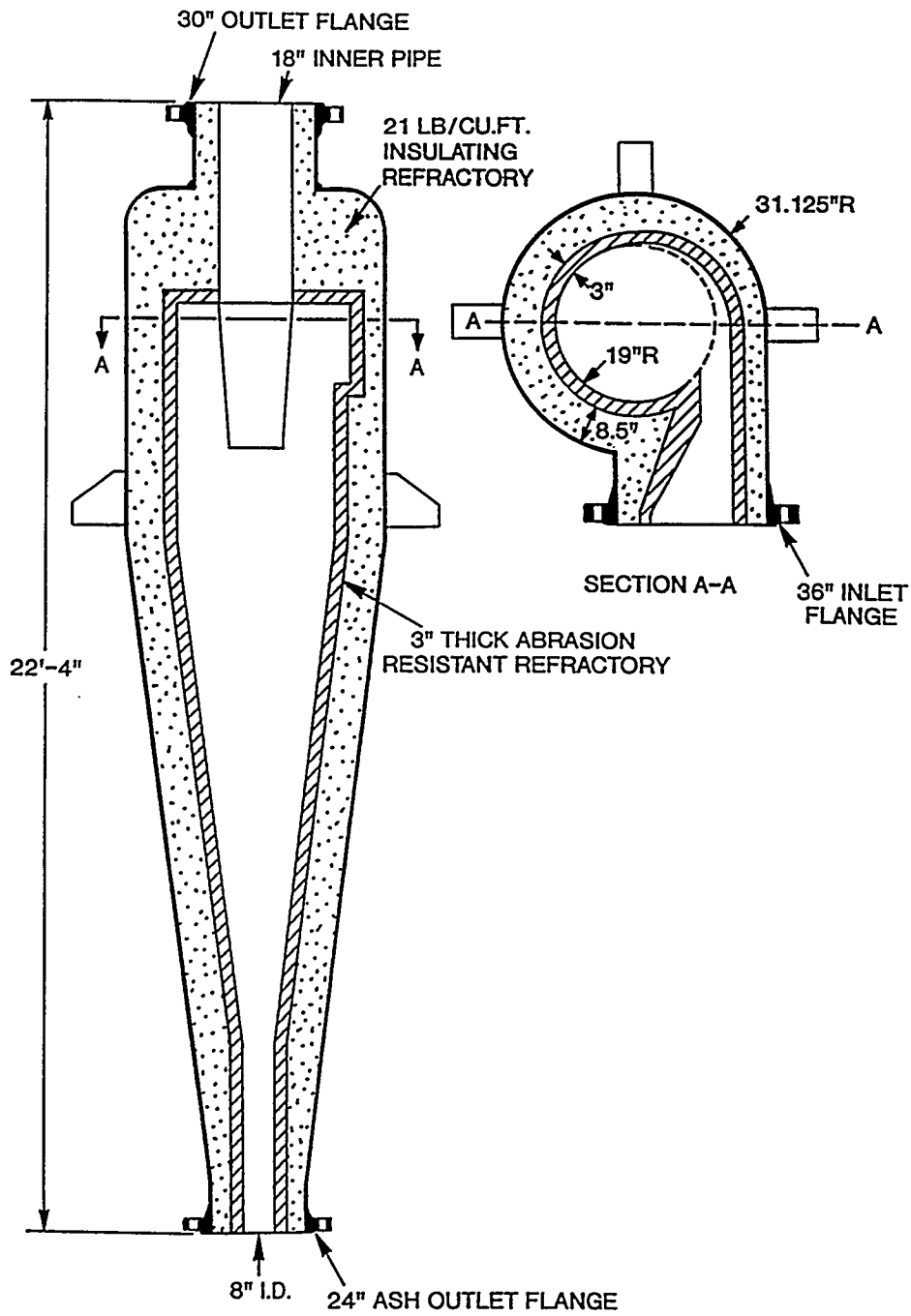


Figure 3.5 - Cross Section of Backup Cyclone

## Project Description

---

### 3.6 Ash Removal System

The function of the ash removal system was 1) to remove ash from the advanced particle filter vessel and cool, depressurize and convey the ash to an ash silo; and 2) to convey ash from the backup cyclone and cool, depressurize, and discharge the ash to the economizer outlet duct where it was collected by the precipitator.

A schematic diagram of the system is shown in Figure 3.6.

The system consisted of the following systems and components:

- Ash Screw Cooler
- Hydraulic Fluid System
- Gear Box Lubricating System
- HGCU Closed Cycle Cooling Water System
- Ash Surge Hopper
- Ash Lockhopper
- Lockhopper Isolation Valves
- Material Cycling Valve
- Lockhopper Pressure Equalizing Valves
- Ash Transport Piping and Valves
- Cyclone Ash Collection Vessels
- Cyclone Ash Transport Piping

Ash collected in the APF vessel was removed and cooled by the screw cooler, depressurized in the lockhopper assembly, and conveyed to an ash silo via a 4" vacuum ash transport line. A hydraulic fluid system was used to provide power to the screw cooler hydraulic drive unit. A closed cycle cooling water system was used to provide cooling water to the screw cooler.

Ash collected in the backup cyclone was conveyed to the economizer outlet duct using conveying air from the combustor vessel. The ash was cooled by mixing with conveying air in the cyclone ash collection vessel. The ash was depressurized in the cyclone ash transport line prior to being discharged into the economizer outlet duct. The ash then mixed with the flue gas and entered the precipitator where it was collected and discharged to an ash silo for disposal via truck.

## Project Description

---

An emergency pneumatic ash removal system was provided at the screw cooler outlet to facilitate ash removal in case the lockhopper system malfunctioned. Following bypassing of the primary cyclone in December 1994, an additional alternate ash transport line was installed to handle the heavy ash loading from the APF. The alternate ash line ran from the screw cooler outlet and tied into the ash line from the other primary cyclones. When the alternate ash line was in service, the lockhopper system was not used. The emergency and alternate ash lines used conveying air from the combustor (process air) in the same manner as the ash line from the backup cyclone.

The system was originally designed to handle an ash loading of 1000 lbm/hr from the APF vessel. The screw cooler was designed to cool ash from 1550F to 400F using closed cycle cooling water at 200 psig, 340F, and 36 gpm at the design ash loading. When the primary cyclone was bypassed in December 1994, the APF ash loading increased to about 2000 lbm/hr at full load. Consequently, the screw cooler outlet temperature was higher than design, typically in the range of 600-650F. However, this did not present a significant operating problem.

# Project Description

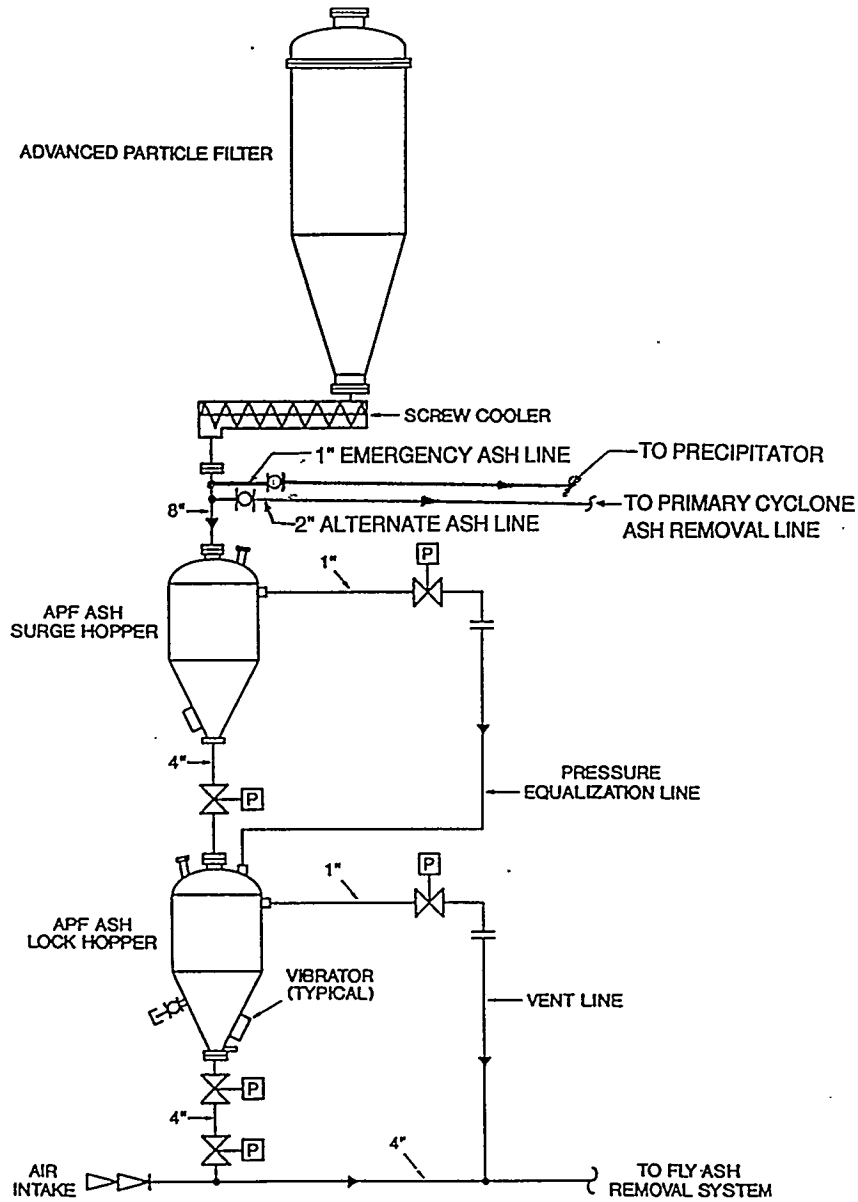


Figure 3.6 - Ash Removal System Schematic

## Project Description

---

### 3.6.1 Screw Cooler

The screw cooler was comprised of a cylindrical housing (trough), water-cooled screw, and a hydraulic drive unit. As ash was conveyed through the screw cooler, heat was transferred to the cooling water. There were three parallel cooling water circuits in the screw cooler. Figure 3.6.1 shows a schematic diagram of the screw cooler.

The screw cooler was supplied by Denver Equipment Company and was designed and stamped according to ASME pressure vessel standards.

The screw flights and stem pipe were hollow, and together they formed a cooling water loop. Most of the heat from the ash was transferred to the cooling water circuit in the screw. The screw pads and flights were made of 304 stainless steel and constructed of a "twin-pad" design to ensure a high structural integrity. This design consisted of a steel ribbon (or pads) wrapped around the stem pipe in a helical fashion and welded to the pipe at the ends only. The screw flights were positioned so they bridged the gap of the steel pads. This design offered free torsional movement of the pad and flights and room for longitudinal expansion under high temperature gradients.

The housing was a cylindrical pressurized water-cooled jacket with inspection ports. It allowed for pressurized ash operation and accounted for 10-15% of the total heat transferred. The housing diameter was larger than the screw diameter and the screw was offset from the housing centerline. This permitted relatively large objects to pass through the screw cooler without jamming. (When candles broke during operation, the screw cooler was able to continue to operate without jamming.) The housing contact surface was made of 304 stainless steel.

## Project Description

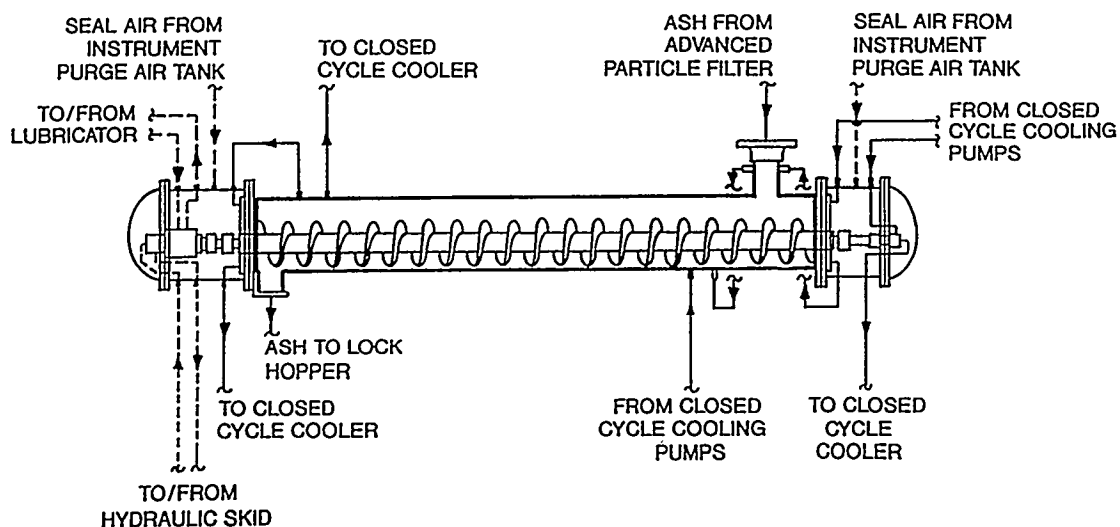


Figure 3.6.1 - Screw Cooler Schematic

The screw was driven through a reduction gear (36:1 gear reduction ratio) by a variable speed, 5 hp, hydraulic drive unit; both the reduction gear and drive unit were totally enclosed within the north end housing. The function of the reduction gear was to transfer power from the hydraulic motor to the screw at reduced speed and increased torque. Based on the maximum hydraulic fluid flow and pressure, the maximum output torque of the gear reducer was approximately 36,720 in.- lbf. If the screw became jammed, stalling occurred at the maximum torque value. The reduction gear was continuously lubricated by the gear box lubricating system located on the hydraulic skid. The hydraulic skid included the hydraulic fluid system, the gear box lubricating system, and the associated control circuitry and control panel for the screw cooler. Seal air was provided to each end housing to keep ash out of the shaft seals. The air pressure was maintained at 0.5 to 2 psi above the system gas pressure.

### 3.6.2 Surge Hopper and Lockhopper

The ash surge hopper had 3.34 cubic feet of net storage capacity and was used to store ash collected from the screw cooler during unloading of the ash lockhopper. The hopper was heat

## Project Description

---

traced and insulated. The hopper was provided with an electric vibrator to assist with hopper unloading and was fabricated of 304 stainless steel with 2B finish to ensure smooth surfaces. Steep hopper cone angles, 10 and 20 degrees (included), ensured good ash flowability.

The ash lockhopper had 12.25 cubic feet of net storage capacity and was used to collect ash from the screw cooler through the surge hopper. During unloading, the lockhopper was isolated from the surge hopper, depressurized, and the ash was emptied into the ash transport line through the two lower isolation valves. This hopper was provided with a compound pressure gauge, a level switch, an ash temperature indicator, heat tracing, insulation, an electric vibrator, and was fabricated of 304 stainless steel with 2B finish and similar cone angles as the surge hopper.

Two lockhopper isolation valves and one material cycling valve were provided on the lockhopper assembly. The upper isolation valve was used to isolate the lockhopper from the surge hopper during the unloading cycle. The two valves provided below the lockhopper were for pressure seal and material cycling. The valves were manufactured by the Everlasting Valve Co. and were 4" rotating disc type, ANSI Class 300, flanged, with a cast Stellite #6 disc and seat.

### 3.7 Hot Gas Piping

The hot gas piping was originally designed with an outer carbon steel pressure-retaining shell, an inner 316 stainless steel liner, and alumina-silica ceramic fiber blanket insulation between the liner and the shell. The inside of the carbon steel pipe shell was lined with an epoxy coating (Plasite 4300) for corrosion protection. Table 3.7 provides design parameters of the piping. Cast refractory rings were used at the ends of each pipe section to support the inner liners, which were designed to allow for thermal expansion at each connection. The system also required eight expansion joints to allow for thermal expansion and relative movement between the combustor vessel and the HGCU components. The expansion joint bellows were made of 321 stainless steel.

The piping and expansion joints were redesigned following initial system operation in May, 1992, as is discussed in Section 4.2.1.

## Project Description

---

**Table 3.7 - Hot Gas Piping Design**

	Upstream of Filter	Downstream of Filter
Gas Velocity	60 fps	75 fps
Outer Pipe	36 in. OD	30 in. OD
Inner Liner	20 in. OD	18 in. OD

### 3.8 Controls and Data Acquisition

There were three control modes available for the filter system, namely manual mode, automatic DP mode and automatic timer mode. The manual mode was generally only used after backpulse cleaning had been interrupted for some reason, and a large ash cake had accumulated on the candles. In this case it was advantageous to use the manual mode so the filter cleaning could be spread out over some time period to avoid overwhelming the ash removal system. During manual mode, the system internally checked the permissives for proper sequencing and operation of the solenoid valves and advised the operator of any malfunction.

The system was normally operated in the timer mode. In this mode, filter cleaning occurred at uniform time intervals, typically thirty minutes. In the timer mode, filter cleaning would be initiated by a DP override if the override setting was reached prior to the next timed cleaning. During test periods IV and V when ash loading to the filter was very heavy, the filter timer sequence was set up for continuous cleaning wherein all nine plenums were cleaned over a fifteen minute time period with backpulses occurring every 1.67 minutes. This was done to even out the ash flow to the ash removal system.

In the DP mode the filter was cleaned when the filter differential pressure reached a preset level. A timer override could be set to clean the filter if backpulsing had not occurred for a specified time period. This control mode was not used.

The cleaning sequence was programmable to allow the cleaning to occur by cluster or by level. For example, all upper level plenums could be cleaned first, then all middle level plenums, and finally all bottom level plenums. In the cluster mode, all plenums in a given cluster were cleaned before moving

## Project Description

---

to the next cluster. In this mode, the cleaning generally occurred in the sequence top, middle, bottom in a given cluster. The cluster mode of cleaning was normally used throughout the test program.

A Bailey Net 90 control system was used to monitor and control the system parameters and provide operator interfaces. System data and alarms were transmitted into the Net 90 system to allow continuous monitoring of the system. In addition, many of the important parameters were recorded in a POPS data system which provided digital and graphical displays of data which could be monitored in real time and printed out for specified time periods. The graphs shown later in this report were generated from data collected in the POPS system.

Data collected included pressure, temperature, flowrate, differential pressure, level, etc. throughout the system. POPS also displayed calculated parameters such as face velocity, gas viscosity, and filter permeability. Due to the huge volume of data collected during this program, it is not practical to summarize all of it in this report. Section 4 of this report presents the most important variables in graphical format.



## Results

---

### 4.0 RESULTS

#### 4.1 Proof-of-Concept Testing

During the design phase of the project, Westinghouse conducted proof-of-concept testing to verify the design basis of various system components. During this test phase, two types of filters were being considered for the Tidd APF, namely, candle and cross-flow. Proof-of-Concept tests were conducted on both types to determine the best choice for this program. Test results are as follows:

##### 4.1.1 Thermal Transient Tests

Both candle and cross-flow filter elements were subjected to thermal transient tests, which imposed a transient of 1550F to 1370F in 200 seconds, followed by a transient of 1370F to 1300F in 400 seconds. These transients simulated expected Tidd trip conditions. After 10 cycles, one cross-flow filter delaminated. Ninety start-up simulations were then conducted, and an additional filter failed. Three of the remaining cross-flow filters were subjected to a 600 hour durability test with no additional failures.

Three Schumacher SiC candles were subjected to 10 trips, 90 start ups, and 1000 blow back cycles with no visible degradation or failures.

##### 4.1.2 HTHP Array Backpulse Tests

Eleven candles were tested with PFBC ash for 368 hours at a face velocity of 3.4 fpm, for 47 cycles; cleaning was excellent. Five candles were tested for 51 hours at a face velocity of 5.7 fpm for 58 cycles; cleaning was also excellent. Three candles were tested with Tidd ash with a 1/2-inch back-pulse nozzle; the baseline pressure drop increased from 22 to 45 inches of water at 500 psig back pulse pressure. The nozzle size was increased to 3/4-inch. With the larger nozzle size, the baseline pressure drop remained below 35 inches of water at 500 psig back pulse pressure. Subsequent testing of the Tidd APF validated these test results by demonstrating the ability to clean up to 52 candles with a single backpulse.

## Results

---

### 4.1.3 Alkali Attack

The silicon carbide ceramic media was subjected to 400 hours of exposure to gas-phase alkali in the presence of steam at temperatures of 1550F to 1600F. No physical degradation of the material was observed, however, the hot strength of the material was reduced to less than 30% of its original design value. These results were confirmed during later testing at Tidd when the silicon carbide candles exposed to the PFBC flue gas exhibited a loss of strength of about 50%.

### 4.1.4 Pulse Valve Testing

An Atkomatic pulse valve was subjected to 101,000 cycles without any degradation in performance. The performance declined during the next 5000 pulses. This life well exceeded the cycle life specified for the Tidd APF system. In spite of these good results, galling problems in the valves were encountered later during system operation.

### 4.1.5 Cold Flow Modelling

Cold model tests were conducted on an 18-candle array to provide input to the APF vessel design. The cold flow testing also provided a verification of the selection of a radial inlet to the APF compared to a tangential inlet. Cold model testing of a 52 candle array showed less than 10% variation in the back pulse flow distribution. No evidence of flow maldistribution was seen during subsequent operation of the full scale Tidd APF, thus validating the cold flow modelling tests.

### 4.1.6 Gasket Tests

The fibrous ceramic material used for gaskets at the connection between the candles and the tube sheet were subjected to 15,000 cold-gas pulses at 1550F for 50 days, 1800F for 8 days, and cycled from ambient to 1800F for 15 days. No degradation was observed. In subsequent operation of the Tidd APF, the gaskets performed very well, again validating the proof-of-concept tests.

## Results

### 4.1.7 Filter Cake Properties

Filter cake properties were checked for three types of ash. Table 4.1.7 provides a summary of those results.

**Table 4.1.7 - PFBC Ash Properties**

Ash Source	Cake Density (gm/cc)	Mean Flow Resistance (Relative)	Mass Mean Particle Size ( $\mu\text{m}$ )	Backpulse Intensity Required (Relative)
Coarse PFB Ash	0.4	1.0	7.8	Lowest
Grimethorpe Ash <sup>(1)</sup>	0.6	1.8	5.3	Medium
Tidd Ash	0.3	2.7	3.5	High
Grimethorpe Ash <sup>(2)</sup>	0.2	6.8	4.0	Highest

(1) With Limestone as sorbent

(2) With Dolomite as sorbent

The actual Tidd PFBC ash cake proved much more difficult to remove from the filter candles than was expected based on the proof-of-concept tests. Therefore, these ash cake results were somewhat misleading.

### 4.1.8 Karhula Testing

While most of the testing of the Tidd APF utilized Schumacher silicon carbide candles, two other materials were tested during Test Periods IV and V, namely, Coors alumina/mullite and Refractron Vitropore silicon carbide filter candles. Proof-of-Concept testing for these two materials was conducted between the fall of 1992 and summer of 1994 at a 10 MWt PCFB test facility in Karhula Finland. This testing was conducted by A. Ahlstrom Corporation and funded by DOE as part of the Tidd HGCU Cooperative Agreement. The Coors candles underwent 716 hours of coal fire operation, and the Vitropore candles experienced 1340 hours of coal fire operation. Results of the Karhula testing increased the level of confidence for using the Coors and Vitropore filter candles in Test Periods IV and V of the Tidd HGCU program. Results of the Karhula test program are documented in a paper by T. E. Lippert, et al., published in the Proceedings of the 13th International Conference on Fluidized Bed Combustion, pp. 251-261, 1995.

## Results

---

### 4.2 Initial System Operation

Initial operation of the system using the bypass cyclone occurred during May 21-23, 1992. The APF was not connected to the system for this initial test. The performance of the bypass cyclone, and the operation of the ash removal system from the bypass cyclone was satisfactory. However, several hot spots developed on the piping system, expansion joints, and cyclone as unit load was increased.

On May 23, 1992, an expansion joint bellow ruptured, forcing the unit to be shut down after 35 hours of operation on coal. Another expansion joint bellows was found to have pinhole leaks on the bottom side of some convolutions. The failures were determined to be due to stress corrosion in the 321 stainless steel bellows due to chlorides in an aqueous solution of sulfuric acid. The solution formed from condensation of the moisture in the flue gas on the inside of the bellows.

Following the expansion joint failure, a complete engineering review of the system was undertaken. As a result of this review, several enhancements were made to the system.

From observations made during and after initial operation of the system, certain deficiencies became evident in the design of the hot gas piping system, as listed below:

- Hot spots appeared at various points in the system, indicating that the insulation was not packed tightly enough in those areas or that a gas leak path into the piping annulus had formed.
- Several expansion joint bellows exhibited elevated temperatures (250F to 670F) during operation, again indicating inadequate insulation or gas flow into the piping annulus.
- Corrosion of type 321 stainless steel expansion joint bellows was evident upon disassembly of the joints. The failure of one joint was attributed to stress corrosion cracking, while the pinholes found in another bellows was due to pitting corrosion. Chlorides were found in the condensed flue gas in the insulation material.

## Results

---

- Corrosion was also found on carbon steel surfaces that did not have the Plasite (epoxy) coating which was applied to the inside of the outer pipe. These areas included flange faces inside the gasket area, and various nozzles on the cyclones. This corrosion is believed to be from sulfuric acid formed from the flue gas condensation.
- The Plasite coating was burned off at locations where hot gas reached the carbon steel pipe.

### 4.2.1 System Modifications (5/92-10/92)

After reviewing the above problems and lengthy discussions with other users of hot gas piping systems, consultants, and others, the following piping modifications were undertaken:

- The expansion joint bellows material was changed from 321 SS to Hastelloy C-22. This is a high nickel alloy that has excellent resistance to pitting, crevice corrosion, and stress corrosion cracking in the presence of oxidizing agents and chlorides.
- A 2-ply expansion joint bellows was used with pressure monitoring capability between the plies. The inner ply was 0.038" thick and the outer ply was 0.062" thick. Failure of the inner ply would not result in failure of the joint and could be detected with local pressure gauges.
- The ceramic fiber insulation was replaced with a cast insulating refractory. It was concluded that a cast refractory would present a superior barrier to prevent gas from flowing behind the inner liner in the annulus compared to the ceramic fiber blanket insulation. (In order to retain freedom of movement in expansion joint spools, a small portion of fibrous insulation was used at the bellows location.) It was further decided to retain the inner liner (except in two instrument spools) to preclude the possibility of refractory spalling off and getting carried into the gas turbine. The liner also served as a form during the installation of the refractory. As additional enhancement, 1/4" thick ceramic fiber rollboard insulation was used on the ID of the cast refractory for expansion and cushioning. The refractory selected had a density of 50 lbs/ft<sup>3</sup> and a thermal conductivity which would keep the outer pipe temperature below 250F. The refractory was shop installed.
- The inside surfaces of all piping and flange faces were clad with Hastelloy C-22 material. The cladding was 16 gauge (1/16" thick) and was applied to the pipe ID by plug welding. The

## Results

---

function of this inner liner was to protect the inside of the outer pipe from the possibility of corrosion from condensed acid. Figure 4.2.1 is a photograph of a typical pipe spool following installation of the Hastelloy C-22 liner. The anchors used to secure the refractory in the pipe are also shown in the photograph.

- The liner end connection collars were modified where possible to minimize gas leaking behind the liner. One end of the collar was seal-welded to the liner where possible.
- The liners in the expansion joint assemblies were modified to include a bellows at the same location as the bellows in the outer pipe. This was necessary to allow the outer pipe, refractory, and liner to move together while still permitting freedom of movement at the bellows area. (Most of the expansion joints underwent angular rotation, not axial movement.) Figure 4.2.2 is a drawing of a typical expansion joint after the modifications.
- The flow liner tees were modified to function as 90° elbows where possible. The blind end of the tee was cut off and a curved plate was welded onto the tee to form an elbow. The end of the outer tee was filled with cast insulating refractory in order to better insulate the blind flange. This change reduced the possibility of ash collecting in the dead end of a tee and becoming dislodged and being carried into the gas turbine.

Figure 4.2.3 provides a comparison of the original and modified designs of the pipe internals.

The modifications described above proved successful, and the piping system performed very well during subsequent testing. However, corrosion of expansion joint bellows remained a problem until additional steps were taken later in the project as discussed in Section 4.3.5.

Following initial operation of the system, both cyclones were opened and inspected by the manufacturer, refractory supplier, and refractory installer. Some cracking of the refractory was apparent, but was not considered to be serious. Some corrosion was evident on the man way nozzle and flange. As a result, Plasite (epoxy) coating was applied to nozzles and flange faces on the cyclones and the APF vessel.

## Results

---



**Figure 4.2.1 - Photograph of Hastelloy Liner in Hot Gas Pipe Spool**

# Results

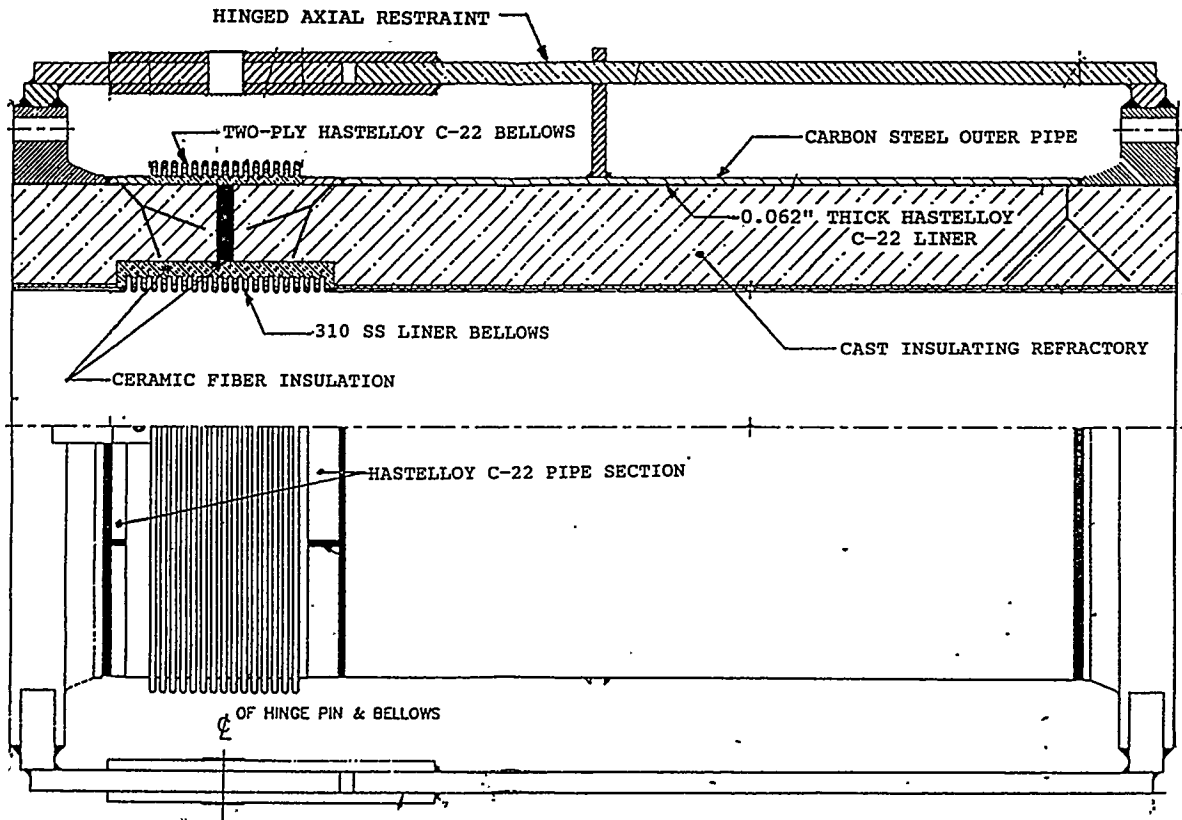


Figure 4.2.2 - Typical Expansion Joint After Modifications

# Results

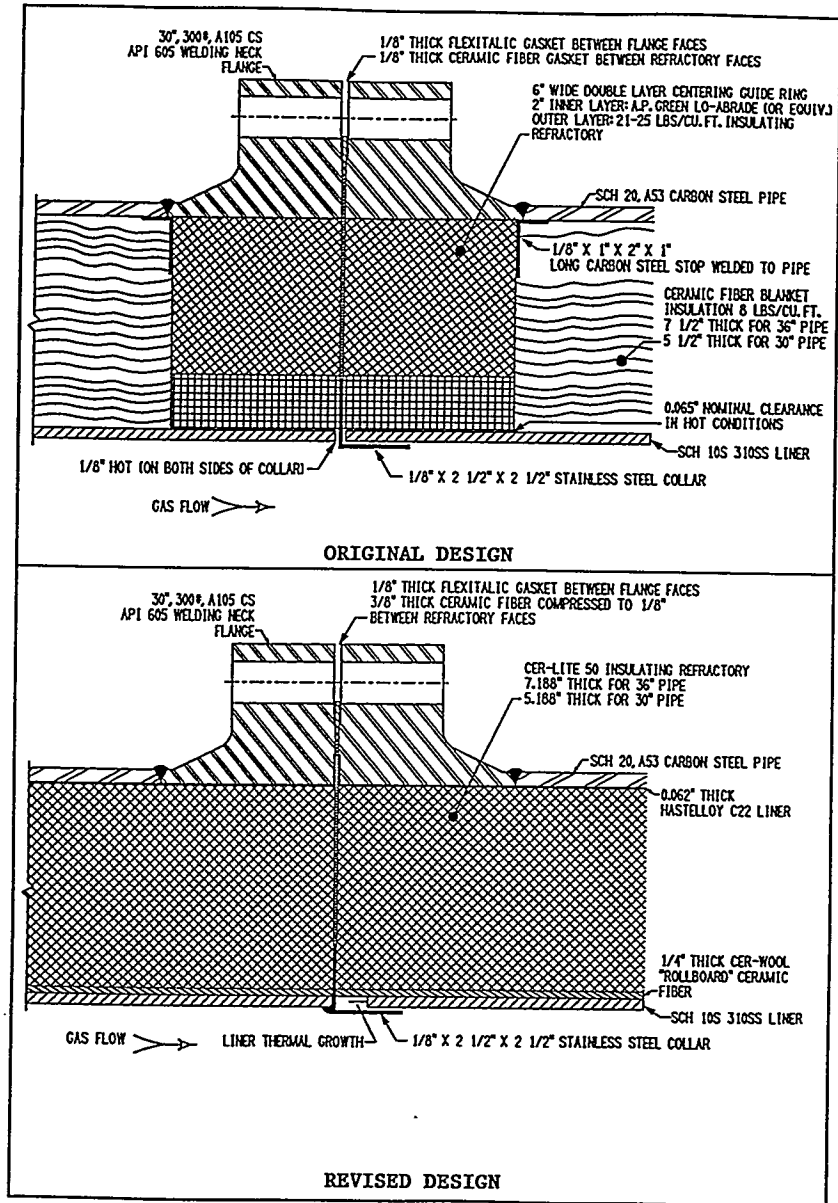


Figure 4.2.3 - Cross Section of Typical Hot Gas Piping Joint

## Results

### 4.3 Test Period I: 10/92 - 12/92

Table 4.3 summarizes the operating conditions and observations from Test Period I.

**Table 4.3 - Summary of HGCU Operation - Test Period I**

	Operating Hours	Cumulative Hours	Operating Temp.	Pressure Drop	Inspection Observations
Run 1	101	101	1150°-1400°F	25-75 in. H <sub>2</sub> O Stable	● No filter issues
Runs 2 & 3	77	178	1000°-1450°F	40-180 in. H <sub>2</sub> O	_____
Run 4	286	464	1300°-1490°F	45-170 in. H <sub>2</sub> O	● 21 Broken candles in bottom plenums

#### 4.3.1 Test Run 1 - 10/28 to 11/1/92

First operation of the advanced particle filter on coal fire occurred on October 28, 1992. The first test of the APF included over 101 hours of operation on coal. During the initial operation, the APF exhibited a stable pressure drop over a range of plant conditions corresponding to the predicted values. Although the APF was operated to approximately 90 percent of the design flow with the PFBC at 80 to 85 percent of full load, full plant load was not achieved due to hot spots on the backup cyclone vessel and APF outlet nozzle. The plant was ultimately shut down due to ash pluggage of valves and instrument lines associated with the control of the APF ash removal system.

Following shutdown, the filter was visually inspected through access ports in the APF pressure vessel head and ash hopper. The inspection, while limited to the clean gas side of the tubesheet and the three bottom plenums of the three cluster assemblies, indicated the system to be in excellent condition with no evidence of filter failure or dust breach to the clean side of the filter. Furthermore, the filters appeared to be uniformly clean with no indication of ash buildup or bridging. Figure 4.3.1 shows a photograph of the bottom filter candles following Test Run 1.

Following repair and maintenance of the APF outlet nozzle and backup cyclone to eliminate local hot spots and to incorporate continuous instrumentation air purges, operation of the PFBC plant was resumed.

## Results

---

### 4.3.2 Test Run 2 - 11/17/92

This run was terminated after 1.3 hours of coal fire due to plugged primary cyclones, and will not be discussed.

### 4.3.3 Test Run 3 - 11/21 to 11/24/92

In Test Run 3, the APF was operated for approximately 76 hours on coal, reaching a maximum operating temperature of 1450F and 90 percent of the design flow. Again, stable filter pressure drops were demonstrated over a range of operating conditions.

Approximately 36 hours into this test, the fourth stage of the APF backpulse compressor failed, thus limiting the ability to clean the filter for 24 hours. During this period, the filter pressure drop reached a value of 180 inches of water. Once a pressurized nitrogen supply system was installed, a stable filter pressure drop was once again achieved. However, the original APF baseline pressure drop was never reestablished.

Following the compressor outage and reestablishment of stable filter operation, the performance of the APF was indirectly checked by briefly opening a vent valve on the backup cyclone ash discharge line. Visual inspection of the short burst of gas discharged from the vent valve showed no evidence of dust. This result, along with other operating data, supported the conclusion that no serious damage to the filter resulted from the compressor outage. In this test, the PFBC was shut down due to a paste feed pump issue unrelated to the APF. No visual inspection of the filter was made at this time.

## Results

---

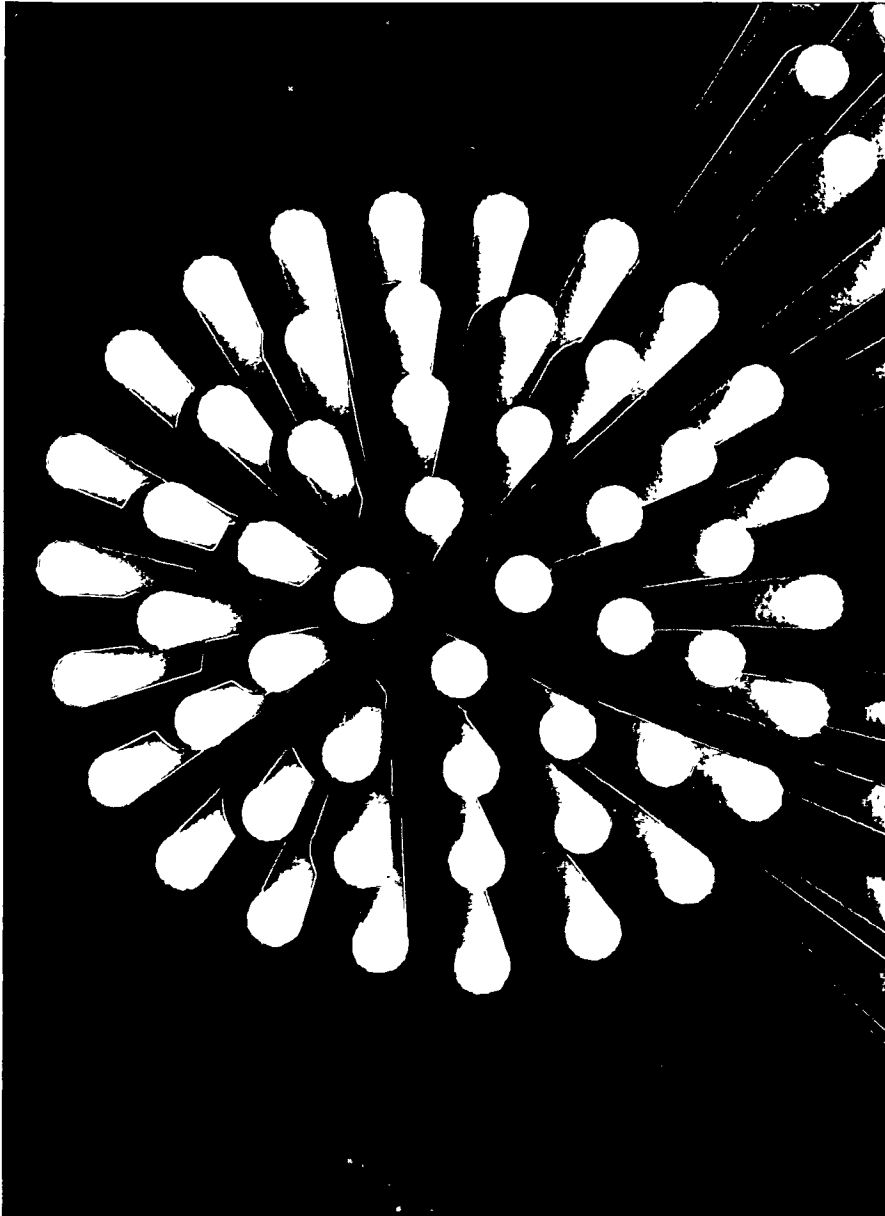


**Figure 4.3.1 - Photograph of Bottom Filter Candles Following Test Run 1**

## Results

---

### 4.3.4 Test Run 4 - 11/25 to 12/7/92

Test Run 4 was a hot restart of the plant following Test Run 3. Test Run 4 accumulated an additional 286 hours of operation on coal. At the start of this test, a nominally low baseline pressure drop was established, apparently due to pulse cleaning during the shutdown of Test Run 3 and prior to restart. During this test, several major events occurred, including high ash level alarm in the APF hopper, a second loss of the backpulse compressor, indications of an unstable pressure drop at temperatures above 1400F, first indications of dust breach, and the first identifiable change in pressure drop indicating a possible loss of filter elements. This test was eventually terminated due to a leak in a pipe expansion joint unrelated to the APF technology.

### 4.3.5 Posttest Inspection and Modifications (12/92-6/93)

Following the conclusion of Test Run 4 and a visual inspection of the filter internals, the tubesheet and cluster assemblies were removed from the pressure vessel. Figures 4.3.2 through 4.3.10 are photographs of the filter internals following Test Run 4. Based on a detailed inspection of the filter, the following observations were made:

- A total of 21 broken candle filters were identified occurring only on the bottom three plenums. Seventeen of the broken filters apparently failed near the transition from the dense-to-porous filter region. Plenum A had 15 failed elements, while Plenum B had 2 and Plenum C had 4.
- No broken candles were detected in the top or middle plenums. Some ash bridging was observed on the top and middle plenums between the inner ring of filters and the cluster support pipe.
- Bowing of filters was detected for some elements in the bottom plenums, as well as for broken filters removed from the ash hopper.

A possible failure scenario would conclude that ash, unable to properly discharge from the hopper, built up and reached the candle filters of the bottom plenums. Ash at this level then began to fill and pack the interstitial spacing, forming ash bridges between the candle filter elements. As cleaning continued, more ash was packed into the interstitial filter spacing with additional accumulation of ash in the hopper.

## Results

---

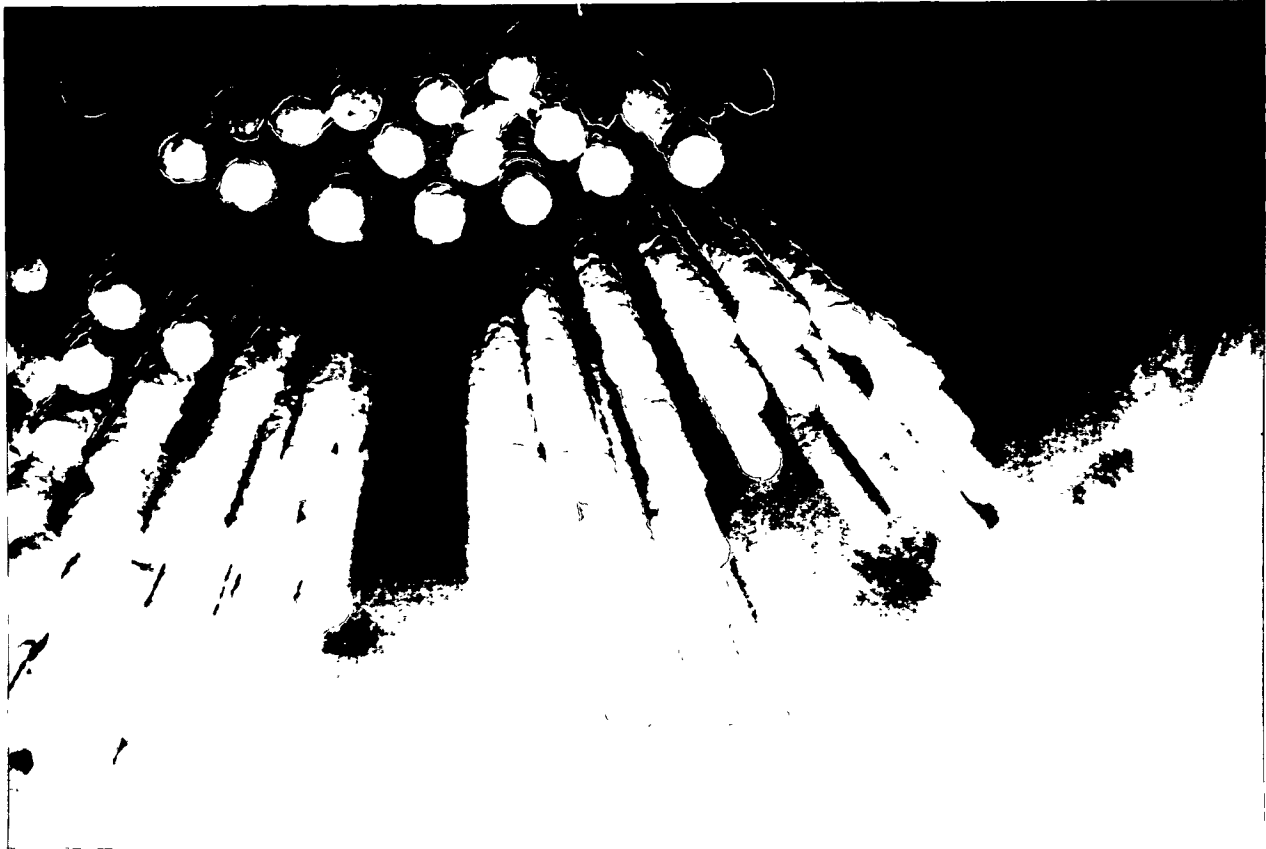


**Figure 4.3.2 - Photograph of Filter Internals Following Test Run 4**

## Results

---

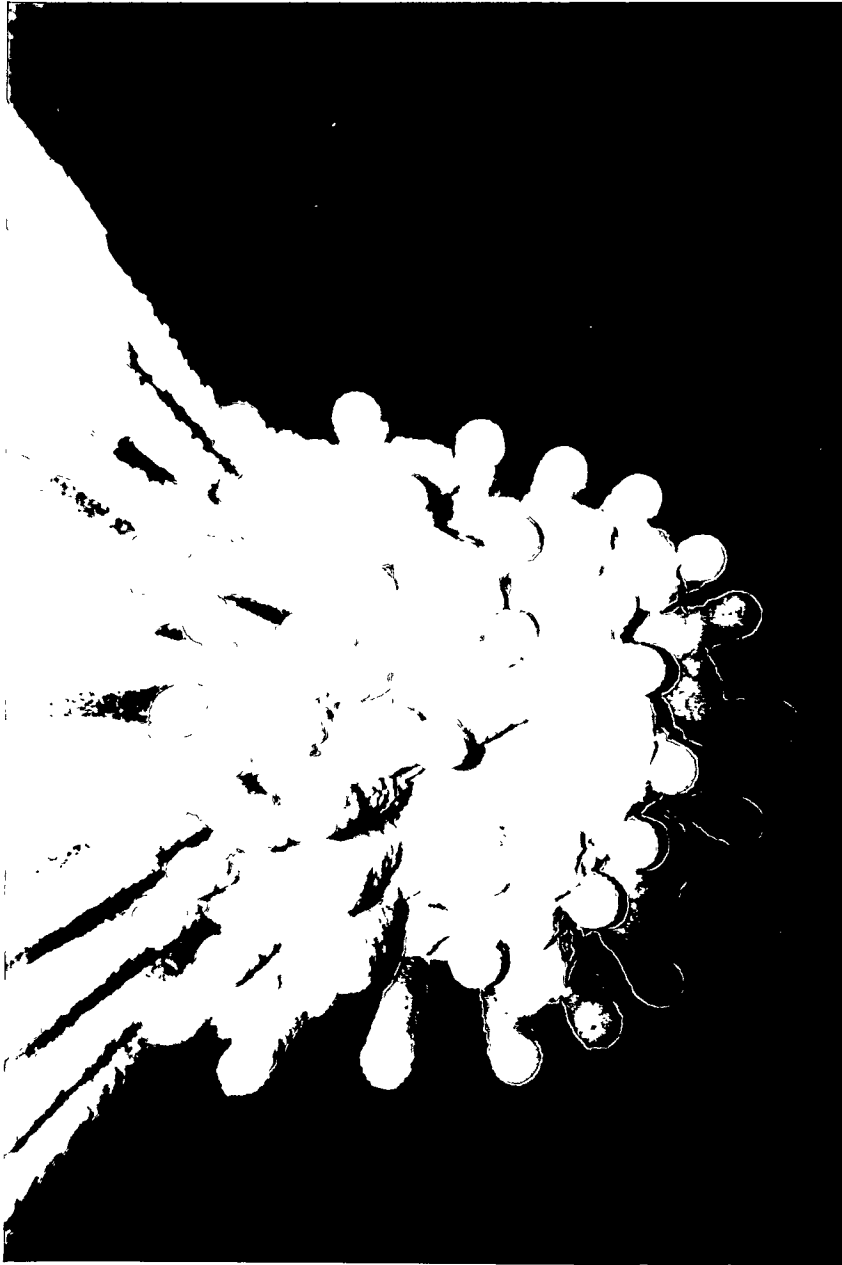
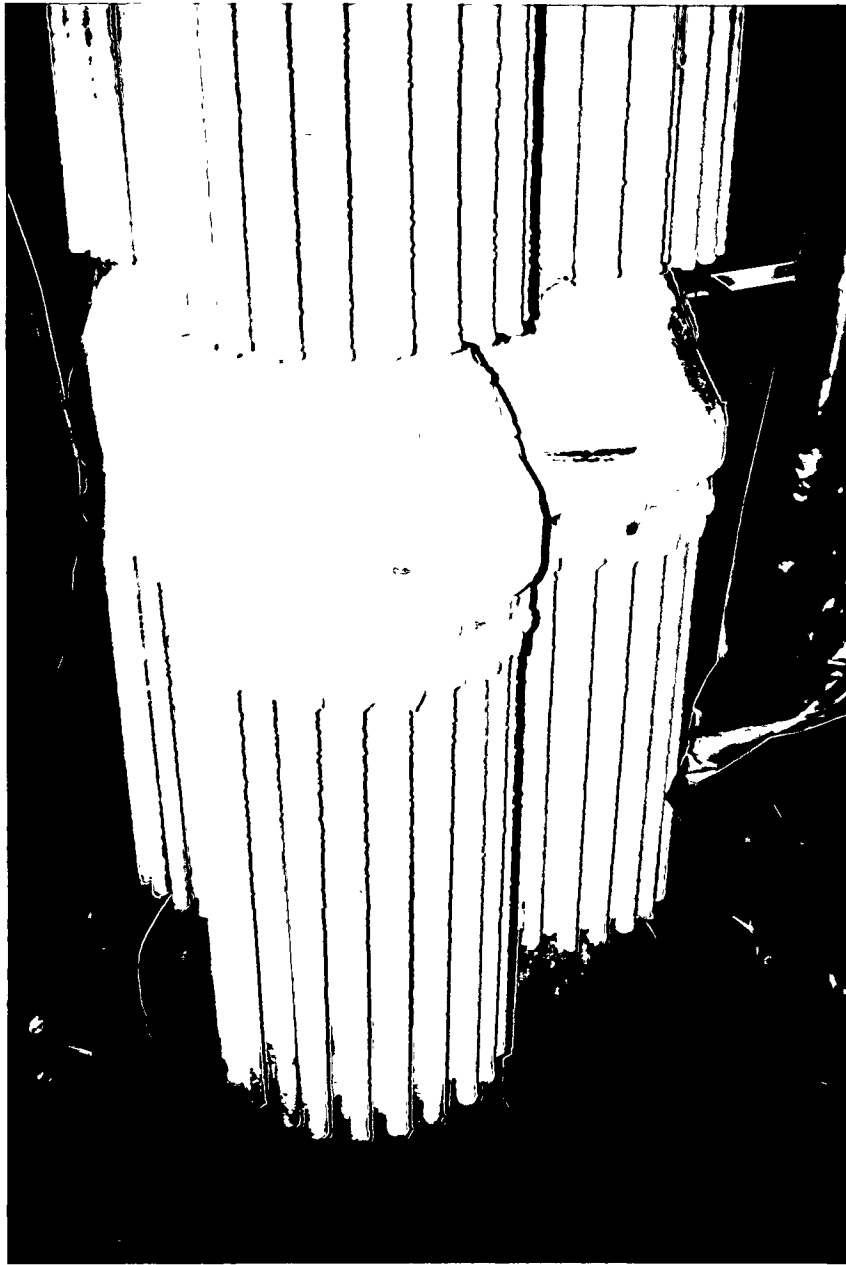


Figure 4.3.3 - Photograph of Filter Internals Following Test Run 4

## Results

---



**Figure 4.3.4 - Photograph of Filter Internals Following Test Run 4**

## Results

---

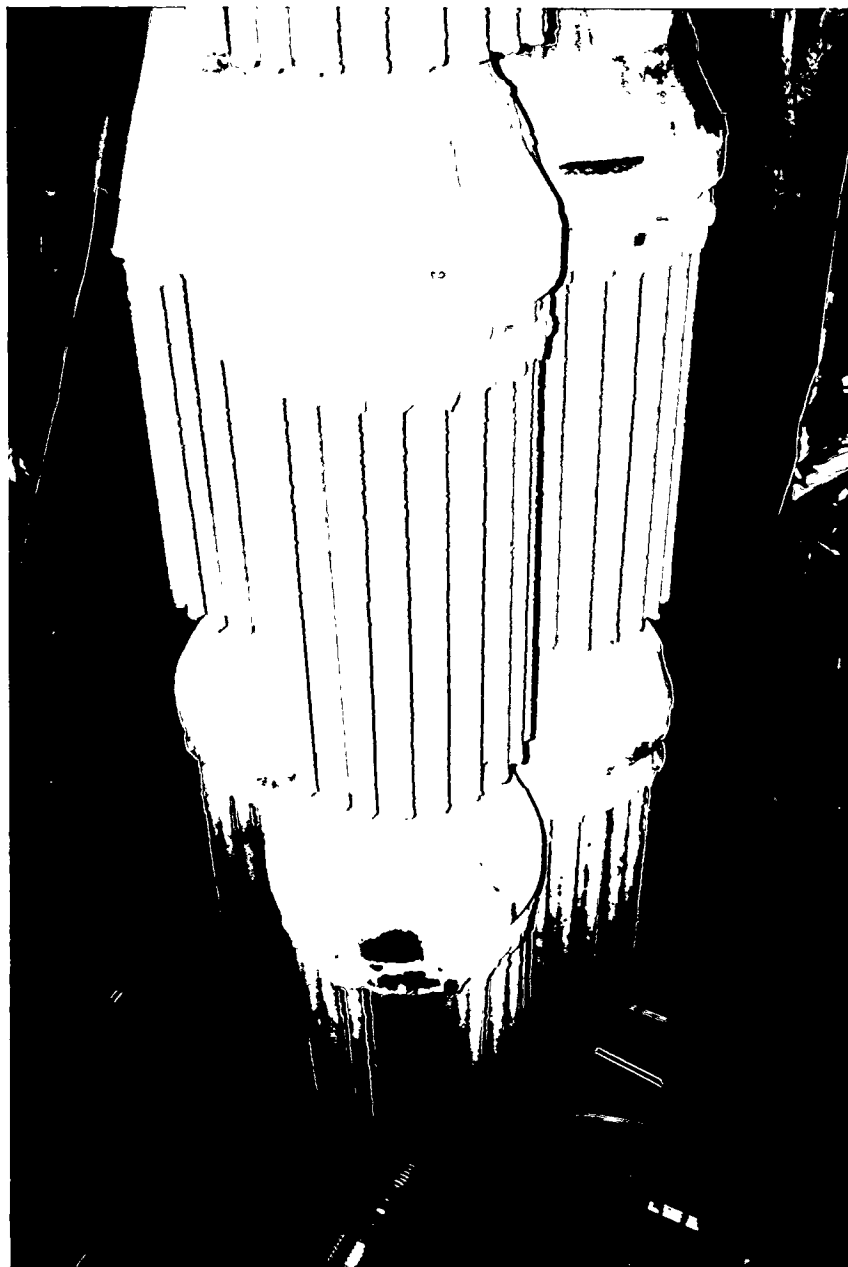


**Figure 4.3.5 - Photograph of Filter Internals Following Test Run 4**

## Results

---

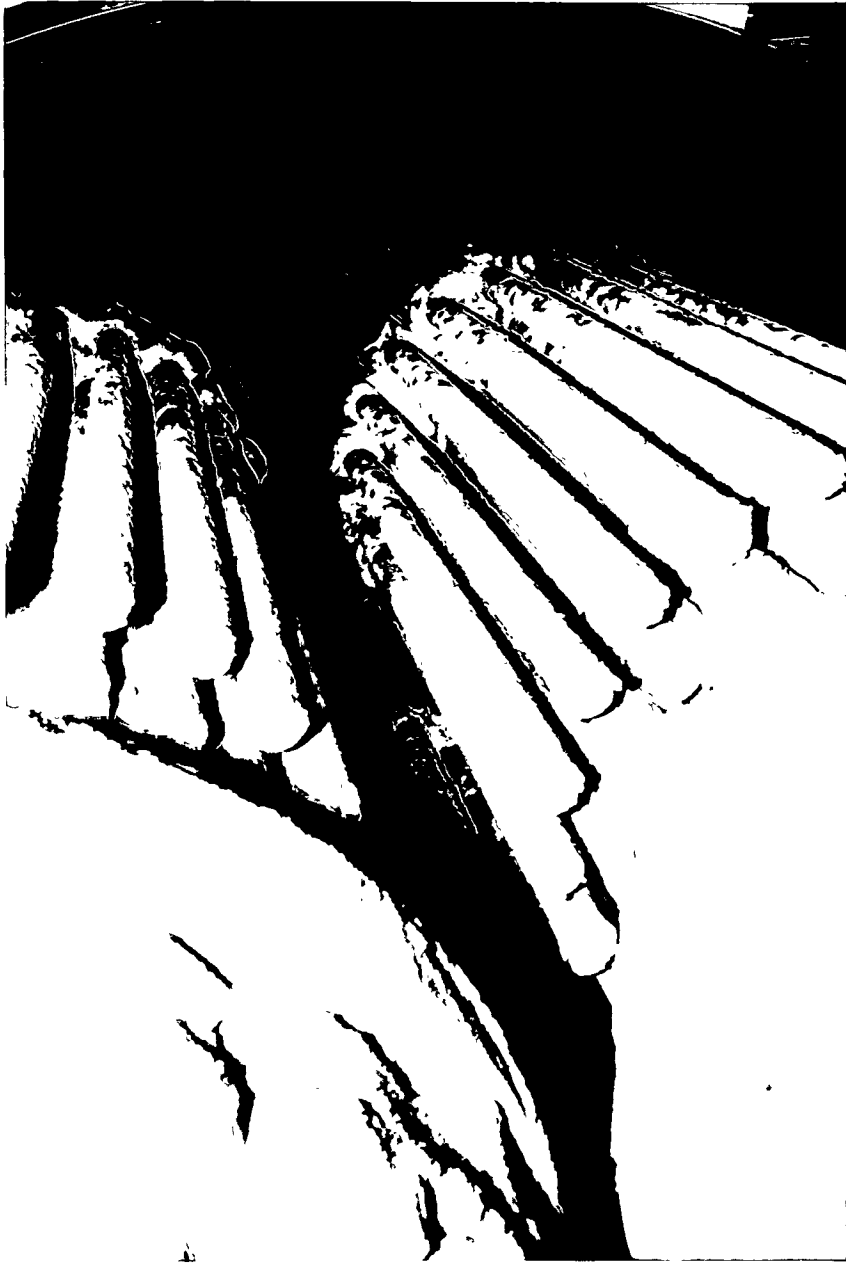


**Figure 4.3.6 - Photograph of Filter Internals Following Test Run 4**

## Results

---



**Figure 4.3.7 - Photograph of Filter Internals Following Test Run 4**

## Results

---

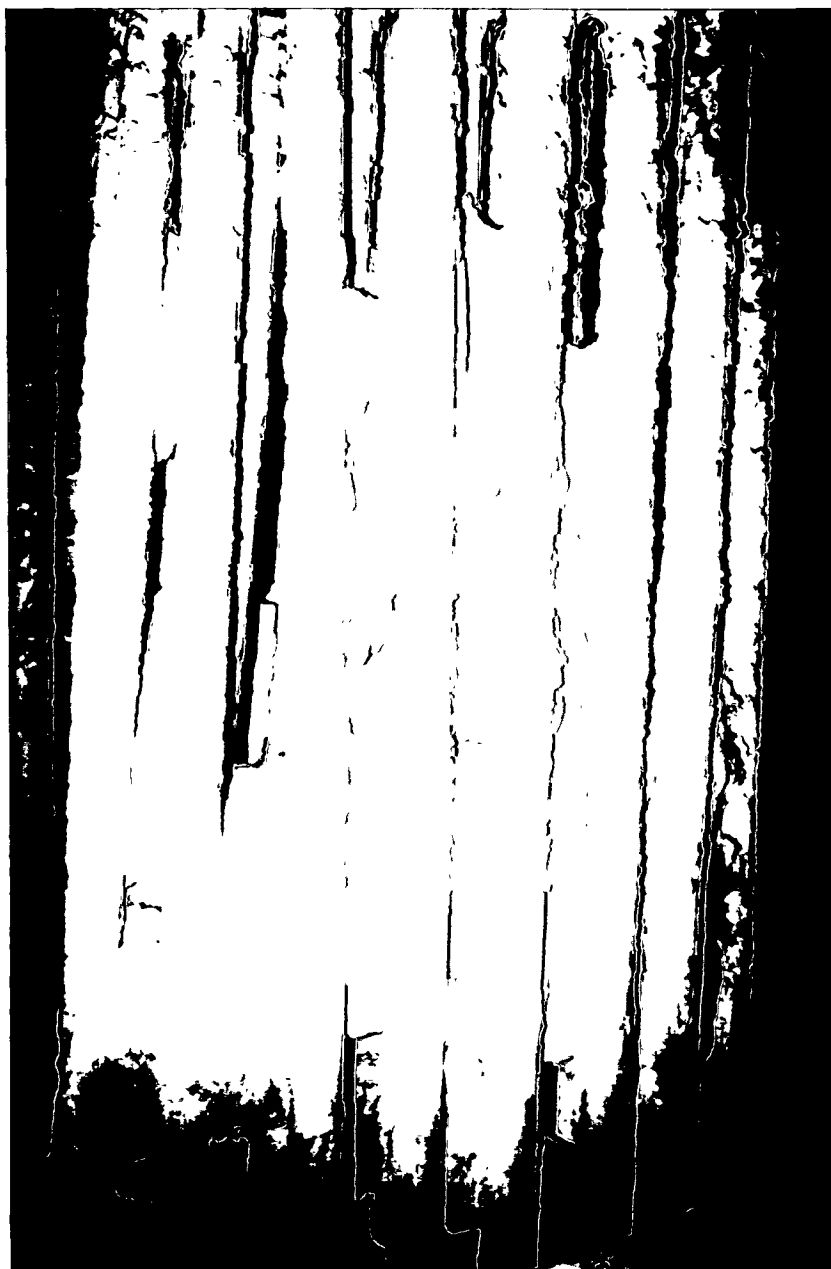


**Figure 4.3.8 - Photograph of Filter Internals Following Test Run 4**

## Results

---

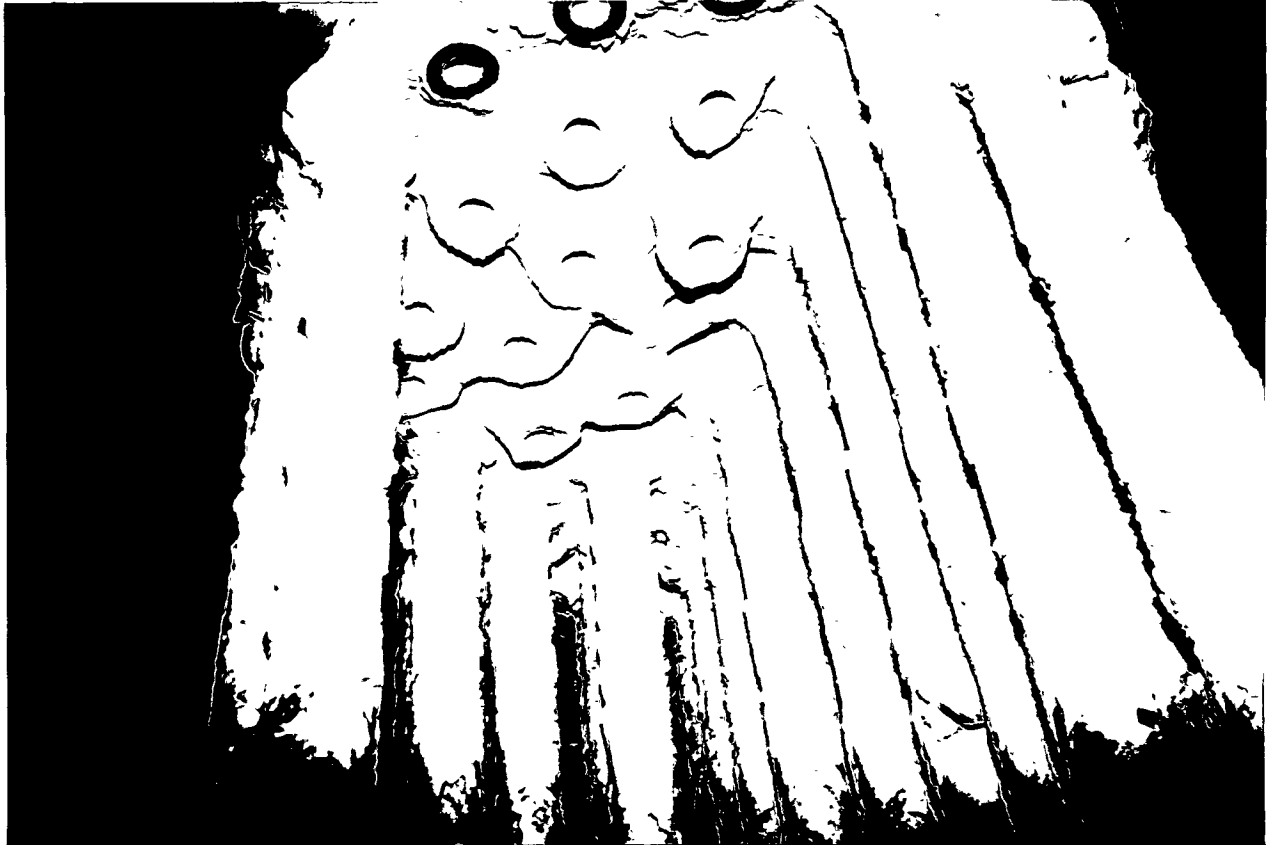


**Figure 4.3.9 - Photograph of Filter Internals Following Test Run 4**

## Results

---



**Figure 4.3.10 - Photograph of Filter Internals Following Test Run 4**

## Results

---

The high cohesive strength of this ash allowed lateral forces to develop on the filter elements. The lateral forces resulted in filter bowing and high shear loads. The concentration of stresses near the top of the filters resulted in a mechanical failure of the filter elements.

The initial operation of the HGCU system revealed some problems with the system. Since this was the first test of a large-scale hot gas clean up system, it is not surprising that problems arose. Most of the problems discussed below did not involve the APF. Other than the problems of hot spots on the shell of the APF and the ash accumulation in the hopper, the APF performed very well. It was necessary to overcome the problems associated with the balance of the system in order to achieve successful long-term operation. A summary of the problems encountered and corrective actions is discussed below.

**Hot Spots.** Hot spots were observed on the backup cyclone, APF vessel head and outlet nozzle, and several instrument nozzles on the hot gas piping. Following Test Run 1, the backup cyclone was heated internally and externally to remove any residual moisture from the refractory lining, and all refractory cracks were repaired. In subsequent tests, the cyclone skin temperature was much lower; however, it still exceeded the nameplate design rating of 200F at several locations. At our request, the cyclone manufacturer recertified the cyclone to 750F by resubmitting ASME code calculations based on this design temperature. Hot spots on the cyclone shell observed in subsequent testing remained well below the revised design temperature.

Also following Test Run 1, all instrument nozzles that exhibited hot spots were opened and inspected. In all cases, it was found that gaps between the refractory and insulation or instrument device allowed hot gas to reach the nozzle/pipe connection. Insulating caulking was added at these locations to seal the gaps. In subsequent tests, none of these hot spots, with one exception, reappeared. One nozzle reached about 400F, and it was reworked again prior to the resumption of testing.

The APF outlet nozzle and several locations on the top of the APF head exhibited high temperatures (up to 800F) during Test Run 1. Between Test Runs 1 and 2, the insulation in the outlet nozzle was revised to eliminate a likely gas flow path, and potential holes around head liner penetrations were repacked with insulation. The following test showed that the outlet nozzle had been successfully repaired, as well as most of the original hot spots on the top of the APF head. However, a new hot area appeared around the head knuckle. Upon disassembly following testing, this hot area was found to be caused by distortion of the brim of the dome liner which opened up a gap between it and the insulation. The brim was eliminated and the insulation repaired.

## Results

---

**Ash Accumulation in the APF Hopper.** Following Test Run 1, the APF hopper was inspected. Some ash was observed on the sides of the hopper near the outlet. However, it appeared to be less than one inch thick. It was cleaned out prior to Test Run 2. During Test Run 3, after approximately 19 hours on coal, the APF liner temperature began dropping, indicating ash buildup near the hopper outlet. Subsequent purging with air corrected the problem. Later in the test run, the backpulse air compressor failed and filter cleaning was abnormally low or completely interrupted for about 33 hours. Following resumption of cleaning, the high ash level annunciator alarmed, and the hopper liner temperatures decreased. During Test Run 4, several instances of low liner temperature and/or high ash level alarm occurred. Upon inspection of the APF hopper following the last test, the entire hopper was found to be full of ash. In some areas the ash level was higher than the bottom of the candles, leading to candle breakage.

Subsequent inspection revealed a solid plug of material in the 8-in. diameter APF hopper outlet pipe. It is unknown when this plug formed. Chemical analysis indicated that it was calcium sulfate and magnesium sulfate. Condensation of sulfuric acid from the flue gas in the relative cool outlet pipe is thought to have contributed to the formation of the plug. This was exacerbated by cool seal air from the screw cooler flowing upward into the filter ash outlet nozzle.

Several options were considered for improving ash flow through the hopper. These included installing purge air pipes or manifolds in the hopper, increasing the hopper angle, mounting the hopper liner supports on vibrators, and installing a pneumatic vibrator in the APF manway nozzle and linking it to the hopper. The purge air option was rejected since it was considered likely to move ash only in localized areas and cool the gas below the dew point causing the ash to become more sticky. Changing the hopper angle was rejected because laboratory flow tests indicated that the dimensional constraints of the APF vessel would make this impractical. The last alternative was chosen and preliminary testing at Tidd using a vibrator showed it to be effective in moving ash down the hopper wall. A detailed design was completed by Westinghouse and the vibrator and related hardware were installed prior to the next test. The screw cooler water temperature was increased in the next test series from 320 to 340F (the limit of the system) in order to increase the ash temperature at the screw cooler inlet.

**Ash Pluggage in the Lockhopper System.** Test Run 1 was terminated due to ash buildup in a lockhopper isolation valve and instrument lines. It was found that the valve purge air contained enough moisture to harden the ash in the valve body. The pressure sensing lines on the ash removal system became plugged with ash, causing erroneous pressure data which resulted in the logic

## Results

---

interrupting the sequence of operation. The lockhopper pressure equalization line also became plugged with ash. As a result, ash removal was sporadic during Test Run 1.

Several improvements were made to the ash removal system between Test Runs 1 and 2. The source of air for all valve purging was switched to a drier source. Blowdown valves were added to the purge air lines to remove any residual moisture accumulation. Constant flow regulators were installed to provide continuous instrument air purge to all pressure sensing lines. The lockhopper pressure equalizing line was revised to utilize clean process air instead of gas in the surge hopper for repressurization in order to keep ash from plugging the equalizing line. The ash removal system logic was revised to reduce the number of interruptions in the ash unloading sequence. Finally, as a backup, an emergency ash removal system was added downstream of the screw cooler. This system used process air to transport ash from the screw cooler discharge pipe in a manner similar to the method used for the backup cyclone ash removal. Ash removal during Test Runs 3 and 4 was much better than during Test Run 1. However, system logic enhancements continued to be made during and after Test Runs 3 and 4. Visual inspection of the system following Test Run 4 revealed that the lockhoppers were clean.

**Expansion Joint Bellows Leak.** The expansion joint bellows material was changed from 321 stainless steel to Hastelloy C22 (UNS N06022) following the failure of two expansion joints in May 1992, during initial operation of the system using only the bypass cyclone as previously discussed. The failures were attributed to stress corrosion and pitting corrosion due to sulfuric acid and chlorides. Hastelloy C22 was believed to be the best candidate material for the corrosive conditions created by condensation of the Tidd PFBC flue gas. Also, the revised expansion joints were made with a two-ply bellows, 0.038" (inner) and 0.062" (outer) in thickness. A pressure gauge was installed at each bellows to monitor the interply pressure and thereby detect a leak in the inner ply. A pinhole leak formed in the inner ply of one bellows during Test Run 4. A hot spot ( $\approx 540\text{F}$ ) was also observed at a localized area in the outer bellows. When the leak was confirmed, the plant was shut down. Subsequent failure analysis confirmed that a pinhole leak was formed by pitting corrosion from hydrochloric acid. The bellows was replaced. A second bellows was removed and examined as well. It also exhibited some pitting corrosion, but to a much lesser degree. It was not replaced. Thus, it was concluded that even Hastelloy C22 was not impervious to corrosion in this system, although it was far superior to stainless steel.

As a result of the failure, it was decided to heat trace and insulate all expansion joints in the hot gas piping system to maintain a temperature of 450F, well above the acid dew point ( $\approx 370\text{F}$ ) of the flue

## Results

---

gas. Necessary instrumentation and controls were installed prior to the next test series to monitor and control the temperature of the bellows.

**Loss of Backpulse Air Compressor.** The backpulse air compressor failed on two occasions, once during Test Run 3 and again during Test Run 4. Both failures were believed to be due to insufficient lubrication to the fourth stage cylinder. The manufacturer subsequently modified the fourth stage cylinder liner to relocate the oil port to eliminate the problem. However, excessive wear of fourth stage piston rings remained an intermittent problem for the remainder of the test program. The second failure also resulted in a broken crosshead which connected the second/ third stage pistons to the crank shaft. The manufacturer suggested that this failure might have been due to excessive oil and moisture building up in the first stage moisture separator and carrying over into the second stage. Therefore, all four moisture separators were equipped with larger drain lines and drain valves, and the first stage separator drain valve was left open continuously in subsequent tests.

In addition, two spare compressors, each with approximately half the capacity of the original, were rented and placed on standby for use during the remainder of the program. They were used for brief periods when the main compressor had to be shut down for maintenance.

**Backpulse Valves.** Piston actuated ball valves were used on the backpulse valve skid to control flow paths during backpulsing. One valve failed during Test Run 4 due to excessive wear at the valve stem coupling. The valve was replaced during the test. Other ball valves also exhibited wear at the couplings. Between Test Runs 1 and 2, bracing was added to the valve operators to reduce misalignment of the stem and coupling during stroking. However, the couplings continued to wear. Following Test Run 4, all couplings, valve bodies, and actuator brackets were replaced with an improved design.

On several occasions backpulse valves failed to operate. In all cases, the parallel backup valve operated successfully. Post-test examination revealed some axial scratches and galling on the piston and cylinder wall. Atkomatic modified all of the solenoid valves in an effort to eliminate galling during valve actuation. However, additional modifications were required later in the program to overcome this problem.

**Unstable Filter DP Above 1400F.** Operating experience, both at Tidd and Westinghouse Test Facility, demonstrated that the filters are difficult to clean, particularly when the ash temperature

## Results

---

approaches 1500F. During Test Runs 1 and 3, filter pressure drop increased moderately (indicative of good cleaning). However, after failure of the backpulse compressor, baseline pressure drop increased considerably. After nitrogen was brought onto the site for backpulsing, the baseline pressure drop did not recover. Upon visual inspection, many candles had a "splotchy" appearance. Some intercandle and candle-to-plenum ash bridging was also observed.

Figure 4.3.11 shows the increase in filter baseline pressure differential over an 18-hour time period during Test Run 4. The temperature in the APF ranged from 1425 to 1450F during this time period. It is not clear whether the inability to clean effectively during this phase was due to a temperature effect on the ash or the result of a thick ash cake on the candles that had been partially cleaned by low pressure backpulsing. Once the candles became "splotched," subsequent cleaning may have been ineffective on the previously uncleaned areas. It should be noted that the filter pressure differential stabilized during portions of Test Runs 1 and 3 (prior to the backpulse compressor failure) at temperatures above 1400F, but below 1500F.

During Test Run 4, unit load was reduced to decrease gas temperature and flow to maintain the APF tubesheet pressure differential below the maximum limit. In order to increase the allowable pressure differential of the filter, stiffener bars were subsequently welded across the bottom filter plenums above the candle holders. The plenum bottoms were the limiting components of the maximum allowable pressure drop of the filter assembly. This modification increased the tubesheet allowable pressure differential from 7 to 9 psi.

In addition, a method of detuning the primary cyclone upstream of the APF was devised. The method involved injecting air from the sorbent system upwards into the cyclone dip leg, thereby reducing the cyclone efficiency. The purpose of cyclone detuning was to increase dust loading and the proportion of larger dust particles to the APF in order to improve filter cleaning and/or ash removal and transport. An analysis was performed to determine the proper air line size to obtain the required air velocity in the cyclone. The system included a manual globe valve and flow metering orifice outside the combustor to allow the detuning air flow to be adjusted or shut off. The system was installed prior to the next start-up, but was not tested until the latter part of Test Run 11.

## Results

---

Prior to the resumption of testing, all of the filter candles in the bottom plenums were replaced and all of the ash accumulation on the filter candles and metal surfaces in the upper and middle plenums was removed, as shown in Figures 4.3.12 through 4.3.15.

# Results

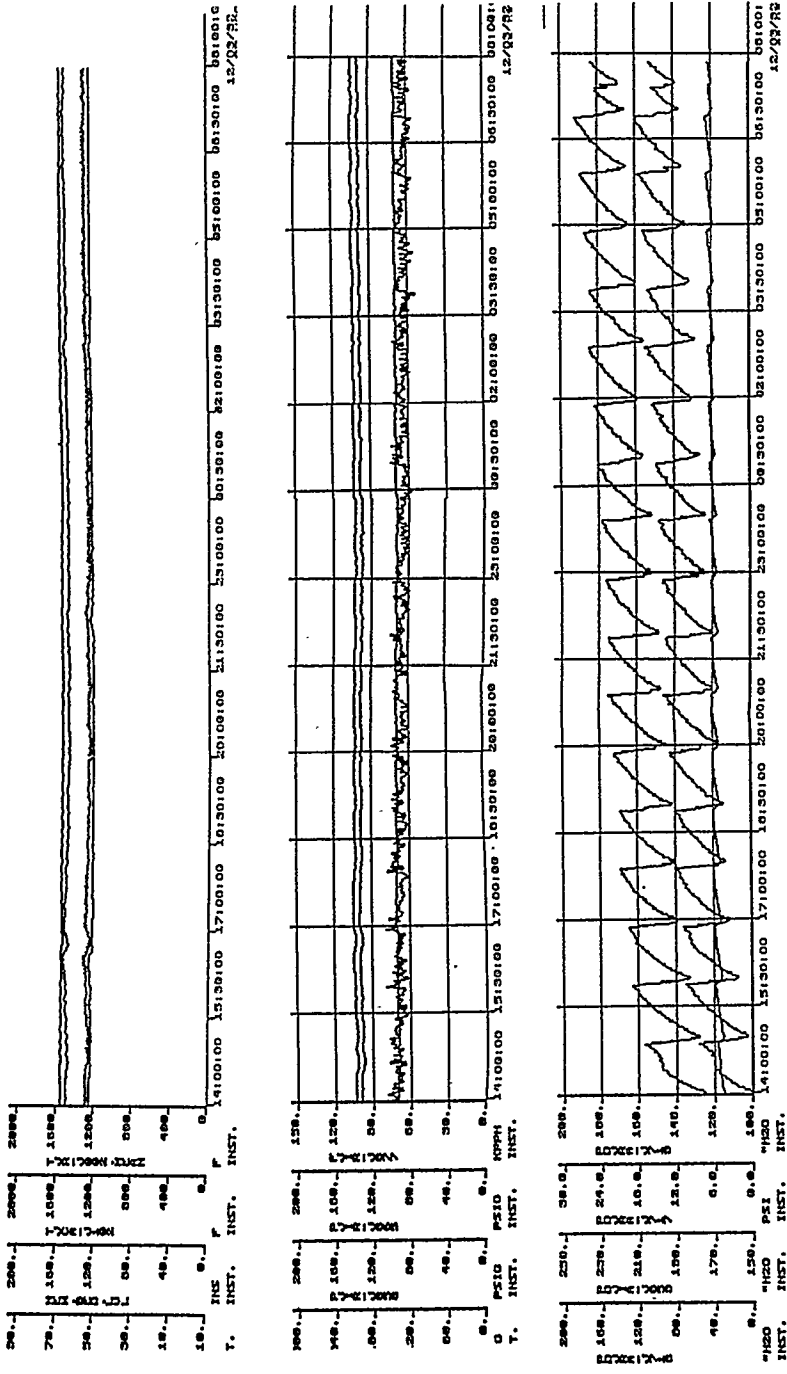


Figure 4.3.11 - Graphs of Filter Parameters During Test Run 4

**Top Set of Graphs:**  
 Top Line: Mean Bed Temperature: 1540F  
 Second Line: Freeboard Temperature: 1490F  
 Third Line: Unit Load: 53 MW  
 Bottom Line: Bed Level: 123\*

**Second Set of Graphs:**  
 Top Line: APF Inlet Pressure: 138 psig  
 Second Line: APF Outlet Pressure: 130 psig  
 Third Line: Freeboard Pressure: 139 psig  
 Bottom Line: APF Gas Flow: 65,000 - 70,000 lb./hr.

**Bottom Set of Graphs:**  
 Top Line: APF DP: Baseline Climbing from 125° H<sub>2</sub>O to 165° H<sub>2</sub>O  
 Second Line: HGCU System DP: Baseline Climbing from 150° H<sub>2</sub>O to 190° H<sub>2</sub>O  
 Bottom Line: APF Tubesheet DP: Climbing from 5 psi to 6 psi

**NOTE:** APF DP as measured between filter outlet nozzle and bottom of vessel cone.  
 Tubesheet DP as measured between filter outlet nozzle and lower cylindrical portion of vessel.  
 HGCU System DP as measured between inlet and outlet piping.

## Results

---



**Figure 4.3.12 - Photograph of Filter Internals Before Test Period II**

## Results

---

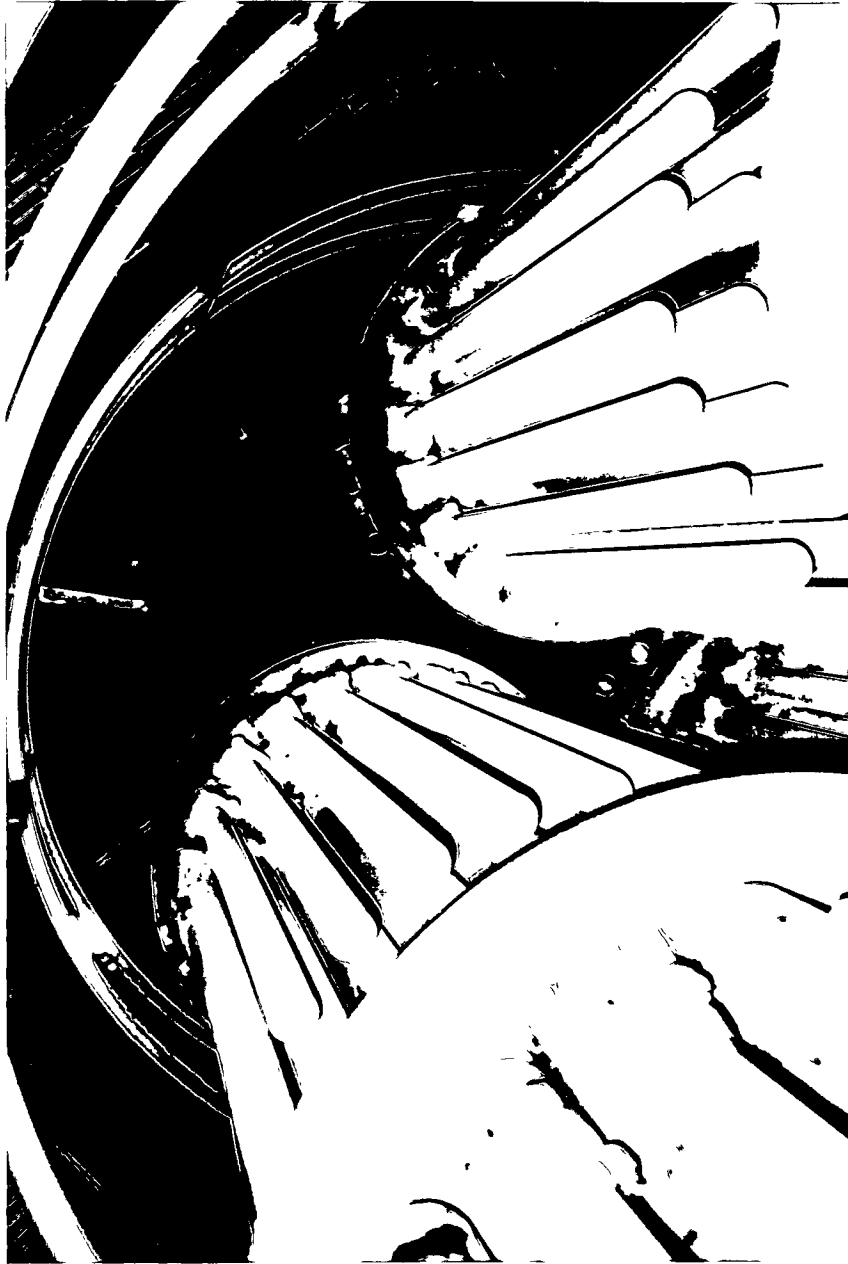


**Figure 4.3.13 - Photograph of Filter Internals Before Test Period II**

## Results

---

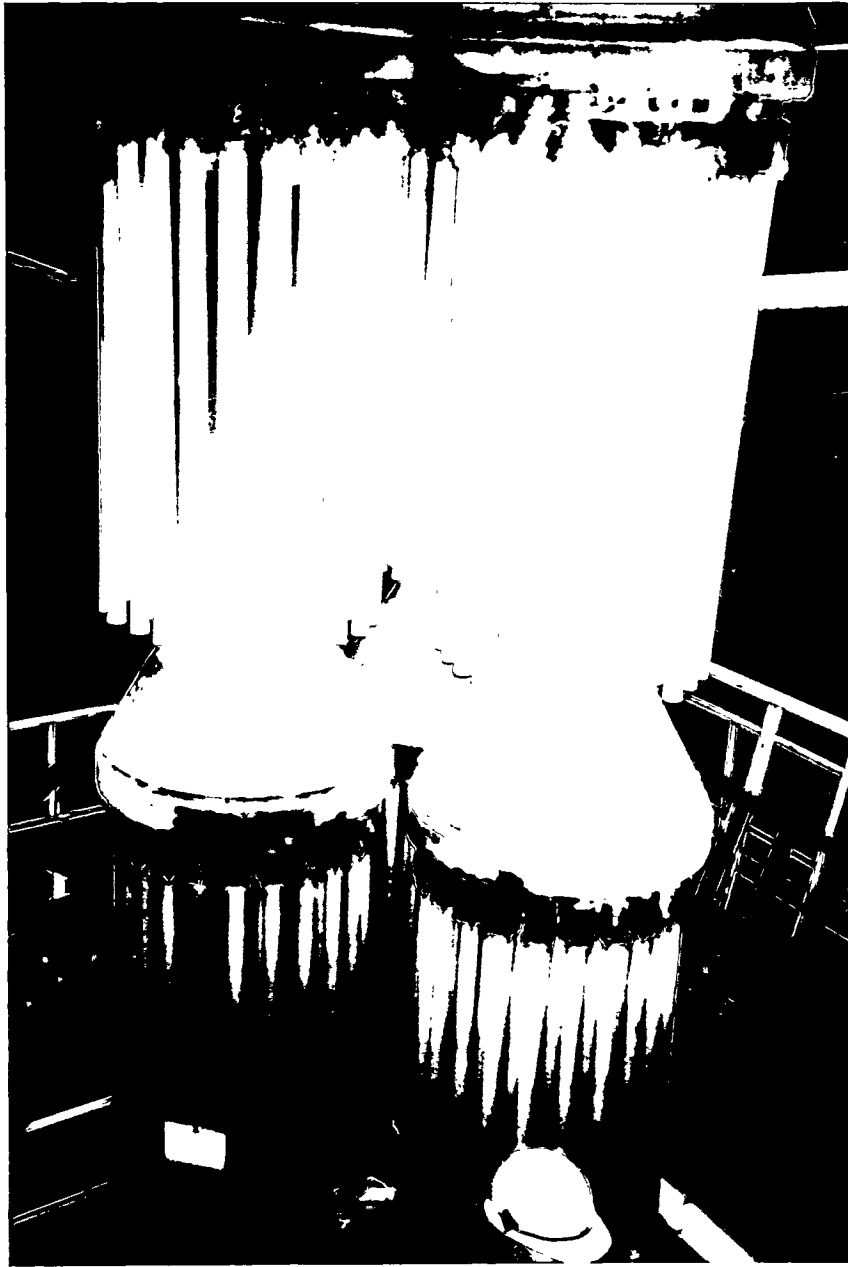


**Figure 4.3.14 - Photograph of Filter Internals Before Test Period II**

## Results

---



**Figure 4.3.15 - Photograph of Filter Internals Before Test Period II**

## Results

### 4.4 Test Period II: 6/93 - 9/93

Table 4.4 summarizes the operating conditions and observations from Test Period II.

**Table 4.4 - Summary of HGCU Operation - Test Period II**

	Operating Hours	Cumulative Hours	Operating Temp.	Pressure Drop	Inspection Observations
Run 5 & 6	77	541	<1400°F	Stable	● No filter issues
Run 7	426	967	1150°- 1350°F	Stable	● No filter issues
Run 8 & 9	80	1047	1450°F	Increasing $\Delta p$ , pulse pressure from 800 to 1000 to 1200 psig	● Patchy cleaning ● No ash bridging
Run 10	116	1163	1450°F	Slowly increasing $\Delta p$ , pulse pressure at 1200 psig	● Patchy cleaning ● No ash bridging
Run 11	596	1759	1450°F  1200°F	Increasing $\Delta p$ $\Delta p = 240$ in wg Stable $\Delta p$	● Outlet dust first detected (after 300 hours) ● Significant ash bridging, failed candles

#### 4.4.1 Test Runs 5 and 6 - 6/30 to 7/5/93

The unit was operated for 60 hours on coal fire during Run 5, and 17 hours during Run 6. While burning Pittsburgh No. 8 coal and Plum Run Greenfield dolomite, the unit achieved a maximum load during Run 5 of 53 MW and 116-inch bed level resulting in an APF gas temperature of approximately 1400F. The APF differential pressures remained stable during these runs and reached a maximum of 90 inches at 1400F gas temperature.

#### 4.4.2 Test Run 7 - 7/18 to 8/5/93

The unit was operated for 426 hours on coal fire burning Pittsburgh No. 8 coal and Plum Run Greenfield dolomite. PFBC performance tests were conducted at 95-inch and 80-inch bed levels and at 85%, 90%, and 95% sulfur retention. Due to problems with gas turbine vibration, the maximum unit load obtained was 46 MW at 110-inch bed level resulting in 1350F APF gas temperature.

## Results

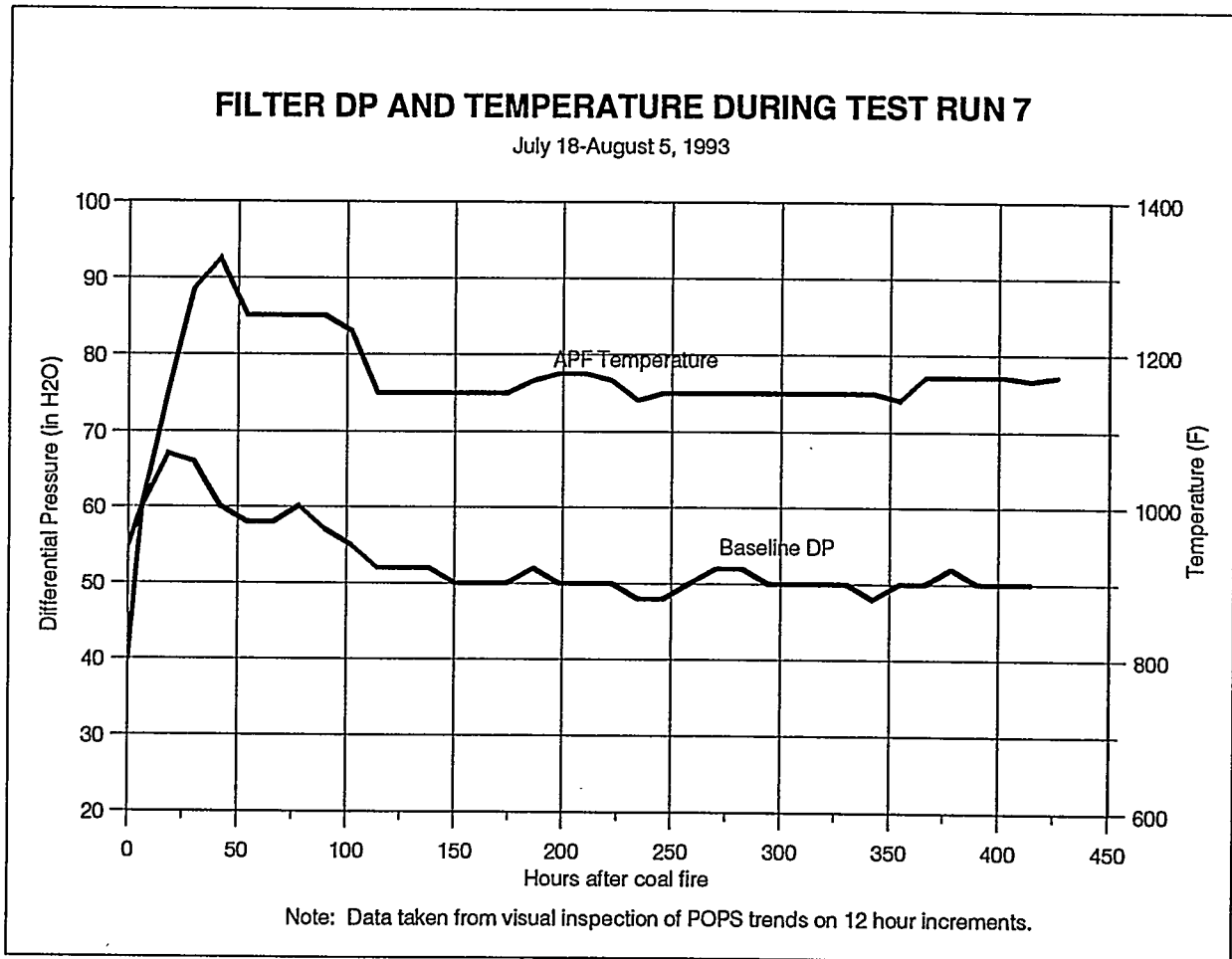


Figure 4.4.2 - Filter DP and Temperature During Test Run 7

## Results

---

Most of the operating time during this run was at 80-inch bed level and 1150F gas temperature. During these operating conditions, the APF DPs were stable at approximately 60-inches trigger and 50-inches baseline. The maximum DP obtained during this run was 105 inches during an excursion at 100-inch bed level and 1250F gas temperature. Figure 4.4.2 shows a graph of filter DP and temperature for the entire run.

The unit was shut down on 8/5 due to ash buildup in the APF hopper that was approaching levels up to the candles. Following shutdown, an inspection revealed three to four inches of ash buildup in areas on the hopper walls. Additionally, a large amount of ash fell off the hopper walls during unit shutdown. Prior to this test series, a pneumatic vibrator was installed in the APF vessel manway and linked to the hopper liner in an effort to keep ash from accumulating on the wall of the hopper. The vibrator, however, did not prove to be effective. Therefore, it was replaced with a larger single impactor-type pneumatic vibrator following this run.

Post-test inspection revealed a small amount of ash buildup on the candles; however, there was no splotching. In general, the candles appeared to be in good shape.

### 4.4.3 Test Runs 8 and 9 - 8/9 to 8/14/93

During most of the run the unit was operated at 115-inch bed level resulting in 1400 and 1450F APF gas temperatures. The APF DPs were unstable at this load. The trigger DP increased from 90 inches on the afternoon of 8/11 to 150 inches on the morning of 8/14. On 8/12, the backpulse pressure was increased from 800 to 1000 psig. On 8/13, the pressure was increased to 1200 psig and the backpulsing time interval was increased from 30 minutes to 60 minutes. Prior to the unit trip on 8/14, the APF DP reached 150 inches trigger and 115 inches baseline.

### 4.4.4 Test Run 10 - 8/19 to 8/24/93

The unit was operated for 116 hours burning Pittsburgh No. 8 coal. The unit was started up using Plum Run Greenfield dolomite, and on 8/24 sorbent feed was switched to Delaware limestone. The unit was shut down 13 hours later due to unstable bed and evaporator conditions experienced while burning limestone. Sulfur retention was maintained at 95% from start-up through the morning of 8/22 and then at 90% for the remainder of the run. The unit was operated at 115-inch bed level and 1450F APF gas temperature for most of the run. The maximum unit load was 52 MW at the conditions stated above.

## Results

---

During operation at 115-inch bed level and 1450F gas temperature, the APF DPs were somewhat unstable; however, not as severe as in Run 9. The trigger DP increased from 95 inches on 8/21 to 115-inches on 8/24, while backpulsing at 1200 psig. When sorbent feed was switched over to Delaware limestone, the baseline DP increased from 90 to 100 inches over a four-hour period while the trigger DP remained fairly constant.

Post-test inspection revealed splotchy areas of ash buildup on the candles. The candles were backpulsed during unit shutdown with little success in removing the ash buildup. The APF hopper walls also had areas of ash buildup.

### 4.4.5 Test Run 11 - 8/29 to 9/23/93

The unit was operated for 596 hours burning Pittsburgh No. 8 coal. The maximum unit load achieved during this run was 55 MW at 125-inch bed level, resulting in an APF gas temperature of 1500F. During start up while increasing load to 115-inch bed level and 1450F gas temperature, sorbent fines (Plum Run Greenfield dolomite, 100% less than 75 microns) were added to the coal water paste while reducing the pneumatic sorbent feed rate by approximately 50%. During this time period the APF DPs started to increase at a rate greater than had been experienced during previous load increases. While at temperatures over 1400F, the APF trigger DP increased from 100 to 168 inches over a period of two days. The baseline DP increased from 84 to 154 inches during this same time period. It is unknown whether this increase in DPs was due to the sorbent fines or whether it was a more aggressive deterioration of APF performance (due to some other phenomenon) than what had been experienced previously at temperatures above 1400F.

On 9/9, the APF trigger DP reached 250 inches, at which time it was decided to reduce unit load to 50-inch bed level, 1000F gas temperature to backpulse the APF. The APF DP was reduced to 145 inches by load reduction and dropped to 36 inches after minimum load backpulsing. However after unit load was brought back to 115-inch bed level, 1450F gas temperature, the APF trigger DP reached a level of 250 inches in less than two days. Load was reduced to 80-inch bed level, 1200F gas temperature to maintain DPs within acceptable limits.

On 9/12 and again on 9/13, indications of candle breaks were noticed by a sudden decrease in APF DP (by approximately 10 in. H<sub>2</sub>O) and a sudden increase in individual plenum gas flow which occurred simultaneously while backpulsing. Later on 9/13, fragments of broken candles were recovered from the

## Results

---

ash removal system. The total fragments recovered could not positively account for more than one candle. Figure 4.4.5 shows a graph of filter pressure drop and temperature for the entire run. On 9/17 the spoiling air to the primary cyclone was turned on to test the system. No problems arose during the initial operation of the system. On 9/21, the unit load was increased to 116-inch bed level and the spoiling air was put into service. The unit was removed from service on 9/23 due to a leak in the sorbent transport pipe caused by erosion. The effects of detuning were inconclusive due to the condition of the filter at the time it was used.

## Results

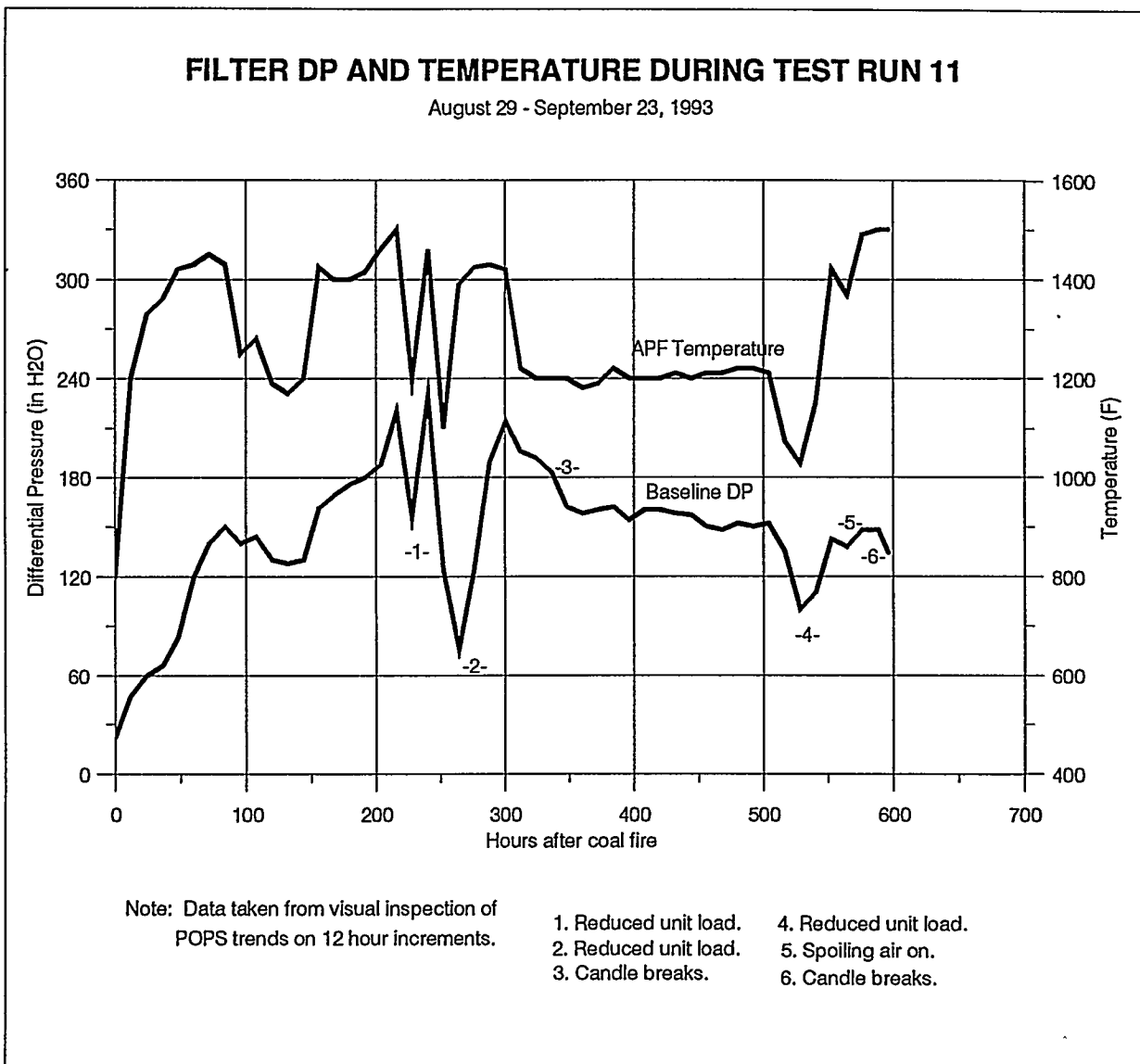


Figure 4.4.5 - Filter DP and Temperature During Test Run 11

## Results

### 4.4.6 Posttest Inspection and Modifications (9/93-1/94)

The APF internals were inspected through instrument nozzles and the manway nozzle on 9/27 and 9/28. During this inspection approximately 24 candles were observed to be broken. The ash hopper was filled with ash and broken candles to a level approximately 6 to 12 inches above the manway nozzle.

On 9/30, the APF internals were removed from the APF. Upon inspection, 62 candles were found to be broken. Approximately three candles were broken during removal from the APF vessel. The following table shows a summary of the location of the broken candles.

Location of Broken Candles  
September 1993

	Plenum A	Plenum B	Plenum C
Top	3	1	2
Middle	6	24	5
Bottom	0	1	20

Very heavy ash bridging was apparent between candles and between candles and support pipes. Figures 4.4.6 through 4.4.11 are photographs of the filter internals following Test Period II. The deposits were very hard and difficult to break into smaller pieces. Many candles were also found to be bowed. During subsequent cleaning of the ash deposits from the candles, approximately 40 more candles broke.

Two surveillance candles were recovered by Westinghouse and tested for remaining hot strength. One candle from the original set, which had been exposed to operating conditions for 1,759 hours, exhibited a 37 percent loss of its original strength. The second candle, which had been installed in December 1992 and had experienced 1,295 hours of operation, had lost 51 percent of its strength.

All filter candles were replaced with new silicon carbide candles between Test Series II and III, except for nine surveillance candles which were reused.

The backpulse solenoid valves exhibited random failures to actuate during these tests. In all cases, the backup valve functioned properly. Following Test Period II, the backpulse solenoid valves were

## Results

---

inspected and found to be galled on both the piston and cylinder walls. The valve pistons were stellite coated and the valve body bores were nickel-boron plated to improve resistance to galling. Following these modifications, the valves successfully underwent accelerated cycle testing to verify the design. Operation of the valves during Test Period III was much improved, and subsequent inspections revealed no galling.

At the end of Test Period II, one backpulse tube was cut up and examined for degradation. Microcracking was evident on the inside surface of the tube, with cracks as deep as 0.020". Based on this observation it was decided to replace the Incoloy 800HT material with Haynes 230 alloy, which has better resistance to thermal fatigue. The new backpulse tubes were fabricated and installed prior to the start of Test Period III. (As discussed in Section 4.6.8, two of the Haynes 230 backpulse tubes also cracked later in the test program.)

Between Test Series II and III, nine additional air purge nozzles were installed on the APF hopper to facilitate the removal of ash accumulation in the hopper. The hopper vibrator was moved from inside the APF nozzle to outside the nozzle because it proved to be unreliable inside the nozzle. It was mechanically linked to the hopper liner.

In an effort to improve the filter performance, it was decided to detune the primary cyclone upstream of the filter during the next test series. It was believed that the resulting coarser ash would be easier to remove from the filter candles and less likely to accumulate on the hopper walls. The system used to accomplish the detuning was described in Section 4.3.5. All testing during Test Period III was conducted with the cyclone detuned.

It was noted in previous runs that the filter DP sometimes became unstable at gas temperatures over 1400F. To prevent limiting the load on the unit because of the 1400F limit, a tempering air line was installed upstream of the filter which allowed 580F process air at a slightly higher pressure to be mixed with the gas to reduce the gas temperature by as much as 150F.

## Results

---

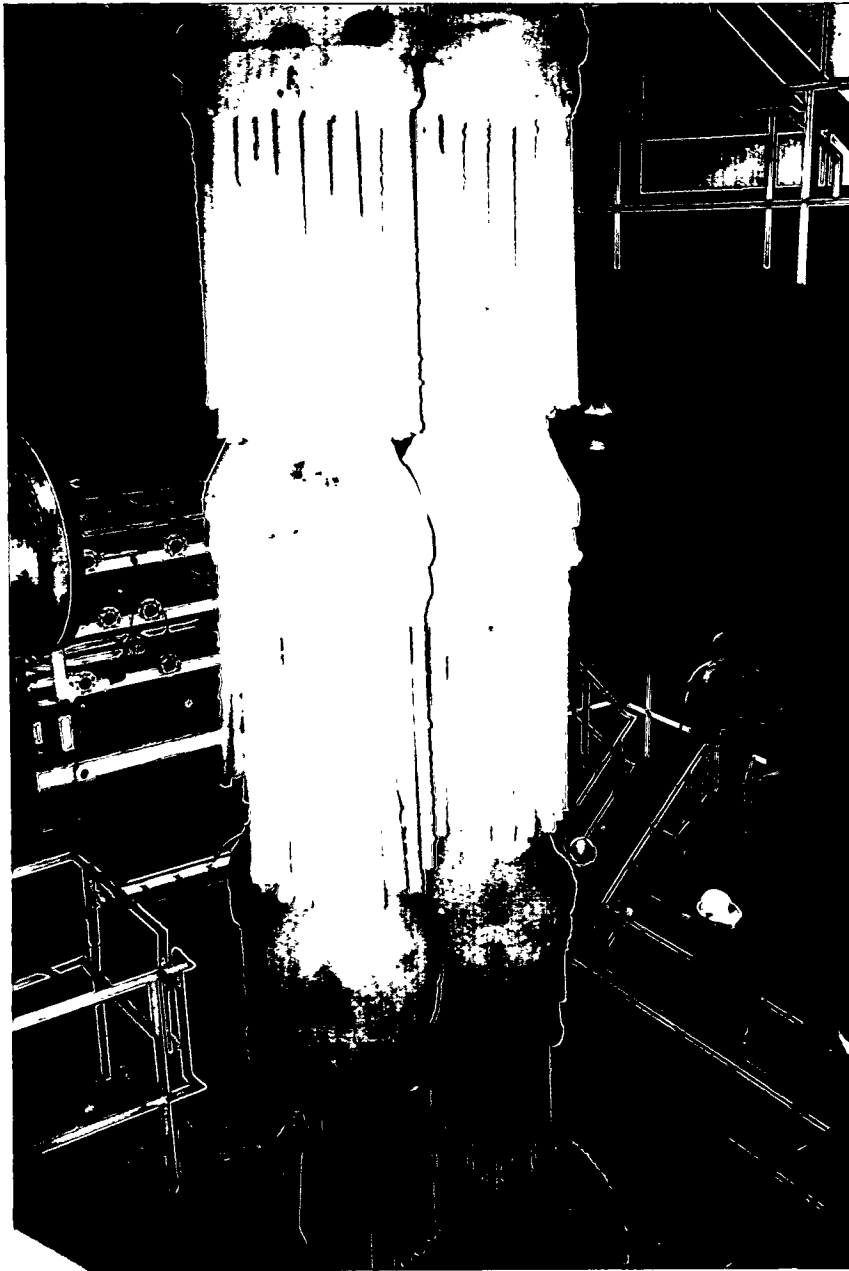


**Figure 4.4.6 - Photograph of Filter Internals Following Test Run 11**

## Results

---



**Figure 4.4.7 - Photograph of Filter Internals Following Test Run 11**

## Results

---

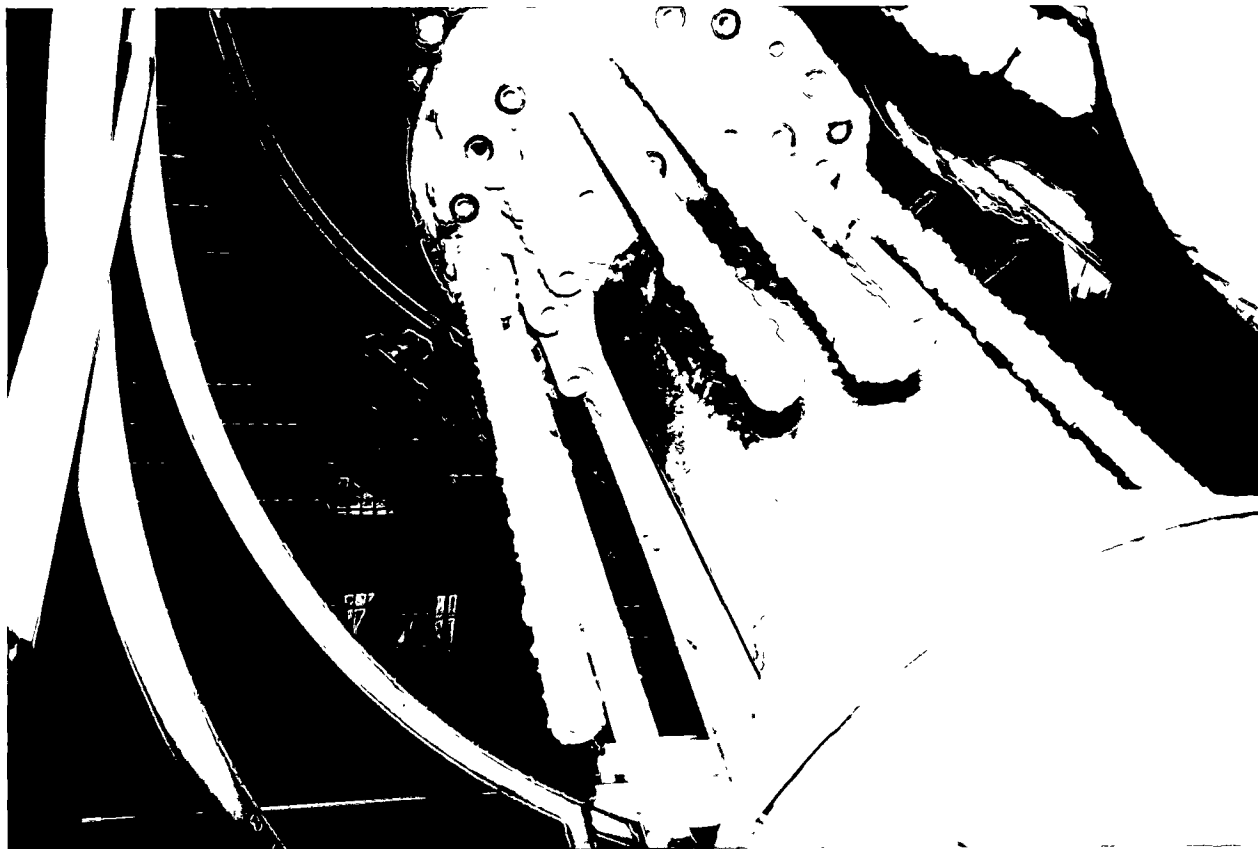


**Figure 4.4.8 - Photograph of Filter Internals Following Test Run 11**

## Results

---



**Figure 4.4.9 - Photograph of Filter Internals Following Test Run 11**

## Results

---



**Figure 4.4.10 - Photograph of Filter Internals Following Test Run 11**

## Results

---

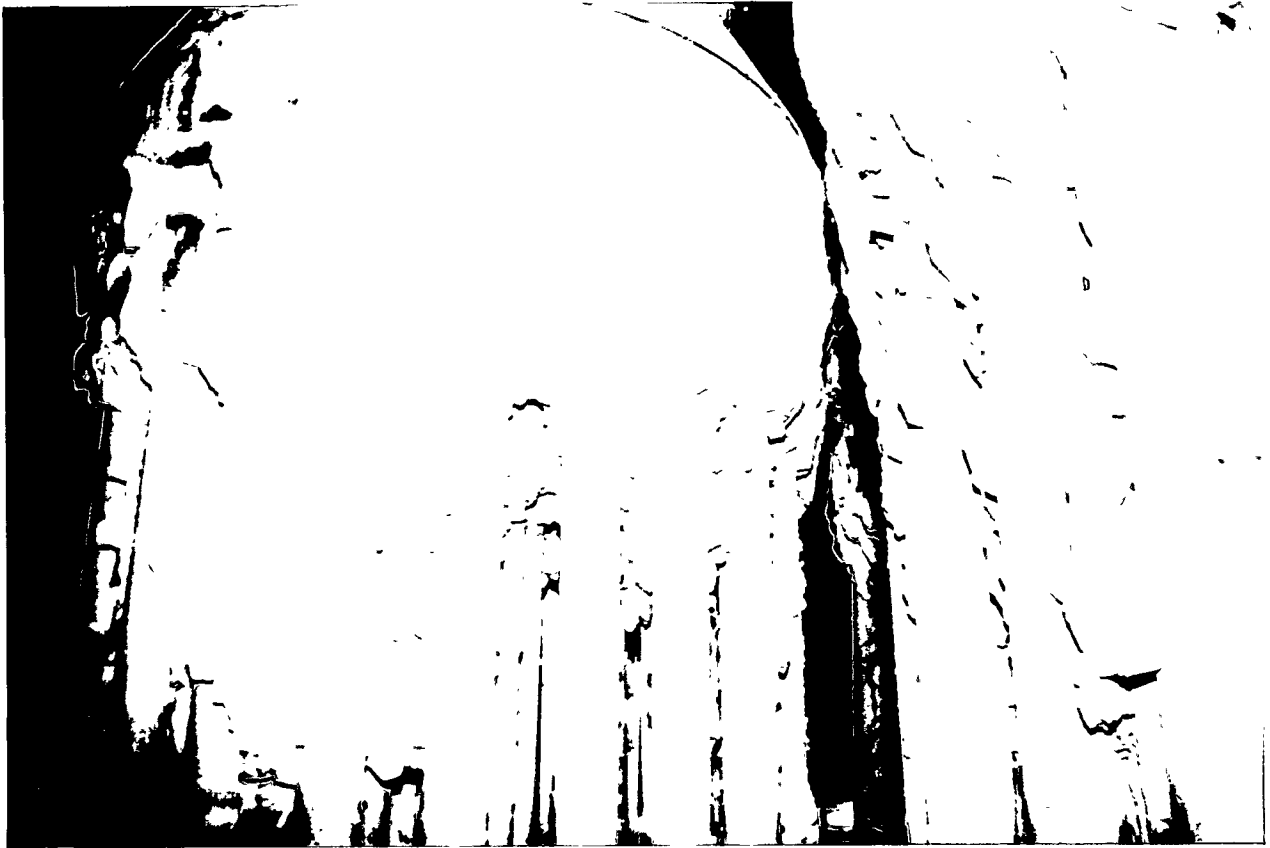


**Figure 4.4.11 - Photograph of Filter Internals Following Test Run 11**

## Results

### 4.5 Test Period III: 1/94 - 4/94

Table 4.5 summarizes the operating conditions and observations from Test Period III.

**Table 4.5 - Summary of HGCU Operation - Test Period III**

	Operating Hours	Cumulative Hours	Operating Temp.	Pressure Drop	Inspection Observations
Run 12	19	1778	1300-1400 °F	Stable	_____
Run 13	333	2111	1300-1400 °F	Stable	<ul style="list-style-type: none"> <li>● Uniform residual ash cake</li> <li>● No failures</li> <li>● Ash accumulated on dust sheds</li> </ul>
Run 14	23	2134	1200-1300 °F	Stable	_____
Run 15	151	2285	1250-1370 °F	Stable	_____
Run 16	145	2430	1350-1400 °F	Stable	_____
Run 17	164	2594	1300-1425 °F	Gas flow rate decreased during run	<ul style="list-style-type: none"> <li>● Ash cake about ¼" thick</li> <li>● No failures</li> <li>● Ash accumulation on sheds</li> </ul>
Run 18	444	3038	1350-1450 °F	Baseline $\Delta p$ increased $\approx$ 20 in. wg	<ul style="list-style-type: none"> <li>● 28 broken candles</li> <li>● Inner rows of top and middle plenums heavily bridged</li> </ul>

#### 4.5.1 Test Run 12 - 1/10 to 1/11/94

This test run was terminated after 19 hours of coal fire when several primary cyclones became plugged. Due to the brevity of this run and lack of steady state operation near design conditions, it will not be discussed further.

## Results

---

### 4.5.2 Test Run 13 - 1/15 to 1/29/94

The unit was operated for 333 hours on coal fire burning Pittsburgh No. 8 coal and Plum Run Greenfield dolomite. The primary objective of this run was to assess the performance of the APF while operating with the primary cyclone ahead of the filter detuned to produce a coarser ash and higher ash loading. The tempering air system was commissioned during this run and functioned without any problems.

During the run ash sampling was performed upstream and downstream of the APF using specially designed sampling probes. The results showed that by detuning the primary cyclone, the ash loading to the filter increased from a design value of 600 ppmw to about 3400 ppmw, and the mass mean particle size of the ash increased from about 3 to 7 microns. The higher ash concentration resulted in significantly higher ash loading. Despite the higher ash loading, the filter performed very well.

Figure 4.5.2 shows a graph of filter pressure drop and temperature for Run 13. The unit load was reduced at about 200 and 250 hours into the run due to bed sintering problems, which accounts for the dips in temperature and DP during these periods. During the remaining periods of this run, the filter pressure drop remained stable and exhibited the usual trend of following gas temperature. During the last 50 to 75 hours of the run, the unit bed height was increased to the maximum (142 inches), and the filter DP increased somewhat due to higher gas flow and dust loading.

Following shutdown of the unit, the filter was inspected via nine 3-in. nozzles on the side of the vessel. In general the candles looked in good condition with very little residual ash accumulation. However, some ash bridging was seen between the bottoms of the inner rows of candles and the dust sheds on the plenum support pipes.

### 4.5.3 Test Run 14 - 2/17 to 2/18/94

This test run was terminated after 23 hours of coal fire when a 1" nipple on the HGCU piping developed a leak that could not be repaired in service. Although the nipple was made from Hastelloy C-276 material, it experienced corrosion because it was used for gas sampling which exposed it to flowing flue gas and it operated below the acid dew point. The nipple was replaced with thicker wall Hastelloy C-22 material and was heat traced and insulated in subsequent operation. Following these modifications, no further problems were encountered with the nipple.

## Results

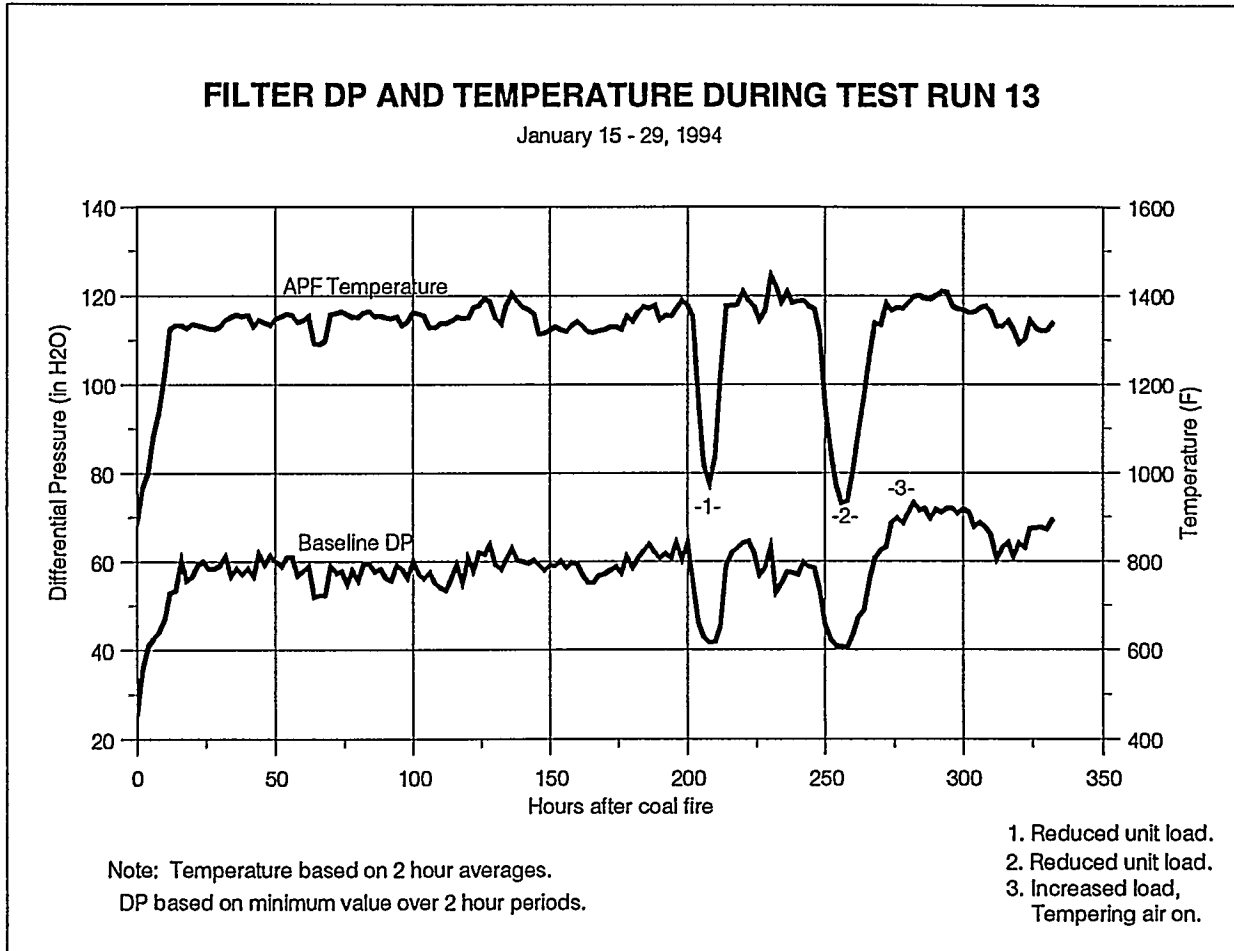


Figure 4.5.2 - Filter DP and Temperature During Test Run 13

# Results

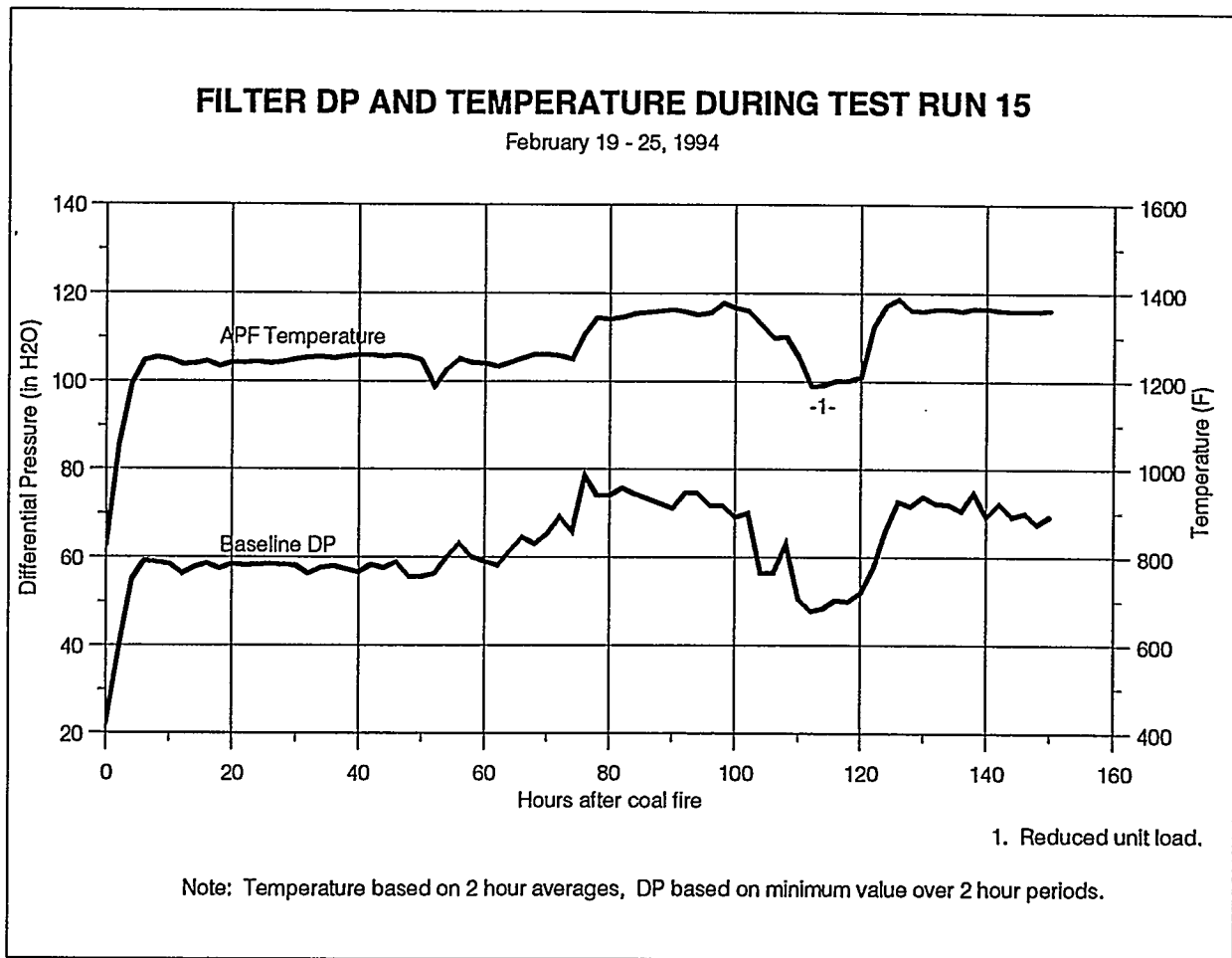


Figure 4.5.4 - Filter DP and Temperature During Test Run 15

## Results

---

### 4.5.4 Test Run 15 - 2/19 to 2/25/94

This run was a hot restart of the previous run. The APF performed without any major problems during this run. Some minor problems, however, arose. Shortly after start-up, the APF head exhibited elevated temperatures (up to 730F) near the gas outlet nozzle. The gas temperature was held to the 1250F range in order to keep the hot areas below 750F. On 2/21 an on-line repair was successfully made which reduced the hot areas to below 300F in some areas and to below 400F in others. The repair involved drilling and tapping three 1/4" holes in the outlet nozzle near the head and pumping in 45 gallons of pumpable insulation. Following this repair, the unit was brought up to full bed height (142 inches).

Tempering air was again used to limit the gas temperature in the APF to 1400F. Figure 4.5.4 shows a graph of APF DP and temperature versus time for this run. The unit load was reduced about 110 hours into the run when a coal paste pump stopped working. After the bed again stabilized, the unit was returned to full load. The HGCU system functioned without further problems from this point until the unit tripped due to loss of the sorbent booster compressor.

### 4.5.5 Test Run 16 - 3/3 to 3/9/94

Most of this test run was conducted at 142 and 150-inch bed levels. As in the previous run, tempering air was used to limit the filter gas temperature to 1400F. This run was the smoothest so far the HGCU system. The system operated for over 145 hours without any major problems. Figure 4.5.5 shows a plot of APF DP and temperature during Run 16. Figure 4.5.6 shows DP and flowrate. The APF DP exhibited a gradual decline throughout this run. The reason for this is unknown. The test conditions throughout Run 16 were the most steady of all the runs. Therefore, data from this run should be considered a good baseline reference for APF operation at 1400F. This run was terminated when the unit tripped due to the loss of two coal paste pumps.

### 4.5.6 Test Run 17 - 3/16 to 3/23/94

This was another relatively uneventful run on the HGCU system. The unit operated for approximately 164 hours on coal fire. Most of the run was conducted at 128-inch bed level, with portions at 142-inch and 115-inch. Due to bed sintering problems, the bed level could not be maintained at 142 inches. The tempering air was turned off during this run which allowed the APF to operate up to 1450F. The filter pressure differential was relatively stable throughout the run as shown in Figures 4.5.7 and 4.5.8.

## Results

---

However, the gas flowrate through the filter decreased throughout the run. During this run additional insulation was pumped into the APF head to lower the surface temperature in one area from 550F to 400F. The unit tripped due to a low oil pressure indication on the gas turbine.

The APF internals were inspected through the nine instrument nozzles following Test Run 17. No broken candles were observed. The residual ash layer on the candles was somewhat thicker than seen following Test Run 13 and appeared to be about 1/8" to 1/4" thick. The ash coating was uniform from candle to candle but also very rough looking on all the candles. The ash bridging previously seen between the dust sheds and the inner rows of candles was still evident, but not obviously worse than before. The amount of ash accumulation on the dust sheds varied considerably (1/2" to 4") among the six dust sheds. No candle-to-candle bridging was seen.

### 4.5.7 Test Run 18 - 3/31 to 4/18/94

This was the longest run of this test period with almost 444 hours of coal fire. The bed height during most of the run was 115 inches and the APF temperature was generally in the 1350 to 1400F range. The temperature was approximately 1450F for about 30 hours of the run. Due to a corroded instrument tube, flowrate data were not obtained during this run. Hazardous air pollutant sampling was conducted during this run. No major problems arose with the APF during this test. The baseline pressure differential increased during this run from about 70 to 90 inches as shown in Figure 4.5.9. This was the first run of this test series in which the DP increased noticeably from the beginning to the end of the run.

Hazardous Air Pollutant sampling was performed by Radian Corporation during Test Run 18. The results of the testing are documented in Radian Report Number DCN 94-633-021-03, dated October, 1994. As part of Hazardous Air Pollutant testing, SO<sub>2</sub> data were obtained upstream and downstream of the APF. Preliminary results indicated that the SO<sub>2</sub> level in the gas was reduced approximately 40% by the APF. Post-test analysis of ash samples retrieved from the APF and precipitator hoppers confirmed this observation. The percent sulfation (calculated as moles of SO<sub>3</sub>/moles of CaO) of the APF hopper ash was 78.6% as compared to 50.0% for ash that did not pass through to APF sampled from the precipitator hopper.

## Results

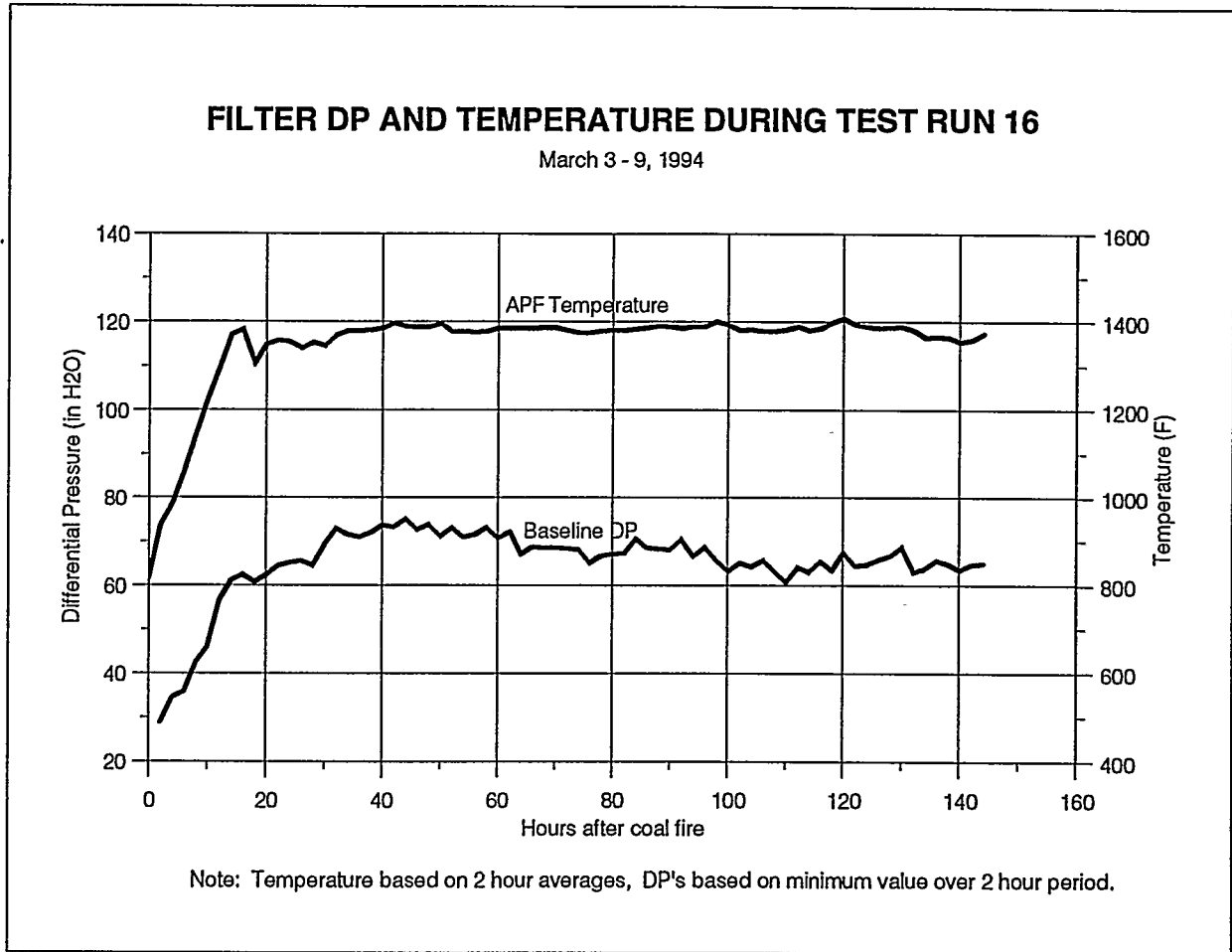


**Figure 4.5.5 - Filter DP and Temperature During Test Run 16**

## Results

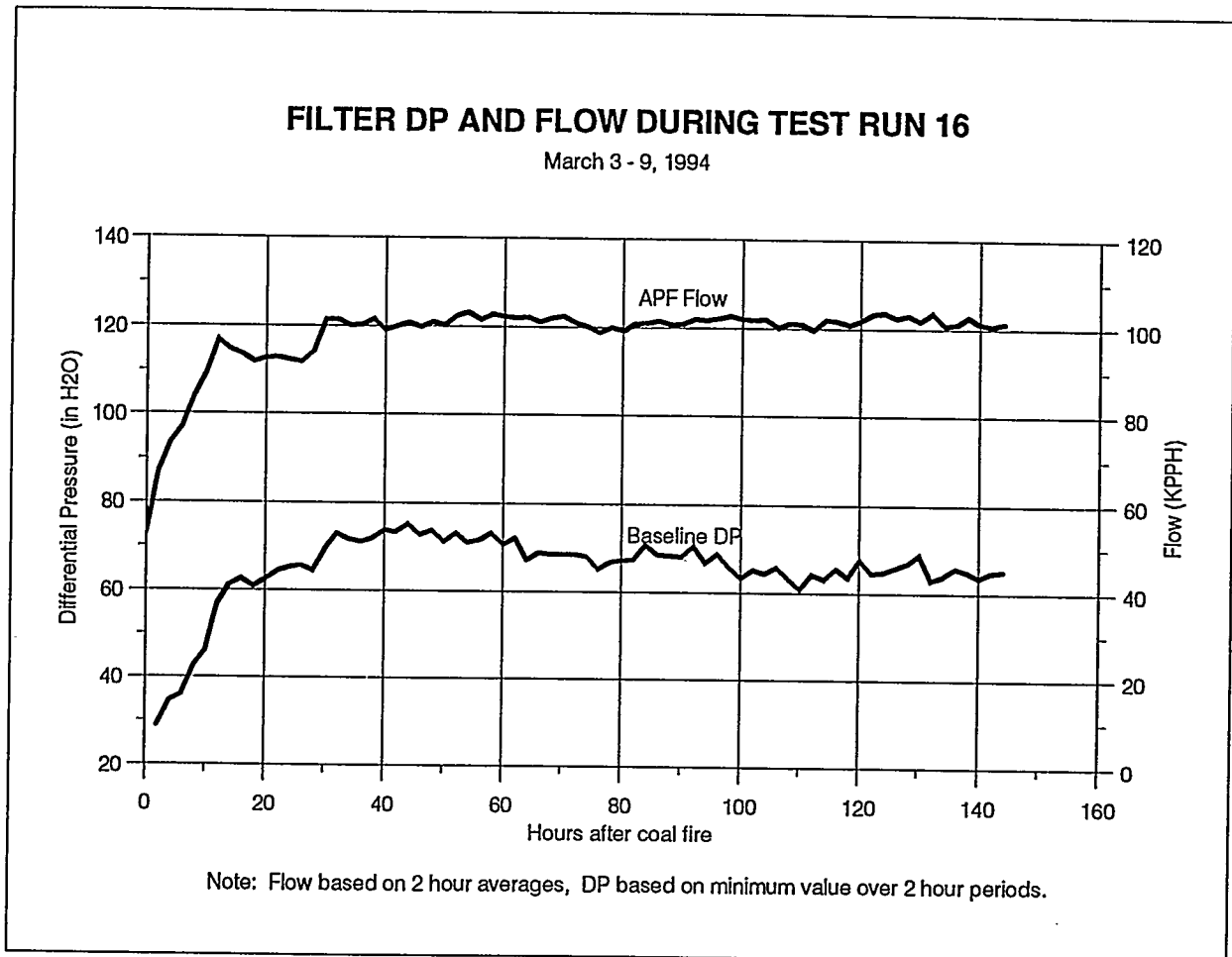


**Figure 4.5.6 - Filter DP and Flow During Test Run 16**

## Results

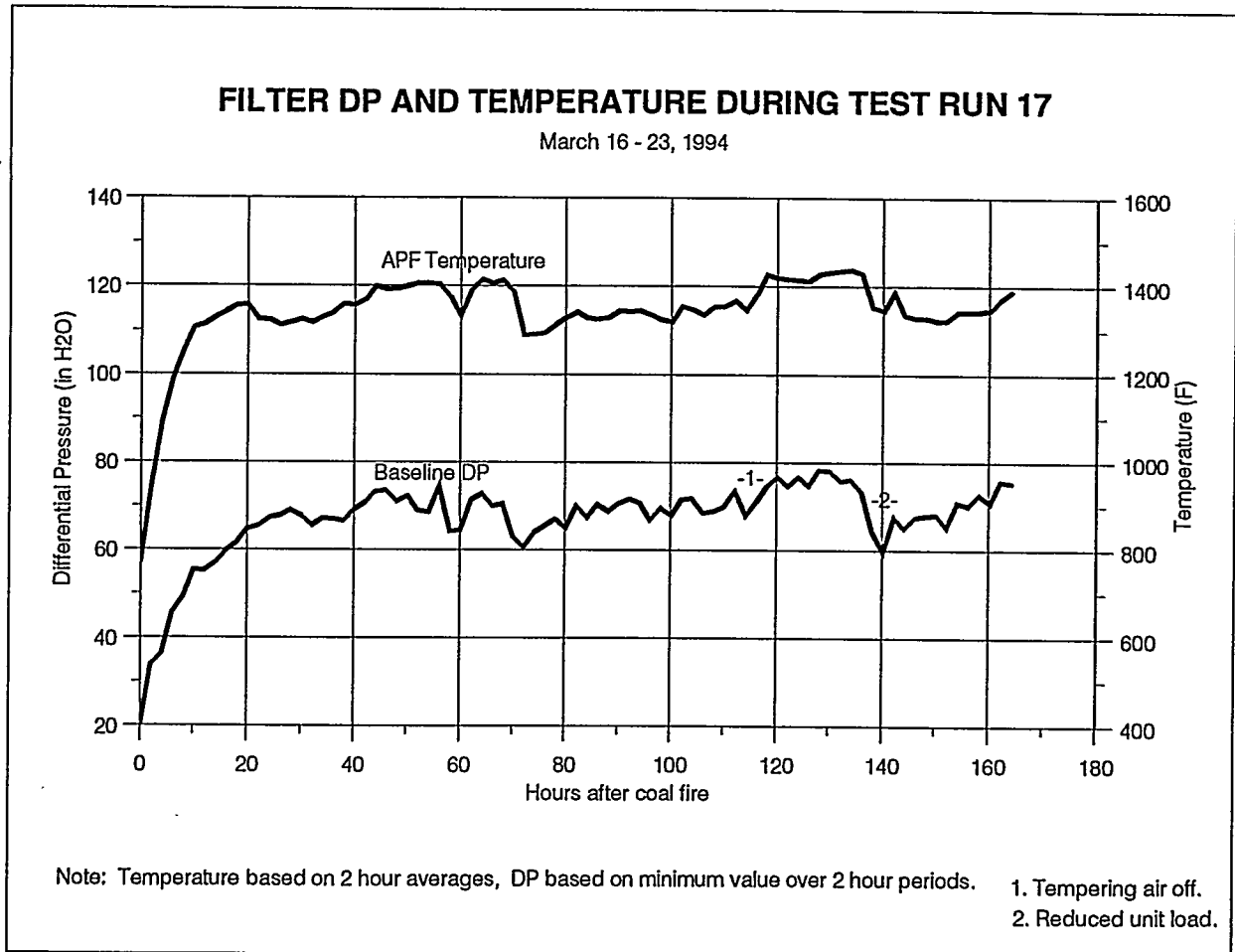


**Figure 4.5.7 - Filter DP and Temperature During Test Run 17**

# Results

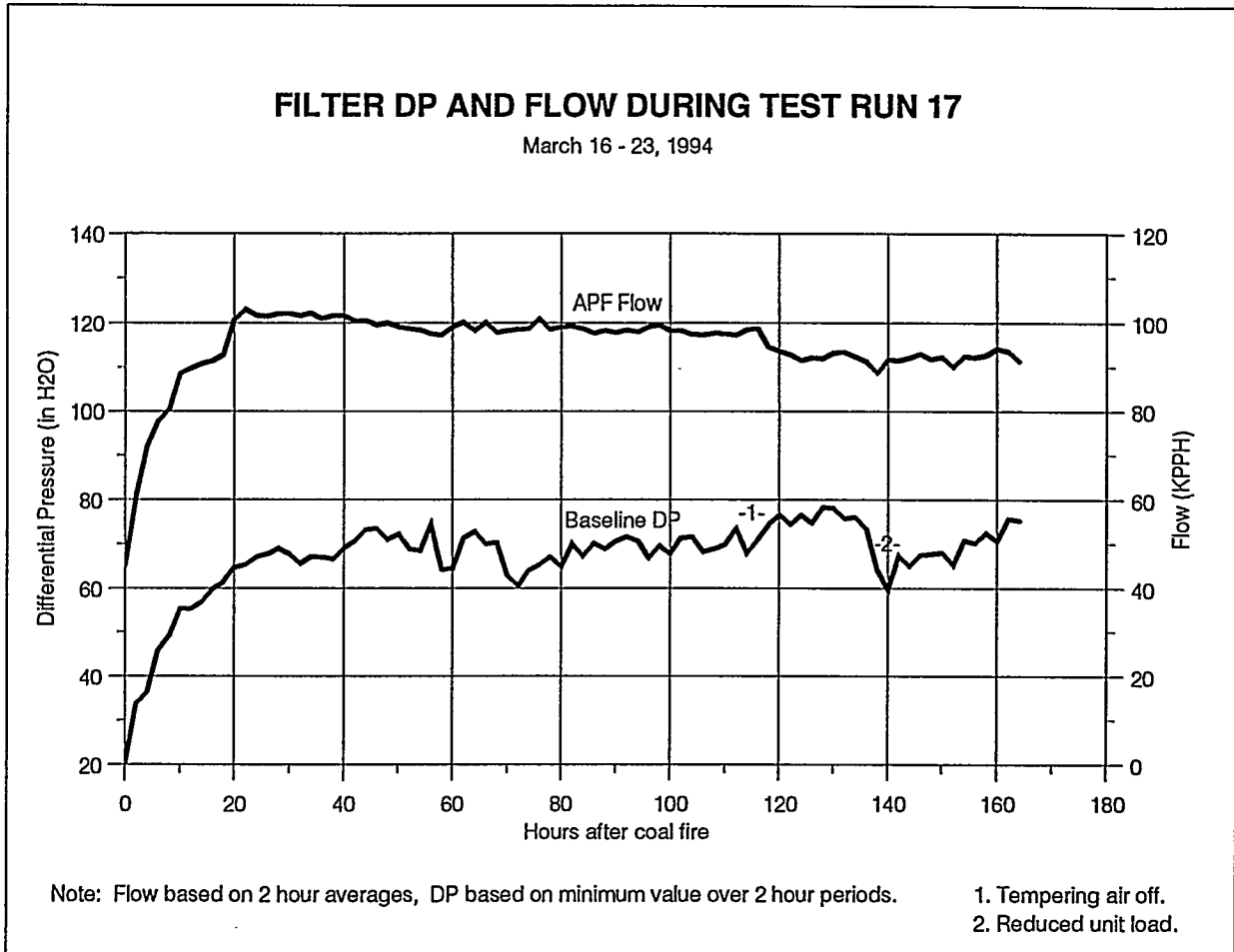


**Figure 4.5.8 - Filter DP and Flow During Test Run 17**

## Results

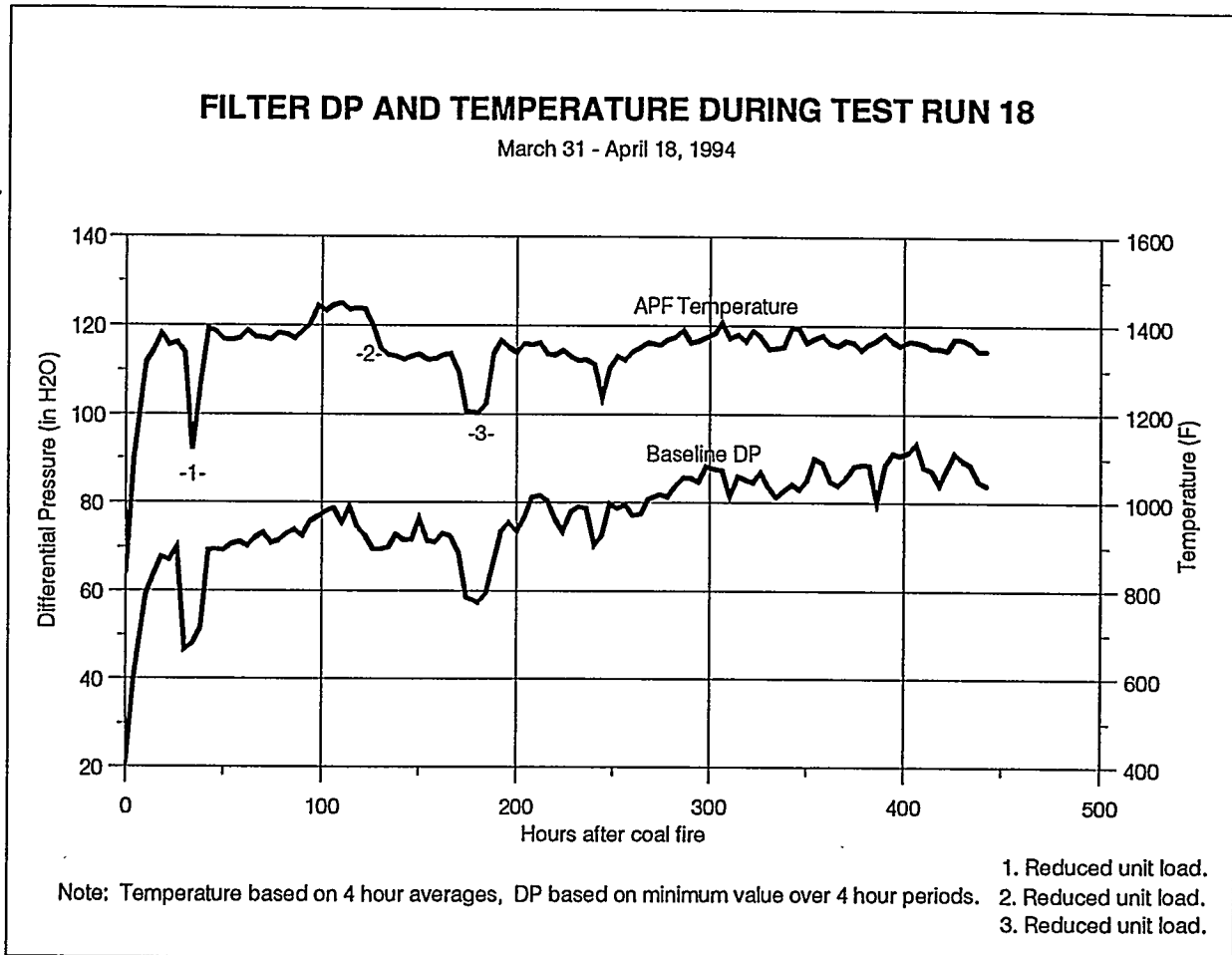


Figure 4.5.9 - Filter DP and Temperature During Test Run 18

## Results

### 4.5.8 Posttest Inspection and Modifications (4/94-7/94)

The APF internals were inspected via the instrument ports after this run. The filter candles had a thin layer (about 1/8") of residual ash, however broken candles were observed during this inspection. The filter internals were removed from the APF vessel on 5/5/94 and a more detailed inspection was performed. A total of 28 broken candles were found at the following locations:

Location of Broken Candles  
May 1994

	Plenum A	Plenum B	Plenum C
Top	7	7	2
Middle	0	2	8
Bottom	0	2	0

The two breaks in the bottom plenum are believed to have occurred during removal of the filter internals from the filter housing. Very heavy ash bridging was observed between the inner rows of candles and the support pipe on the top and middle plenums. Figures 4.5.10 through 4.5.18 are photographs of the candle clusters following Test Period III. The ash build-up extended over the entire length of the inner candles. In some cases the ash bridging extended into the outer rows of candles. Many of the inner candles were bowed outward and in some cases almost contacted the candles in the outer row. All of the candle breaks except one appeared to be fresh breaks judging from the clean fracture surfaces. All of the breaks occurred at the top of the candle just below the candle holder. The breaks appeared to result from bending forces from ash bridging from the inner candles to the outer candles. Only one break was in an inner row; the remainder were in outer rows.

The outlet side of the filter was very clean with virtually no ash deposits. This is further indication that the failures occurred during or after plant shutdown, and that the filter was not leaking ash to the clean side during operation.

All of the candles in the upper and middle plenums were removed, cleaned, and inspected. The bottom plenum candles were not removed and cleaned since they did not exhibit significant bridging. There was, however, about 1/8 in. thick ash layer remaining on these candles. The upper and middle plenums

## Results

---

were reassembled with an assortment of new and used candles. In an effort to expand the knowledge base of candle materials, 30 of the candles installed following this test series were second generation materials and included 8 Coors alumina/ mullite, 8 Schumacher FT 20 second generation clay bonded silicon carbide, 8 Pall Vitropore clay bonded silicon carbide, 3 3M silicon carbide composite, and 3 Dupont filament wound mullite structure candles.

In an effort to overcome the ash bridging problem between the support pipe and inner row of candles, it was decided to remove the inner row of candles from the six upper and middle plenums. This reduced the number of candles from 384 to 288 and increased the face velocity from 7.1 ft/min to 8.9 ft/min. In addition, provisions were added to totally spoil the primary cyclone ahead of the filter to evaluate operation with a higher mean particle size.

Figures 4.5.19 through 4.5.24 are photographs of the filter internals prior to Test Period IV.

## Results

---



**Figure 4.5.10 - Photograph of Filter Internals Following Test Run 18**

## Results

---



**Figure 4.5.11 - Photograph of Filter Internals Following Test Run 18**

## Results

---

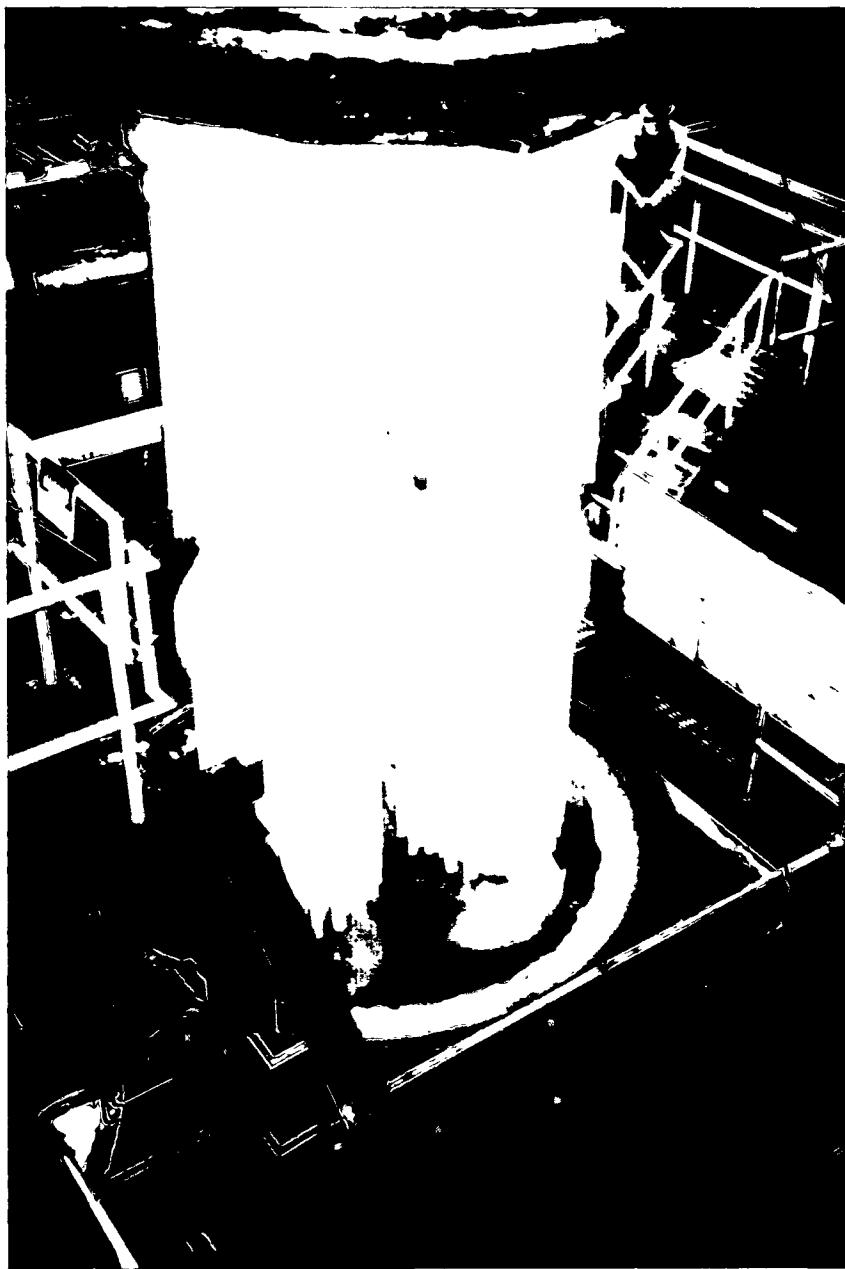


**Figure 4.5.12 - Photograph of Filter Internals Following Test Run 18**

## Results

---



**Figure 4.5.13 - Photograph of Filter Internals Following Test Run 18**

## Results

---



**Figure 4.5.14 - Photograph of Filter Internals Following Test Run 18**

## Results

---



**Figure 4.5.15 - Photograph of Filter Internals Following Test Run 18**

## Results

---



**Figure 4.5.16 - Photograph of Filter Internals Following Test Run 18**

## Results

---

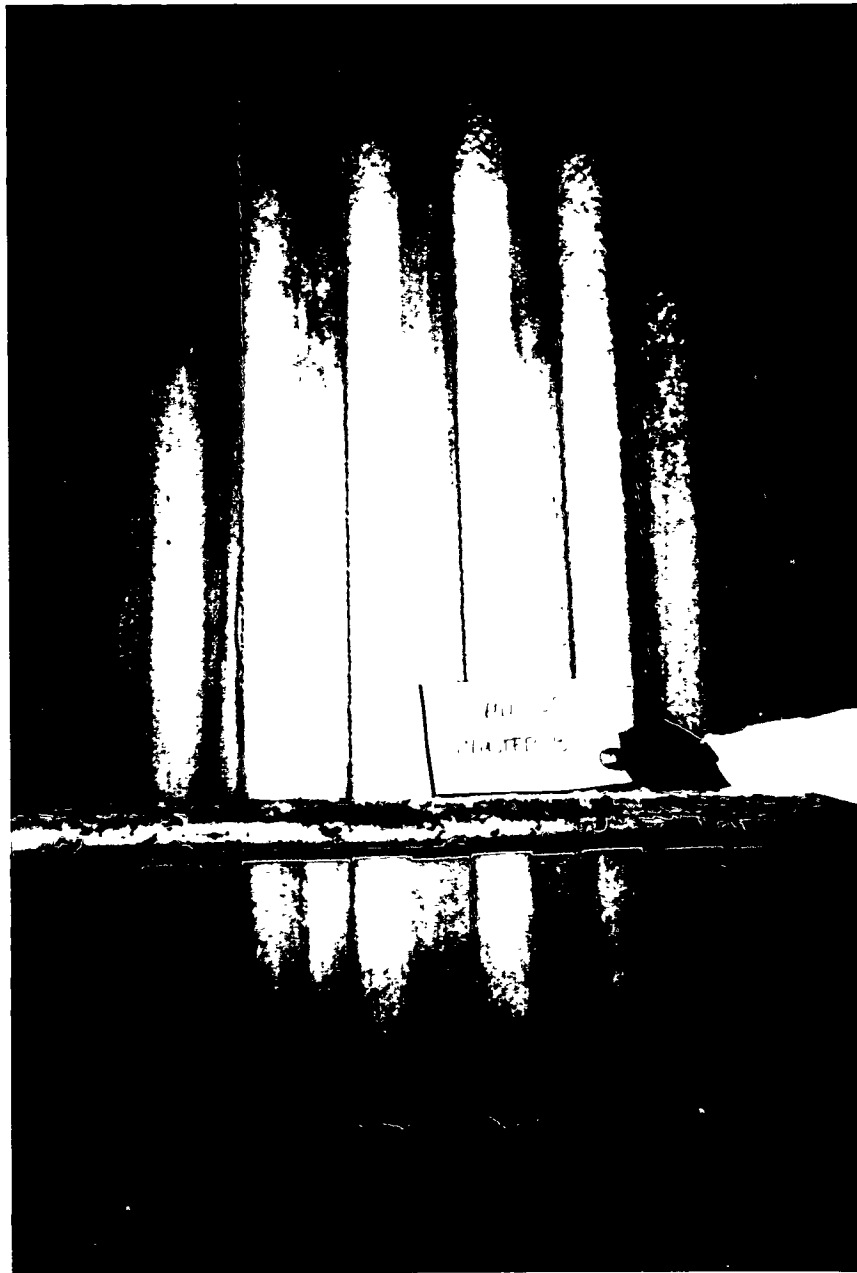


**Figure 4.5.17 - Photograph of Filter Internals Following Test Run 18**

## Results

---

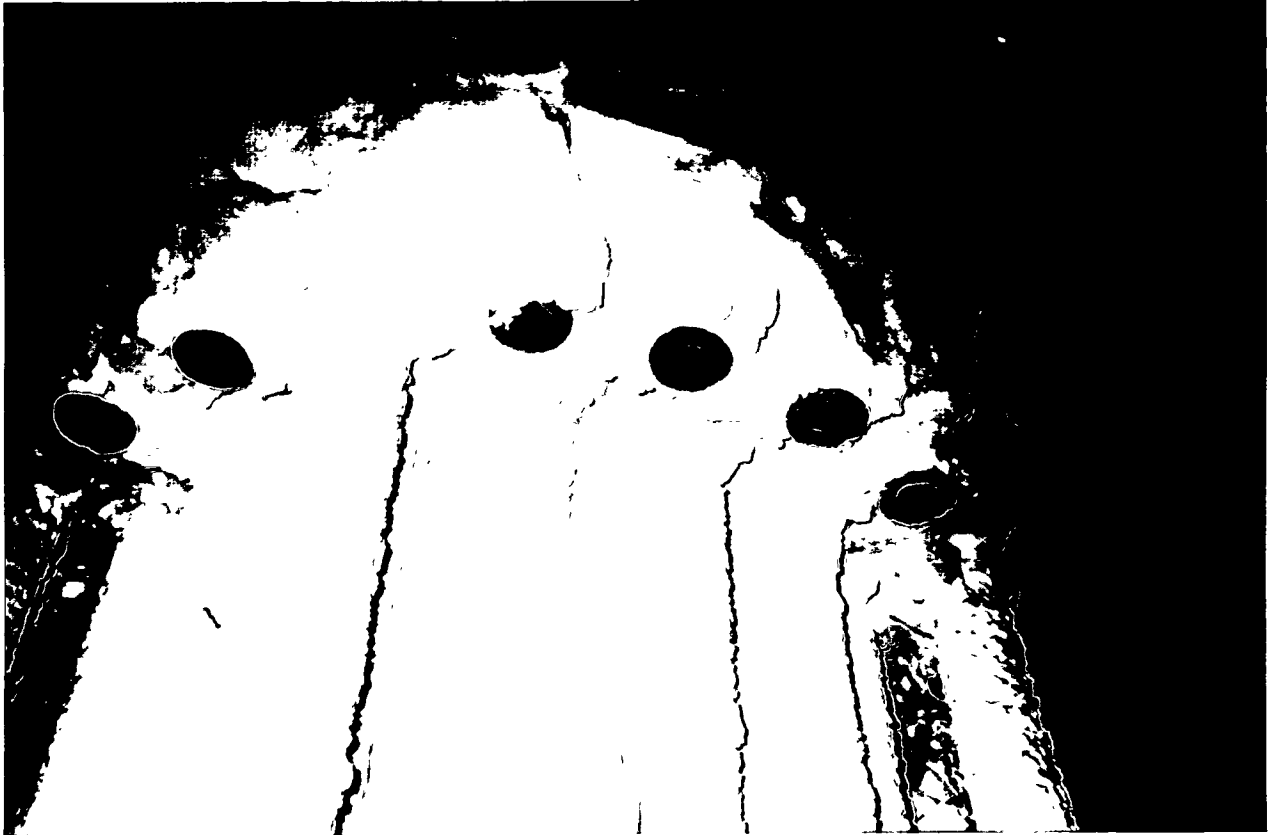


**Figure 4.5.18 - Photograph of Filter Internals Following Test Run 18**

## Results

---



**Figure 4.5.19 - Photograph of Filter Internals Before Test Period IV**

## Results

---



**Figure 4.5.20 - Photograph of Filter Internals Before Test Period IV**

## Results

---



**Figure 4.5.21 - Photograph of Filter Internals Before Test Period IV**

## Results

---

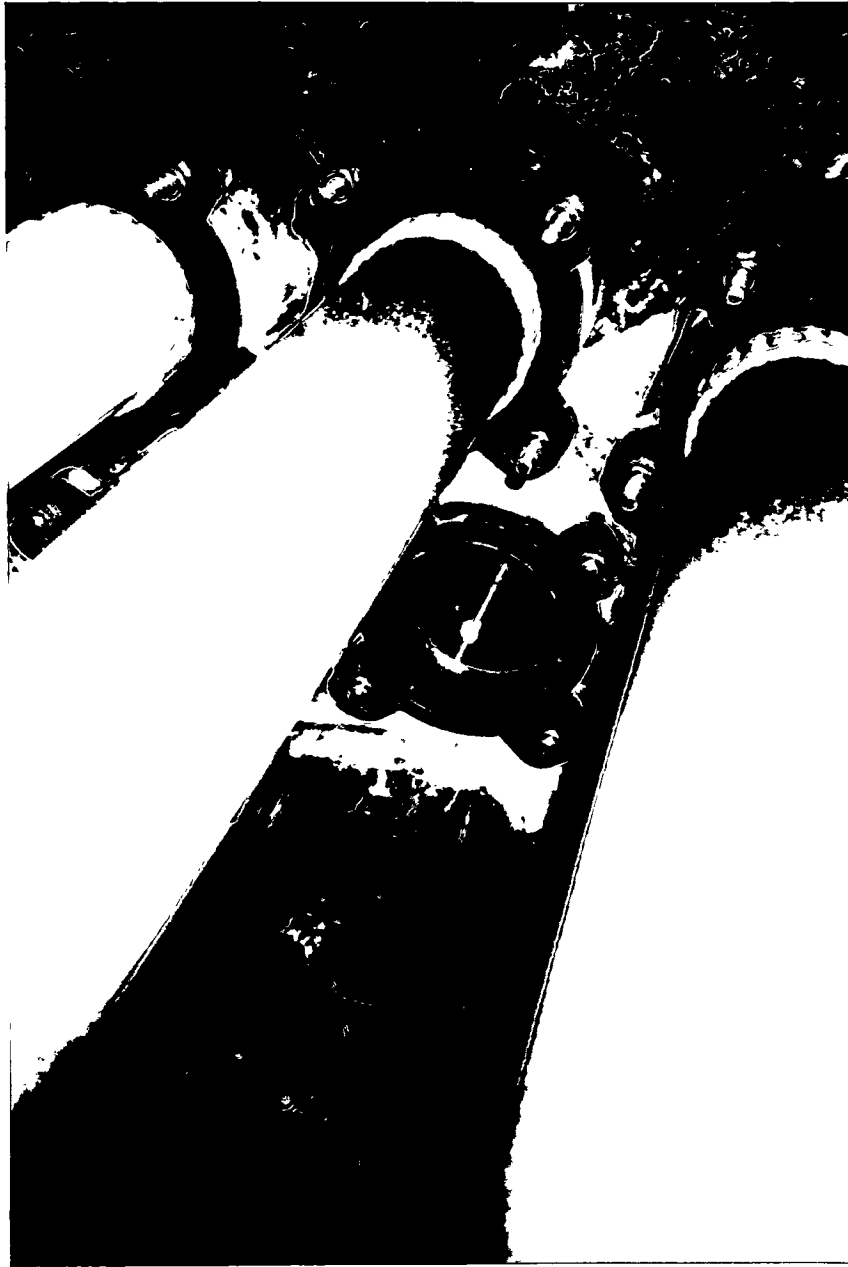


**Figure 4.5.22 - Photograph of Filter Internals Before Test Period IV**

## Results

---



**Figure 4.5.23 - Photograph of Filter Internals Before Test Period IV**

## Results

---



**Figure 4.5.24 - Photograph of Filter Internals Before Test Period IV**

## Results

### 4.6 Test Period IV: 7/94 - 10/94

Table 4.6 summarizes the operating conditions and observations from Test Period IV.

**Table 4.6 - Summary of HGCU Operation - Test Period IV**

	Operating Hours	Cumulative Hours	Operating Temp.	Pressure Drop	Inspection Observations
Run 19 & 20	3	3041	_____	_____	_____
Run 21	161	3202	1125-1150 °F	Stable	
Run 22	680	3882	1200-1400 °F	Baseline $\Delta p$ increased $\approx$ 40 in. wg	<ul style="list-style-type: none"> <li>● Bridging from dust shields</li> <li>● 14 candles broken 3 days after shutdown (not replaced)</li> </ul>
Run 23	171	4053	1170-1400 °F	Stable $\Delta p$ with cyclone spoiled	<ul style="list-style-type: none"> <li>● Ash bridging much less than at start of run</li> </ul>
Run 24	691	4744	1300-1450 °F	Baseline $\Delta p$ increased $\approx$ 60 in. wg without cyclone spoiled	<ul style="list-style-type: none"> <li>● 30 broken candles (including previous 14)</li> <li>● Some ash bridging from dust sheds</li> </ul>

#### 4.6.1 Test Runs 19 and 20 - 7/16/94

These two runs together totaled only three hours and therefore will not be discussed.

#### 4.6.2 Test Run 21 - 7/20/94 to 7/27/94

This 161-hour run was terminated to repair a vibration problem on the gas turbine. Because of the turbine limitation, the APF temperature was in the 1125-1150F range during most of this run. The APF differential pressure remained stable during the run, as shown in Figure 4.6.2.

Between Test Runs 21 and 22 a second nuclear level device was installed on the APF hopper at a higher level than the first level detector, and served as an extreme high alarm. The detector at the lower elevation was revised to produce a digital signal indicative of the ash thickness on the APF hopper wall. The signal from this detector which was trended on POPS provided early indication of ash buildup in the hopper and was useful in alerting the plant operators when to use the air purges and air cannon.

## Results

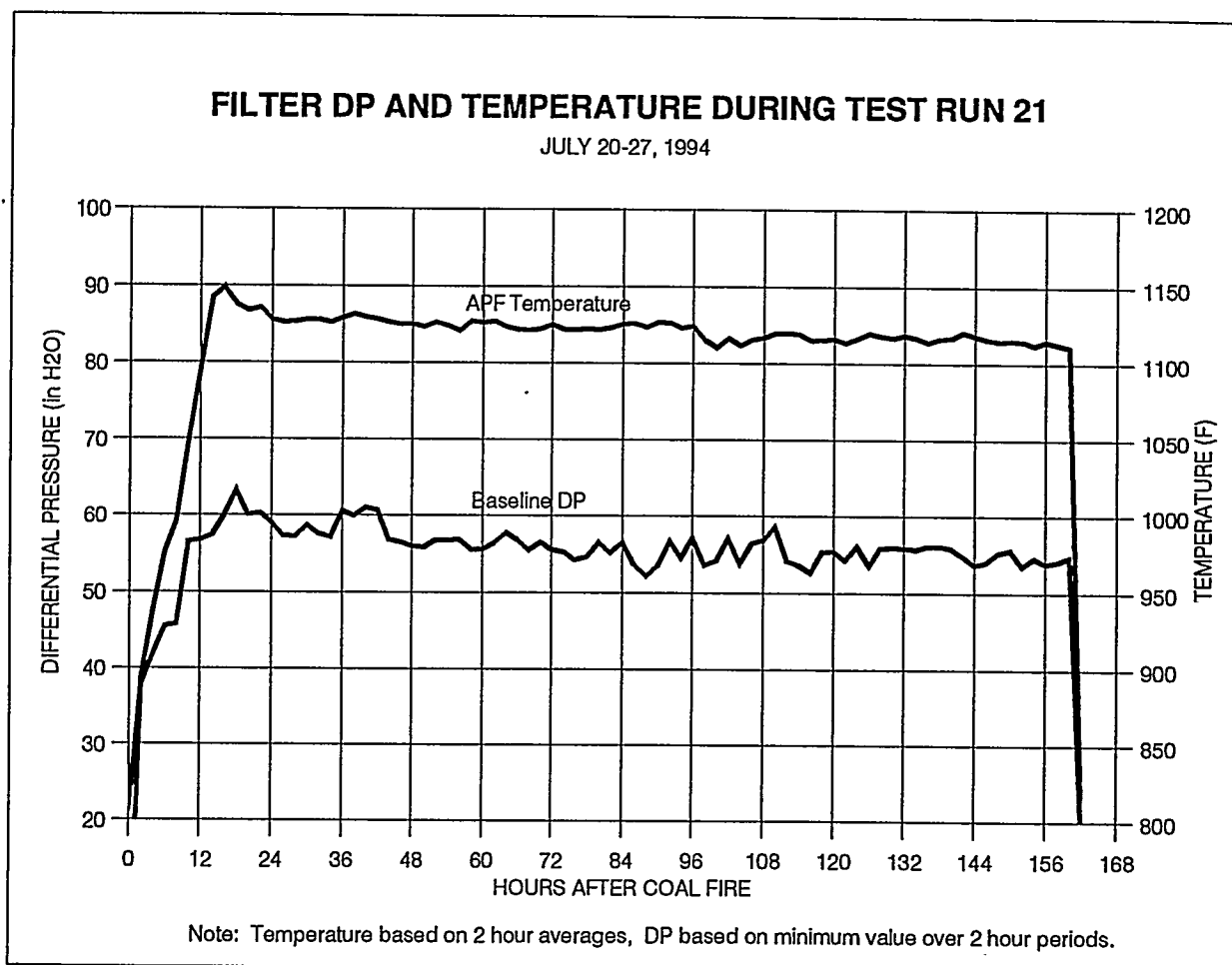


**Figure 4.6.2 - Filter DP and Temperature During Test Run 21**

## Results

### 4.6.3 Test Run 22 - 7/28/94 to 8/25/94

This was hot restart from the previous run. This was the longest run to date for the HGCU system at just under 680 hours. Unit load was reduced on 8/1 to limit hot spots on the APF head. After insulation was pumped in, the hot spots were reduced to below 500F. Several performance tests were conducted during this run using Pittsburgh #8 coal and various sorbents as shown in Figure 4.6.3 which is a plot of the APF DP, temperature, and flowrate for this run. The DP exhibited periods of instability during this run. On 8/5 the ash removal system became plugged and several candles fragments were removed from the ash line. On 8/6 hot spots again appeared on the APF head and tempering air was used to control the hot spot temperatures. On 8/9 the hot spots were pumped with insulation.

### 4.6.4 Posttest Inspection (8/94)

At the end of Run 22 the APF had logged 844 hours of operation since it was reconfigured with 288 candles. The objective of this test series was to determine if removal of the inner rows of candles from the upper and middle plenums would eliminate ash from accumulating on the ash sheds and bridging over to the candles. An inspection on 8/29 revealed that ash bridging, while less than before, had still occurred. The APF hopper was clean two days following shutdown, but when inspected again four days following shutdown, ash was found in the hopper. During the inspection with a boroscope, 14 broken filter candles were seen, and candle pieces were later removed from the hopper. A total of nine candle bottoms were recovered in the hopper. A possible explanation for the candle breakage would be that ash, bridged between the ash sheds and candles, expanded slightly during cooling and absorbed moisture from the air, thereby inducing bending moments on the candles which all failed near the top. Another possible explanation is that the metal support pipe contracted more than the ceramic candles upon cooling and thereby induced bending stresses in the candles due to ash that was wedged between the candle bottoms and sloping dust shed surfaces.

Location of Broken Candles  
August 1994

	Plenum A	Plenum B	Plenum C
Top	4	0	0
Middle	4	0	6
Bottom	0	0	0

# Results

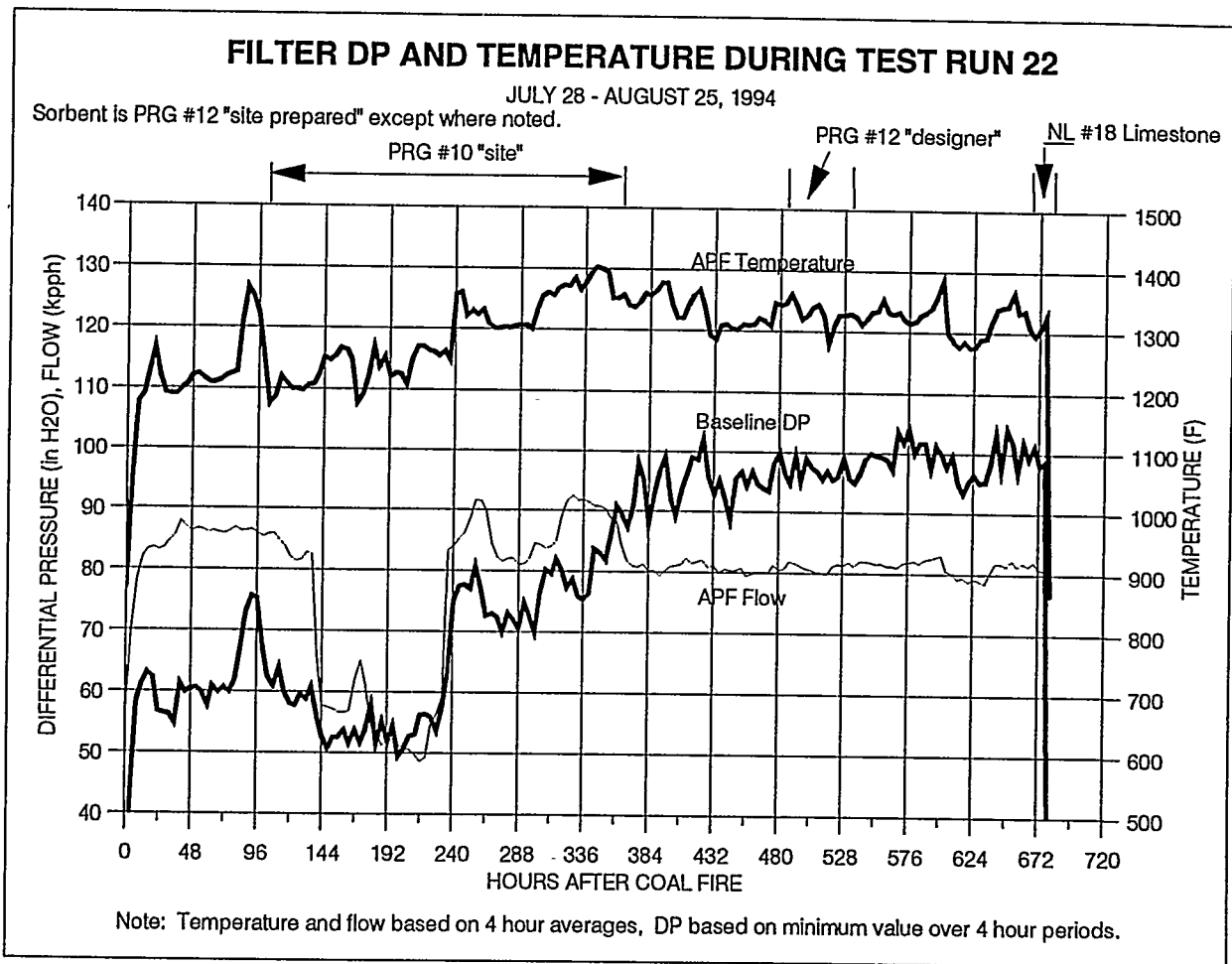


Figure 4.6.3 - Filter DP and Temperature During Test Run 22

## Results

---

It was decided to continue this test series with 14 broken candles rather than take the system out of service at this time to replace them. It was planned to replace all of the candles in the fall of 1994.

### **4.6.5 Test Run 23 - 9/3/94 to 9/10/94**

During the last 90 hours of this 171-hour run, the primary cyclone was spoiled by injecting air into the ash pickup nozzle to reduce the ash transport ability and force the ash to build up in the dip leg of the cyclone. In order to even out the ash discharge from the APF, the backpulsing sequence was changed to produce uniform cleaning. Each plenum was backpulsed every 15 minutes with backpulses occurring every 1.67 minutes. During this period the APF temperature was in the 1300F to 1400F range and the DP was stable as shown in Figure 4.6.5. Ash removal during this run was difficult since the lockhopper system could not keep up with the approximately 1700 lb/hour of ash flow. A new alternate ash removal line was successfully used to overcome this problem.

### **4.6.6 Posttest Inspection (9/94)**

The APF was inspected using a boroscope on 9/14. This inspection revealed that most of the ash bridges seen in the previous inspection had disappeared, and the few that remained appeared smaller. This indicated that the coarser ash was cleaning the ash accumulation from the ash sheds. The liner and hopper also were very clean of ash deposits. No additional broken candles were observed. The backup cyclone ash removal line was found to be eroded near the first two bends as a result of coarser ash and missing candles. A new line was designed with lower velocities and installed following this test series.

### **4.6.7 Test Run 24 - 9/22/94 to 10/21/94**

Due to the problem with the erosion of the BUC ash line, it was decided to operate the unit with the primary cyclone only partially detuned for the first three weeks of this scheduled four-week run, and the cyclone was totally spoiled during the last four days of the run. Figure 4.6.7 shows the trend of filter DP and temperature throughout this longest run of 691 hours. The DP increased significantly during the first 300 hours, increased gradually over the next 300 hours, and increased dramatically when the cyclone was spoiled due to the increased ash loading. Unit performance tests were conducted during this run at various bed levels and sulfur retention, using various sorbents as shown in Figure 4.6.7.

## Results

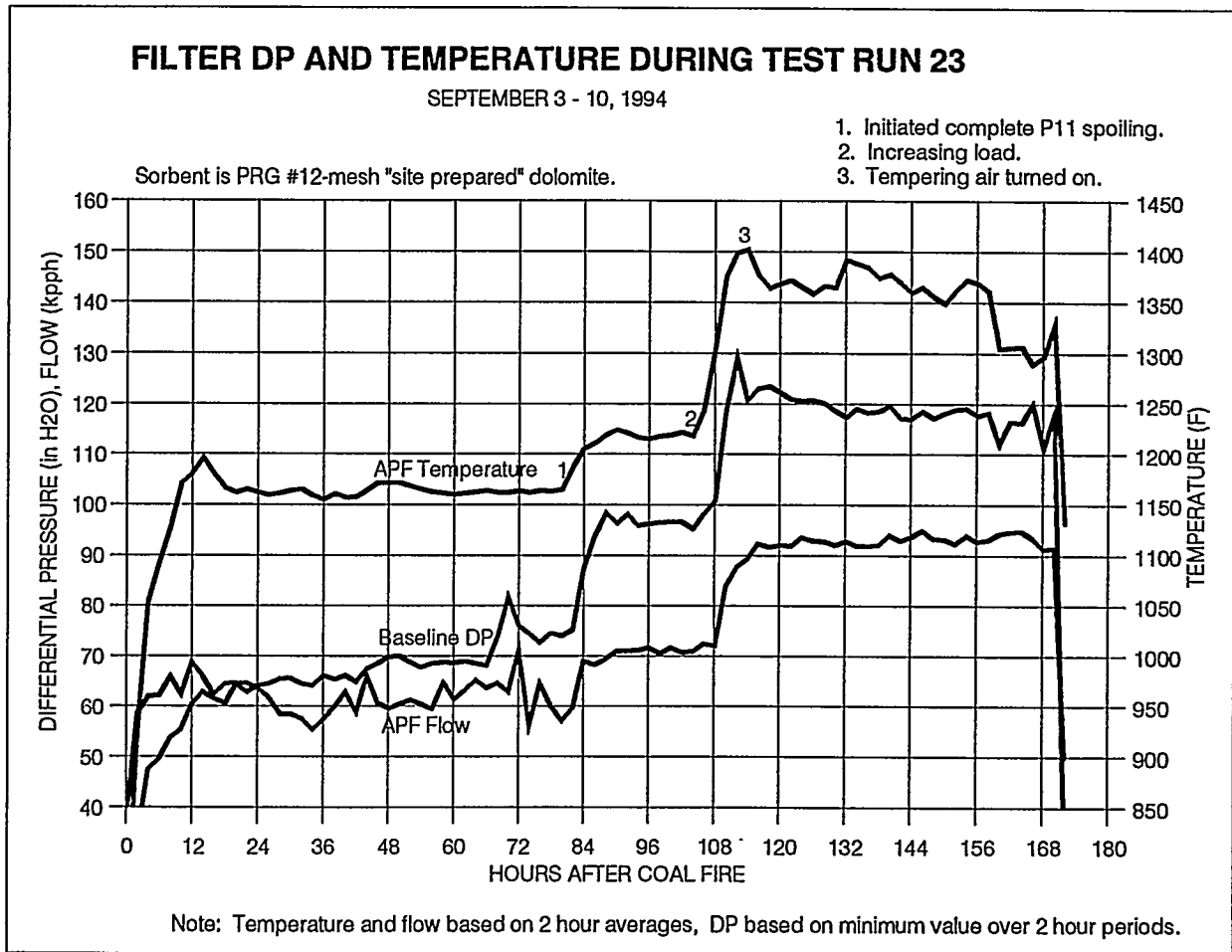


Figure 4.6.5 - Filter DP and Temperature During Test Run 23

# Results

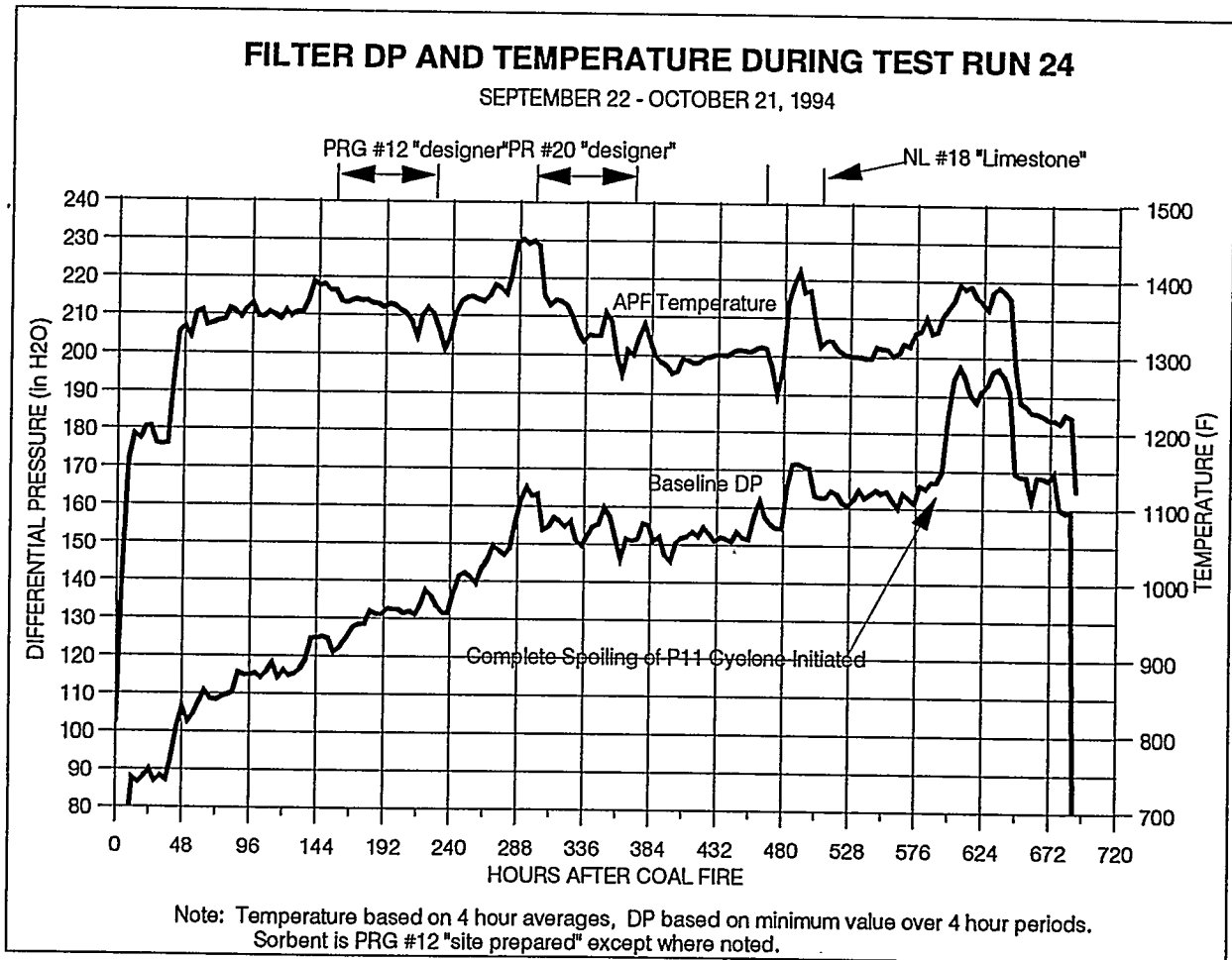


Figure 4.6.7 - Filter DP and Temperature During Test Run 24

## Results

### 4.6.8 Posttest Inspection (10/94)

On 10/27/94 the APF internals were removed from the vessel for inspection and candle replacement. A total of 30 candles were observed to be broken, as listed below.

Location of Broken Candles  
October 1994

	Plenum A	Plenum B	Plenum C
Top	6	1	7
Middle	4	2	6
Bottom	2	1	1

Ten of the 30 breaks had clean fracture surfaces indicating that the breaks occurred after shutdown or during removal from the vessel. Heavy ash bridging was apparent near the bottoms of candles in clusters B Top and B Middle, while light to moderate ash bridging was seen in clusters C Top, A Bottom, and B Bottom. Figure 4.6.8 through 4.6.16 are photos of the candle clusters following Test Period IV. It was evident that the ash accumulation that occurred during the first 600 hours of this run was not removed during the last 90 hours of operation with the cyclone spoiled.

Two of the nine backpulse tubes were found to have longitudinal cracks through the wall about 12 to 16 inches long (see Figure 4.6.17). The cracks occurred only on two of the bottom plenum tubes which were backpulsed at a higher pressure (1300 psig) than the upper and middle plenums (1000 psig). The cracks were believed to be due to thermal fatigue. All nine tubes were replaced in kind following Run 24. The tube material was Haynes Alloy 230.

All of the filter candles in the APF were replaced between Test Periods IV and V. In order to broaden the base of candle filter material testing, the filter was fitted with a combination of silicon carbide, alumina mullite, and two other second generation materials, namely, Dupont PRD66 and 3M CVI-SiC. Figure 4.6.18 shows the location of the various candle materials as installed for the last test period. The inner rows of candles in the upper and middle plenums were left out, the same as in the prior test series. Figures 4.6.19 and 4.6.20 are photos of the candle clusters showing the different candle materials installed prior to the start of Test Period V.

## Results

---

In order to protect the gas turbine from erosion by the coarse ash in case the filter leaked during the next test series, fail-safe devices were installed above each filter candle. The devices were designed to plug up when exposed to ash, but not impose a significant restriction to the normal flow of gas and backpulse air. These devices also functioned as heat regenerators for the backpulse air in order to mitigate the thermal shock of the backpulse air on the filter candles. Appendix II is a discussion of the performance of the fail safe devices prepared by Westinghouse STC.

During removal of the filter internals on 10/27/94, it was noted that the top of the shroud inside the APF was distorted inward at its four support brackets (Figure 4.6.21) which made removal of the clusters difficult due to interference between the shroud and the plenums. There was concern over the ability to reinstall the candle clusters due to this interference. Consequently, prior to the next test series, the upper 26" of the shroud was replaced with thicker material with stiffener rings at top and bottom (Figure 4.6.22). The four shroud support brackets were also replaced as they were found to be distorted. The distortion was attributed to thermal creep.

The primary cyclone upstream of the APF was modified between Test Periods IV and V to force all the gas and ash to flow through it and not collect any ash. This was done to demonstrate that the APF would operate at full load gas temperature (1550F) without ash bridging and without the formation of hard ash cake deposits on the filter candles which had caused the filter DP to become unstable in prior tests runs.

## Results

---

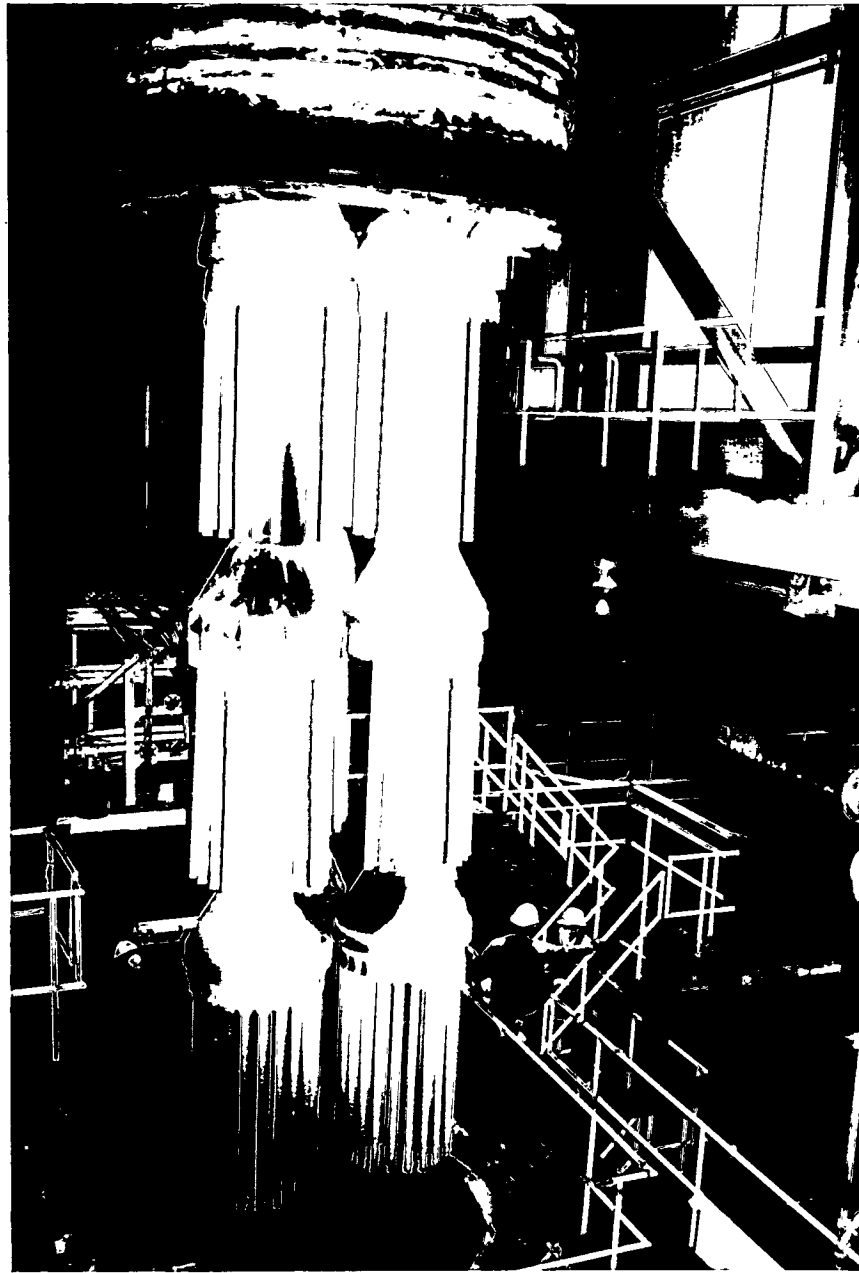


**Figure 4.6.8 - Photograph of Filter Internals Following Test Run 24**

## Results

---



**Figure 4.6.9 - Photograph of Filter Internals Following Test Run 24**

## Results

---



**Figure 4.6.10 - Photograph of Filter Internals Following Test Run 24**

## Results

---



**Figure 4.6.11 - Photograph of Filter Internals Following Test Run 24**

## Results

---

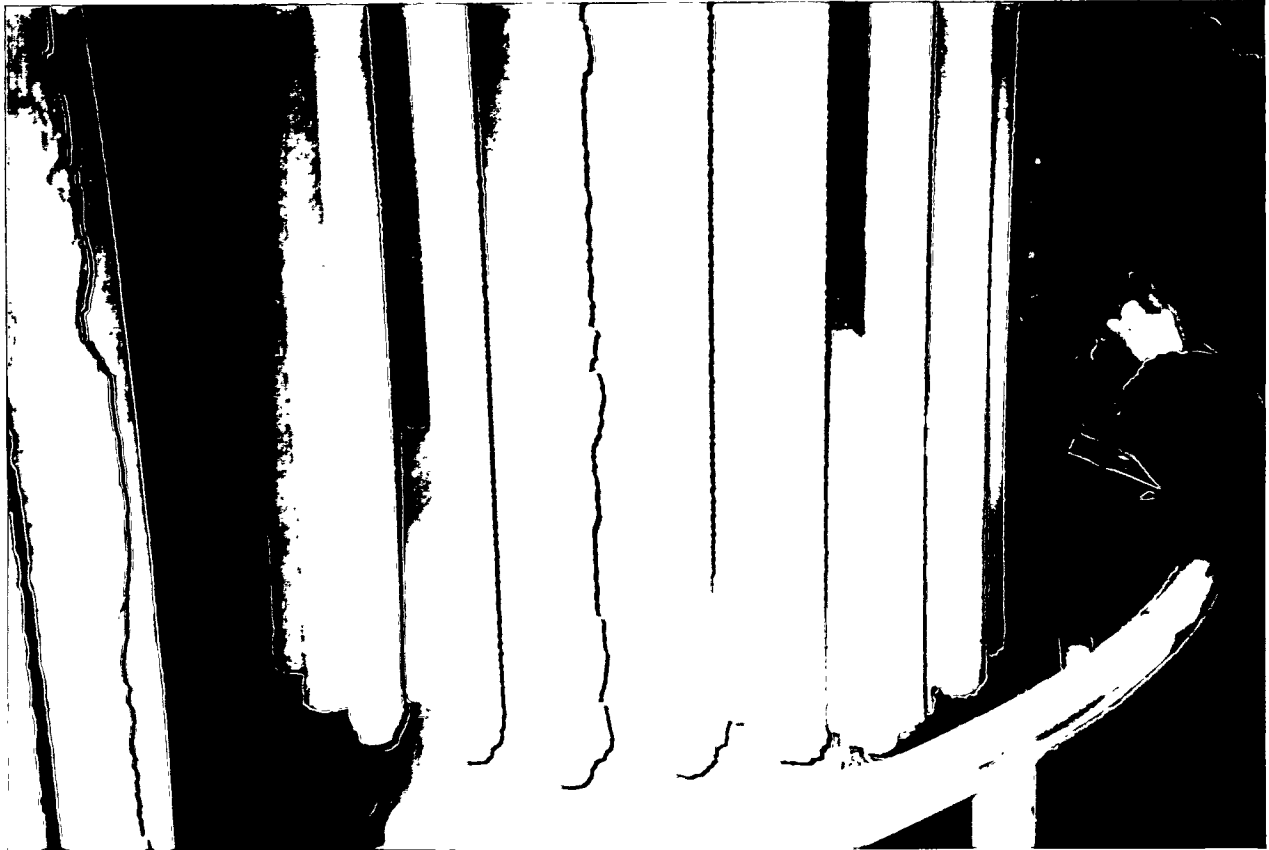


**Figure 4.6.12 - Photograph of Filter Internals Following Test Run 24**

## Results

---

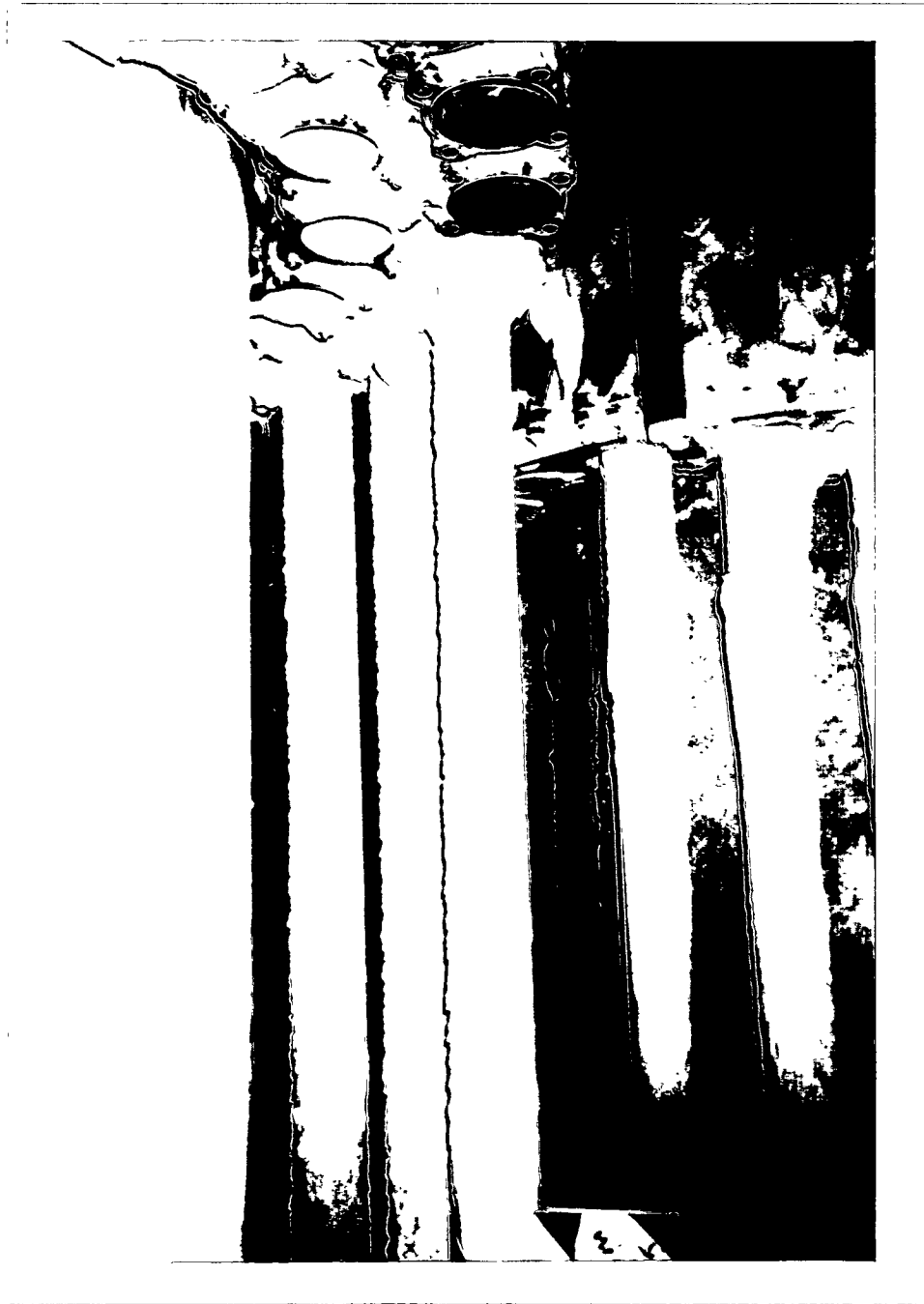


**Figure 4.6.13 - Photograph of Filter Internals Following Test Run 24**

## Results

---



**Figure 4.6.14 - Photograph of Filter Internals Following Test Run 24**

## Results

---



**Figure 4.6.15 - Photograph of Filter Internals Following Test Run 24**

## Results

---



**Figure 4.6.16 - Photograph of Filter Internals Following Test Run 24**

## Results

---



**Figure 4.6.17 - Photograph of Crack in Back Pulse Tube**

# Results

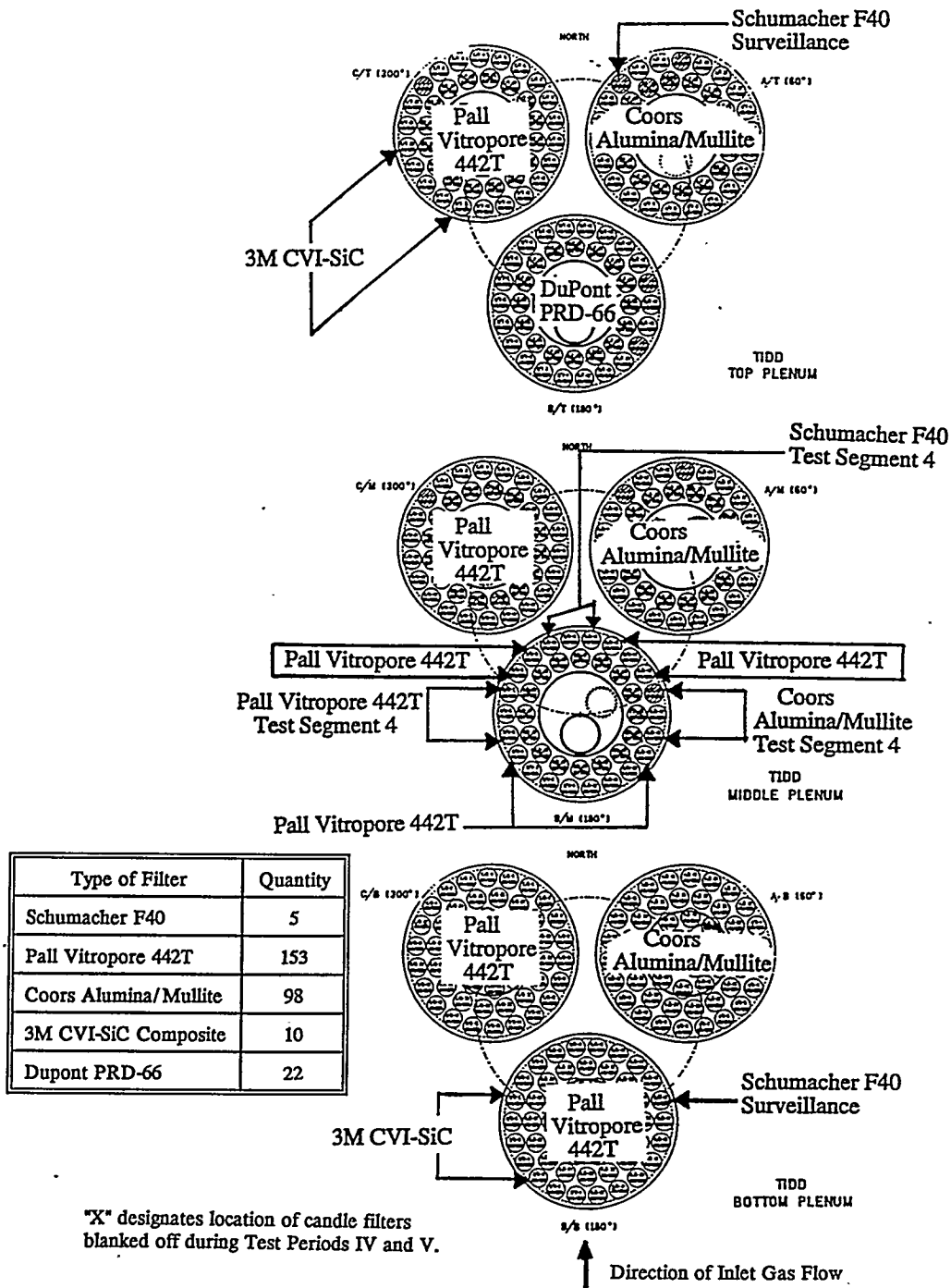
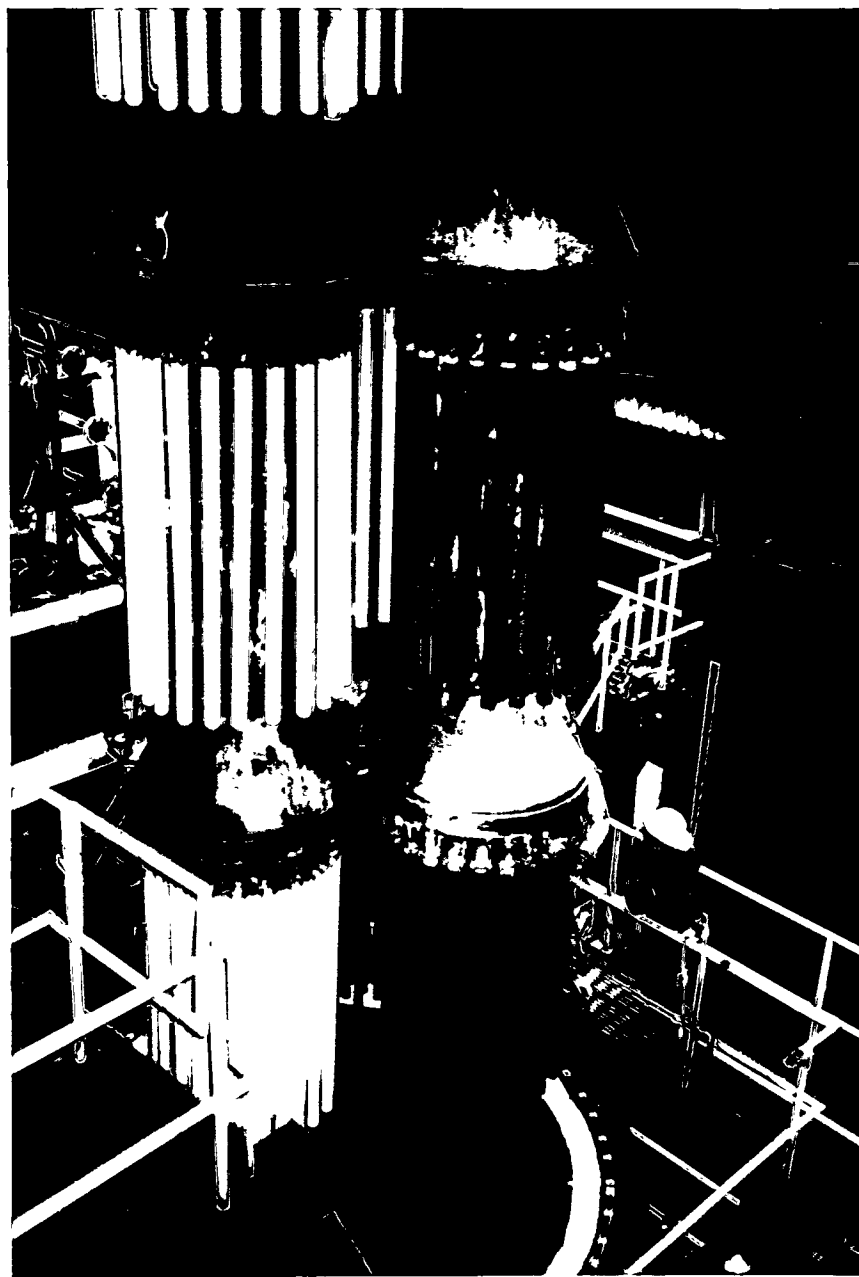


Figure 4.6.18 - Location of Filter Candle Materials Before Test Period V

## Results

---



**Figure 4.6.19 - Photograph of Filter Internals Before Test Period V**

## Results

---



**Figure 4.6.20 - Photograph of Filter Internals Before Test Period V**

## Results

---



**Figure 4.6.21 - Photograph of APF Shroud Following Test Run 24**

## Results

---



**Figure 4.6.22 - Photograph of APF Shroud After Replacement of Upper Portion**

## Results

### 4.7 Test Period V: 1/95-3/95

Table 4.7 summarizes the operating conditions and observations from Test Period V, the final test period.

**Table 4.7 - Summary of HGCU Operation - Test Period V**

	Operating Hours	Cumulative Hours	Operating Temp.	Pressure Drop	Inspection Observations
Run 25, 26, and 27	28	4772	_____	_____	_____
Run 28	145	4917	1350-1525 °F	Stable	● Filter internals very clean
Run 29 and 30	29	4946	_____	_____	_____
Run 31	32	4978	1420-1540 °F	Stable	_____
Run 32	73	5051	1240-1540 °F	Stable	_____
Run 33	427	5478	1275-1560 °F	Slight increase	_____
Run 34	375	5854	1275-1425 °F	Slight increase near end of run	● No ash bridging ● 22 Broken candles

#### 4.7.1 Test Runs 25, 26, and 27 - 1/13/95 to 1/21/95

These test run durations were 4.4, 16.8, and 7.1 hours, respectively. In each case the unit was shut down due to a problem not related to the HGCU system. Due to the brevity of these runs, they will not be discussed.

#### 4.7.2 Test Run 28 - 1/27/95 to 2/2/95

This run lasted 145 hours and was terminated when insulation came off the surface of a blind flange and the flange temperature exceeded 1350F at one point. It was found upon inspection that the anchor pins

## Results

---

which held a stainless steel cover plate over the insulation boards corroded which allowed the plate to fall away from the insulation. The gas flow entrained the insulation and carried it through the gas turbine. Portions of four anchor pins also were carried into the turbine and one of them passed through the turbine causing minor blade damage. (The blind flange was downstream of the backup cyclone.) During the early part of this run, problems with ball valves and pressure regulators on the backpulse skid interrupted filter cleaning for some periods which resulted in abnormally high DP as shown in Figure 4.7.2. During the last half of the run, the filter DP was stable with the gas temperature at 1500F. The drop in DP and flow late in the run is due to the effects of the restriction in flow downstream of the APF caused by the blind flange insulation cover plate falling partially into the gas steam. During the run approximately 11 gallons of Fiberfrax insulation were pumped into the APF head to control three hot spots.

## Results

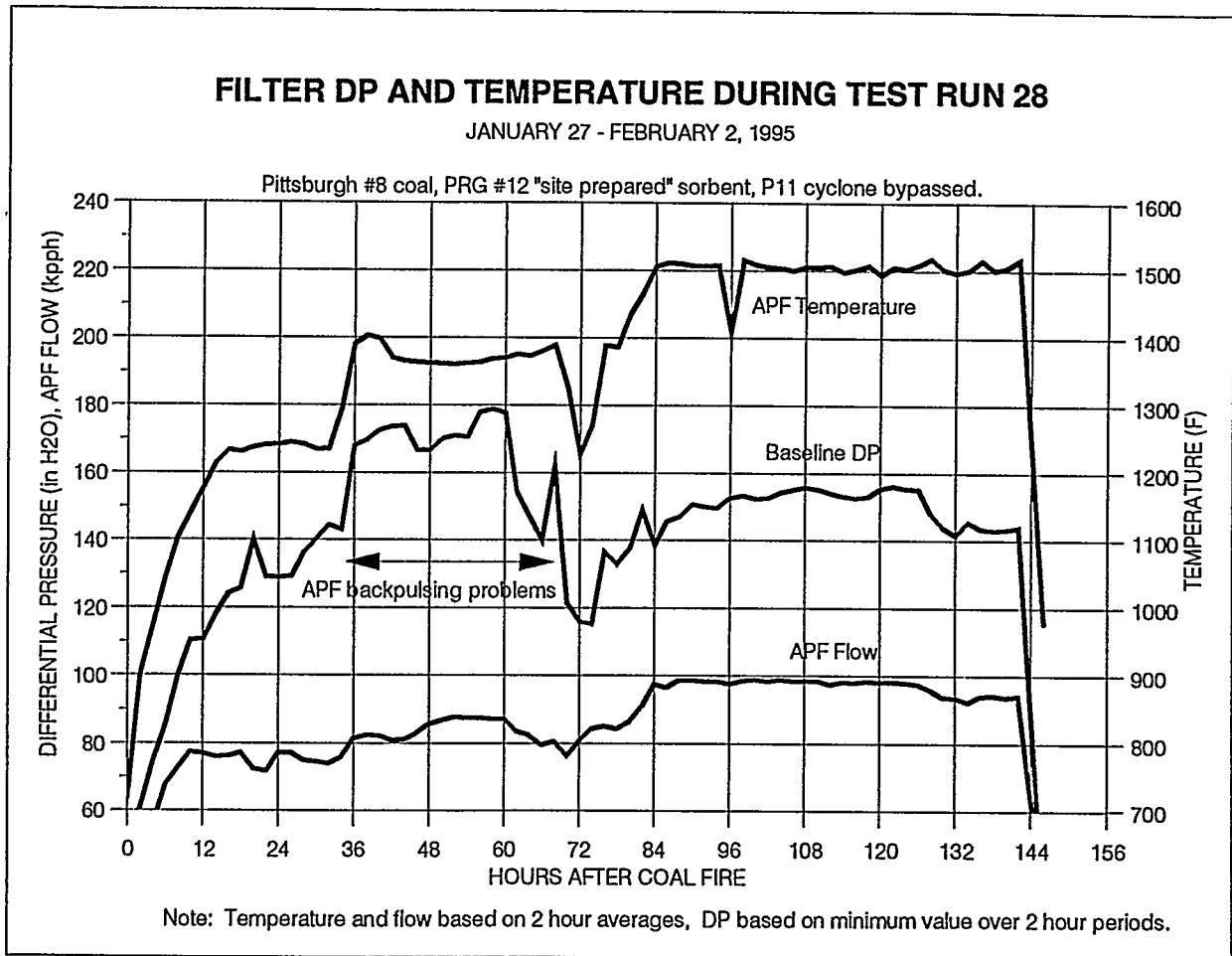


Figure 4.7.2 - Filter DP and Temperature During Test Run 28

## Results

---

### 4.7.3 Posttest Inspection (2/95)

Following Run 28 the APF was inspected using a boroscope passed through three instrument nozzles on the side of the filter vessel. The filter internals were found to be very clean with no ash bridging seen between the candles and the ash sheds. One very minor ash accumulation was seen between two candles in a bottom plenum, but overall, the filter looked cleaner than it had since the inspection following Test Run 1. The bottom of the APF hopper was also without significant ash deposits. Very little (less than 1/8") ash coating was observed on the candles. It was obvious that the coarser ash resulting from bypassing the primary cyclone was much easier to remove from the candles and did not tend to stick to the sides of the hopper, thereby making ash removal a non-issue.

### 4.7.4 Test Runs 29 and 30 - 2/9/95 to 2/10/95

These test run durations were 14.7 and 14.4 hours, respectively. Run 29 was terminated due to a failure unrelated to HGCU, and Run 30 was terminated to repair a gasket leak at the inlet of the ash surge hopper. Due to their brevity, they will not be discussed.

### 4.7.5 Test Run 31 - 2/11/95 to 2/12/95

This 32-hour run was terminated when the alternate ash line became plugged and the APF hopper began filling with ash. During the run candle fragments were found in the ash line from the lockhopper. Additional fragments were found upon shutdown in the alternate ash line while it was being cleaned. It is believed that a candle fragment became lodged in the orifice in the alternate ash line causing it to plug. The candle was a second generation Dupont PRD66 candle.

### 4.7.6 Test Run 32 - 2/13/95 to 2/16/95

Run 32 was a hot restart of the previous run. This test duration was 73 hours and was terminated due to plugged coal paste pumps. Early in the run the APF head exhibited additional hot spots and another 50 gallons of Fiberfrax insulation were pumped in to correct the problem. Once the gas temperature reached 1450-1500F, the APF DP remained fairly stable as shown in Figure 4.7.6.

# Results

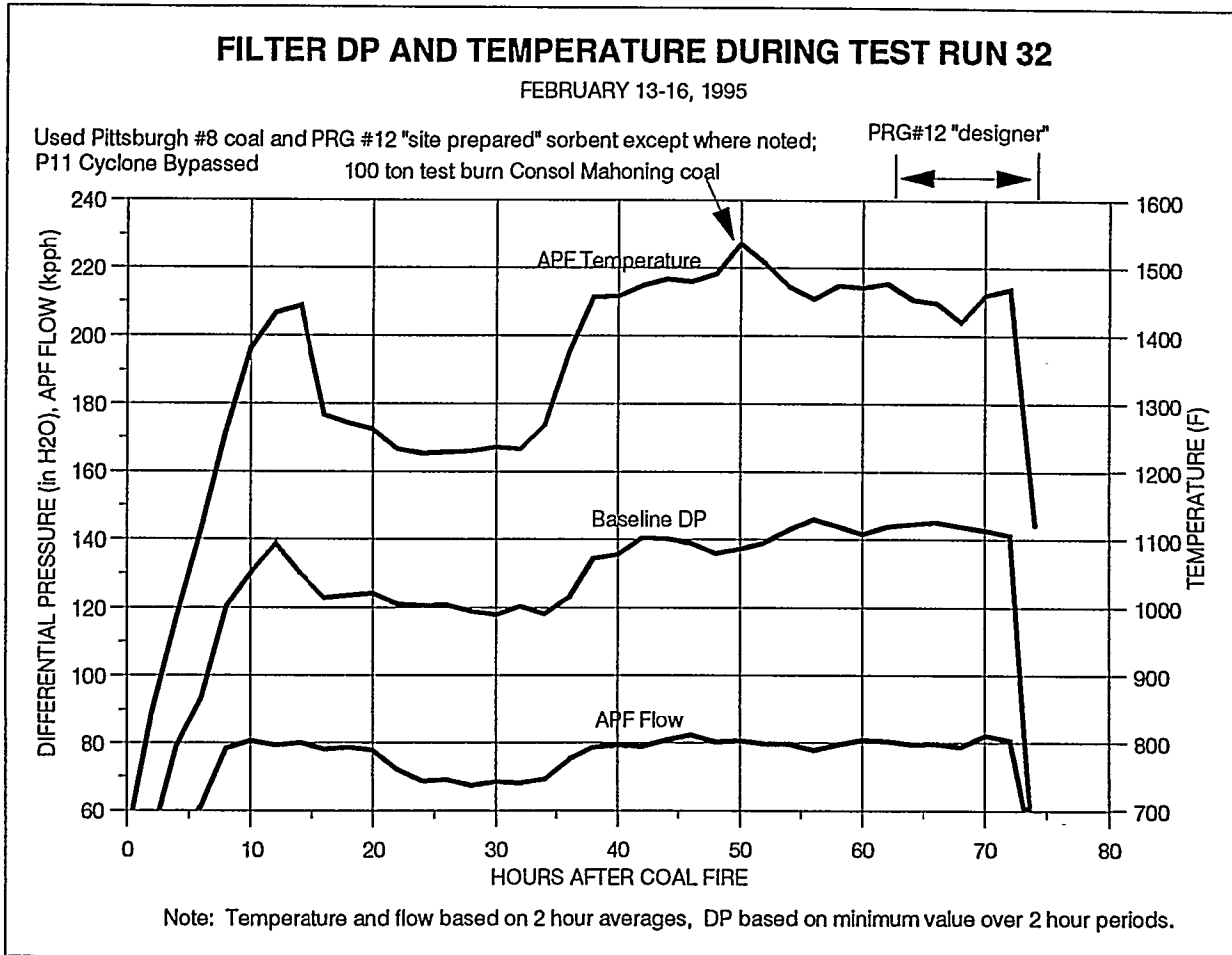


Figure 4.7.6 - Filter DP and Temperature During Test Run 32

## Results

---

### 4.7.7 Posttest Modifications (2/95)

Following shutdown another candle fragment was found in the lockhopper isolation valve. This fragment was the same material as the earlier fragments, and is believed to be from the same broken candle. In order to prevent the alternate ash line from becoming plugged by a candle fragment, a perforated plate was added at the inlet of the ash line between Run 32 and 33.

### 4.7.8 Test Run 33 - 2/18/95 to 3/8/95

Test Run 33 was one of the longest runs of the program at 427 hours. It was also the first run during which the filter operated at or above 1550F for significant time periods. Figure 4.7.8 shows the filter performance trends for this run. The Tidd unit reached its maximum output during this run, and the APF operated above 1550F during three separate time periods as shown by the temperature data in Figure 4.7.8. Portions of this run were conducted using two different coals, namely Minnehaha (from Indiana) and Consol coal. The remainder of the run used Pittsburgh 8, the same coal as in all other runs. The dolomite was also changed from Plum Run to Mulzer during part of the run. These periods are noted in Figure 4.7.8. The APF DP remained relatively stable during this run, but there was a noticeable increase in the DP following the last test at 1550F. The plant did not operate at full load for longer than about 20 hours at a time, so it is not known if the filter DP would have become unstable at 1550F for longer time periods.

During this run the APF head had to be pumped again with 20 additional gallons of insulation to control hot spots. On 2/24 the ash line from the Backup Cyclone became plugged, and for the remaining twelve days of the run no ash could be removed from the cyclone.

The run ended when the coal paste pumps plugged. Following shutdown, the Backup Cyclone was opened and found to be nearly full of ash. The ash was removed with a vacuum truck.

### 4.7.9 Test Run 34 - 3/14/95 to 3/30/95

This was the final test run of the HGCU system as the Tidd Plant was shut down permanently at the end of this run. The run time exceeded 375 hours which was the second longest of the test period. Two days after the start of this test run, APF candle fragments were removed from the lockhopper system.

# Results

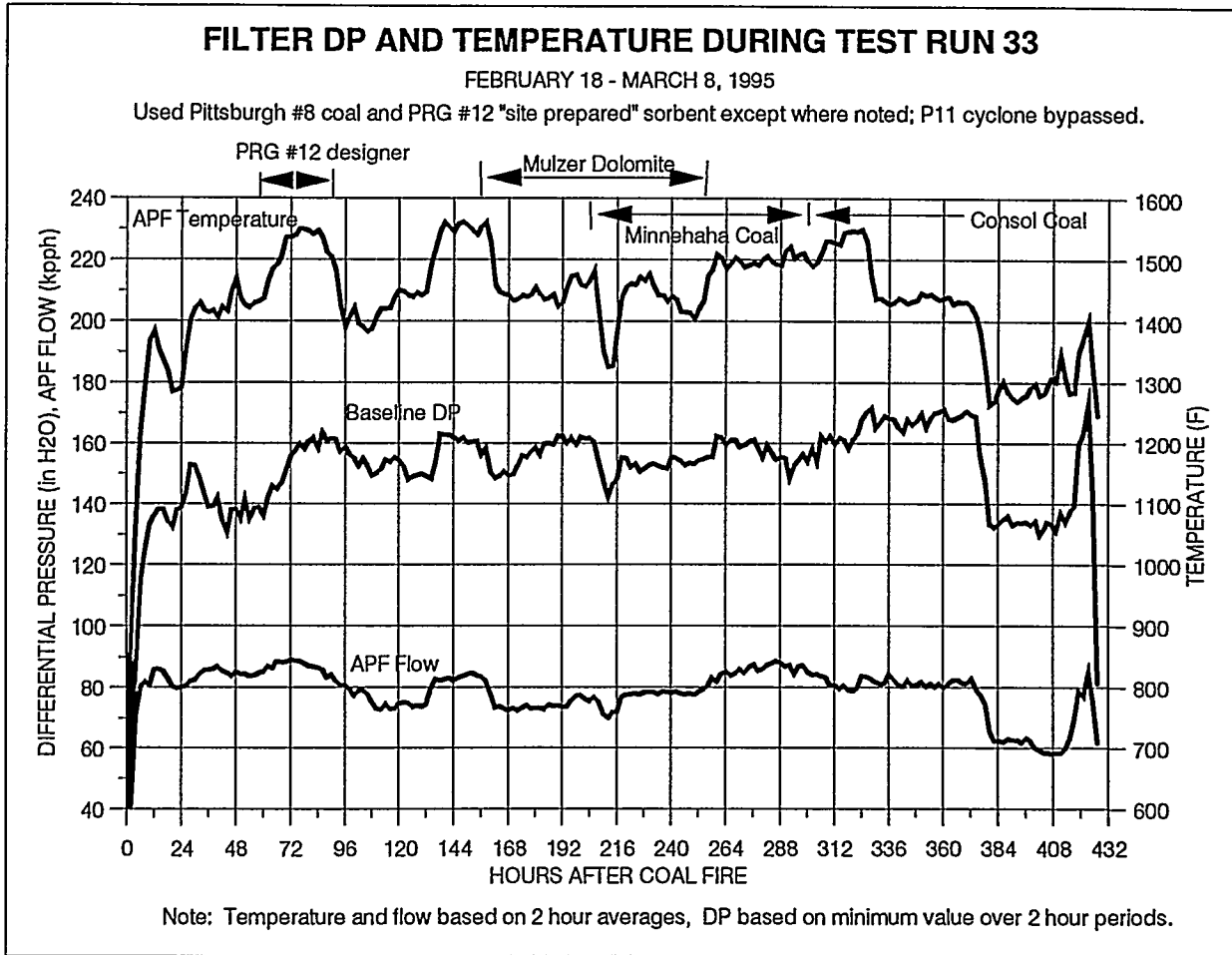


Figure 4.7.8 - Filter DP and Temperature During Test Run 33

## Results

---

The fragments were examined, and it was determined that they came from one Coors alumina-mullite and two Dupont PRD66 candles. The candle breaks apparently occurred during the first two days of this run. No other candle fragments were found for the remaining 13 days of the run. Most of this run was conducted at 90" and 115" bed level, and as a result, the APF temperatures ranged from 1250 to 1400F during most of the run. Figure 4.7.9 shows APF DP and temperature for this run. The DP was constant at a given temperature, but showed a slight increase during the last two days of the run. During the final week of operation, limestone was used as the sorbent instead of dolomite.

### 4.7.10 Posttest Inspection (4/95-5/95)

On 4/26 the internals of the APF were inspected with a boroscope. The internals were very clean with no ash bridges observed. All but two of the 22 Dupont PRD66 experimental filter candles appeared to be missing or were partially broken off. In addition, one Coors alumina-mullite candle was observed partially broken off. The remaining candles appeared in good condition.

On 5/11 the APF internals were removed from the filter vessel. Figures 4.7.10 through 4.7.18 are photographs of the filter internals after removal. As observed by the boroscopic inspection, 20 of 22 of the Dupont PRD66 candles were broken, all in plenum B Top. In addition, two Coors alumina-mullite candles were broken (rather than one), one near the top in plenum A Top and the other about 2/3 down from the top in plenum A Middle. No ash bridging was seen. The residual ash cake layer thickness on the candles ranged from about 1/8" on the Coors alumina-mullite candles to about 3/8" on the Vitropore silicon carbide candles. During removal, cracks were seen in two candles (Figure 4.7.18), one alumina-mullite the other an original Schumacher silicon carbide surveillance candle. Both candles broke during removal and handling. Hard ash deposits were found in the bottom 6 to 12 inches of these cracked candles. In addition, a 3M candle was found to be cracked near the bottom after it was removed. No indication of an ash leak path was seen at the gasket area of any of these candles, but it appeared that ash accumulated in the bottom portion of these candles which resulted in cracking of the candles.

# Results

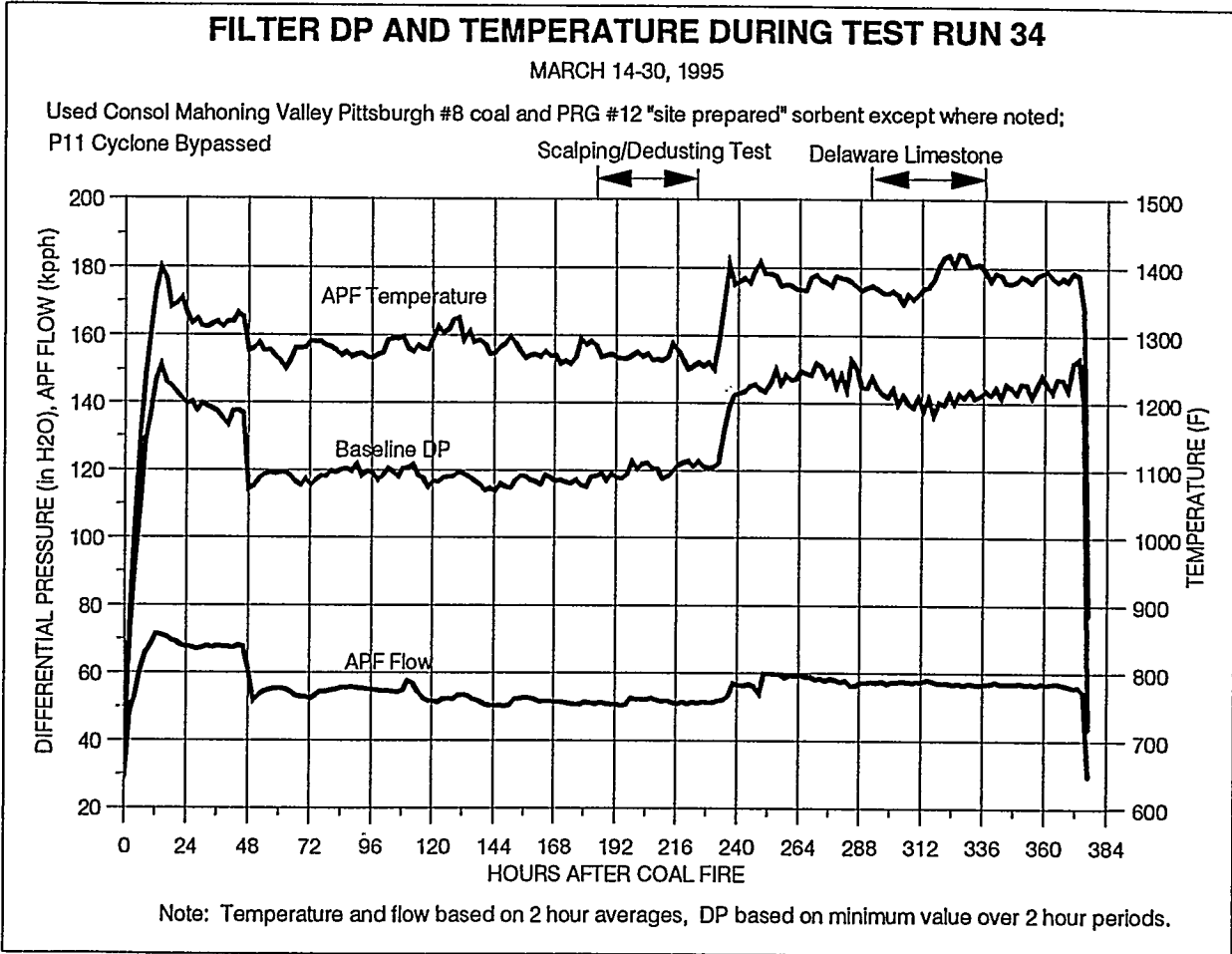
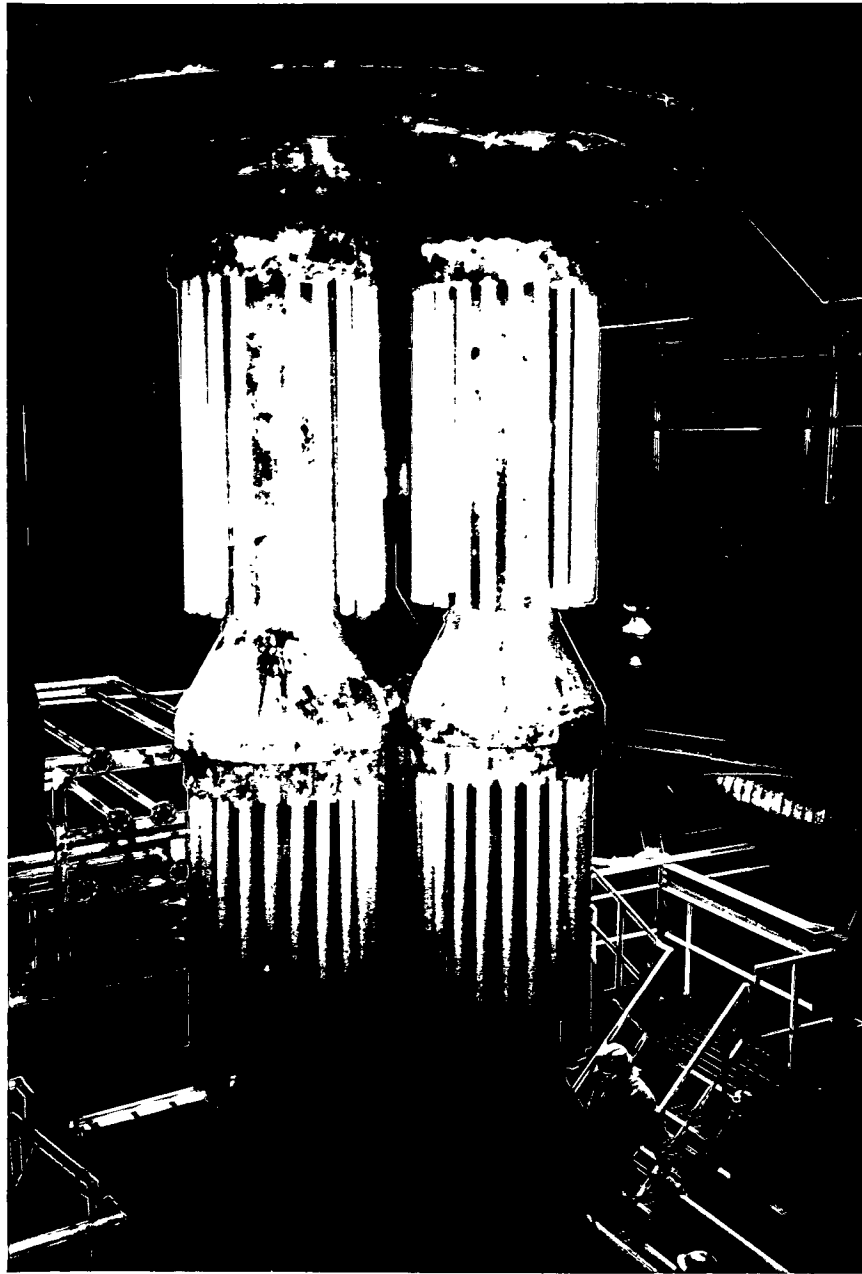


Figure 4.7.9 - Filter DP and Temperature During Test Run 34

## Results

---



**Figure 4.7.10 - Photograph of Filter Internals Following Test Run 34**

## Results

---

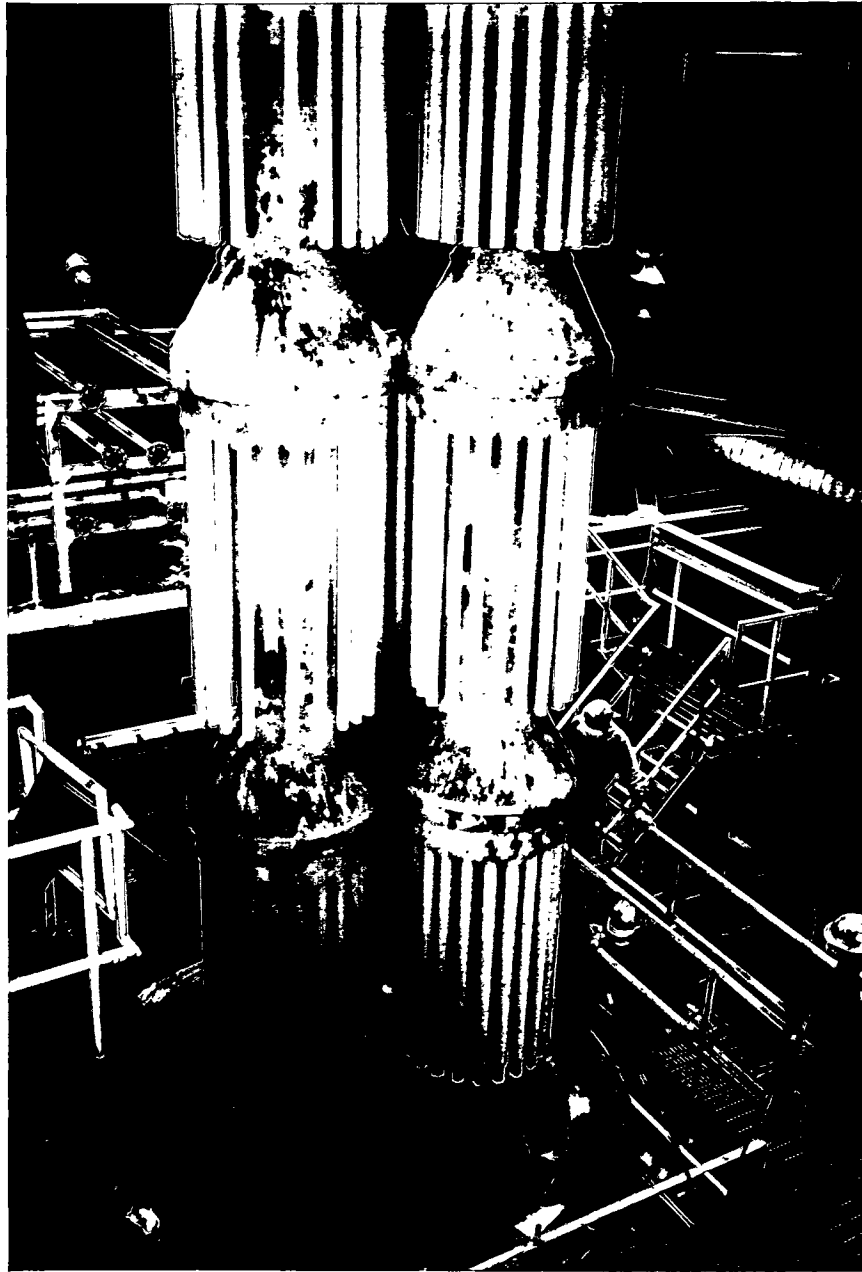


**Figure 4.7.11 - Photograph of Filter Internals Following Test Run 34**

## Results

---



**Figure 4.7.12 - Photograph of Filter Internals Following Test Run 34**

## Results

---

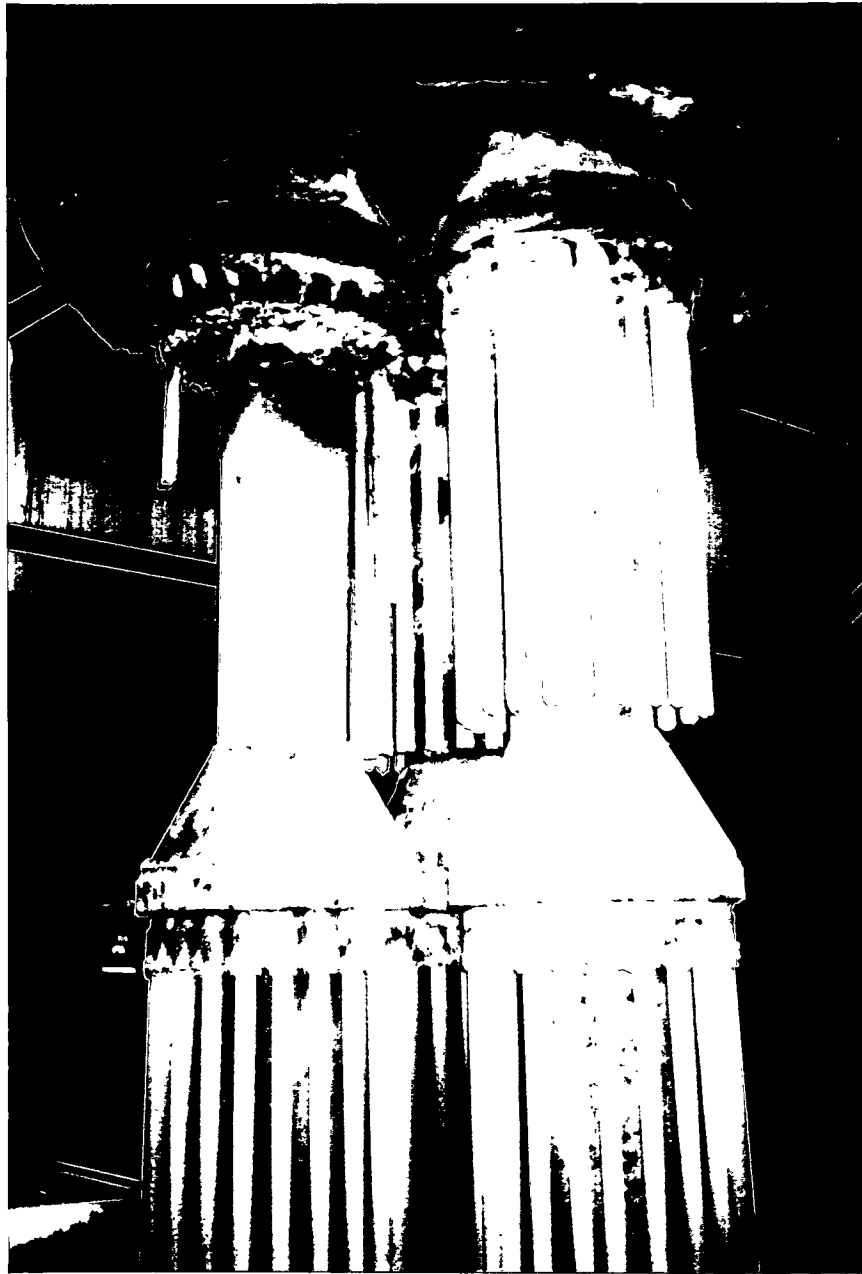


**Figure 4.7.13 - Photograph of Filter Internals Following Test Run 34**

## Results

---

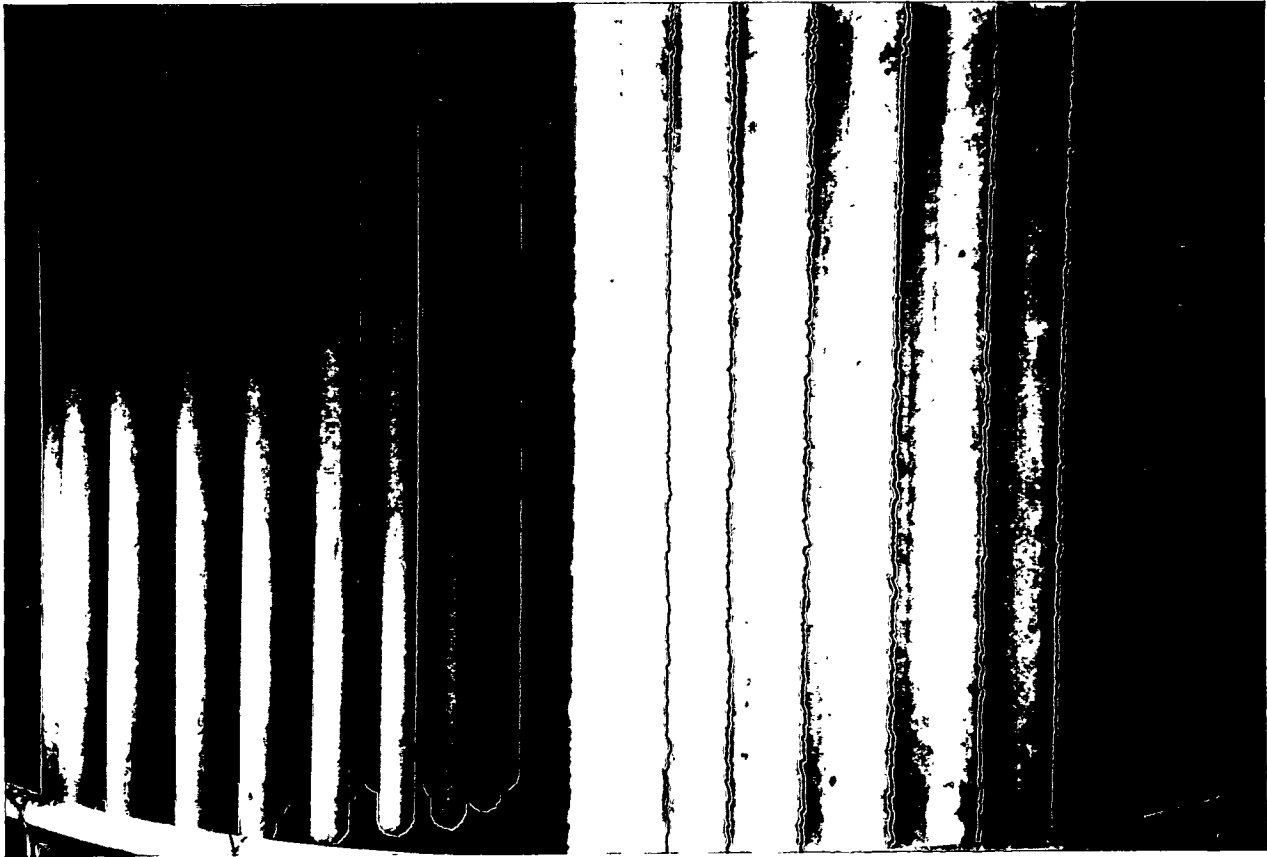


**Figure 4.7.14 - Photograph of Filter Internals Following Test Run 34**

## Results

---

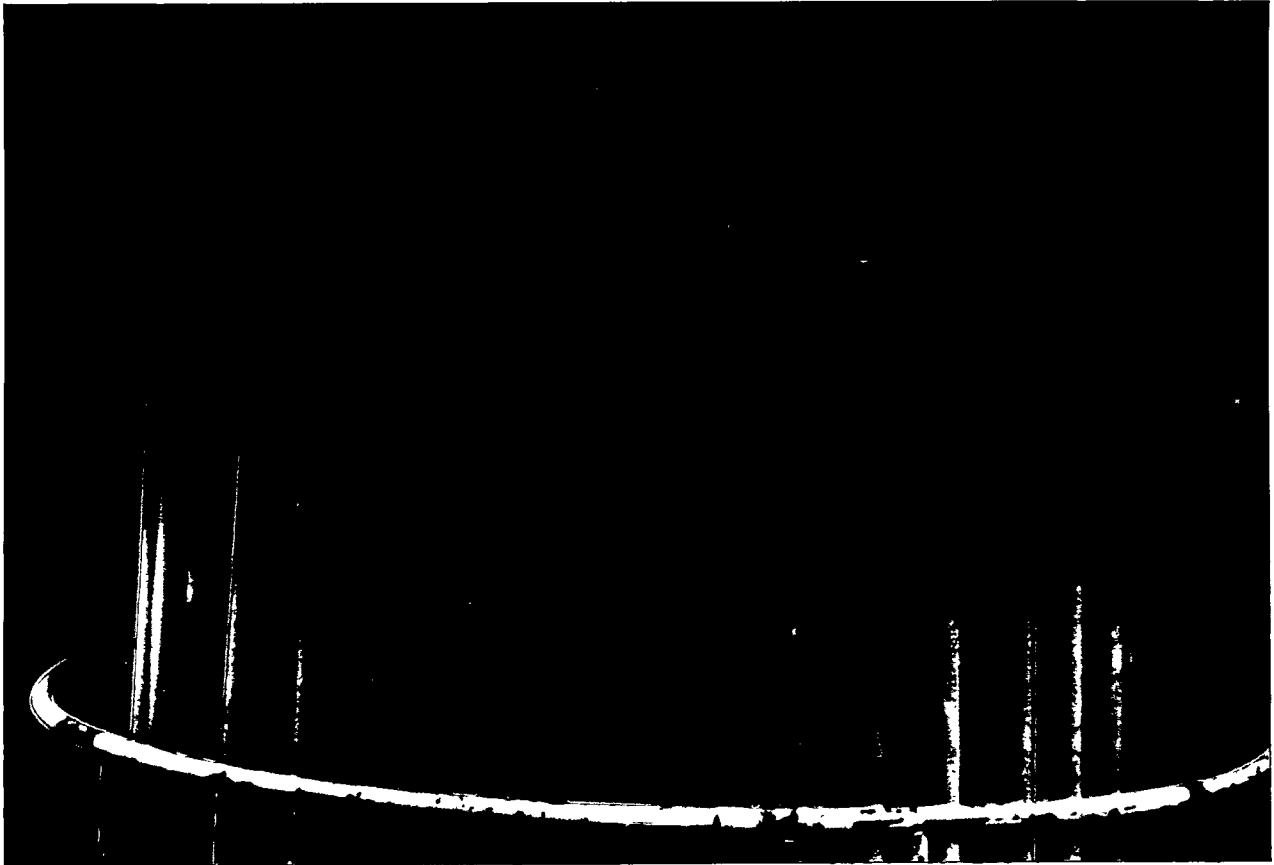


**Figure 4.7.15 - Photograph of Filter Internals Following Test Run 34**

## Results

---



**Figure 4.7.16 - Photograph of Filter Internals Following Test Run 34**

## Results

---



**Figure 4.7.17 - Photograph of Filter Internals Following Test Run 34**

## Results

---

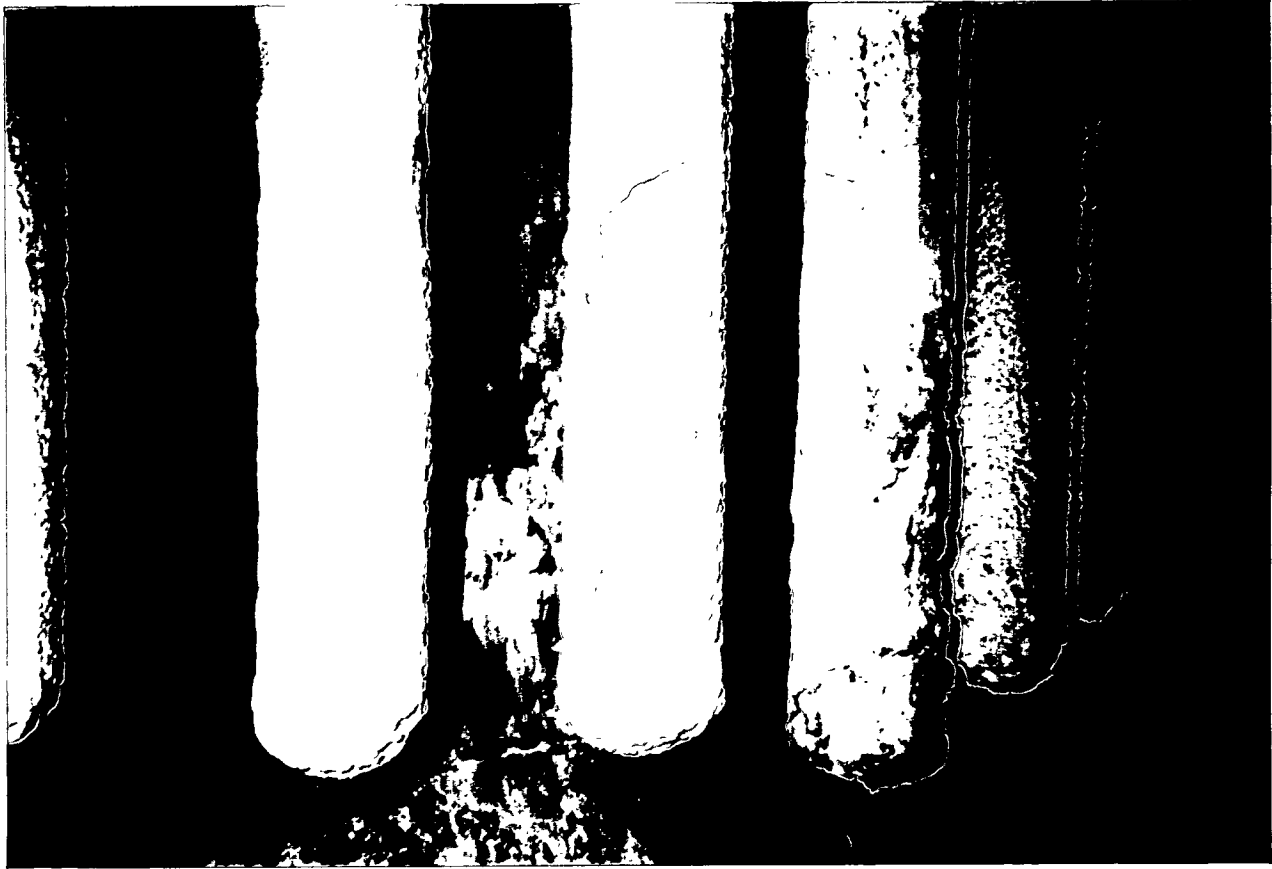


**Figure 4.7.18 - Photograph of Filter Internals Following Test Run 34**

## Results

---

### 4.8 Final Equipment Inspections

Following completion of the test program, inspections were conducted on system components to assess their condition. This section of the report describes the results of those inspections.

#### 4.8.1 Filter Vessel

During much of the test program, the APF head exhibited hot spots near the outlet nozzle and the backpulse piping nozzles. The hot spots were corrected by drilling small holes through the head and pumping in insulation. Experience has shown that hot gas flowing against a cold metal surface promotes rapid corrosion. Therefore, the inside surface of the APF head was inspected following completion of the test program. A section of the head liner and Z-Block insulation was removed to expose the inside surface of the head. Heavy corrosion was apparent, as shown in Figure 4.8.1. Portions of the metal were so corroded that large (3 to 4 inch) pieces of corroded metal about 1/16 to 1/8-inch thick would flake off the surface by pulling with one finger. Following this observation, shell thickness data were obtained using an ultrasonic instrument. It was found that thickness of the top portion of the head averaged 7.6% below the nominal 1.50 inches, and was 12.2% below nominal at the thinnest point measured. The thickness of the bottom portion of the outlet nozzle near the nozzle-to-head weld was found to be 4.5% to 7.8% below the nominal 7/8 inch. It was evident that the carbon steel exposed to the flowing hot gas experienced significant corrosion. The remainder of the APF head which did not exhibit hot spots due to flowing hot gas was in excellent condition with the epoxy surface coating still intact.

#### 4.8.2 Filter Internals

The shroud was removed from the vessel for inspection. It appeared to be in generally good condition as shown in Figure 4.8.2. No erosion was seen on the impingement plate opposite the inlet nozzle. This was of concern after the ash loading and particle size were increased during the last test period. The ash tended to form a deposit and flake off on the impingement plate as shown in Figure 4.8.3. One problem was noted with the shroud. The four support brackets were bent upward due to deformation of the shroud. This occurred even after the shroud material thickness was increased to 1/4 inch and a stiffening ring was added at the top of the shroud to mitigate this problem prior to the last test period. It was apparent that the shroud thickness was still insufficient to prevent distortion.

## Results

---

Upon removal of the shroud, the filter liner was exposed for better inspection. The upper portion of the liner was in generally good condition, except near the very top where it had been distorted by the weight of the shroud support brackets. However, severe distortion and warpage was apparent in the lower half of the liner as shown in Figure 4.8.4. This distortion was much worse than observed in previous inspections and probably resulted from operating the APF at very high temperatures (above 1550F) during the last test period. It appeared that the liner could not expand properly and buckled inward as a result. The hopper cone appeared to be in good condition; only the cylindrical sections were warped. Ash had accumulated behind the liner at points where it had buckled inward and this may have prevented the liner from returning to its original position upon cooling.

The tubesheet support cone was inspected by removing some of the insulation from the upper side of the cone. The expansion cone and tubesheet appeared in excellent condition, as shown in Figures 4.8.5 and 4.8.6. Dye penetrant tests were conducted on the seam and circumferential welds on the inner cone, and no indications were noted.

The insulating plug used in the APF manway deteriorated severely. The 310 stainless steel metal used to contain the insulation corroded to such a degree that it essentially fell apart upon removal. The plug was exposed to flue gas below the dew point which aggressively attacked the stainless steel in the plug. However, the manway nozzle which had been coated with epoxy was in good condition.

### 4.8.3 Backpulse System

Two of the Atkomatic solenoid valves and the COAX valve (used in the last test period) were disassembled for inspection. The COAX valve did not show any signs of degradation. The two Atkomatic valves appeared to be in excellent condition. Some very minor surface scratches were seen in localized areas on the pistons indicating that the Stellite coating held up very well. The valve body bores showed very minor surface pitting, but felt very smooth. Figures 4.8.7 and 4.8.8 are photographs of the valve internals.

## Results

---



**Figure 4.8.1 - Photograph of Corrosion of APF Head Under Insulation Near Outlet Nozzle**

## Results

---



**Figure 4.8.2 - Photograph of APF Shroud During Final Removal**

## Results

---



**Figure 4.8.3 - Photograph of Shroud Impingement Plate**

## Results

---



**Figure 4.8.4 - Photograph of APF Liner**

## Results

---

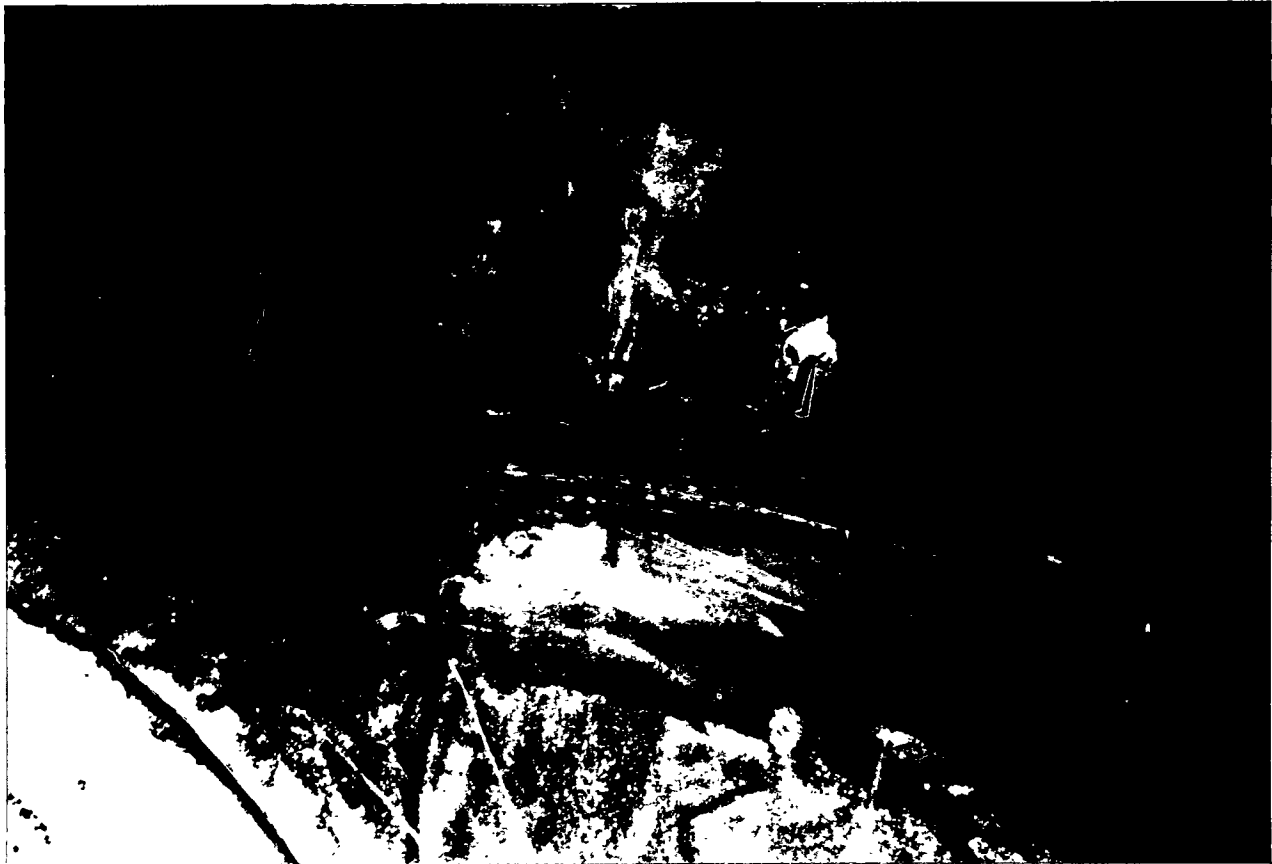


Figure 4.8.5 - Photograph of Tubesheet Cone

## Results

---



**Figure 4.8.6 - Photograph of Tubesheet Cone**

## Results

---

### 4.8.4 Backup Cyclone

The backup cyclone was inspected through the manway nozzle and found in good condition. Figures 4.8.9 - 4.8.11 are photographs of the internals of the cyclone. Cracks in the refractory noted after the first test period did not appear to be much worse. However, a portion of the refractory liner used at the level detector location appeared to be eroded away as shown in Figure 4.8.10. The stainless steel sheet metal used to contain the refractory on the manway door was pitted but still in one piece. The ash line outlet and air nozzles at the bottom of the cyclone were in good condition. A solid plug of ash about 4 inches deep was found in the bottom of the ash removal vessel as seen in Figure 4.8.12.

### 4.8.5 Ash Removal System

A section of the alternate ash line was removed and sectioned to determine if it had experienced erosion. No erosion was noted. This indicated that ash conveying lines can be properly sized to handle heavy ash loading with coarse particles without experiencing erosion. The restrictive orifice in the alternate ash line was removed and inspected. The orifice, which was a tungsten carbide nozzle, appeared in excellent condition, as shown in Figures 4.8.13 and 4.8.14. Also, the tee downstream of the orifice was inspected and it also was undamaged.

The screw cooler internals were inspected using a boroscope. No problems were noted, however, fibrous material apparently from broken second generation filter candles was wrapped around the screw in several locations. The screw cooler end housings were removed to expose the hydraulic motor and bearings. No problems were apparent. However, ash was seen in both end housings indicating that the pressure sealing system had not been totally effective in keeping ash out of the housings.

### 4.8.6 Hot Gas Piping

Corrosion of the hot gas piping system was a concern following the failure of the expansion joint during initial system operation. Major effort was made to improve the design of the piping system to overcome this problem as previously discussed. In order to determine how successful these modifications were, a section of a pipe spool including a portion of an expansion joint bellows was cut out for inspection. The Hastelloy liner between the refractory and the outer pipe was in excellent condition as shown in Figure 4.8.15. The outer bellows was also in excellent condition. The carbon steel surface under the Hastelloy was not corroded at all (Figure 4.8.16). The refractory was not cracked and was intact. In

## Results

---

fact, it was very difficult to remove from the pipe. Figures 4.8.17 - 4.8.20 are photographs of the inside of the pipe spool after removal of the section. This expansion joint had been pumped with insulation which could be seen in the expansion joint convolutions.

## Results

---



**Figure 4.8.7 - Photograph of Backpulse Valve Internals**

## Results

---

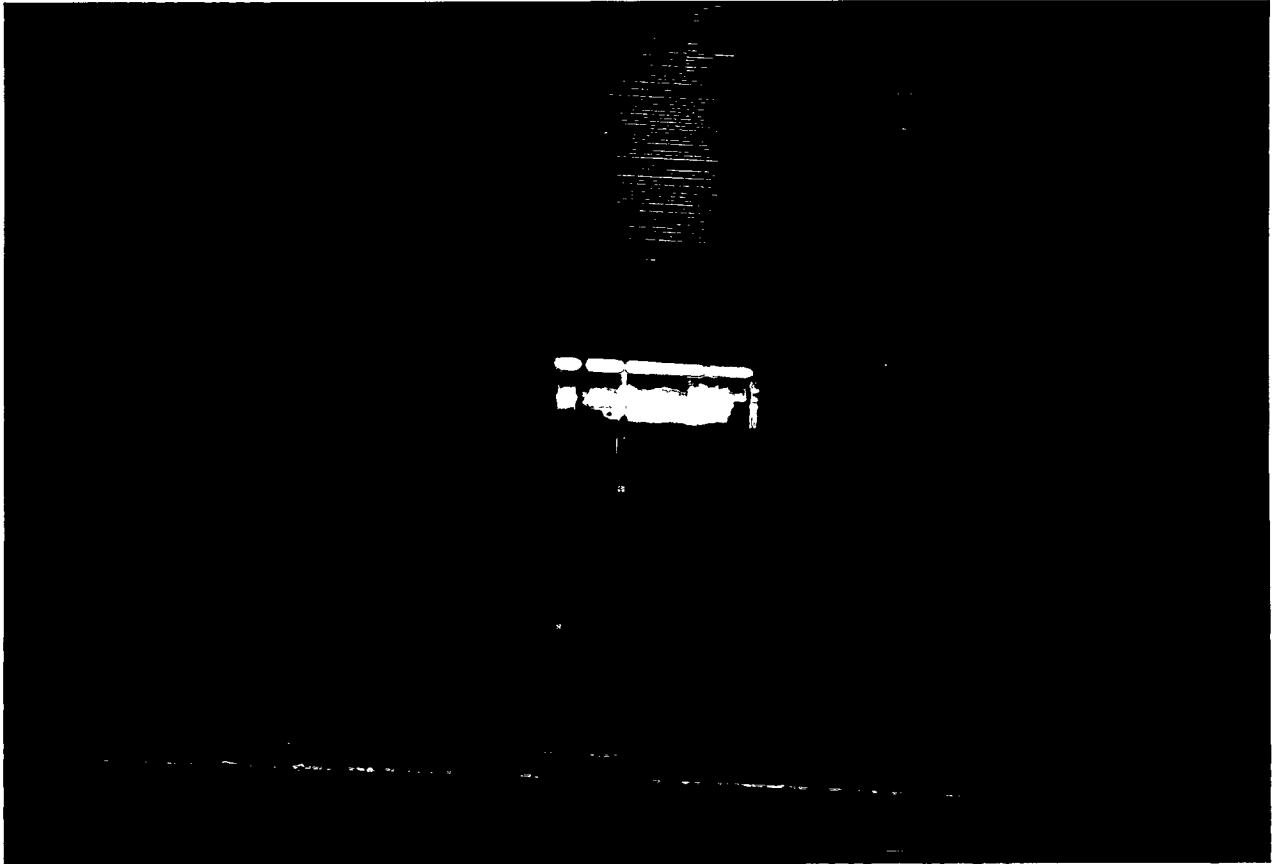


**Figure 4.8.8 - Photograph of Backpulse Valve Internals**

## Results

---

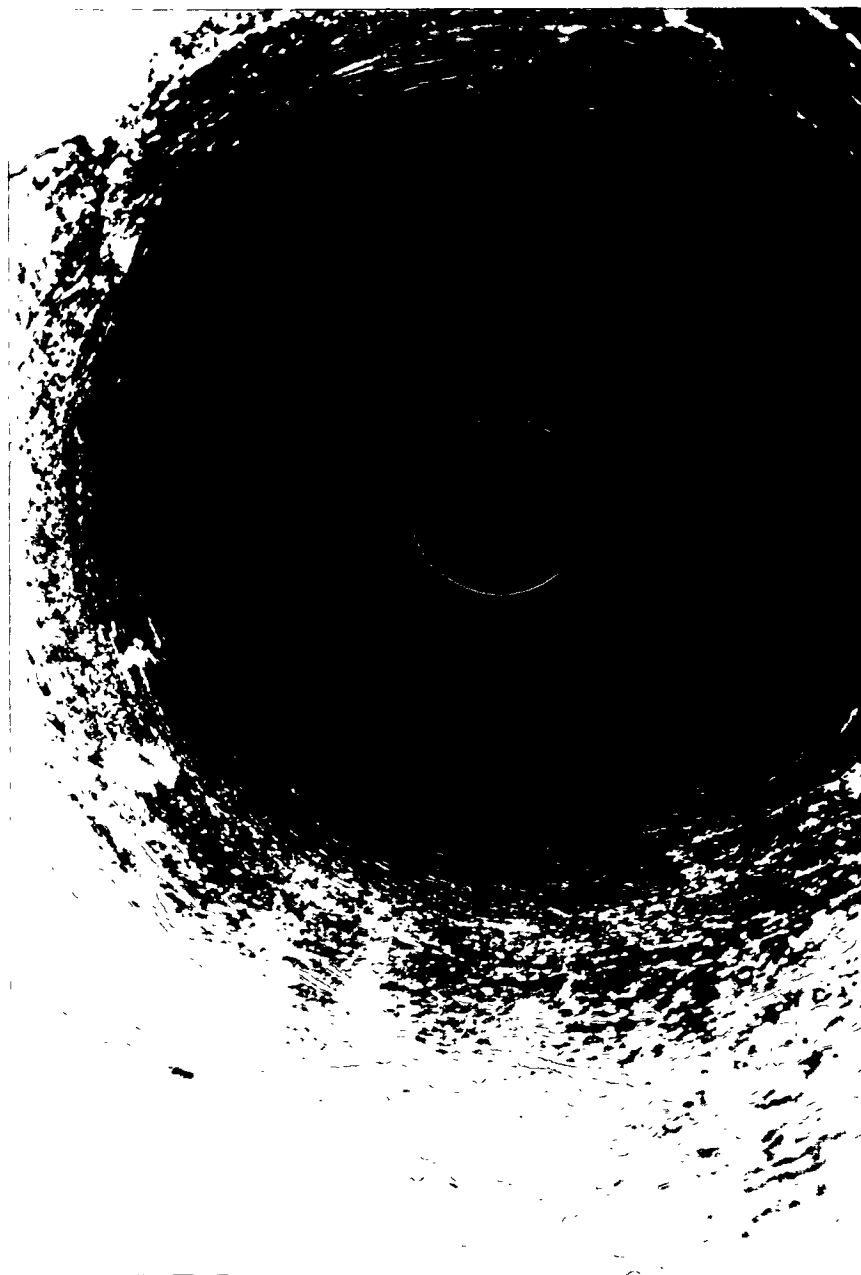


**Figure 4.8.9 - Photograph of Backup Cyclone Internals**

## Results

---



**Figure 4.8.10 - Photograph of Backup Cyclone Internals**

## Results

---



**Figure 4.8.11 - Photograph of Backup Cyclone Internals**

## Results

---



**Figure 4.8.12 - Photograph of Backup Cyclone Internals**

## Results

---

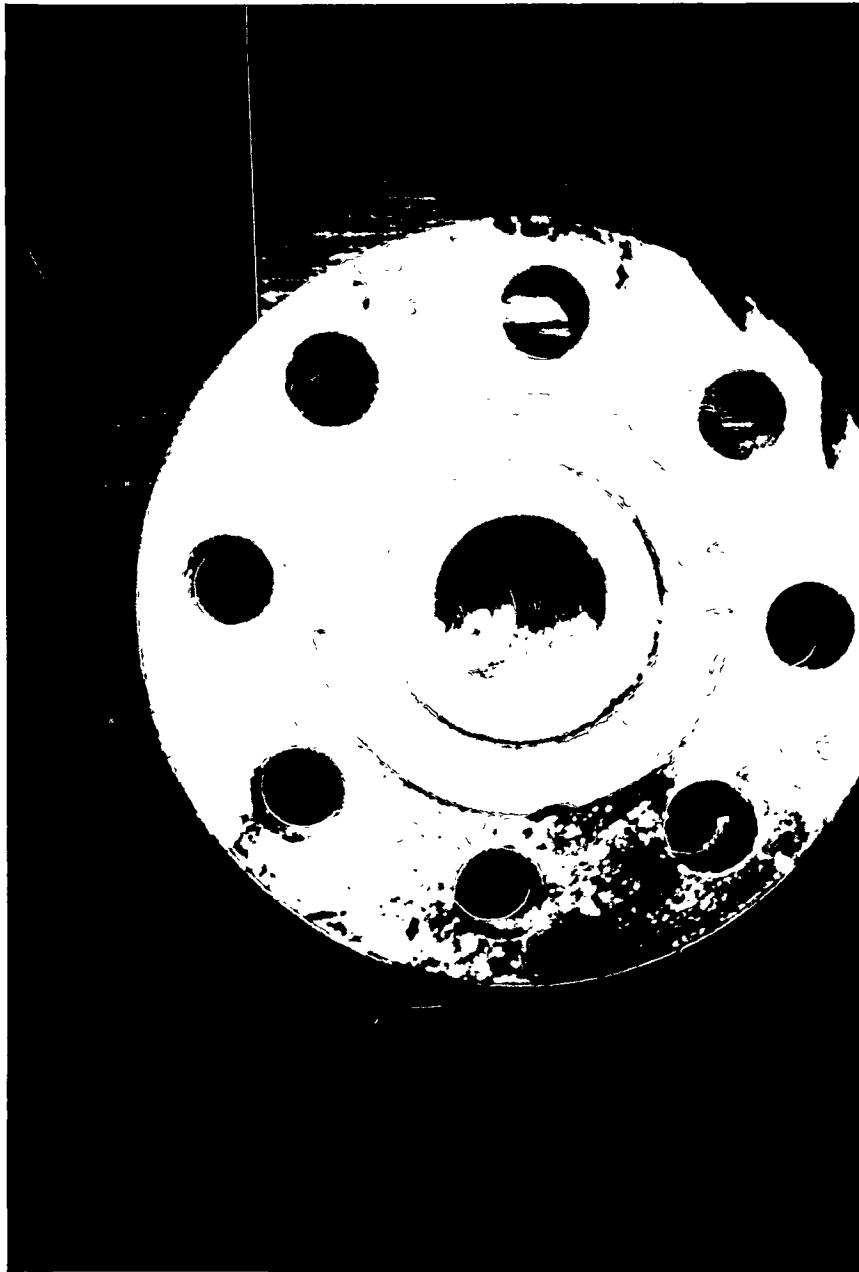


**Figure 4.8.13 - Photograph of Alternate Ash Line Restrictive Orifice**

## Results

---

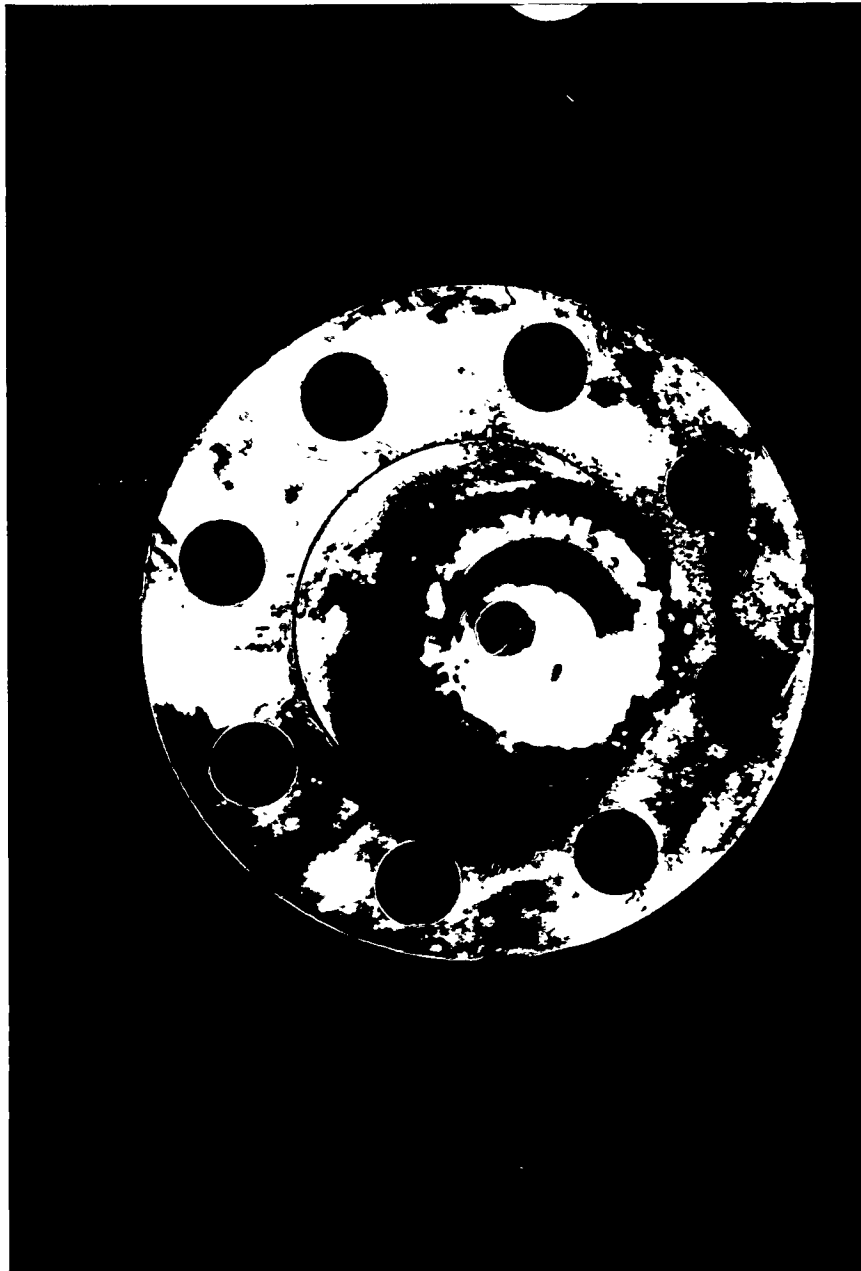


**Figure 4.8.14 - Photograph of Alternate Ash Line Restrictive Orifice**

## Results

---



**Figure 4.8.15 - Photograph of Hastelloy Liner After Removal From Pipe Section**

## Results

---

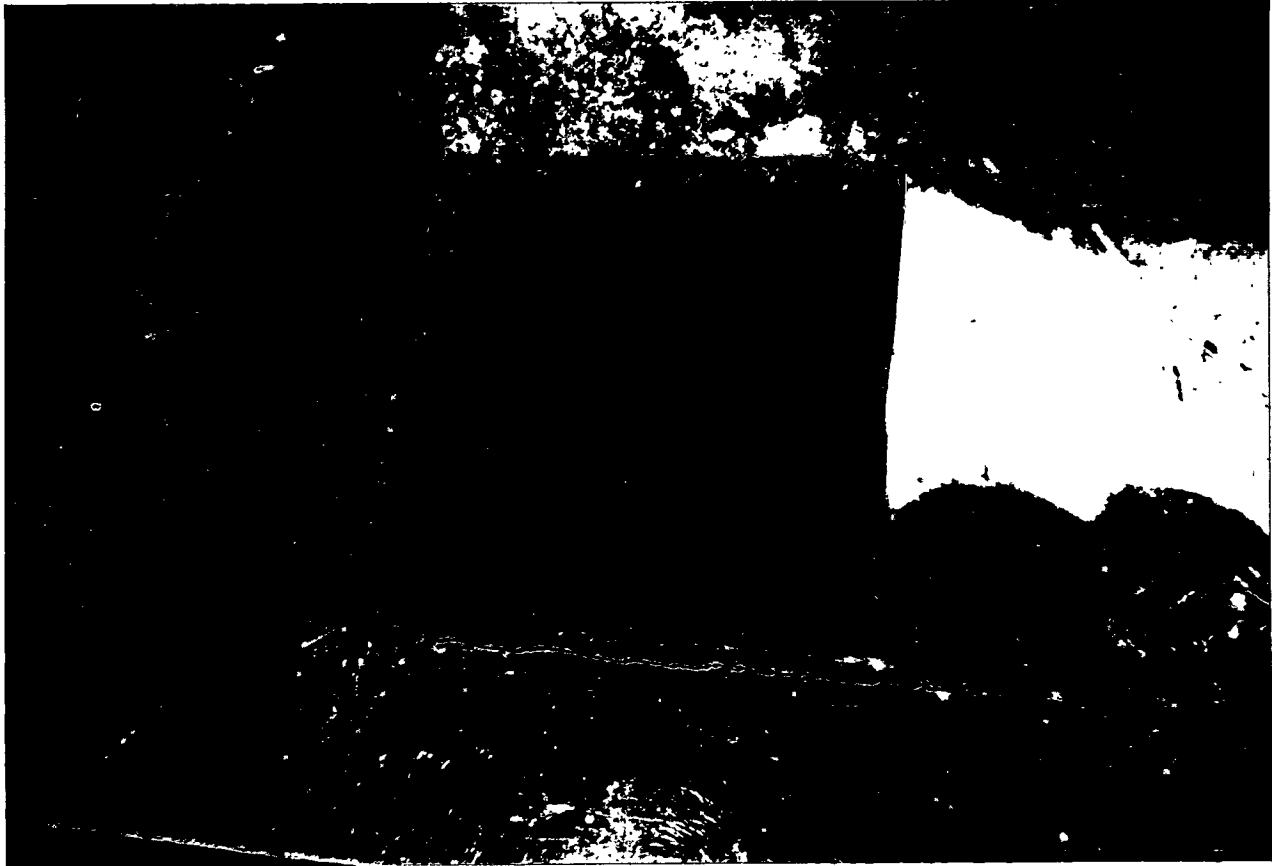


**Figure 4.8.16 - Photograph of Inside Surface of Carbon Steel Pipe Under Hastelloy Liner**

## Results

---



**Figure 4.8.17 - Photograph of Inside of Pipe Spool Following Removal of Section**

## Results

---



**Figure 4.8.18 - Photograph of Inside of Pipe Spool Following Removal of Section**

## Results

---



**Figure 4.8.19 - Photograph of Inside of Pipe Spool Following Removal of Section**

## Results

---



**Figure 4.8.20 - Photograph of Inside of Pipe Spool Following Removal of Section**

## Results

---

### 4.9 Materials Surveillance Test Results

In order to put the results of the material surveillance tests in the proper perspective, the operating temperature history of the Tidd APF is presented below.

Figure 4.9 is a bar graph which depicts the operating temperature history of the APF. It can be seen that two-thirds of the operating time was in the 1250-1500F range, and about one-fourth of the operating time was in the 1000-1250F range. A comparatively small percentage of the operating time was above 1500F. At the beginning of the project it was planned to operate the APF at full load conditions (1550F) as much as possible during the test program. However, a number of factors limited the operating time at full load conditions. First, Tidd PFBC could not achieve full load except during cold ambient air conditions due to the gas turbine/compressor limitations. Second, much of the operating time, the fluidized bed experienced sintering and/or fluidizing problems which precluded reaching full bed height and load. Third, hot spots on the APF limited unit load on some occasions. Two other factors caused the APF temperature to be lower than the freeboard temperature during much of the test program. Spoiling air supplied from the sorbent air system injected into the dip leg of the primary cyclone for detuning purposes lowered the gas temperature to the APF about 70 to 90F. Tempering (cooling) air was injected upstream of the APF to limit the gas temperature to 1400F during some test periods to mitigate the problem of filter pressure drop instability above this temperature. Only during the final test period when the primary cyclone was bypassed and the ash particle size was much larger did the APF operate above 1550F for sustained periods. It should be recognized that the limited operating time near the full load temperature of 1550F reduced the opportunity to observe long-term high-temperature effects on both ceramic filter elements and the metallic components inside the APF.

## Results

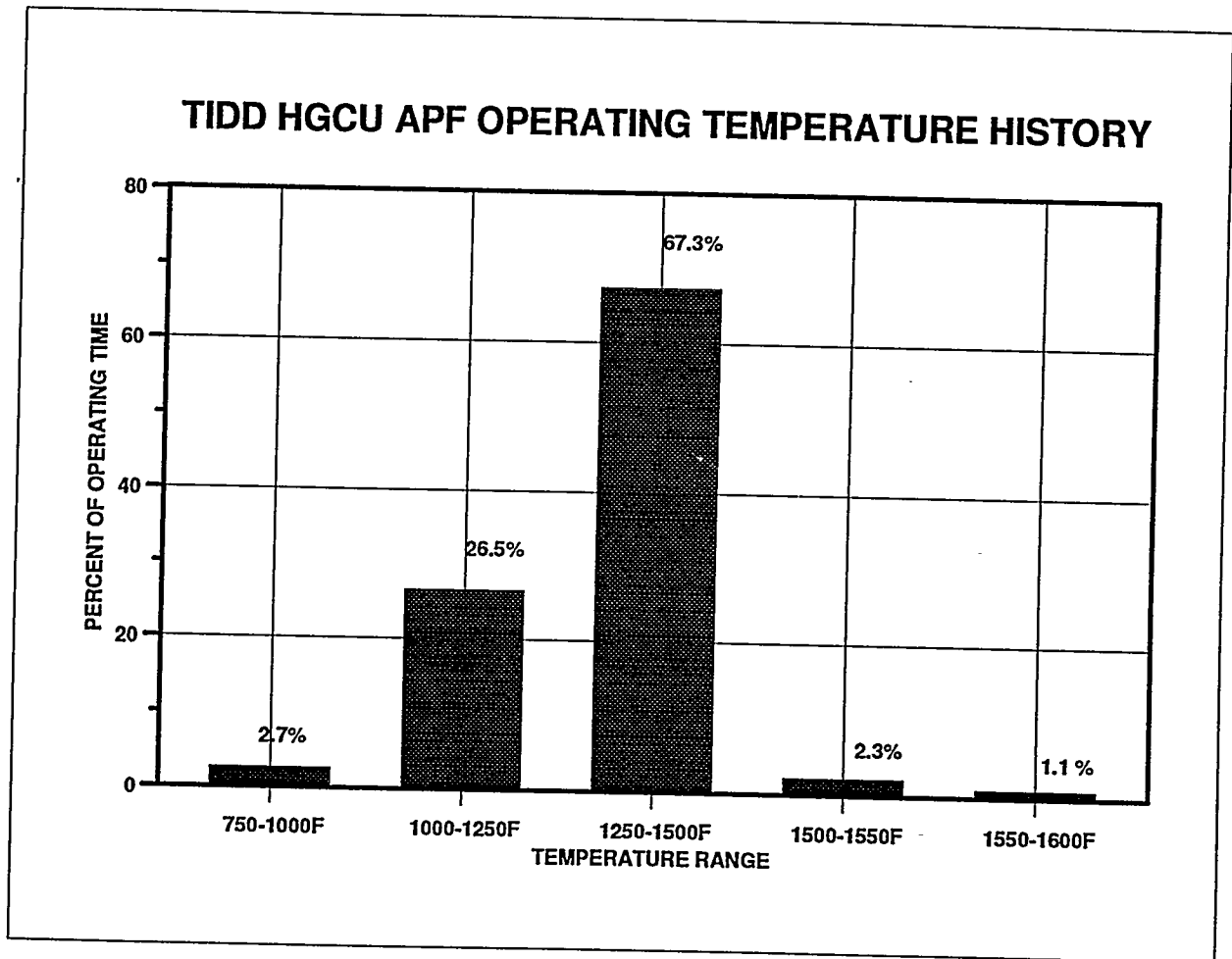


Figure 4.9 - Tidd HGCU APF Operating Temperature History

## Results

---

### 4.9.1 Metal Structures and Test Coupons

Internal structural components of the APF were inspected during a number of plant outages. The key results of these inspections are summarized in Table 4.9.1. This section provides a summary of findings observed during the test program and description of final inspections on an individual component basis. A metallurgical evaluation is described for the critical fine wire mesh used in the fail-safe regenerators. Finally, additional tests, observations and resulting conclusions are summarized for final evaluation of surveillance coupons.

**Cluster.** Type 310S stainless steel was chosen for the Tidd cluster fabrication because of the alloy's good high temperature mechanical properties and resistance to oxidation. On the other hand, it is recognized that type 310S embrittles and hardens due to sigma formation over a range of temperatures encompassing the temperature of Tidd operation.

The principal concern with respect to the expected cluster property changes was the ability to retrofit and/or repair the cluster after operation. For example, during recandling of the filter, it was found desirable to enlarge holes in the filter holder lower cast nuts. (Larger holes enhanced alignment of bolting during assembly.) Redrilling of exposed nuts (1760 hours of operation) was accomplished at Westinghouse with the use of cobalt drill bits. Other evidence of such hardening was encountered after final shutdown (5854 hours of operation) when a few filter holders were removed. Removal of the holders by grinding was found more practical than by sawing because of the hardening that had occurred.

An opportunity to retrofit the cluster was encountered in December 1992 (465 hours of operation) when it was deemed desirable to weld bars across the bottom plates of the bottom plenums to stiffen them and thereby to effect the ability to run a higher differential pressures. Prior to such retrofit, weldability testing was conducted using surveillance coupon material that had been stored in the head of the APF. Simulation welds with significant imposed restraint were prepared, metallographically examined and penetrant tested. The welds were found to be acceptable and successful retrofit was subsequently achieved.

An opportunity for cluster repair was encountered in October 1993 (1760 hours of operation). Several filter holders were found to be out of plumb and an attempt was made to mechanically straighten one at room temperature. The filter holder neck cracked in a circumferential orientation for a length of

## Results

---

approximately one inch. The type 310S (cast HK) material had evidently embrittled during exposure. Again, surveillance material that had been stored in the APF head was weldability tested. Visual and penetrant examination confirmed soundness of the test weld and heat affected zone. The filter holder crack was then repair welded.

Cluster A was chosen for visual and penetrant inspection of welds. No relevant indications were detected after 3039 hours of operation. Also no evidence of creep elongation could be detected. Cluster A was again chosen to verify the post service integrity of critical structural welds. Approximately three feet of top plenum circumferential weld joining top plate to side plate were penetrant tested. No relevant indications were found. Approximately three feet of support pipe joining top plenum to middle plenum were also penetrant tested. Again no relevant indications were found.

**Tubesheet.** Permanent distortion after prolonged high temperature exposure was possible in the thin member (1/4 inch) inner cone near to its juncture with the tubesheet inner disk. Alloy 333 was chosen for this application and analytically judged to have appropriate resistance to such creep.

Surveillance verification of creep effects was provided in the following manner. At the time of manufacture rows of fiducial marks (1/2 inch spacing) were placed parallel and perpendicular to the tubesheet inner disk-to-inner cone circumferential weld at the locations where inner cone to inner cone radial welds intersect the circumferential weld. Then three dimensional as-manufactured Silastic replicas were made at these junctures. Following shutdown, another replica was made at one of the junctures.

## Results

**Table 4.9.1 -Summary of Internal Structural Component Performance Issues and Corrective Actions**

Aberrant Component Condition	Corrective Action and Result
<p><b>Filter Holder Embrittlement</b>            Attempt to straighten a filter holder at room temperature caused cracking of the neck of the holder. The 1760 hours of operation are speculated to have precipitated sigma phase and embrittled the type 310 stainless steel.</p>	<p>Performed Weldability Test on Surveillance Coupon.            Repaired (Welded) Crack.            While the repair was successful, subsequent straightening operations were avoided.</p>
<p><b>Pulse Pipe Cracking</b>            Longitudinal cracks were noted in Incoloy 800HT pulse pipes after approximately 1760 hours. The problem is attributable to thermal fatigue.</p>	<p>Replaced Pipes using Haynes 230            NOTE: Alternate thermally sleeved design performed without incident at Karhula.</p>
<p><b>Thermocouple Sheath Degradation</b>            Embrittlement and/or corrosion of type 310 stainless steel sheathing caused thermocouple failure in times less than 3039 hours.</p>	<p>Performed Service Exposure of Matrix of Alloys:            1. Incoloy 825            2. Hastelloy C276            3. Inconel 600            Subsequent operation for approximately 2815 hours showed best performance for Inconel 600.</p>
<p><b>Linear Indication in Tubesheet Lift Lug Weld (3039 hours)</b></p>	<p>Ground Out and PT.            It is speculated that this indication is not service related because the lug is not stressed during operation.</p>
<p><b>Corrosion Under Tubesheet Outer Ring</b>            Significant corrosion of the type 310 stainless steel liner and more shallow corrosion of the Alloy 330 outer ring was noted after 3039 hours.</p>	<p>None.            Acid resistant coating is recommended in areas of condensate formation for prolonged operation.</p>
<p><b>Pulse Pipe Centering Device Broke</b>            Vibrations and fatigue may have caused welds to break (3039 hours).</p>	<p>Replaced Component.            NOTE: Alternate spring-loaded fixture used at Karhula has performed relatively well.</p>
<p><b>Venturi Broke</b>            Tack welds and cap screws holding venturi in place broke causing dislodging of venturi (3039 hours).</p>	<p>Replaced Venturi and Seal Welded the Entire Circumference of all Venturis.            Venturis remained intact and in place during subsequent operation for 2815 hours.</p>
<p><b>Shroud Rotation</b>            After approximately 3039 hours of operation, significant shroud rotation was noticed. Further rotation could cause shroud to drop.</p>	<p>Welded angle Stops to Shroud Bracket.            Subsequent operation showed rotation was effectively limited.</p>
<p><b>Shroud Distortion</b>            After approximately 4745 hours of operation, distortion near the shroud top encumbered removal of internals.</p>	<p>Reinforced Top Section.            Additional operation for approximately 1109 hours showed the newly reinforced shroud to reduce distortion.</p>

## Results

---

Careful measurements were taken to compare fiducial mark spacing as manufactured and after shutdown. No evidence of creep could be detected. In fact, purely due to limitations in measurement accuracy/precision, it can be concluded that creep was no more than one tenth of one percent. The replicas were also used to compare inner cone to inner disk angles. Using an optical comparator, as manufactured and post service angles were both measured to be  $13^{\circ}-50'$ . The tubesheet may therefore be judged to have resisted detectable creep during its 5854 hours operation at Tidd.

Following final shutdown the tubesheet top liner and localized Fiberfrax insulation were removed to expose: (1) the entire inner cone-to-tubesheet inner disk circumferential weld, (2) one (of three) inner cone-to-inner cone radial welds, (3) one (of three) outer cone-to-outer cone radial welds, and (4) a limited length (about one foot each) of top cap-to-cone and outer cone-to-outer ring welds. Penetrant examination of the aforementioned welds revealed no relevant indications.

**Pulse Pipes.** The performance of pulse pipes was considered a particularly relevant issue of metal ally performance for the Tidd APF. Incoloy 800 HT was chosen for Tidd's original pulse pipe fabrication because of its superior performance relative to type 310S stainless steel at Grimethorpe.

All nine of the Tidd pulse pipes were 100% dye penetrant inspected on their outside surface at site and prior to installation in the APF head. No relevant indications were detected. In December 1992 (465 hours of operation) one Incoloy 800 HT pulse pipe was inspected by dye penetrant examination and radiography. While dye penetrant examination was found to be inconclusive, radiography indicated satisfactory pulse pipe performance.

In December 1993 (1760 hours of operation) one Incoloy 800 HT pulse pie was removed from Tidd and examined by multiple destructive sectioning and metallography. Cracking was noted to have initiated on the pipe's inside surface similar to cracking found in Incoloy 800 HT in the APF at Karhula. The Karhula pulse pipe cracking was attributed to thermal fatigue arising from repetitive "cold" pulsing of this normally hot structure. All nine pipes were replaced with pipes made of a potentially more fatigue resistant material -Haynes Alloy 230.

The Haynes 230 pulse pipes were examined by borescopic, visual and penetrant examination in October 1994 (2985 hours of operation for these pipes). Two of the three bottom plenum pulse pipes showed through-wall longitudinal cracks. While exposed to more hours of operation than the Incoloy 800 HT pulse pipes, the Haynes 230 material was evidently not sufficiently resistant to fatigue for prolonged

## Results

---

service at Tidd operating conditions. The pipes were again replaced with Haynes 230 and performed without macroscopic cracking for the balance of Tidd operation (1109 hours of additional operation).

Geometric constraints and issues of material availability were key elements in the decisions at Tidd to utilize relatively fatigue resistant materials for the back pulse pipes. In contrast, the larger pulse pipe size at Karhula permitted a design alternative, i.e., use of a sacrificial thermal barrier sleeve inserted inside of the primary pulse pipe. This design, consisting of a thin Alloy 333 sleeve within an Alloy RA 253MA pulse pipe, has thus far performed without visually detectable problems in the APF at Karhula.

**Fail-Safe Regenerators.** The fail-safe regenerators used at Tidd were comprised of type 310 stainless steel Raschig rings sandwiched between two Haynes Alloy 25 (Alloy L 605) fine mesh screens using a type 310 stainless steel body. The fine mesh was the most delicate member of this package. Degradation of the 0.0055 inch diameter wire used for this mesh may result from high temperature corrosion (e.g., oxidation) and/or thermal shock during back pulsing. Appendix II presents additional discussion of the performance of the fail-safe regenerators.

Fine mesh used at both Karhula and Tidd was compared to as manufactured mesh. Samples of these three conditions were silver flash coated and nickel electroplated (to preserve edge and/or oxide), mounted in cross section and prepared metallographically. Photo micrographs of unetched cross sections of individual wires are shown in Figure 4.9.1, 4.9.2 and 4.9.3. A thin (0.0001 to 0.0008 inch) layer speculated to be oxide developed on the surface and/or into the substrate of the exposed wires. In addition, reaction is evident in a zone within approximately 0.0015 inches of the surface. Both Karhula and Tidd samples appeared to be of similar condition even though the times and temperatures of exposure were somewhat different. Protracted exposure would need to be conducted to verify if the oxidation/precipitation has stabilized and reached a steady state.

**Coupon Examinations.** High temperature oxidation/corrosion of alloys chosen for Tidd structures (Alloy 333 and Type 310 stainless steel) and of candidate alloys for retrofit and/or future filter applications (Alloys 617, 556, 188 and 253 MA), was monitored using a surveillance tree which suspended such alloy coupons on the top side of the tubesheet inner disk during the entire 5854 hours of Tidd operation.

## Results

Nominal compositions and weight comparisons of the samples are shown in Table 4.9.2. All alloys showed slight weight loss except for Alloy 556 which showed a slight weight gain.

Samples of all coupons were silver flash coated and nickel electroplated (to preserve edge and/or oxide), mounted in cross section and prepared metallographically. Photo micrographs comparing unetched cross sections are provided in Figures 4.9.4 through 4.9.9. The nickel based alloys 333 and 617, cobalt based alloy 188 and type 310 stainless steel all showed surface reaction (0.0005 to 0.001 inch thick) and near surface grain boundary reaction up to 0.004 inch deep. Alloy 253 MA showed no grain boundary reaction but developed approximately 0.001 inch thick surface product. Alloy 556 showed a relatively thick (0.003 inch) surface layer and approximately 0.006 inch deep grain boundary reaction.

The reaction of all alloys studied is considered to be modest in the context of their thick section structural applications. Several mils of affected substrate represents a percentage of the substrate of the order of only 1%. Furthermore, the slight weight changes suggest that the reaction is relatively stable after 5854 hours.

**Table 4.9.2 - Surveillance Tree Coupon Weight Comparisons**

Alloy	Nominal Composition							Weight			
	Ni	Cr	Fe	Si	Mo	Co	W	Original, gm	Final, gm	Change, gm	% Change
333	45	25	18	1.0	3	3	3	32.76	32.67	-.09	-0.3
617	45	22	3	1	9	12		33.22	33.12	-.10	-0.3
556	21	22	31	0.5	3	18	3	32.49	32.54	+.05	+0.2
188	22	22	3	0.35		37	14	35.81	35.68	-.13	-0.4
253MA	11	21	65	1.7				31.02	30.92	-.10	-0.3
310	20	25	52	0.5				30.77	30.70	-.07	-0.2

## Results

---

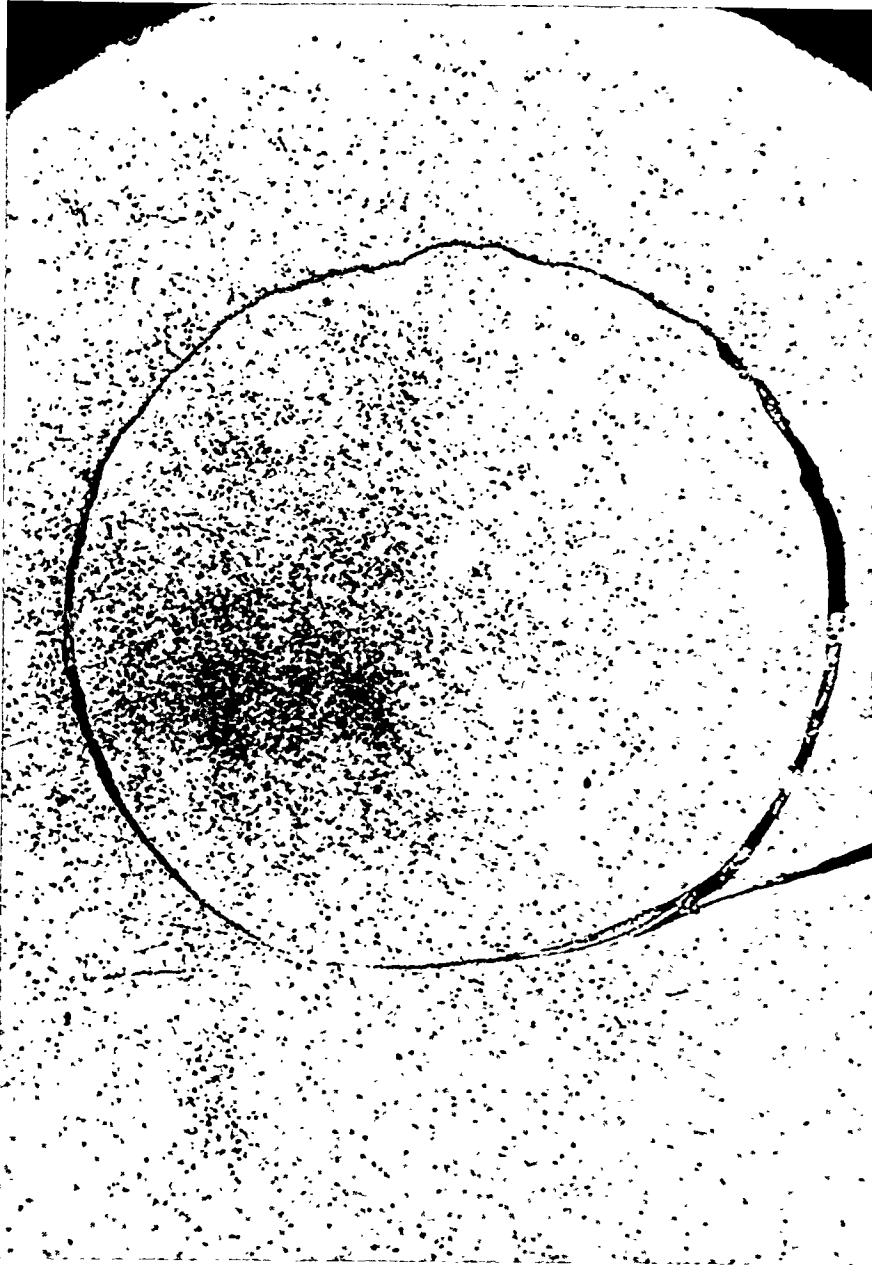


**Figure 4.9.1 - Cross Section of 0.005-inch Wire from Fine Fail-safe Mesh As New-700X**

## Results

---

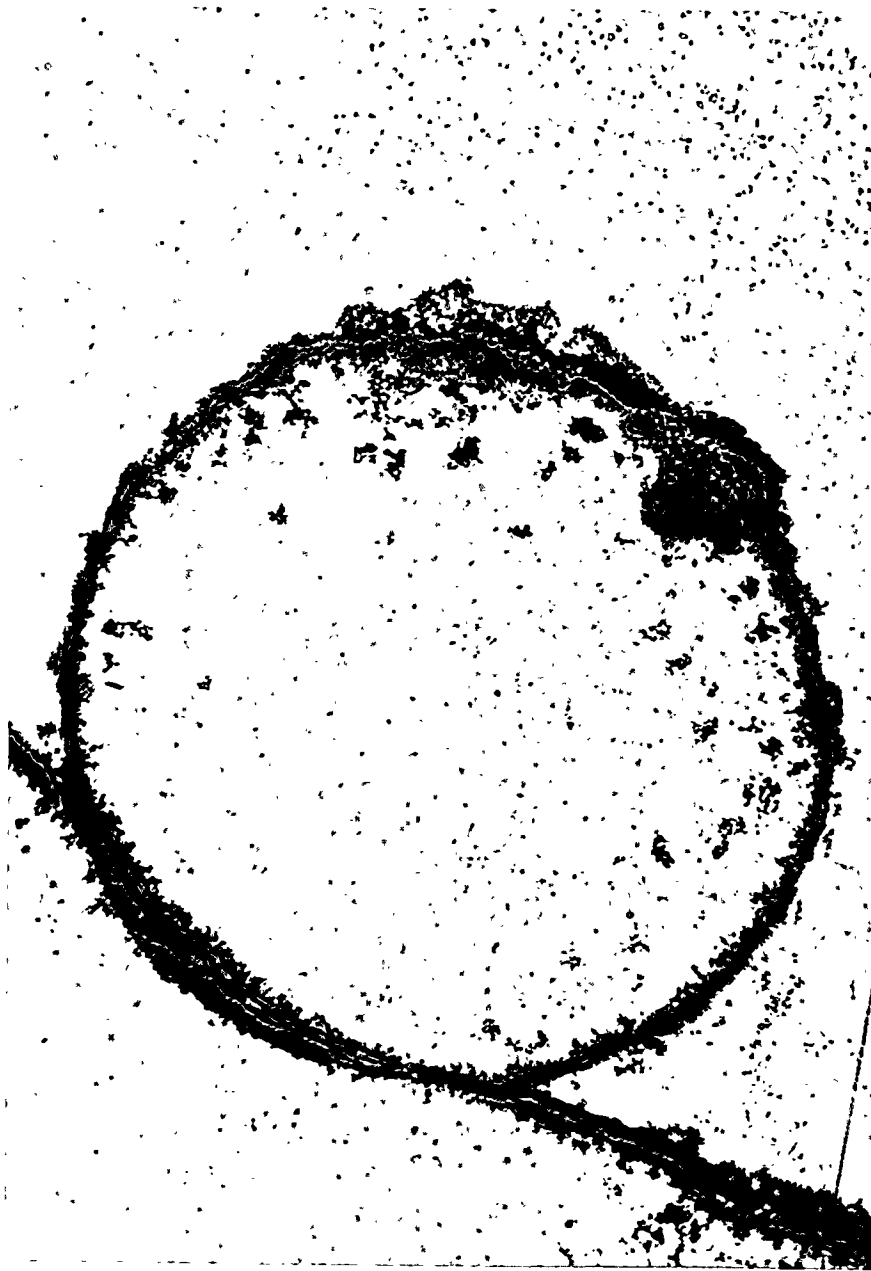


**Figure 4.9.2 - Cross Section of 0.005-inch Wire from Fine Fail-safe Mesh After 1329 hours at Karhula-700X**

## Results

---

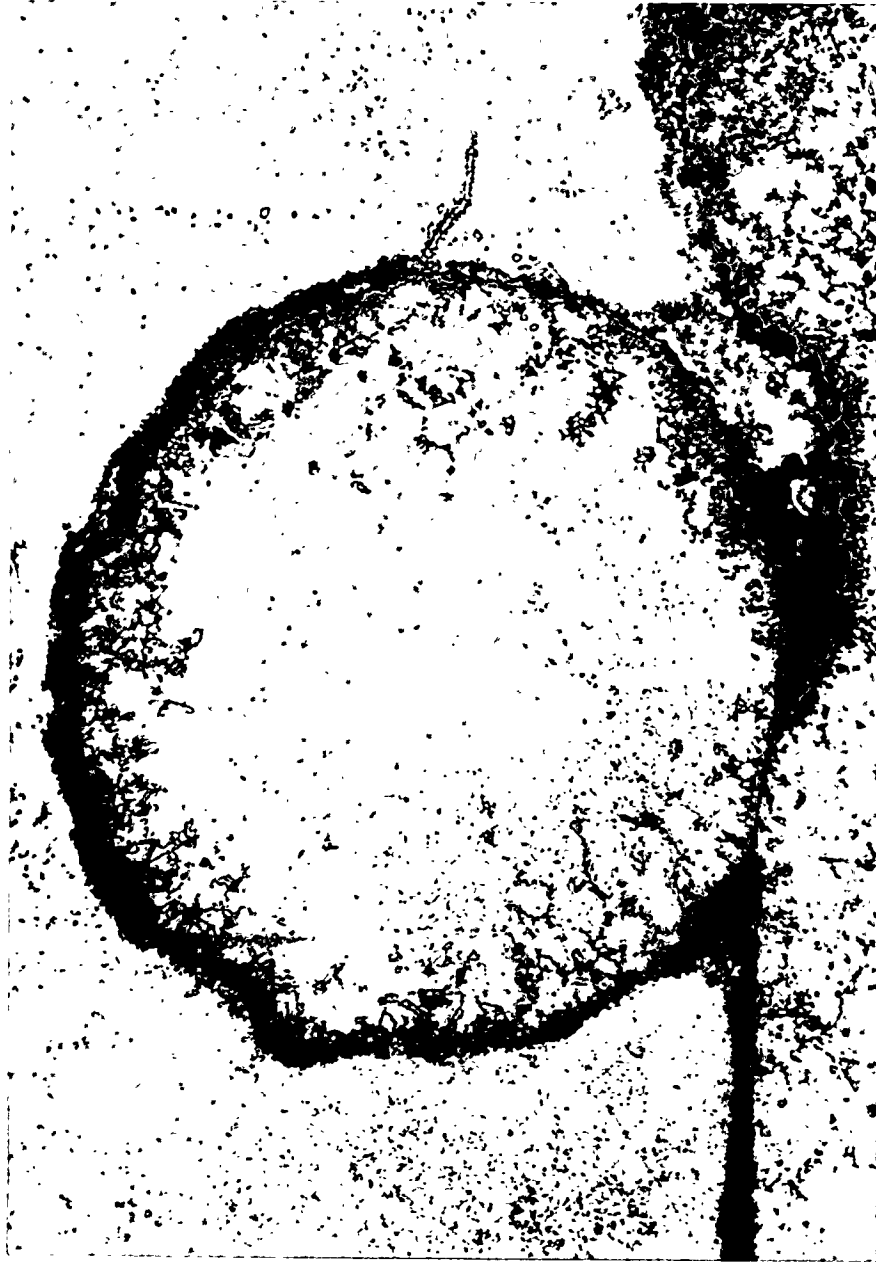


**Figure 4.9.3 - Cross Section of 0.005-inch Wire from Fine Fail-safe Mesh After 1110 hours at Tidd-700X**

## Results

---

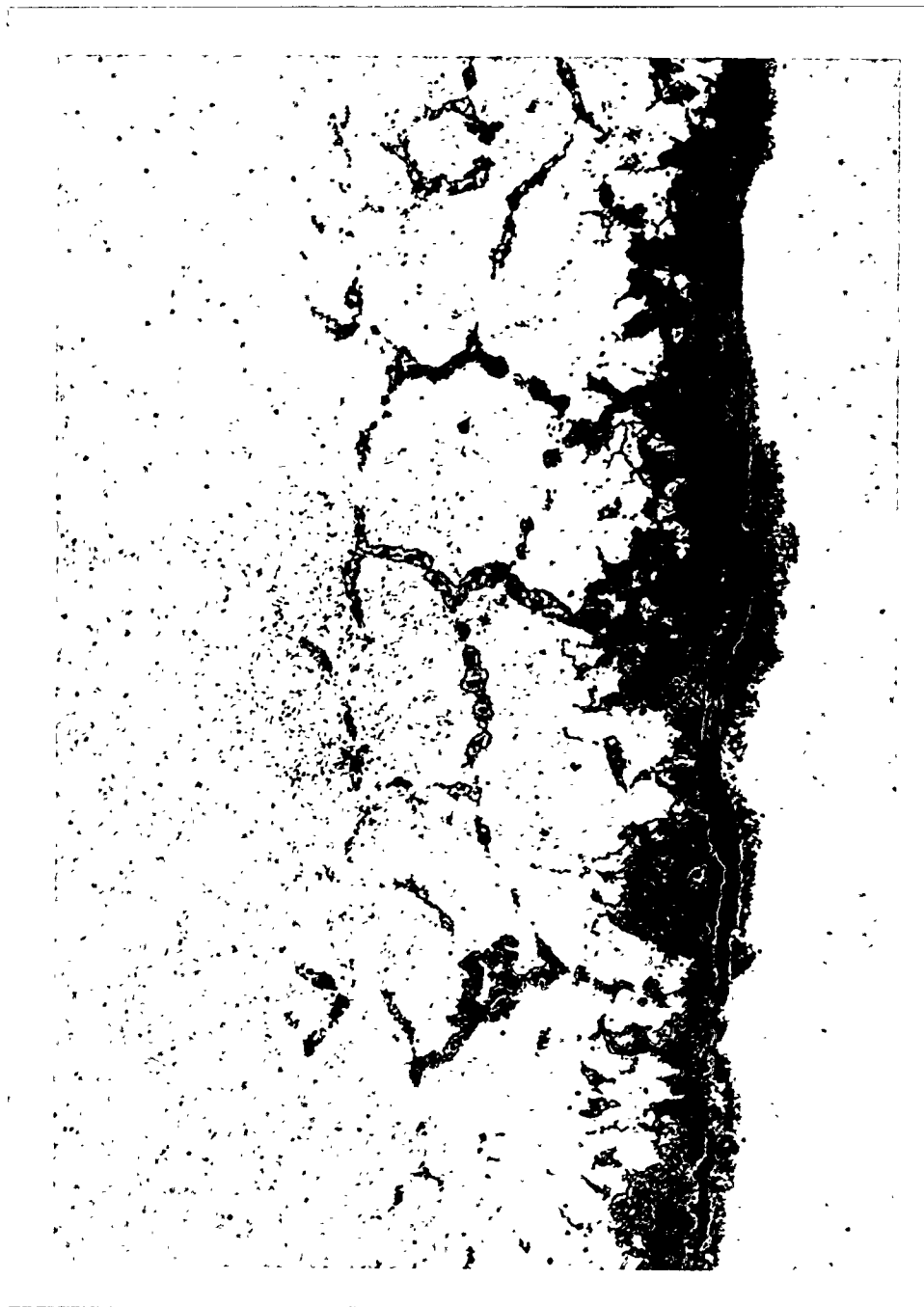


**Figure 4.9.4 - Cross Section of Alloy 333 Coupon-700X**

## Results

---



**Figure 4.9.5 - Cross Section of Alloy 617 Coupon-700X**

## Results

---

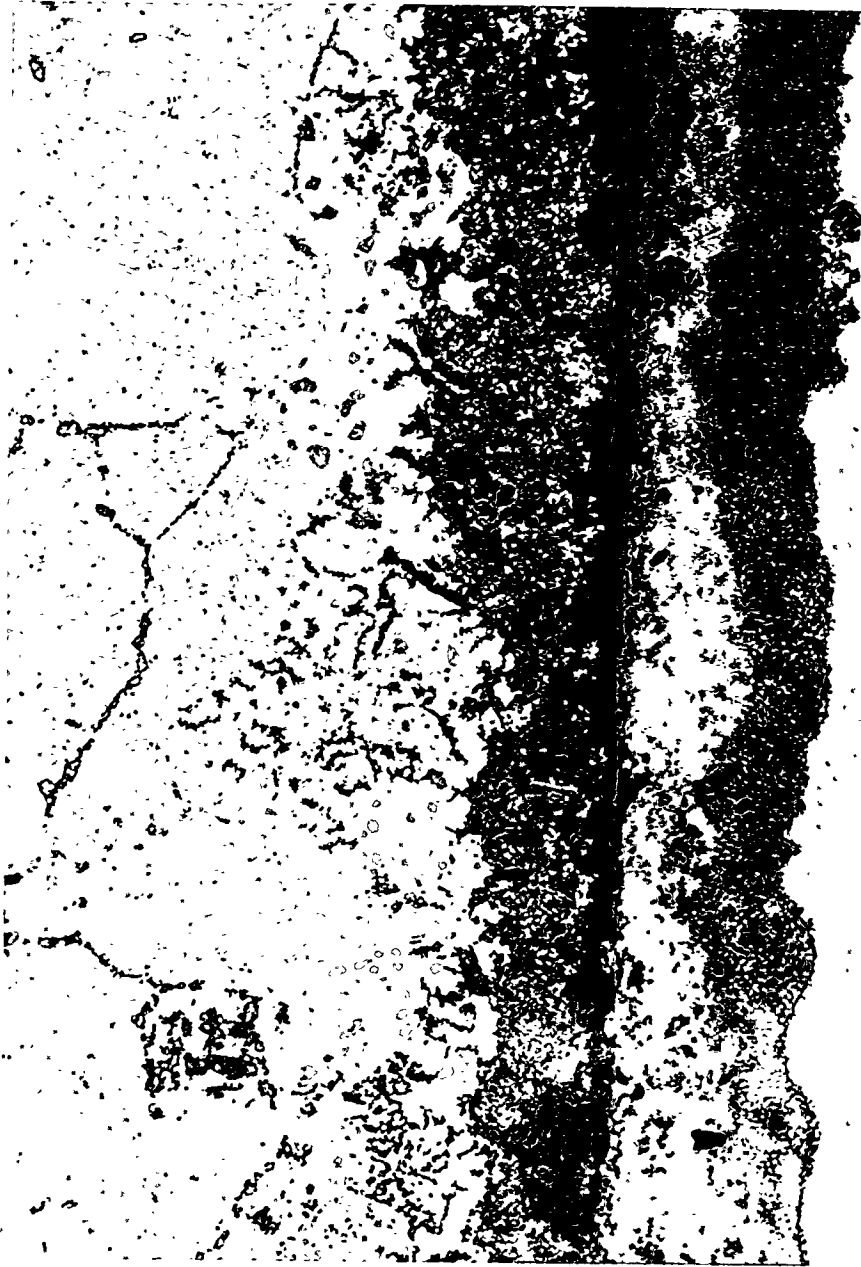


Figure 4.9.6 - Cross Section of Alloy 556 Coupon-700X

## Results

---

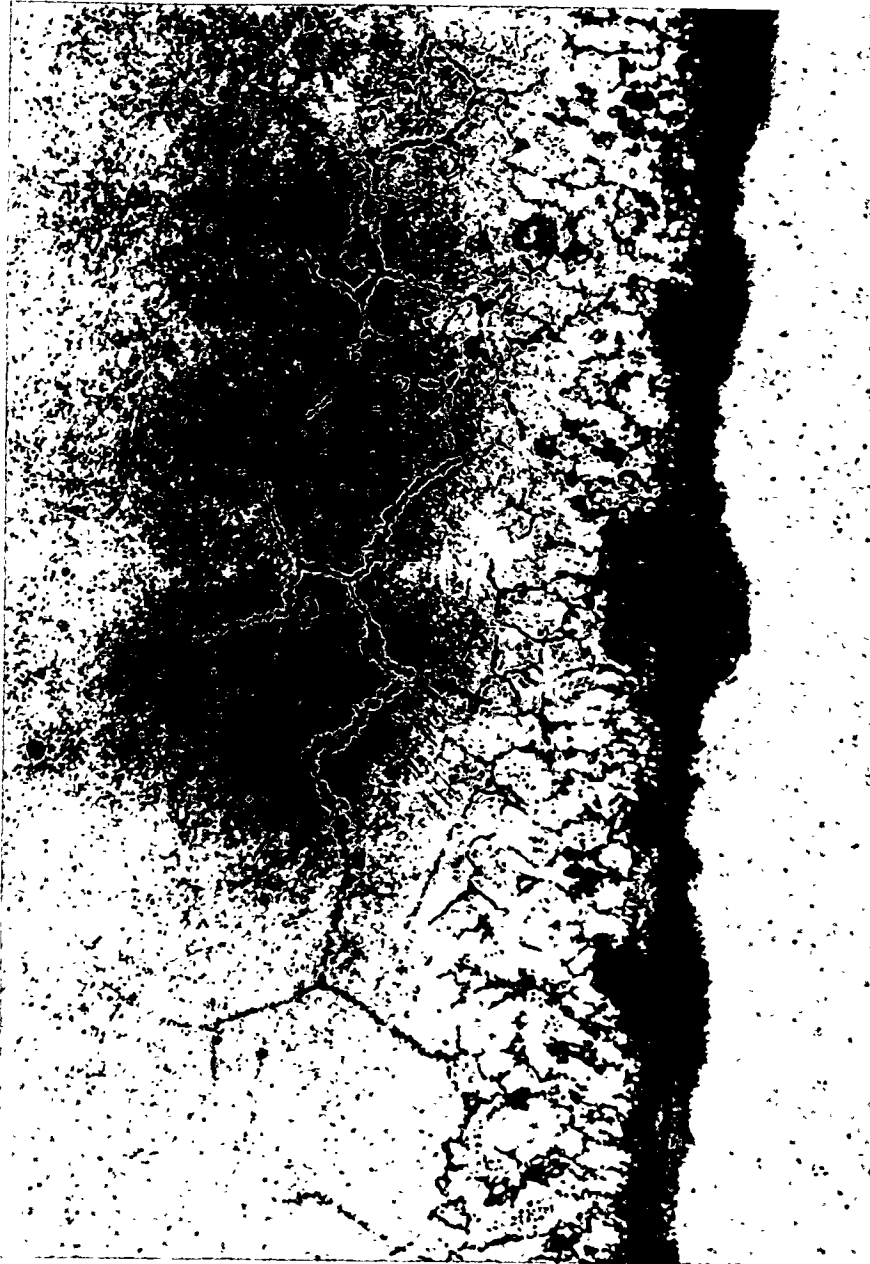


Figure 4.9.7 - Cross Section of Alloy 188 Coupon-700X

## Results

---

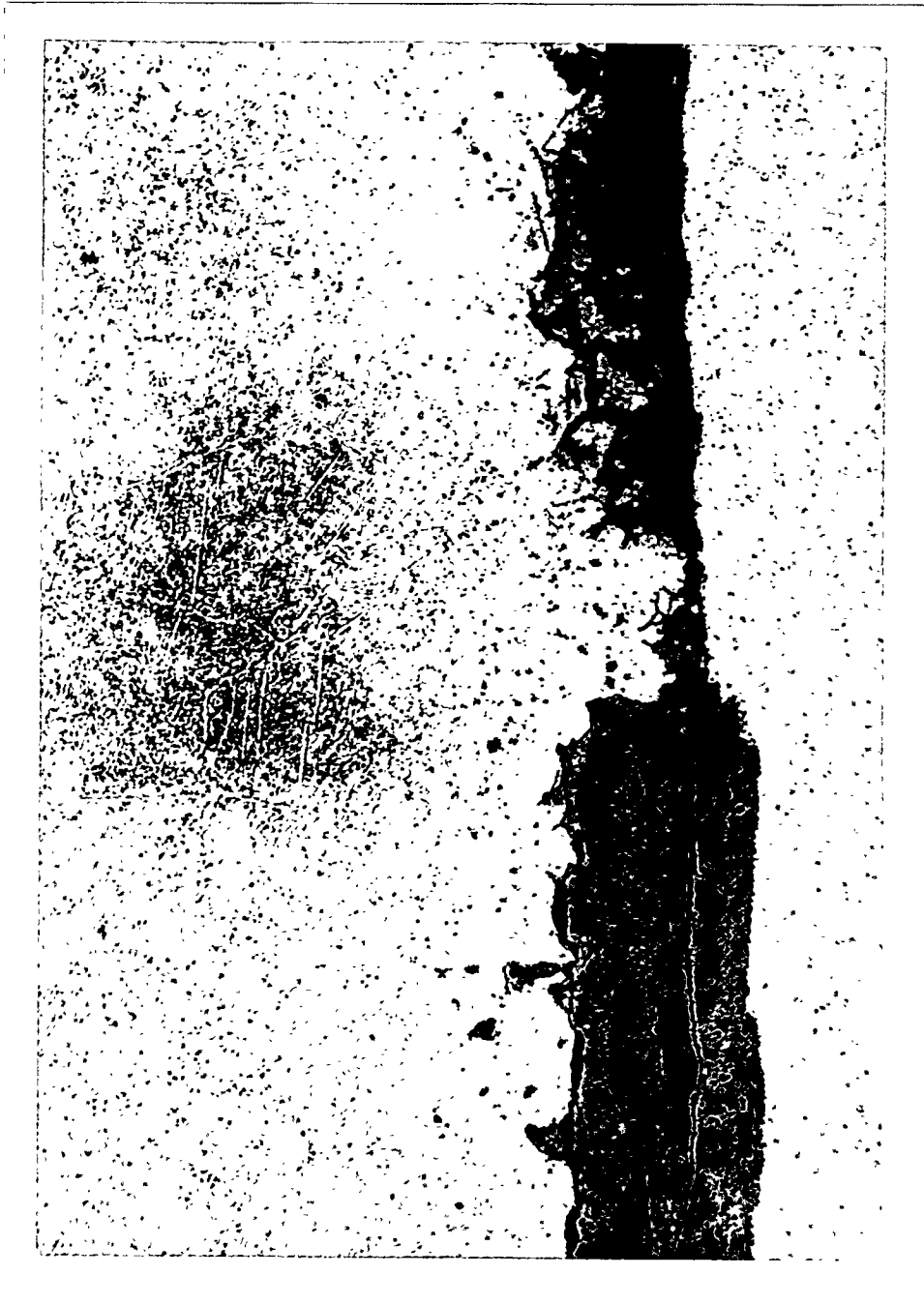
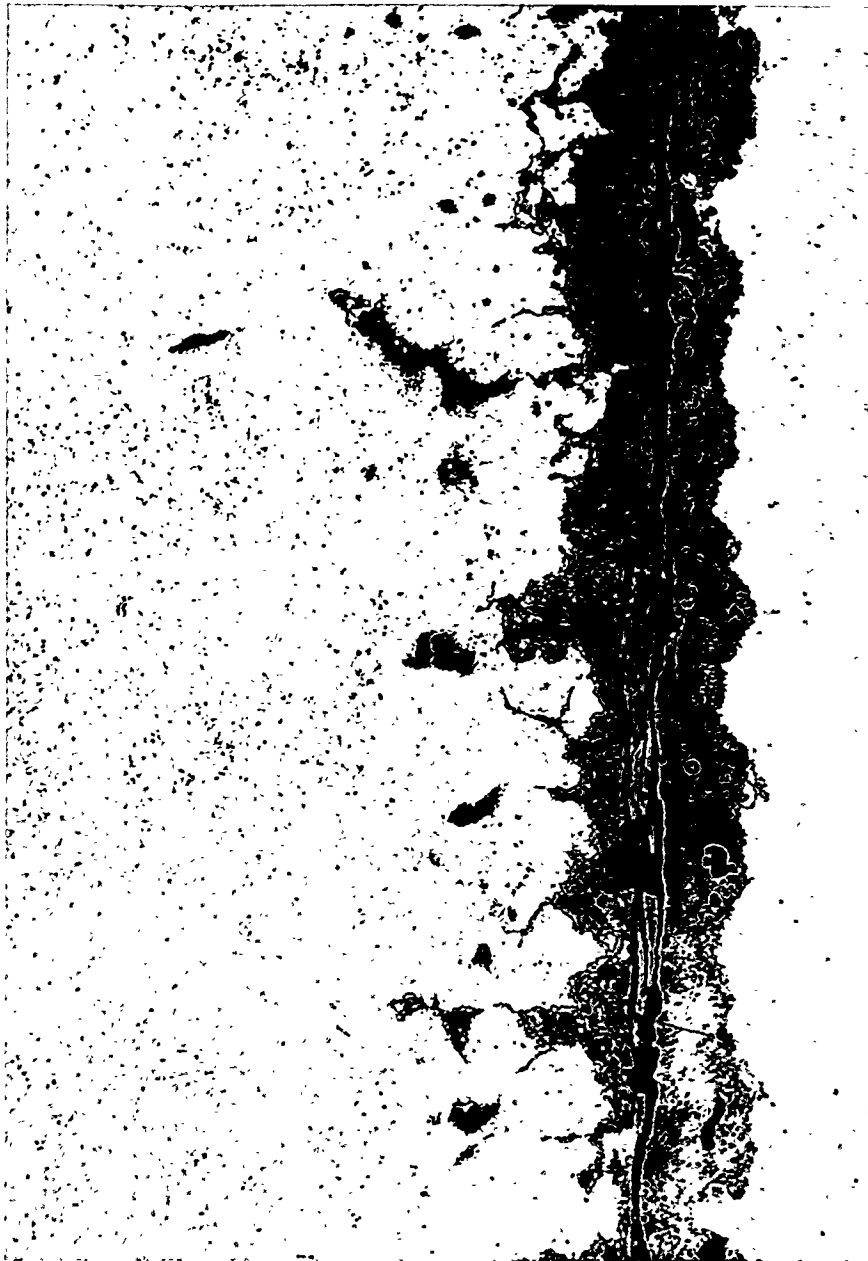


Figure 4.9.8 - Cross Section of Alloy 253MA Coupon-700X

## Results

---



**Figure 4.9.9 - Cross Section of Alloy 310 Coupon-700X**

## Results

---

### 4.9.2 Candle Filters

Westinghouse conducted material surveillance tests on selected candle filters throughout the HGCU program. This section presents a discussion of candle surveillance testing and summarizes the conclusions reached during the surveillance program.

All filter candles were subjected to a formal QA/QC program both at the supplier sites and at Westinghouse or Tidd Plant. The surveillance program included post-test non-destructive inspection and characterization of selected filter candle properties, such as gas flow resistance, measurements of creep and bow, and time-of-flight measurements. Destructive testing to determine residual bulk strength and morphological changes was also performed.

#### Filter Selection and Qualification

Throughout this program, it was the responsibility of the filter suppliers to meet defined material tolerance specifications for filter length, outer body diameter, flange diameter and length, concentricity, perpendicularity, gas flow resistance, and particle collection efficiency. Generally, re-inspection of filter elements either on an entire production batch or on a randomly selected basis was conducted prior to final selection and installation within the filter in order to confirm production quality and uniformity.

The material properties of the filter matrix defined the required composition, construction, porosity, membrane thickness and manner of its application in order to achieve a desired gas flow resistance, particle collection efficiency and bulk matrix strength. Similarly, the specific manufacturing process defined the component wall thickness, flange and end cap assembly, and final weight of an individual filter element. Post-manufacturing QA/QC testing frequently included a final visual inspection to screen for not only unwanted cracks, chips, voids and/or bumps, but also a smooth and uniform texture of the outer filter wall surface. Both bubble and/or burst testing were conducted by the suppliers to ensure the as-manufactured integrity of the filter element, and ultimately to identify and reject elements which had inherent cracks, flaws or an inadequately coated membrane surface, prior to shipment and installation.

As shown in Figure 4.9.10, current monolithic and advanced second generation candle filters have achieved acceptable gas permeability tolerances (i.e., 1 in. H<sub>2</sub>O / fpm at 70°F) for use in advanced coal-fired applications. Pre-qualification testing was frequently conducted at Westinghouse to assure that a

## Results

>99.99% particle collection efficiency was achieved by the filter elements at simulated steady-state PFBC process operating conditions, prior to acceptance for field use. Pre-qualification testing was designed to qualify the performance and integrity of filter elements under extreme conditions such as accelerated pulse cycling which monitors the performance of the matrix with respect to thermal fatigue, or exposure to thermal transient events which simulated rapid start-up or shut-down ramps experienced during process upset conditions. During pre-qualification testing, the as-manufactured strength of the flange was evaluated, and mechanical sealing and mounting of the element within the filter holder were assessed. Candle filters were required to have an as-manufactured bulk material strength of >1800 psi. During conduct of this program, residual or conditioned strengths of 800-1200 psi were observed after 3000-6000 hours of operation of the Schumacher Dia Schumalith F40 filters. The conditioned strength of the Schumacher filters was adequate to permit retention of the candle's physical integrity, and continued process operation of the filter elements.

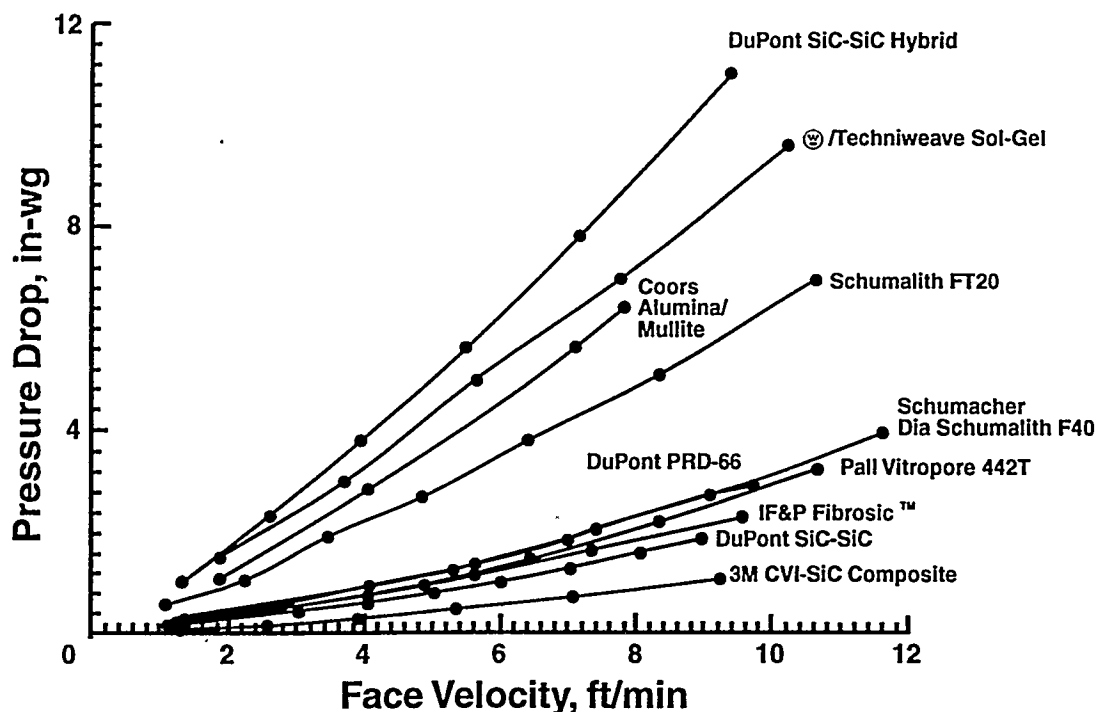


Figure 4.9.10 - Room Temperature Gas Flow Resistance of the First Generation Monolithic and Advanced Second Generation Candle Filters

## Results

---

### Posttest Inspection And Characterization

Filter elements were randomly subjected to posttest gas flow resistance measurements, overall length measurements to detect creep within the matrix, bow and/or perpendicularity measurements prior to conducting destructive testing which determined the residual bulk matrix strength, and phase and morphological changes that resulted within the filter matrix.

**Gas Flow Resistance Measurements.** During operation, fines accumulated along the surface of the candles which increased the pressure drop across the porous ceramic filter elements. In order to remove the collected dust cake layer, pulse gas was delivered to the ID of the candles, which permeated through the filter wall, releasing the deposited fines from the filter element surface. After each pulse cycle event, a conditioned layer of fines was expected to remain along the element, while the majority of the deposited ash was collected in the ash hopper.

Frequently, ash nodules 1 cm diameter x 0.5-1.0 cm high formed along the filter surface during operation. Similarly, continuous dust cake layers formed which ranged from 1-2 mm to 1-1.5 cm. When ash bridging events resulted within the filter array prior to detuning or bypassing of the primary cyclone, the nodules or dust cake layer were observed to be separated from the bridged mass of ash which formed between adjacent candles, or between candles and the plenum pipes or dust sheds.

As shown in Figure 4.9.11, the pressure drop or gas flow resistance through the filter element increased as fines collected and remained along the outer surface of the filter elements. Following normal operating conditions, the as-manufactured gas flow resistance was regenerated by simply washing the elements with water and drying. In the event that candles failed and process operation continued, fines released into the clean gas stream were pulsed back into the inner wall of the remaining intact filter elements. Posttest washing of these elements generally did not permit regeneration of the as-manufactured gas flow resistance, since the fines typically blinded the inner wall of the coarse support matrix. Since the ID fines generally could not be removed, the elements were eliminated for continued use.

## Results

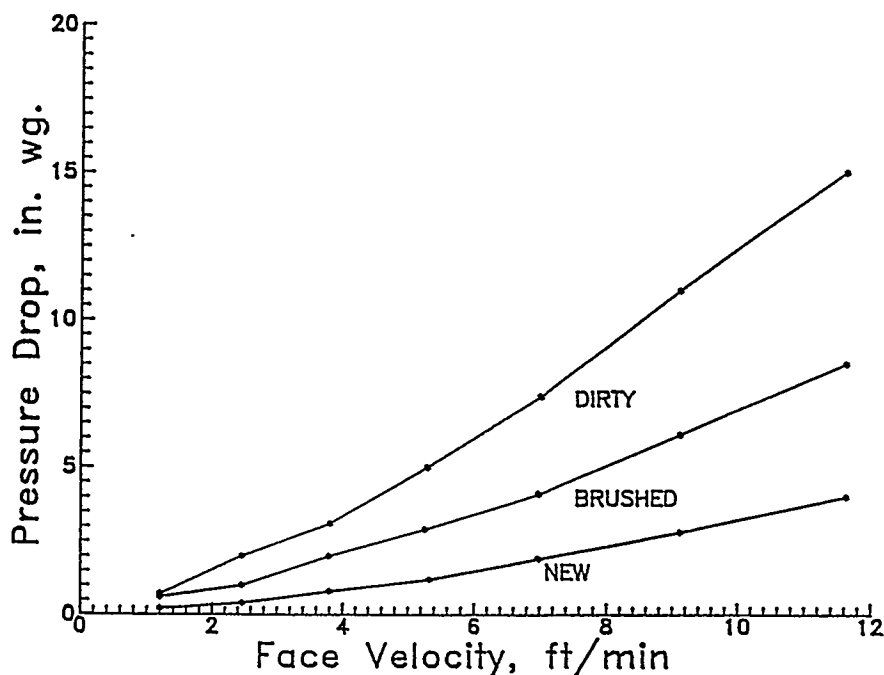


Figure 4.9.11 - Room Temperature Gas Flow Resistance Measurements Across As-Manufactured Clay Bonded Silicon Carbide Filter Elements. Measurements Were Repeated After Operation at Tidd.

**Bow and Creep Measurements.** During normal operation, overall straightness of the candle filters was maintained. When ash bridging events occurred within the filter, bowing of the clay bonded silicon carbide elements resulted (see Figure 4.3.8). Following 464 hours of operation in Test Period I, a maximum bow of 17 mm was observed along the length of the Schumacher Dia Schumalith F40 candle filter body. This significantly exceeded the 3 mm as-manufactured Westinghouse tolerance for allowable bow.

Bowing which occurred in the clay bonded silicon carbide filters resulted from softening or plastic deformation of the binder in the Schumacher Dia Schumalith F40 filter matrix when it was subjected to an applied load. In addition to bowing, softening of the binder phase resulted in the elongation of the filters during operation as shown in Table 4.9.3. The extent of elongation of either the Schumacher Dia

## Results

Schumalith F40 or Pall Vitropore 442T clay bonded silicon carbide candles was not sufficient to fail the elements through the creep crack growth mechanism that had been identified for the Pall Vitropore 442T elements during operation in Ahlstrom's pressurized circulating fluidized-bed combustion test facility.

**Time-Of-Flight and Burst Strength Measurements.** During this program, Westinghouse focused its efforts on conducting a filter material surveillance program which monitored the residual bulk strength and phases present within the various elements after each Test Period. After Test Period I, time-of-flight (TOF) measurements were also performed on 32 filters prior to subjecting select filter elements to destructive materials characterization. As shown in Table 4.9.4, with the exception of two candles, each filter element experienced an increase in its TOF measurement after exposure to the Tidd operating conditions. Although ash and sorbent fines remained along the surface of the candles (i.e., a portion of the non-removable conditioned layer) and through the filter wall (i.e., ID wall pulse cycled fines) after each element had been vacuumed brushed, the presence of fines did not appreciably impact the resulting TOF measurements.

**Table 4.9.3 - Elongation of Clay Bonded Silicon Carbide Candle Filters**

Filter Type	Test Period	Operating Time, Hours	Elongation, mm
Schumacher F40	I	464	1
	I, II, III, IV	4744	3
	I, II, III, IV, V	5854	5-7
Pall Vitropore 442T	IV	1706	ND
	IV, V	2816	17-20
	V	1110	0-4

ND: Not Determined.

## Results

**Table 4.9.4 - Posttest Candle Filter Time-Of-Flight Measurements**

Candle	Position	Tag Number	TOF, $\mu$ sec				
			Initial	Vacuumed Brushed	$\Delta$ TOF	Vacuumed Brushed Washed/Dried	$\Delta$ TOF
1	A/T-1 *	492	330	337	7	337	7
2	B/T-1 *	504	332	339	7	331	-1
3	B/T-23	459		338		333	
4	A/M-1 *	367	332	340	8	339	7
5	B/M-1 *	436	336	343	7	343	7
6	B/M-23	244		344		334	
7	A/B-5 *	028	343	353	10		
8	A/B-6 *	065	348	362	14		
9	A/B-7 *	019	340	356	16		
10	A/B-8 *	083	339	342	3		
11	A/B-16 *	075	343	351	8		
12	A/B-17 *	172	342	349	7		
13	A/B-18 *	164	338	347	9	346	8
14	A/B-19 *	002	339	353	14		
15	A/B-35 *	056	346	357	11		
16	A/B-36 *	071		352		351	
17	B/B-1 *	193	323	335	12	334	11
18	B/B-5 *	343	345	356	11		
19	B/B-6 *	297	334	341	7		
20	B/B-7 *	115	335	340	5		
21	B/B-8 *	238	331	339	8		
22	B/B-16 *	089	350	342	-8		
23	B/B-17 *	328	339	344	5		
24	B/B-18 *	253	335	344	9	346	11
25	B/B-19 *	213	323	342	19		
26	B/B-34	127		340			
27	B/B-45	106		348			
28	C/B-5	187		347			
29	C/B-6 *	178	333	344	11		
30	C/B-7 *	129	347	356	9		
31	C/B-17 *	314	332	338	6		
32	C/B-18 *	097	351	345	-6	347	-4

\* Initial Surveillance Candles.

## Results

As shown in Figure 4.9.12, a direct correlation between room temperature C-ring compressive and burst strength of the 464 hr PFBC-exposed clay bonded silicon carbide filter matrix resulted particularly for candles that were located in a common cluster or location within the system. As the TOF value for a given filter element increased, the room temperature C-ring compressive strength of the clay bonded silicon carbide filter matrix decreased, again for candle filters that were located in a common cluster. Cluster A candles and the bowed Cluster B candles tended to deviate from the TOF/C-ring compressive and burst strength/C-ring compressive relationship.

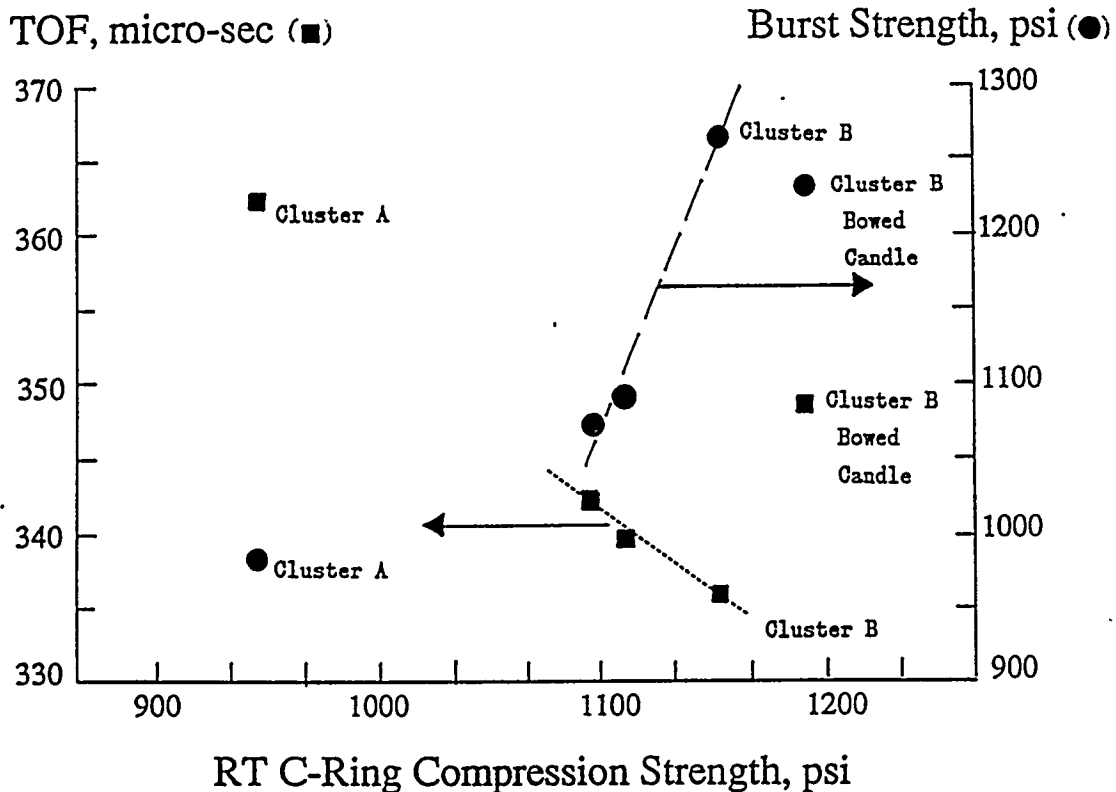


Figure 4.9.12 - Correlation of Time-of-Flight and Burst Strength with Room Temperature C-Ring Compressive Strength for Candle Filters Exposed for 464 Hours of PFBC Operating Conditions in Test Period I.

## Results

Table 4.9.5 lists the number of each type of candle filter used in the five test periods. First generation, monolithic, Schumacher Dia Schumalith F40 clay bonded silicon carbide candle filters were primarily used during the first four test periods. During the last two test periods, advanced, second generation candle filter elements were used.

With the exception of ash bridging which failed the filter elements, the stability and long-term viability of the "aged" or "conditioned" candle filter materials were demonstrated during operation in the PFBC gas environment. A summary of the residual strength, microstructural and phase changes which occurred during operation of the first and second generation candle filter materials is presented in this section. Table 4.9.6 presents a summary of the candle filter failure mechanisms experienced during operation at Tidd.

**Schumacher Dia Schumalith F40.** The Schumacher Dia Schumalith F40 filter matrix consists of an aluminosilicate binder phase that encapsulates and bonds together silicon carbide grains, forming 40-50  $\mu\text{m}$  pores within a 15-mm thick support wall. An  $\sim 100 \mu\text{m}$  thick, aluminosilicate fibrous membrane is applied to the outer surface of the filter body, in order to prevent fines penetration into and/or through the porous ceramic filter wall. During test operation, the integrity of the membrane was retained, imparting complete barrier filtration characteristics to the Schumacher Dia Schumalith 40 filter matrix.

**Table 4.9.5 - Filter Candle Materials**

Test Period	I	II	III	IV	V
Type of Filter	Number of Filter Elements				
Schumacher F40	384	384	384	258	5
Schumacher FT20	—	—	—	8	—
Pall Vitropore 442T	—	—	—	8	153
Coors Alumina/Mullite	—	—	—	8	98
3M CVI-SiC Composite	—	—	—	3	10
DuPont PRD-66	—	—	—	3	22

## Results

**Table 4.9.6 - Candle Filter Failure Mechanisms Experienced During Operation at Tidd**

Filter Element	Maximum Hours of Operation/ (Test Period)	Failure Mechanism	Comments
Schumacher Dia Schumalith F40	5854 (I, II, III, IV, V)	Ash Bridging	Maximum elongation of 5-7 mm; Reduction of strength; Conditioned strength of 800-1200 psi; Binder crystallization; Bowing under load; Failure at base of the flange during bridging; Failure along end cap when ID filled with ash
Schumacher Dia Schumalith FT20	1706 (IV)	None-Experienced	Improved high temp. creep resistant binder; No loss of strength identified
Pall Vitropore 442T	2816 (IV, V)	None-Experienced	Maximum elongation of 17-20 mm; Strength reduction
Coors Alumina/Mullite	2816 (IV, V)	Possible Thermal Fatigue	Mid-body or failure at the base of the flange for isolated elements; End cap failure when ID filled with ash; Loss of strength experienced at elevated operating temperatures
3M CVI-SiC	1706 (IV)	Ash Bridging	Failure at the base of flange during bridging; Failure along end cap when ID filled with ash; Apparent strength increase due to fines filling matrix wall
DuPont PRD-66	1706 (IV)	Divot Formations Mid-Body Failure	Failure occurred at the base of the flange when ash encapsulated the filter holder mount; Body thinned where divots formed; Divots may be responsible for mid-body fracture; Apparent strength increase due to fines filling matrix wall; Minimal adherence of ash along outer filtration surface; Bridging and ash ID bore filling did not cause failure

## Results

Within the entire candle filter assembly, generally 5-16% of the Schumacher Dia Schumalith F40 filter elements failed during operation in Test Periods I through IV, primarily as a result of ash bridging. After removal of the primary cyclone from service in Period V, ash bridging, as well as candle failure were mitigated. Schumacher Dia Schumalith F40 surveillance candles, however, successfully achieved 5854 hours of operation. The residual bulk strength of the Schumacher Dia Schumalith F40 matrix was determined via room temperature and process temperature C-ring compressive and tensile testing. As shown in Figure 4.9.13, the process temperature bulk strength of the Schumacher Dia Schumalith F40 matrix decreased during the initial 1000-2000 hours of PFBC operation. With continued operation, however, the bulk strength of the Schumacher Dia Schumalith F40 matrix remained constant. The residual or "conditioned" strength was considered to result from the complete or nearly complete crystallization of the binder phase that encapsulated the silicon carbide grains, as well as the bond posts or ligament surfaces as shown in the photo micrograph in Figure 4.9.14.

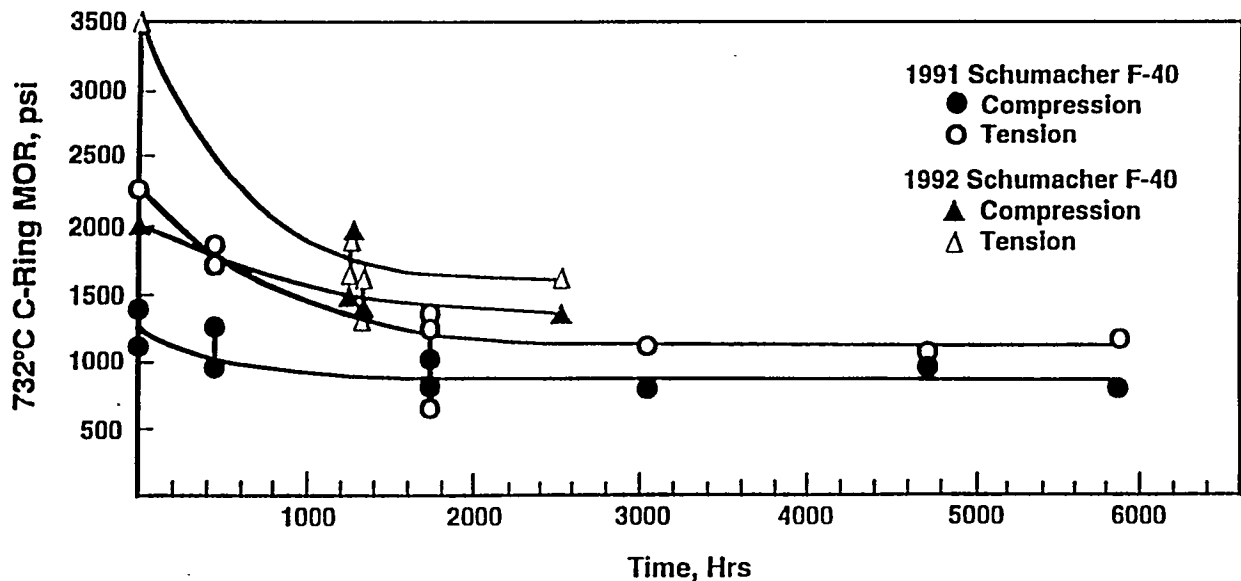


Figure 4.9.13 - Schumacher Strength Profile

## Results

---

Previous use of alternate clay bonded silicon carbide candle filters indicated that creep crack growth occurred primarily at the base of the flange, and failure of the elements resulted after 500-1000 hours of operation in ~ 1525F, circulating pressurized fluidized-bed combustion environment. In order to ascertain whether the Schumacher Dia Schumalith F40 filter matrix experienced creep during operation, the overall lengths of the surveillance filter elements were measured after the various test campaigns, and compared to their initial, as-manufactured lengths. After 5854 hours of operation, two surveillance filters were observed to have elongated by 5-7 mm. Cracks as a result of high temperature creep were not evident along the external surface of the filter elements, particularly within and/or below the densified section of the flange.

**Pall Vitropore 442T.** The Pall Vitropore 442T matrix also consists of silicon carbide grains that are bonded together via an oxide-based binder to form the 10 mm filter support wall. A finer grit silicon carbide layer is applied to the outer surface of the filter element, forming the barrier filter's membrane. During Test Period IV, eight Pall Vitropore 442T, clay bonded silicon carbide candle filters were installed and operated in the system. Similar to the "conditioning" experienced by the Schumacher Dia Schumalith F40 filters, the Pall Vitropore 442T clay bonded silicon carbide filters experienced a loss of bulk material strength after 1706 hours of operation in the PFBC gas environment as shown in Table 4.9.7.

Three of the Pall Vitropore 442T filter elements which had been used during Test Period IV were reinstalled and acquired an additional 1110 hours of operating life in Test Period V. Post-test inspection indicated that the 2816 hour PFBC-exposed Pall Vitropore 442T filters elongated by 17-20 mm. Cracks which are an indication of high temperature creep were not evident along the external surface of the filter elements, particularly in the area of the filter directly below the flange.

During Test Period V, 150 new Pall Vitropore 442T candle filter elements were installed in the APF. All candles remained intact after 1110 hours of operation. Posttest characterization of seventeen elements indicated that the filters elongated by 0-4 mm. Since all of the Pall Vitropore 442T filter elements had been identically manufactured, the difference in elongation which resulted between the two test periods was considered to reflect "aging" or the time lag required to initiate high temperature creep in the Vitropore 442T clay bonded silicon carbide candle filter matrix.

## Results

### Table 4.9.7 - Candle Filter Bulk Matrix Strength

Filter ID No.	Filter Location	Test Period No.	Operating Time, Hrs.	Room Temperature Strength, psi C-Ring Testing		High Temperature (732°C) Strength, psi C-Ring Testing	
				Compression	Tension	Compression	Tension
Schumacher Dia Schumalith F40 - 1991 Production Lot				Compression	Tension	Compression	Tension
S153/317B	—	—	—	1300±213	1907±111	1416±127	2328±228
S504/322B	B/T-1	I	464	1120±123		1226±116	
S436/321B	B/M-1	I	464	1096±116		1172±134	
S193/318B	B/B-1	I	464	1147±119		1245±108	
S065/314B	A/B-6	I	464	940±60		1056±131	
S106/317B	B/B-45	I	464	1180±98		1230±127	
S324/319B	B/B-9	I	464	1083±148	1438±108	1137±101	1778±246
S109/317B	B/B-41	I	464	1140±120	1424±162	1132±112	1873±174
S215/378B	B/M-22	I, II	1760	908±72	1117±91	1064±72	1418±122
S447/322B	A/T-22	I, II	1760	794±50	709±71	1028±94	973±121
S455/322B	B/T-22	I, II	1760	793±58	711±89	989±77	885±54
S523/322B	C/T-22	I, II	1760	793±39	1016±134	968±96	1252±241
S418/321B	B/T-16	I, II, III	3038	720±57	944±172	890±65	1284±199
S422/322B	B/B-16	I, II, III, IV	4734	870±145	816±112	1031±105	1139±160
S228/318B	A/T-16	I, II, III, IV, V	5854	592±56	763±87	777±57	1208±99
						891±52(a)	966±47(a)
Schumacher Dia Schumalith FT20							
S199/315E	—	—	—	2296±261	2268±167	3034±148	2708±360
S039/312E	C/M-15	IV	1706	2283±184	2370±238	3041±238	3102±272
Pall Vitropore 442T							
R2-325	—	—	—	2857±186	2574±177	3430±221	3029±149
R5-325	B/M-20	IV	1706	2311±231	2034±139	2453±187	2138±180
R2-360	C/T-1	V	1110	2569±132	2277±156	2721±138	2201±212
						2454±214(a)	2115±238(a)

## Results

### Table 4.9.7 - Candle Filter Bulk Matrix Strength (Cont'd.)

Filter ID No.	Filter Location	Test Period No.	Operating Time, Hrs.	Room Temperature Strength, psi C-Ring Testing		High Temperature (732 °C) Strength, psi C-Ring Testing	
				Compression	Tension	Compression	Tension
<b>Coors Alumina/ Mullite</b>				Compression	Tension	Compression	Tension
DC-013	—	—	—	2575 ± 182	2721 ± 415	3107 ± 276	3353 ± 231
DC-003	B/M-16	IV	1706	2475 ± 189	2903 ± 289	2738 ± 161	3291 ± 246
DC-056	A/T-17	V	1110	2079 ± 140	2392 ± 130	2368 ± 93	2636 ± 238
						2512 ± 107(a)	2717 ± 167(a)
DC-068	A/T-1	V	1110	1958 ± 68	2544 ± 214	1800 ± 135	2542 ± 196
						2079 ± 85(a)	2659 ± 109(a)
DC-002	B/M-17	IV, V	2816	2097 ± 119	2063 ± 178	2200 ± 141	2146 ± 362
						2360 ± 116(a)	2287 ± 251(a)
<b>DuPont PRD-66</b>							
D-99	—	—	—	1219 ± 162	1265 ± 188	1277 ± 178	1304 ± 327
D-132	B/M-7	IV	1706	1830 ± 238	1725 ± 320	1884 ± 142	1642 ± 401
D-237	B/M-8	V	1110	1533 ± 202	1380 ± 188	1897 ± 256	1356 ± 104
						1872 ± 230(a)	1460 ± 197(a)
<b>Diametral O-Ring Testing</b>							
Filter ID No.	Filter Location	Test Period No.	Operating Time, Hrs.	Room Temperature Strength, psi		High Temperature (732 °C) Strength, psi	
				Composite	Triaxial Braid	Composite	Triaxial Braid
<b>3M CVI-SiC Composite</b>							
43-1-2	—	—	—	1341 ± 254	14026 ± 2012	1060 ± 219	11012 ± 1795
43-1-6	B/M-15	IV	1706	1696 ± 195	18220 ± 1356	1429 ± 159	15599 ± 2246
45-18-02	C/T-18	V	1110	2333 ± 415	18975 ± 3117	2225 ± 361	18001 ± 3745
						1850 ± 299(a)	16173 ± 2245(a)

(a) High Temperature Strength Testing Conducted at 843 °C

## Results

---

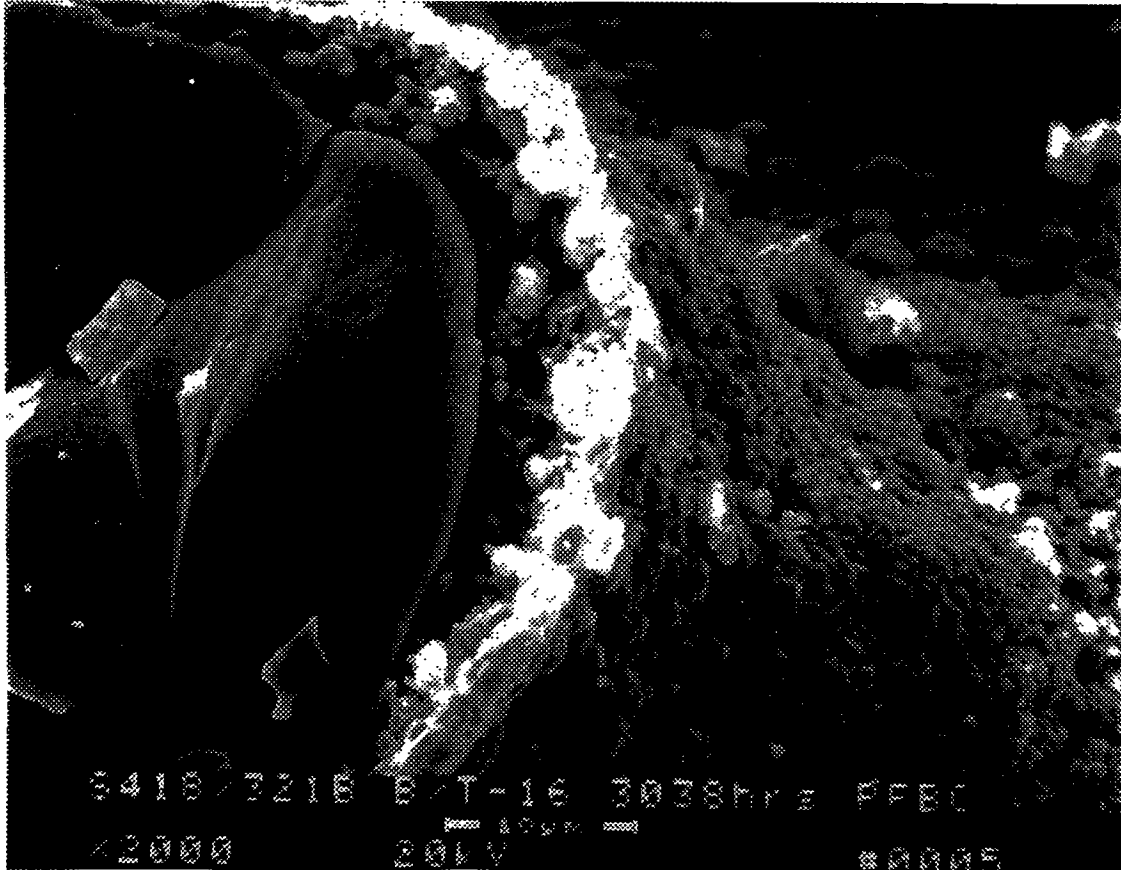


**Figure 4.9.14 - Photo Micrograph Showing Crystallization of the Schumacher Dia Schumalith F40 Filter Matrix**

## Results

---

**Schumacher Dia Schumalith FT20.** Eight improved, high temperature, creep resistant Schumacher Dia Schumalith FT20 clay bonded silicon carbide candles were installed and operated during Test Period IV. The initial bulk strength of the 10-mm wall Schumacher Dia Schumalith FT20 matrix was comparable to the higher strength, 15-mm wall, Schumacher Dia Schumalith F40 filters which had been manufactured in 1992. As shown in Table 4.9.7, the residual bulk strength of the Schumacher Dia Schumalith FT20 matrix after 1706 hours of operation was comparable to that of the initial bulk strength of the filter matrix.

**Coors Alumina/Mullite.** In contrast to the clay bonded silicon carbide candle filters, the alumina/mullite matrix consists of mullite rods that are embedded within an amorphous phase that contains corundum ( $Al_2O_3$ ) and anorthite ( $CaAl_2Si_2O_8$ ). Eight Coors filters were used during Test Period IV. All Coors filter elements remained intact after 1706 hours of operation. The residual bulk strength of the 1706 hour PFBC-exposed Coors filter matrix was comparable to that of the as-manufactured filter matrix as shown in Table 4.9.7.

Three of the Test Period IV Coors filters were reused during test Period V. Post-test inspection indicated that all three of the Coors filters remained intact, achieving 2816 hours of successful operation. In addition, 95 newly manufactured Coors filters were installed for Test Period V. After 1110 hours of operation, two filters failed, while the remaining Coors filters remained intact. One of the Coors filters failed directly below the flange, while the second filter fractured at approximately 1000 mm below the flange.

Characterization of the residual bulk strength of the 1110 hour, PFBC-exposed, Coors alumina/mullite filter elements indicated that they lost strength during operation in the 1400-1550F, oxidizing environment. This implied a sensitivity of the alumina/mullite matrix to higher process operating temperatures which may either induce or accelerate phase changes, or enhance crack propagation properties along the ID surface and/or through the 10 mm filter wall. A further reduction of residual bulk strength along the ID surface and/or through the filter wall was exhibited within the Coors filter matrix after 2816 hours of operation (Test Periods IV and V).

As shown in Figures 4.9.15 and 4.9.16, extensive mullitization resulted along the pore cavity wall of the Coors alumina/mullite filter matrix as both operating time and process temperature increased. As determined by qualitative x-ray diffraction analysis, minor dissociation of mullite that was present in the as-manufactured Coors filter matrix was initiated early during process operation. Simultaneously a

## Results

---

reduction and/or depletion of the as-manufactured anorthite and glass phases resulted, leading to the production of trace and minor concentrations of alumina, cordierite and cristobalite within the bulk matrix. Retention of the bulk matrix strength with time will largely depend on the rate of cristobalite and cordierite grain growth, which could ultimately lead to the formation of microcracks and loss of material strength. Since phase conversion appears to have stabilized within the first 1100 hours of operation, additional microcrack formation and/or loss of bulk material strength would be attributed to thermal fatigue (i.e., increased pulse intensity or duration) and/or thermal shock of the Coors alumina/mullite filter matrix during high temperature PFBC process operation.

**3M CVI-SiC Composite.** The 3M Chemical Vapor Infiltration-Silicon Carbide (CVI-SiC) composite filter consists of three layers – an outer open mesh confinement layer, a middle filtration mat, and an inner triaxial braided fabric layer which forms the structural support matrix of the filter element. Within the confinement and filtration mat layers, an 1-2  $\mu\text{m}$  layer of silicon carbide encapsulates Nextel 312 or alumina-based fibers, while an 100  $\mu\text{m}$  layer of silicon carbide is deposited along the Nextel 312 triaxial braid in the support matrix.

Three 3M CVI-SiC composite filters were used during Test Period IV, and after 1015 hours of operation, two of the elements failed at the base of their flange due to ash bridging. The third 3M filter element, which remained intact, achieved 1706 hours of operation prior to termination of Test Period IV. Post-test, room temperature, gas flow resistance measurements of the intact 3M filter indicated that the pressure drop across the element was 220 in-wg at a gas face velocity of 10 ft/min. The room temperature pressure drop across the ash coated 3M filter was relatively high in comparison to alternate filter elements which were exposed to similar PFBC test conditions. The high pressure drop across the candle filter was attributed to the adherence of the dust cake layer along and within the confinement layer, as well as through the filtration mat, and triaxial support braid.

Characterization of the 3M CVI-SiC matrix via scanning electron microscopy/energy dispersive x-ray analysis indicated that minor changes in the morphology of the filter matrix had occurred after 1705 hours of operation in the 1225-1400F temperature range. Due to deposition of the thin  $<1 \mu\text{m}$  interface coating, it was frequently difficult to discern whether the interface coating had remained intact. A gap or separation was considered to exist between the CVI-SiC coating and the underlying Nextel 312 fibers in several areas of the PFBC-exposed 3M composite filter matrix. In the high temperature PFBC environment, oxidation of the interface coating is expected to occur.

## Results

---

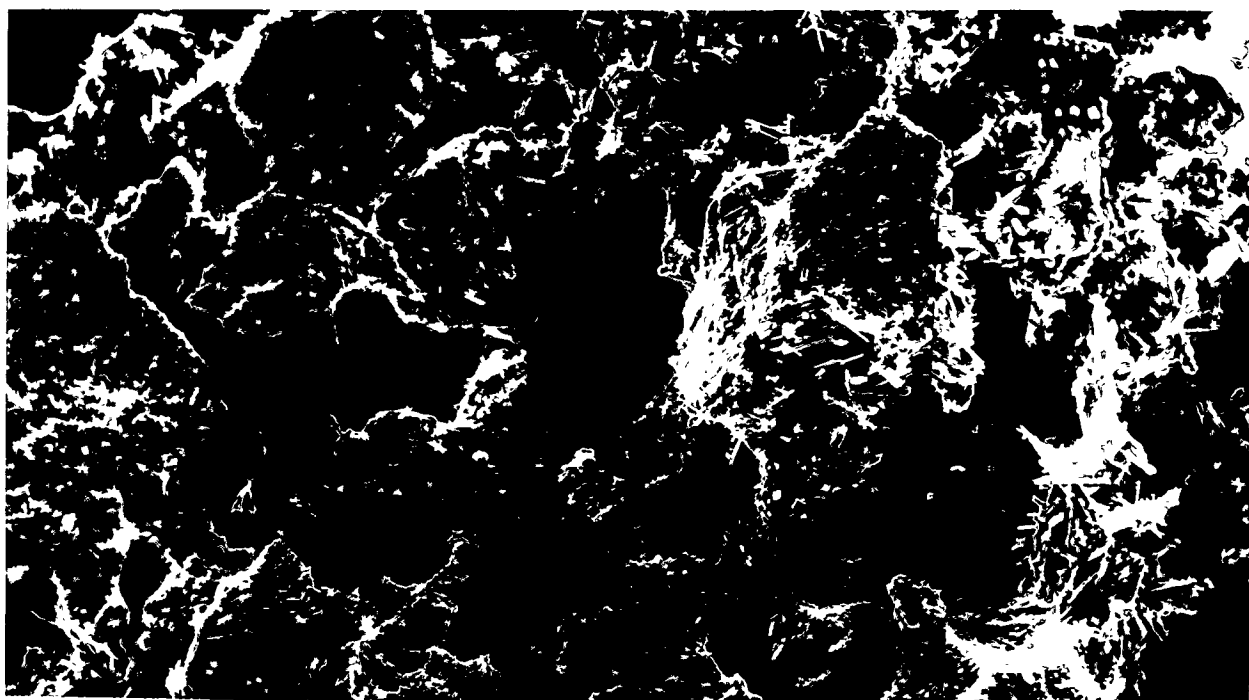


**Figure 4.9.15 - Crystallization of the Coors Alumina/Mullite Filter Matrix after 1110 hrs of Operation in Test Period IV**

## Results

---

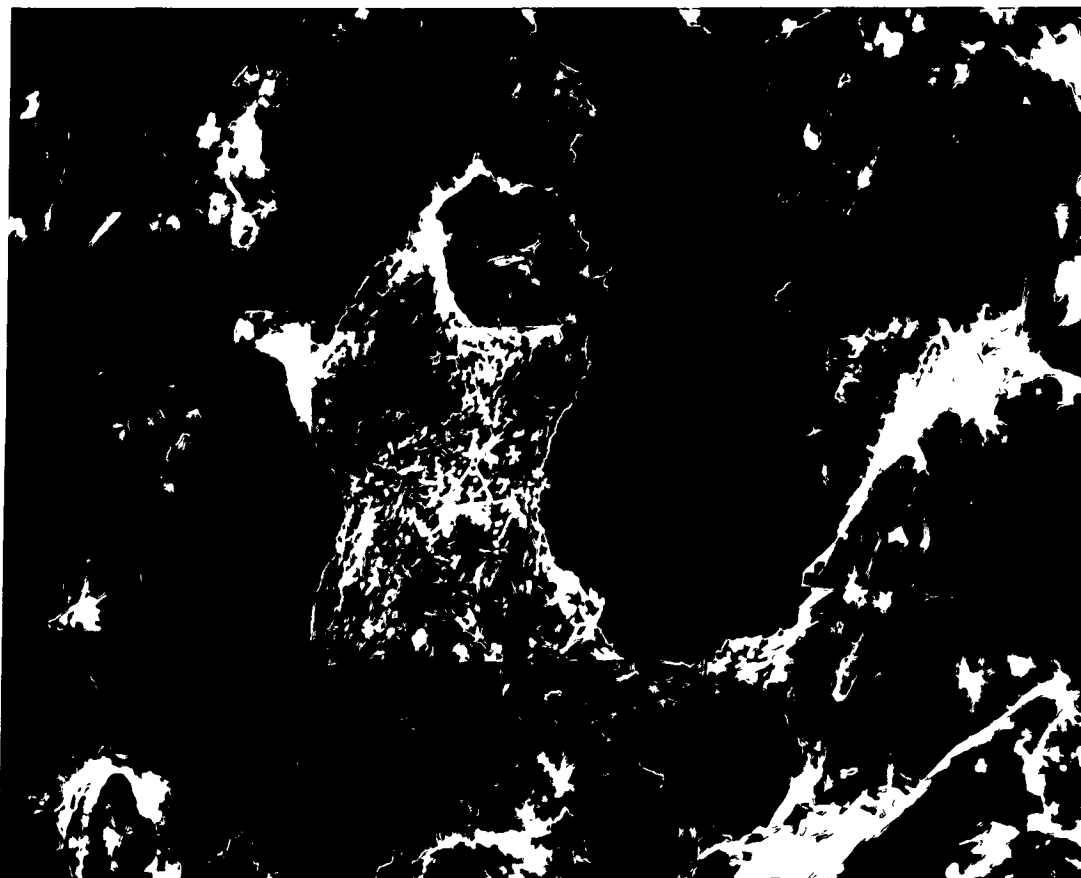


**Figure 4.9.16 - Crystallization of the Coors Alumina/Mullite Filter Matrix after 2816 hrs of Operation in Test Period IV and V**

## Results

---

Post-test O-ring diametral compressive strength testing indicated that the strength of the 3M CVI-SiC composite matrix was greater than that of the as-manufactured filter matrix. Due to the accumulation of fines within the PFBC-exposed matrix, "wedging" of fines in between the SiC coated fibers may require a higher load to be applied to the matrix prior to failure, thus generating what appeared to be a strengthened composite matrix. Alternate secondary mechanisms have been considered which include phases changes within the matrix which provide additional strength during process operation. During diametral compressive strength testing, the relatively low load bearing, PFBC-exposed, 3M CVI-SiC matrix generally retained the graceful fiber "pull-out" characteristics of the fracture toughened, as-manufactured matrix.

Ten newly manufactured CVI-SiC composite filters were used during Test Period V. After 1110 hours of operation, post-test inspection of the filter cluster indicated that all ten of the 3M CVI-SiC composite filter elements were intact. Assuming that the strength of the as-manufactured 3M filters which were used for testing in Test Period V was equivalent to the strength of the as-manufactured filter elements which were used in Test Period IV, characterization of the 1110 hour, 3M CVI-SiC composite filter elements indicated that the strength of the ash-filled matrix once again appeared to increase.

**DuPont PRD-66 Filament Wound Filters.** The oxide-based, filament wound, DuPont PRD-66 matrix consists of a layered cordierite ( $Mg_2Al_4Al_5O_{18}$ ), mullite ( $3Al_2O_3 \cdot 2SiO_2$ ), cristobalite ( $SiO_2$ ), and corundum ( $Al_2O_3$ ) microstructure. An amorphous phase is also present in the as-manufactured PRD-66 filter matrix. Due to the differences in the thermal coefficient of expansion for mullite, cordierite, and corundum which are present in the PRD-66 matrix, a microcracked structure is formed after firing.

The "diamond" pattern weave of the polycrystalline refractory oxide-based fibers forms the ~7 mm structural support layer of the DuPont PRD-66 filter matrix. A thin membrane layer is wrapped along the outer surface of the support matrix, producing a light weight, bulk filter element.

During Test Period IV, three DuPont PRD-66 filter elements were installed in a middle array. After 1706 hours of operation, all three filters remained intact. During C-ring preparation of the Tidd-exposed PRD-66 filter element, magnesium sulfate crystallized along the outer surface of the filter, as a result of leaching of the ash that was contained within the filter ID bore and wall during wet cutting with a diamond wheel. Posttest strength characterization of the PRD-66 matrix indicated that the bulk strength of the ash filled matrix tended to increase after 1706 hours of operation.

## Results

---

Twenty-two DuPont PRD-66 candle filters were installed in a top array for operation in Test Period V. After 232 hours of operation, sections of the PRD-66 matrix were identified in the ash hopper discharge, implying that failure had occurred. Testing continued, and after ~775 hours of operation, additional sections of the PRD-66 filter matrix were evident in the ash hopper discharge.

Testing was terminated after 1110 hours of operation. Only two of the DuPont PRD-66 filter elements remained intact, four had suffered either mid-body fracture or failure at a location that was approximately three-quarters of the candle length below the flange, and sixteen filters had fractured at the base of the flange. The outer surface of the intact and fractured filters was generally "ash free", particularly along the portion of the body that was adjacent to the plenum pipe, and to approximately mid-way down the length of the filter element. Alternately 1-2 mm of ash was deposited along the outer surface of the PRD-66 candles, near the bottom end cap. "Divot-like" formations resulted in lines which ran parallel down both sides of the remaining intact and fractured filter elements. Localized "divoting" was also observed underneath the outer protected gasket sleeve, as well as in alternate, isolated areas along the filter body. The mechanisms leading to "divoting", flange fracture, and mid-body failure of the DuPont PRD-66 filter elements are under investigation. The formation of divots is believed to be either thermal and/or mechanical in nature, as opposed to a response of the DuPont PRD-66 filter matrix to the process gas chemistry and/or particulate fines. Since the PRD-66 filter array had suffered failure after 232 hours of operation, ash filled the inside bore of the remaining PRD-66 candles (i.e., 120 mm and 350 mm) during pulse cycling. Unlike the 3M CVI-SiC matrix and alternate filter elements, failure of the ash-filled PRD-66 end cap region was not observed.

Assuming that the strength of the PRD-66 elements used in Test Period V was equivalent to the strength of the PRD-66 elements used in Test Period IV, post-test strength characterization of the 1110-hour Tidd-exposed PRD-66 filter matrix indicated that an increase in strength appeared to have occurred along the ash-filled OD surface, while virtually no change in strength was detected along the ID or pulse cycled surface of the filament wound matrix.

With the exception of ash bridging which failed the filter elements, the stability and long-term viability of the "aged" or "conditioned" candle filter materials were generally demonstrated during operation in the pressurized fluidized-bed combustion gas environment. Due to the differences in the thermal coefficient of expansion of the PFBC ash and ceramic filter matrices, as shown in Figure 4.9.17, the clay bonded silicon carbide Schumacher Dia Schumalith F40, Coors alumina/mullite, and 3M CVI-SiC

## Results

composite filters frequently failed due to ash bridging. Failure of the filters also occurred when a densified plug of fines was embedded within the ID bore of the filter elements.

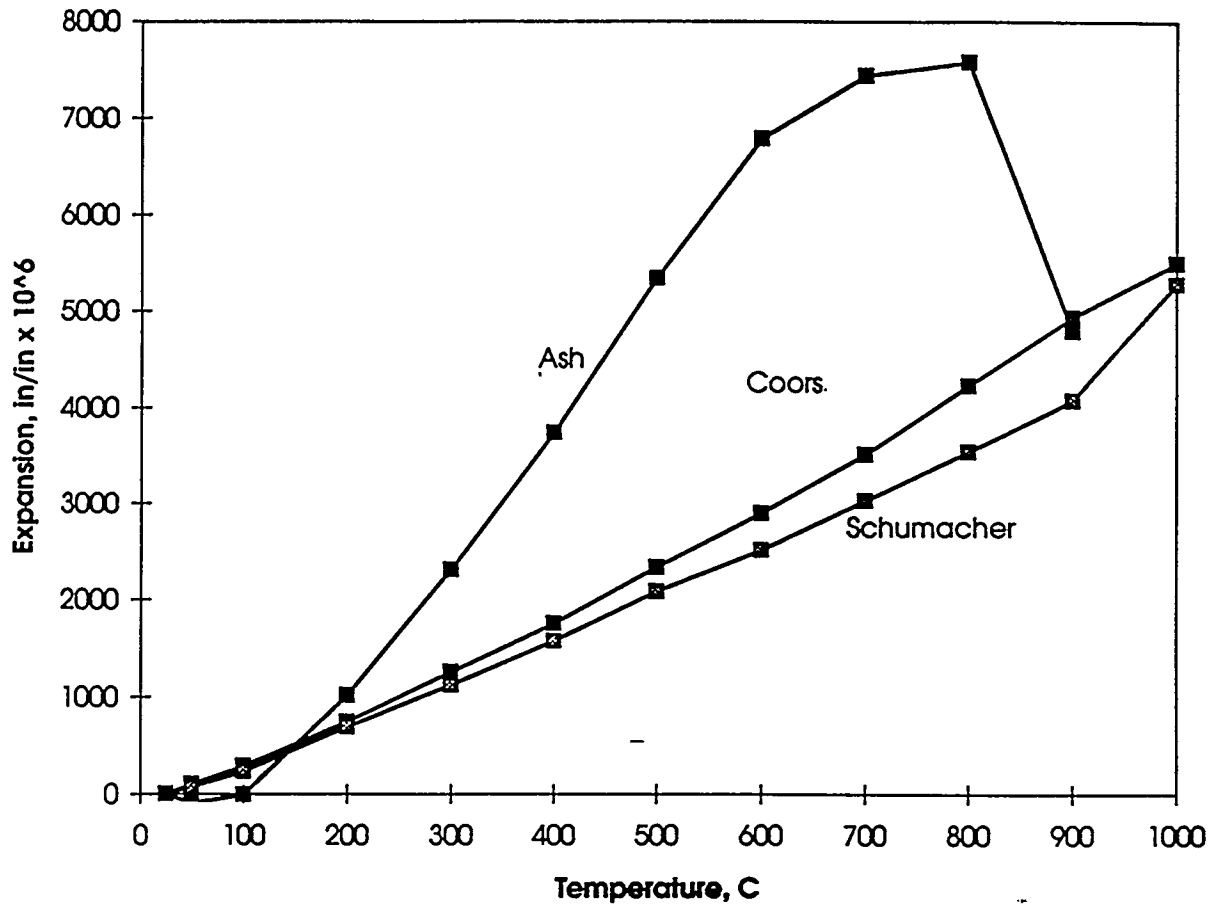


Figure 4.9.17 - Thermal Coefficient of Expansion of the Tidd PFBC Ash and Select Porous Ceramic Filter Materials

## Conclusions

---

### 5.0 CONCLUSIONS

The Tidd Hot Gas Clean Up Program provided valuable information for the future design and operation of ceramic barrier filters in a PFBC flue gas environment. The most important conclusions reached from this program are listed below.

1. The basic design of the candle-based APF was structurally adequate. The hot metal structure of tubesheet, plenums, and candle holders operated without problems.
2. Clay-bonded silicon carbide candle material exhibited an approximately 50% loss of strength after 1000-2000 hours of exposure to the PFBC environment. The strength level stabilized upon further exposure time. The candles maintained their functionality after undergoing the loss of strength.
3. Nearly all of the silicon carbide candle breakage observed in this program was attributed to ash bridging in the APF. Ash bridging was strongly affected by the size and temperature of the ash entering the filter. Very small ash (1 to 3 microns) passing through a well-tuned cyclone formed an ash cake on the filter candles that was extremely difficult to remove at operating temperatures over 1400F. Ash from a partially detuned cyclone (about 7 microns) was more easily removed than the smaller ash, but still difficult to remove at operating temperatures over 1450F. Ash from a completely spoiled cyclone (above 27 microns) was easily removed and did not tend to bridge. The coarse ash was also much easier to handle in the ash removal system.
4. It is important to prevent ash from contaminating the inside of filter candles to avoid blinding them on the inside surfaces which have larger pore size than the outside surfaces. Also, ash accumulation in the bottom of candles can induce candle cracking.
5. The design of hot gas piping is critical. Cast refractory thermal insulation was required to protect the pipe from the hot gas. Ceramic fiber insulation proved unsatisfactory as internal thermal insulation in the hot gas piping.
6. Flue gas which contacts metal surfaces below the acid dew point forms a very corrosive liquid. Metal surfaces that were not protected from contact with the gas experienced corrosion. Stainless steel and Hastelloy C-22 experienced pitting attack while carbon steel exhibited

## Conclusions

---

generalized corrosion. Carbon steel exposed to flowing gas exhibited up to 12% loss of wall thickness over the duration of the test program. Expansion joint bellows proved to be the most troublesome elements in the piping system.

7. The head of the Tidd APF was plagued by hot spots throughout the program due to hot gas flowing behind the ceramic fiber insulation. On-line pumping of insulating refractory was demonstrated to be effective in controlling these hot spots. Temperature sensitive paint used on the filter vessel and piping system proved useful in detecting hot spots.
8. It is important to have reliable continuous ash removal from the filter. Ash buildup in the APF hopper resulted in candle breakage. High level alarms in the hopper were important in preventing additional failures. Continuous discharge of ash with gas and cooling air through carefully sized lines proved more reliable than a lockhopper system.
9. Based on very limited data, the APF reduced the SO<sub>2</sub> concentration in the gas passing through it approximately 45%. This is believed to result from the gas reacting with ash cake on the filter candles as evidenced by a higher degree of sulfation of the APF ash than the precipitator ash.

## **Recommendations**

---

### **6.0 RECOMMENDATIONS**

1. In future HGCU applications on PFBC flue gas, it is recommended to not utilize a cyclone upstream of the filter to reduce the filter inlet dust loading. The advantage of coarse ash in improving filter cleaning and ash removal outweighs the disadvantage of higher ash loading to the filter and higher backpulse frequency.
2. The Tidd PFBC plant design utilized a combustor vessel different from the vessel for the fluidized bed to separate the thermal boundary from the pressure boundary. When this approach is used for the system, it is recommended that the APF be installed inside the combustor vessel. Such an arrangement would eliminate most of the hot gas piping and many of the corrosion problems which were experienced in the HGCU slipstream but not experienced in the Tidd PFBC system. The disadvantage of this arrangement is reduced access to the filter for inspection and servicing.
3. It is recommended that fail-safe devices be included in the APF design to minimize ash penetration in the event of broken elements. Fail-safes will protect the gas turbine from erosion by coarse ash in case of candle breakage and ensure that particulate emission limits can be maintained. Fail-safe devices need to be improved to reduce the amount of ash entering the filter outlet under a broken candle scenario to prevent ash from being entrained with back pulse air and accumulating in other candles which could result in candle failures.
4. A means to detect filter leakage on line should be developed. At Tidd the only method available for this purpose was to briefly open a valve downstream of the filter and look for dust in the gas. However, this method was crude and unreliable unless the filter leakage was large.
5. The APF vessel should include a sufficient quantity of adequately sized nozzles for inspection of all filter clusters. A means to safely enter the filter vessel to replace broken filter elements should be developed. Removing the filter internals for this purpose was costly and time consuming.
6. In future filter designs with plenums arranged vertically, ash sheds below the filter candles should include provisions for pneumatically removing ash accumulations from them. The

## Recommendations

---

distance between ash sheds and candle bottoms should be increased to minimize the possibility of ash bridging between them.

7. The filter vessel ash hopper angle should be steep enough to ensure good ash flow. Flow testing with the ash is recommended to confirm the design prior to fabrication. The hopper should contain an adequate number of nozzles for air purging.
8. A minimum of two level detectors (high and extreme high) should be installed at the filter hopper to detect ash build up.
9. Continuous pneumatic ash removal is recommended in lieu of a screw cooler and lockhopper arrangement. This type of system was found to be reliable in removing ash from the primary and secondary cyclones in the PFBC combustor and was effectively used as an alternate means of ash discharge from the Tidd APF.
10. Cast refractory is recommended as the internal insulating material for the filter vessel head and piping. Fibrous (Z-Block) insulation is suitable for the body of the filter vessel. Expansion joints in the piping system should be avoided or at least minimized.
11. If a hot gas filter system is installed external to the combustor and the piping system operates below the acid dew point of the flue gas, it is imperative that internal corrosion protection be addressed in the design.
12. Conduct additional long-term high temperature testing of clay bonded silicon carbide candles to confirm that their loss of strength is not a serious disadvantage for commercial applications. Alumina-mullite material also merits additional testing.
13. All pressure sensing lines in the HGCU system should have continuous air purge to prevent pluggage.
14. Conduct further investigations into the chemistry of high temperature ash agglomeration.
15. Conduct additional research into the phenomenon of SO<sub>2</sub> removal through ash cakes.

## Appendix I

---

### APPENDIX I (Prepared by Southern Research Institute)

#### ANALYSES OF ASH SAMPLES FROM THE TIDD ADVANCED PARTICLE FILTER

##### Background

The Tidd Advanced Particle Filter (APF) was designed to perform as a barrier filter with periodic reverse pulses of high pressure air used to remove ash from the filtering surface of the ceramic candle filter elements. In its initial configuration, the APF was preceded by a cyclone designed to capture most of the entrained particulate matter. As operating experience with the APF accumulated, this cyclone was first derated, and then completely bypassed in order to alter the characteristics of the ash entering the filter vessel.

The operating history of the Tidd APF has demonstrated the importance of ash characteristics in determining the overall performance of the filter. Although the performance of the different types of candle filter elements that were tested varied considerably, the ash deposits that formed in the APF were the primary factor that determined the integrity of the barrier filter. Almost all of the ashes removed from the filter vessel comprise relatively fine particles, and are highly cohesive. Observations of the APF made throughout its operating history, coupled with laboratory analyses of the bulk ash and ash deposits collected in the filter assembly, have shown how strong, tenacious ash deposits form in the APF, and how these deposits often led directly to bent and broken candle filter elements. Analyses of various Tidd ashes indicate that after the ash particles are initially deposited, the ash deposit undergoes a physical restructuring or consolidation that significantly reduces the overall porosity of the ash deposit.

Although the filtration of particulate matter from flue gas streams is an established technology for conventional pulverized-coal-fired plants, the environment within the APF and the specific characteristics of the PFBC ash being collected presented unique challenges for this installation. The high temperatures in the filter vessel combined with the chemistry and morphology of the ash entering the filter vessel to form ash deposits that severely limited APF operation.

##### On-Site Observations

Southern Research Institute personnel made four site visits to the Tidd APF to inspect and document the condition of the filter vessel and to collect representative samples of the various deposits of ash found in the APF

## Appendix I

---

for analysis. When the filter assembly was opened during the first of these site visits on September 30, 1993, extensive deposits of ash were found on candle surfaces, bridged between candles, and on non-filtering surfaces. The deposits found on non-filtering surfaces formed by the gradual deposition of particles as a result of turbulent diffusion. Some of these passive deposits were up to six inches thick with high mechanical strength. Many of the candle filter elements were covered by filter cakes up to one inch thick. Like the passively deposited agglomerates of ash, these filter cakes also had high mechanical strength.

The filter vessel was again opened for inspection and refitting on May 5, 1994. Despite the relative cleanliness of the candles, significant deposits of ash were observed at several other locations in the assembly. For each of the nine clusters, the underside of the tube sheet was coated with a deposit of ash about eight inches thick. Although the outer (presumably the most recently deposited) portions of these deposits were fairly fluffy, the inner regions were hard, strong, and well consolidated. Similar deposits were apparent on the ash sheds above the middle and bottom plenums. These deposits were about three inches thick, and were also strong and well consolidated. Strong, thick deposits were present on the center support conduits that are part of the top and middle plenum assemblies. These deposits were thick enough (over four inches) in most areas to envelop the inner ring of candles in these plenum assemblies. Many of the innermost candles in the top two plenums were bent away from the center plenum support conduits. The region between these candles and the center support conduits was almost completely filled with ash.

Observations of the APF during this refitting indicated that severe bridging of ash between adjacent candles was still a serious problem. Many ash bridges were present, some of which extended from the deposit on the underside of the tube sheet all the way down to the conical surface of the ash shed below the bottom ends of the candles. Ash bridges were identified in many different stages of formation. Most ash bridges were found in the top and middle plenums, which are also the locations where most of the severely bent candles were found. The bottom plenum had the fewest ash bridges, and the fewest bent or broken candles. As was observed previously, the ash deposits throughout the APF had high mechanical strength. However, the filter cakes observed during this second site visit were only about 0.4 inch thick, compared with the one inch thick cakes present in September 1993.

From May 1994 until the shutdown of the facility in the spring of 1995, operation of the APF focused on two separate approaches to eliminating the ash bridges previously formed between candle filter elements and nearby surfaces. The first approach involved increasing the mean size of the entrained particles entering the filter vessel by derating the cyclone located just upstream of the filter. The other approach was to remove the inner ring of candle filter elements from the top two plenum assemblies. Although this latter approach involved removing

## Appendix I

---

25 % of the ceramic candle filter elements, and consequently 25 % of the active surface area, it was implemented to increase the separation between the candle filter elements and the ash sheds and center support conduits, reducing the likelihood that ash bridges would form at this location.

When the APF was opened on October 27, 1994 a significant number of candle filter elements were broken, and ash deposits were present at various locations throughout the filter assembly. As observed in two previous site visits, the region under each tube sheet where the candle filter elements are mounted to the tube sheet was completely packed with ash deposits. Although the number of ash bridges adjacent to the filter elements was reduced compared to the two prior observations, there were still a few large ash bridges formed between the lower portion of filter elements in the top two plenums and the ash sheds and/or the plenum support conduits. In general, the filtering surfaces of the intact filter elements were relatively clean, except for regions of the candles just below the tube sheet deposits mentioned above. The surfaces of the center support conduits and the ash sheds were cleaner than previously observed; however, several thick ash deposits were present on portions of these surfaces. Bridging of ash between filter elements in the bottom plenum did not seem to be a serious problem.

The APF was opened once more on May 11, 1995 after the final shutdown of the Tidd Demonstration Plant. During this last operating period, the cyclone upstream of the APF was entirely bypassed in order to get as many relatively large particles into the filter vessel as possible. In general, the filter assembly was quite clean. The only significant deposits of ash were on the underside of the tube sheets, much like the deposits found in these locations during prior inspections. Most of the broken candle filter elements were of a particular experimental design. Most of the other filter elements were intact.

Early observations of the Tidd APF led to the conclusion that tenacious ash deposits can form in the filter vessel and induce stresses that result in bent and/or broken ceramic candle filter elements. The proximity of these bent and broken candle filter elements to large, strong ash deposits emphasized the need to prevent or control the growth of these deposits, facilitate their on-line removal, and/or to redesign the filter to lessen their effects on individual filter elements. The approach that proved most successful in eliminating the deposits was the total bypassing of the cyclone upstream of the APF.

### Laboratory Analyses

During each of the four site visits described above, Southern Research Institute personnel collected a suite of ash samples from various locations in the APF for analysis. These samples included large pieces of the various

## Appendix I

---

types of deposits present throughout the filter vessel, as well as samples of loose ash that were found at several places in the APF. Analyses performed on the ash deposits included SEM examinations of their structure and chemical composition, as well as measurements of their porosity and strength. Measurements on loose bulk ash or deagglomerated (broken up) deposits included size distribution, chemical composition, specific surface area, uncompacted bulk porosity, tensile strength, solubility studies, and SEM photographs to assess particle morphology.

In general, analyses of the ash samples from the Tidd APF showed that the ash that collects at various places throughout the filter vessel initially forms loose, weak, uncompacted deposits that are 85 to 90 % porous. (After the cyclone was completely bypassed, the ash formed deposits that were initially around 80 % porous.) In almost all cases, when these deposits were exposed to temperatures like those in the APF (1200-1550 °F), they gradually consolidated, transforming into much stronger structures having porosities as low as 69 %. Various analyses and reviews of pertinent literature indicate that the mechanism responsible for the extreme consolidation of these agglomerates of ash was a physical rearrangement of the ash particles due to the surface tension of melted or partially melted alkali-aluminosilicate eutectic mixture(s) formed at the contact points between adjacent particles after long-term exposure to the temperatures in the APF.

Because the most freshly deposited portions of the filter cakes and passively deposited ash deposits collected during the site visits were so fragile, a number of these samples were encapsulated in low-viscosity epoxy at the plant. This procedure allowed more detailed measurements of the porosity of these deposits as well as preservation of the samples for further analyses. When thick filter cakes were allowed to form on the candle surfaces, they consolidated as a result of eutectic formation, and they also tended to compact under the force of filtering pressure drop. The compaction was greatest in the layer closest to the filtering surface and progressively less pronounced in the outer layers. Measurements of the porosity of filter cakes removed from Tidd in September 1993 verified the existence of a gradient in the porosity of the filter cake. Porosity gradually increased from about 72 % in the 0.1 inch of cake closest to the candle, to about 85 % for the 30 to 40 % of the cake most recently deposited. These compacted filter cakes had comparatively high mechanical strength and high resistance to gas flow. Laboratory data showed that the tensile strength of a fully consolidated filter cake nodule can exceed 12.5 psi.

Stereographic SEM photographs were made of a fresh fracture surface of a nodule taken from an ash shed in October 1994. The stereographic image was very enlightening as to the structure of the nodule. (One of the pair of SEM photographs used to create the stereographic image is shown in Figure I-1.) The nodule appeared to be a concretion composed of discrete fine particles almost completely embedded in a pervasive amorphous

## Appendix I

mass which apparently formed in the APF after the particles were initially collected. The origin of this amorphous mass is discussed in more detail later in this appendix. Passively deposited agglomerates of ash like the one shown in Figure I-1 were found to have porosities around 74 %.

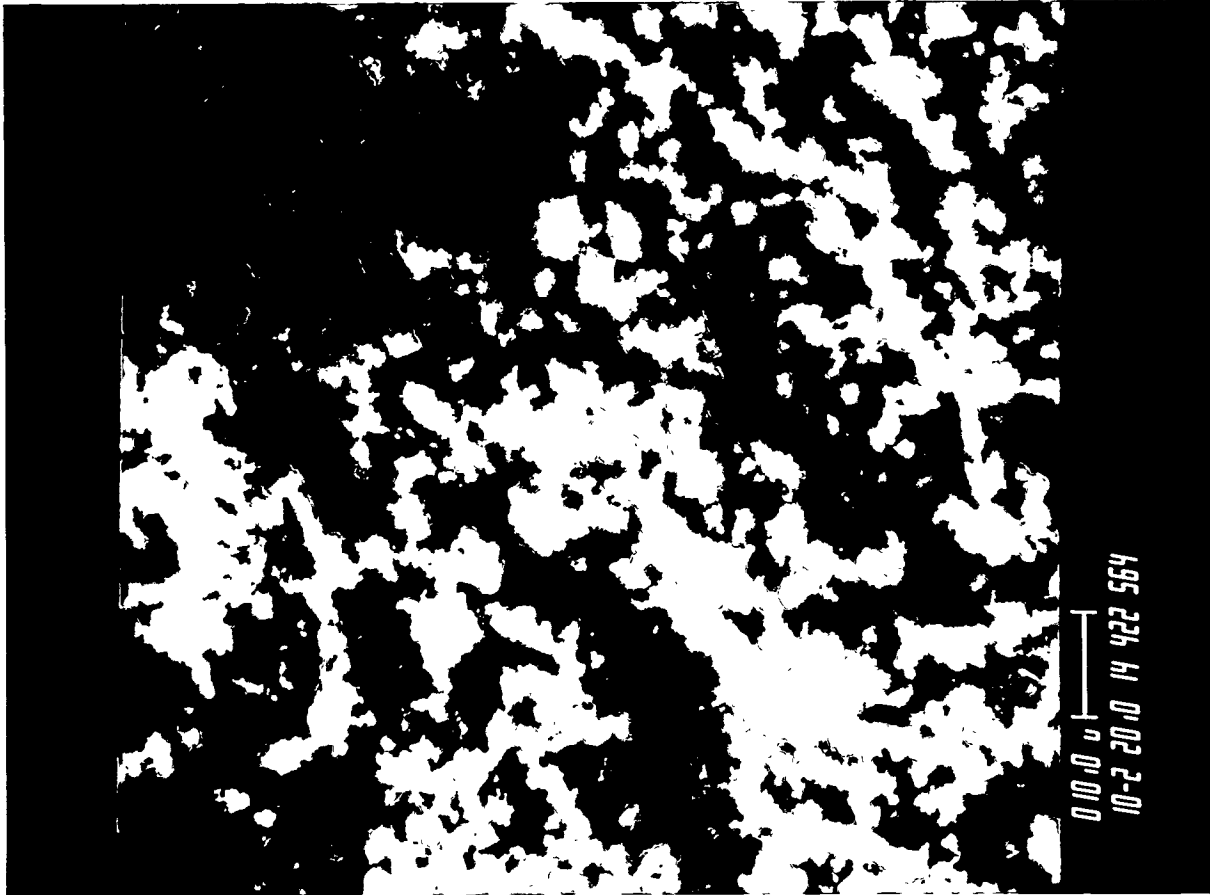


**Figure I-1 - SEM Photograph of a Fresh Fracture Surface of an Ash Agglomerate  
Taken from an Ash Shed in the Tidd APF in October 1994**

## Appendix I

---

An SEM microprobe was used to examine agglomerates of ash obtained from the filter vessel in May 1994. The device performs elemental analyses on selected 1  $\mu\text{m}$  diameter hemispherical regions. There was little consistency from region to region in the various specimens that were examined. Each particle observed was a special case. Some particles were almost completely iron, others were very high in calcium or magnesium. Aluminosilicate particles were also common. The shapes and sizes of the particles also varied considerably. Some particles showed evidence of having been melted and resolidified. Such particles, to the extent that it was possible to determine, were enriched in magnesium because of the formation of  $\text{MgSO}_4$ . The bonds between particles showed some enhanced levels of Mg, accompanied by such other species as Ti, Al, Ca, and S. Although conclusions are hard to verify because of the limitations of the technique and the heterogeneity of the samples, particles rich in Mg and S apparently softened during combustion and/or collection and residence in the filter vessel. The presence of significant amounts of Mg and S in the ash particles may have enhanced the chances for eutectic formation between particles.

Tidd ash nodules that were slowly covered with water rapidly disintegrated. When this same procedure was performed with ethanol, the nodules maintained their shape, and when they dried, they seemed to recover all of their initial strength. Apparently the hydration of various compound(s) in the ash or the dissolution of soluble compounds into the water broke apart the interparticle bonds in the nodules.

The most useful information describing the bulk ash samples was derived from determinations of size distribution, chemical analyses, and uncompact bulk porosity measurements. Size distributions were measured by sieving and sedigraphic analysis. Prior to derating and eventually bypassing the cyclone upstream of the APF, the ash particles collected in the filter vessel were very fine, with MMD's around 3 to 5  $\mu\text{m}$ . As efforts to increase the size of the ash entering the APF by derating the cyclone progressed, somewhat larger MMD's were observed. However, the major changes in the size distributions of the ashes collected in the APF did not occur until the last period of operation, during which the cyclone was completely bypassed.

Sedigraphic and sieve analyses were performed on ashes collected in October 1994, after derated cyclone operation, and May 1995, after operation with the cyclone completely bypassed. These data, which are summarized in Tables I-1 and I-2, show that bypassing the cyclone between October 1994 and May 1995 significantly increased the size distributions of ash collected in the APF. The sieving process used on these five ashes separated a portion of the original ashes into three size fractions: particle diameters  $> 45 \mu\text{m}$ , particle diameters  $> 15 \mu\text{m}$ , but smaller than  $45 \mu\text{m}$ , and ash particles with diameters  $< 15 \mu\text{m}$ . (The sieving process caused this last, smallest fraction to be discarded along with the isopropanol used to wash the particles through the  $45 \mu\text{m}$  and  $15 \mu\text{m}$  sieves.)

## Appendix I

### Table I-1 - Sedigraphic Analyses of Tidd Ashes

Location, Date	Size Range Measured, $\mu\text{m}$	Stokes' MMD, $\mu\text{m}$
Bottom Plenum Tube Sheet, Oct. 1994	1.0 - 40	7.0
Middle Plenum Ash Shed, Oct. 1994	1.0 - 40	3.6
Top Plenum Tube Sheet, May 1995	0.4 - 40	17
Top Plenum Filter Cake, May 1995	0.6 - 40	11
Middle Plenum Tube Sheet, May 1995	0.6 - 40	16

### Table I-2 - Sieve Analyses of Tidd Ashes

Location, Date	% weight		
	dia > 45 $\mu\text{m}$	45 $\mu\text{m}$ > diam > 15 $\mu\text{m}$	diam < 15 $\mu\text{m}$
Bottom Plenum Tube Sheet, Oct. 1994	4.03	17.3	78.6
Middle Plenum Ash Shed, Oct. 1994	0.64	3.84	95.5
Top Plenum Tube Sheet, May 1995	28.9	50.7	20.4
Top Plenum Filter Cake, May 1995	30.1	34.3	35.6
Middle Plenum Tube Sheet, May 1995	44.8	33.3	21.9

In Figure I-2, the size distribution data for these five samples obtained with the sieves have been combined with size distribution data obtained with the sedigraph. These data clearly show the increase in particle size induced by bypassing the cyclone. The ash corresponding to the last row in Tables I-1 and I-2 behaved much more like a free flowing powder than the other samples collected on the same site visit. Based on our sieving measurements, this free flowing ash exhibited the largest particle size distribution of those ashes that were analyzed. When this ash was removed from the tube sheet, it was loose and fluffy, unlike the other ash samples that were consolidated into nodules and strong deposits. This type of difference is common with fine powders. All other conditions the same, powders tend to become more free flowing as their particle size distribution becomes coarser.

## Appendix I

Chemical analyses of this free flowing ash and one of the nodular ashes were performed to determine if differences other than particle size might account for the tendency of the coarser ash to behave like a free flowing powder. Chemical analyses of these two ashes and the size-separated portions generated from them during sieving are summarized in Table I-3.

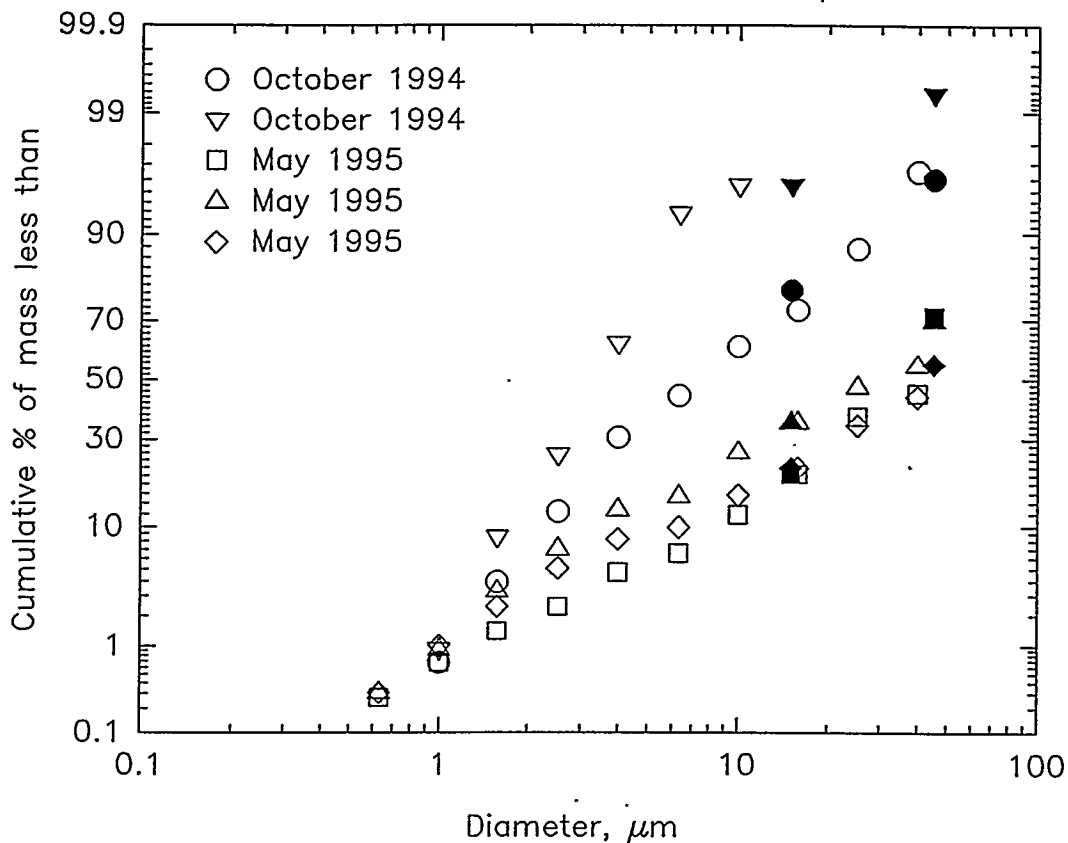


**Figure I-2 - Cumulative Size Distribution Data Measured with a Sedigraph and Sieves for Five Ashes Collected from the Tidd APF**

The hollow data points represent sedigraphically obtained Stokes' diameters. The filled data points represent data obtained in the sieve analyses.

## Appendix I

**Table I-3 - Chemical Analyses of Tidd Ashes Collected in May 1995, % wt.**

Constituent	Nodular Ash (Filter Cake)			Free Flowing Ash (Tube Sheet)		
	all diameters	d > 45 $\mu\text{m}$	15 $\mu\text{m}$ < d, d < 45 $\mu\text{m}$	all diameters	d > 45 $\mu\text{m}$	15 $\mu\text{m}$ < d, d < 45 $\mu\text{m}$
$\text{Li}_2\text{O}$	0.01	0.01	0.01	0.01	0.01	0.01
$\text{Na}_2\text{O}$	0.29	0.16	0.23	0.27	0.13	0.20
$\text{K}_2\text{O}$	1.3	0.83	1.3	1.2	0.77	1.1
$\text{MgO}$	8.3	11.3	8.5	13.2	16.5	13.5
$\text{CaO}$	14.1	18.1	15.0	20.5	24.7	21.0
$\text{Fe}_2\text{O}_3$	7.1	4.8	7.5	8.0	6.2	9.9
$\text{Al}_2\text{O}_3$	11.7	7.5	10.8	10.8	7.2	9.5
$\text{SiO}_2$	26.1	17.6	26.0	25.1	19.6	25.6
$\text{TiO}_2$	1.2	0.41	0.46	1.1	0.33	0.49
$\text{P}_2\text{O}_5$	0.15	0.12	0.14	0.14	0.10	0.14
$\text{SO}_3$	30.1	38.5	28.5	19.5	22.9	17.4
LOI	13.5	19.6	15.3	1.5	2.4	1.1
soluble $\text{SO}_4^{=}$	29.7	36.0	29.8	22.4	26.3	20.6

These analyses demonstrated that the larger ash particles in both samples contain more Mg, Ca,  $\text{SO}_3$ , and have higher LOI values than the smaller particles. The smaller particles are richer in Al, Na, K, Fe, Ti, and Si. These results suggest that the larger ash particles are derived mainly from the sorbent used in the combustion process, while the smaller particles are derived mainly from the coal. This is supported by comparisons of the concentrations of calcium and magnesium in the two parent samples and their corresponding size fractions. The coarser ash contains about 50% more calcium and magnesium than the finer filter cake ash. These differences suggest that the sorbent-derived ash particles are somewhat larger than the coal-derived ash particles in these samples.

Another difference in these two samples is evident in the acid/base ratios as defined in Table I-4.

## Appendix I

**Table I-4 - Acid/ Base Ratios of Ashes Collected at Tidd on May 11, 1995**

Location	SO <sub>3</sub> /(Ca+Mg)	Soluble SO <sub>4</sub> <sup>=</sup> /(Ca+Mg)
Top Plenum Filter Cake	1.3	1.3
Middle Plenum Tube Sheet	0.58	0.66

The differences in these ratios are due to the exposure of the filter cake ash to much more flue gas than the ash obtained from the passive deposit under the tube sheet. As flue gas is filtered through the filter cake, additional SO<sub>2</sub> in the flue gas is captured by calcium and/or magnesium still remaining in the ash. Although unreacted sorbent present in the passive ash deposits can still react with SO<sub>2</sub> in the flue gas, the reaction is diminished because the flue gas in direct contact with the ash particles in the deposit is exchanged or refreshed relatively slowly. The higher LOI of the filter cake ash is attributed to the presence of the increased amounts of sulfur captured by chemical absorption in the filter cake. The comparisons discussed above suggest that it is possible that the increased flowability of the tube sheet ash may be partially due to chemical differences as well as differences in size distribution.

Standard mineral analyses of two bulk hopper ash samples and two filter cake ash samples (Table I-5) found that, like other Tidd ashes that have been analyzed, the primary elemental constituents of these ash samples were calcium, magnesium, aluminum, silicon and sulfur. Most of the calcium and magnesium in the ash in these samples is derived from use of limestone and/or dolomite in the fluidized bed. The other major constituents of the ash are derived from the coal. These chemical comparisons of hopper ashes and filter cake ashes have also helped to identify the mechanism controlling the consolidation of ash deposits in the APF, as discussed below.

## Appendix I

**Table I-5 - Chemical Analyses of Tidd Ashes Collected in 1993, % wt.**

Constituent	Hopper Ashes		Filter Cake Ashes	
Na <sub>2</sub> O	0.30	0.31	0.30	0.27
K <sub>2</sub> O	1.6	1.42	1.73	1.77
MgO	9.9	9.63	8.77	7.96
CaO	15.3	15.48	14.16	13.67
Fe <sub>2</sub> O <sub>3</sub>	5.3	6.49	4.79	5.63
Al <sub>2</sub> O <sub>3</sub>	13.4	11.80	13.01	13.63
SiO <sub>2</sub>	19.2	21.29	23.03	22.89
TiO <sub>2</sub>	0.50	0.56	0.61	0.07
P <sub>2</sub> O <sub>5</sub>	0.08	0.12	0.11	0.10
SO <sub>3</sub>	33.6	31.10	31.06	31.38
LOI	1.5	2.96	1.45	1.84
Soluble SO <sub>4</sub> <sup>=</sup>	48.3	—	—	40.2

In other chemical analyses, a sample of Tidd ash was leached with water. These analyses indicated that large proportions, but not all, of the Mg, Ca, K, Na, and SO<sub>4</sub> were leached out of the ash in this procedure. Analyses of the leachate showed that the leachable sulfate ions were almost totally bound up as magnesium sulfate and calcium sulfate. At least 30% by weight of the ash was soluble in water.

A variety of physical analyses were also performed on several of the ashes collected in May, 1995. The results of these analyses are presented in Table I-6.

## Appendix I

**Table I-6 - Physical Analyses of Ashes Collected at Tidd on May 11, 1995**

Location (Size Range)	Nodule Porosity, %	Uncompacted Bulk Porosity, %	Specific Surface Area, m <sup>2</sup> /g
Top Plenum Tube Sheet, (all diameters)	73	80	—
Top Plenum Filter Cake (all diameters)	70	84	—
Middle Plenum Tube Sheet, (all diameters)	—	81	—
Top Plenum Filter Cake (diameter >45 μm)	—	—	6.9
Top Plenum Filter Cake 15 μm < diameter < 45 μm	—	—	5.1
Middle Plenum Tube Sheet (diameter > 45 μm)	—	—	1.7
Middle Plenum Tube Sheet 15 μm < diameter < 45 μm	—	—	1.8

The relative coarseness of ash removed from the middle plenum tube sheet, as indicated by the sieve analyses, is evident in the values of specific surface area data measured for the two samples comprising particles with diameters larger than 45 μm.

### Mechanisms Controlling the Consolidation of Ash Deposits

Studies of the buildup of boiler tube deposits in conventional pulverized-coal fired boilers describe a mechanism which may account for the apparent consolidation of the Tidd ash deposits. Many of the ash particles collected in HGCU filter assemblies are derived directly from coal particles. These ash particles often contain a large percentage of aluminosilicate compounds. The other main source of ash particles is the sorbent used in the PFBC process. Sorbent-derived ash particles contain relatively large amounts of magnesium and/or calcium.

## Appendix I

---

Once these two types of ash particles come in contact with each other in the agglomerates formed in the filter vessel, the aluminosilicate compounds in the coal fly ash tend to react with alkali and alkaline metals in the sorbent ash particles to form eutectics that melt at relatively low temperatures<sup>1</sup>. The progress of these reactions is supported by the intimate contact of the ash particles in the agglomerate and by long-term exposure of the ash particles to the temperatures in the filter vessel.

Most of the research into the formation of these eutectics has examined the formation of calcium aluminosilicate compounds (e.g.  $2\text{Ca}\cdot\text{Al}_2\text{O}_3\cdot\text{SiO}_2$  or  $\text{CaO}\cdot\text{Al}_2\text{O}_3\cdot 2\text{SiO}_2$ ). Although pure forms of these compounds do not melt at the temperatures encountered in HGCU filter vessels (pure  $2\text{Ca}\cdot\text{Al}_2\text{O}_3\cdot\text{SiO}_2$  and  $\text{CaO}\cdot\text{Al}_2\text{O}_3\cdot 2\text{SiO}_2$  melt at around 2800 °F), impurities that would almost certainly be present in these compounds because of the heterogeneous nature of coal fly ash particles would lower their melting points. It is likely that this reduction in melting points could combine with long-term exposure to the temperatures in the filter vessel to create relatively soft, sticky layers on the surfaces of the ash particles<sup>2,3</sup>. As the viscosity of the outer layer of the ash particles decreases, the bonds between the particles become stronger. Also, the surface tension of the near-liquid layer on the particles tends to pull adjacent ash particles closer together, thereby eventually consolidating the structure of the entire ash agglomerate. This mechanism may be further enhanced by the relatively small size of the ash particles in the agglomerate.

Chemical reactions, such as the formation of calcium sulfate and/or magnesium sulfate on the surfaces of incompletely reacted sorbent particles in the agglomerate, may increase the strength of interparticle bonds and contribute to another mechanism for eutectic formation. Sulfate salts which form on the surfaces of the ash and sorbent particles result primarily from the reaction of gaseous  $\text{SO}_2$  with solid calcium oxide and/or magnesium oxide. Pure calcium sulfate melts at around 2600 °F, and pure magnesium sulfate decomposes at around 2000 °F. Therefore, it is possible, even with the effects that impurities have on melting points, that these salts do not melt in the filter vessel. Because these sulfate salts may remain in the solid state, they could act as solid bridges between adjacent particles. Such salt bridges can increase particle bonding strengths by several orders of magnitude<sup>4</sup>. Because filter cake ash contacts much more flue gas than passively deposited ash, this type of reaction would be accentuated in the filter cake. However, passive ash deposits can remain in the filter vessel for extended periods since there is no effective means for their periodic on-line removal. Therefore this type of reaction may also occur to a significant extent in these passive deposits.

Additionally sodium, although present in only small amounts in the sorbent and coal fly ash particles, may react with sulfur compounds in the flue gas to form sodium sulfate. Although the melting point of sodium sulfate is over 1600 °F, it may form eutectic mixtures with calcium sulfate, thereby lowering the melting point of the

## Appendix I

---

eutectic mixture into the range of temperatures encountered in barrier filters. (A parallel reaction may also occur with sodium sulfate and magnesium sulfate.) Once this eutectic mixture is formed, it could then act to consolidate the ash agglomerate in the same way as does the calcium aluminosilicate eutectic mixture described above. The same consolidating mechanism would apply to any other eutectic mixture that melted or significantly softened at the temperatures within the filter vessel.

A review of the chemical analyses of hopper and filter cake ashes from Tidd was performed to assess whether additional material that might be condensed out of the flue gas or adsorbed onto the collected particles could account for the apparent consolidation of the various agglomerates of ash present in the filter vessel. The data show that the degree of consolidation of these agglomerates can not be accounted for by condensation and/or adsorption of materials from the flue gas. The mechanism responsible for the extreme consolidation of these agglomerates of ash is most likely a physical rearrangement of the ash particles due to the surface tension of melted or partially melted alkali-aluminosilicate eutectic mixture(s) that form at the contact points between adjacent particles after long-term exposure to the temperatures in the APF.

As can be seen in the SEM photograph of an aggregate of ash removed from the Tidd APF in October 1994 (Figure I-1), the primary ash particles are nearly completely imbedded in a pervasive amorphous mass. Based on various observations of the behavior of these aggregates, it is apparent that the amorphous mass in which the particles are embedded is derived directly from the primary coal ash particles and sorbent particles originally deposited on the surface of the aggregate. The first observation that supports this contention is based on the difference between the porosity of newly-deposited regions of ash aggregates (85 % or higher) and the porosity of portions of the aggregates that have been exposed to the temperatures in the APF for extended periods (around 74 %). In other words, the newly-deposited regions of the agglomerates are no more than 15 % solid, whereas the solid content of older portions is at least 26 %. This means that as the aggregates age in the APF, either the amount of mass has been nearly doubled from some source other than the primary particles (condensation or adsorption from the flue gas), or the primary particles have rearranged themselves to occupy about 58 % of their original total volume.

If the flue gas contributed large amounts of mass to the aggregate through condensation or adsorption, the chemical constituents of this added mass would be limited to compounds that could exist as a vapor at the normal operating conditions of the APF. Although many compounds could satisfy these requirements, some of the major constituents found in the fly ash do not. Three major constituents that will not be found in a gaseous state in the APF are iron, aluminum and silicon. When we compare the mineral analyses of Tidd APF hopper ashes with mineral analyses of aged Tidd filter cake ashes (see Table I-5), the iron, aluminum, and silicon

## Appendix I

---

contents of the two types of samples are very similar. Since the amounts of these three non-volatile elements are not significantly lower in filter cake ash than in hopper ash, it is apparent that essentially all of the mass of the filter cake is due to the original ash particles, and not to any significant deposition of gas-phase constituents from the flue gas.

By examining the SEM photograph of an aggregate of ash taken from the ash shedding cone below the middle plenum at Tidd (Figure I-1), it is apparent that a significant portion of the mass of the ash particles has been transformed into the amorphous material mentioned above. The physical appearance of the amorphous mass is clearly distinct from the appearance of the small ash particles. The appearance of the amorphous mass can best be described as concretion formed from individual ash particles embedded in what appears to be a large, interconnected molten mass. This appearance also supports the contention that eutectics have formed in the ash aggregate.

### Modification of Ash Characteristics

It is doubtful that process changes such as slightly lowering the temperature in the APF, sorbent switching, or addition of a conditioning agent will be able to significantly affect the formation of these eutectics and the subsequent consolidation and strengthening of the ash aggregates. The minimum operating temperature of the APF is strictly limited by the economics of the PFBC process. Past operation at reduced temperatures around 1250 °F have not been able to prevent the formation of consolidated ash aggregates. Since magnesium and calcium are both excellent fluxing agents, altering the type of sorbent used in the PFBC process is not likely to alter the tendency for eutectic formation. Finally, the addition of any conditioning agent to the eutectic system is only likely to lower its melting point even further.

In an attempt to prevent the development of excessive pressure drop at Tidd, efforts have recently been made to alter the characteristics of the filter cake. The approach used has been to decrease the efficiency of the cyclone upstream of the filter assembly. This method, known as derating, can be used to increase the mean diameter of particles exiting the cyclone. For this approach to be effective the size distribution of the entrained ash at the inlet to the filter vessel must be shifted toward larger particle sizes, and this altered size distribution entering the vessel must result in an altered size distribution of particles being deposited on the filter cake and in other locations where tenacious ash deposits have been observed to form. The extent to which relatively large particles entering the APF are actually transported to these locations could not be accurately assessed until samples of actual filter cake ash from derated-cyclone operation had been obtained and analyzed.

## Appendix I

---

### Conclusions

Operation of the Tidd APF has demonstrated the importance of ash characteristics in determining overall filter performance. Ash deposits that formed in the APF were the primary factor that determined the integrity of the barrier filter. The high temperatures in the filter vessel combined with the chemistry and morphology of the ash to form strong, tenacious deposits that often led directly to bent and broken candle filter elements.

The optimum solution to the problems in the Tidd APF caused by the ash aggregates that have been consolidated and strengthened by pervasive eutectic formation is the removal of these aggregates from the APF before the eutectics have had enough time to develop. A large measure of success has been achieved by bypassing the cyclone upstream of the APF. This increases the size distribution of the particles forming the various ash deposits (filter cakes and passive deposits), thereby decreasing their inherent cohesivity. Although particle size is probably the primary reason for these decreases in cohesivity, the somewhat different chemical composition of these larger particles may also influence cohesivity. These agglomerates of lower cohesivity do not have sufficient strength to remain in the APF long enough to undergo consolidation. Gravity and/or vibration cause them to fall off the surface on which they initially formed.

### References

1. O'Gorman, J.V. and P.L. Walker, Jr. "Thermal behavior of mineral fractions separated from selected American coals," Fuel **52**, 71 (1973).
2. Wibberley, L.J. and T.F. Wall. "Alkali-ash reactions and deposit formation in pulverized-coal-fired boilers: experimental aspects of sodium silicate formation and the formation of deposits," Fuel **61**, 93 (1982).
3. Helble, J.J., S. Srinivasachar, and A.A. Boni. "Factors influencing the transformation of minerals during pulverized coal combustion," Prog. Energy Combust. Sci. **16**, 267 (1990).
4. Williams, R. and R.W. Nosker. "Adherent dust particles," RCA Engineer **28**, 76 (1983).

## Appendix II

---

### APPENDIX II (Prepared by Westinghouse STC)

#### FAIL-SAFE DEVICE PERFORMANCE

##### Background

Westinghouse has developed and tested a patented fail-safe regenerator device (FSRD). The device, one of which is installed in the filter holder above each ceramic candle filter, is intended to both minimize thermal shock of the ceramic during pulse cleaning, and minimize penetration of dust when the ceramic filter has failed. When an intact filter is present, the FSRD should not have a high pressure drop nor interfere with pulse gas delivery, but it should heat the pulse gas. In the event of a filter failure the FSRD should restrict flow so as to minimize dust penetration, eventually plug so that penetration stops, and retain the dust plug when its plenum is back pulsed.

Prior developments featured testing of various candidate components, including porous ceramic foam plugs, wire mesh screens, and metal particle beds. Of these, only the fine mesh screen was demonstrated to plug with dust during high-pressure, high-temperature test facility operation. Consequently, the current design evolved, which includes a layered arrangement of fine mesh screen (dust collection barrier), Raschig Rings (heat storage medium), and coarse screens or perforated plates (layer separation and support). Recommended correlations for heat transfer, pressure drop, and dust collection performance were established from Westinghouse STC in-house testing. Rather than correlating these performance parameters in terms of the devices as a whole, the correlations were established for each component layer. Subsequent to these developments, prototype components were built and installed in the Westinghouse filter units operating at Tidd and at Karhula. Results of this testing are reported in this Appendix.

##### Testing at Tidd

In October of 1993, nine FSRDs were installed, one on each plenum in position number 16. This original design (Design A) had the fine mesh screens close together at the bottom of the device. These ran for 1279 hours from January to April 1994. The devices were examined and found to be in good condition. Those above broken candles and in plenums with broken candles had substantial dust in them. No additional data were collected.

## Appendix II

---

In May of 1994 the nine FSRDs were removed and new FSRDs were installed above each candle in the middle plenum of cluster B (twenty-two total). The new FSRDs were of a design which had been improved by separating the fine screens by the width of the Raschig ring bed, to allow trapping of a thick dust cake in event of function as a fail-safe device (Design B). This plenum was the one fitted with prototype developmental candles from a variety of manufacturers, as discussed in Section 4.6.8. These FSRDs were used for 1706 hours from July to October 1994. FSRDs operating above broken candles were recovered, inspected and observed to have been effectively plugged. The pressure drop across a plugged FSRD and across a clean used FSRD were measured at Westinghouse STC.

In November 1994 FSRDs of the B Design were installed at all 288 positions and were subsequently in place for 1110 hours of testing between January and March of 1995. Physical appearance of the intact devices, and in particular of the fine mesh screen elements, is described in Section 4.7.10 and 4.9.1. Again, some of the plugged (broken filter) and still-clean FSRD devices were returned for pressure drop measurement.

### Testing at Karhula

FSRDs of the A Design were installed at Karhula and tested for 1329 hours from November 1993 until June 1994. Upon removal, the FSRDs corresponding to broken candles were plugged. Upper coarse screens had some broken wires, presumably due to a combination of corrosion and thermal shock. The fine mesh screens were torn in some instances. The pressure drop across several used, clean FSRD devices was again measured at Westinghouse. The pressure drop across a plugged device was also measured by Ahlstrom.

### Pressure Drop Assessment

Pressure drop is important because it must be minimal when an intact filter is in place and very high when a filter is broken. Pressure drop may be characterized in terms of flow resistance, i.e., a number of velocity head (N) lost by gas flowing through the device, based on superficial velocity of gas through the 2.62 inch ID internal channel of the FSRD. The pressure drop  $\Delta P$  is related to number of velocity heads N by:

$$\Delta P = \frac{1}{2} N \rho V^2$$

where  $\rho$  is gas density and  $V$  is gas velocity.

## Appendix II

Table II-1 summarizes pressure drop measurements. The number 36 listed for the "Broken Candle" is the flow resistance from the head of a candle with a 30 mm orifice at the center of the candle head, which is assumed to be still in place. It should be added to any of the other numbers in the Table for a final head loss. The data indicates a maintenance of clean permeability with exposure, as well as a substantial decrease in permeability upon plugging. The actual measured decrease in permeability may be low due to loss of dust during handling.

Figure II-1 shows projected gas flow split that occurs with large numbers of candle failures. The top line, developed from pressure drop modeling, shows what would occur with no FSRDs in place. This curve predicts, for example, that approximately 82% of the total gas flow would pass through the open area left by the 25% broken candle elements. The gas passing through this area carries the inlet dust concentration. The lower line shows the projected gas flow split with the FSRDs in place. The curve is based on dust sampling from the controlled four candle element (3 candles intact, 1 broken) laboratory test run. In this case the flow split is assumed proportional to the ratio of the outlet to inlet dust loading. It is also assumed in this testing that only 50% of the dust feed reaches the test unit. This provides, perhaps by a factor of two, a very conservative basis for predicting the performance of the FSRD device.

**Table II-1 - Head Loss Across Fail-Safe Regenerator Devices**

Design	Where Used	Condition After Use	No. Velocity Heads
Broken candle, no FSRD			36
Design A	Laboratory STC	Unused	110
Design B	Laboratory STC	Unused	150
Design A	Laboratory STC	Used/ Broken Candle	4000
Design A	Tidd	Used/ Intact Candle	190
Design A	Tidd	Used/ Broken Candle	2,000,000
Design B	Tidd	Used/ Intact Candle	122
Design B	Tidd	Used/ Broken Candle	1700
Design A	Karhula	Used/ Intact Candle	100
Design A	Karhula	Used/ Broken Candle	5000*

\* Based on measurement by Ahlstrom

## Appendix II

The field test data, Table II-1, show comparable or better performance levels based on flow resistance measurements than that of the reference laboratory test. It is uncertain as to how the dismantling, handling and transporting of the field tested units may have compromised the flow resistance measurements.

Operating the hot gas filter unit with the FSRD devices in place provides considerable margin for failed candle elements. For example, assuming 1000 ppm inlet dust concentration and the conditions given in Figure II-1, the predicted outlet dust loading from the filter unit with 5% failed elements would be expected to be less than 20 ppm based on the conservative laboratory test and perhaps as low as less than 1 ppm based on the most optimistic field test data.

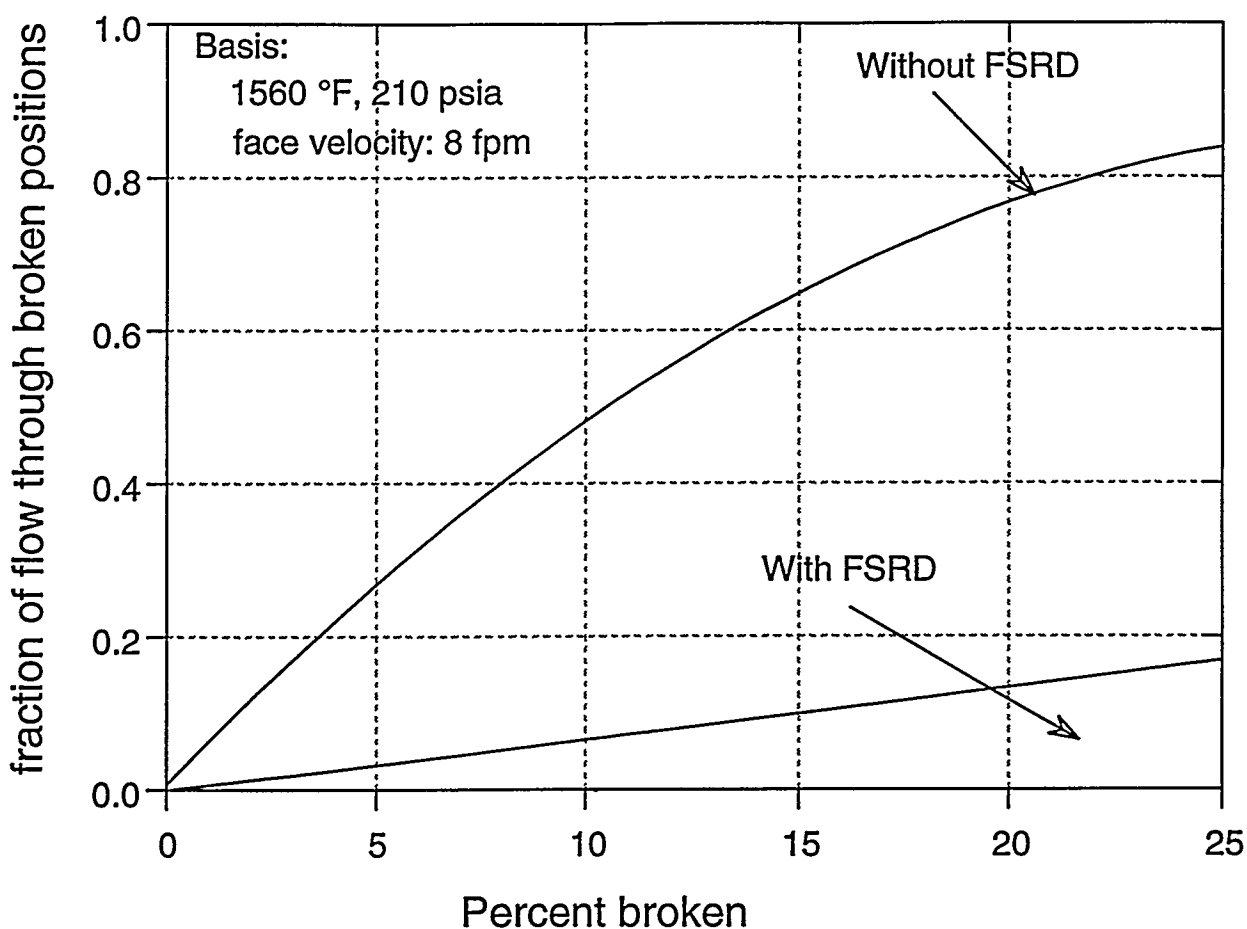


Figure II-1 - Fraction of Flow Through Broken Positions Versus Percent Broken

**Fossil**